STATISTICAL DATA FOR MOVEMENTS ON YOUNG FAULTS OF THE CONTERMINOUS UNITED STATES; PALEOSEISMIC IMPLICATIONS AND REGIONAL EARTHQUAKE FORECASTING

H. R. Shaw, A. E. Gartner
U.S. Geological Survey, Menlo Park, CA 94025
and
F. Lusso*
Sandia Laboratories, Albuquerque, N M 87185

U.S. Geological Survey
OPEN-FILE REPORT

81-946

*Present address: 4301 Livengood Rd., Winston-Salem, NC 27106

Contents

Figures

Tables

Abstract

Fault-activation frequencies in the United States have been derived from U.S. Geological Survey Miscellaneous Field Studies Map 916 for 30 faulting regions and 5 age groups (from 15 m.y. to historical). Three conclusions from this study are: (1) faults are branching systems conforming to geometric laws of self- similarity; (2) slopes of frequency-magnitude plots (b values) can be explained geometrically, (3) regional earthquake forecasting can be geologically quantified. Paleoseismic parallelograms have been constructed representing relations between the given number of activated faults (n), their lengths, and the rupture lengths per year. "Activated length" is the fault length involved in rupture according to the map data; "rupture-length rate" is the rate at which fault rupture occurs according to the age progressions for these data. Earthquake magnitudes and frequencies are calculated using different assumptions about the possible rates at which given numbers and lengths may be activated in a given fault set.

SECTION 1.

1. Introduction; Maps of Young Faults in the United States.

The principal data of our study are histograms for numbers of faults versus fault length taken from a map compiled by Howard and others (1978)[1/] at a scale of 1:5,000,000; it was derived from regional compilations at a scale of 1:250,000 (Figure 1.-1). The map is subdivided into 30 named regions by Howard and others (1978), as listed in Table 1.-1; we have numbered the regions in this report only for bookkeeping purposes according to alphabetical order, avoiding any attempt to group regions genetically.

We have also used data from maps of coastal southern California (Ziony and others, 1974)[1/] at a scale of 1:250,000 as a comparative set to check the relative effects due to map scale, compilation methods, and different ranges in age classifications (see area outlined in Figure 1.-1B).

Although the data for coastal southern California (designated L.A. Area in this report) are basically from the same original sources as the United States map, there are major differences in the length scales and age groups for the faults portrayed, and the boundaries of the geographic regions represented are different. This comparison represents one of the interesting discoveries of this preliminary analysis.

Our purpose in reporting results in this tentative and incomplete manner is to stir interest in carrying the analysis to more definitive conclusions. The conclusions are largely subjective, and they are made so we can describe some of the patterns and ideas that we feel are suggested by the data. We feel that the implications are important enough to launch a major statistical study of faulting in North America. Based on our present approach the next phase of study is to compile data sets for each of the base maps at 1:250,000 and to select within each of these map regions still larger scale areas where faulting resolution and age classifications may be optimized. In subsequent work, a goal is to also classify faults according to their styles of movement and their angular orientations. We did not attempt that kind of sorting for the United States data. That omission, in itself, is the basis for ideas concerning the general nature of faults as branching systems of fractures behaving with a remarkable degree of similarity regardless of style, crustal heterogeneity or age. We believe there is sufficient data on different map scales to test this idea quantitatively, and, if it can be documented, there exists a powerful geological basis for classifying fault regions for a variety of environmental purposes, including earthquake forecasting.

[1/] These maps, Miscellaneous Field Studies Maps MF-585 and MF-916, can be purchased from the Branch of Distribution, U. S. Geological Survey, Box 25286, Federal Center, Denver, CO 80225. MF-916 is also available from the Branch of Distribution, U. S. Geological Survey, 1200 South Eads Street, Arlington, VA 22202.

SECTION 1. FIGURES AND TABLES

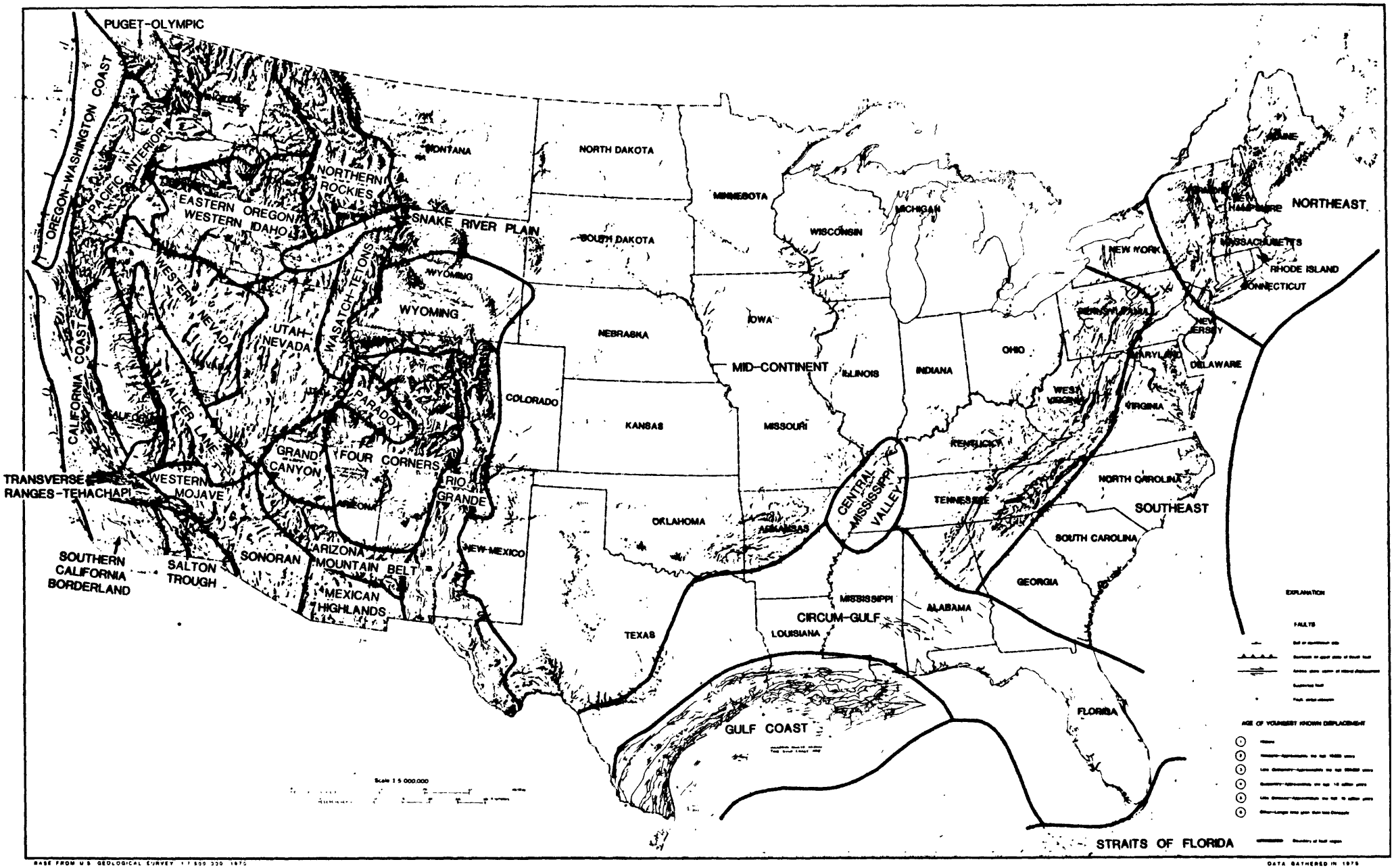

PRELIMINARY MAP OF YOUNG FAULTS IN THE UNITED STATES AS A GUIDE TO POSSIBLE FAULT ACTIVITY

COMPILED BY

R A HOWARD J M AARON, E E BRABB M R BROCK H D GOWER B J HUNT
D J MILTON W R MUEHLBERGER J N NAKATA G PLAFKER
D C PROWELL R E WALLACE AND J J WITHIND

1978

Figure 1.-1. (A)

Reduced photocopy; Preliminary Map of Young Faults in the United States (Howard and others, 1978).

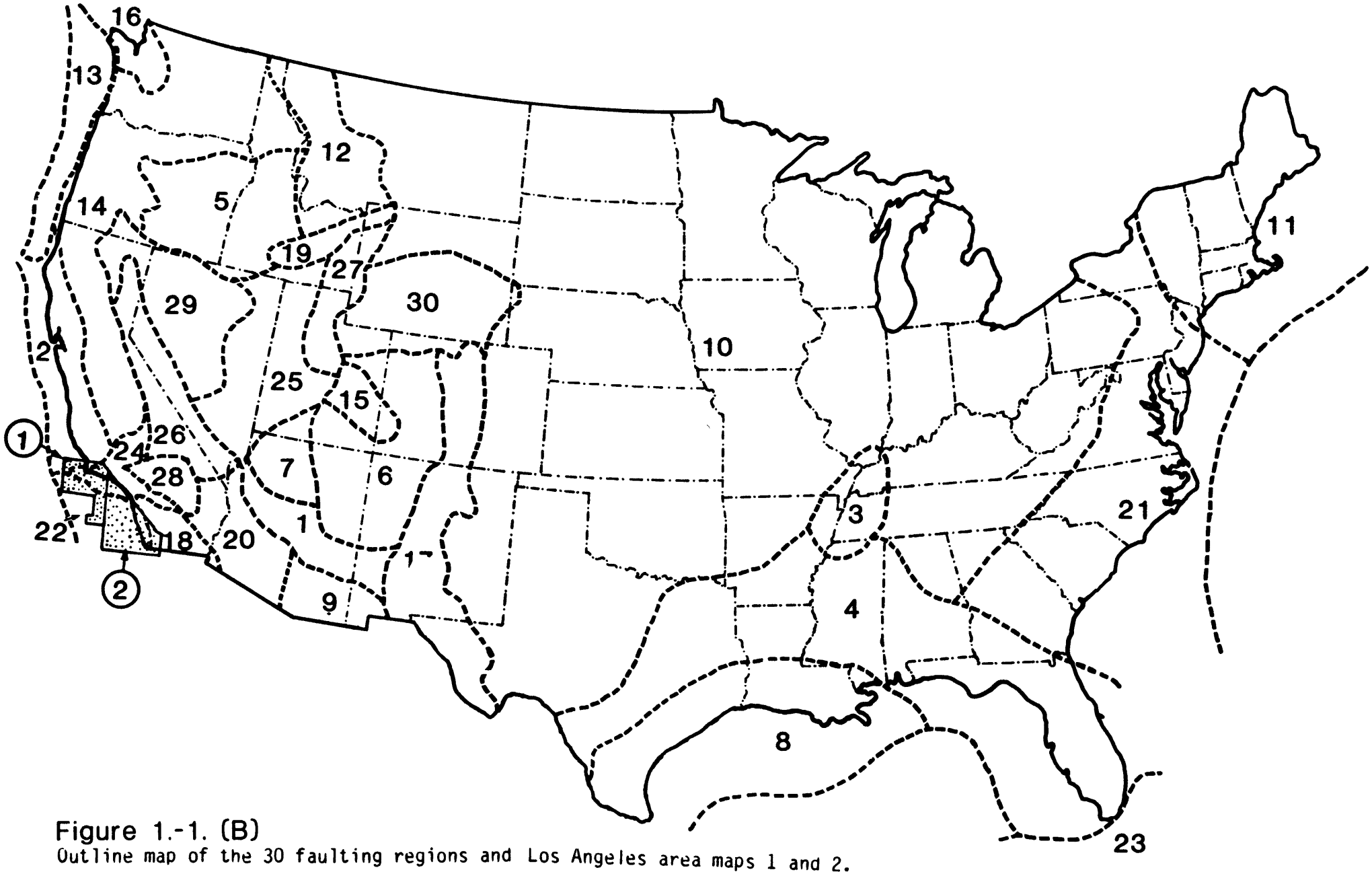

Figure 1.-1. (B)
Outline map of the 30 faulting regions and Los Angeles area maps 1 and 2.

Table 1.-1. Alphabetical list of fault regions for the conterminous United States (from Howard and others, 1978).

Arizona Mountain Belt	[01]
California Coast	[02]
Central Mississippi Valley	[03]
Circum-Gulf	[04]
Eastern Oregon-Western Idaho	[05]
Four Corners	[06]
Grand Canyon	[07]
Gulf Coast	[08]
Mexican Highland	[09]
Mid-Continent	[10]
Northeast	[11]
Northern Rockies	[12]
Oregon-Washington Coast	[13]
Pacific Interior	[14]
Paradox	[15]
Puget-Olympic	[16]
Rio Grande	[17]
Salton Trough	[18]
Snake River Plain	[19]
Sonoran	[20]
Southeast	[21]
Southern Calif. Borderland	[22]
Straits of Florida	[23]
Transverse Ranges-Tehachapi	[24]
Utah-Nevada	[25]
Walker Lane	[26]
Wasatch-Tetons	[27]
Western Mojave	[28]
Western Nevada	[29]
Wyoming	[30]

Brackets give numbers used in compiling data for illustrations.

SECTION 2.

2. Numbers of Faults Distributed by Fault Length.

2.1 Frequency Histograms

The measurements used to classify fault lengths are summarized in Figure 2.1.-1 (individual sets of histograms are numbered in parentheses according to Table 1.-1, including data from the larger scale maps for Coastal Southern California; each set of histograms gives the total numbers for measured faults in each region, as well as the numbers for measured faults in each age group in the region). Table 2.1.-1 lists the age groups for the conterminous U. S. and Los Angeles areas used throughout this report. Counts were made for every 0.02 cm at the scale 1:5,000,000, giving a length interval of 1 km, which is near the resolution limit at this scale. This limit explains why the maximum recorded number occurs at a greater length (near 10 km) for the United States data. The data for the Los Angeles area, however, show maxima near 1 or 2 km at the same length scale and counting interval, because the larger mapping scale (1:250,000) allowed shorter faults to be portrayed on the map. This point is important to interpretating regression curves for frequency versus length in later sections.

The counting interval is also important relative to protraying frequencies as continuous functions. Most of our data are expressed in terms of the 1 km interval. This must be kept in mind when we portray the results as logarithmic and cumulative distributions. Slopes, limiting intercepts and shapes for cumulative distributions are affected by gaps in the data. However, there are strong consistencies in the distributions even where the quantitites of data are poor. This generalization, though crude, is another basis for our inference that, on the average, there is a natural law of branching ratios with a relatively narrow range in functional forms. Anticipating later discussions, these functions appear to represent length frequencies that are inversely porportional to the length raised to a power somewhere between about 1 and 3, with an average a little less than 2. The cumulative frequency, being a summation or integral of these distributions is also an inverse power law with an exponent usually less than 2; the relations between incremental and cumulative distributions are illustrated in section 4.

It is notable that the above forms for the distributions were suggested theoretically by Vere-Jones (1976) on the basis of stochastic models describing fault activation. The average values and ranges in exponents are similar to values he derived. We have also observed that similar functions describe the distributions of microfractures in laboratory test specimens, the distribution in lengths of septa between soap bubbles in froths having heterogeneous bubble sizes, the distributions for stream lengths in drainage systems, and the relation between numbers and crater diameters for meteorite impacts on the planets. These comparisons are given in section 4 discussing cumulative frequencies. Evidently we have rediscovered the wheel in the sense that the distributions apparently

represent some general properties that describe intersecting lines and surfaces. The conditions for, limitations on, and rates of change in these fundamental distributions, however, may bring a new and unifying perspective to our abilities in locating active faults and forecasting related earthquake frequencies.

SECTION 2.1. FIGURES AND TABLES

REGION 1

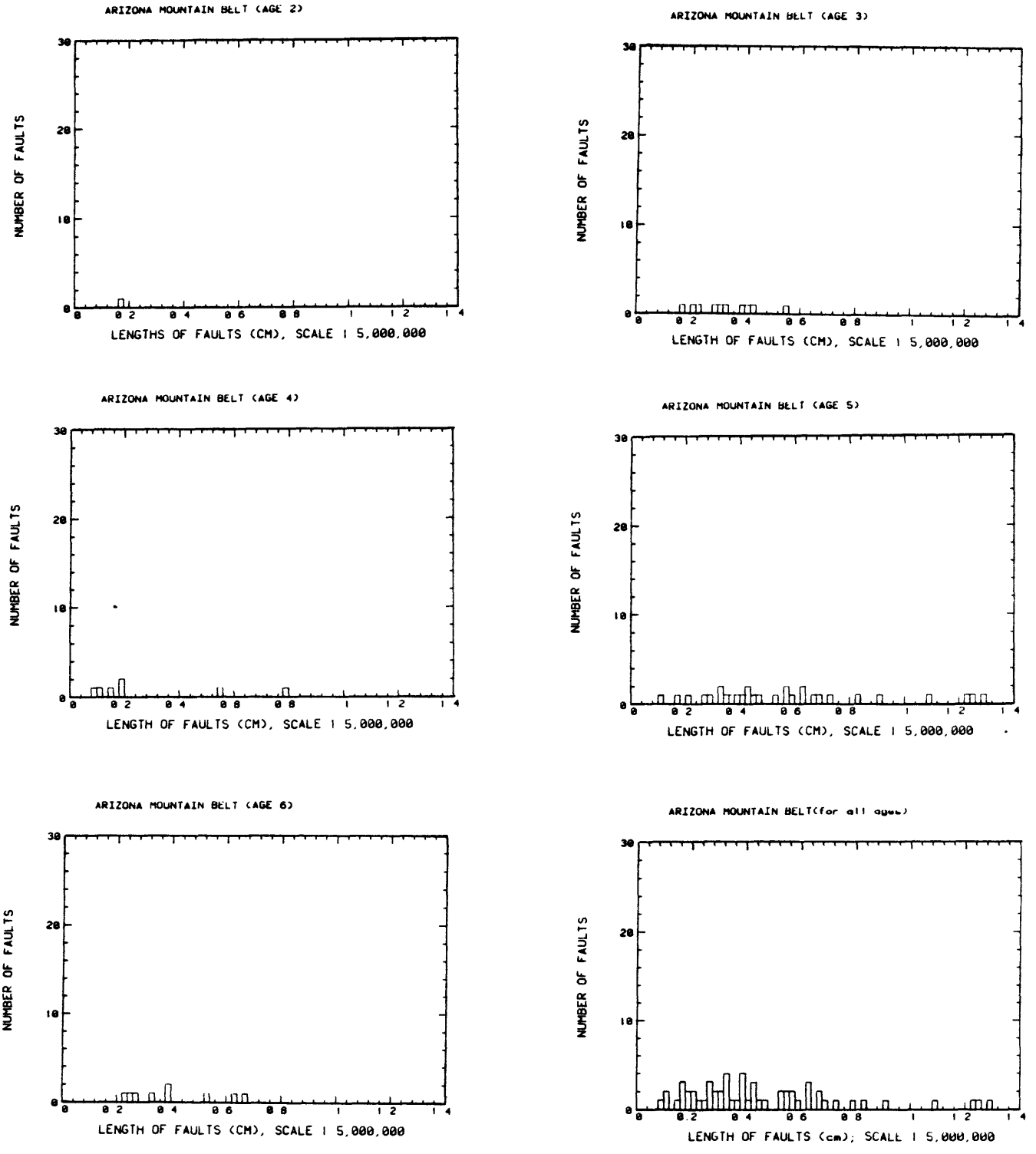

Figure 2.1.-1. (1)
Histograms for number versus fault length in each faulting region of Figure 1.-1 plus the L. A. area; data are given for each age category plus summations of all data in all age categories. Individual diagrams are identified by region numbers in parentheses and by name for L. A. Lengths are in centimeters at the map scale 1:5,000,000 (1 cm equals 50 km); more than one diagram per age group is used for regions with very long faults. In a few instances the histograms show fault counts for an age group that does not appear on the map for that region. This is because we used an unedited version that has a few age distinctions that were eliminated in the published version.

HISTOGRAM OF FAULT LENGTHS, CONTERMINOUS U S

REGION 2

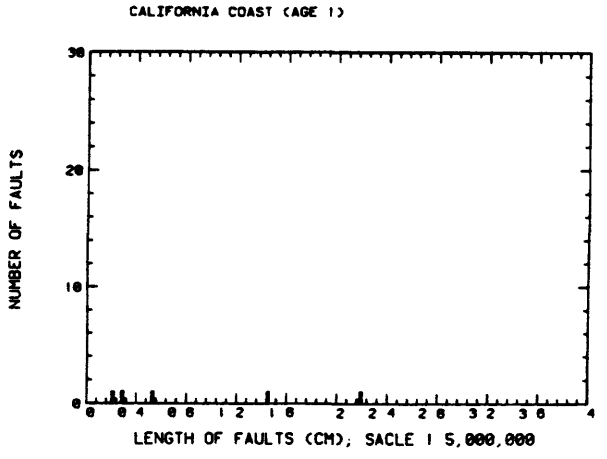

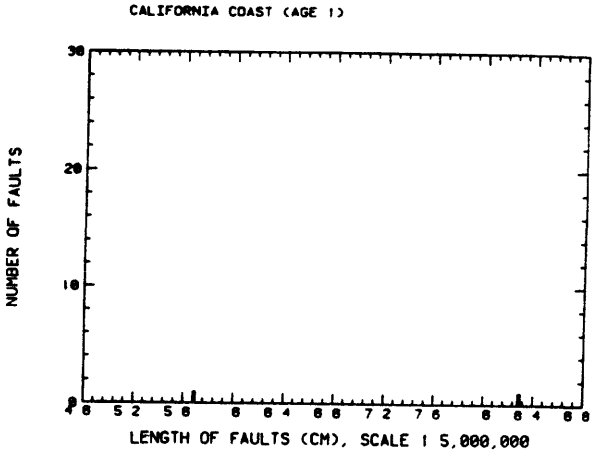

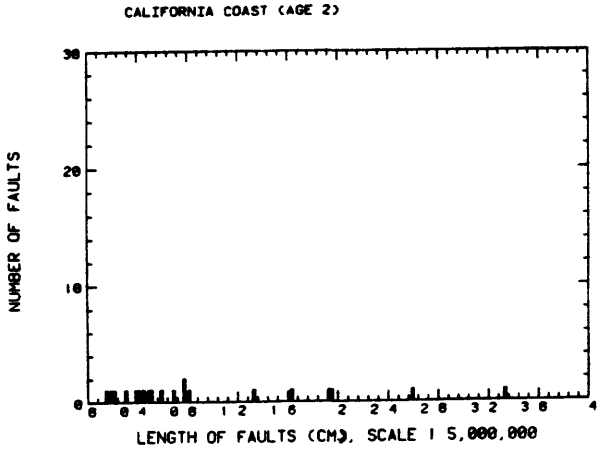

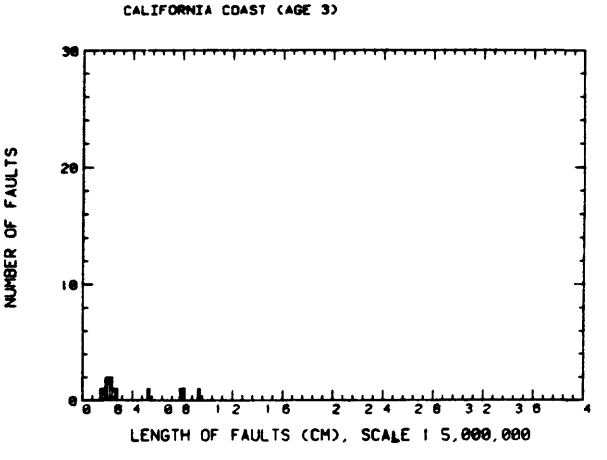

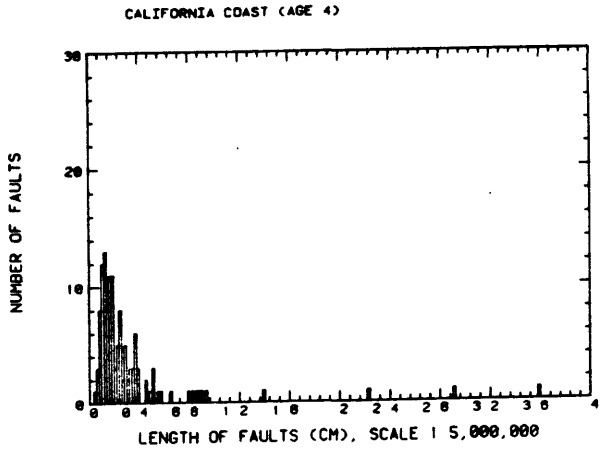

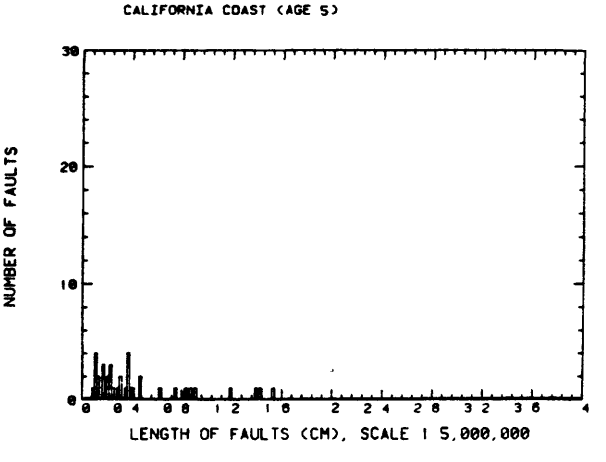

Figure 2.1.-1. (2)

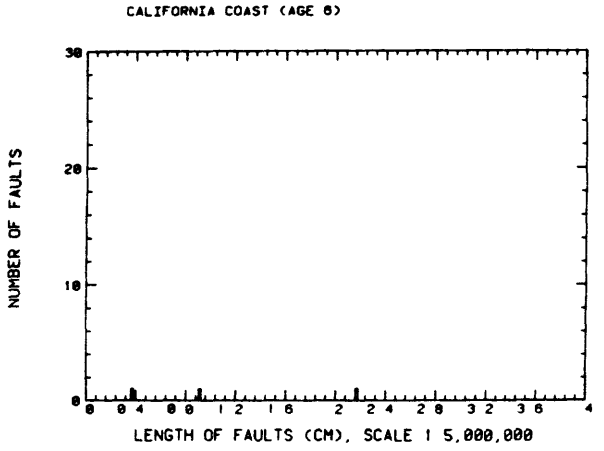
CALIFORNIA COAST (AGE 0)
NUMBER OF FAULTS
30
20
10
0
0 0 4 0 0 1 2 1 6 2 2 4 2 8 3 2 3 6 4
LENGTH OF FAULTS (CM), SCALE 1 5,000,000

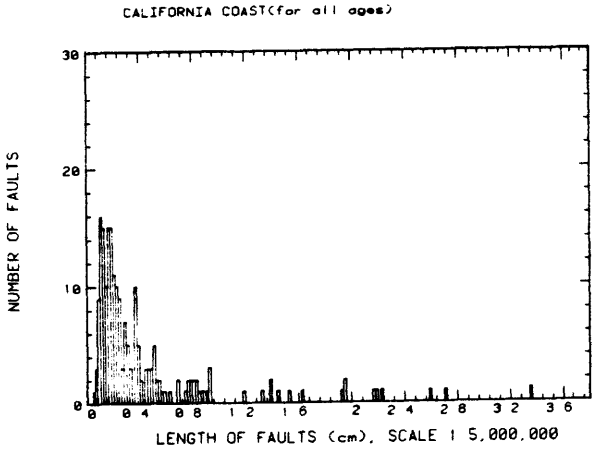
CALIFORNIA COAST(for all ages)
NUMBER OF FAULTS
30
20
10
0
0 0 4 0 8 1 2 1 6 2 2 4 2 8 3 2 3 6
LENGTH OF FAULTS (cm), SCALE 1 5,000,000

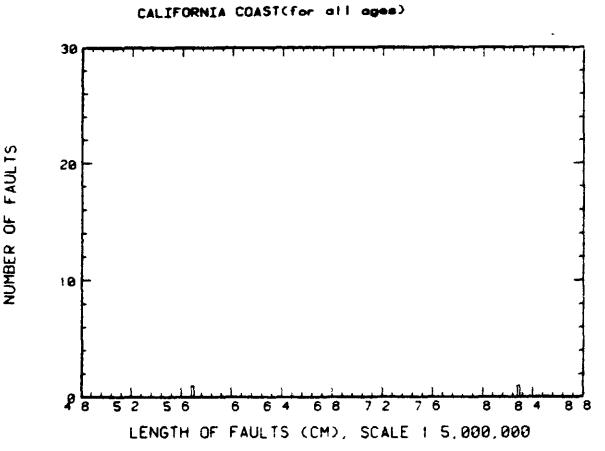
CALIFORNIA COAST(for all ages)
NUMBER OF FAULTS
30
20
10
0
4 8 5 2 5 6 6 6 4 6 8 7 2 7 6 8 8 4 8 8
LENGTH OF FAULTS (CM), SCALE 1 5,000,000

HISTOGRAM OF FAULT LENGTHS, CONTERMINOUS U S.

REGION 3

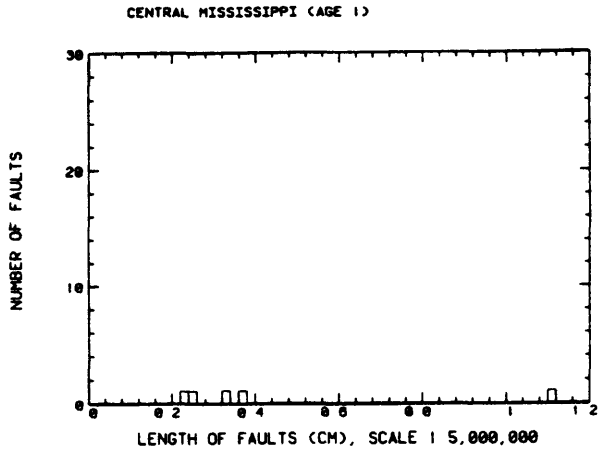

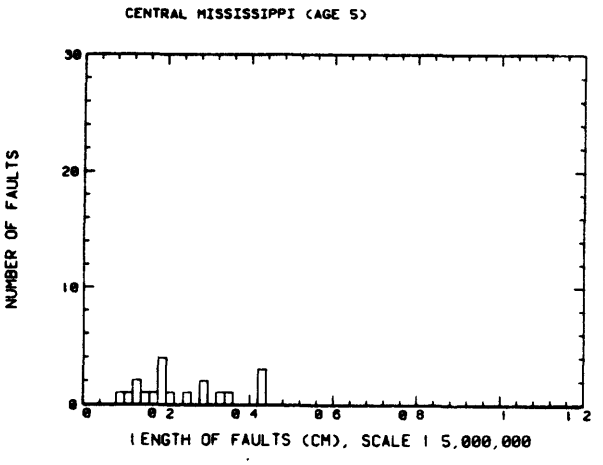

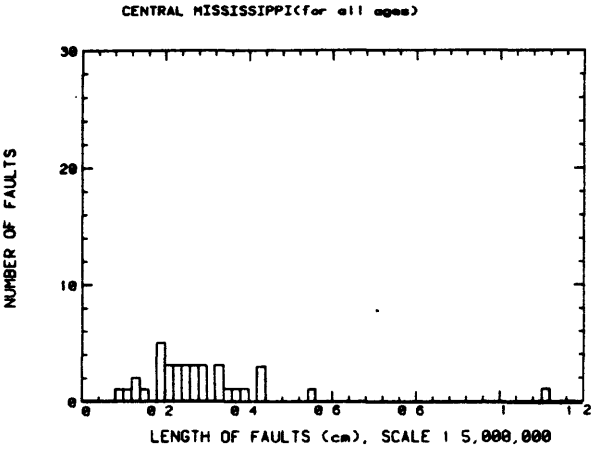

Figure 2.1.-1. (3)

HISTOGRAM OF FAULT LENGTHS, CONTERMINOUS U.S.

REGION 4

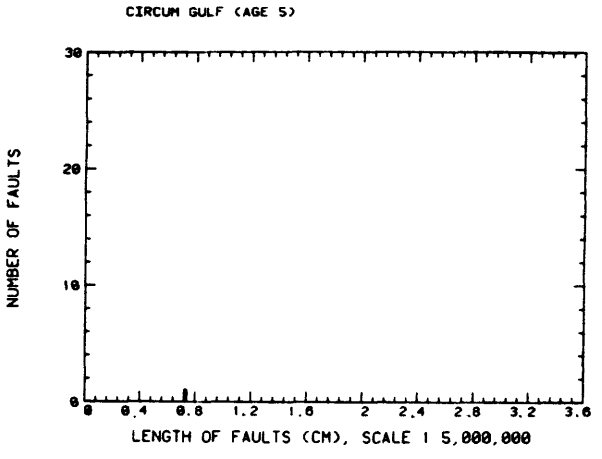

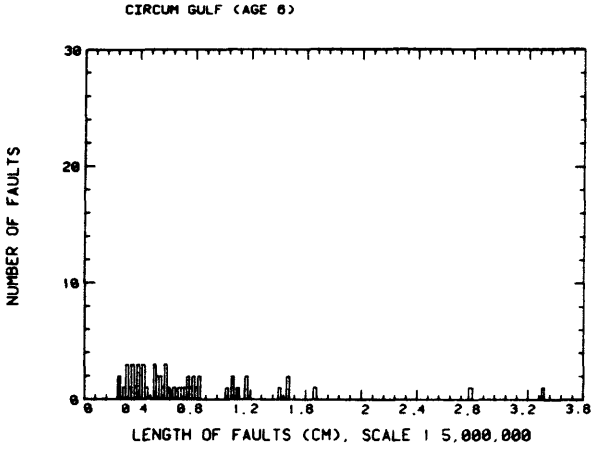

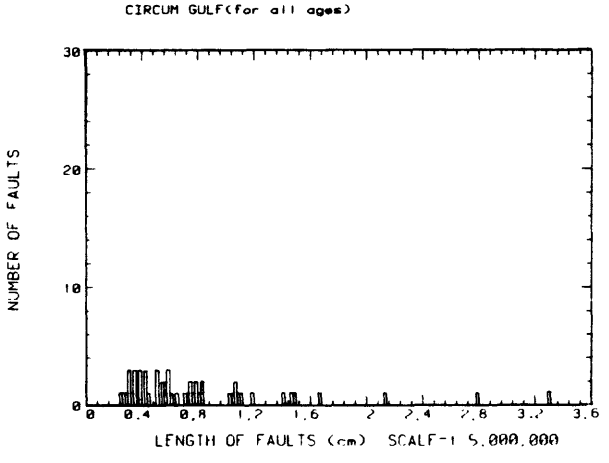

Figure 2.1.-1. (4)

HISTOGRAM OF FAULT LENGTHS, CONTERMINOUS U S

REGION 5

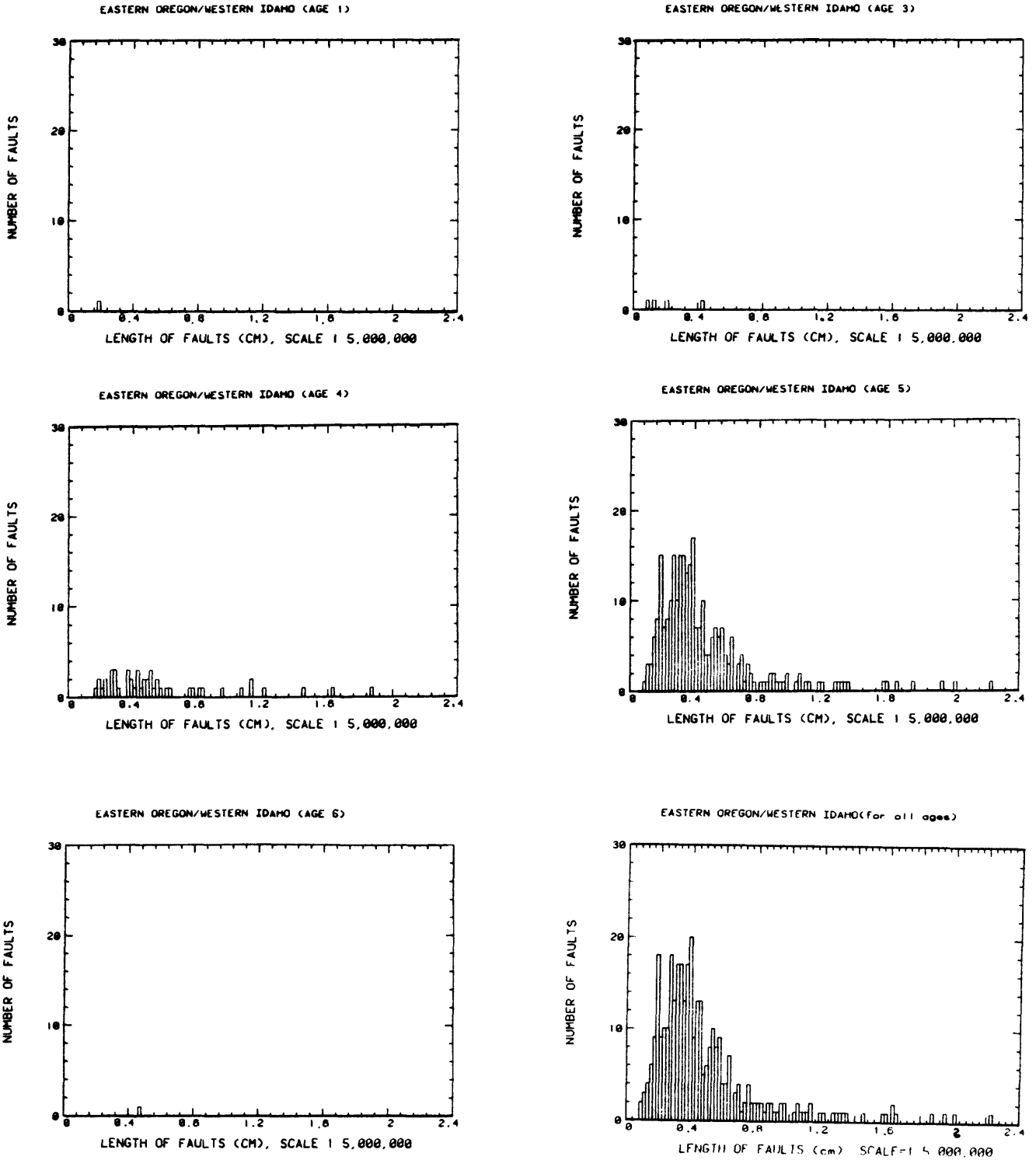

Figure 2.1.-1. (5)

HISTOGRAM OF FAULT LENGTHS, CONTERMINOUS U.S.

REGION 6

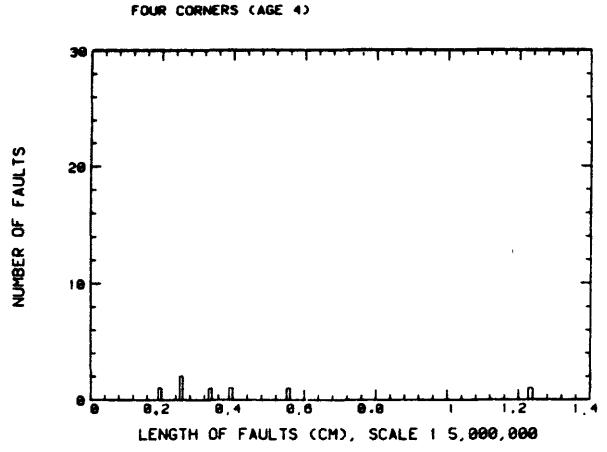

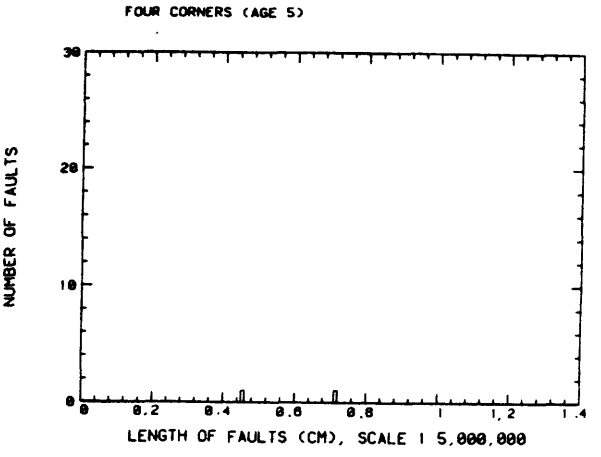

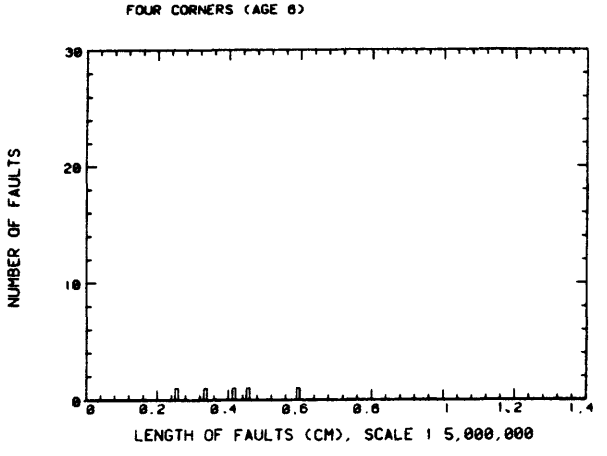

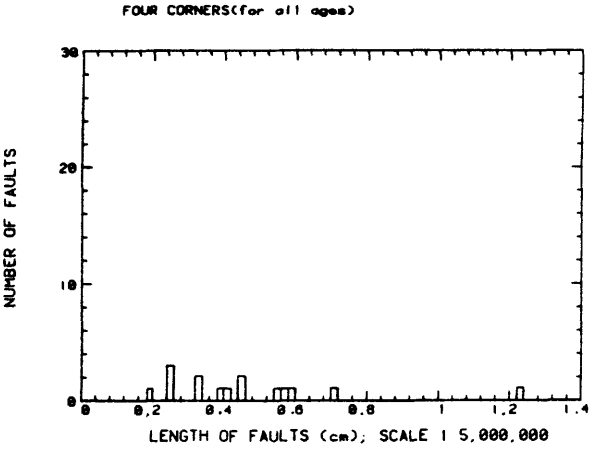

Figure 2.1.-1. (6)

HISTOGRAM OF FAULT LENGTHS, CONTERMINOUS U.S.

REGION 7

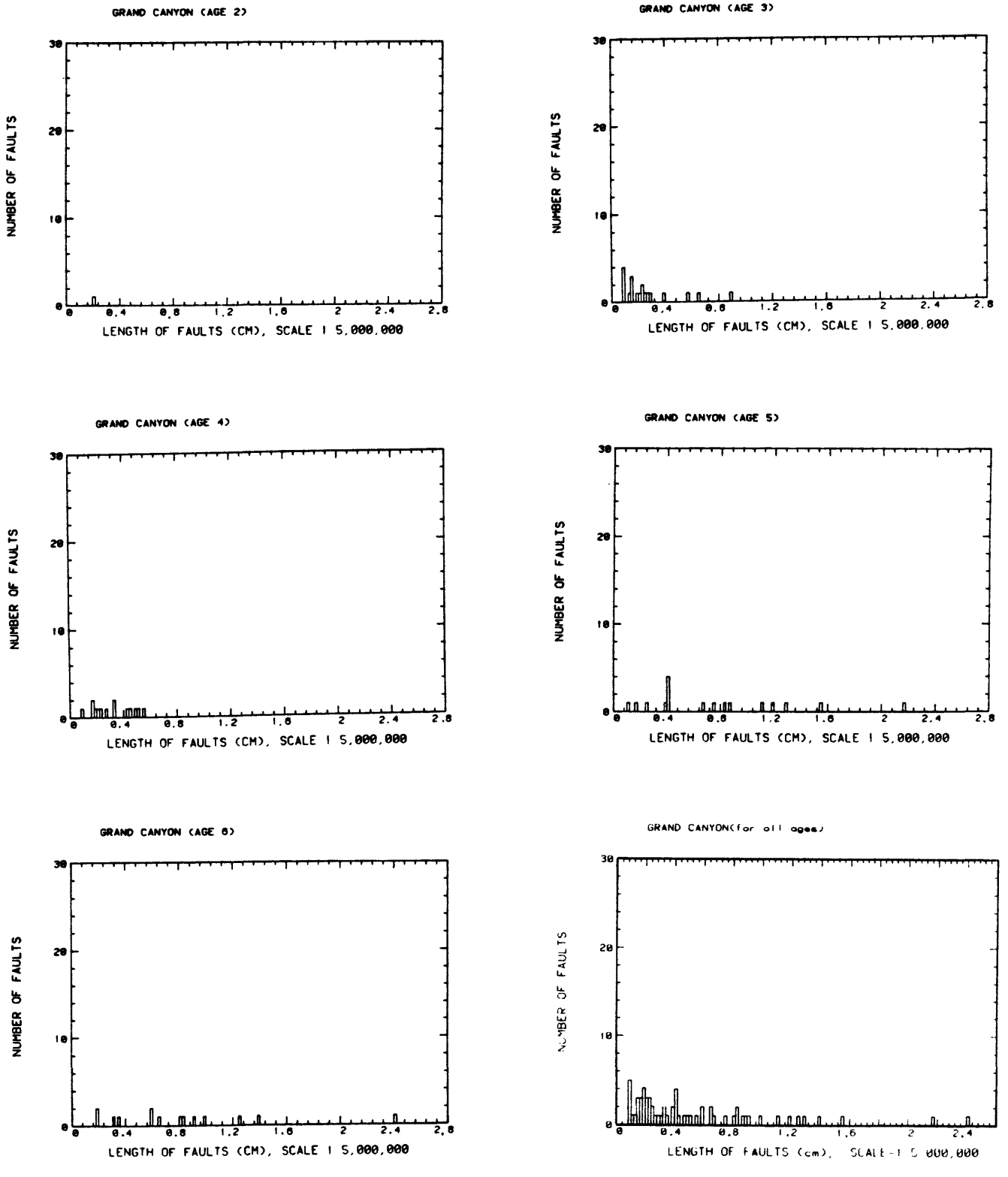

Figure 2.1.-1. (7)

HISTOGRAM OF FAULT LENGTHS, CONTERMINOUS U.S.

REGION 8

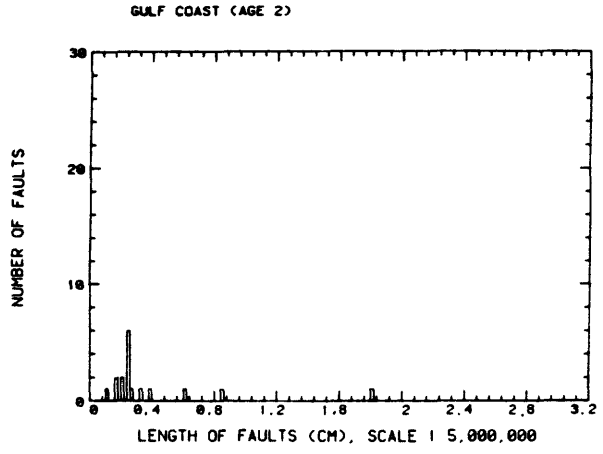

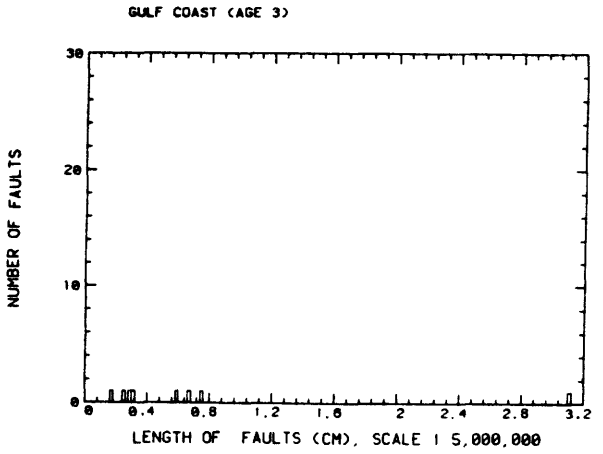

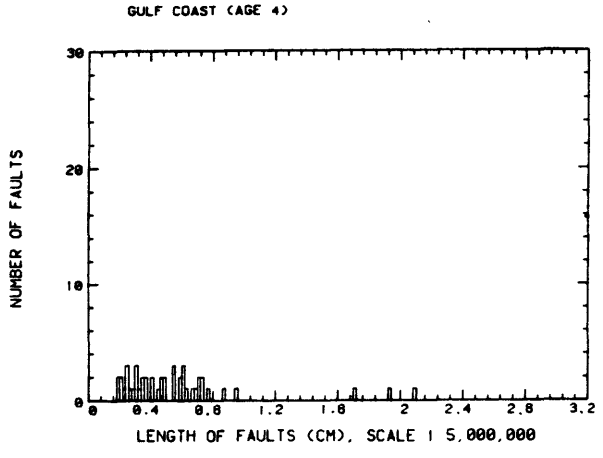

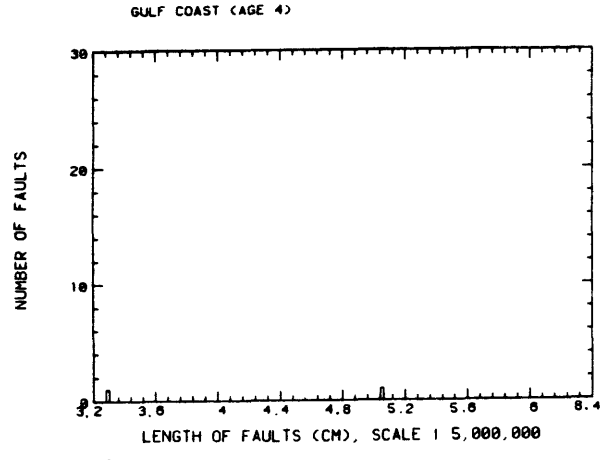

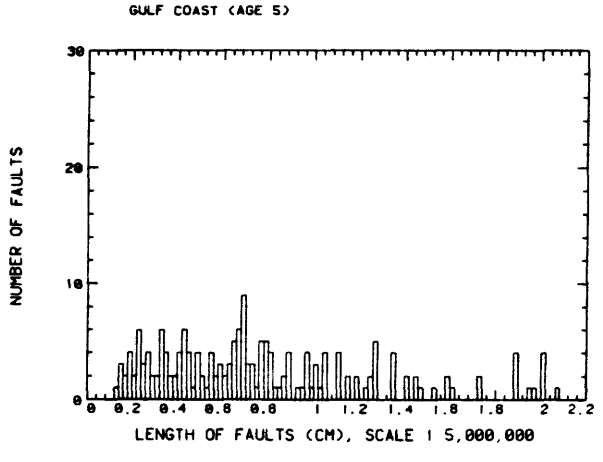

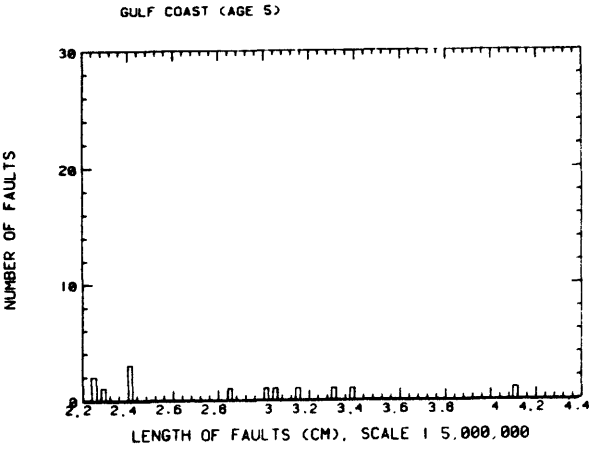

Figure 2.1.-1. (8)

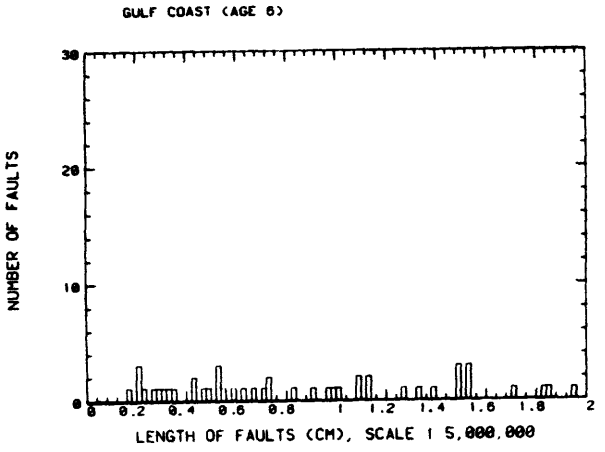
GULF COAST (AGE 6)
NUMBER OF FAULTS
30
20
10
0
0 0.2 0.4 0.6 0.8 1 1.2 1.4 1.6 1.8 2
LENGTH OF FAULTS (CM), SCALE 1 5,000,000

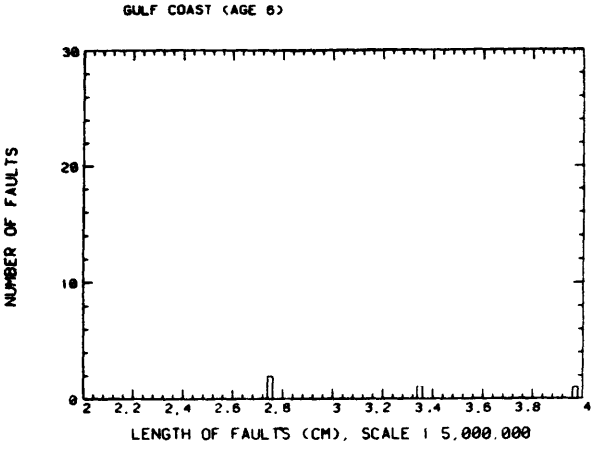
GULF COAST (AGE 6)
NUMBER OF FAULTS
30
20
10
0
2 2.2 2.4 2.6 2.8 3 3.2 3.4 3.6 3.8 4
LENGTH OF FAULTS (CM), SCALE 1 5,000,000

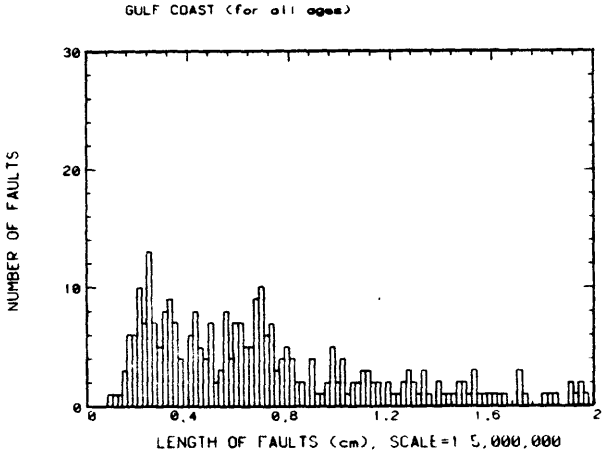
GULF COAST (for all ages)
NUMBER OF FAULTS
30
20
10
0
0 0.4 0.8 1.2 1.6 2
LENGTH OF FAULTS (cm), SCALE=1 5,000,000

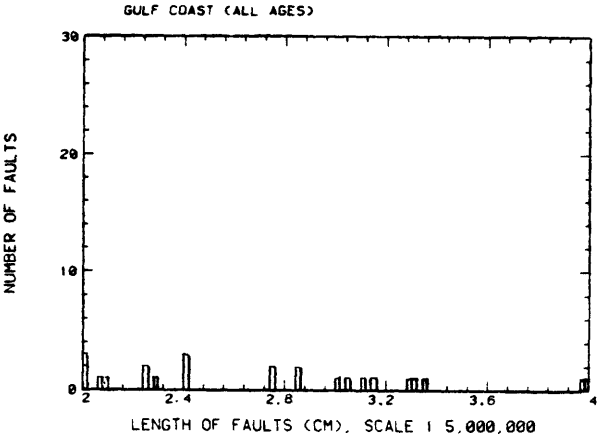
GULF COAST (ALL AGES)
NUMBER OF FAULTS
30
20
10
0
2 2.4 2.8 3.2 3.6 4
LENGTH OF FAULTS (CM), SCALE 1 5,000,000

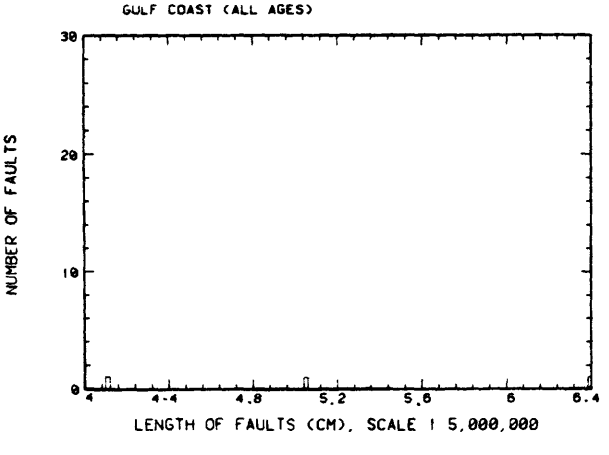
GULF COAST (ALL AGES)
NUMBER OF FAULTS
30
20
10
0
4 4.4 4.8 5.2 5.6 6 6.4
LENGTH OF FAULTS (CM), SCALE 1 5,000,000

HISTOGRAM OF FAULT LENGTHS, CONTERMINOUS U S

REGION 9

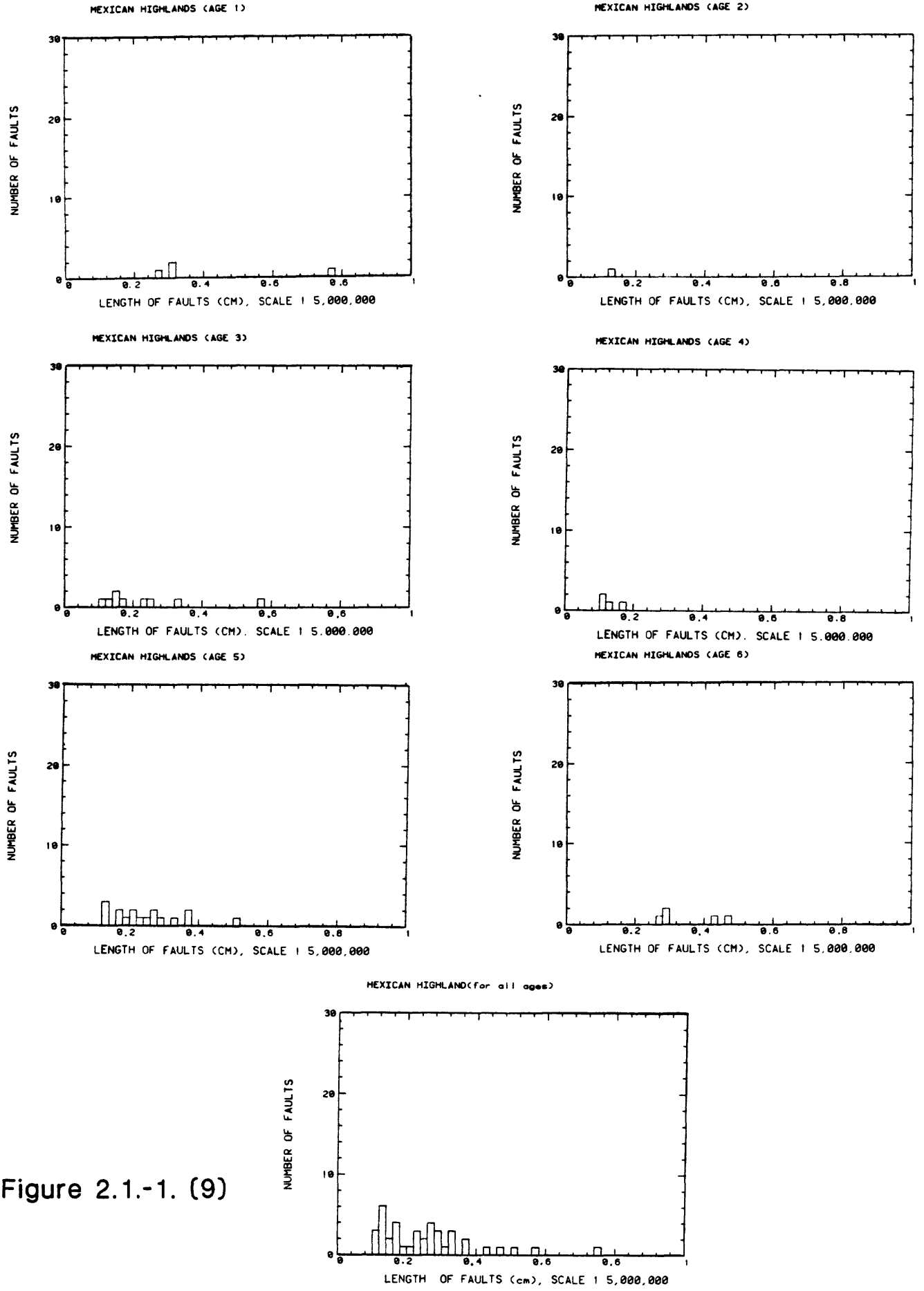

Figure 2.1.-1. (9)

HISTOGRAM OF FAULT LENGTHS, CONTERMINOUS U.S.

REGION 10

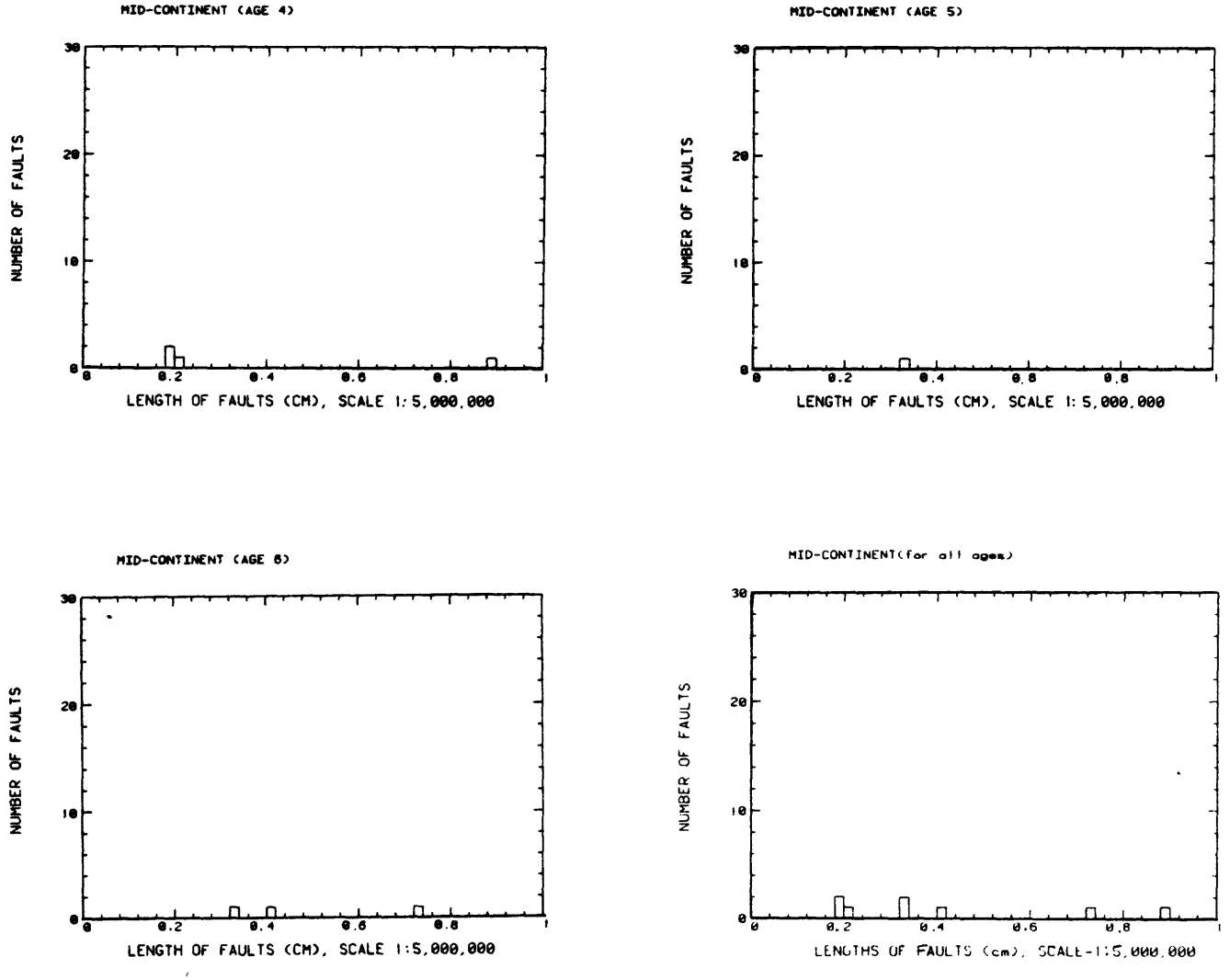

Figure 2.1.-1. (10)

HISTOGRAM OF FAULT LENGTHS, CONTERMINOUS U.S.

REGION 11

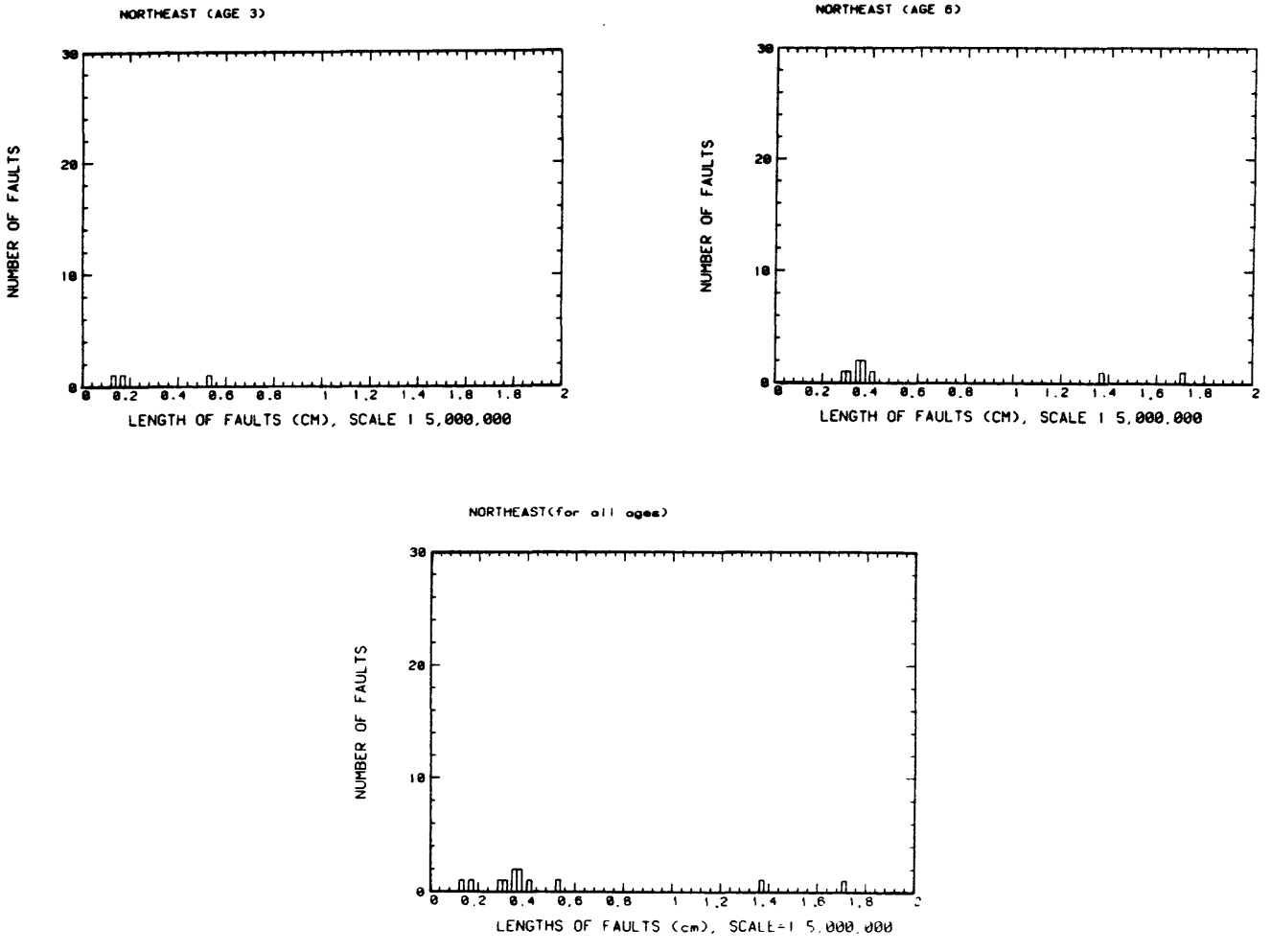

Figure 2.1.-1. (11)

HISTOGRAM OF FAULT LENGTHS, CONTERMINOUS U.S

REGION 12

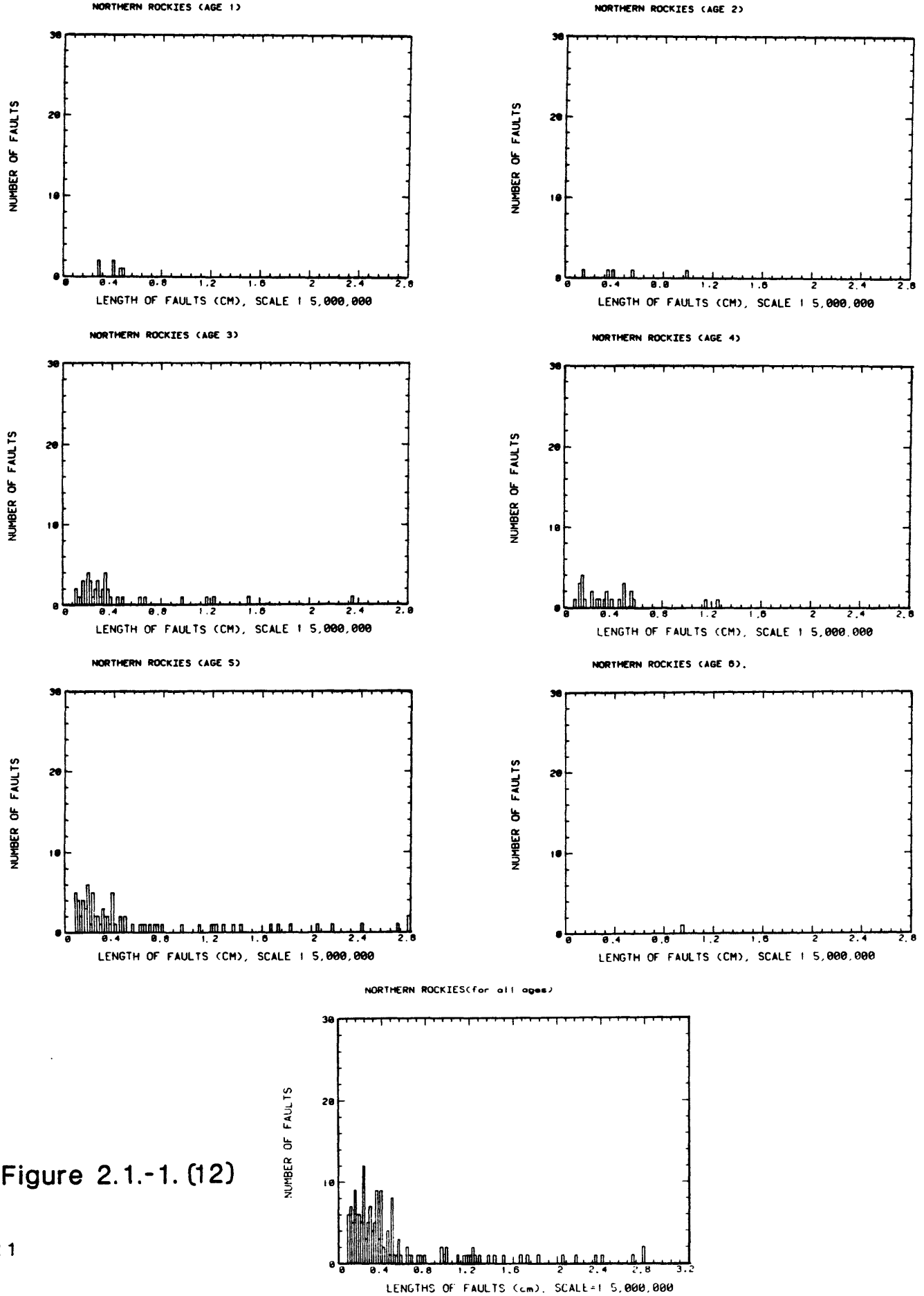

Figure 2.1.-1. (12)

HISTOGRAM OF FAULT LENGTHS, CONTERMINOUS U.S.

REGION 13

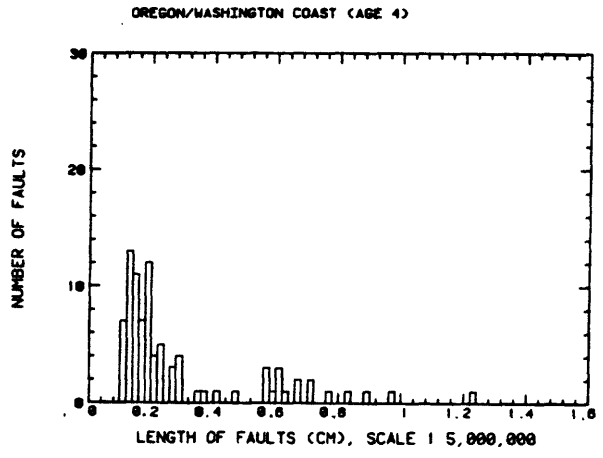

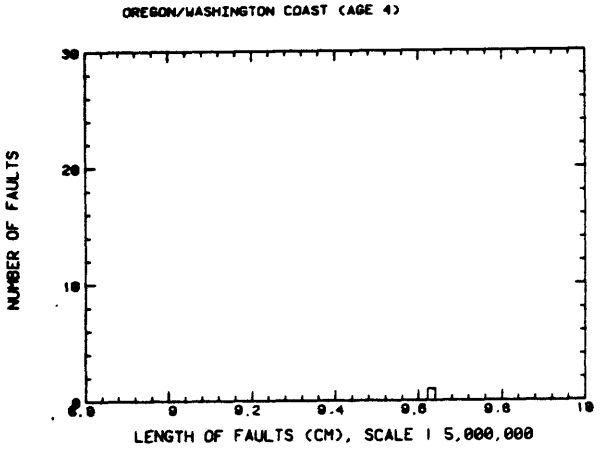

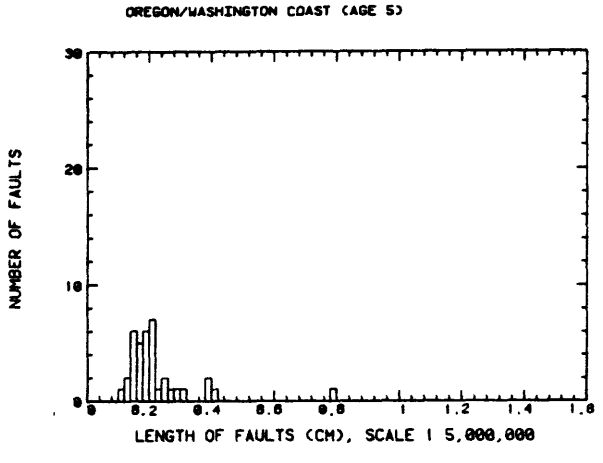

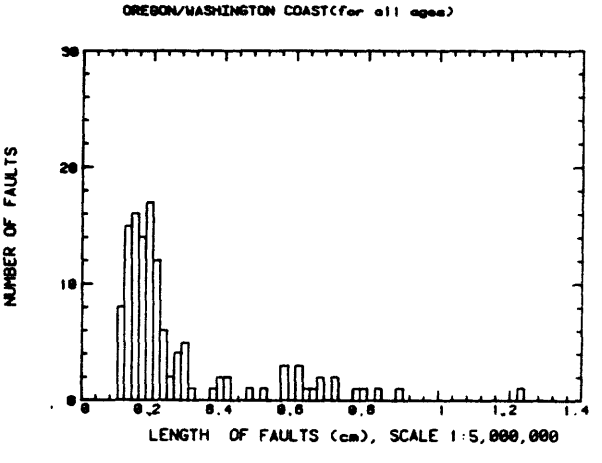

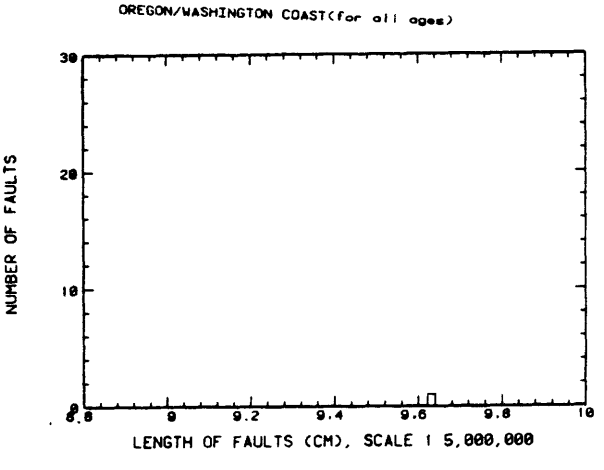

Figure 2.1.-1 (13)

HISTOGRAM OF FAULT LENGTHS, CONTERMINOUS U.S.

REGION 14

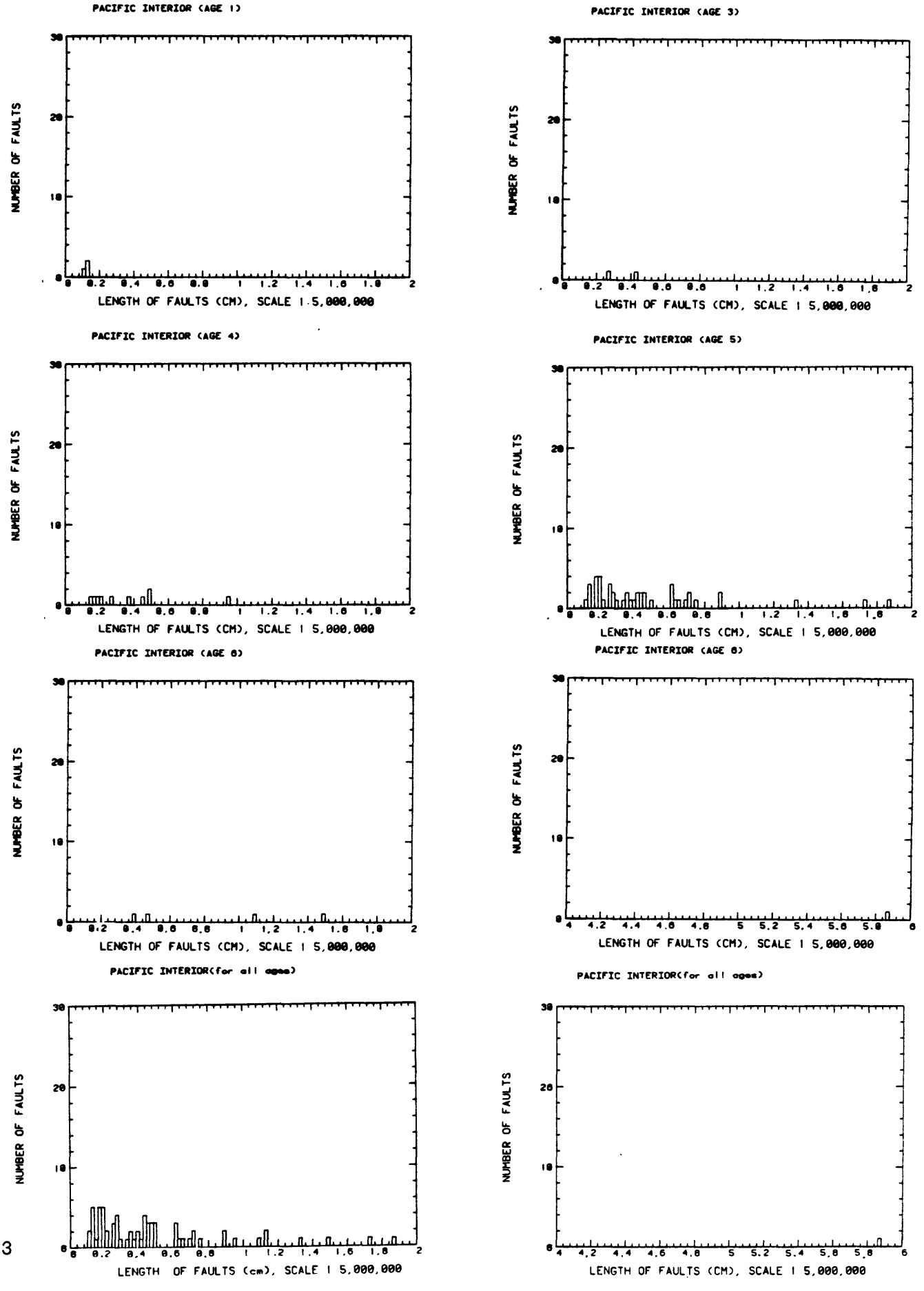

Figure 2.1.-1. (14)

HISTOGRAM OF FAULT LENGTHS, CONTERMINOUS U.S.

REGION 15

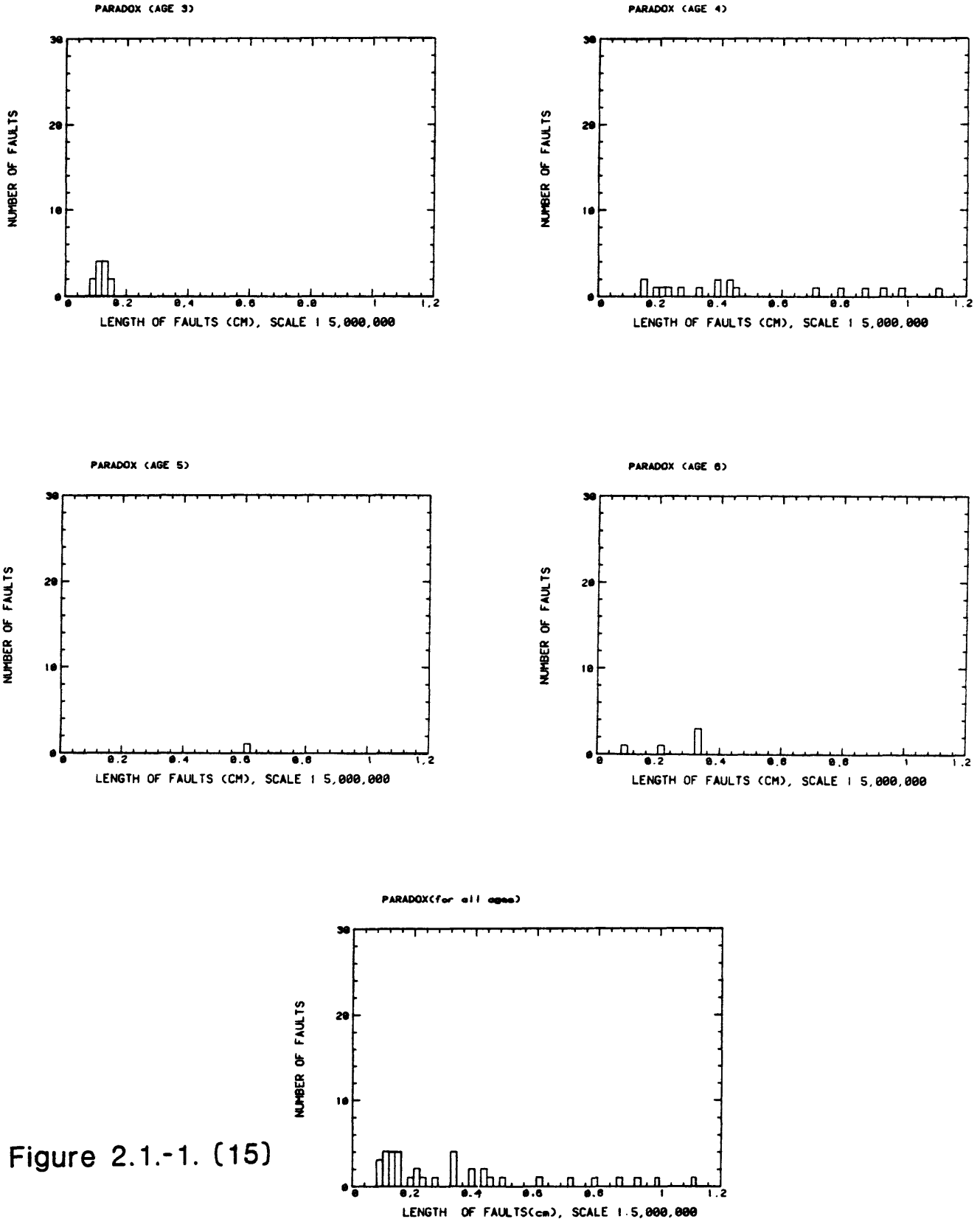

Figure 2.1.-1. (15)

HISTOGRAM OF FAULT LENGTHS, CONTERMINOUS U.S

REGION 16

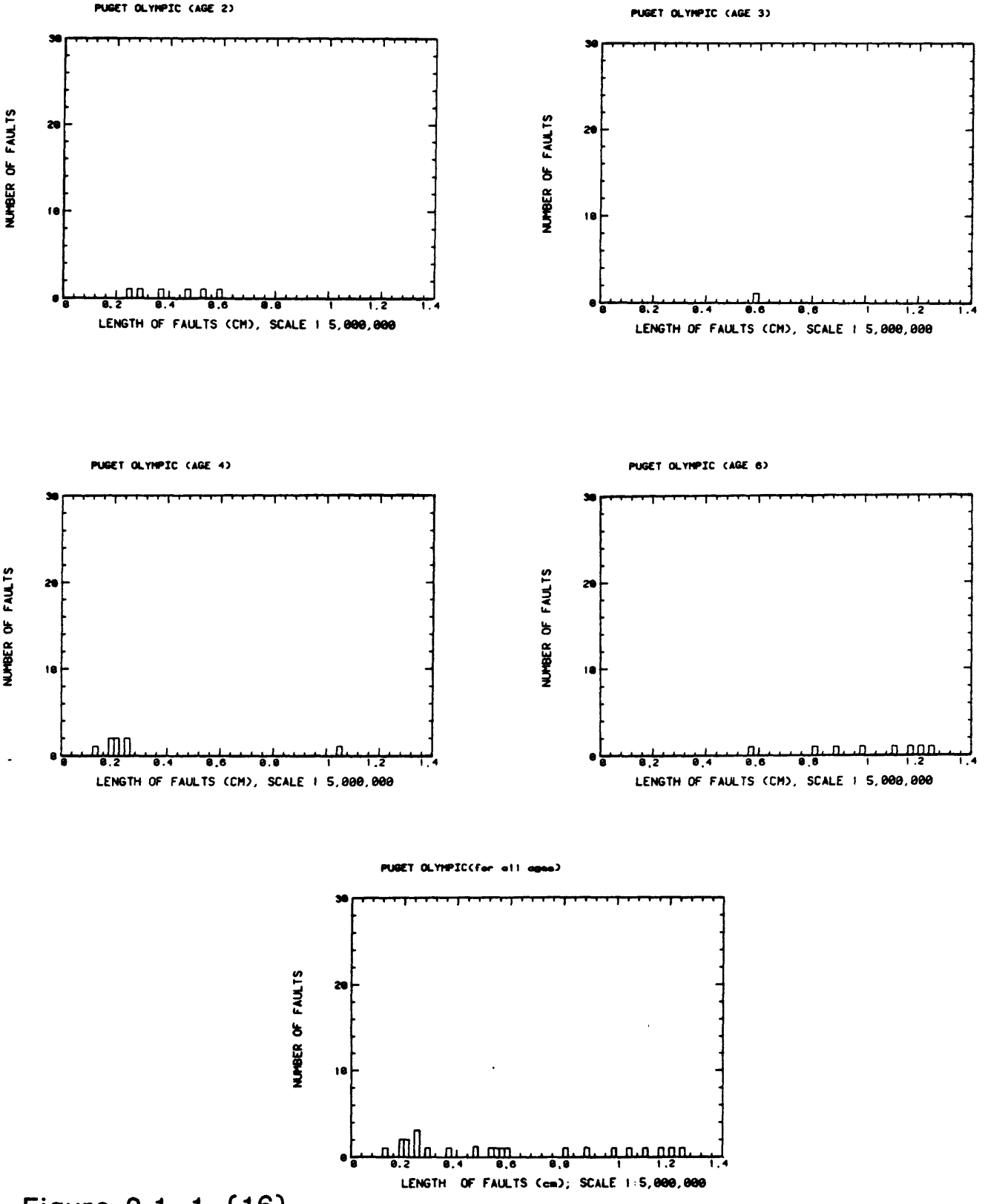

Figure 2.1.-1. (16)

HISTOGRAM OF FAULT LENGTHS, CONTERMINOUS U.S.

REGION 17

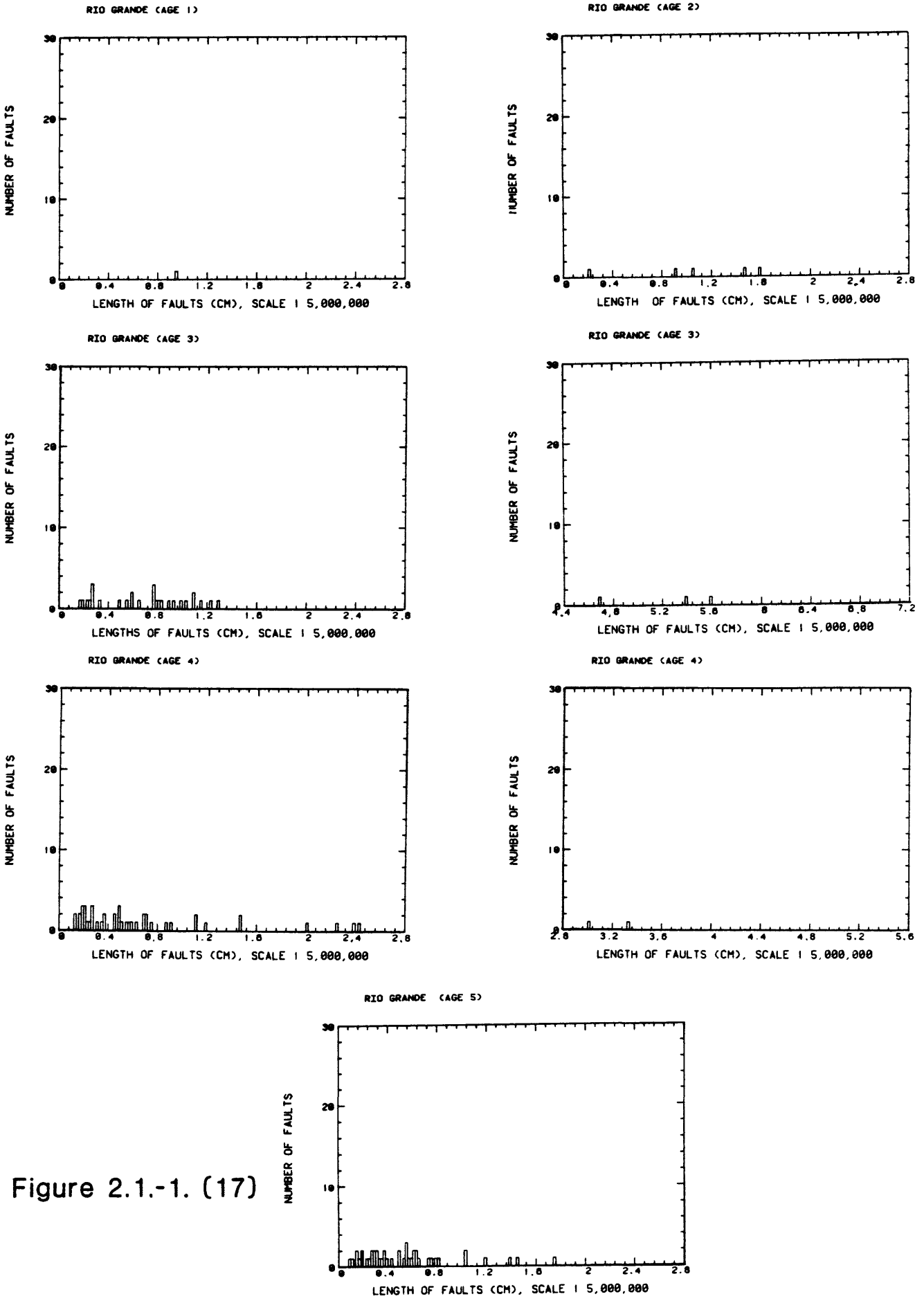

Figure 2.1.-1. (17)

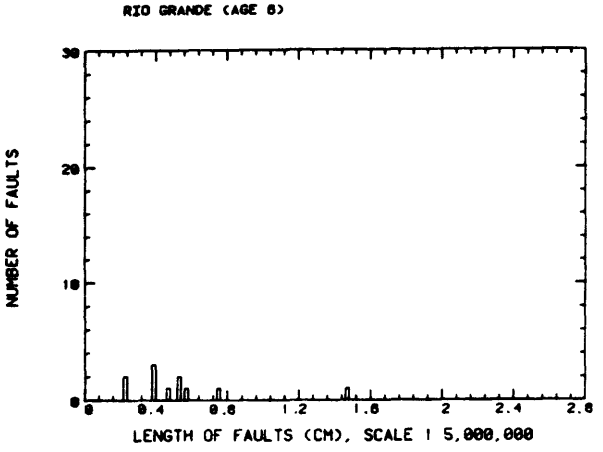
RIO GRANDE (AGE 8)
NUMBER OF FAULTS
30
20
10
0
0
0.4
0.8
1.2
1.6
2
2.4
2.8
LENGTH OF FAULTS (CM), SCALE 1 5,000,000

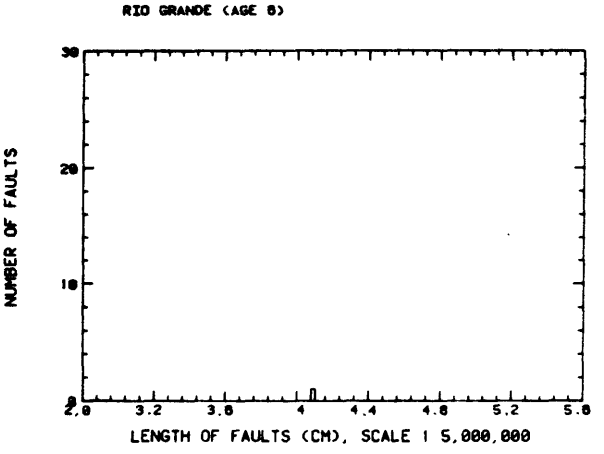
RIO GRANDE (AGE 8)
NUMBER OF FAULTS
30
20
10
0
2.8
3.2
3.6
4
4.4
4.8
5.2
5.6
LENGTH OF FAULTS (CM), SCALE 1 5,000,000

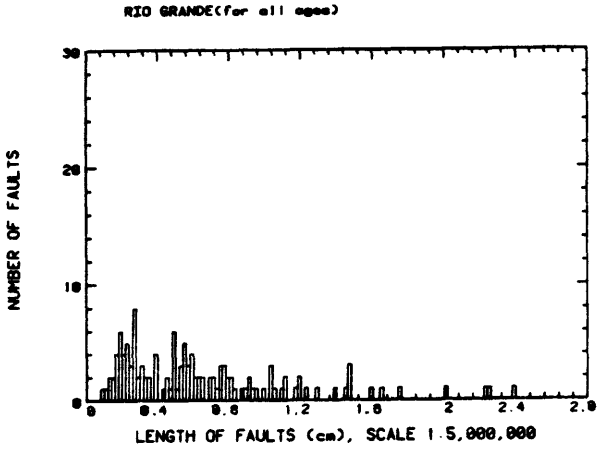
RIO GRANDE(for all ages)
NUMBER OF FAULTS
30
20
10
0
0
0.4
0.8
1.2
1.6
2
2.4
2.8
LENGTH OF FAULTS (cm), SCALE 1 5,000,000

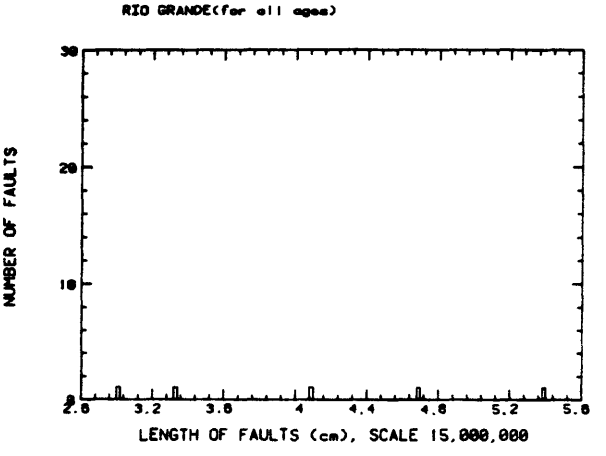
RIO GRANDE(for all ages)
NUMBER OF FAULTS
30
20
10
0
2.8
3.2
3.6
4
4.4
4.8
5.2
5.6
LENGTH OF FAULTS (cm), SCALE 15,000,000

HISTOGRAM OF FAULT LENGTHS, CONTERMINOUS U.S.

REGION 18

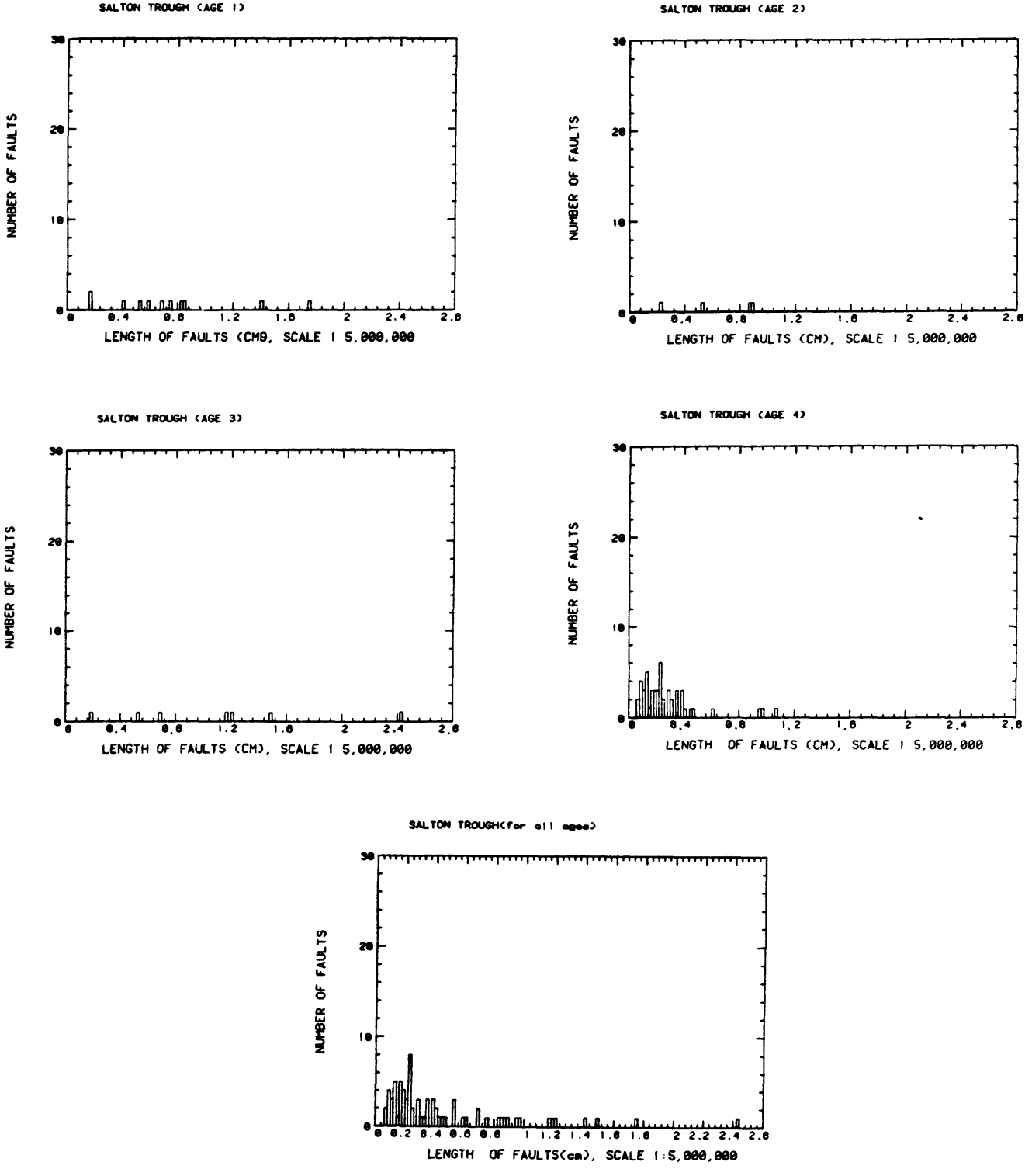

Figure 2.1.-1. (18)

HISTOGRAM OF FAULT LENGTHS, CONTERMINOUS U.S

REGION 19

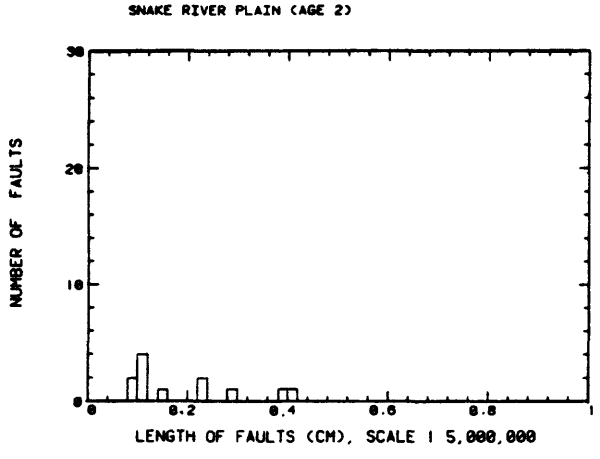

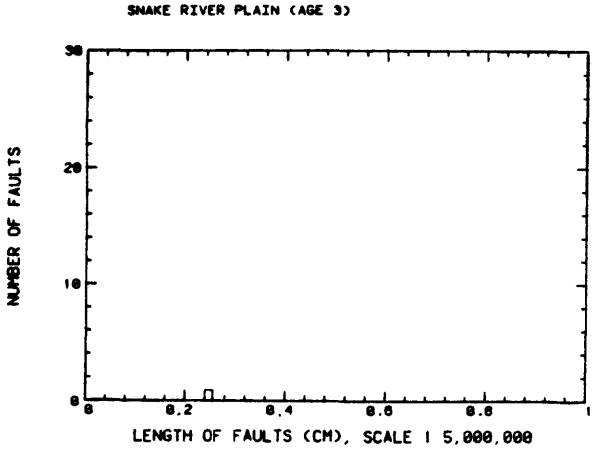

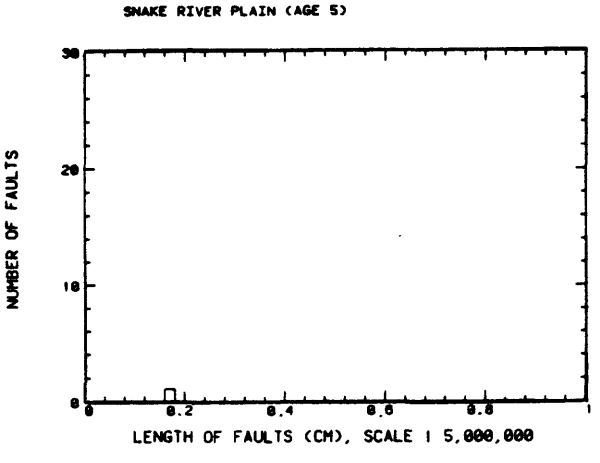

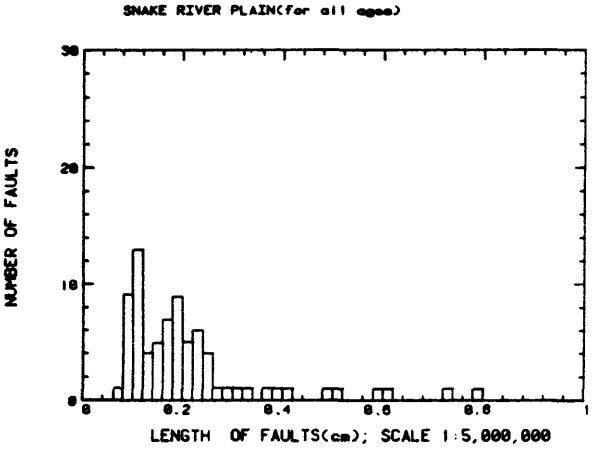

Figure 2.1.-1. (19)

HISTOGRAM OF FAULT LENGTHS, CONTERMINOUS U.S.

REGION 20

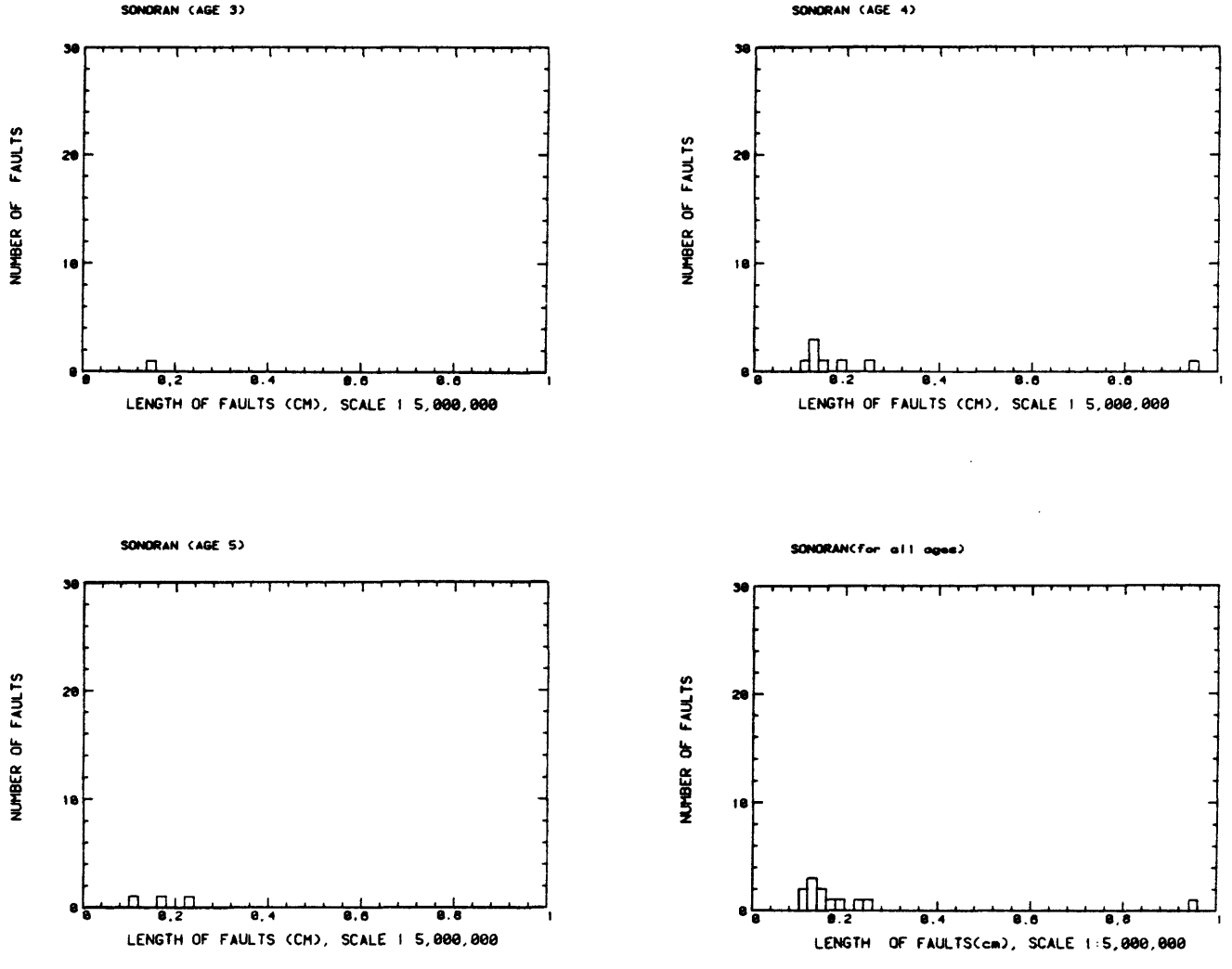

Figure 2.1.-1. (20)

HISTOGRAM OF FAULT LENGTHS, CONTERMINOUS U S.

REGION 21

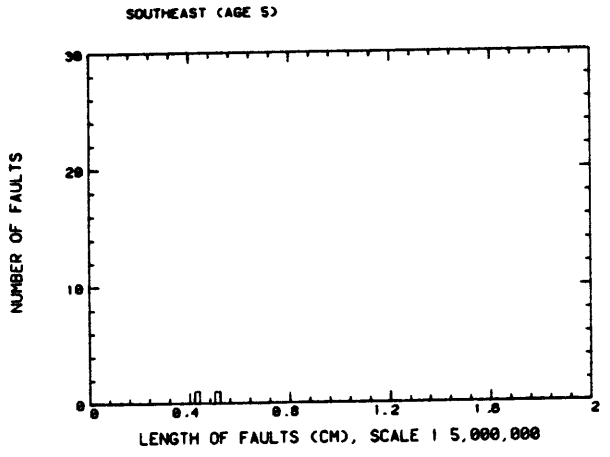

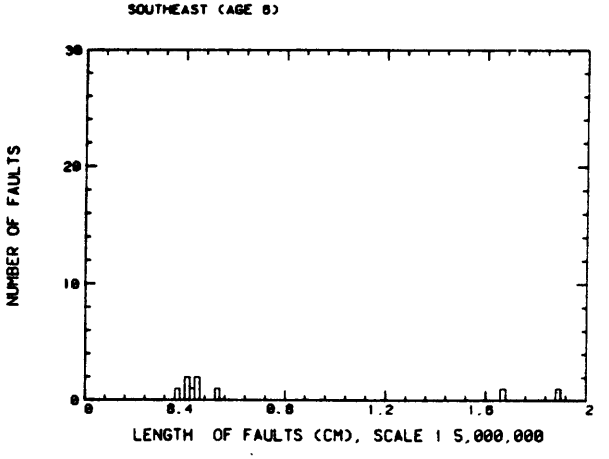

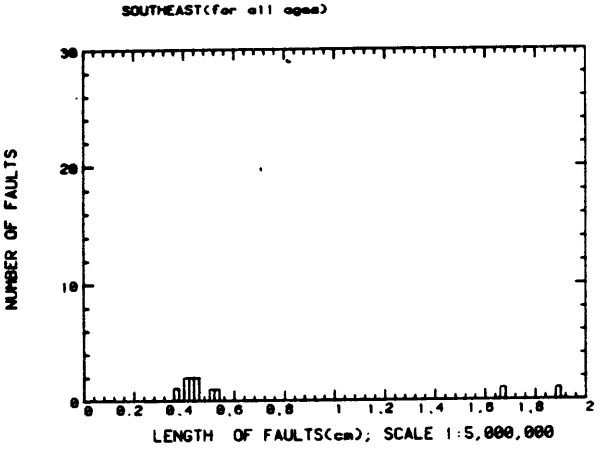

Figure 2.1.-1. (21)

HISTOGRAM OF FAULT LENGTHS, CONTERMINOUS U S

REGION 22

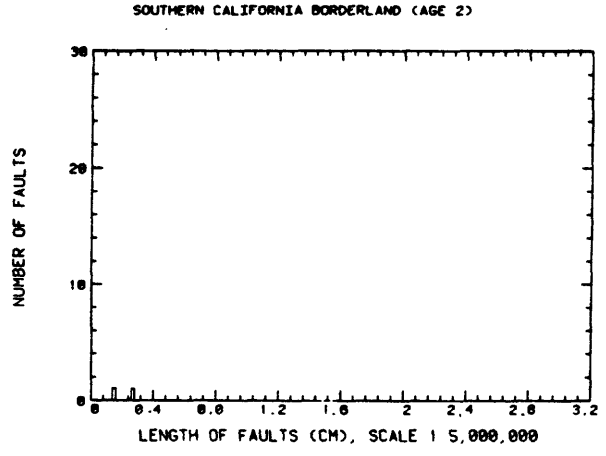

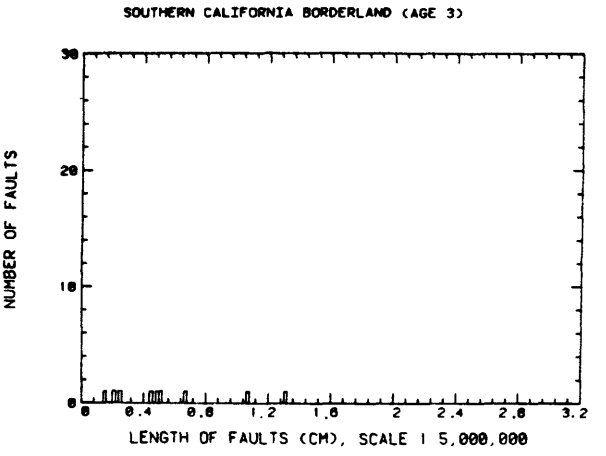

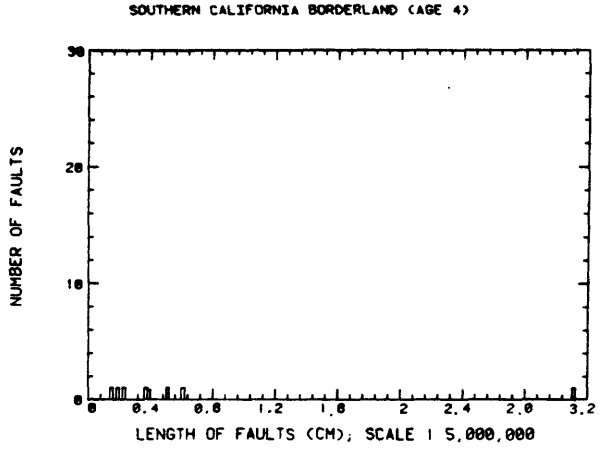

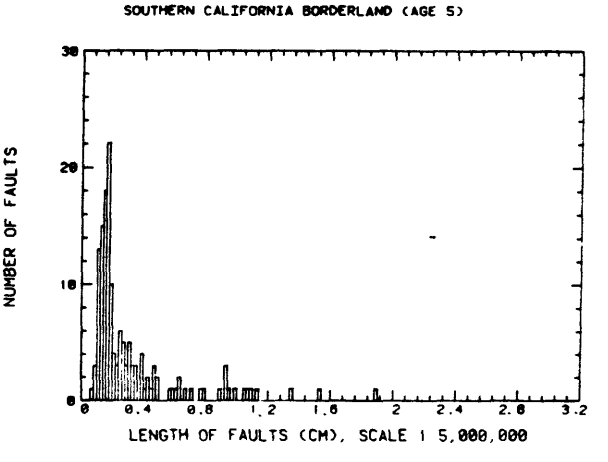

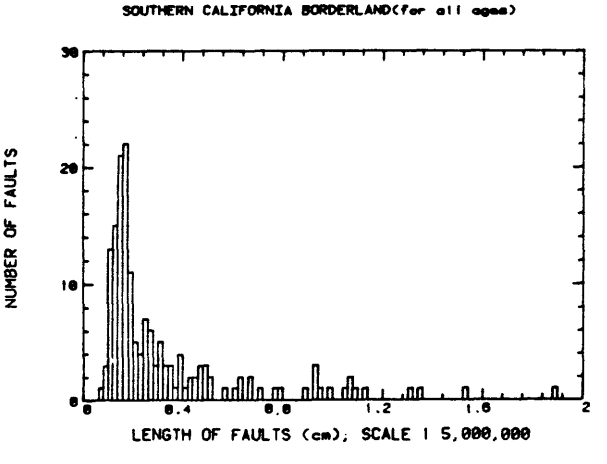

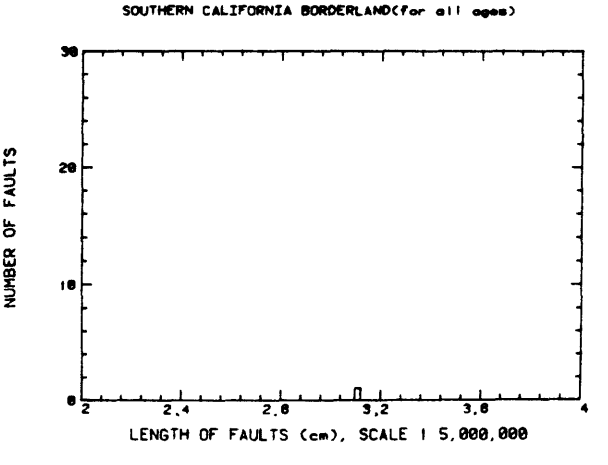

Figure 2.1.-1. (22)

HISTOGRAM OF FAULT LENGTHS, CONTERMINOUS U.S

REGION 23

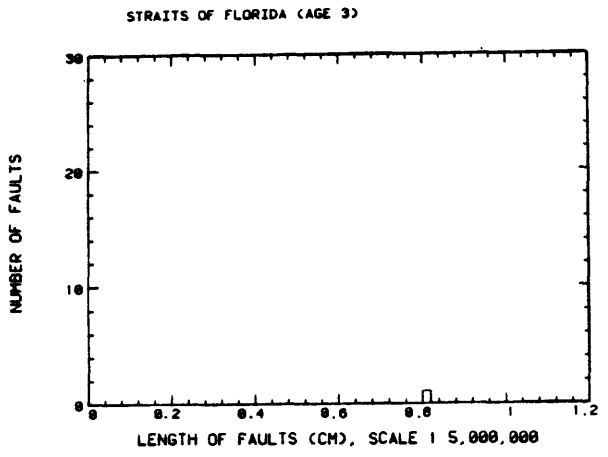

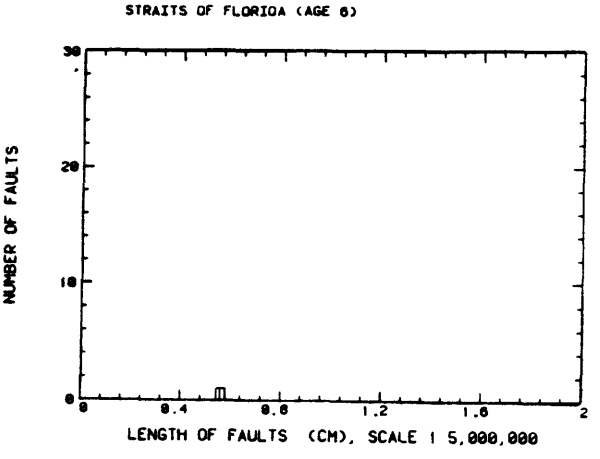

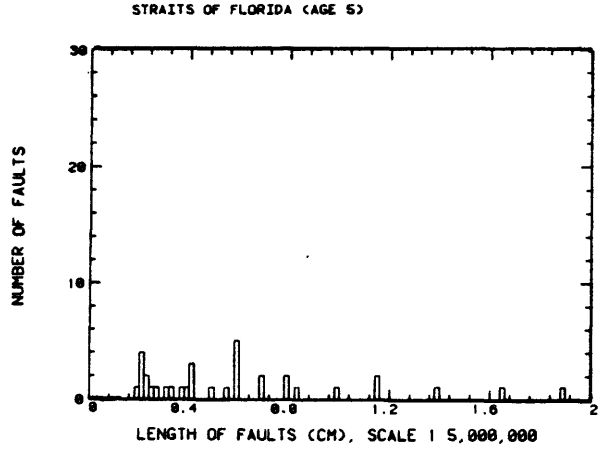

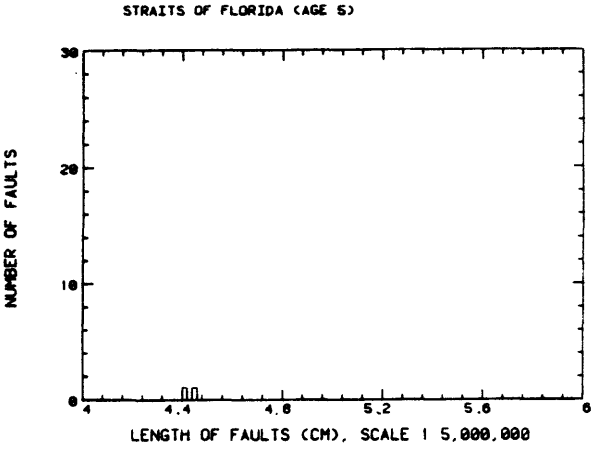

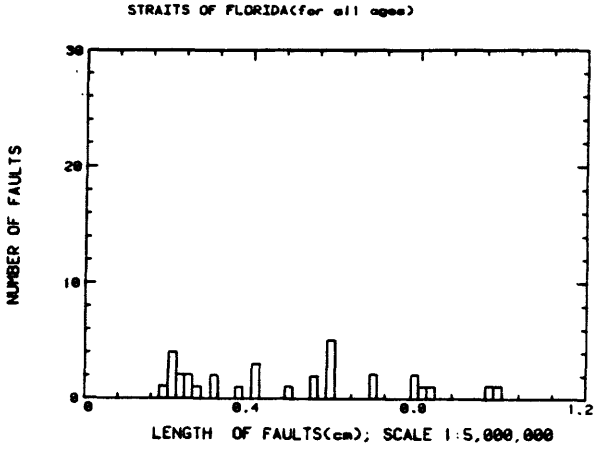

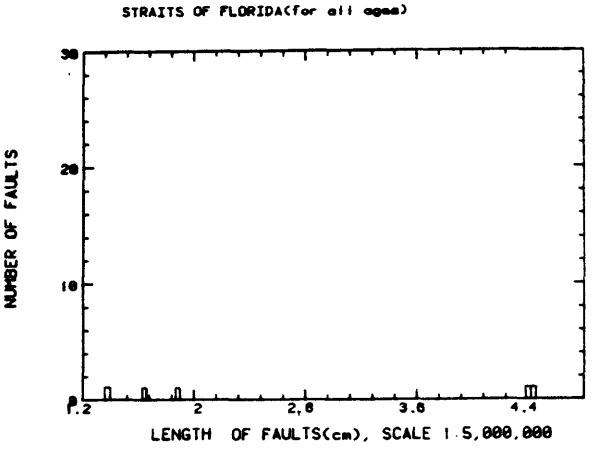

Figure 2.1.-1. (23)

HISTOGRAM OF FAULT LENGTHS, CONTERMINOUS U.S

REGION 24

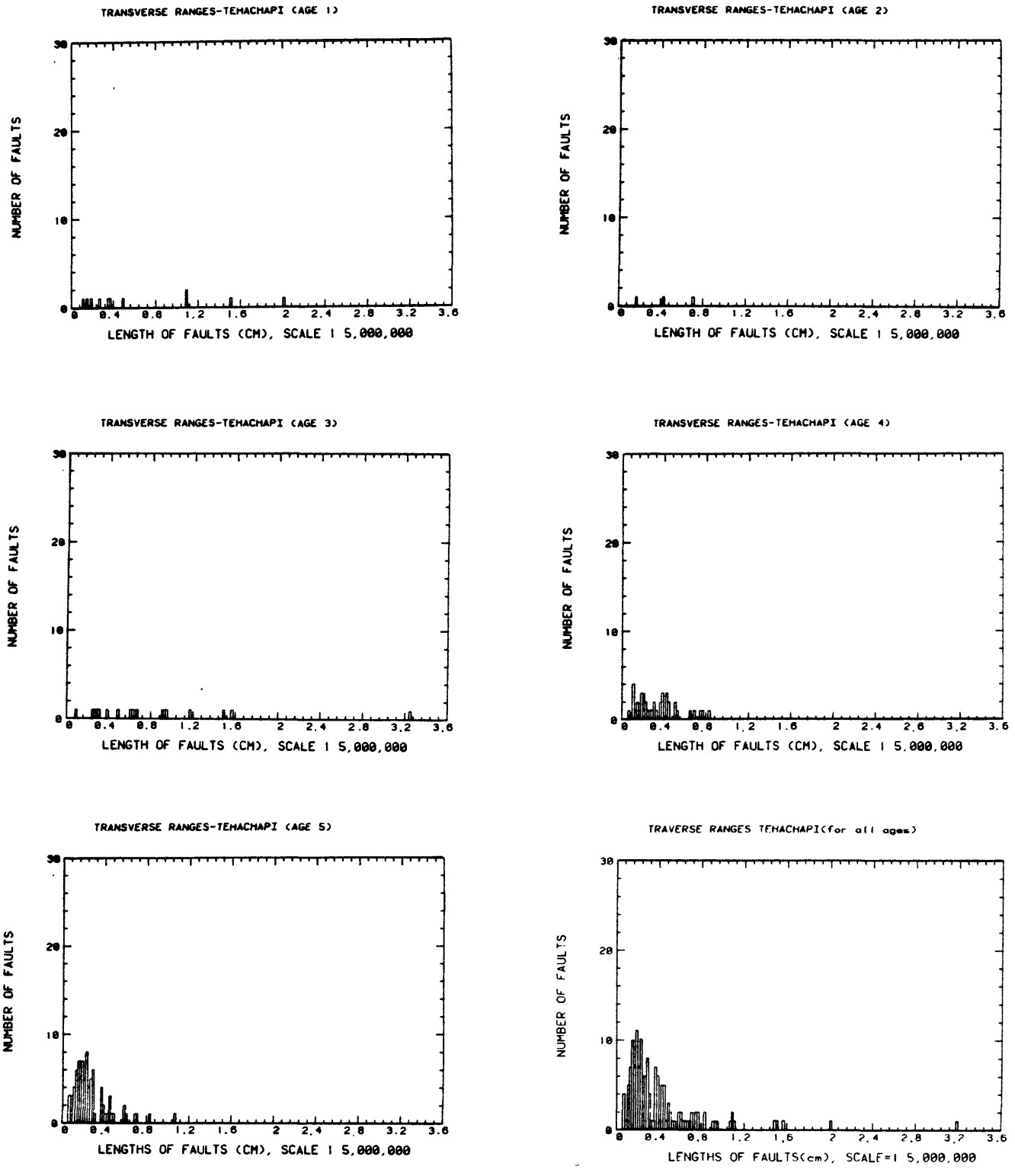

Figure 2.1.-1. (24)

HISTOGRAM OF FAULT LENGTHS, CONTERMINOUS U.S

REGION 25

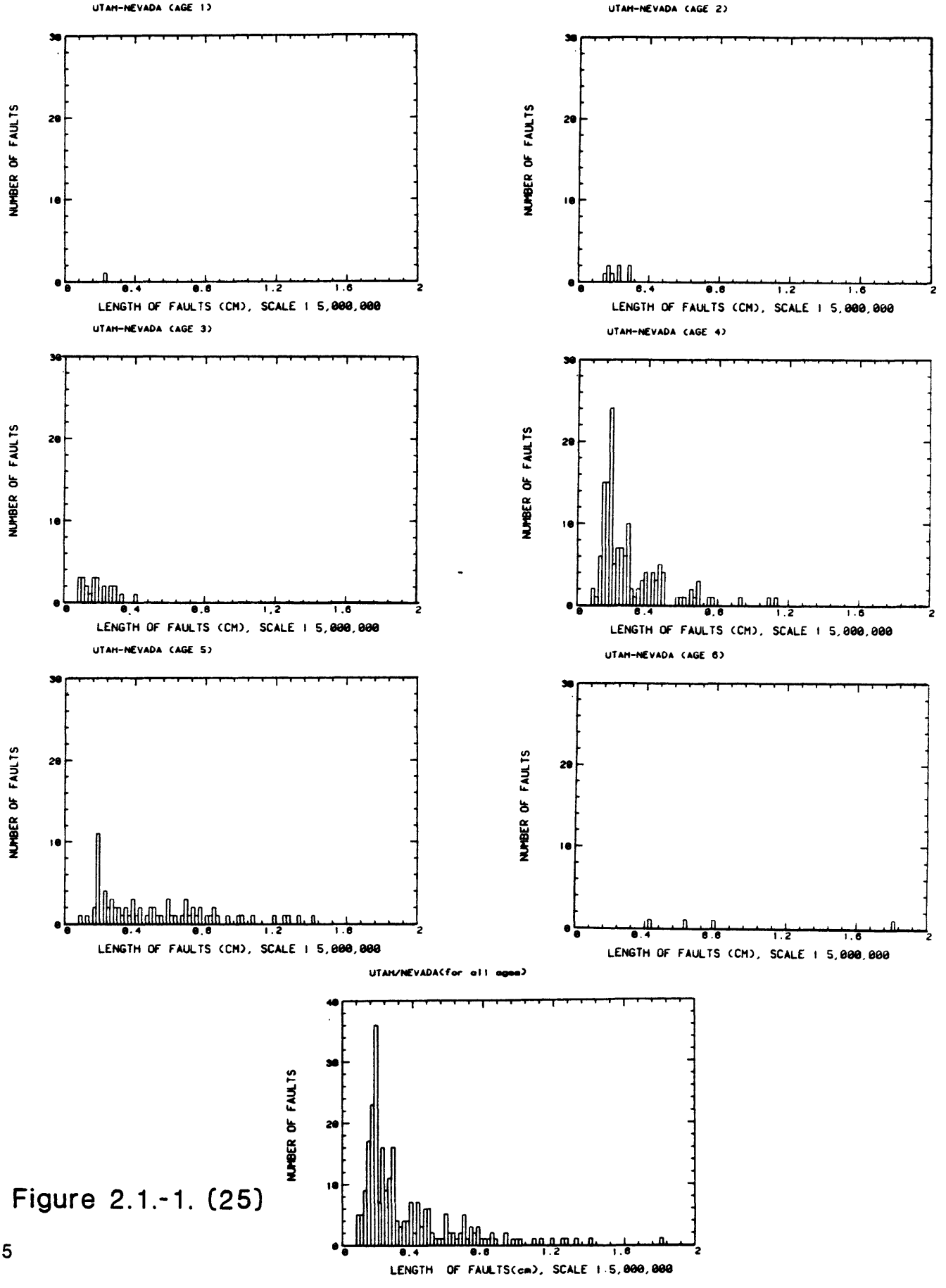

Figure 2.1.-1. (25)

HISTOGRAM OF FAULT LENGHTS, CONTERMINOUS U.S.

REGION 26

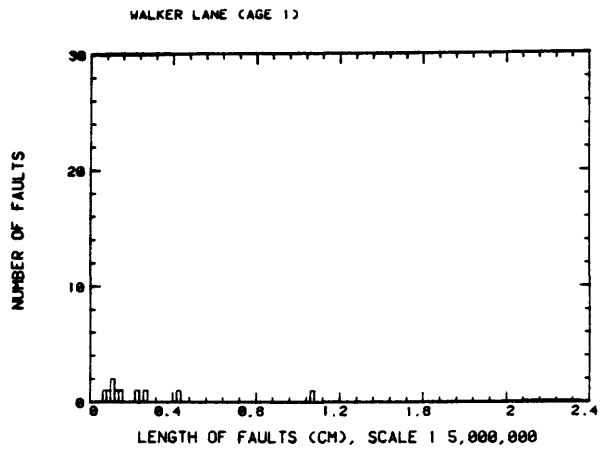

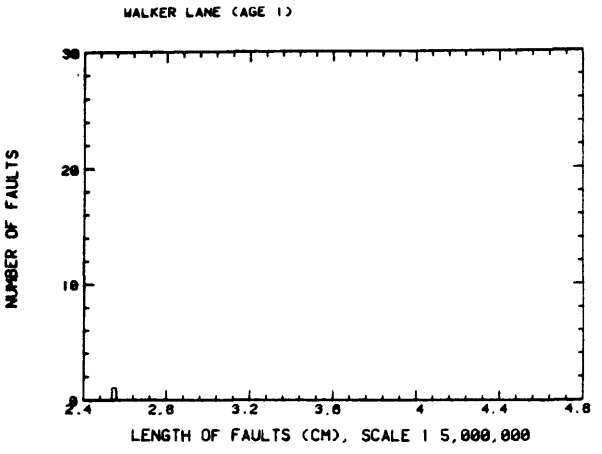

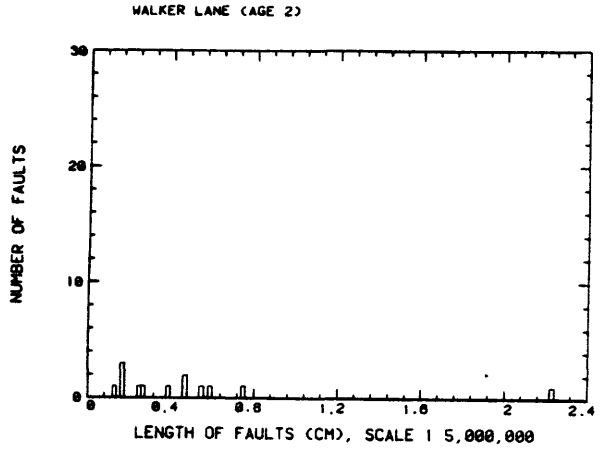

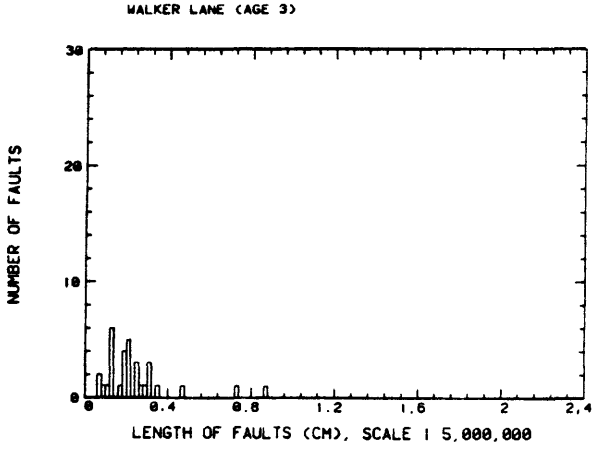

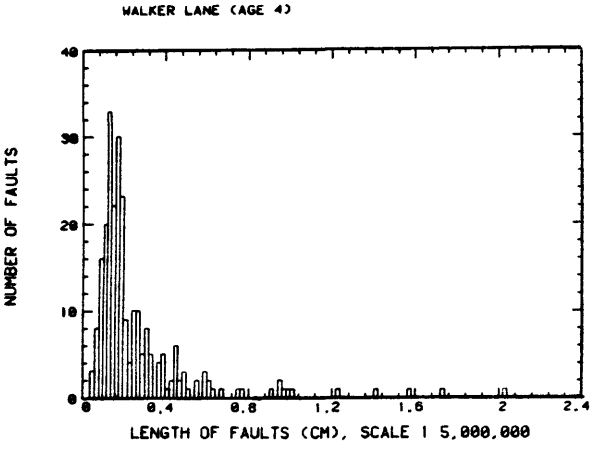

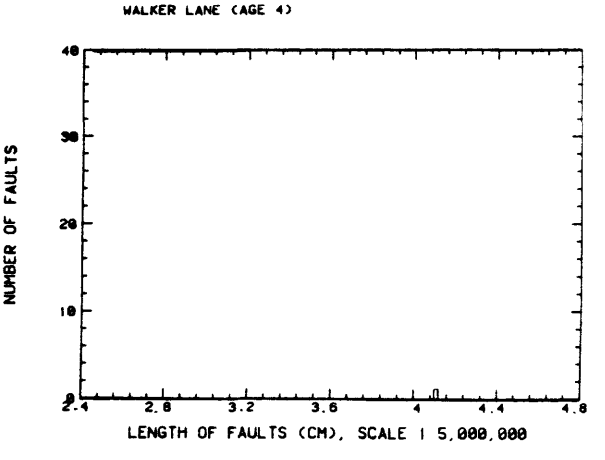

Figure 2.1.-1. (26)

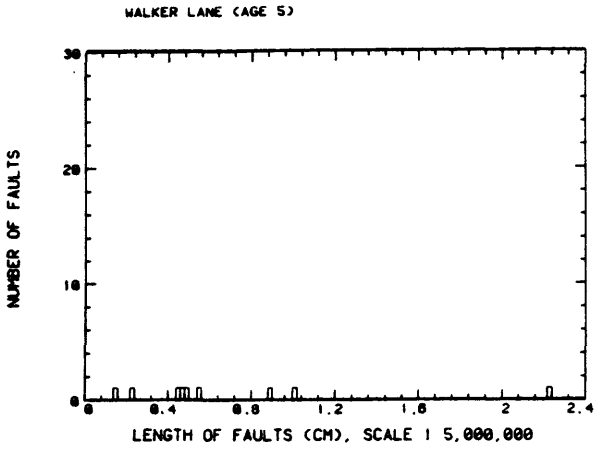
WALKER LANE (AGE 5)
NUMBER OF FAULTS
30
20
10
0
0
0.4
0.8
1.2
1.6
2
2.4
LENGTH OF FAULTS (CM), SCALE 1 5,000,000

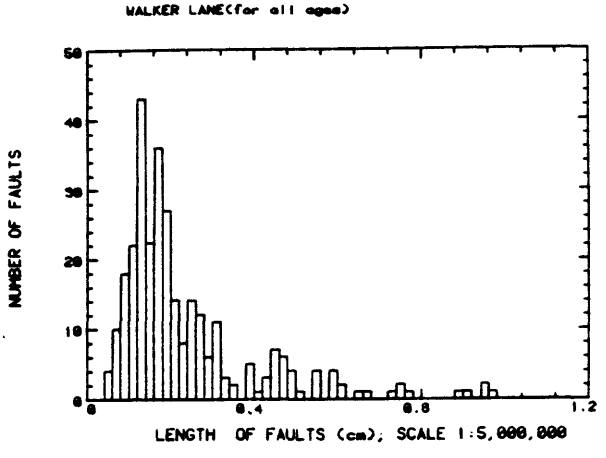
WALKER LANE(for all ages)
NUMBER OF FAULTS
50
40
30
20
10
0
0
0.4
0.8
1.2
LENGTH OF FAULTS (cm), SCALE 1:5,000,000

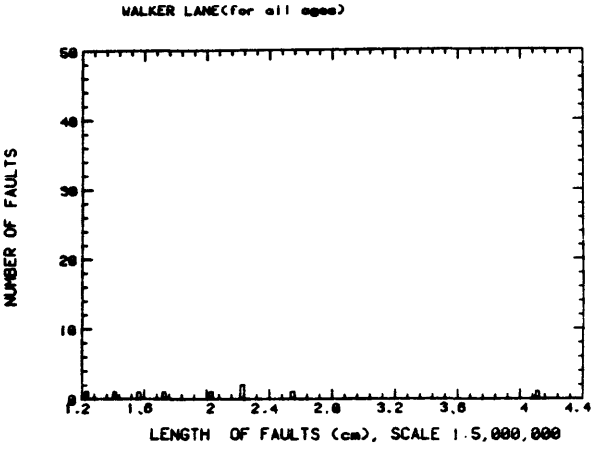
WALKER LANE(for all ages)
NUMBER OF FAULTS
50
40
30
20
10
0
1.2
1.6
2
2.4
2.8
3.2
3.6
4
4.4
LENGTH OF FAULTS (cm), SCALE 1:5,000,000

HISTOGRAM OF FAULT LENGTHS, CONTERMINOUS U S.

REGION 27

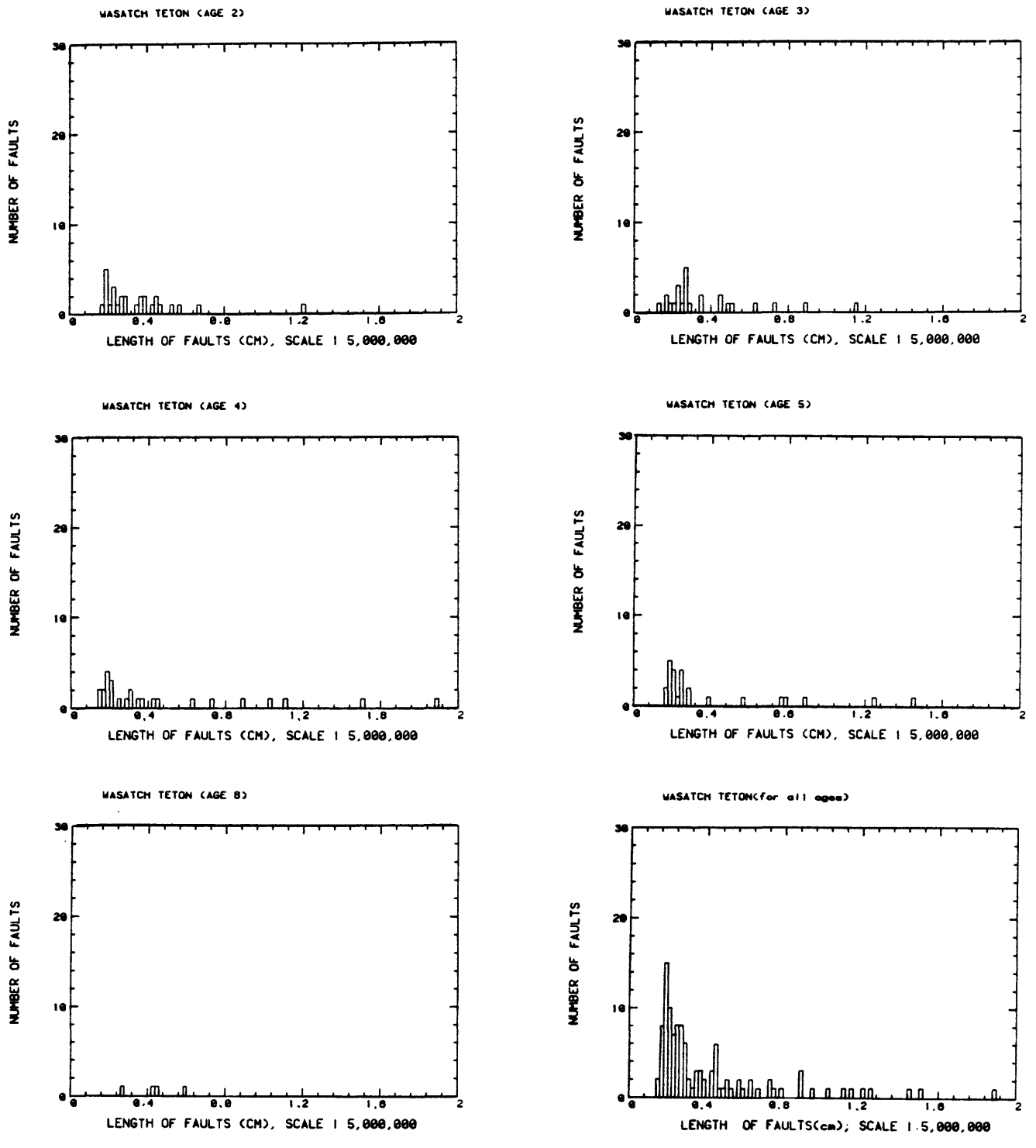

Figure 2.1.-1. (27)

HISTOGRAM OF FAULT LENGTHS, CONTERMINOU U.S

REGION 28

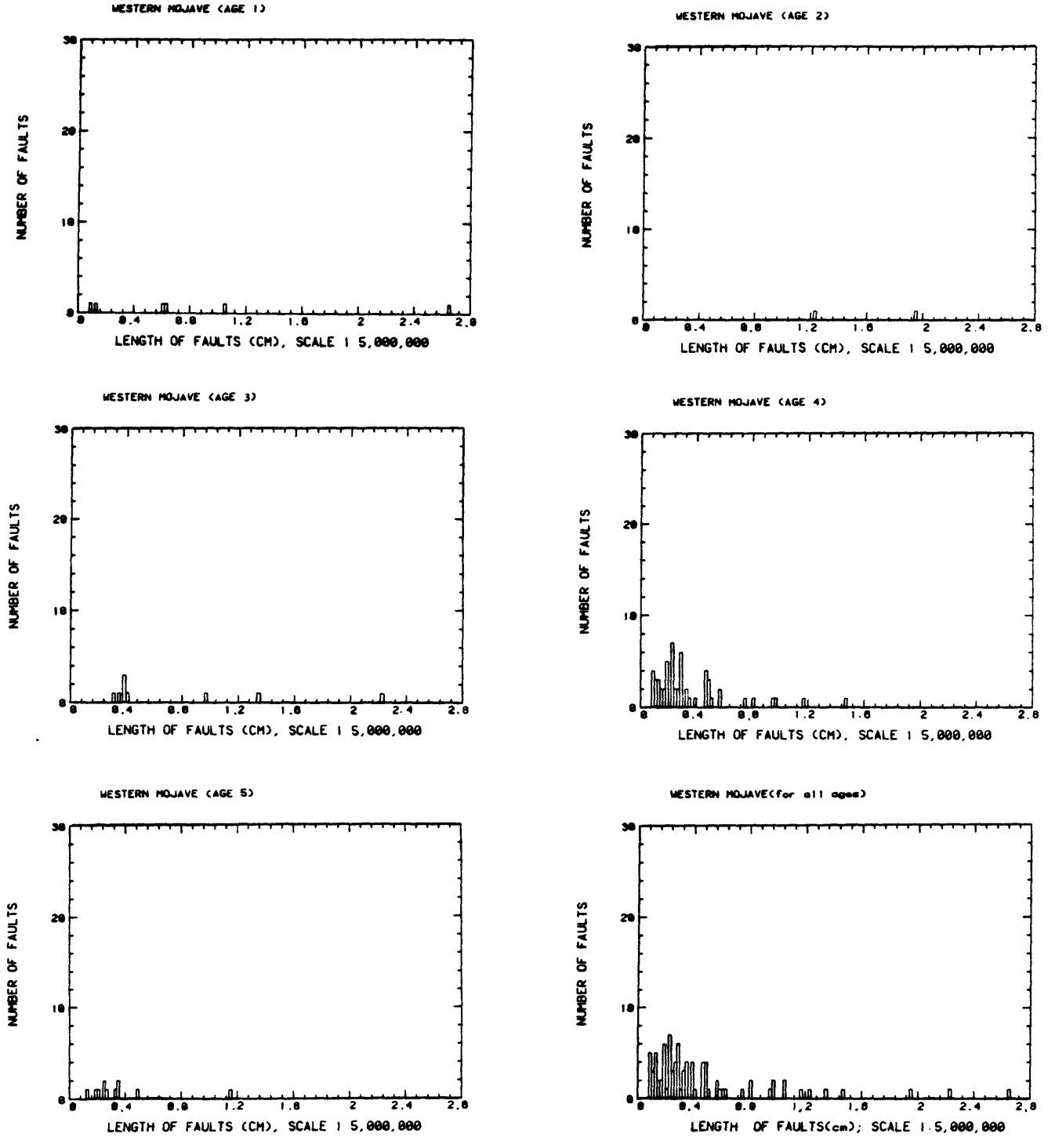

Figure 2.1.-1. (28)

HISTOGRAM OF FAULT LENGTHS, CONTERMINOUS U.S.

REGION 29

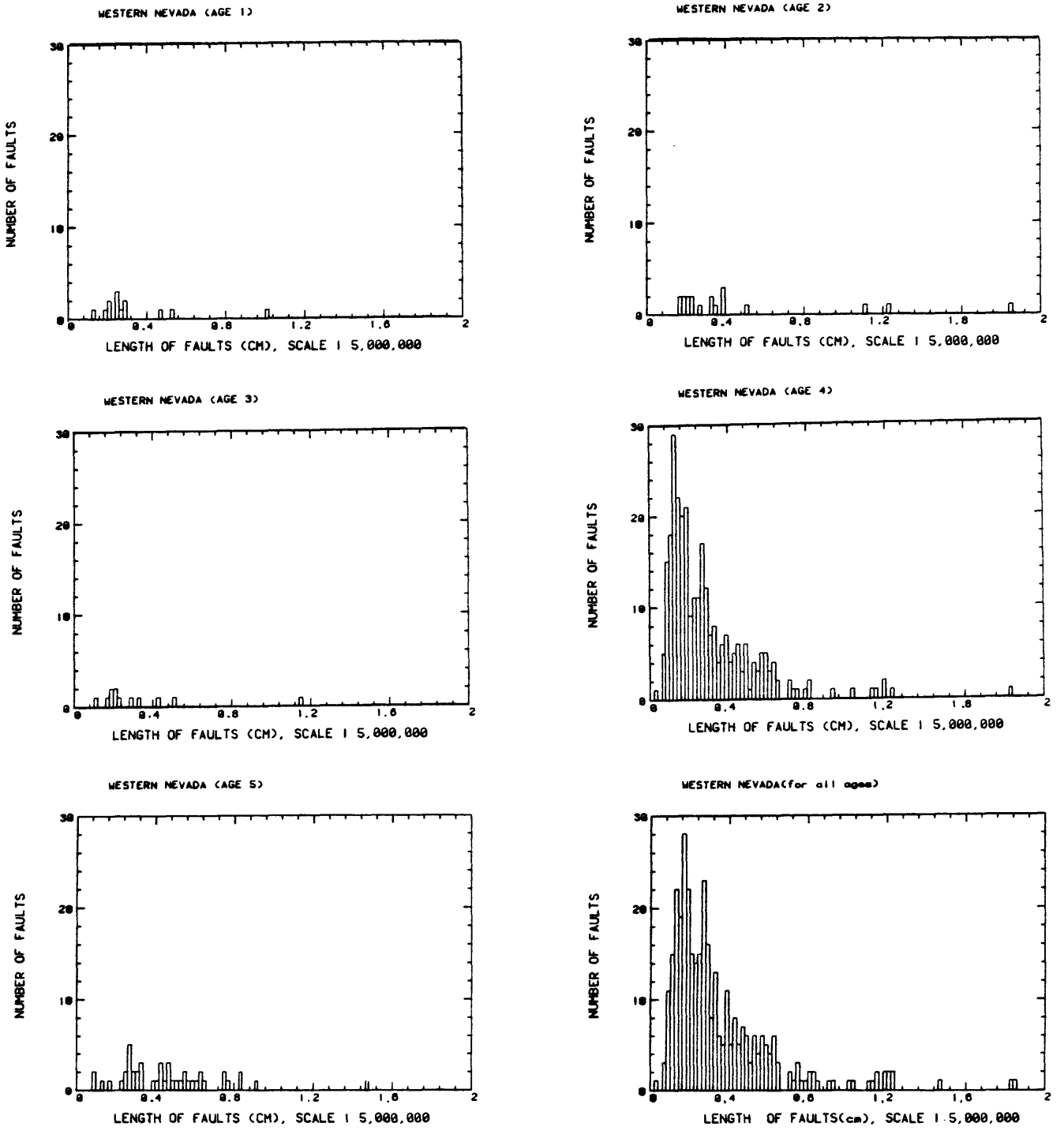

Figure 2.1.-1. (29)

HISTOGRAM OF FAULT LENGTHS, CONTERMINOUS U.S.

REGION 30

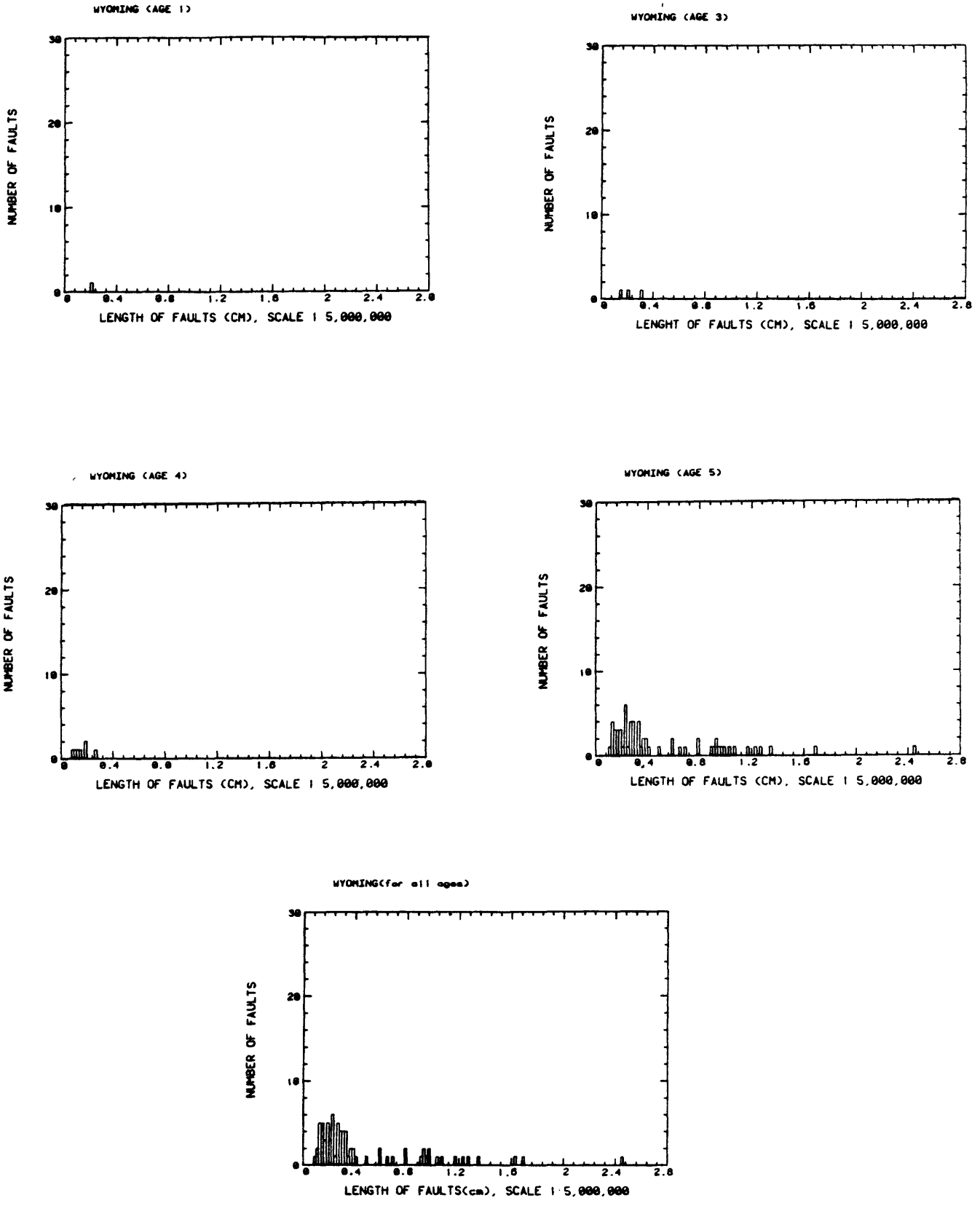

Figure 2.1.-1. (30)

HISTOGRAM OF FAULT LENGTHS, LOS ANGELES AREA

LOS ANGELES MAP 1

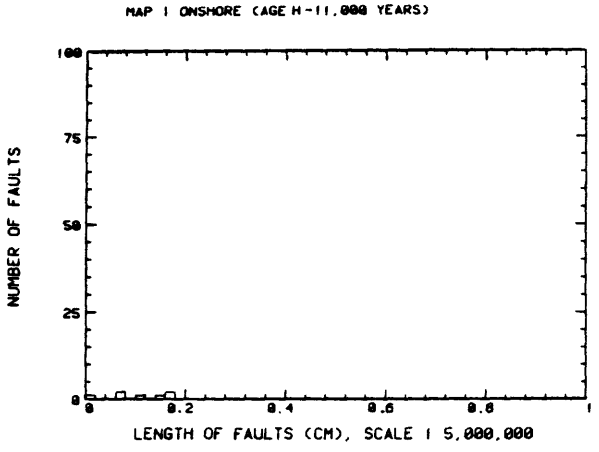

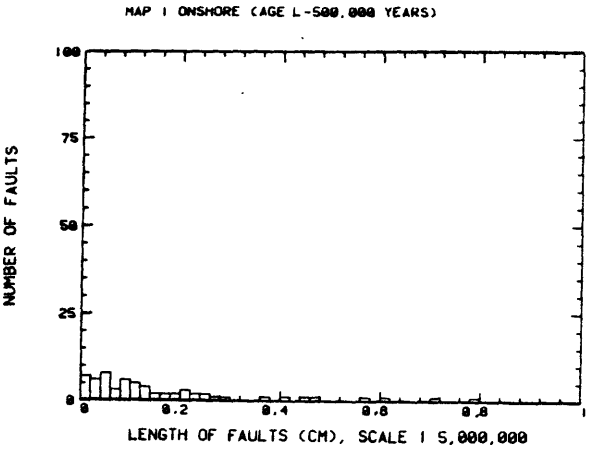

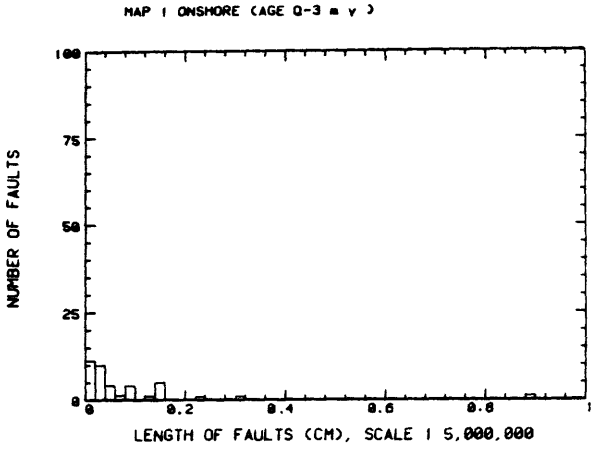

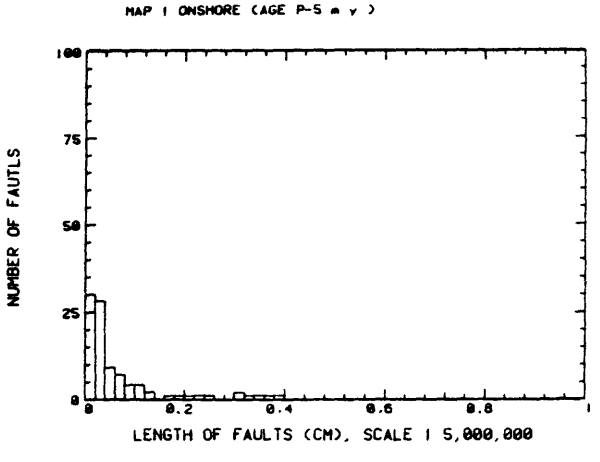

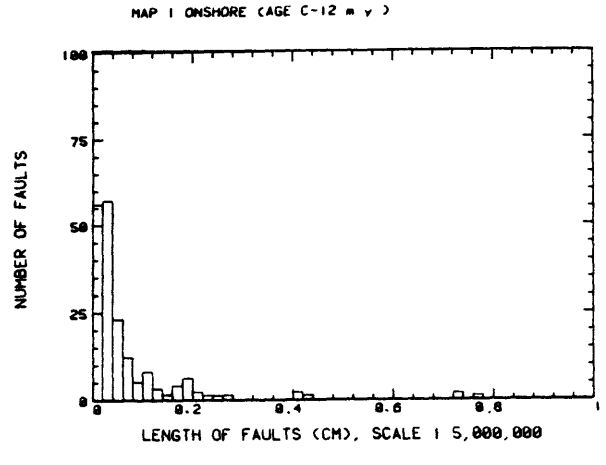

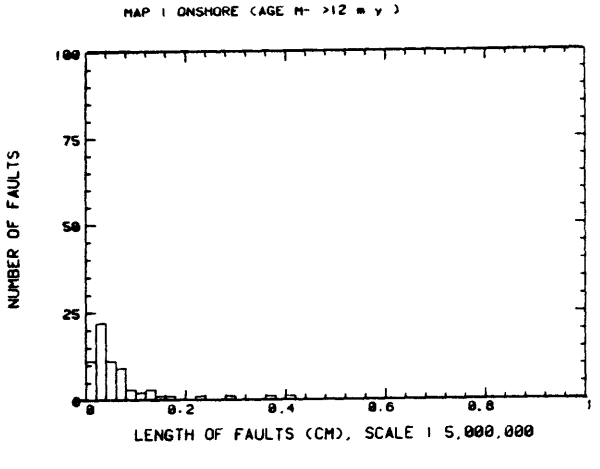

Figure 2.1.-1.(LA MAP 1)

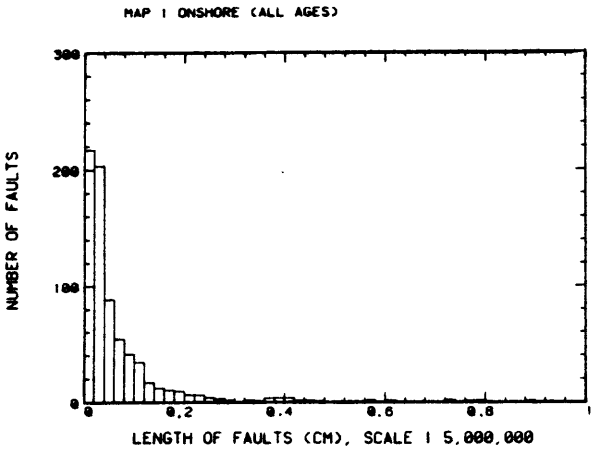
MAP 1 ONSHORE (ALL AGES)
NUMBER OF FAULTS
300
200
100
0
0
0.2
0.4
0.6
0.8
1
LENGTH OF FAULTS (CM), SCALE 1 5,000,000

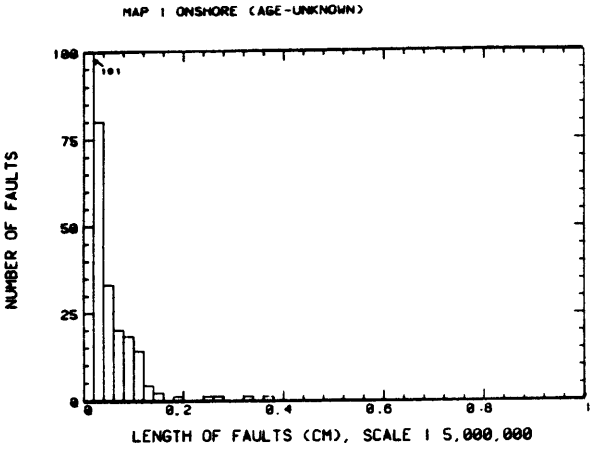
MAP 1 ONSHORE (AGE-UNKNOWN)
NUMBER OF FAULTS
100
75
50
25
0
101
0
0.2
0.4
0.6
0.8
1
LENGTH OF FAULTS (CM), SCALE 1 5,000,000

HISTOGRAM OF FAULT LENGTHS, LOS ANGELES AREA

LOS ANGELES MAP 2

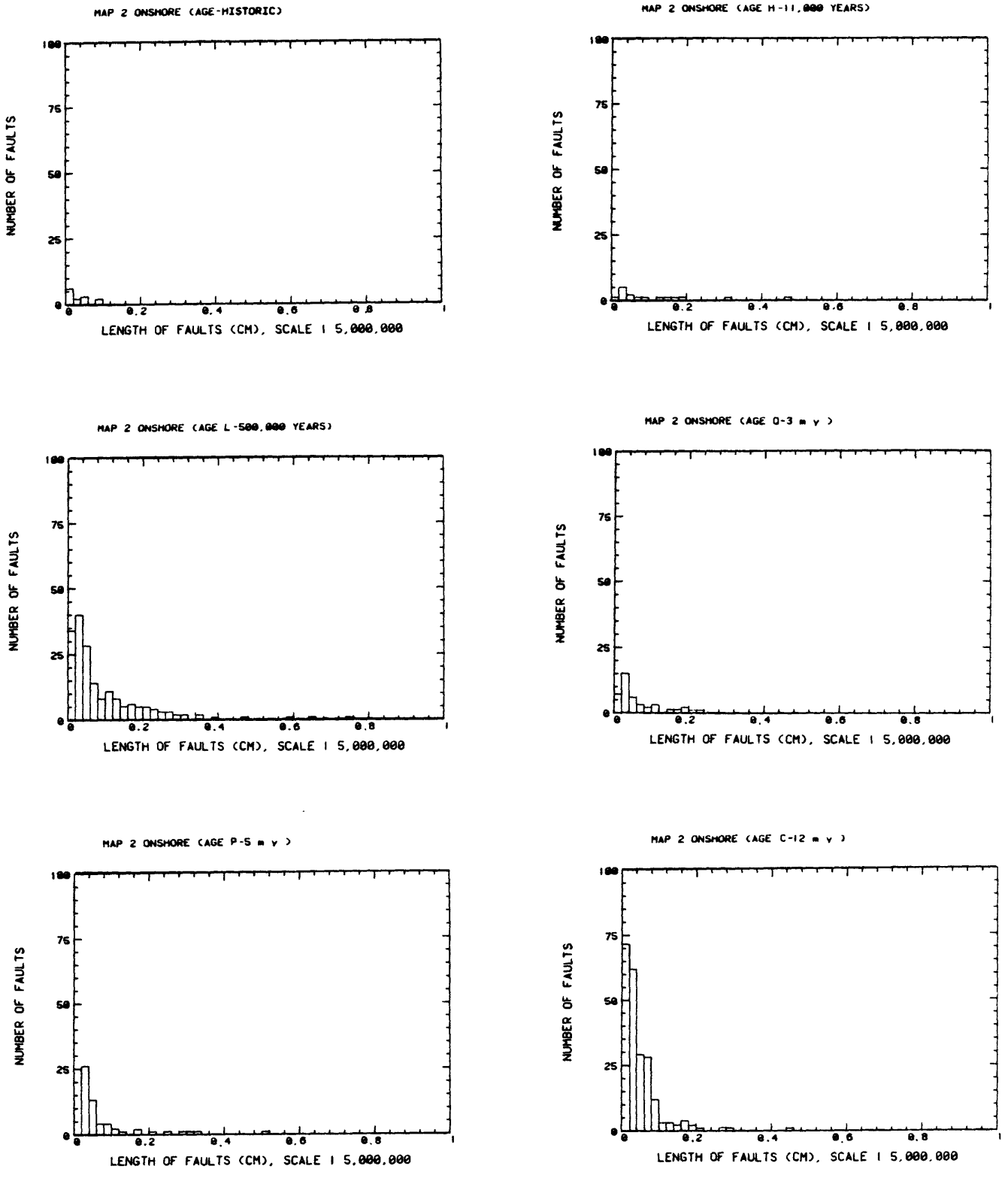

Figure 2.1.-1.(LA MAP 2)

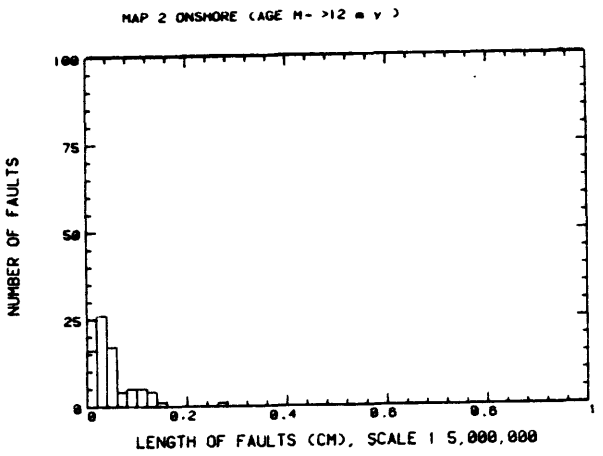
MAP 2 ONSHORE (AGE M- >12 m y)
NUMBER OF FAULTS
100
75
50
25
0
0
0.2
0.4
0.6
0.8
1
LENGTH OF FAULTS (CM), SCALE 1 5,000,000

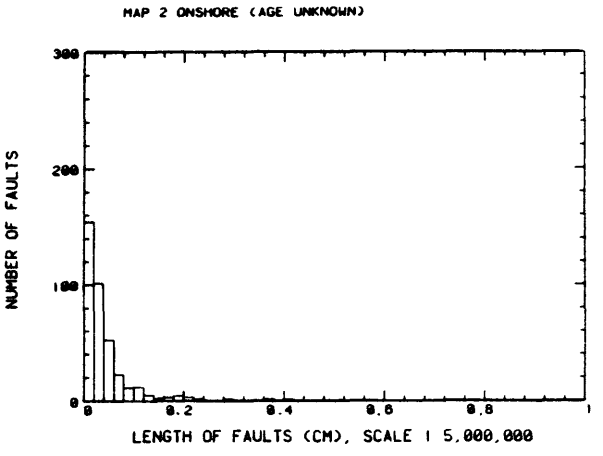
MAP 2 ONSHORE (AGE UNKNOWN)
NUMBER OF FAULTS
300
200
100
0
0
0.2
0.4
0.6
0.8
1
LENGTH OF FAULTS (CM), SCALE 1 5,000,000

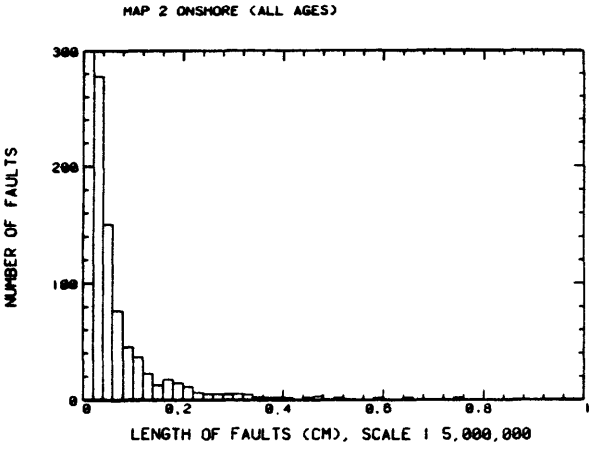
MAP 2 ONSHORE (ALL AGES)
NUMBER OF FAULTS
300
200
100
0
0
0.2
0.4
0.6
0.8
1
LENGTH OF FAULTS (CM), SCALE 1 5,000,000

Table 2.1.-1. Age groups for conterminous U.S. and Los Angeles Region

Conterminous United States [1]

1	Historic[2]
2	Holocene--approximately the last 10,000 years.
3	Late Quaternary--approximately the last 500,000 years.
4	Quarternary--approximately the last 1.8 million years.
5	Late Cenozoic--approximately the last 15 million years.
6	Other--longer time span than late Cenozoic.

Los Angeles region[3]

	Historic[4]
H(1)	Holocene (0-11,000 years).
L(2)	Late Quaternary (11,000-5000,000 years).
Q(3)	Quaternary (500,000-3 million years).
P(4)	Late Pliocene and Quaternary (3-5 million years).
C(5)	Late Cenozoic (5-12 million years).
M(6)	Pre-late Cenozoic (>12 million).
U,Un	Unknown.

[1] from Howard and other (1978).
[2] assumed to be within the last 200 years.
[3] from Ziony and others (1974).
[4] fault movements having specific calendar dates on the map (e.g., 1918, 1963, etc).

2.2 Subjective Searches for Patterns in the Data

We have compiled fault lengths in various ways and have expressed them as relations between the common logarithm of the number of faults plotted against the common logarithm of fault length at the length intervals shown by the histograms. The lengths are all expressed in units of centimeters for the map scale 1:5,000,000; a fault segment 1 cm long in the data therefore represents an actual length of 50 km. Data from the maps of coastal southern California at the scale 1:250,000 also were converted to 1:5,000,000 for uniformity.

The data have been grouped in the following ways:

a. All data for the conterminous United States taken together without regard to regions or age of faulting.

b. Data in (a) subdivided into the five age groups from the United States map.

c. Seven regions selected without regard to age of faulting; selection was arbitrary but with an eye to choosing from regions having high faulting activity.

d. Data in (c) subdivided into the five age groups.

e. All data in (a) with all data for subset (c) removed, designated "All United States Minus Seven Regions."

f. Data in (e) subdivided by the five age groups.

g. Data for each of the 30 regions plotted without regard to faulting age.

h. Data in (g) subdivided, where possible, by age group; in most regions there is insufficient data in a single age category to establish a trend.

i. All data from Coastal Southern California (designated L.A. Area in this report) without regard to faulting age.

j. Data in (i) divided into five age groups; notice that the ages for these groups are somewhat different than for the United States data as a whole.

Graphical data in the various categories are presented in the following two sections, showing least squares regression lines through the data. Subjective lines through the data are also given; the difference between the subjective trends and the regression fits basically reflect how the distributions were weighted by physical intuition concerning data

truncation and other geometric limitations. Faults that are longer than the characteristic dimension for a region are counted for that portion of length within the region. Thus, the statistical data for the longest and the shortest faults are both unrepresentative of the actual distribution. Therefore, the central portion of the data were emphasized in both the regression and subjective fitting.

2.2.1 Frequency Functions; All Ages Taken Together.

To set the stage for subsequent exploration of patterns in the data we first describe the fault length distributions for the conterminous United States as a whole relative to the distribution for coastal southern California (L.A. Area). Figure 2.2.1.-1 gives all data regardless of movement age for the conterminous United States showing the data points and computer regression fits. Figure 2.2.1.-2 shows the data for the United States as a whole compared with data for the Los Angeles Area. The comparative diagram illustrates two points: (1) numbers of faults continue to increase with decreasing length in a region mapped at a scale that gives data for faults too short to be represented on the United States map, and (2) the slope of the distribution for the larger map scale is very similar to that for the United States as a whole. From these observations we infer that the empirical relation for numbers of faults versus fault lengths holds without limit for decreasing lengths less than the mean length for the unit fault (intercept at unit frequency). This implies that the numbers of fractures below mappable lengths on any given map scale are determined by the numbers for mappable lengths at that scale. Hypothetically, this is assumed to apply to the branching pattern for all fractures related to fault movement down to the scale of microfractures. We state this as a hypothesis to be tested by counting fracture lengths at progressively larger map scales.

The analogous distributions for each of the 30 regions, without regard to movement ages, are shown in Figure 2.2.1.-3 (1 through 30). The abundances of data and the forms for their distributions clearly have widely varying quality. Despite this unevenness in the sampling, there is, to us, a strong coherence in the relationship between frequency and length. We attempt to illustrate this coherence by comparisions of slopes and intercepts for trends in the distributions using both subjective fits to the data by eye and computer regressions. Table 2.2.1-1 lists these values for both forms of representation. Figure 2.2.1.-4 (A and B) shows a composite for all the computer and subjective trends; the lengths of the lines indicate the frequency range encompassing the data. In Table 2.2.1-1, the regions with poorer data are indicated by asterisks, and the trends for these regions are shown by dashed lines in Figure 2.2.1-4.

In the next few figures and tables the same data are grouped in various ways to search for patterns, and in the next section we subdivide the data by age group to the extent possible.

Figure 2.2.1.-5 is a histogram showing slope values for the subjective and regression trends. It is not statistically well defined, but it suggests a bimodal distribution, which is also hinted at by the composite plot showing slope trends (Figure 2.2.1.-4). Table 2.2.1.-2 gives a listing for those regions with absolute values for slope less than 1.5, and Table 2.2.1.-3 gives those greater than 1.5. Figure 2.2.1.-6 shows a plot of slope values versus values for the length intercept at unit frequency.

Tables 2.2.1.-1 and 2.2.1.-2 and Figure 2.2.1.-6 illustrate that there is a suggestion of systematic differences between regimes having, respectively, low and high subjective slopes. The regimes with low slopes tend to have somewhat greater fault lengths at unit frequency. Subdividing the data according to quality has little effect on mean slopes, but it reveals a large systematic shift in the length intercept toward more negative values (smaller mean lengths at unit frequency) for the poorer data sets. This reflects the larger gaps in the frequency data, so the total population is suppressed. It is interesting that this happens without an analogous systematic effect on general slope trends in the data. That is, in order to shift a number population without changing the form of the distribution means that the population added or subtracted must have the same form. This could mean either that there are actual unmapped faults that cause the shift, or that for some reason branching distributions may have missing limbs in some cases. The consistency in the more complete data sets suggests the former interpretation.

Figures 2.2.1.-7 and 2.2.1.-8 give outline maps for the conterminous United States showing state boundaries and the arbitrary boundaries for fault regions on which are plotted the areal distributions of slopes and intercepts derived from the logarithmic diagrams illustrating frequency versus length. Figure 2.2.1.-7 shows the locations for regions having absolute slope values falling within one of four equal intervals between 1.0 and 2.6. Figure 2.2.1.-8 shows the analogous locations for regions having four different ranges of intercept values between about 10 and 130 km. It is notable that the regions having the lower absolute slope values tend to be those having the longer systems of major faulting. Some regions, such as the California Coast (2), represent great systems of strike-slip faulting; the Rio Grande region (17), however, is a rift system and also falls in this category (see pl. I for fault patterns). The growth faults along the Gulf Coast (8) also tend to show a similar relation. Regions with high slopes, on the other hand, tend to be those that are tectonically more broken up, or blockier, such as the regions in the Basin and Range province (regions 5, 19, 25, and 29). The relation of the Transverse-Tehachapi (24) to the California Coast and Western Mojave regions (2, 28) is instructive in this regard.

Table 2.2.1.-4 lists the slopes and intercepts for an arbitrary group of seven regions; Figure 2.2.1.-9 shows their locations. These seven regions were selected at an early stage of the study just to see if there was a major distinction in the numerical data for a subset taken from different areas in the western United States relative to the United States as a whole. It turns out that the averages for these regions are not much different than the United States average.

Another region subset shows up by inspecting the composite plot of subjective trends (Figure 2.2.1.-4B). It contains a tightly bunched group with trends centered about a crossover point at a Log frequency at about 0.7 (frequency = 5) and Log length at about -0.35 (length = 22 km).

Nearly all these trends come from the better quality data; they are listed in Table 2.2.1.-5, and their map locations are also shown in Figure 2.2.1.-9. A proposed explanation for the convergence is that rates of creation for shorter faults and rates of coalescence from short to longer faults oscillate from place to place and time to time averaging around the mean slope which is bracketed by the parallel group listed in Table 2.2.1.-5. The present data are insufficient to test this hypothesis quantitatively, although rates derived later support the idea that time-dependent variations are different for different fault lengths. The particular pattern mentioned is not as clearly defined in the regression curves (Figure 2.2.1.-4A), although we feel that the subjective lines are the more consistent representations.

SECTION 2.2.1. FIGURES AND TABLES

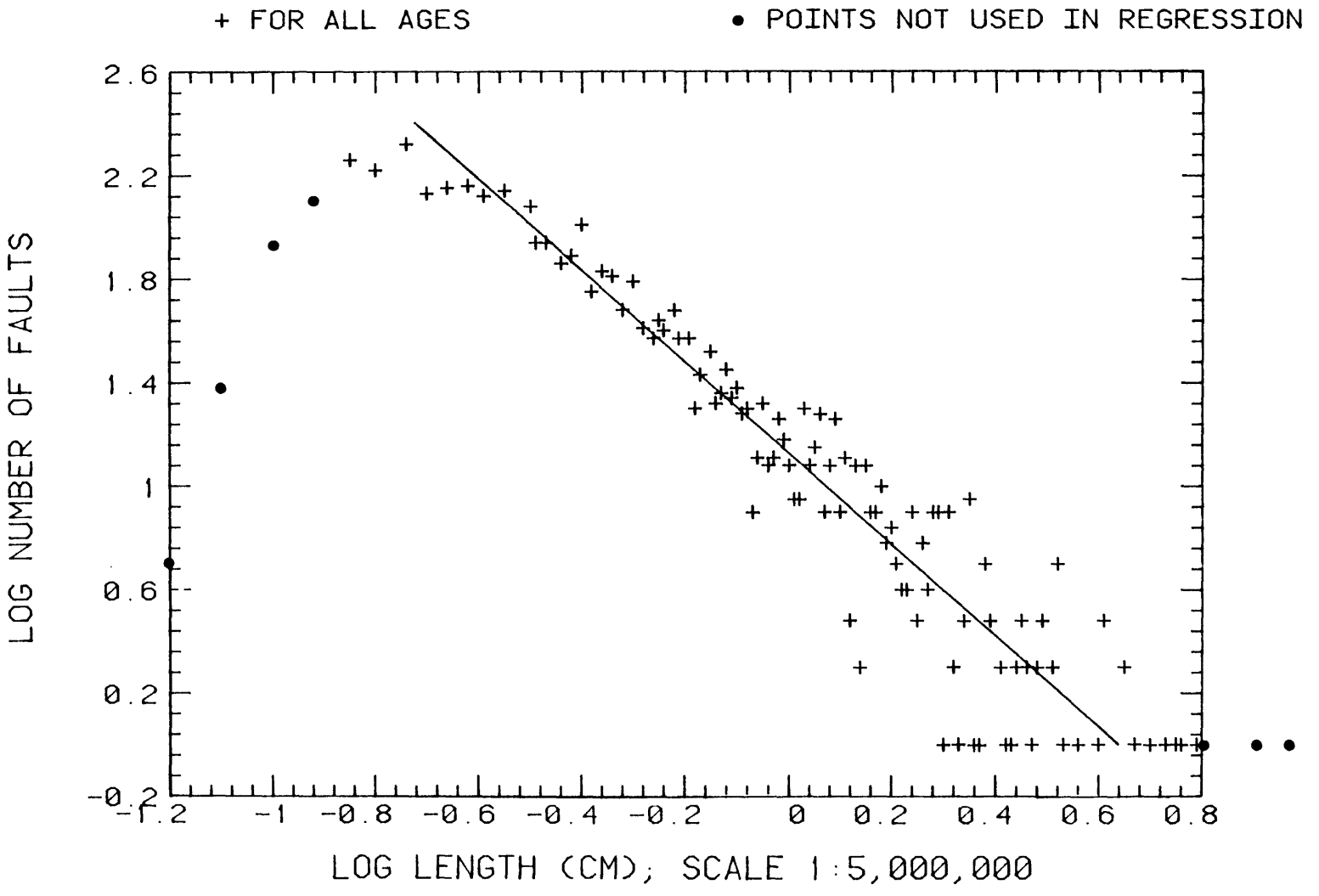

Figure 2.2.1.-1.
Logarithmic data for number versus fault length fitted by linear regression analysis for the total data set in the conterminous United States (all ages taken together).

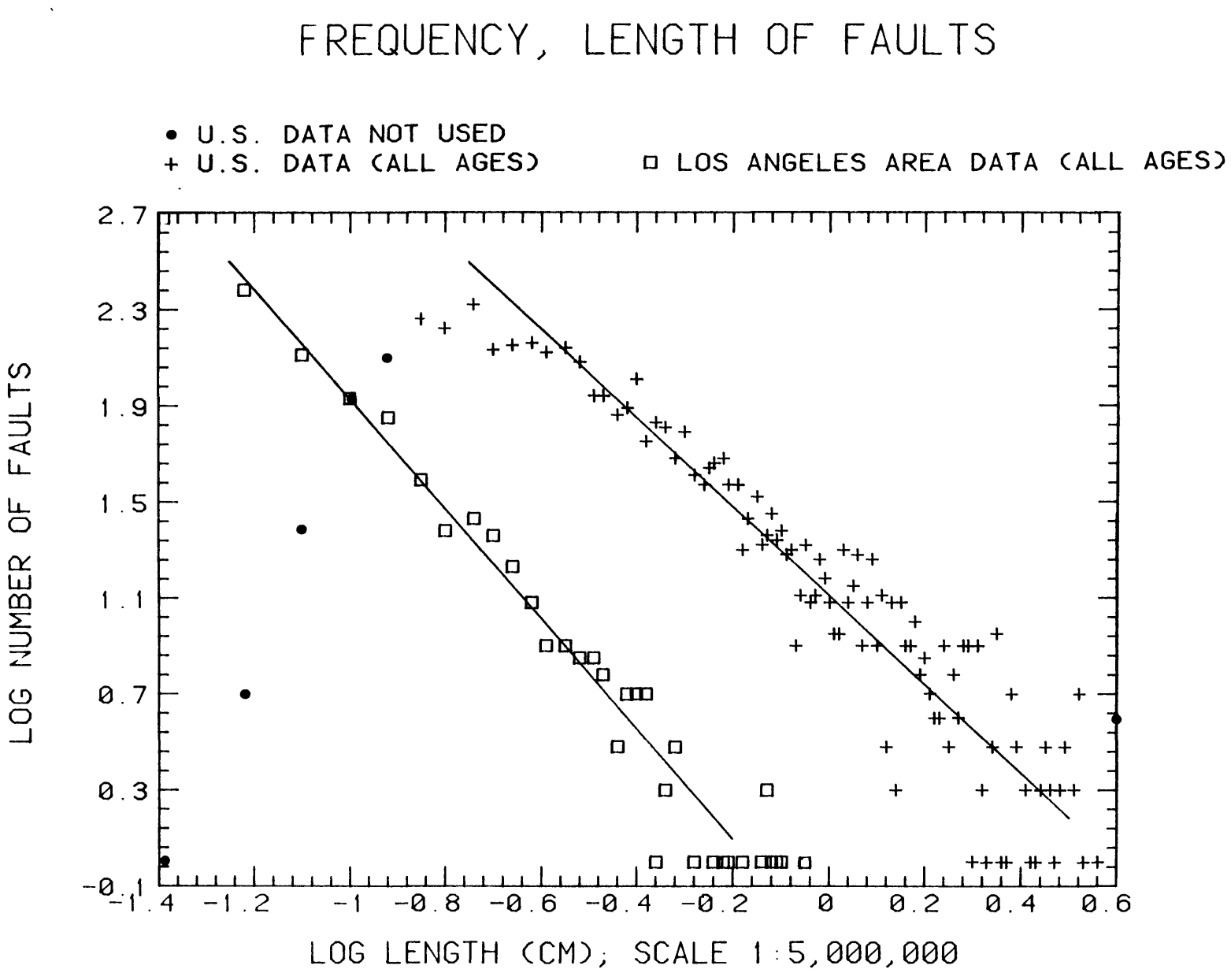

Figure 2.2.1.-2.
Logarithmic data for number versus fault length fitted by linear regression, comparing the U. S. data overall with the data for the L. A. Area (all ages taken together).

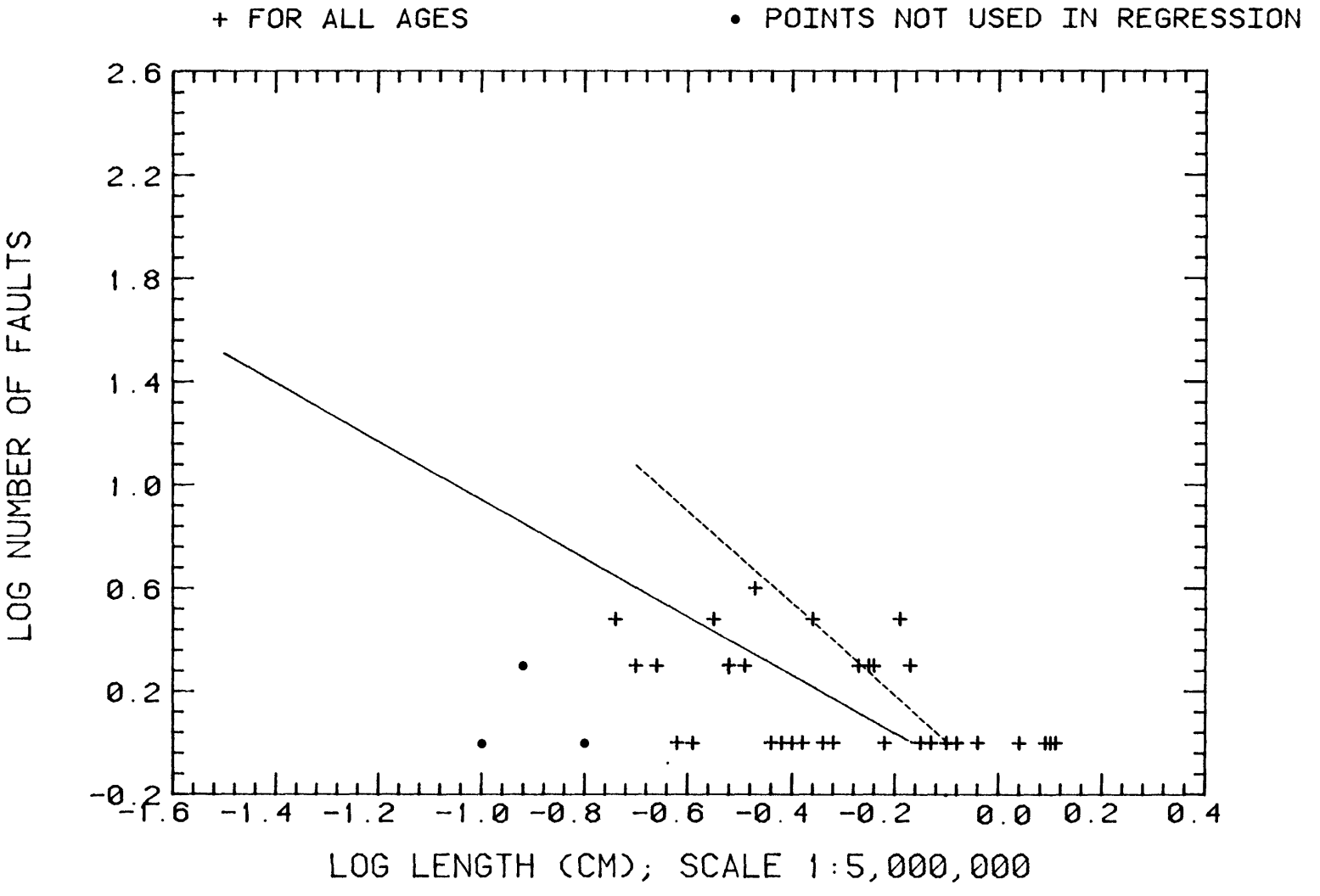

Figure 2.2.1.-3. (1)
Logarithmic data for number versus fault length fitted subjectively (dashed) and by linear regression (solid) for each fault region 1 through 30 (region numbers are indicated in parentheses; all ages taken together).

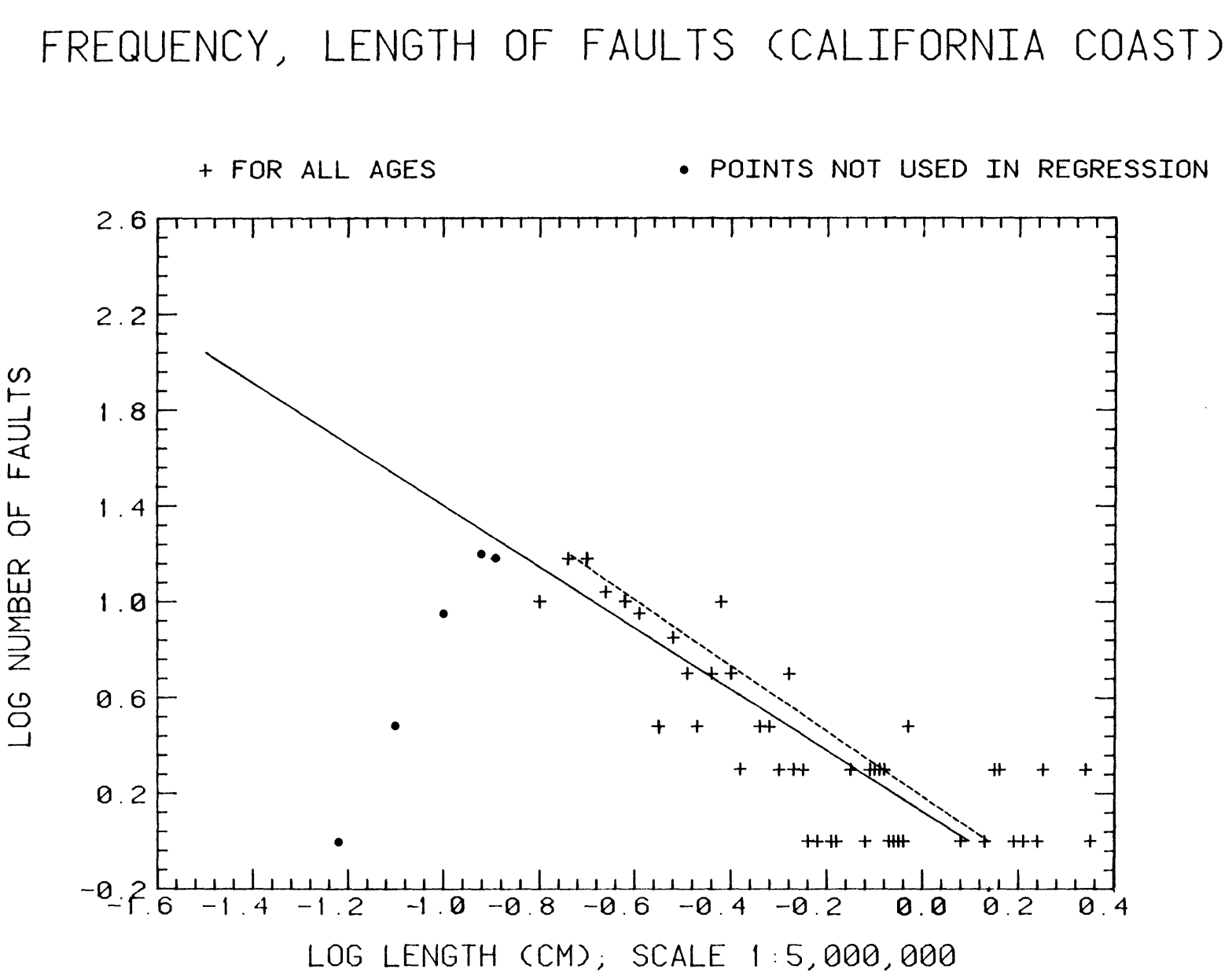

Figure 2.2.1.-3. (2)

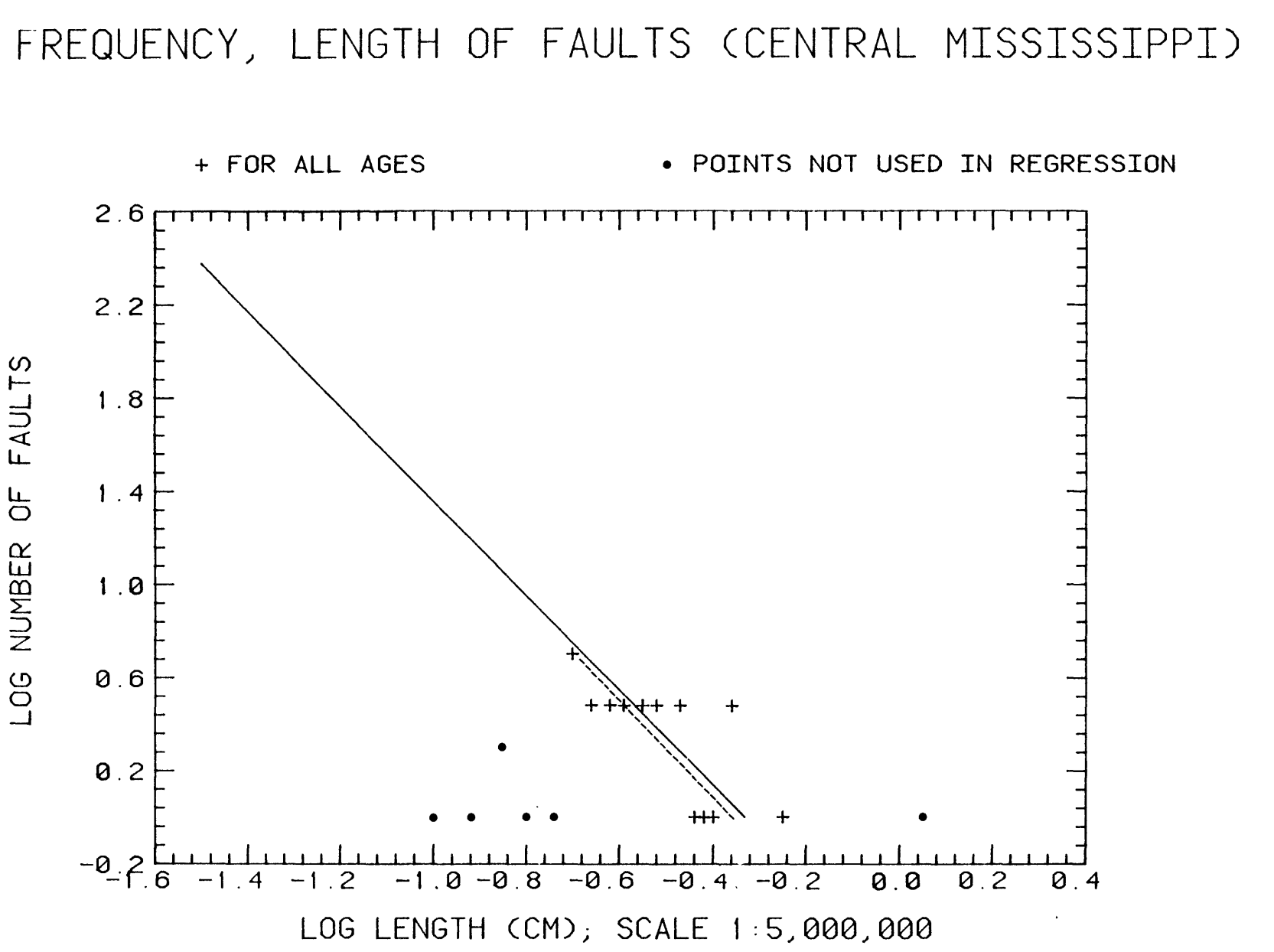

Figure 2.2.1.-3. (3)

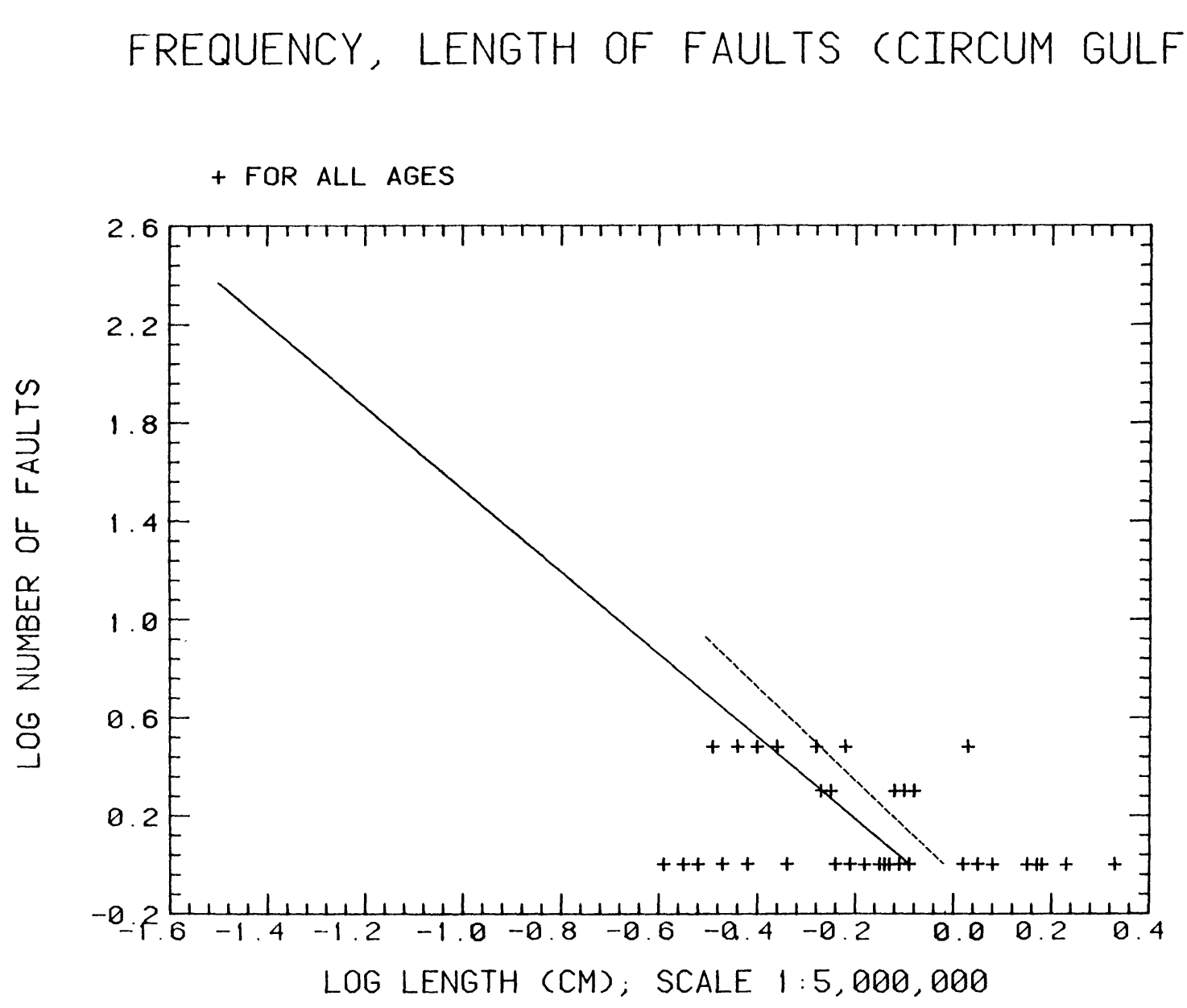

Figure 2.2.1.-3. (4)

FREQUENCY, LENGTH OF FAULTS (EASTERN OREGON/WESTERN IDAHO)

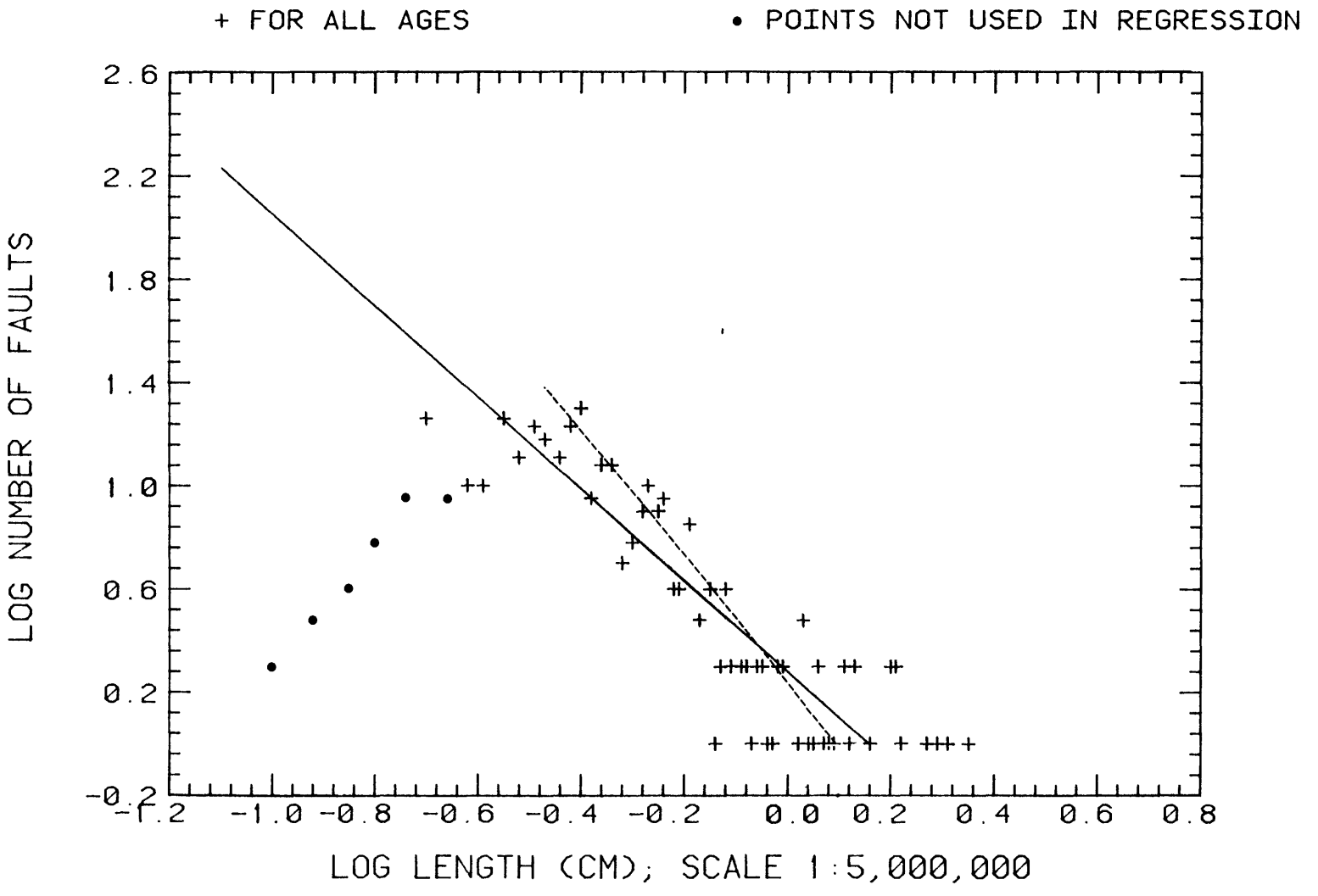

Figure 2.2.1.-3. (5)

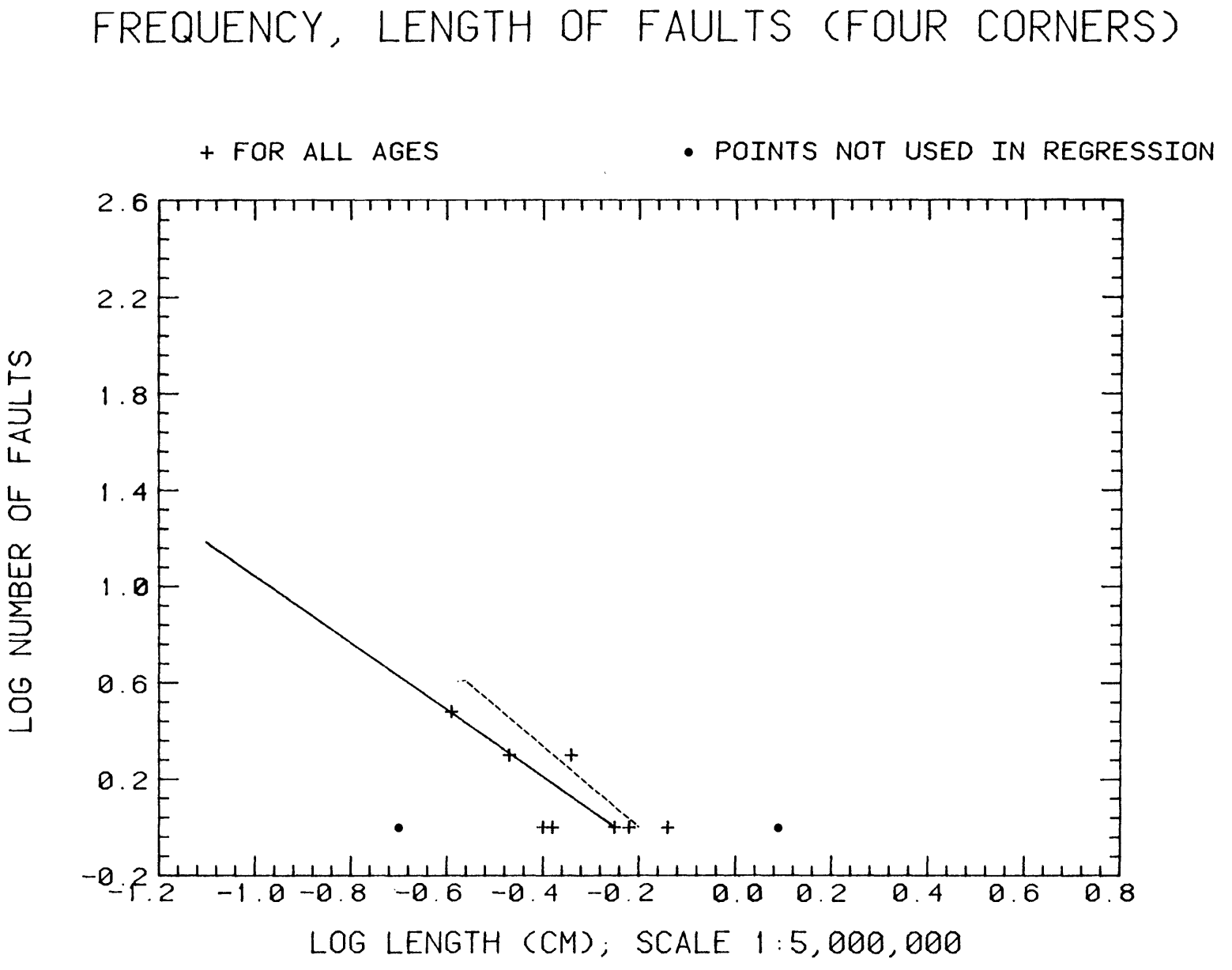

Figure 2.2.1.-3. (6)

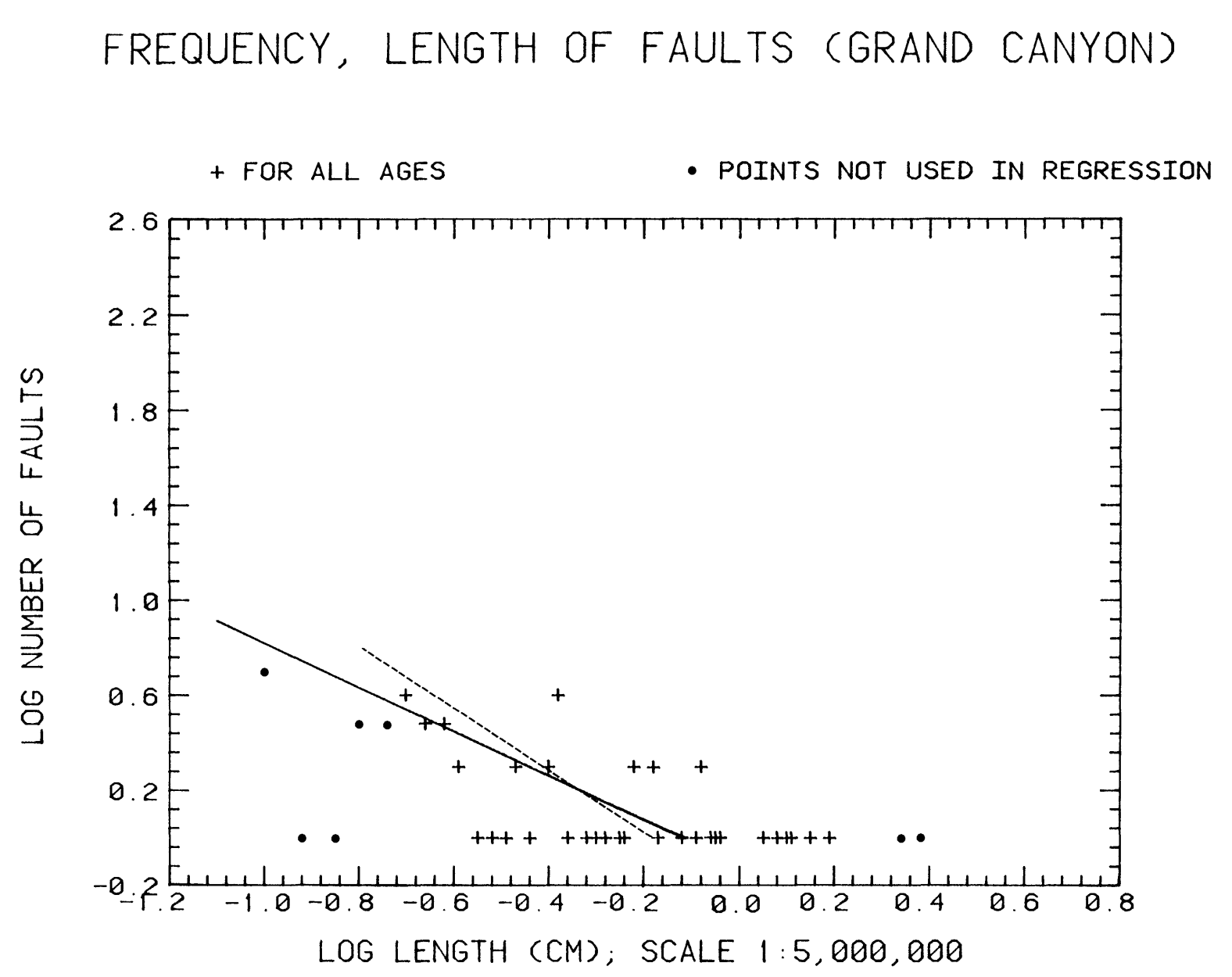

Figure 2.2.1.-3. (7)

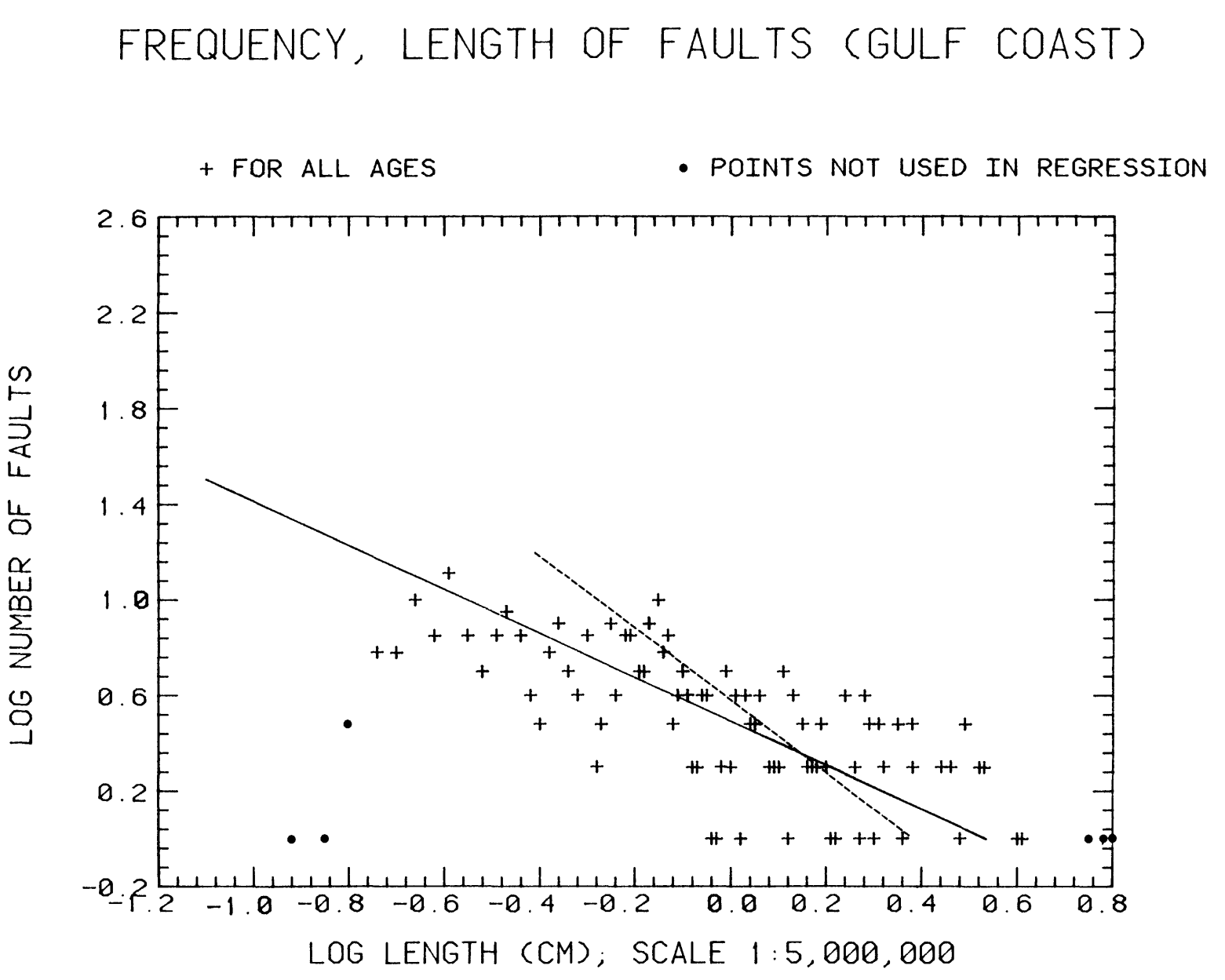

Figure 2.2.1.-3. (8)

FREQEUNCY, LENGTH OF FAULTS (MEXICAN HIGHLANDS)

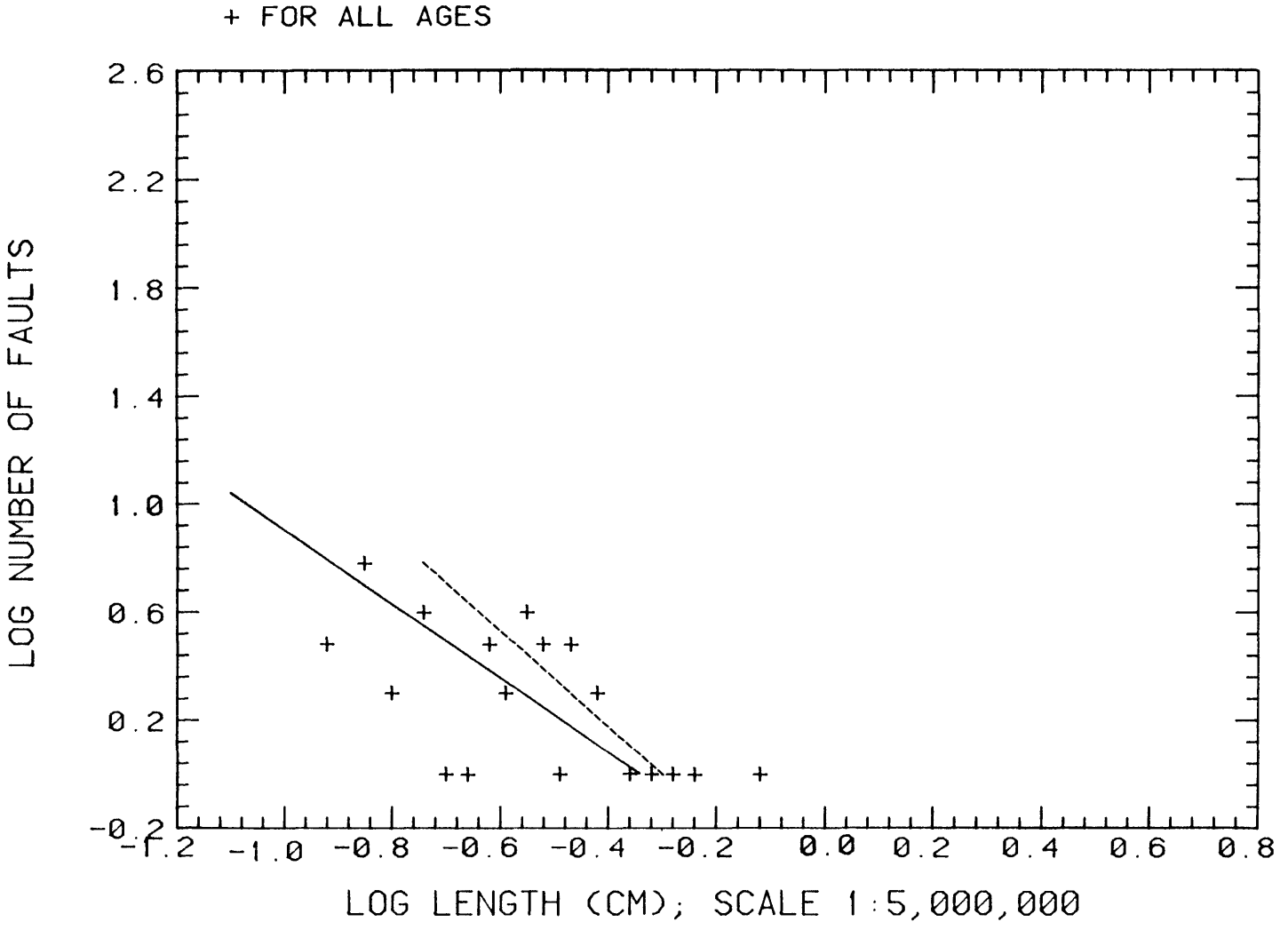

Figure 2.2.1.-3. (9)

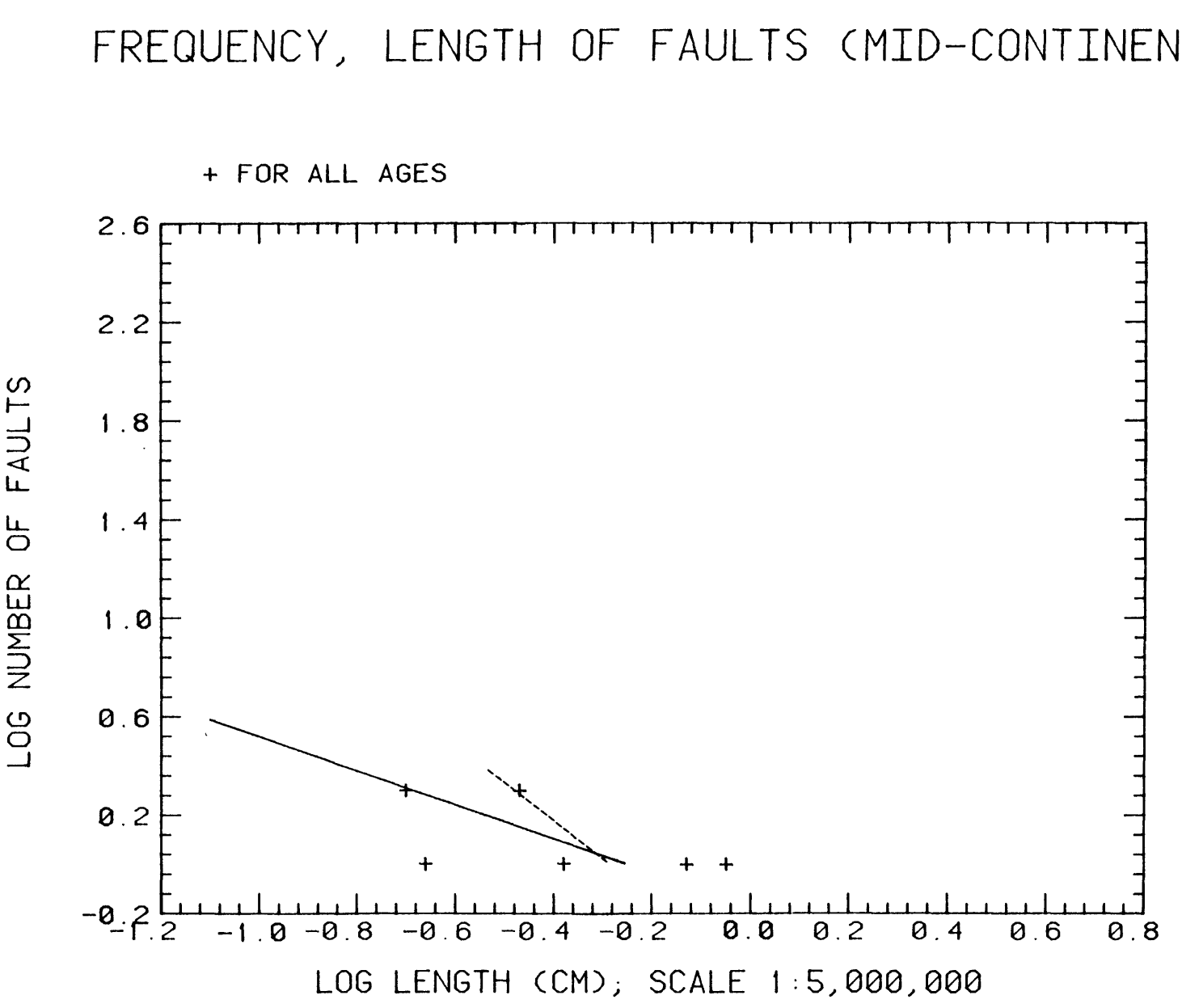

Figure 2.2.1.-3. (10)

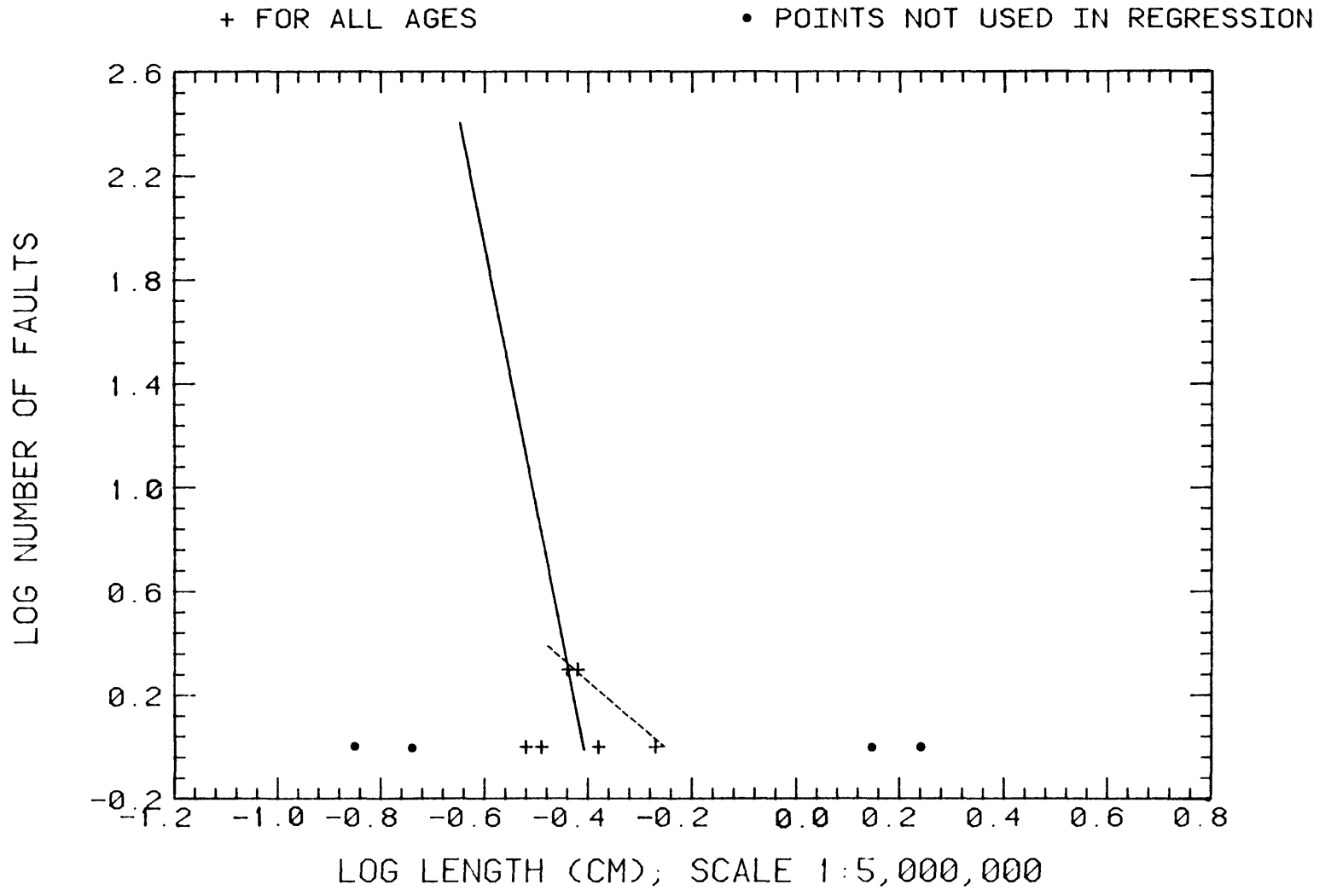

Figure 2.2.1.-3. (11)

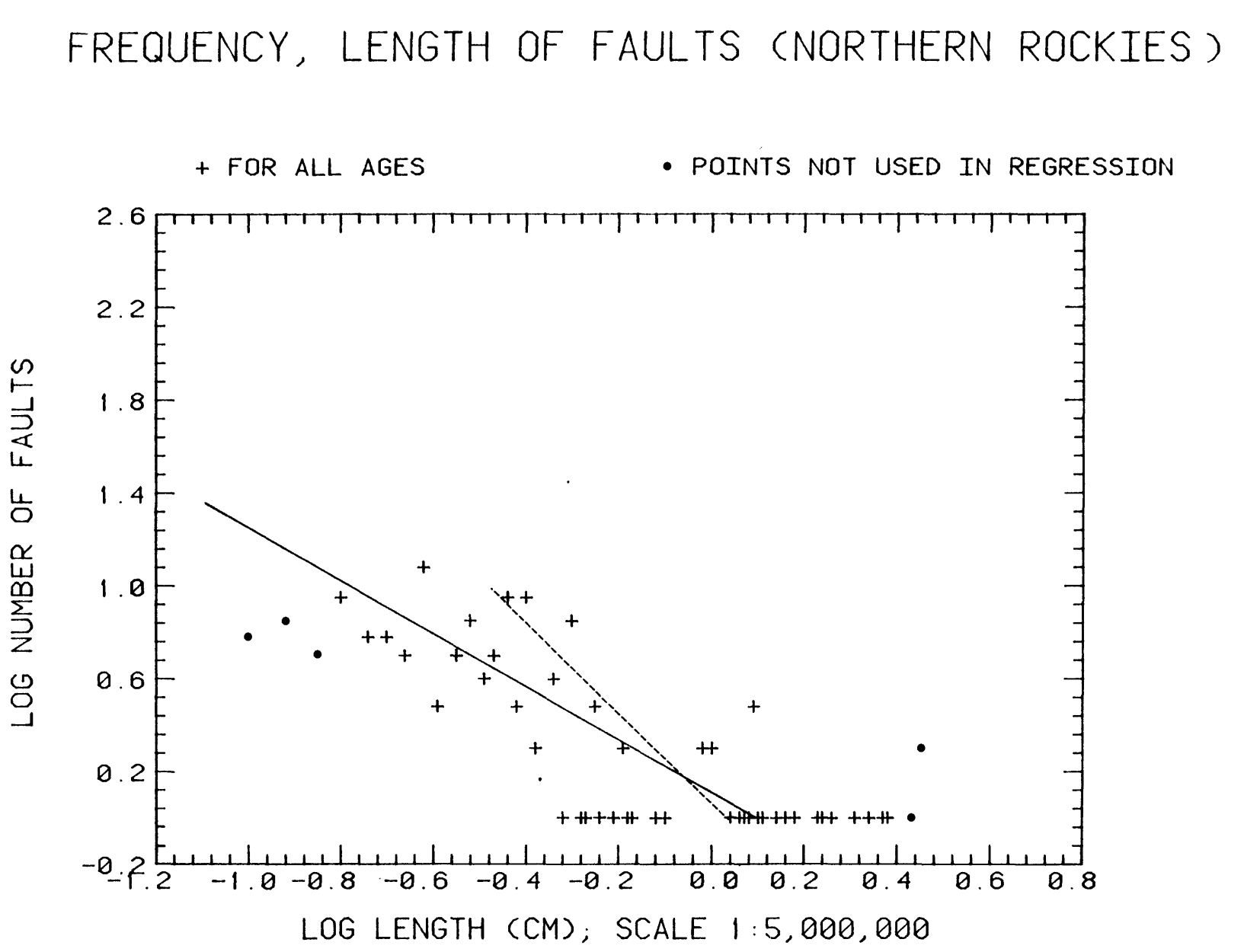

Figure 2.2.1.-3. (12)

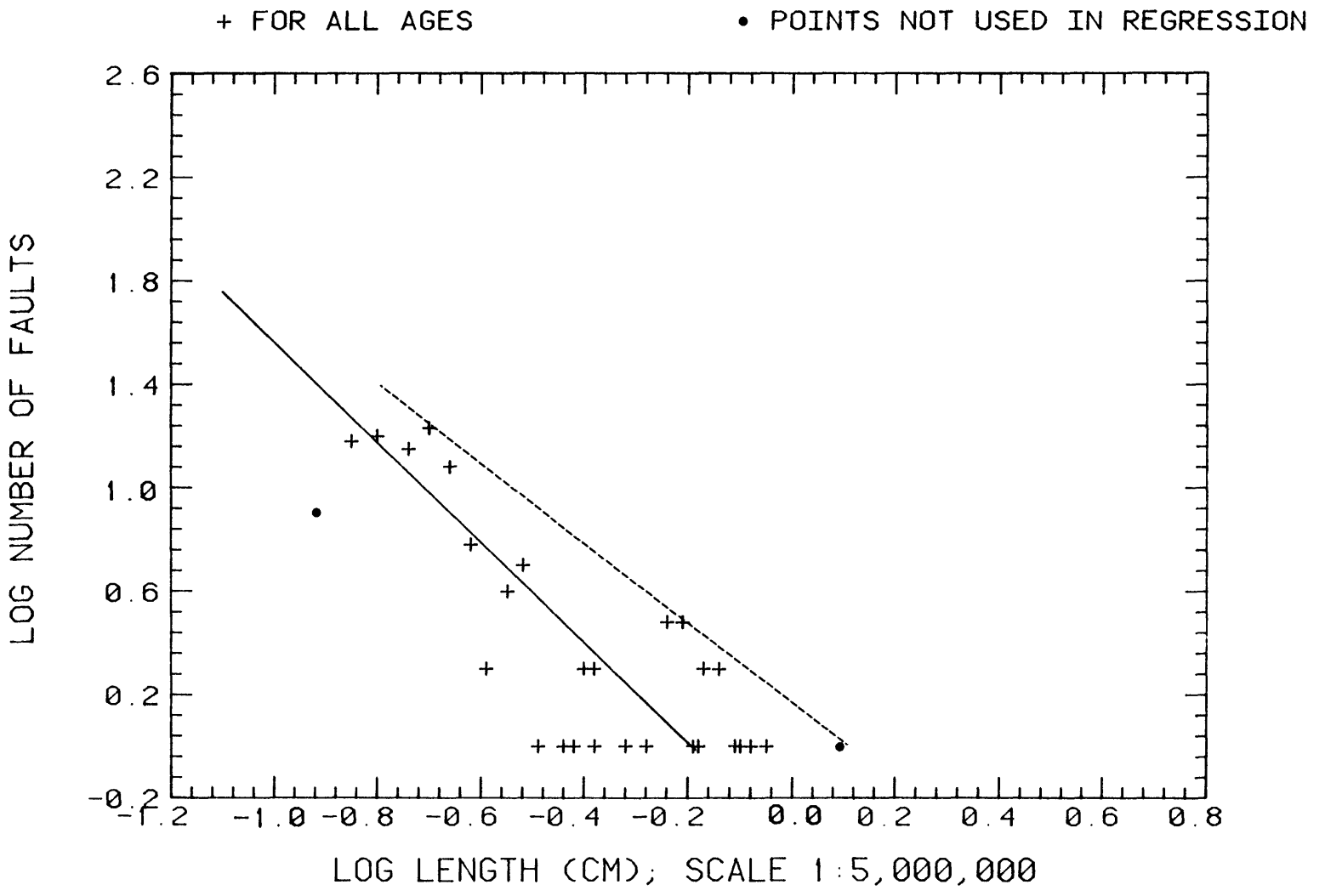

Figure 2.2.1.-3. (13)

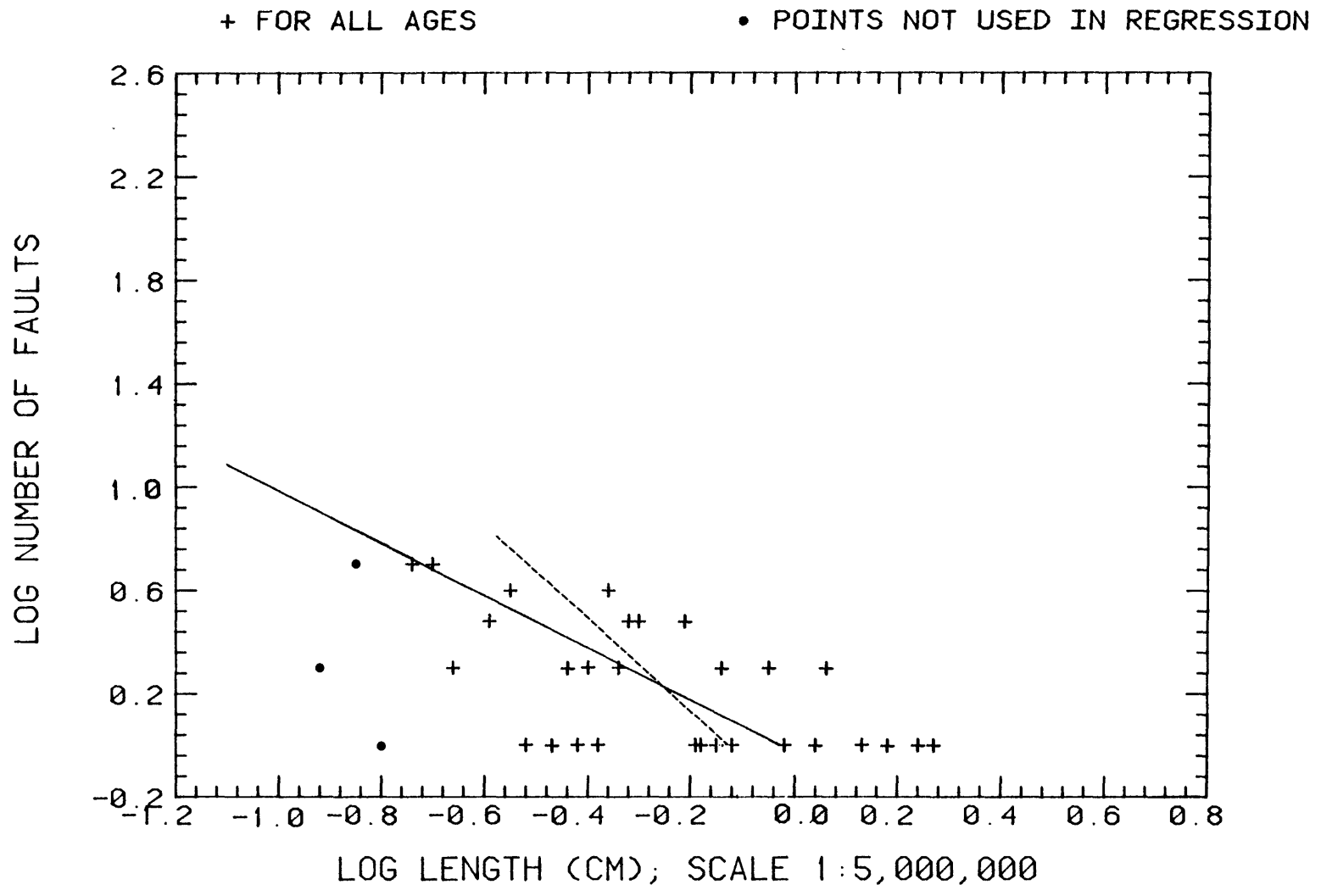

Figure 2.2.1.-3. (14)

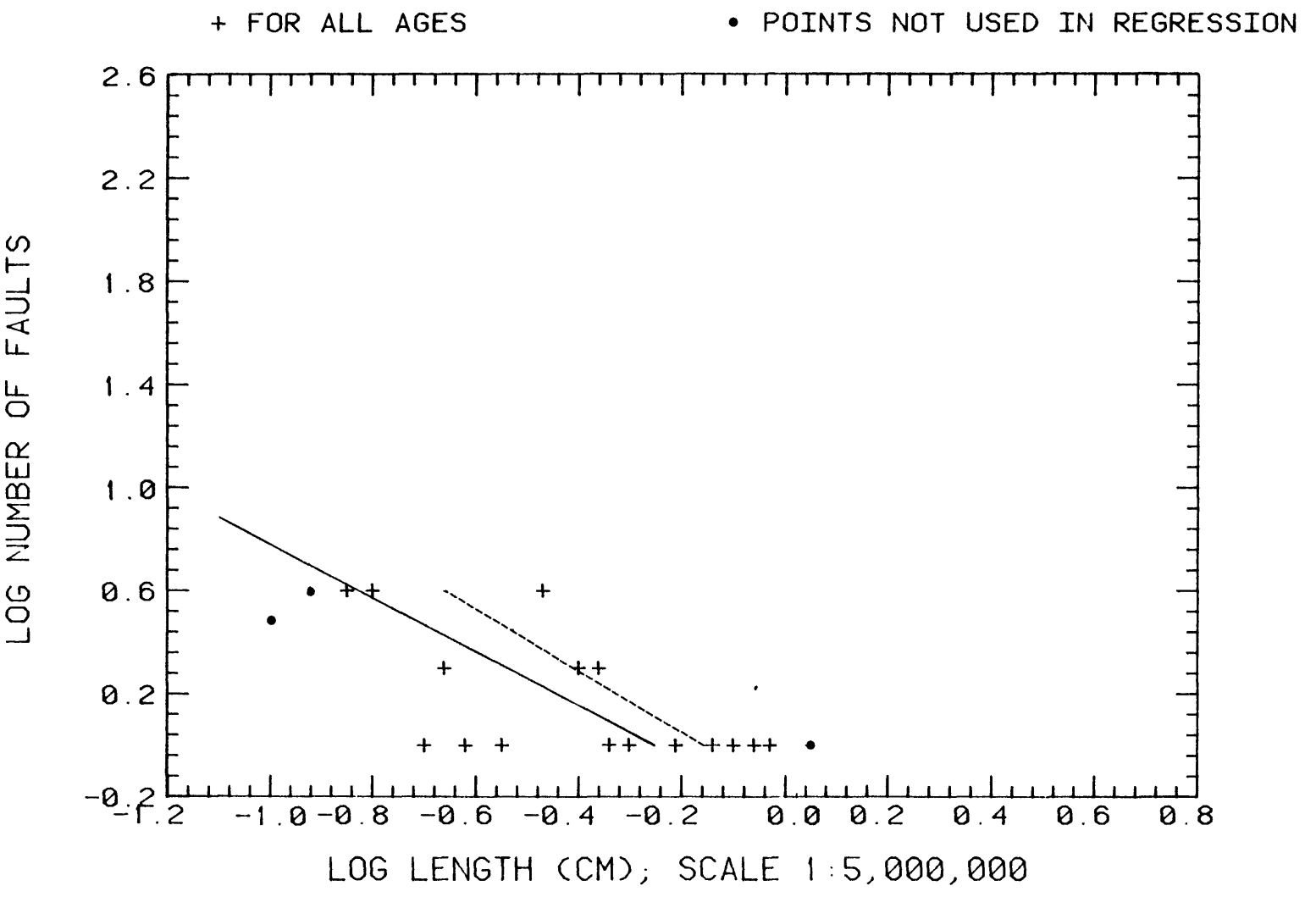

Figure 2.2.1.-3. (15)

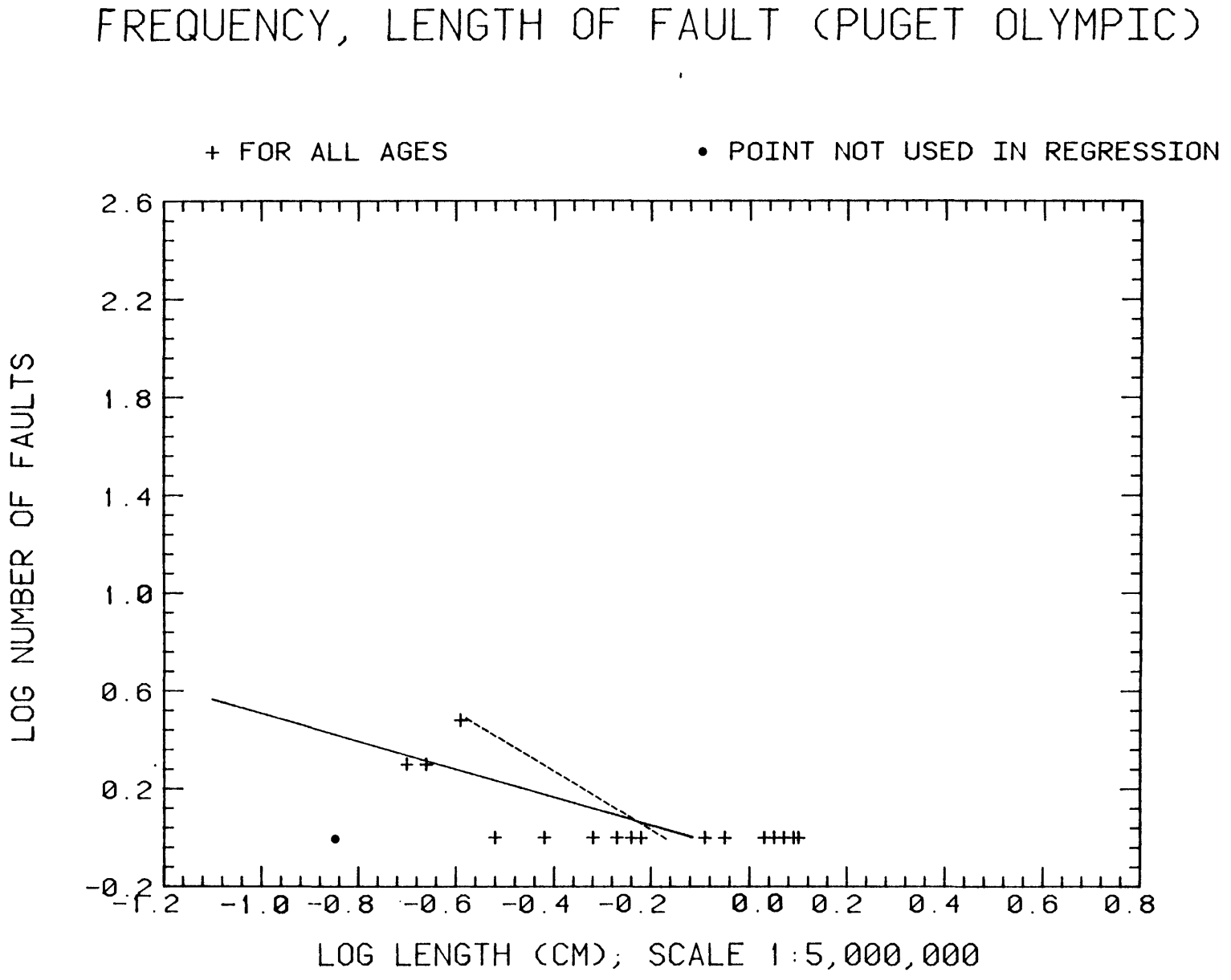

Figure 2.2.1.-3. (16)

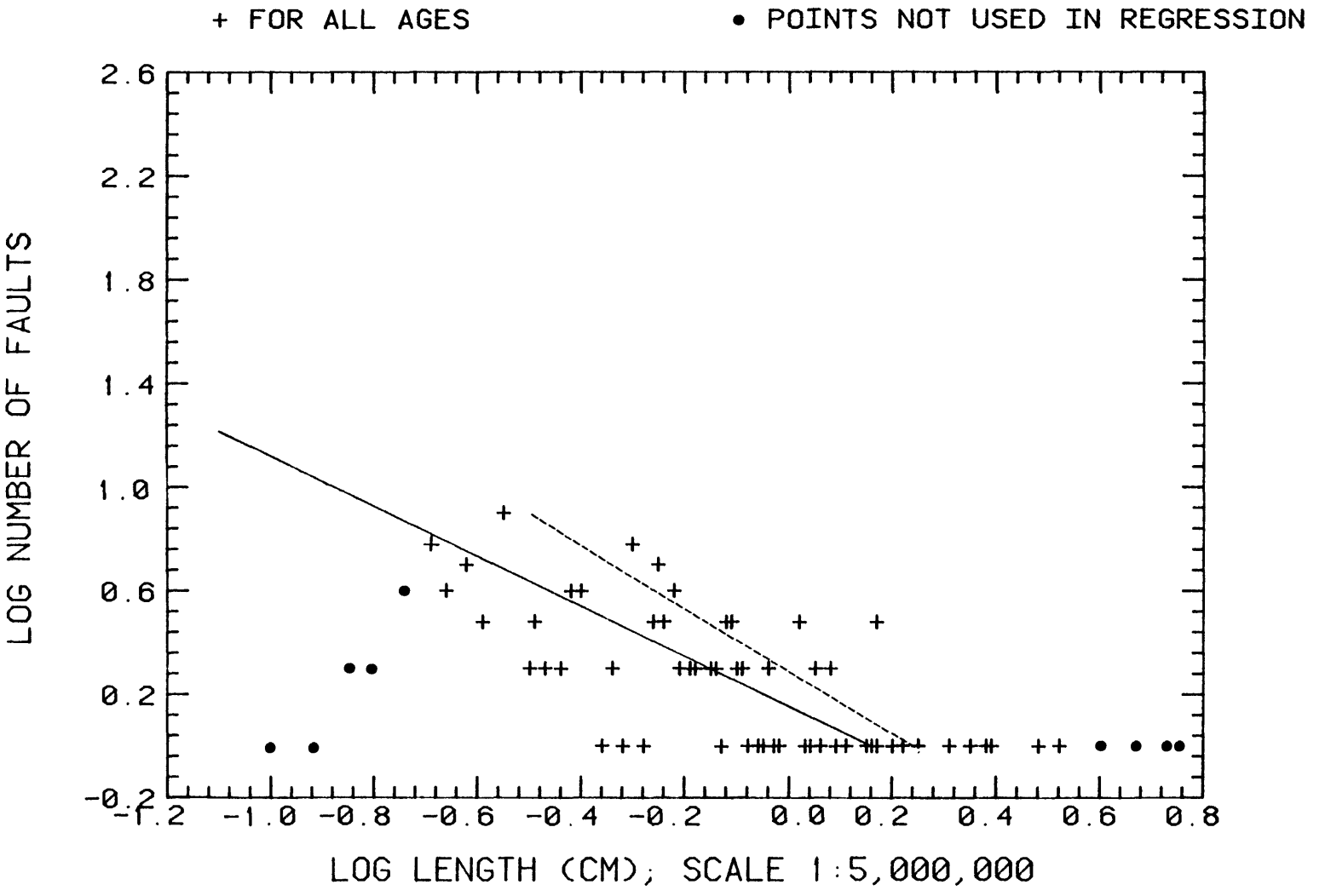

Figure 2.2.1.-3. (17)

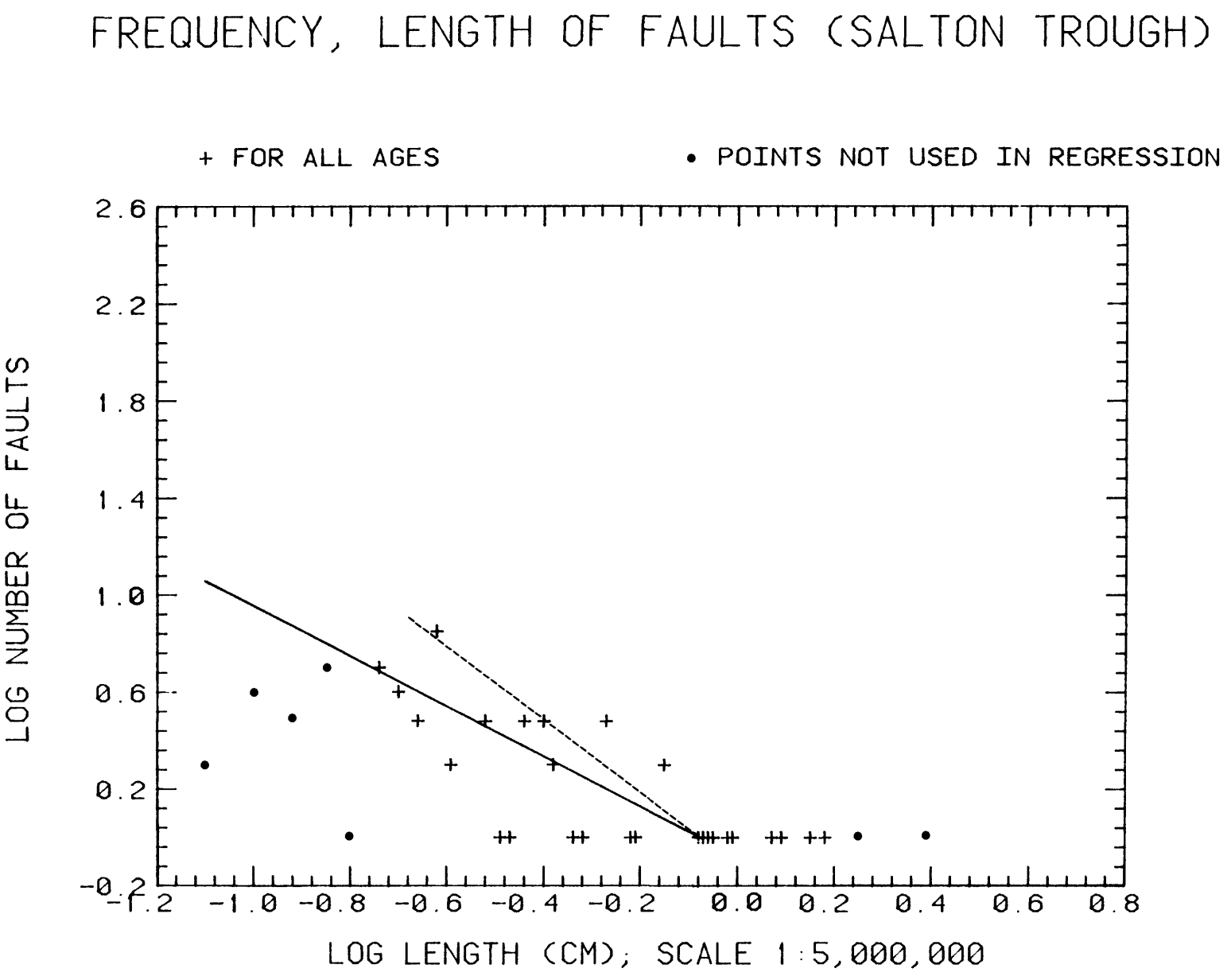

Figure 2.2.1.-3. (18)

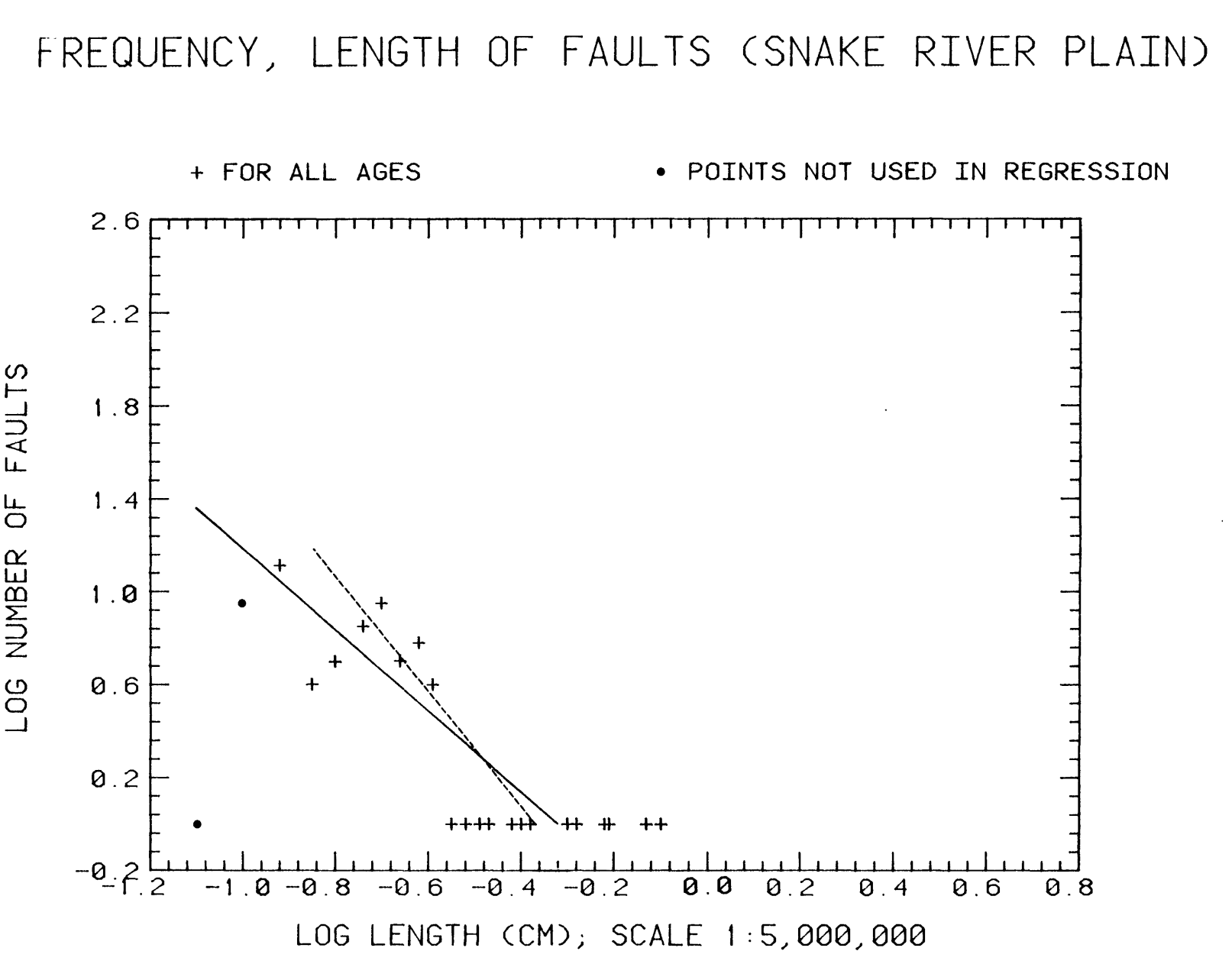

Figure 2.2.1.-3. (19)

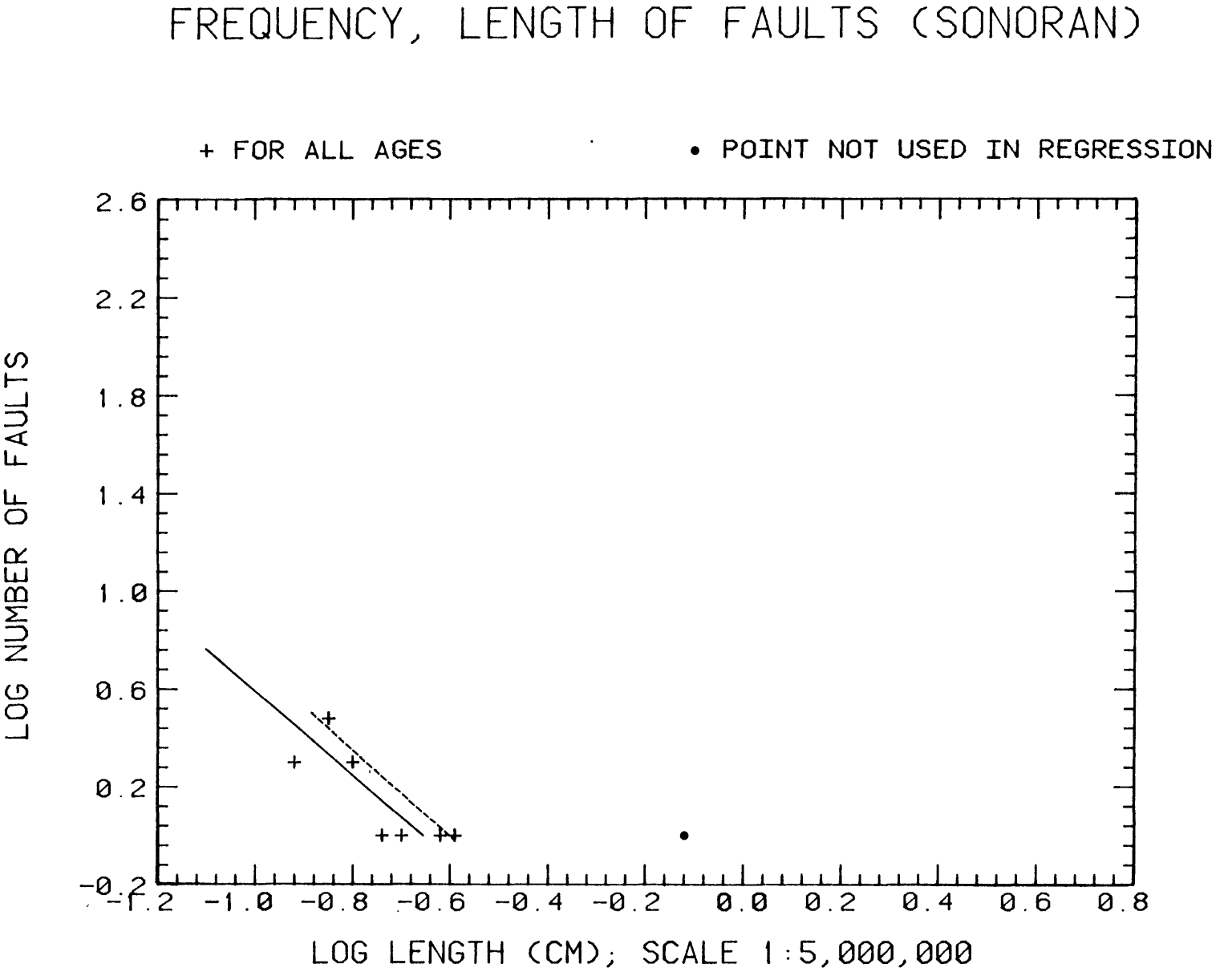

Figure 2.2.1.-3. (20)

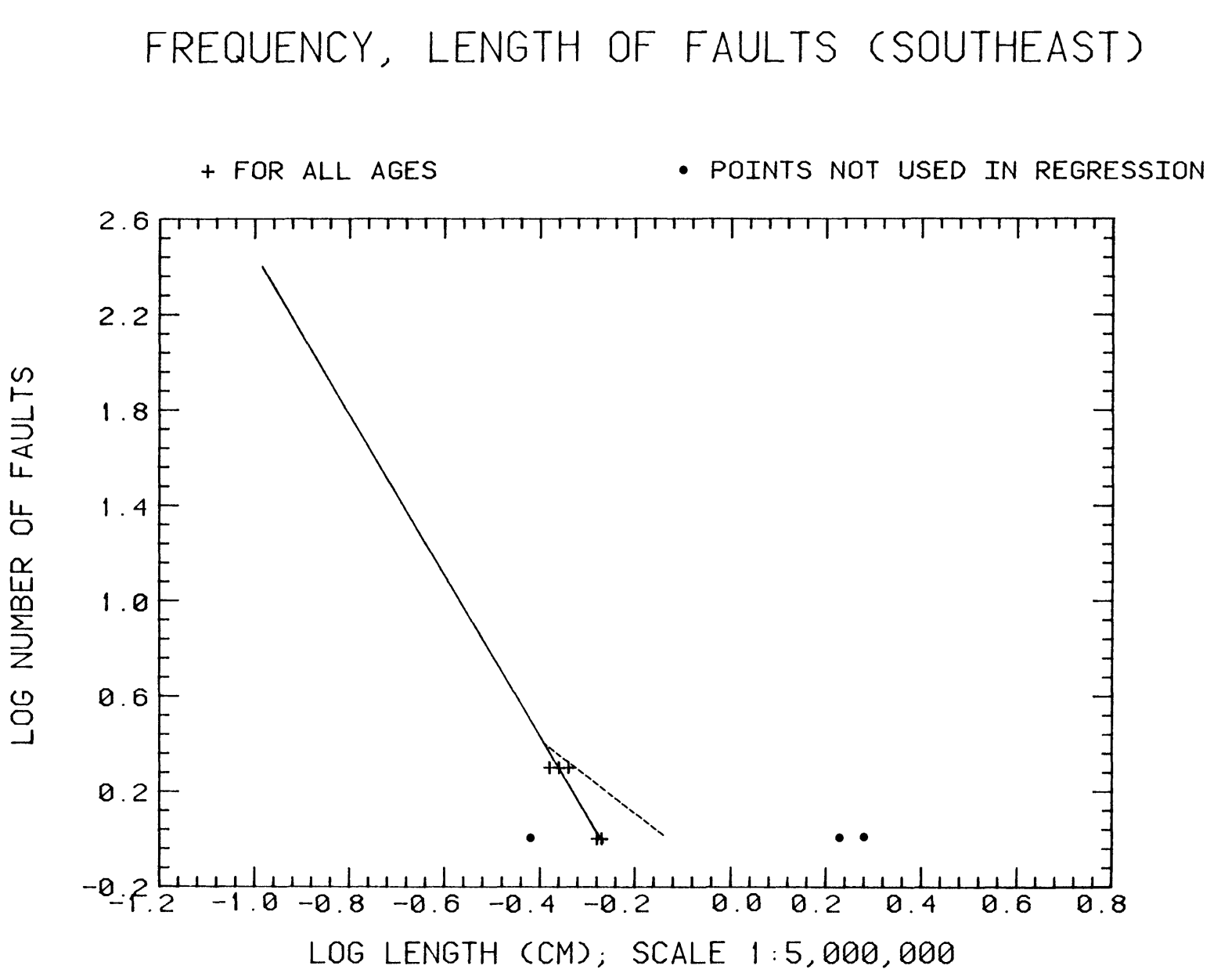

Figure 2.2.1.-3. (21)

FREQUENCY, LENGTH OF FAULTS (SOUTHERN CA. BORDERLAND)

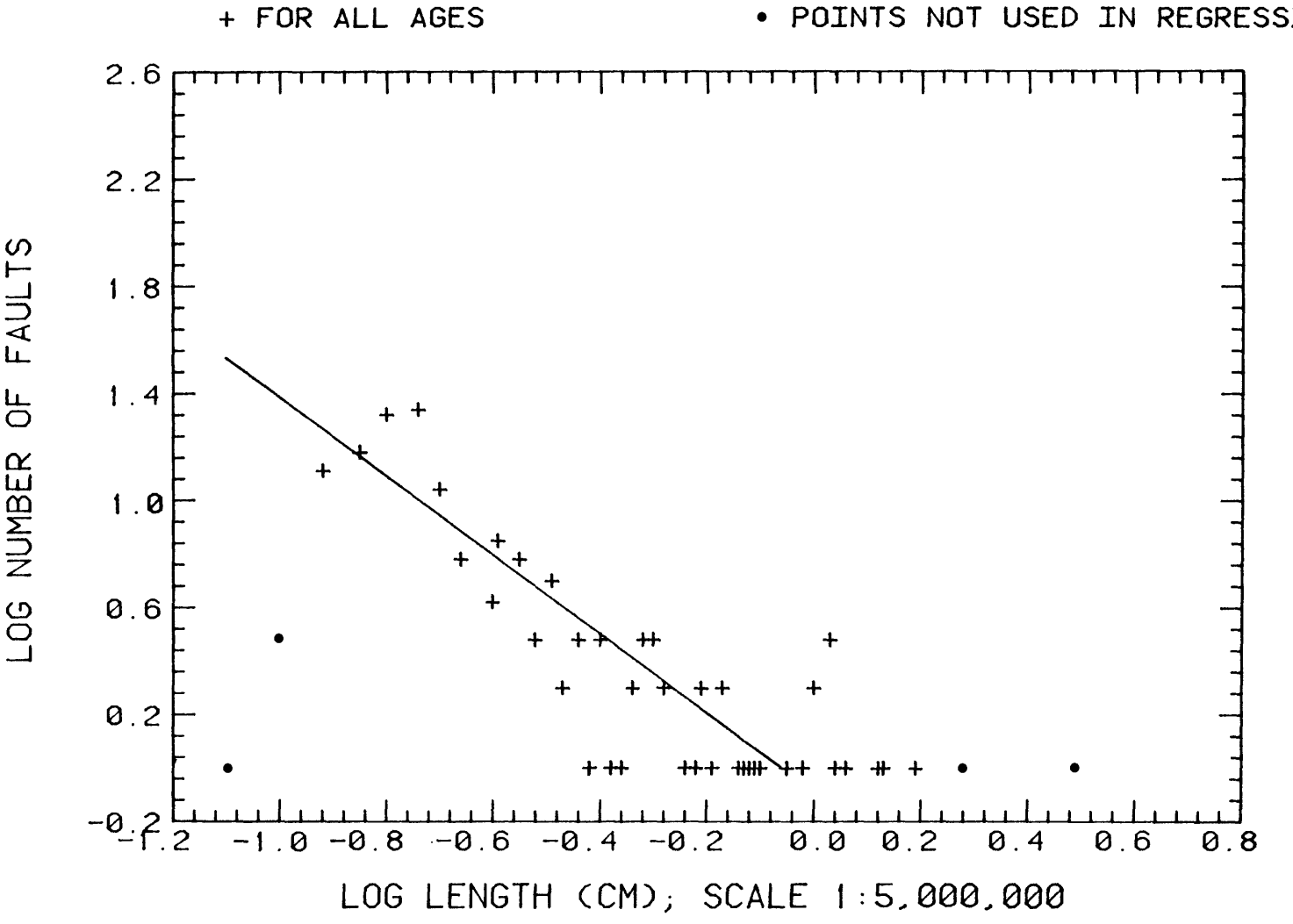

Figure 2.2.1.-3. (22)

FREQUENCY, LENGTH OF FAULTS (STRAITS OF FLORIDA)

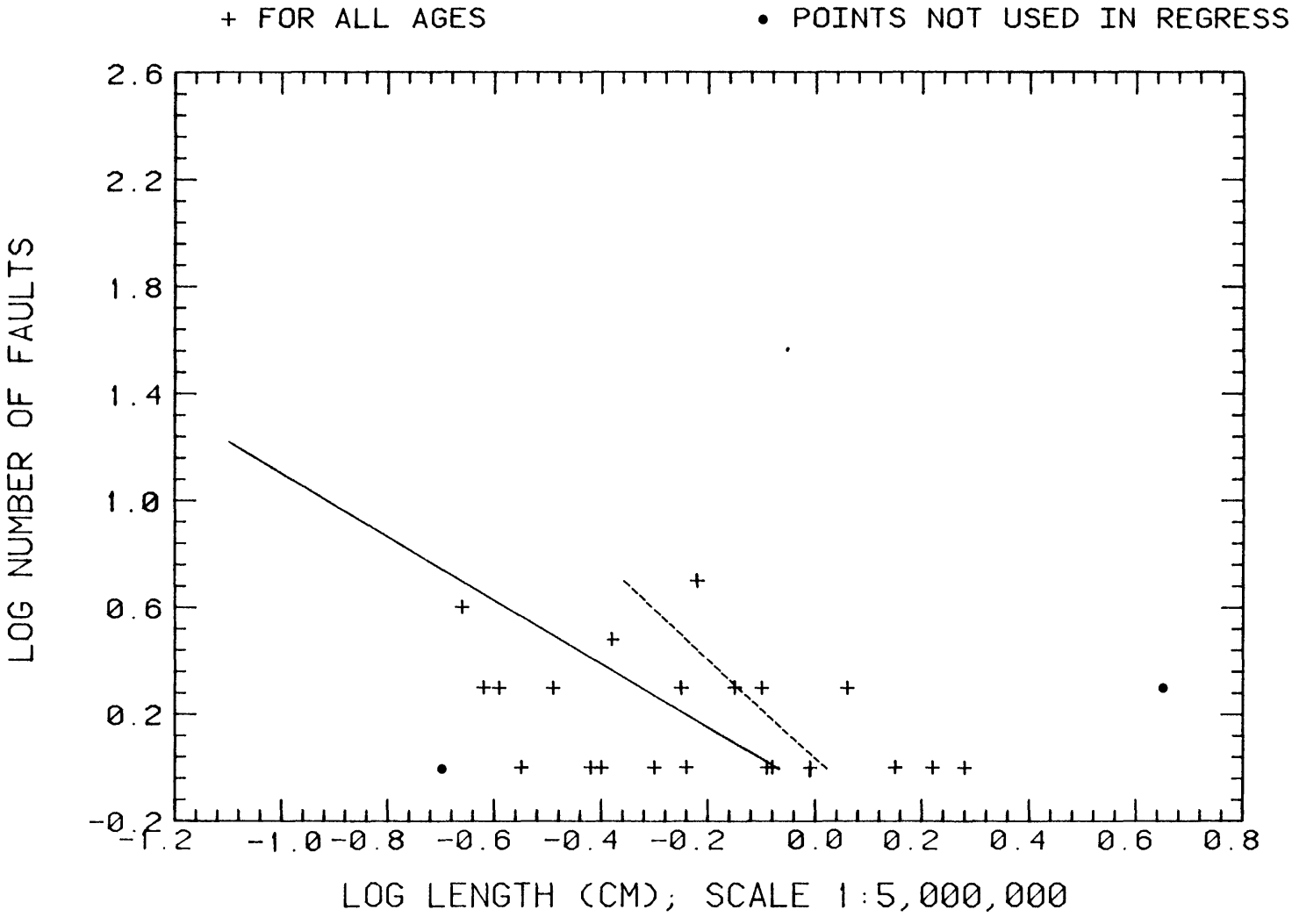

Figure 2.2.1.-3. (23)

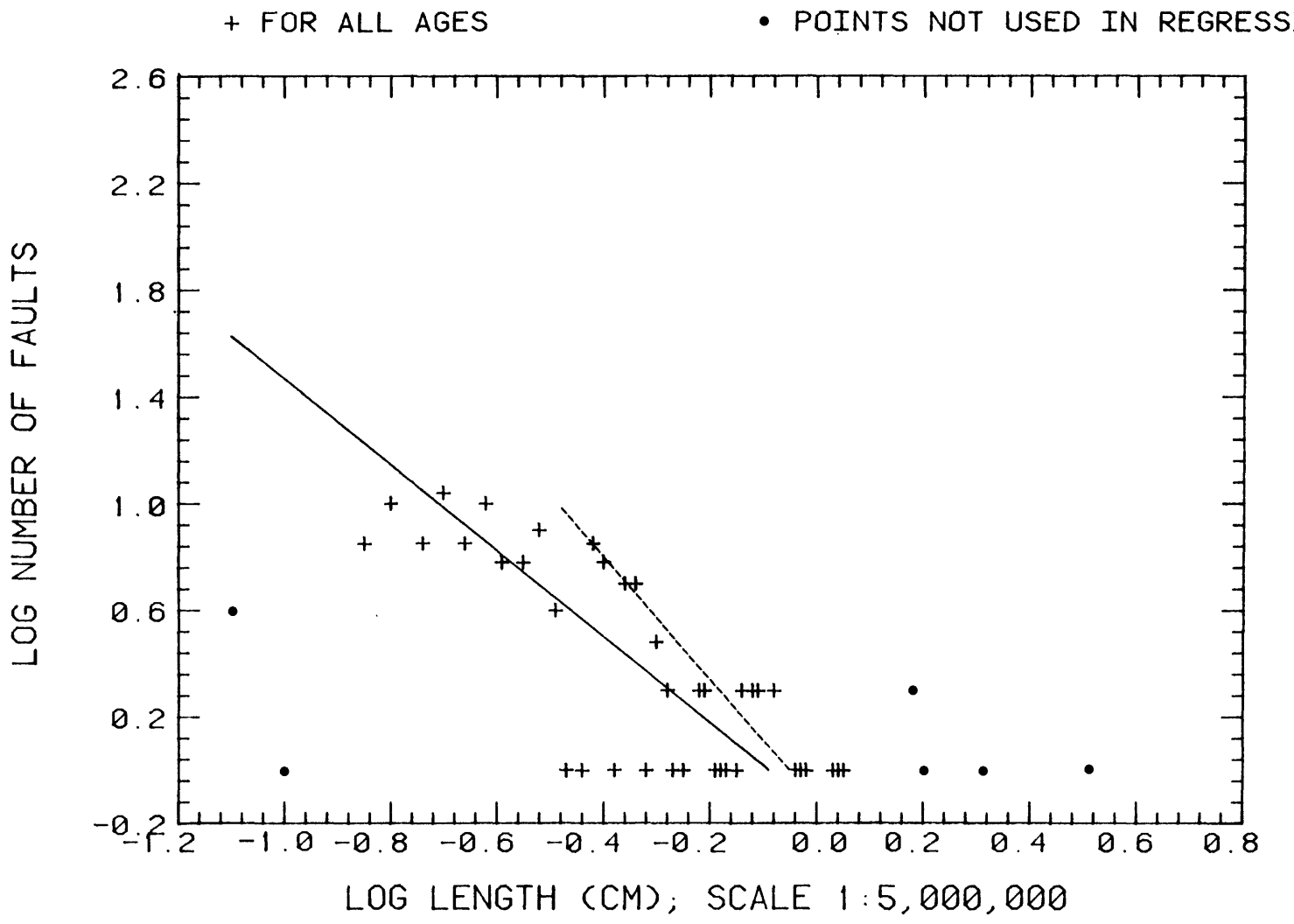

Figure 2.2.1.-3. (24)

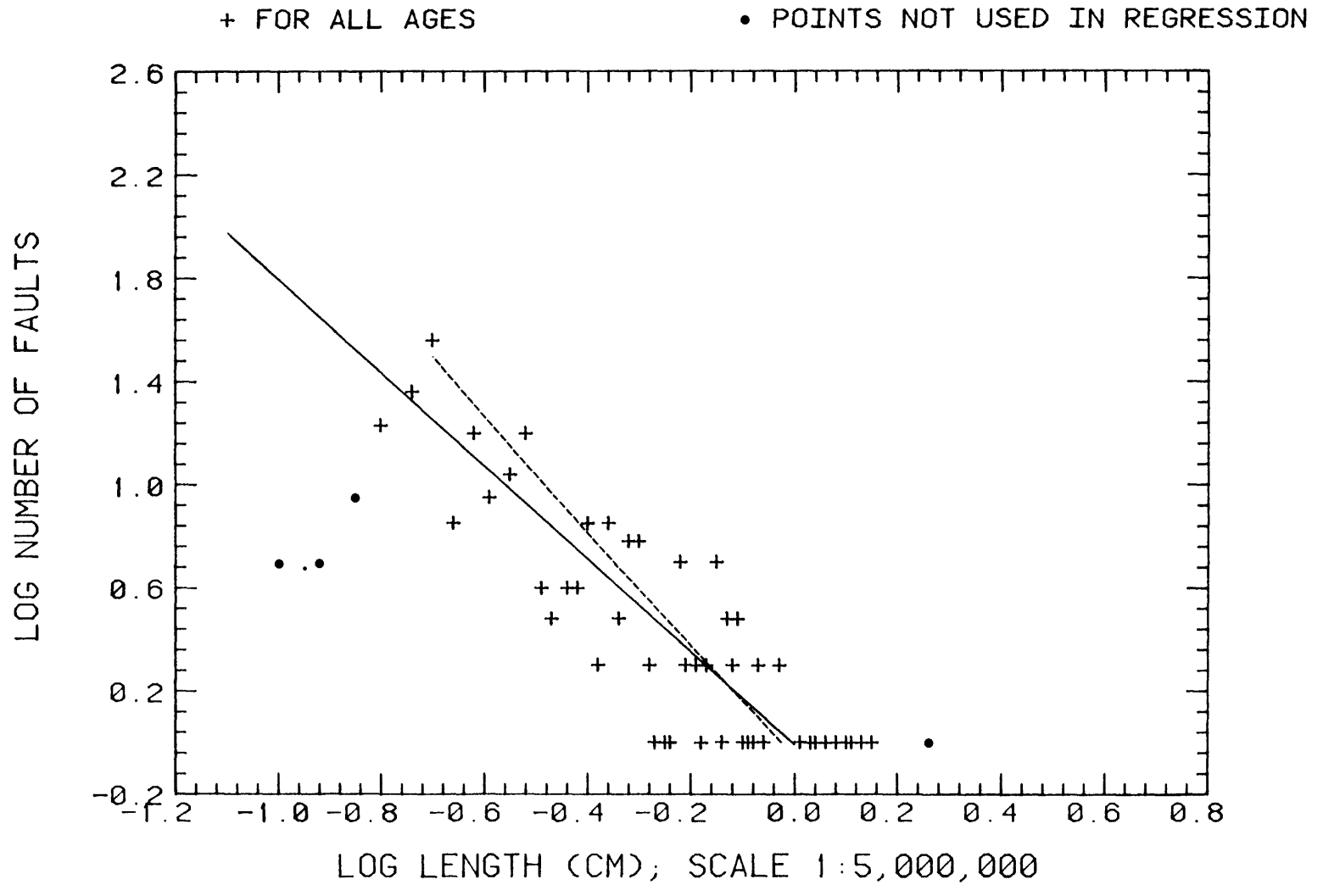

Figure 2.2.1.-3. (25)

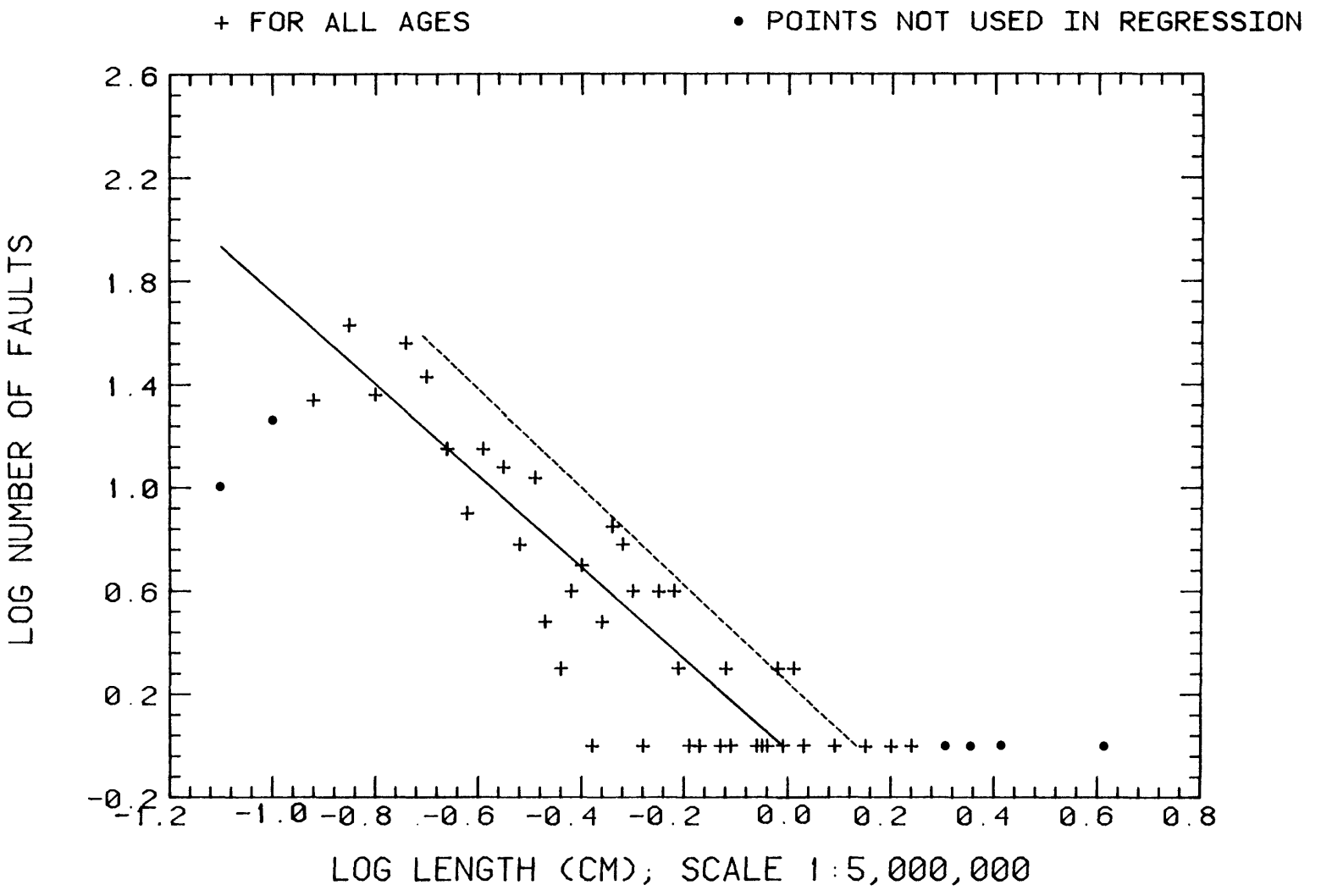

Figure 2.2.1.-3. (26)

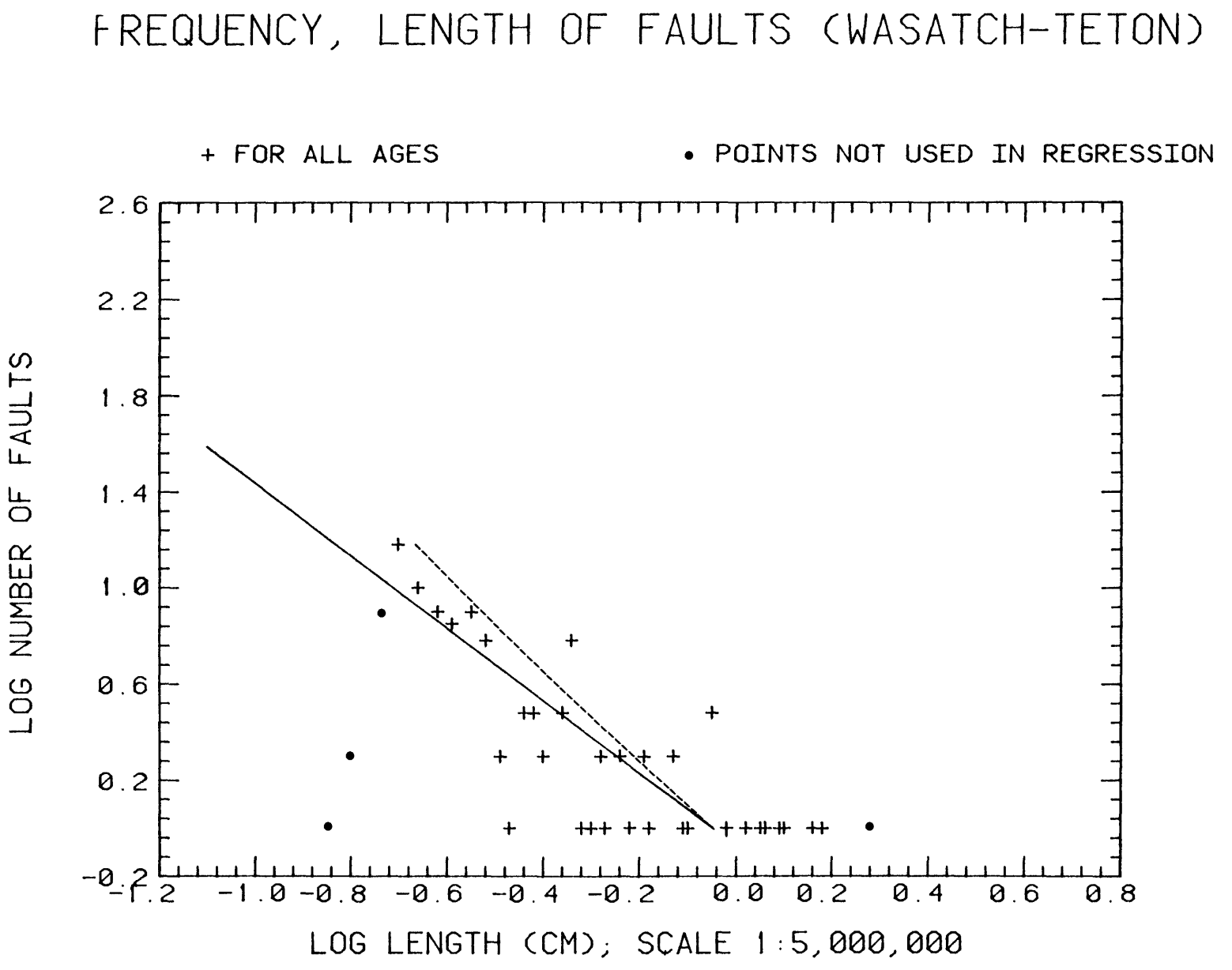

Figure 2.2.1.-3. (27)

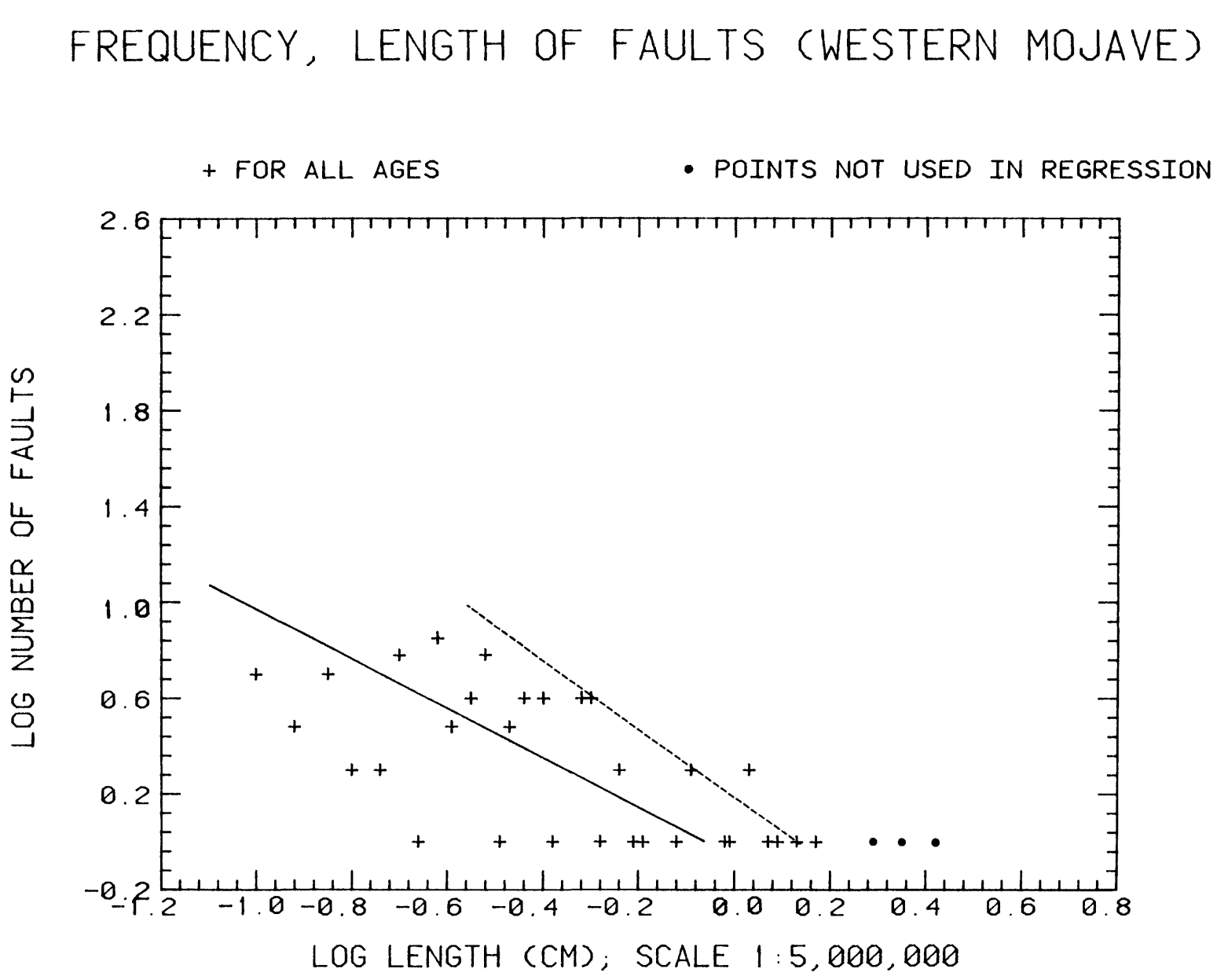

Figure 2.2.1.-3. (28)

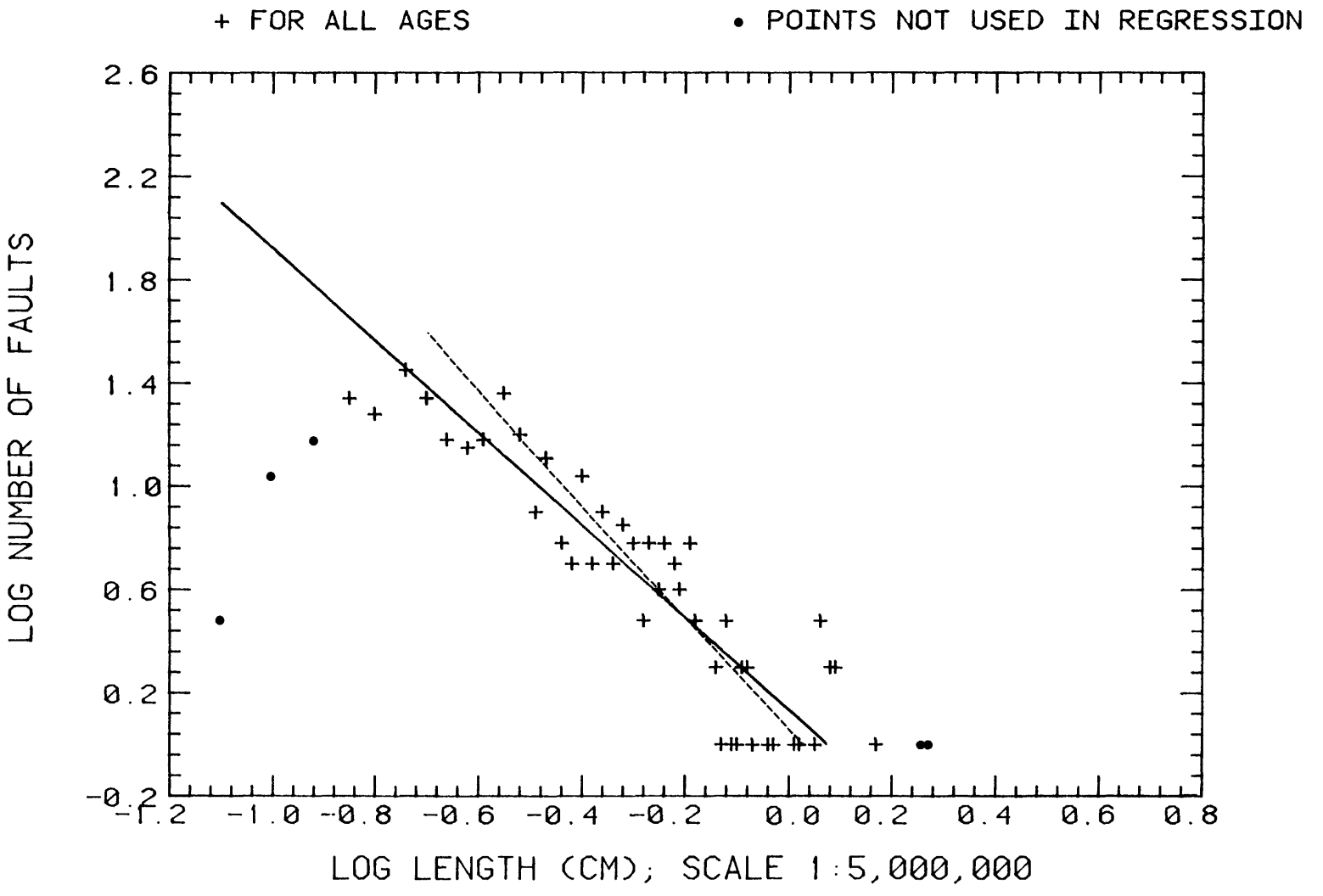

Figure 2.2.1.-3. 2 (29)

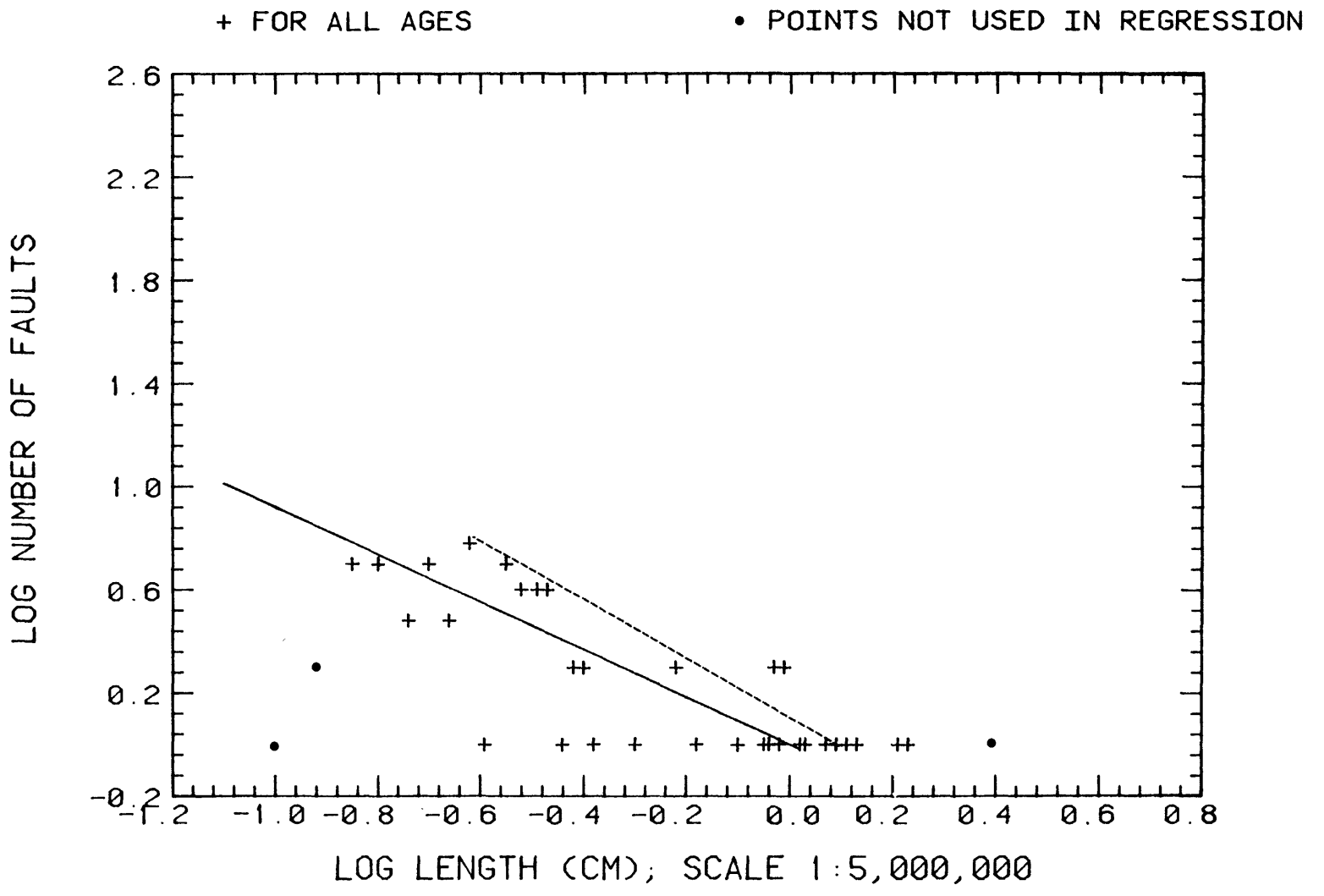

Figure 2.2.1.-3. (30)

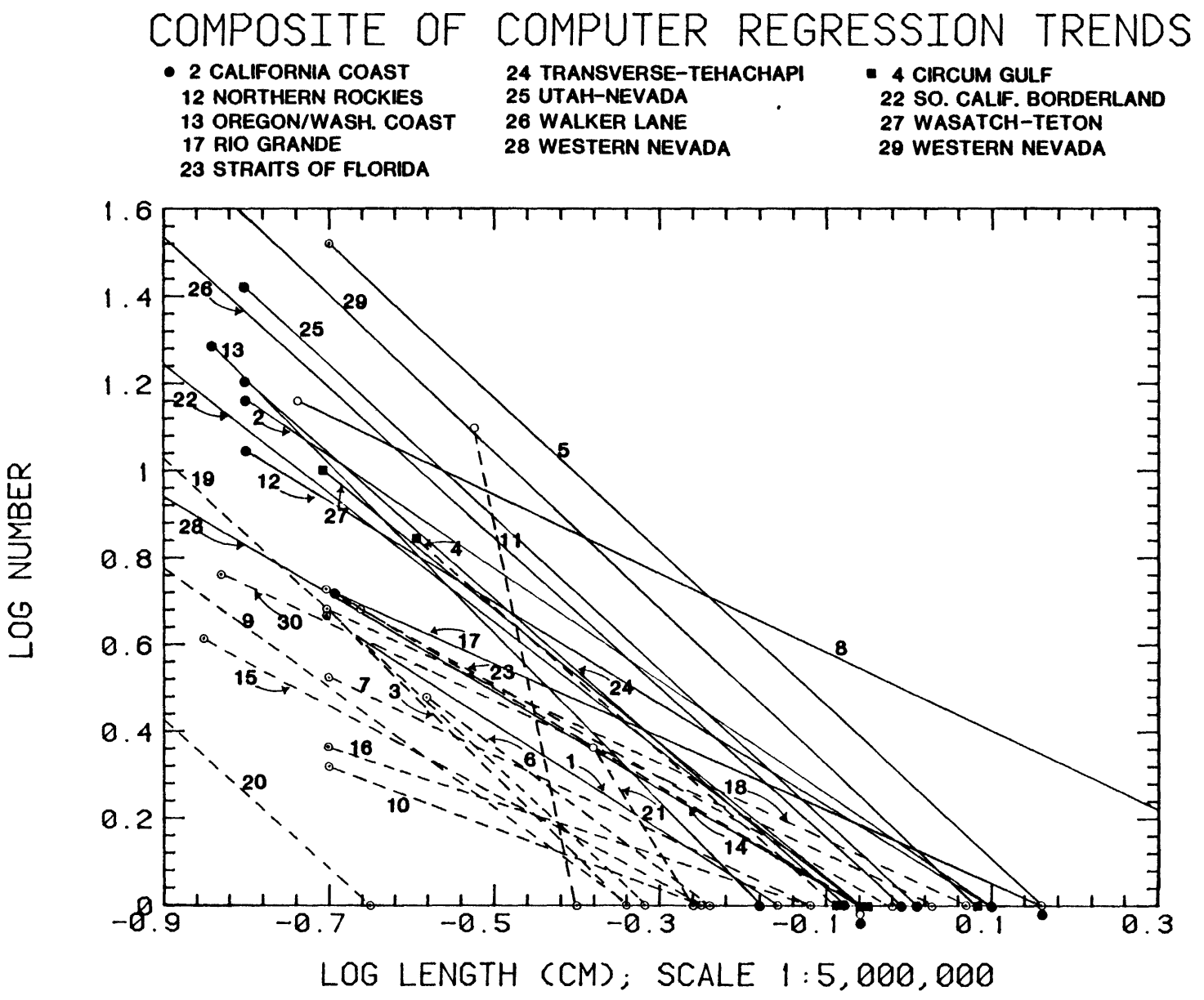

Figure 2.2.1.-4. (A)
Composite of subjectively fitted data for logarithms of numbers and fault lengths for all fault regions in the United States (all ages taken together); A. computer regressions

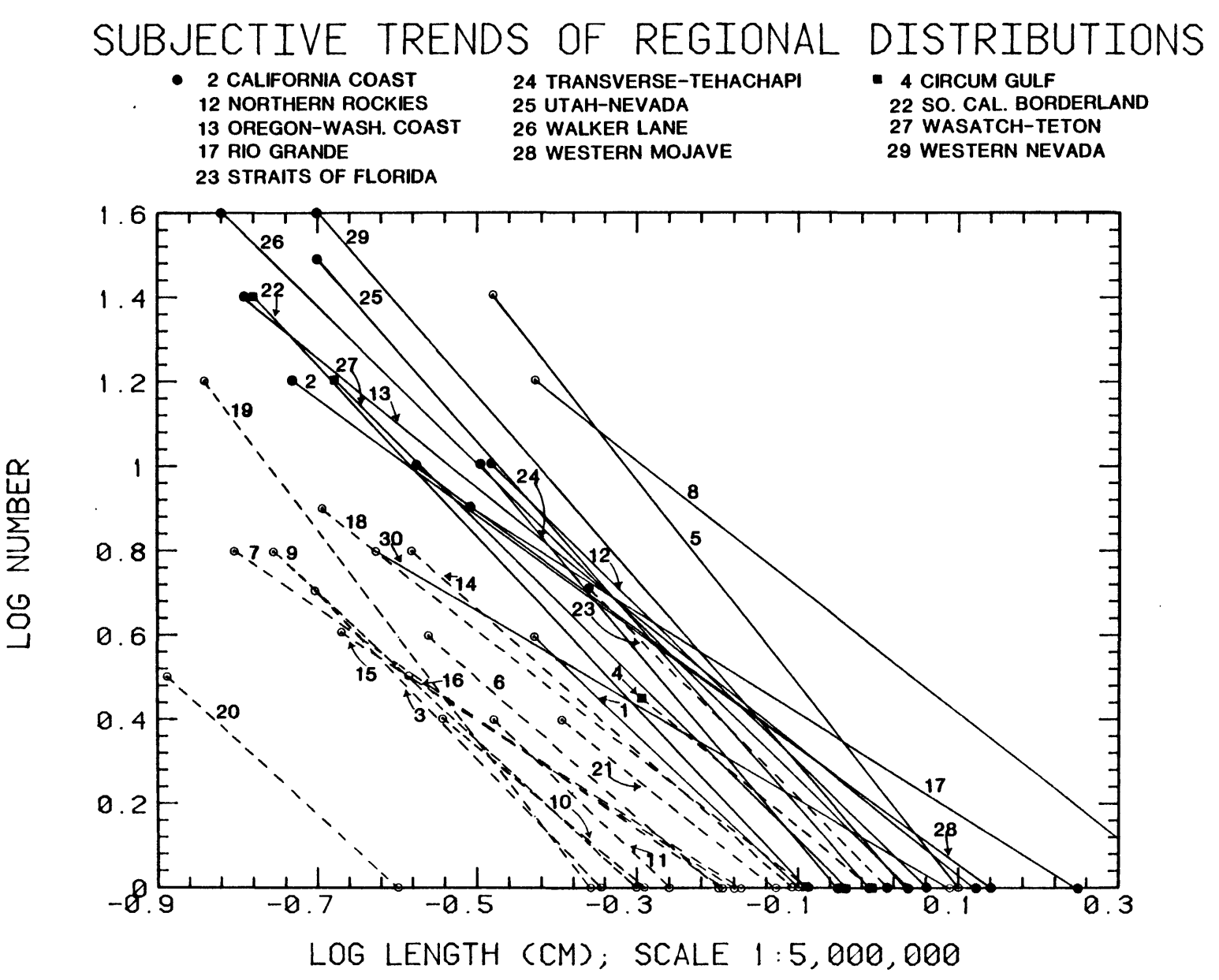

Figure 2.2.1.-4. (B)
subjective regressions.

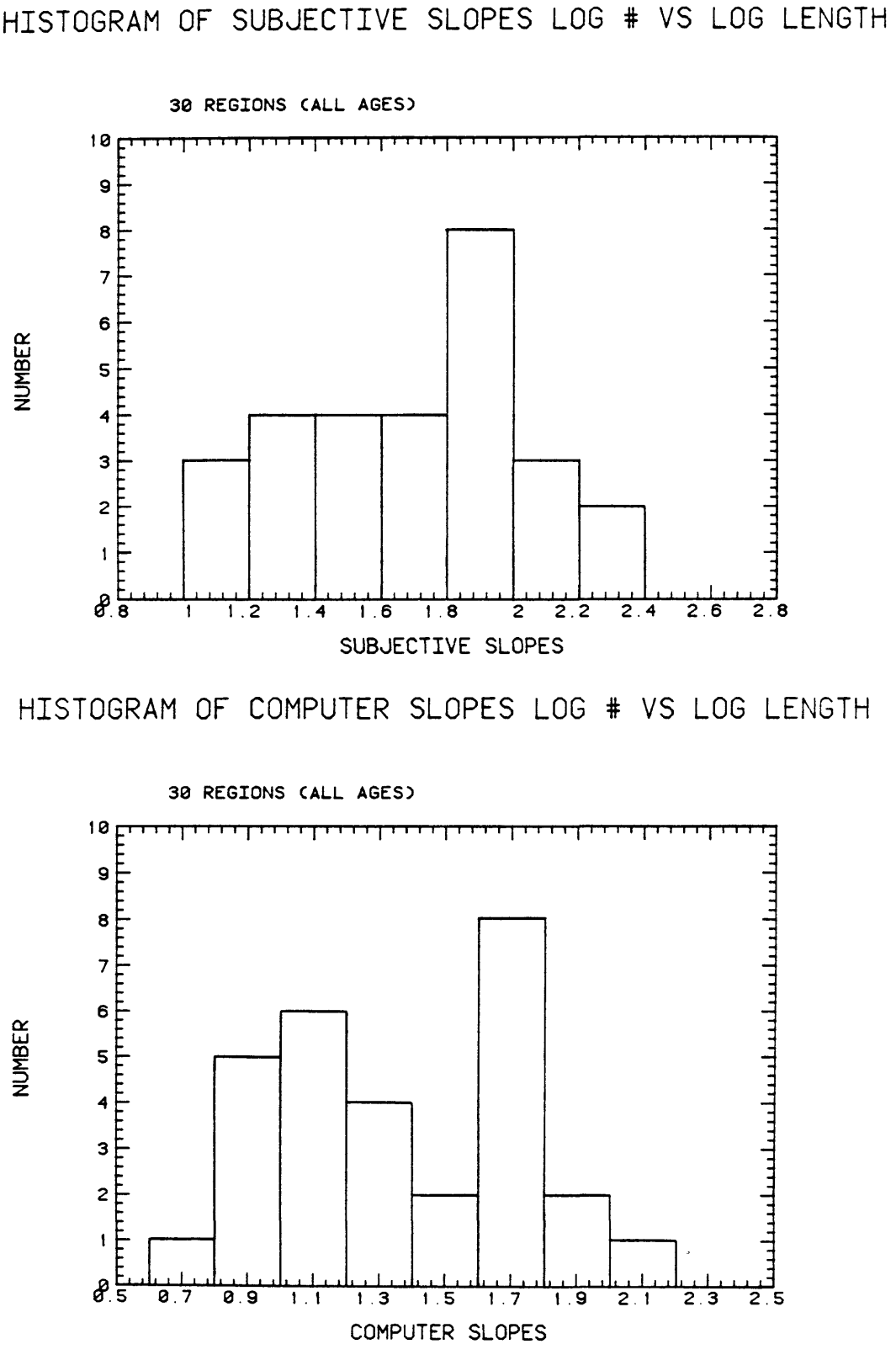

Figure 2.2.1.-5.
Histogram showing the distribution for slopes representing the relation between the logarithms of number versus length for the set of 30 fault regions in the conterminous United States (all ages taken together).

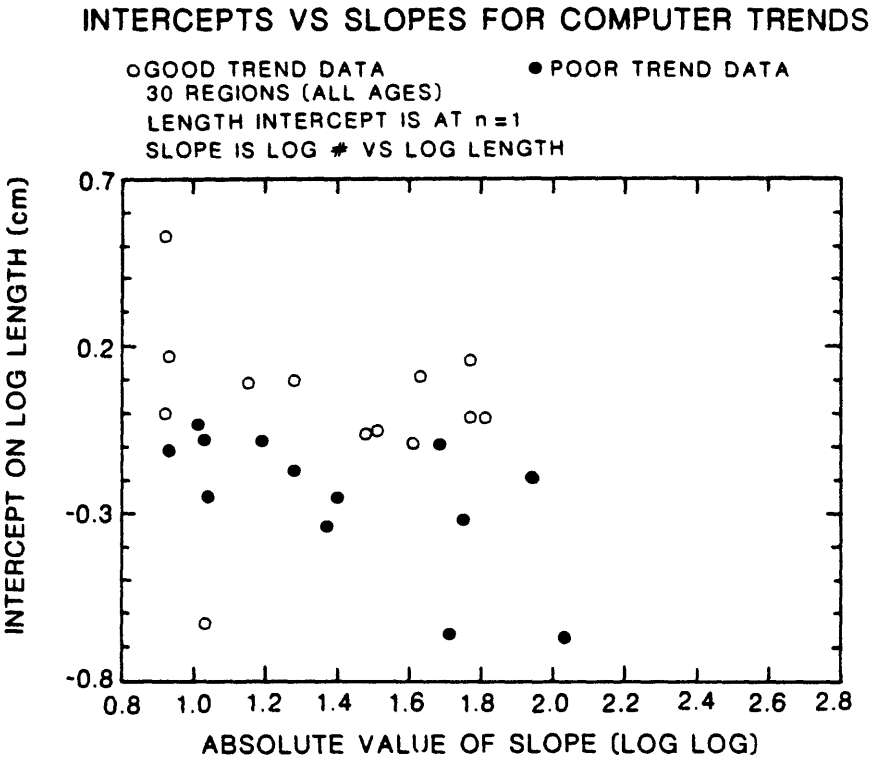

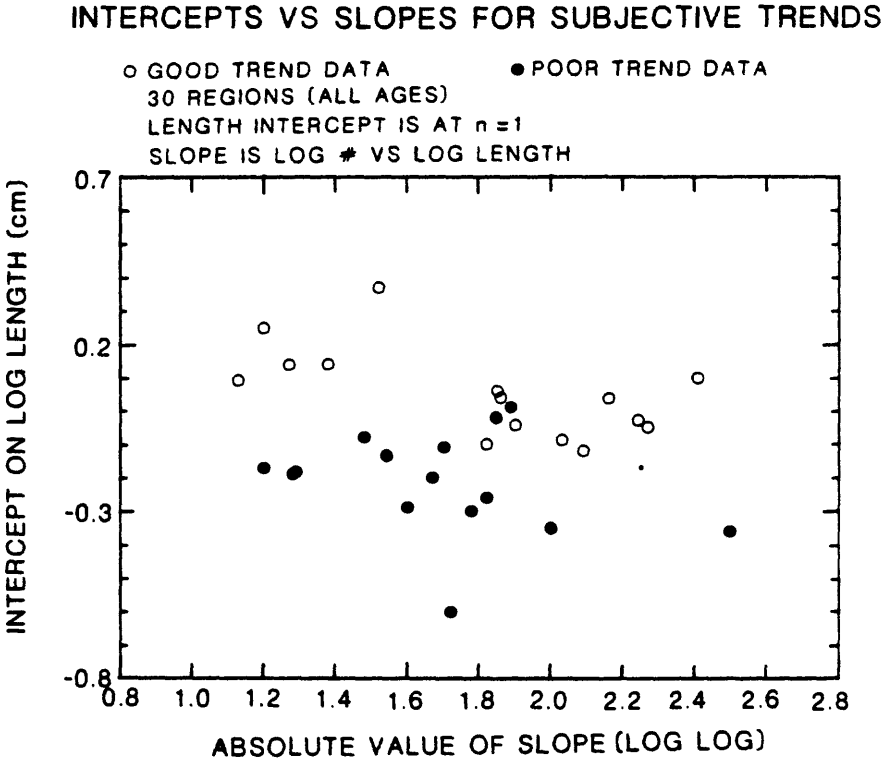

Figure 2.2.1.-6.
Absolute values for slopes versus length intercepts at number n=1 based on subjectively fitted data (Fig. 2.2.1.-4).

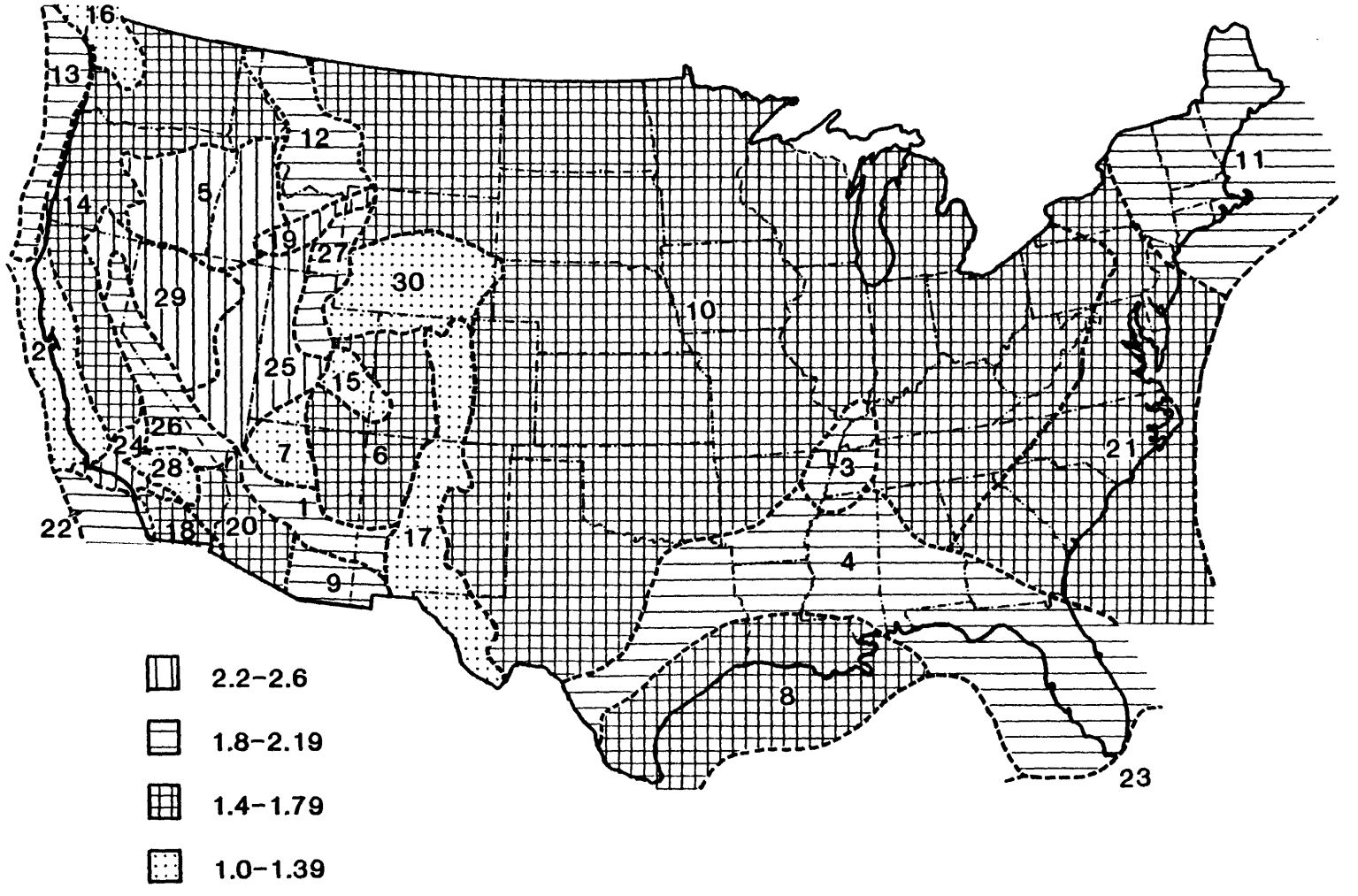

Figure 2.2.1.-7.
Map showing distribution for absolute slope values in conterminous United States based on subjectively fitted data.

MAP DISTRIBUTION OF INTERCEPT LENGTHS FOR SUBJECTIVE TRENDS IN PLOTS OF LOG NUMBER VS LOG LENGTH USING ALL DATA IN EACH REGION

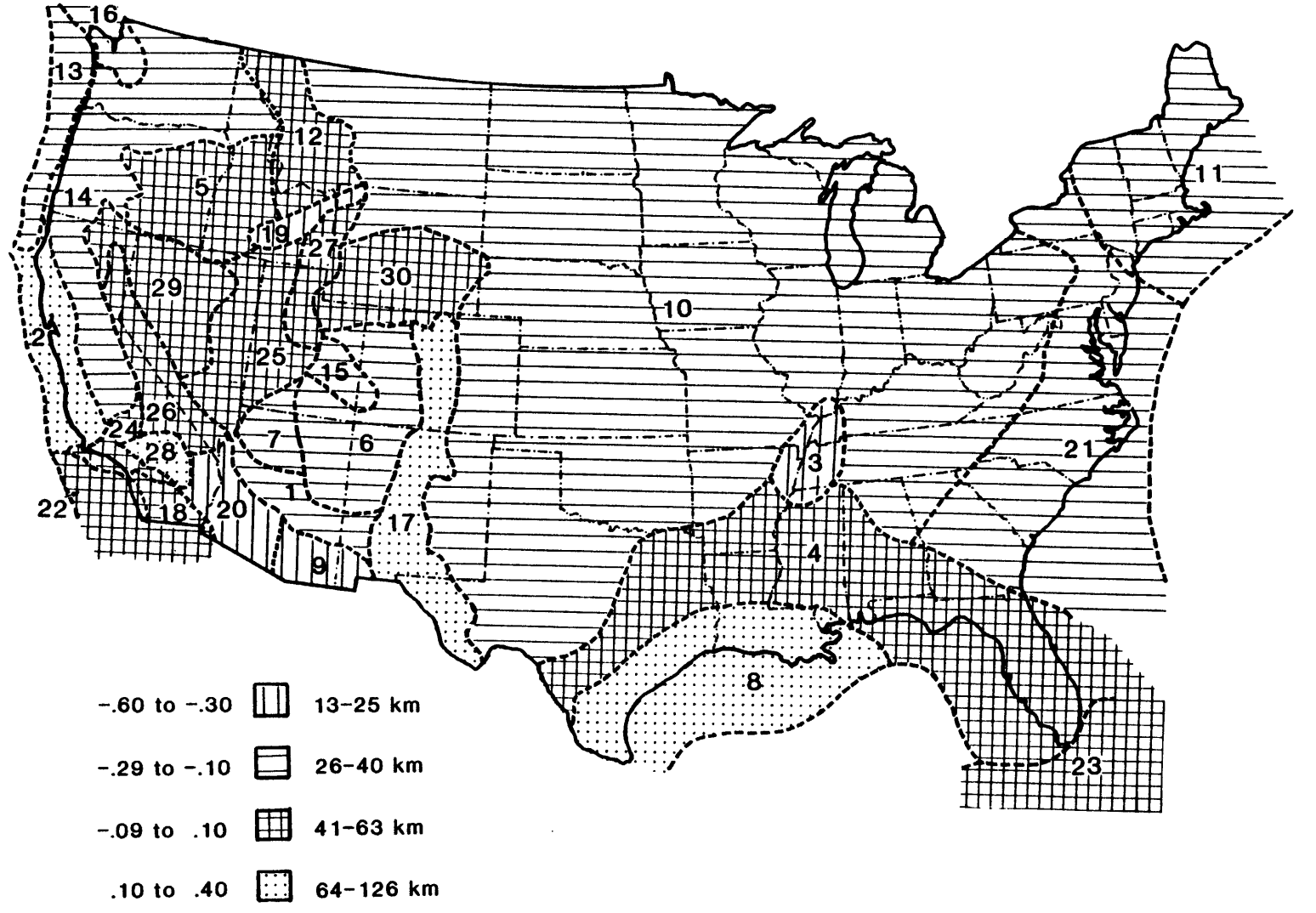

Figure 2.2.1.-8.
Map showing distribution for intercept values at n=1 in the conterminous United States based on subjectively fitted data.

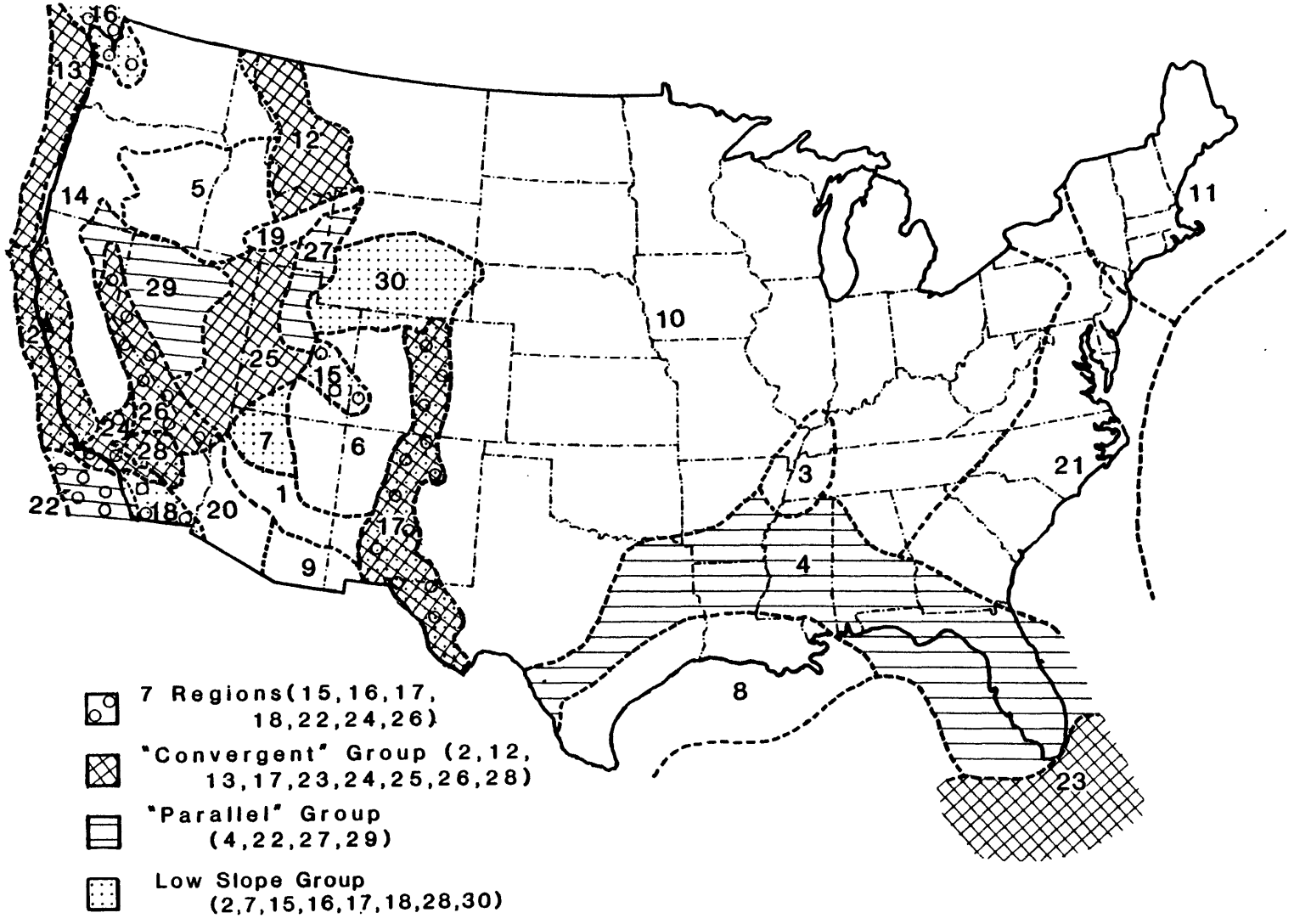

Figure 2.2.1.-9.
Map showing distribution for various selected subgroups of regions (see text).

Table 2.2.1-1. Slopes and intercepts of trends in frequency versus length of faults.

Region Number[1]		Region Name	Slope		Intercepts on X[2]	
			Subjective	Regression	Subjective	Regression
1		Arizona Mountain Belt	-1.82	-1.28	-0.10 (40)	-0.17 (34)
2		California Coast	-1.38	-1.28	+0.14 (69)	+0.10 (63)
3	*	Central Mississippi Valley	-2.00	-2.03	-0.35 (22)	-0.67 (11)
4	*	Circum-Gulf	-1.85	-1.68	-0.02 (48)	-0.09 (41)
5		Eastern Oregon-Western Idaho	-2.41	-1.77	+0.10 (63)	+0.16 (72)
6	*	Four Corners	-1.67	-1.40	-0.20 (32)	-0.25 (28)
7	*	Grand Canyon	-1.29	-0.93	-0.18 (33)	-0.11 (39)
8		Gulf Coast	-1.52	-0.92	+0.37 (117)	+0.53 (169)
9	*	Mexican Highland	-1.78	-1.37	-0.30 (25)	-0.34 (23)
10	*	Mid-Continent	-1.60	-0.69	-0.29 (26)	-0.25 (28)
11	*	Northeast	-1.82	-10.08	-0.26 (27)	-0.41 (19)
12		Northern Rockies	-1.85	-1.15	+0.06 (57)	+0.09 (62)
13		Oregon-Washington Coast	-2.09	-1.94	+0.12 (38)	-0.19 (32)
14	*	Pacific Interior	-1.70	-1.01	-0.11 (39)	-0.03 (47)
15	*	Paradox	-1.20	-1.04	-0.17 (34)	-0.25 (28)
16	*	Puget-Olympic	-1.28	-0.57	-0.19 (32)	-0.12 (38)
17		Rio Grande	-1.20	-0.93	+0.25 (89)	+0.17 (74)
18	*	Salton Trough	-1.48	-1.03	-0.08 (42)	-0.08 (42)
19	*	Snake River Plain	-2.50	-1.75	-0.36 (22)	-0.32 (24)
20	*	Sonoran	-1.72	-1.71	-0.60 (13)	-0.66 (11)
21	*	Southeast	-1.54	-3.37	-0.13 (37)	-0.27 (27)
22		Southern Calif. Borderland	-2.03	-1.48	-0.09 (46)	-0.06 (44)
23	*	Straits of Florida	-1.89	-1.19	+0.01 (51)	-0.08 (42)
24		Transverse Ranges-Tehachapi	-2.27	-1.61	-0.05 (45)	-0.09 (41)
25		Utah-Nevada	-2.24	-1.81	-0.03 (47)	-0.01 (49)
26		Walker Lane	-1.86	-1.77	+0.04 (55)	-0.01 (49)
27		Wasatch-Tetons	-1.90	-1.51	-0.04 (46)	-0.05 (45)
28		Western Mojave	-1.27	-1.03	+0.14 (69)	-0.63 (12)
29		Western Nevada	-2.16	-1.63	+0.04 (55)	-0.11 (39)
30		Wyoming	-1.13	-0.92	+0.09 (62)	-0.00 (50)

	All Data		Best Data		Worst Data	
	Subj.	Reg.	Subj.	Reg.	Subj.	Reg.
Mean values of slopes	1.75	1.70	1.81	1.40	1.69	1.99
Mean values (log) of X intercept	-0.08	-0.13	+0.05	-0.02	-0.22	-0.26
Mean of log lengths at unit frequency in km	42	37	56	48	30	27

1/ Asterisks indicate regions in which the data are sparse.
2/ Numbers in parentheses are fault lengths in kilometers at unit frequency.

Table 2.2.1.-2 Regions having absolute values of slope less than 1.5 in plots of log frequency versus log length (called low-slope group.)

Region Number[1/]		Region Name	Absolute value of slope Subjective	Regression
2		California Coast	1.38	1.28
7	*	Grand Canyon	1.29	0.93
15	*	Paradox	1.20	1.04
16	*	Puget-Olympic	1.28	0.57
17		Rio Grande	1.20	0.93
18	*	Salton Trough	1.48	1.03
28		Western Mojave	1.27	1.03
30		Wyoming	1.13	0.92

	All Data		Best Data		Worst Data	
	Subj.	Reg.	Subj.	Reg.	Subj.	Reg.
Mean values of slopes	1.28	0.97	1.25	1.04	1.31	0.89
Mean values (log) of X intercept	0	-0.12	+0.16	-0.09	-0.16	-0.14
Mean of log lengths at unit frequency in km	50	38	72	4I	34	36

[1/] Asterisks indicate regions with sparse data.

Table 2.2.1.-3 Regions having absolute values of slope greater than 1.5 in plots of log frequency versus log length (called high-slope group).

Region Number[1/]		Region Name	Absolute value of slope Subjective	Regression
1		Arizona Mountain Belt	1.82	1.28
3	*	Central Mississippi Valley	2.00	2.03
4	*	Circum-Gulf	1.85	1.68
5		Eastern Oregon-Western Idaho	2.41	1.77
6	*	Four Corners	1.67	1.40
8		Gulf Coast	1.52	0.92
9	*	Mexican Highland	1.78	1.37
10	*	Mid-continent	1.60	0.69
11	*	Northeast	1.82	10.08
12		Northern Rockies	1.85	1.15
13		Oregon-Washington Coast	2.09	1.94
14	*	Pacific Interior	1.70	1.01
19	*	Snake River Plain	2.50	1.75
20	*	Sonoran	1.72	1.71
21	*	Southeast	1.54	3.37
22		Southern Calif. Borderland	2.03	1.48
23	*	Straits of Florida	1.89	1.19
24		Transverse Ranges-Tehachapi	2.27	1.61
25		Utah-Nevada	2.24	1.81
26		Walker Lane	1.86	1.77
27		Wasatch-Tetons	1.90	1.51
29		Western Nevada	2.16	1.63

	All Data		Best Data		Worst Data	
	Subj.	Reg.	Subj.	Reg.	Subj.	Reg.
Mean values of slopes	1.92	1.96	2.05	1.55	1.76	2.45
Mean values (log) of X intercept	-0.11	-0.14	-0.015	+0.028	-0.23	-0.31
Mean of log lengths at unit frequency in km	39	36	48	53	29	24

[1/] Asterisks indicate regions with sparse data.

Table 2.2.1.-4 Absolute values of slopes for subset of 7 Regions.

Region Number[1/]		Region Name	Absolute value of slope Subjective	Regression
15	*	Paradox	1.20	1.04
16	*	Puget-Olympic	1.28	0.57
17		Rio Grande	1.20	0.93
18	*	Salton Trough	1.48	1.03
22		Southern Calif. Borderland	2.03	1.48
24		Transverse Ranges-Tehachapi	2.27	1.61
26		Walker Lane	1.86	1.77

	All Data		Best Data		Worst Data	
	Subj.	Reg.	Subj.	Reg.	Subj.	Reg.
Mean values of slopes	1.62	1.20	1.84	1.45	1.32	0.88
Mean values (log) of X intercept	-0.04	-0.05	+0.04	+0.002	-0.15	-0.15
Mean of log lengths at unit frequency in km	46	45	55	50	36	36

[1/] Asterisks indicate regions with sparse data.

Table 2.2.1.-5 Subset of regions showing convergence in composite diagram of subjective trends (figure 2.2.1.-4).

Region[1/] Number		Region Name	Absolute value of slope Subjective	Regression
("Convergent" Group)				
2		California Coast	1.38	1.28
12		Northern Rockies	1.85	1.15
13		Oregon-Washington Coast	2.09	1.94
17		Rio Grande	1.20	0.93
23	*	Straits of Florida	1.89	1.19
24		Transverse Ranges-Tehachapi	2.27	1.61
25		Utah-Nevada	2.24	1.81
26		Walker Lane	1.86	1.77
28		Western Mojave	1.27	1.03
("Parallel" Group)				
4	*	Circum-Gulf	1.85	1.68
22		Southern Calif. Borderland	2.03	1.48
27		Wasatch-Tetons	1.90	1.51
29		Western Nevada	2.16	1.63

	All Data		"Convergent"		"Parallel"	
	Subj.	Reg.	Subj.	Reg.	Subj.	Reg.
Mean values of slopes	1.85	1.46	1.78	1.41	1.99	1.58
Mean values (log) of X intercept	+0.03	-0.06	+0.05	-0.07	-0.03	+0.02
Mean (log) length at unit frequency (km)	53	44	56	42	47	48

[1/] Asterisks indicate regions with sparse data.

2.2.2 Frequency Functions; Subdivided by Age of Latest Movement

Table 2.2.2.-1 gives the slopes and intercepts for the United States data by age group according to the various categories identified in the previous section. The subcategories broken down by age involve: (a) regions having low overall slopes; (b) regions having high overall slopes; (c) the "7 Regions" subset; (d) regions with convergent trends; (e) regions with parallel trends; (f) L. A. Area subset. Table 2.2.2.-2 gives the breakdown for those individual regions having enough data in two or more age groups.

The data in Tables 2.2.2.-1 and 2.2.2.-2 are based on the distributions broken down by age category in the following series of diagrams:

Figure 2.2.2.-1. Length-frequency distributions by age for all of the conterminous U.S.

Figure 2.2.2.-2. Length-frequency distributions by age for the 7 Regions.

Figure 2.2.2.-3. Length-frequency distributions by age for the U.S. with the 7 Regions subtracted.

Figure 2.2.2.-4. Length-frequency distributions by age for the regions of lowest slope.

Figure 2.2.2.-5. Length-frequency distributions by age for the U.S. with regions of low slope subtracted.

Figure 2.2.2.-6. Length-frequency distributions by age for the "convergent group."

Figure 2.2.2.-7. Length-frequency distributions by age for the "parallel group."

Figure 2.2.2.-8. Length-frequency distributions by age for sum of convergent and parallel groups.

Figure 2.2.2.-9. Length-frequency distributions by age for the Los Angeles Area.

Figure 2.2.2.-10. Length-frequency distributions by age for individual regions (regions omitted have insufficient numbers to attempt fitting a trend, and many of those shown have poor control).

Figure 2.2.2.-11 summarizes the variations in slope versus age of latest motions. There are trends that we can point to, equivocally, and there appear to be fluctuations in time that are statistically significant. The variations as a whole suggest that most often slopes have

decreased at the younger ages; for the United States as a whole this decrease appears to have been almost continuous over the latest 2 m.y. The decrease could reflect the way sampling is biased in different age groups, but we think the trends and fluctuations are significant.

If the variations of slopes with age of movement are real, the implications are the following: A decrease in the absolute slope with time means that the number of movements on the shorter faults are decreased relative to the longer faults. This could happen by decreased activity on the shorter faults, increased activity on the longer faults, or by coalescence among sets of shorter faults to form longer faults. Conversely, higher absolute slopes with time imply increased activity of the shorter relative to the longer faults. This could mean deactivation on the longer faults, or the possible creation of entirely new sets of shorter faults. Fluctuations in the data, of course, reflect the time dependence among these ratios. In order to resolve such issues we will need to obtain histories for movement on specific fault sets in addition to more detailed data on the ages of latest movement.

Although these interpretations are unsubstantiated, the implications are theoretically intriguing, and we will refer to them again later relative to the implications of some published laboratory experiments on fracture growth in metal fatigue tests.

Figure 2.2.2.-12 gives compilations by age group for the regression lines of length versus age in all the different groups of regions and the U. S. overall. This gives another view of the slope progressions with age. The fact that the numbers for the subsets sometimes exceed the U. S. total indicates that there is a systematic underestimate of the shorter lengths in the regressions for the total U. S. This is because the overall regressions average the data for the low-slope and high-slope groups; the "parallel" group resembles the "high slope" group (30 regions - low slope group; (see Figure 2.2.2.-1, Figures 2.2.2.-5, and Figure 2.2.2.-7).

SECTION 2.2.2. FIGURES AND TABLES

FREQUENCY, LENGTH OF FAULTS (FOR ALL U. S.)

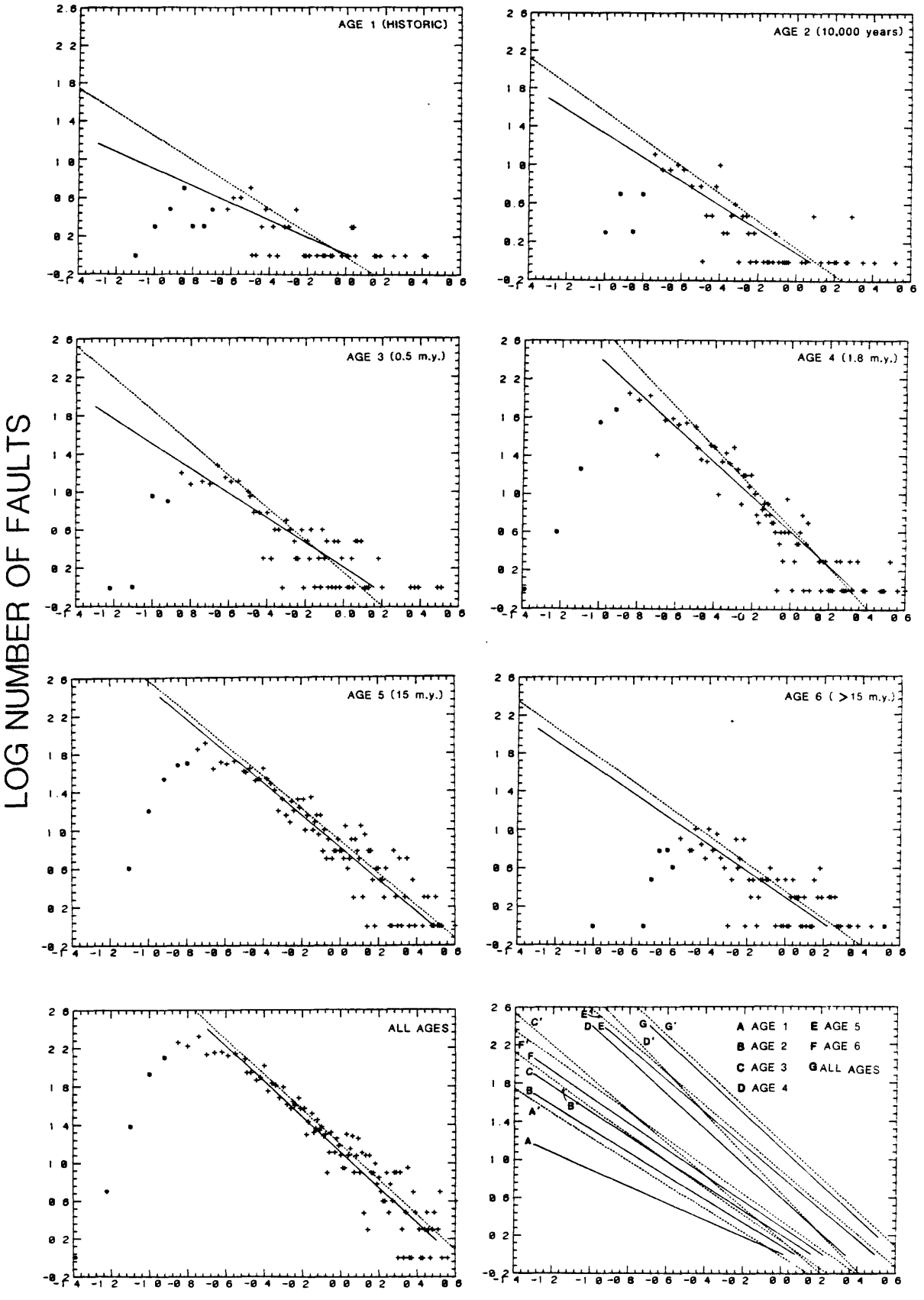

Figure 2.2.2.-1. LOG LENGTH (CM); SCALE 1:5,000,000

Logarithmic data for number versus fault length subdivided by age category; summations for all regions in the conterminous United States.

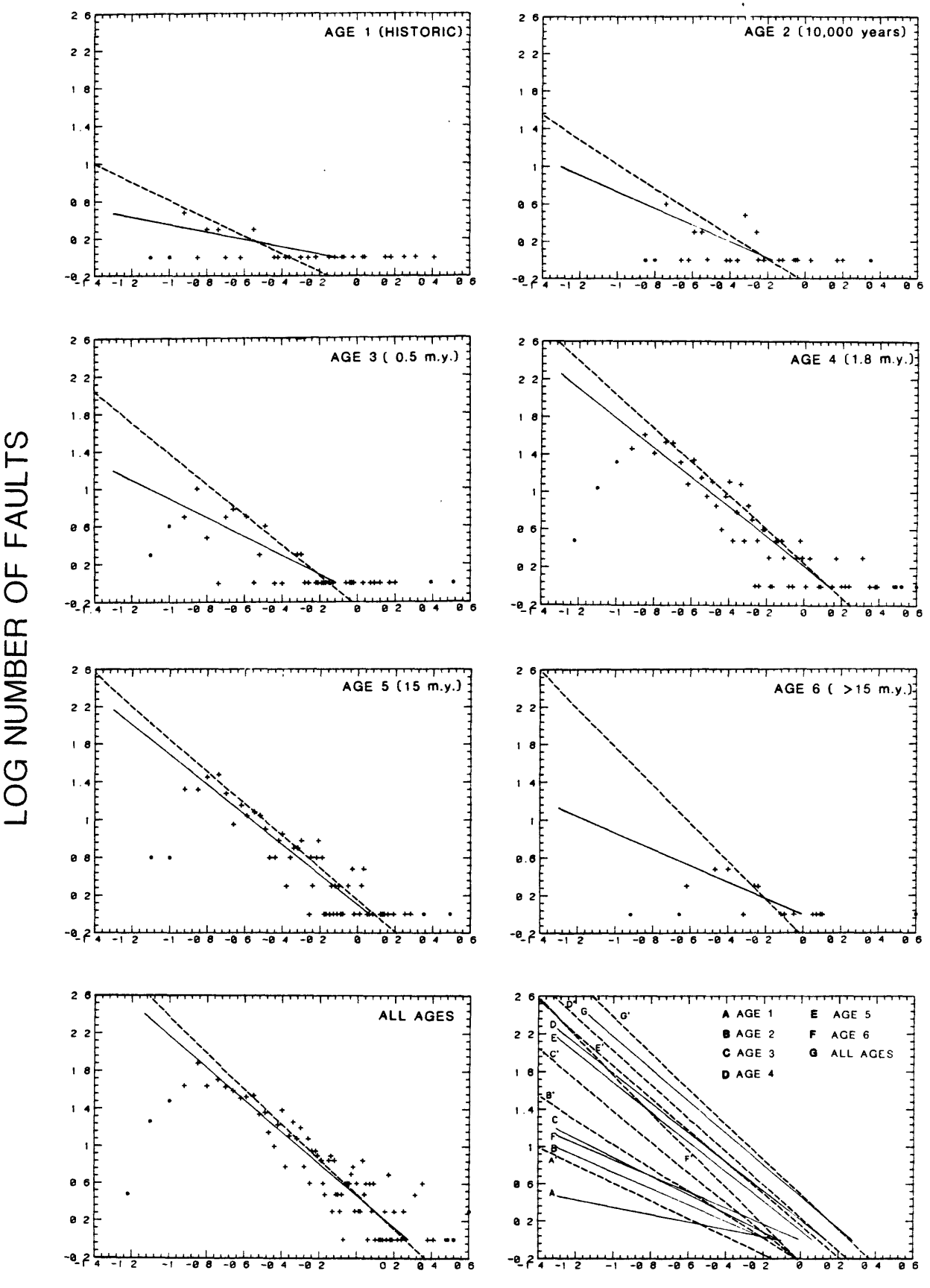

Figure 2.2.2.-2.

99 Logarithmic data for number versus fault length subdivided by age category; summations for data in the "7 Regions."

FREQUENCY, LENGTH OF FAULTS (ALL U.S. - 7 REGIONS)

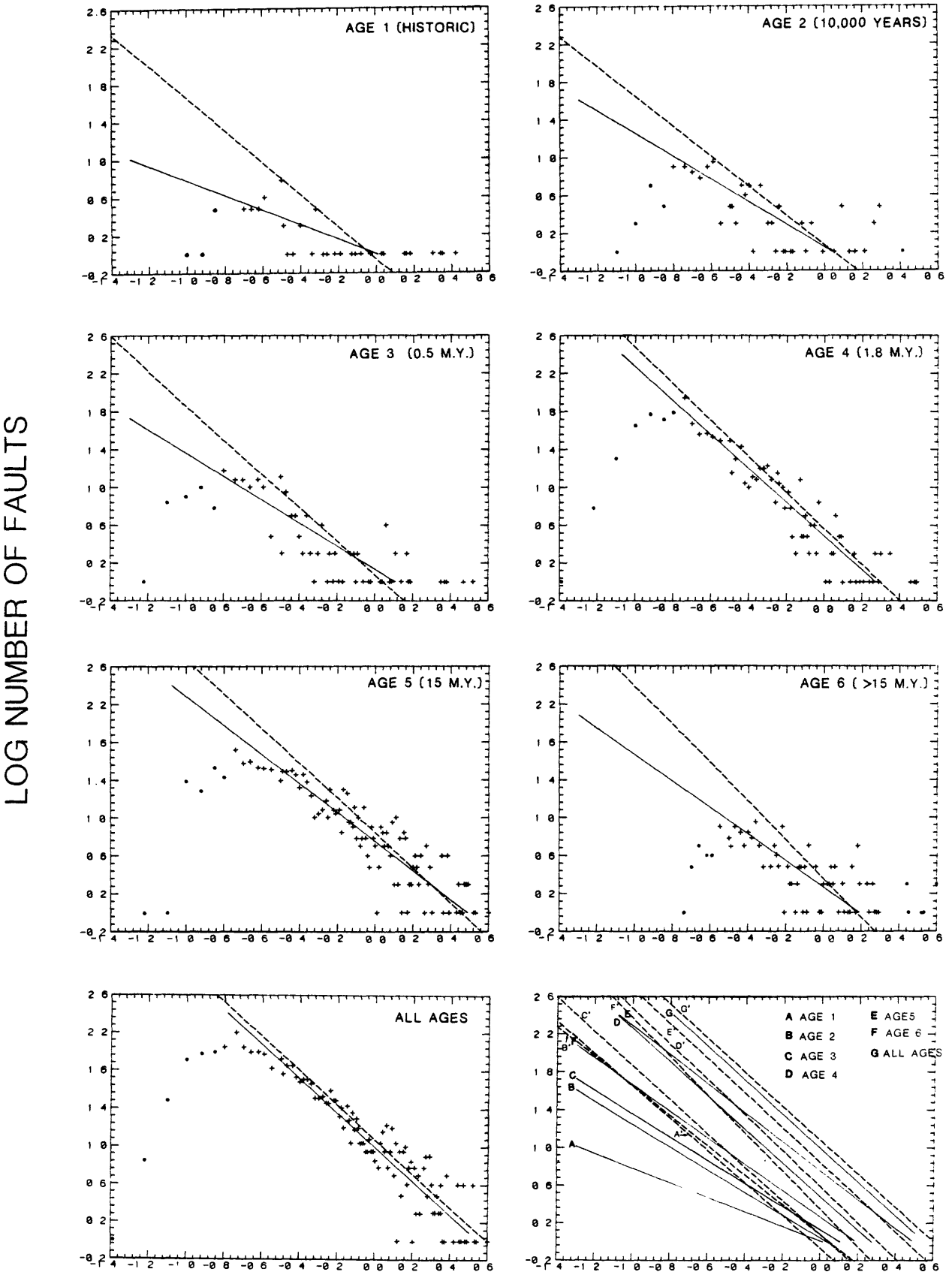

Figure 2.2.2.-3. LOG LENGTH (CM) : SCALE 1:5,000,000

Logarithmic data for number versus fault length subdivided by age category; summations for all U. S. minus "7 Regions."

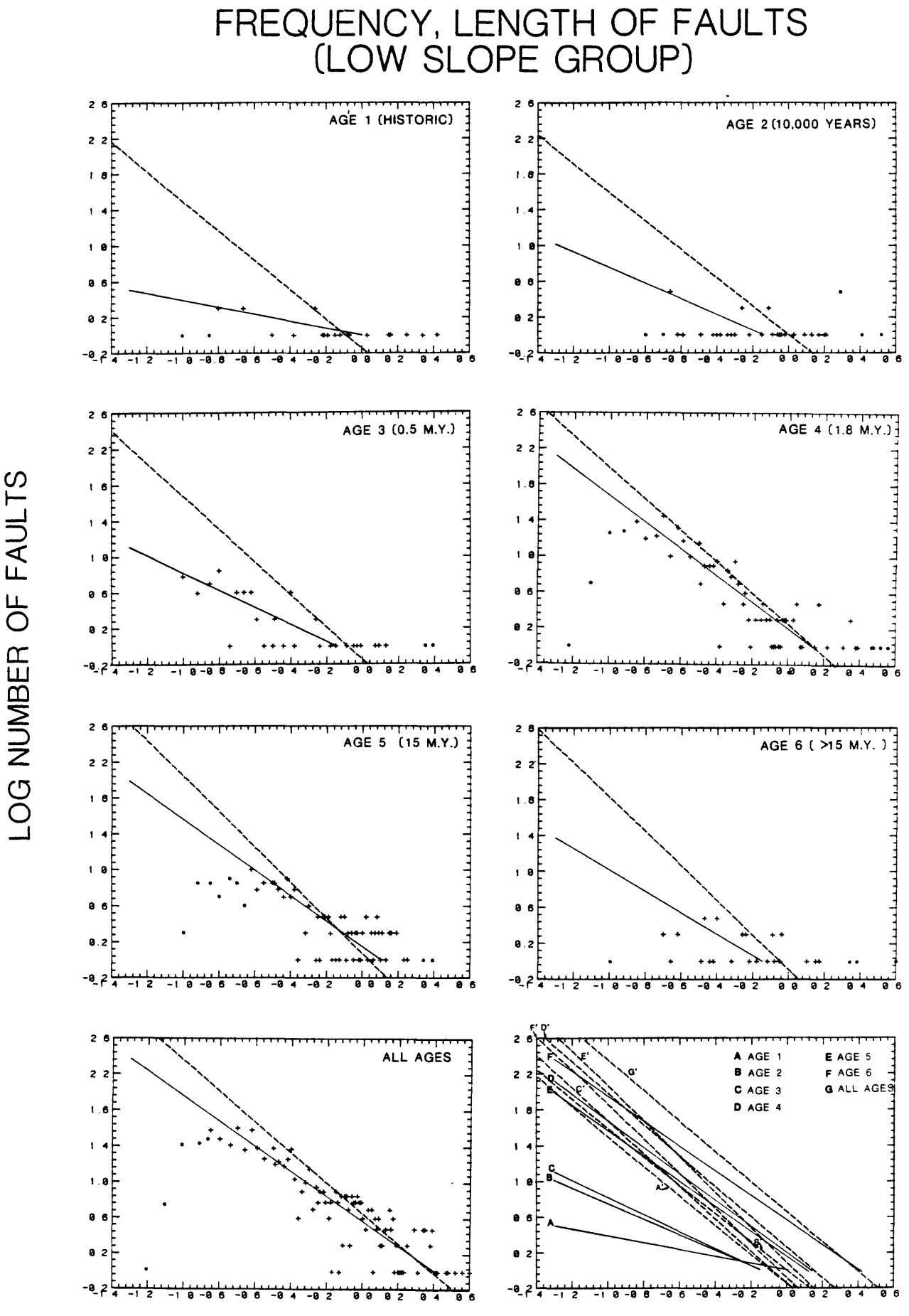

Figure 2.2.2.-4.

101 Logarithmic data for number versus fault length subdivided by age category; summations for data in the "low slope" group.

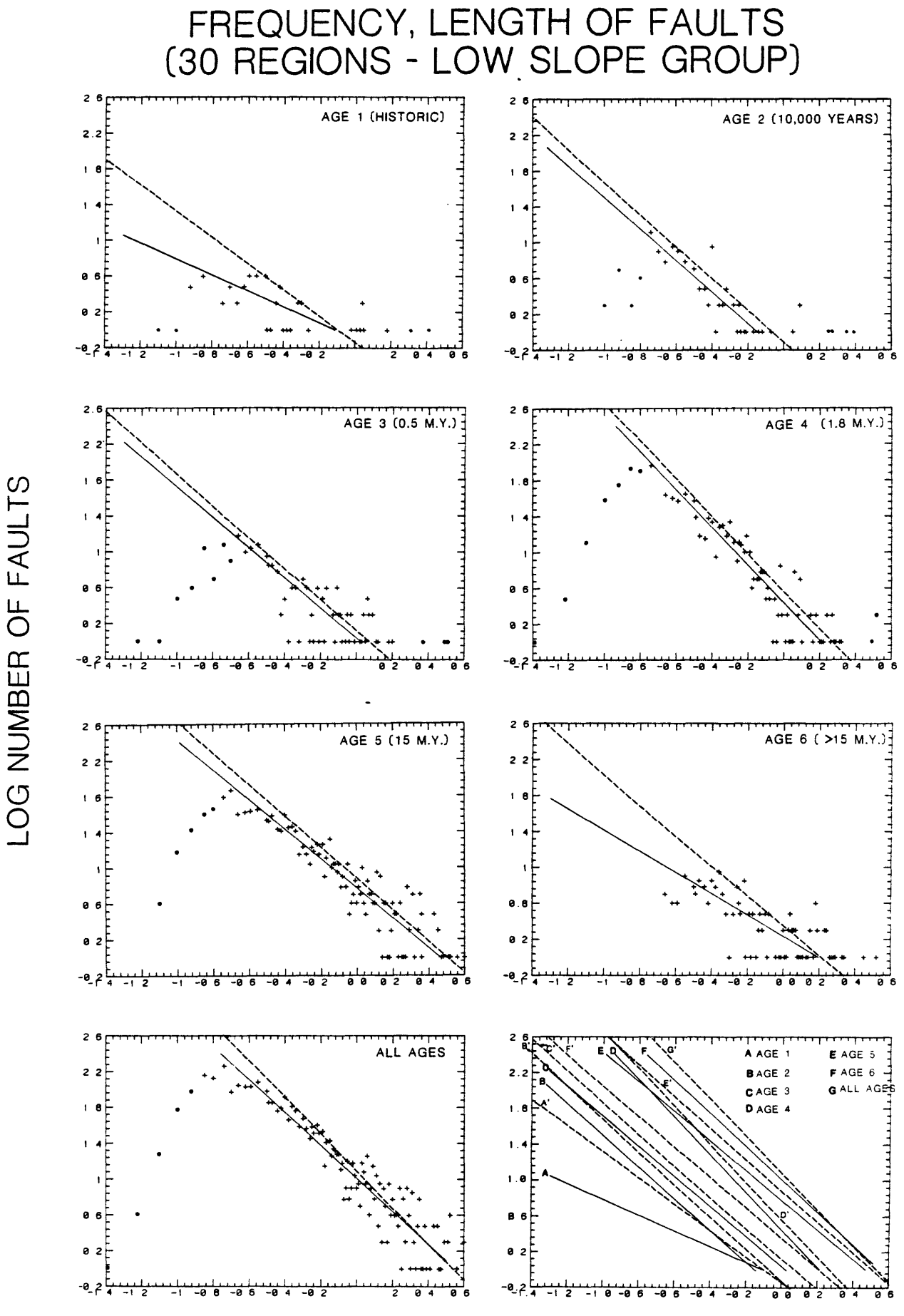

Figure 2.2.2.-5.

Logarithmic data for number versus fault length subdivided by age category; summations for all U. S. minus "low slope" group.

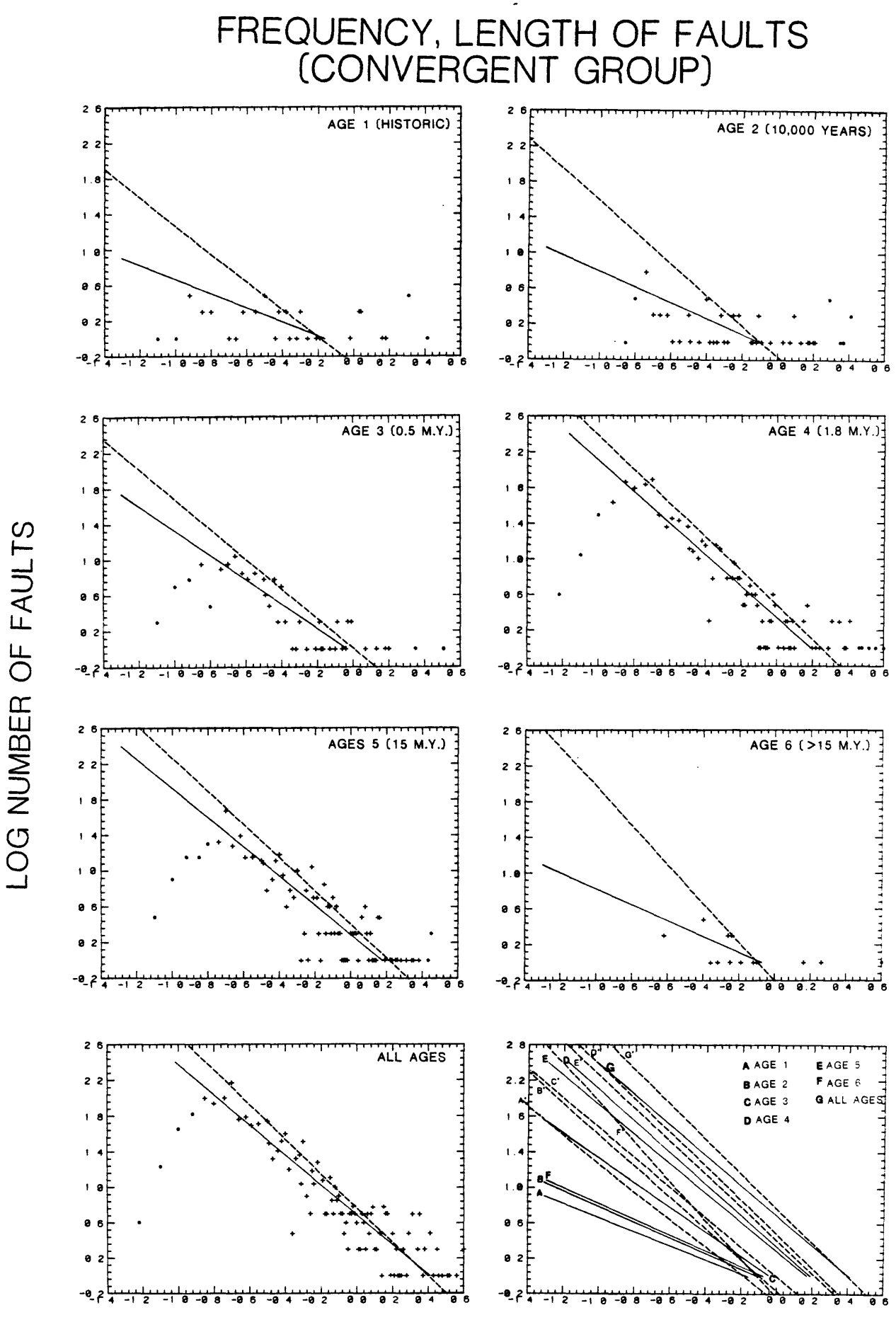

Figure 2.2.2.-6

 Logarithmic data for number versus fault length subdivided by age category; summations for data in the "convergent" group.

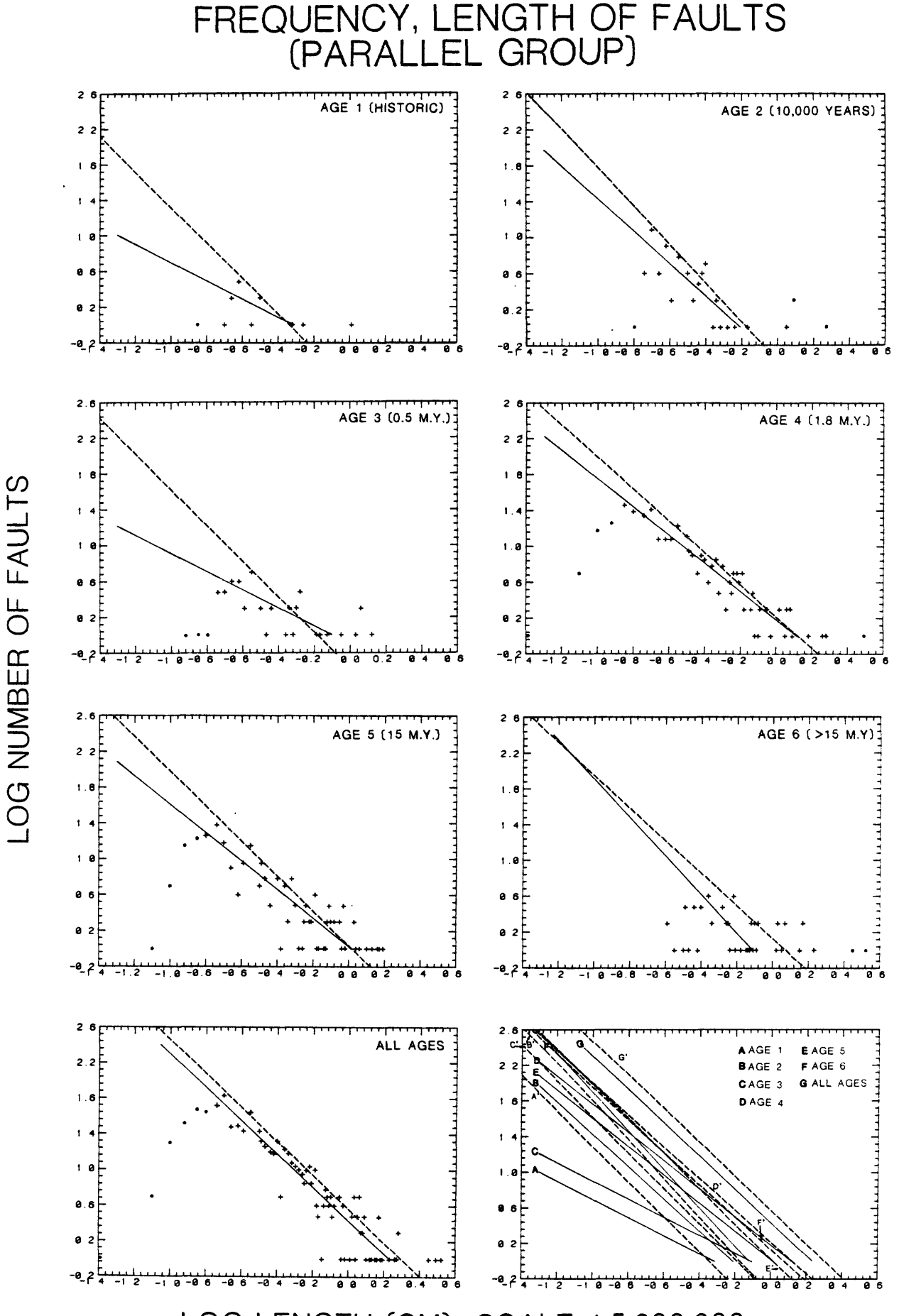

Figure 2.2.2.-7

Logarithmic data for number versus fault length subdivided by age category; summations for data in the "parallel" group.

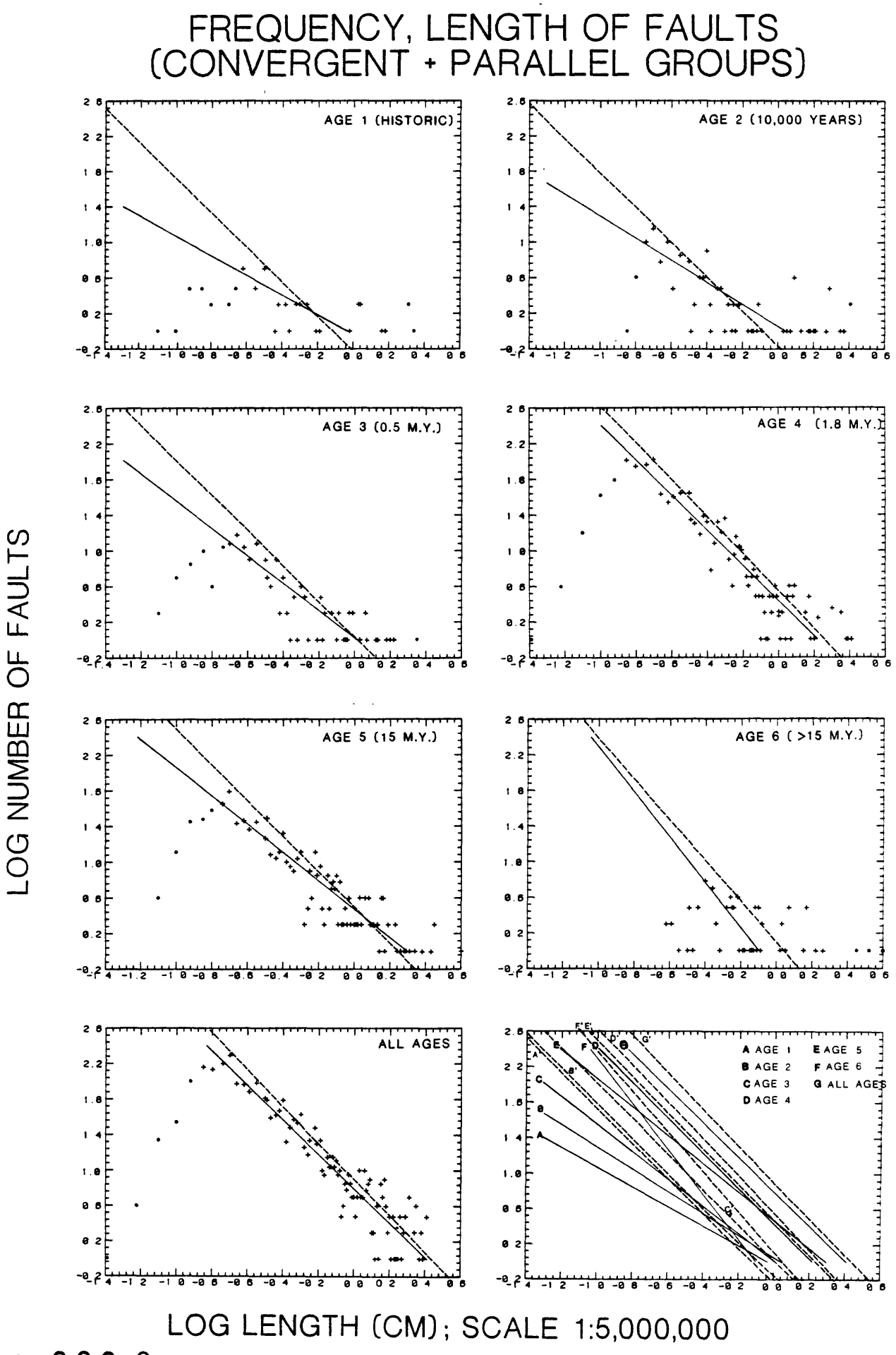

Figure 2.2.2.-8.

105 Logarithmic data for number versus fault length subdivided by age category; summations for data in the "convergent" plus "parallel" groups.

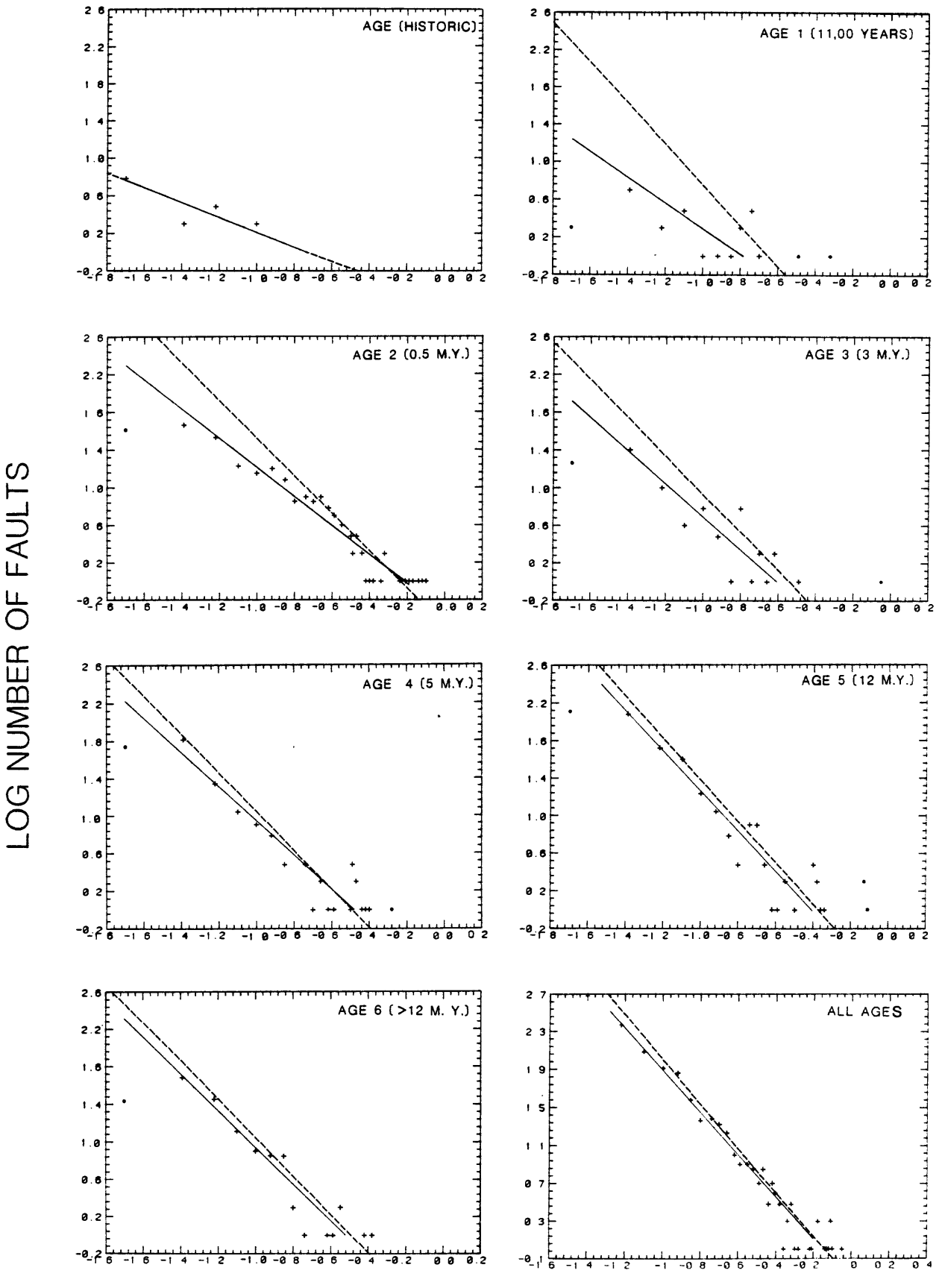

Figure 2.2.2.-9

Logarithmic data for number versus fault length subdivided by age category; summations for data in the L. A. Area.

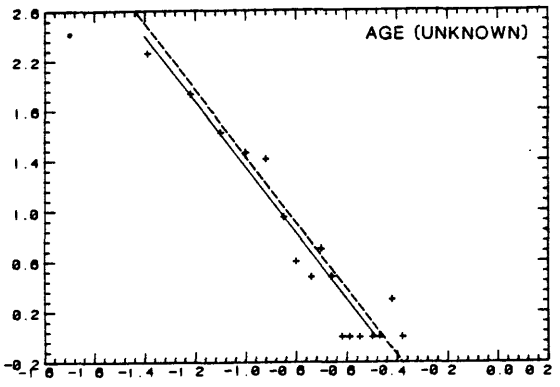
AGE (UNKNOWN)

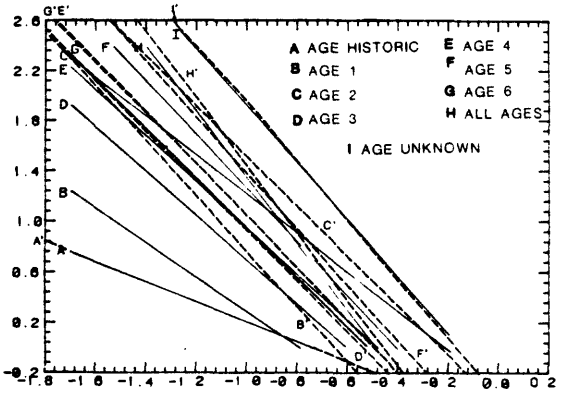
A AGE HISTORIC
B AGE 1
C AGE 2
D AGE 3
E AGE 4
F AGE 5
G AGE 6
H ALL AGES
I AGE UNKNOWN

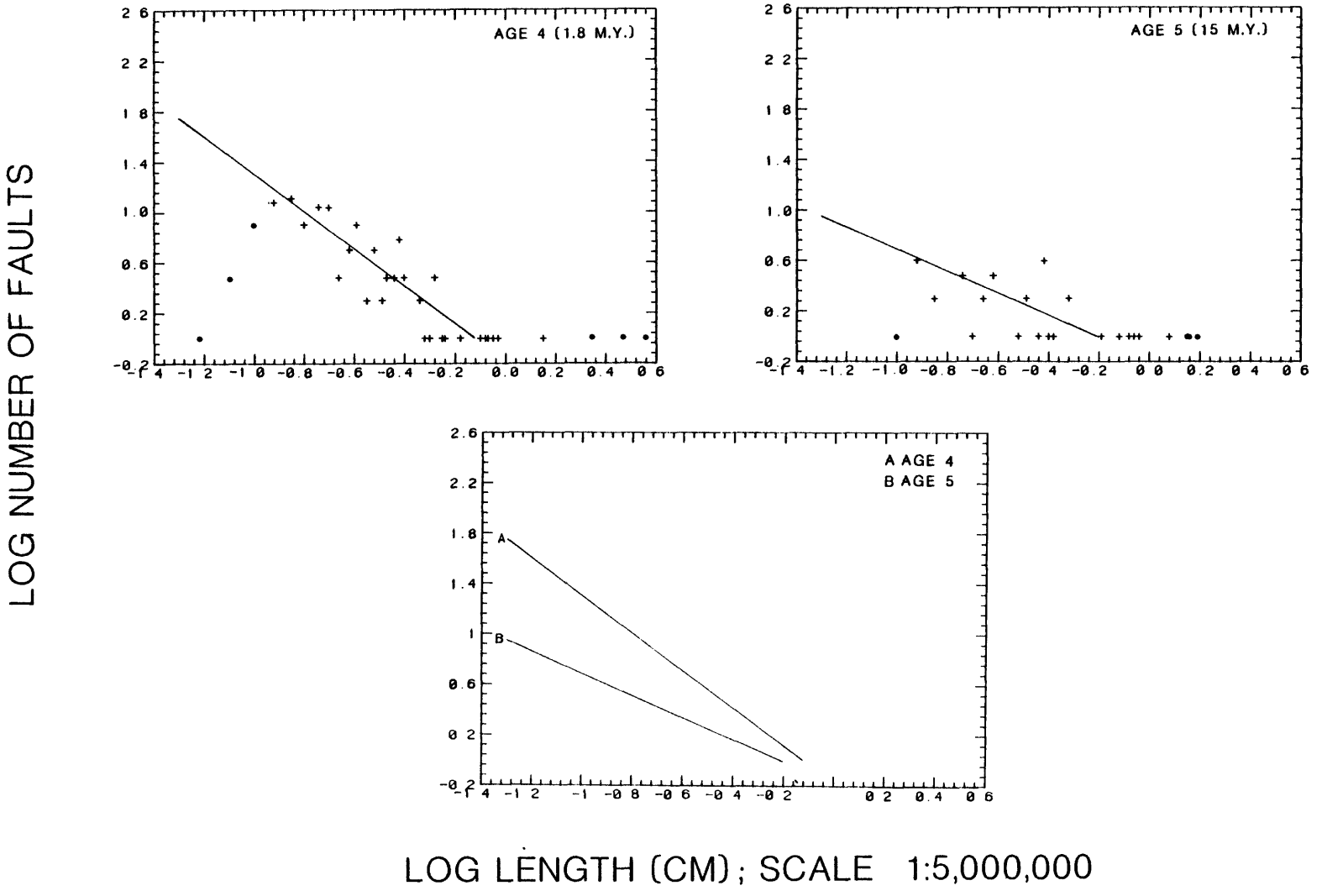

Figure 2.2.2.-10. (2)

Logarithmic data for number versus fault length subdivided by age category; A-E composite showing slopes for regions with data for each age category (dashed line is all U. S. data in that age category).

FREQUENCY, LENGTH OF FAULTS E. OREGON/W. IDAHO

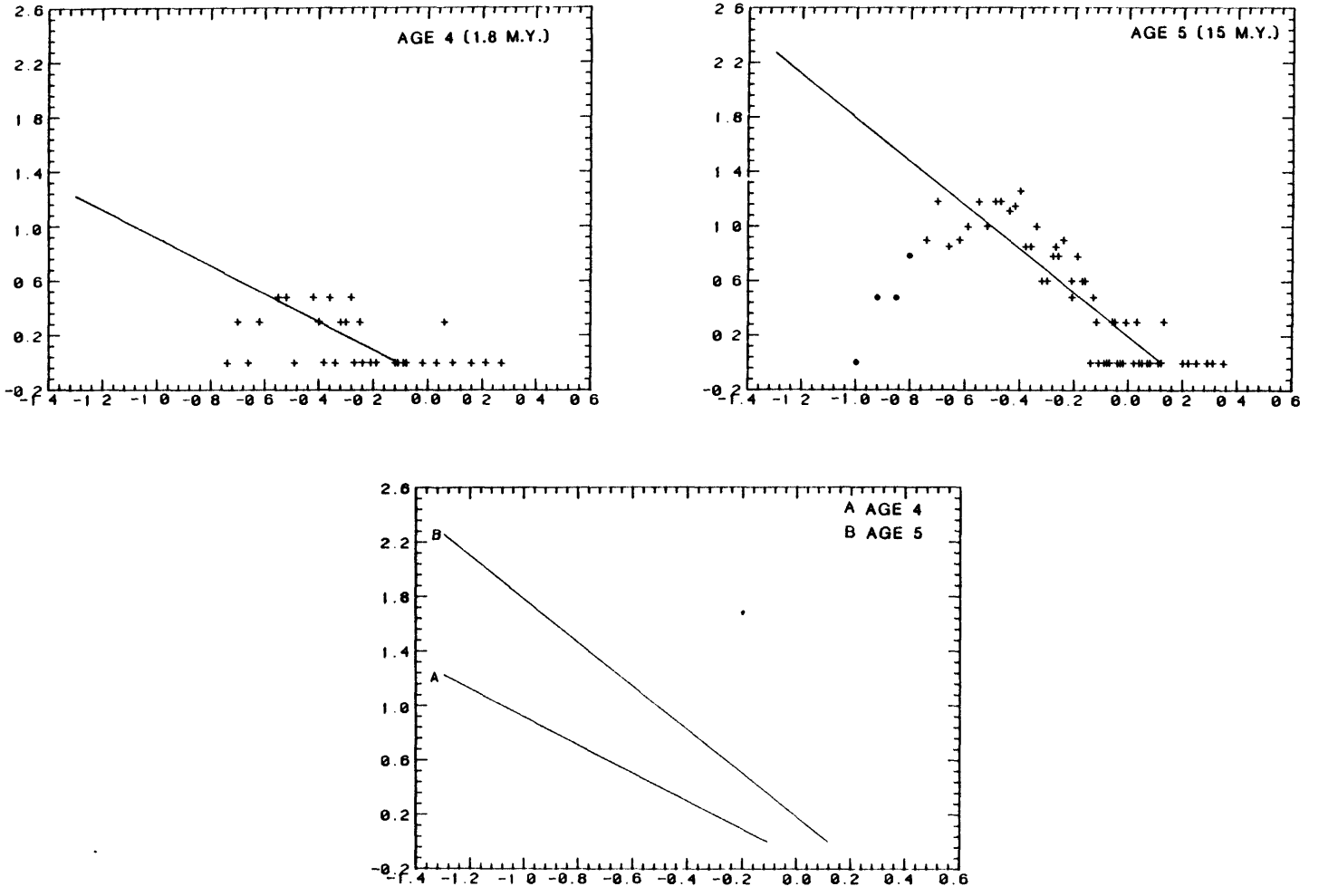

Figure 2.2.2.-10. (5)

FREQUENCY, LENGTH OF FAULTS GULF COAST

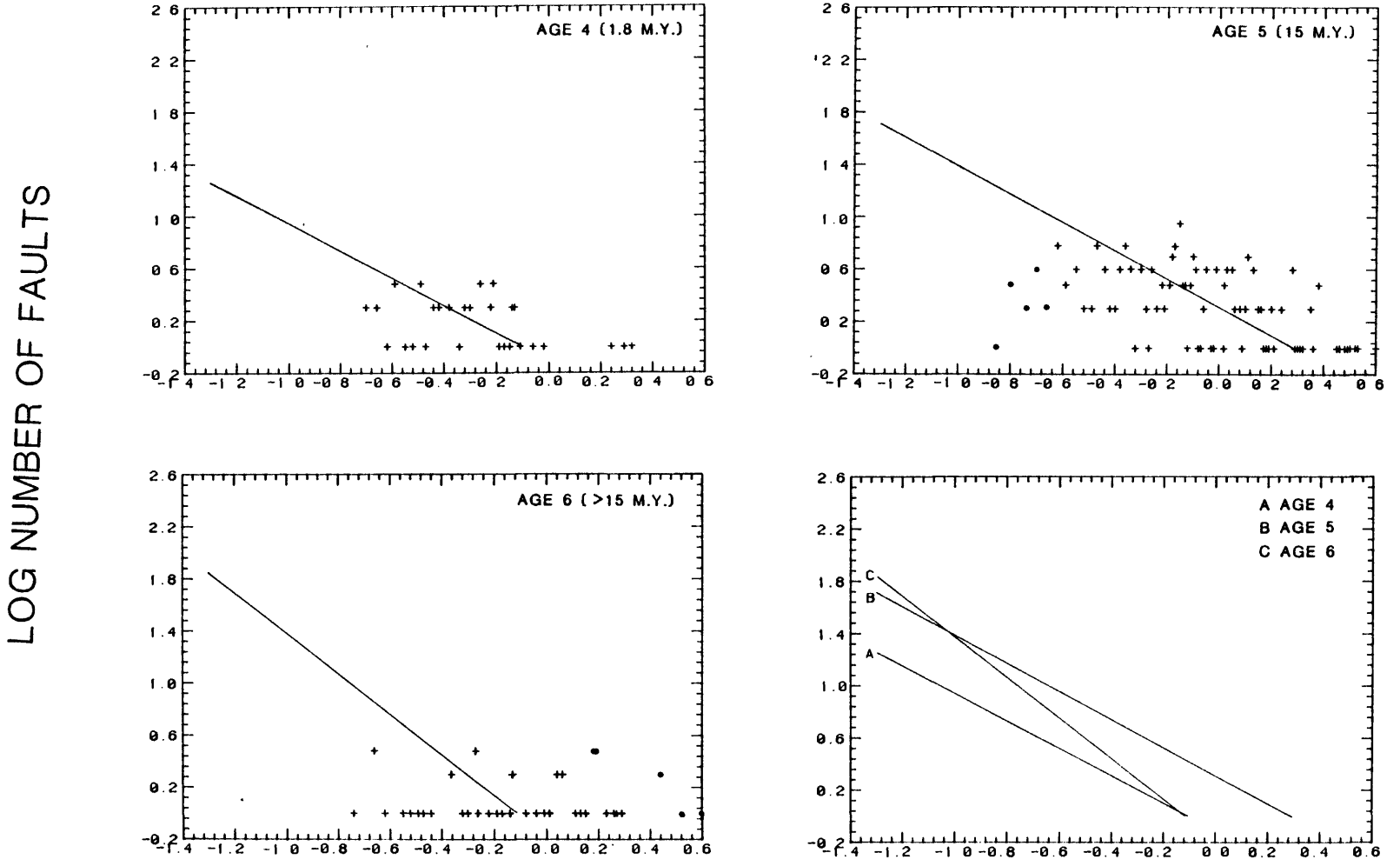

Figure 2.2.2.-10. (8)

FREQUENCY, LENGTH OF FAULTS NORTHERN ROCKIES

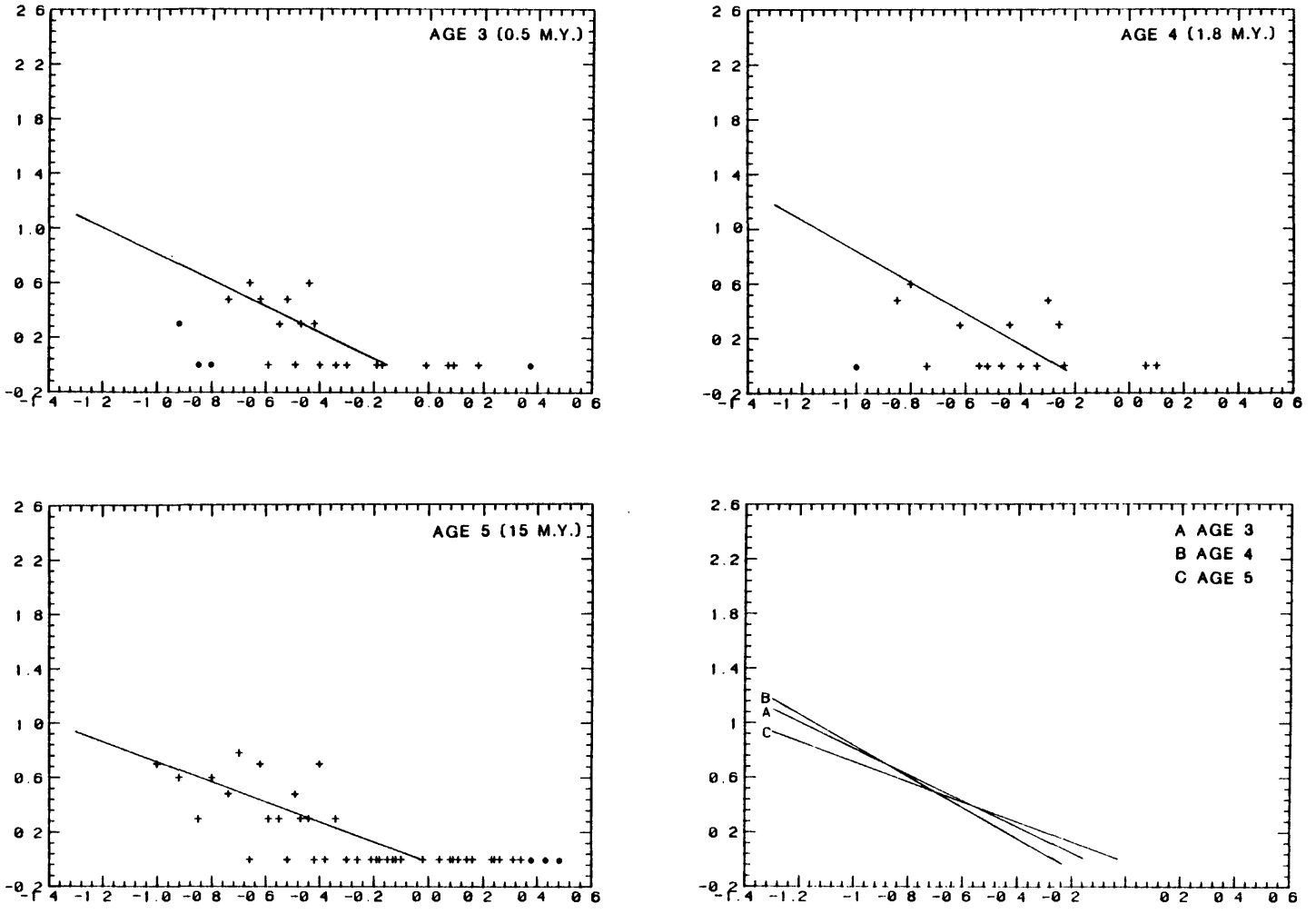

Figure 2.2.2.-10. (12)

FREQUENCY, LENGTH OF FAULTS OREGON/WASHINGTON COAST

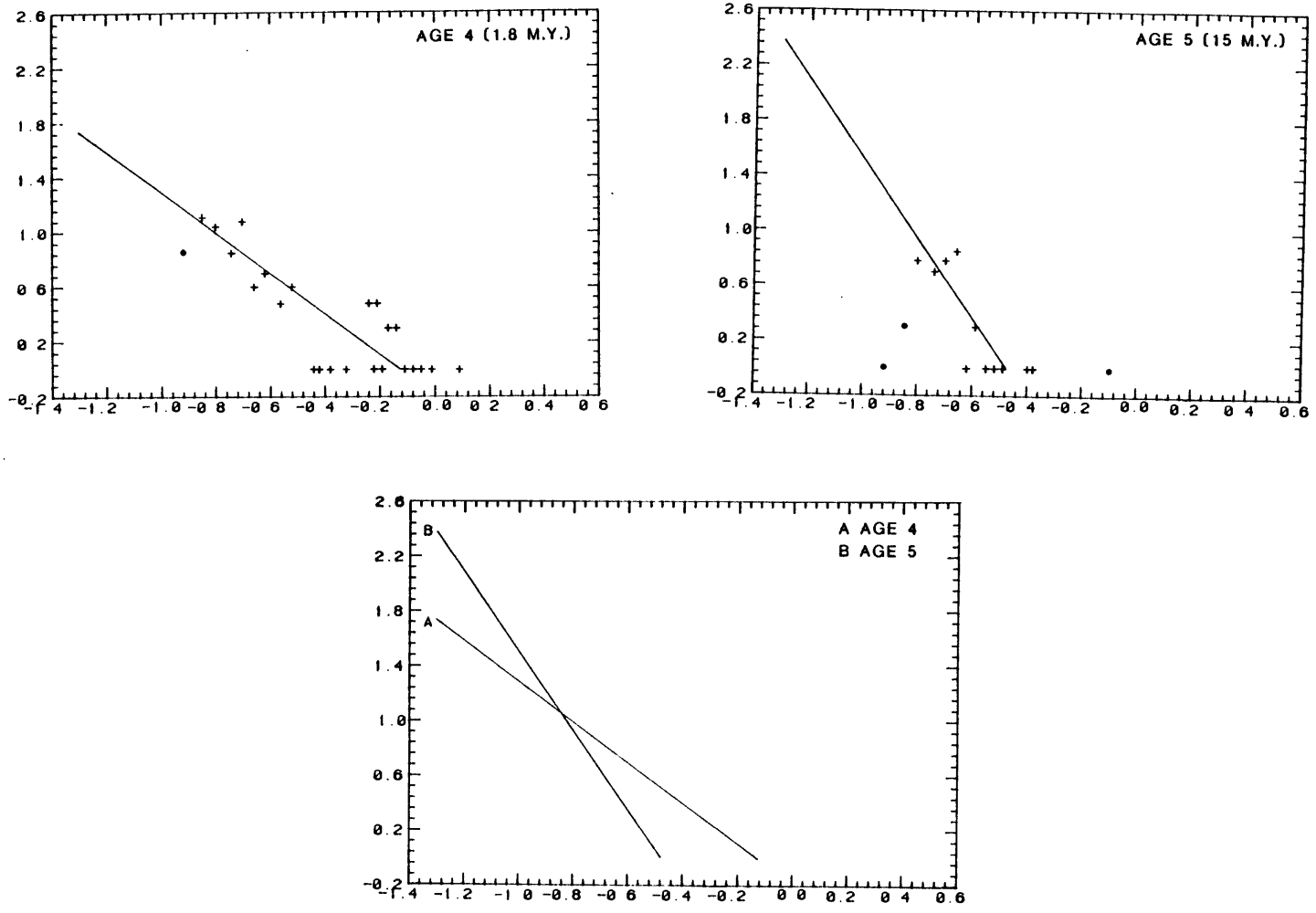

Figure 2.2.2.-10.(13)

FREQUENCY, LENGTH OF FAULTS RIO GRANDE

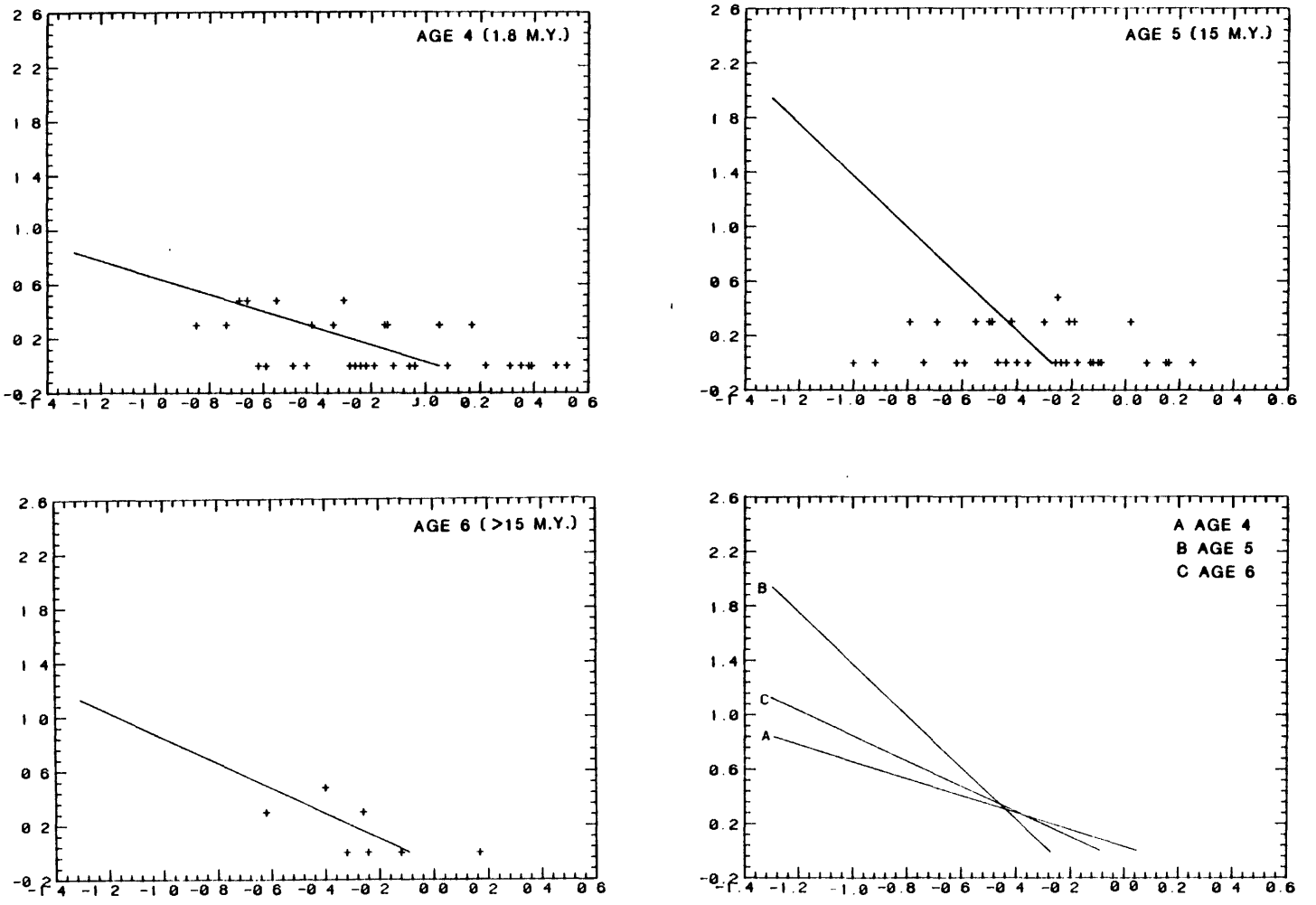

Figure 2.2.2.-10. (17)

FREQUENCY, LENGTH OF FAULTS SNAKE RIVER PLAIN

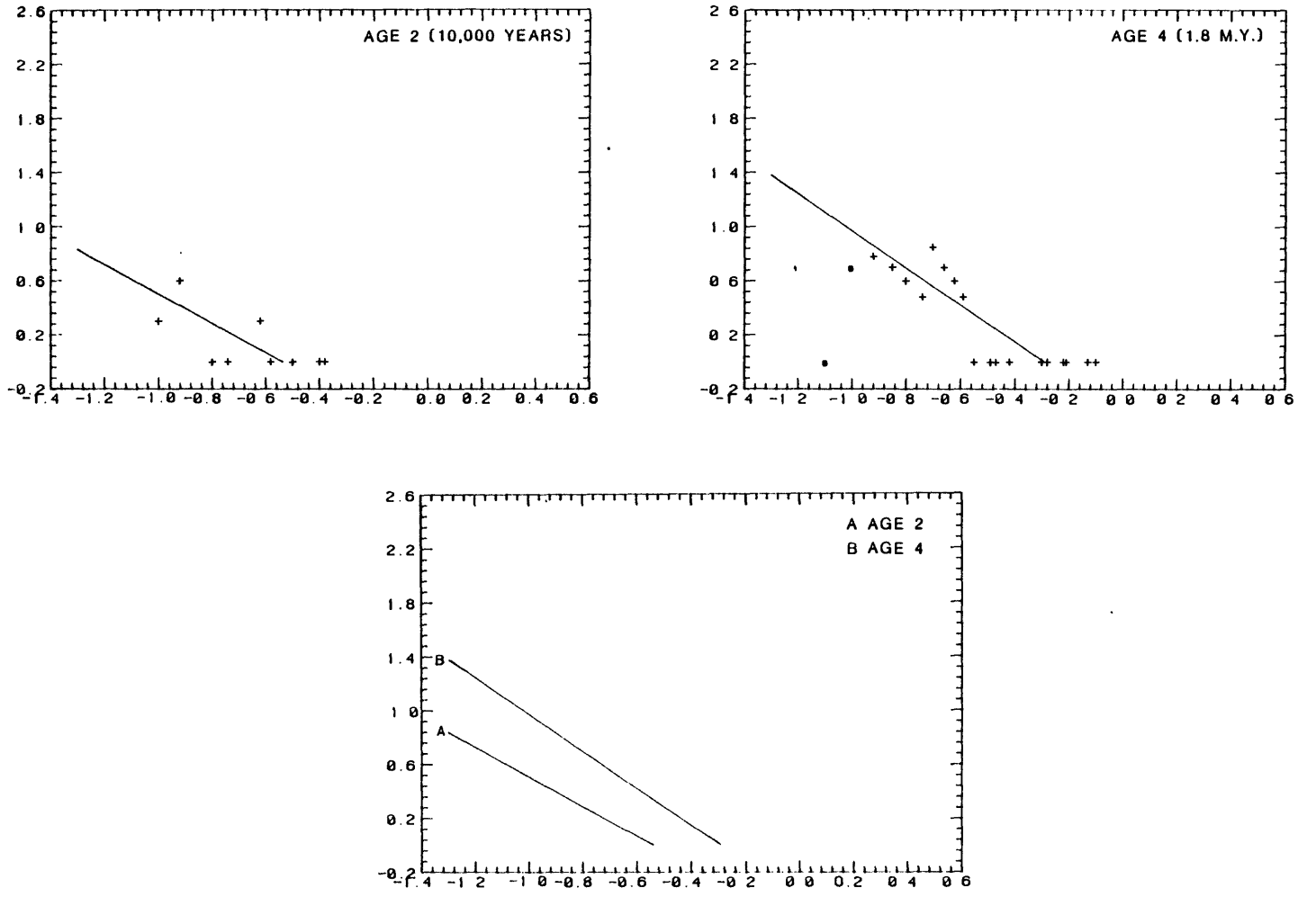

Figure 2.2.2.-10. (19)

FREQUENCY, LENGTH OF FAULTS SO. CALIFORNIA BORDERLAND

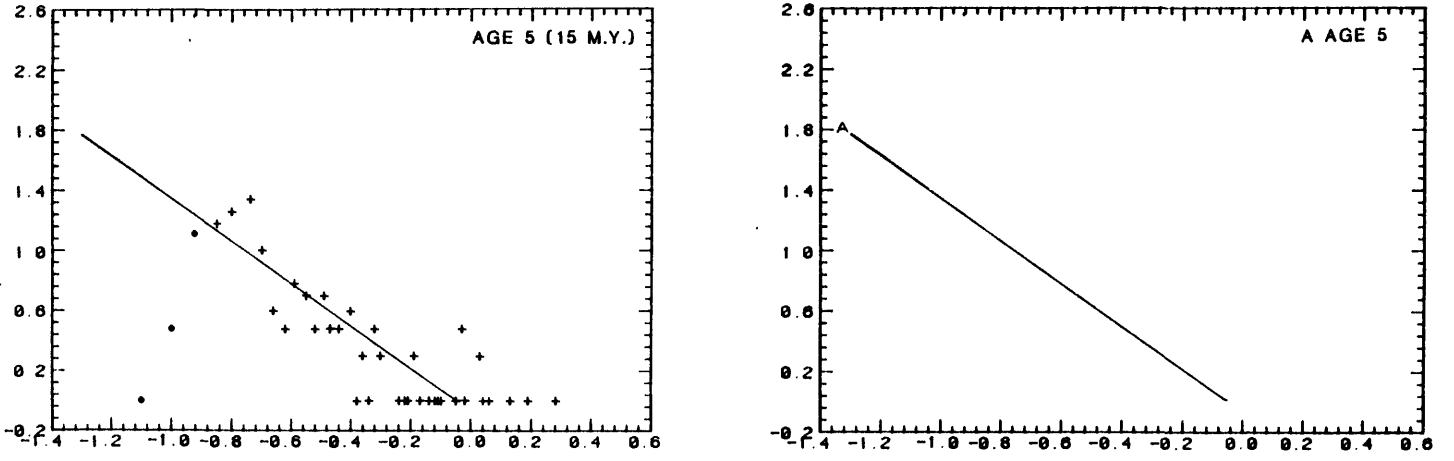

Figure 2.2.2.-10. (22)

FREQUENCY, LENGTH OF FAULTS TRANSVERSE RANGES TEHACHAPI

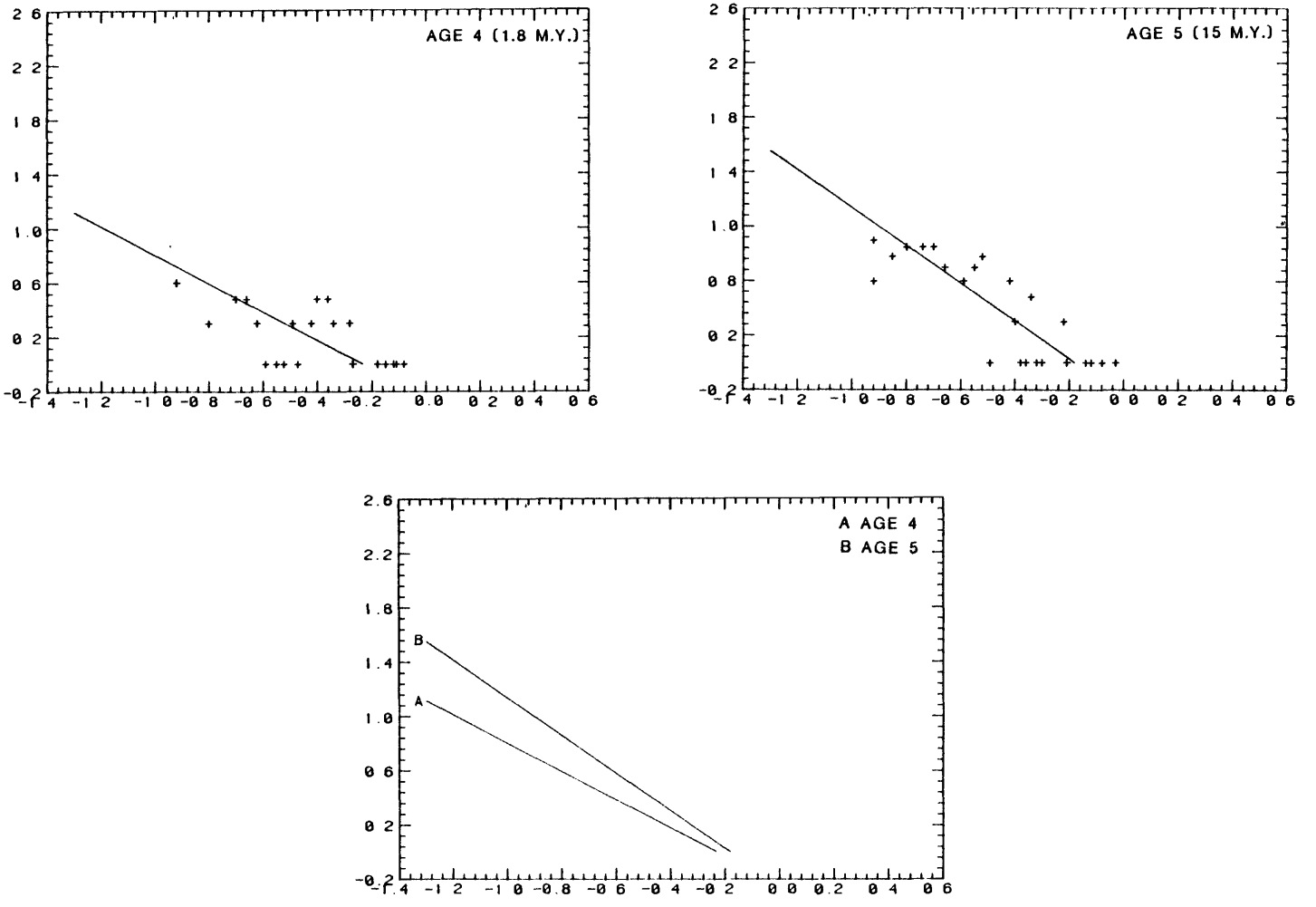

Figure 2.2.2.-10. (24)

FREQUENCY, LENGTH OF FAULTS UTAH-NEVADA

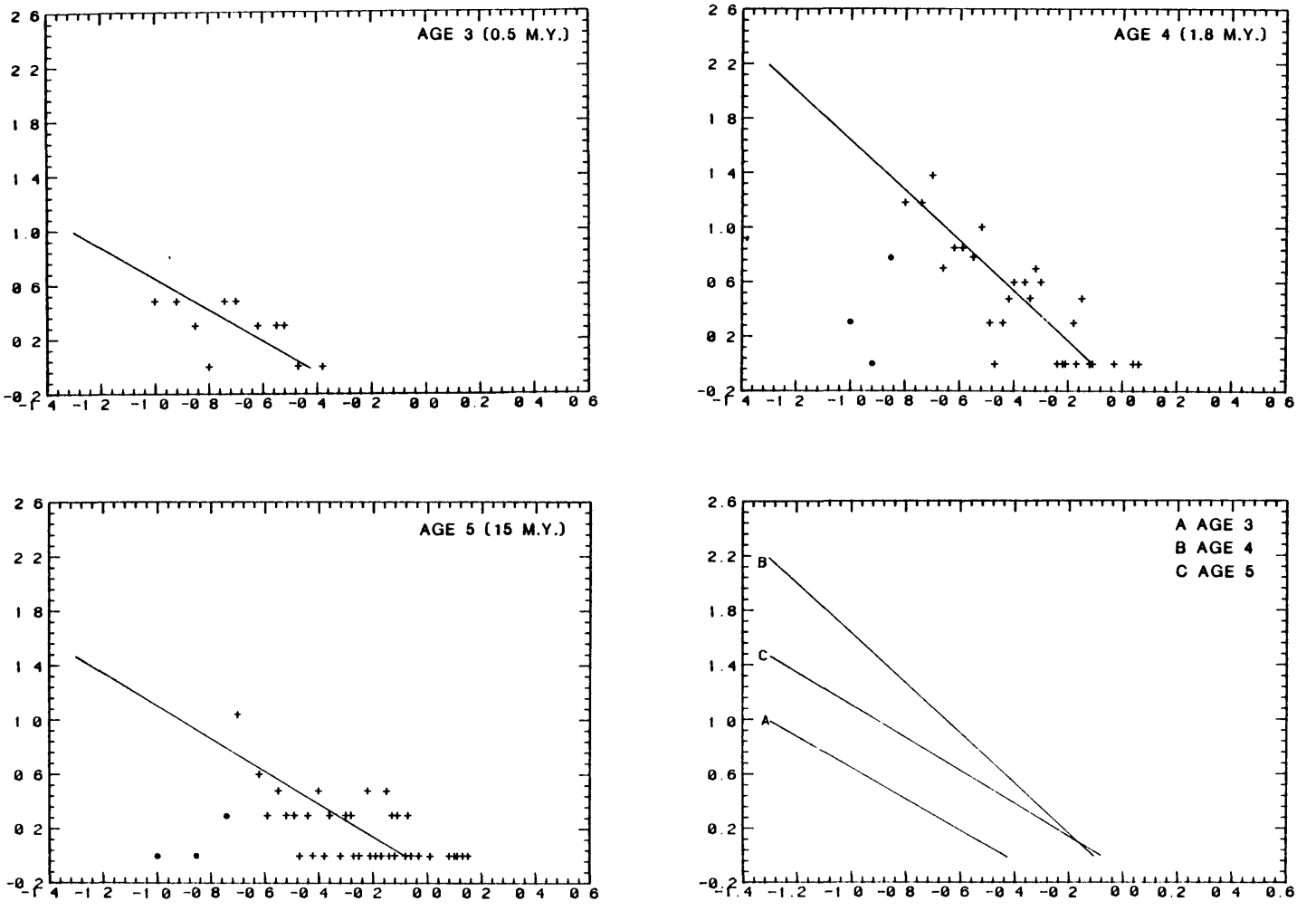

Figure 2.2.2.-10. (25)

FREQUENCY, LENGTH OF FAULTS WALKER LANE

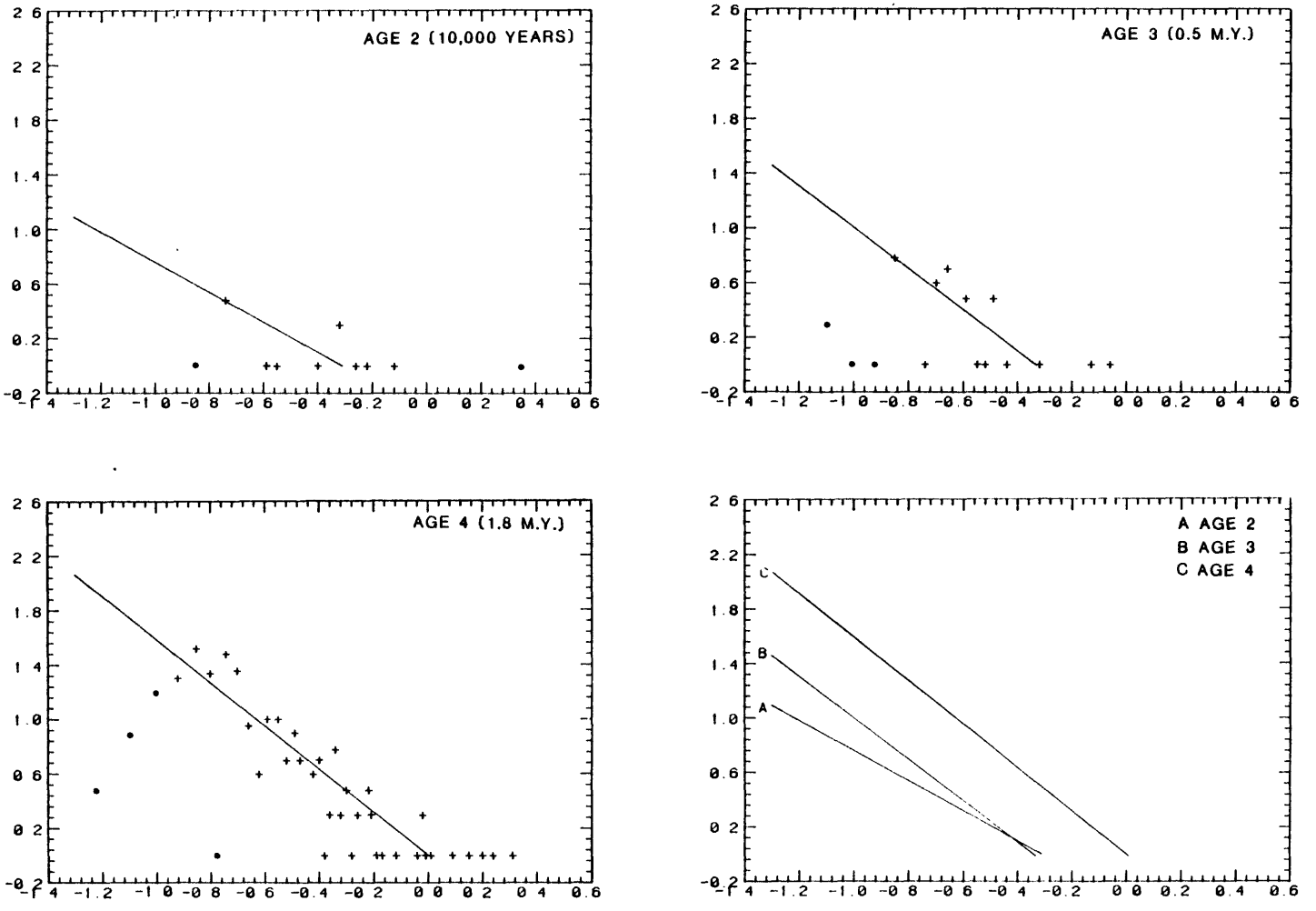

Figure 2.2.2.-10. (26)

FREQUENCY, LENGTH OF FAULTS WASATCH-TETON

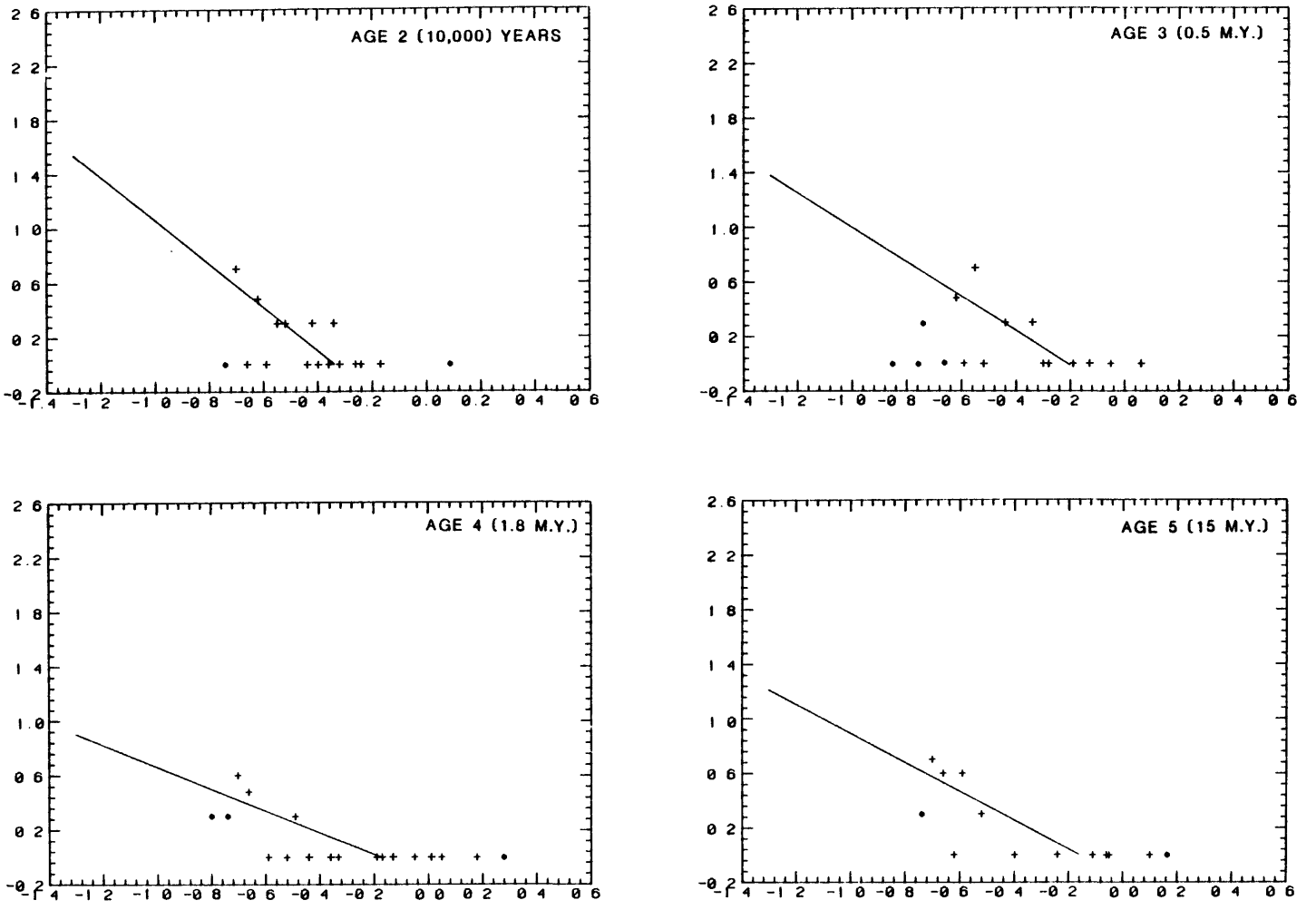

Figure 2.2.2.-10. (27)

FREQUENCY, LENGTH OF FAULTS WASATCH-TETON

LOG NUMBER OF FAULTS

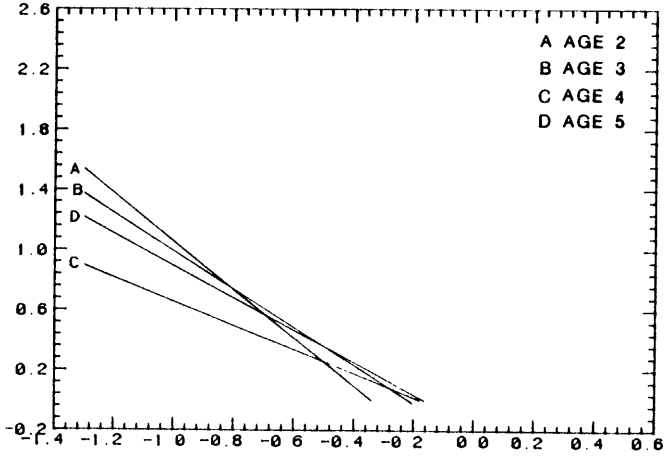

LOG LENGTH (CM); SCALE 1:5,000,000

FREQUENCY, LENGTH OF FAULTS WESTERN NEVADA

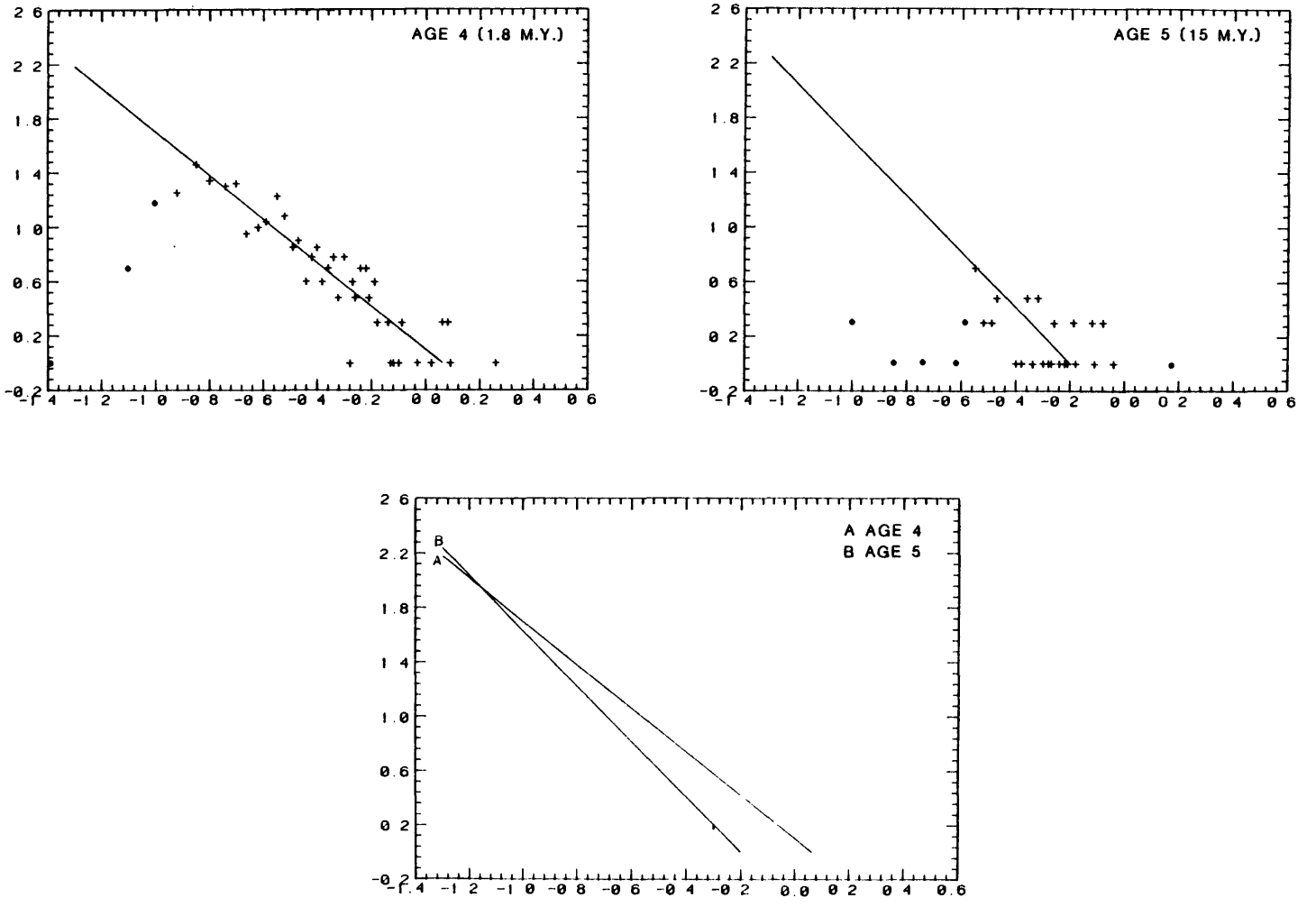

Figure 2.2.2.-10. (29)

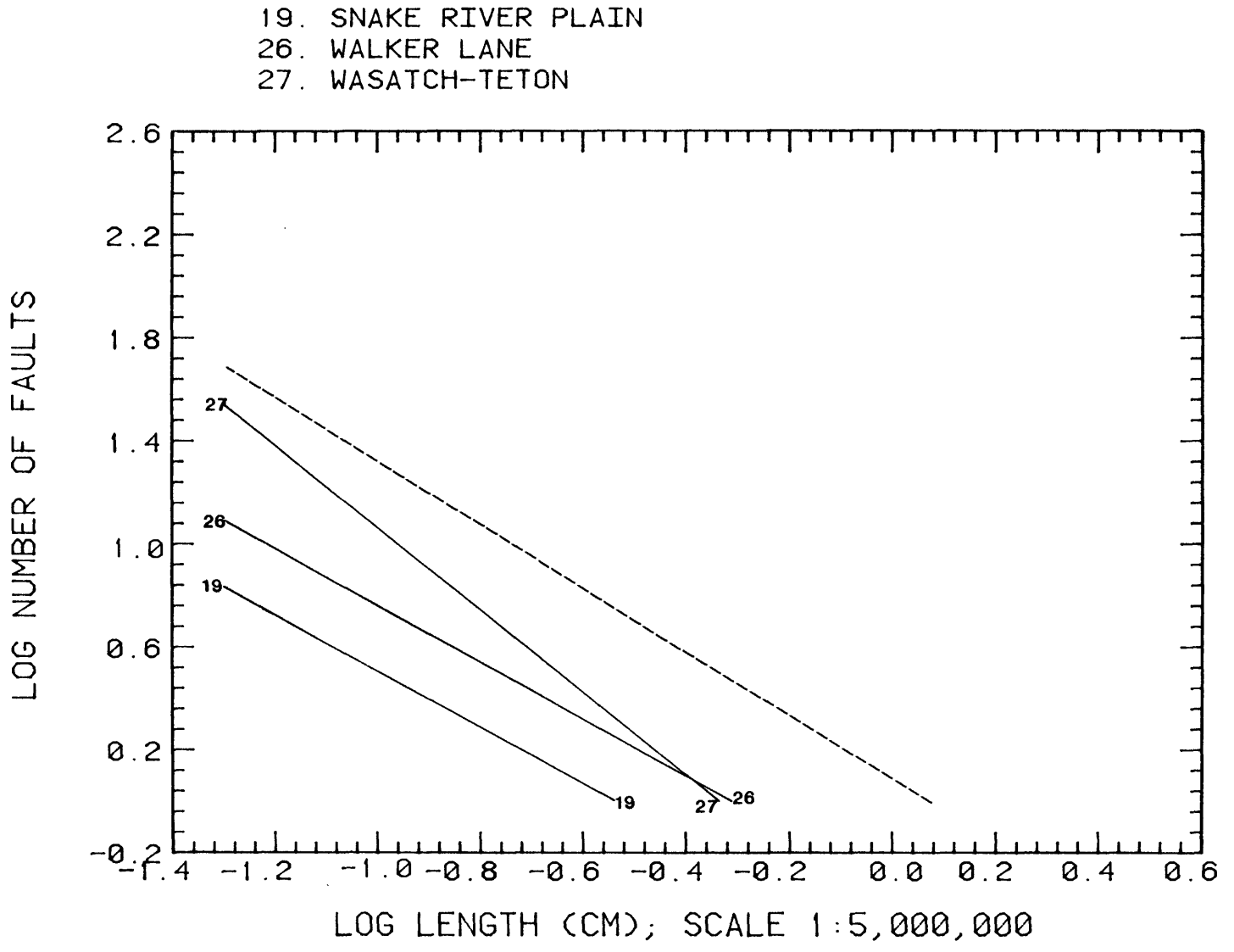

Figure 2.2.2.-10. (A)
(see Figure 2.2.2.-10.(2) caption pg. 108)

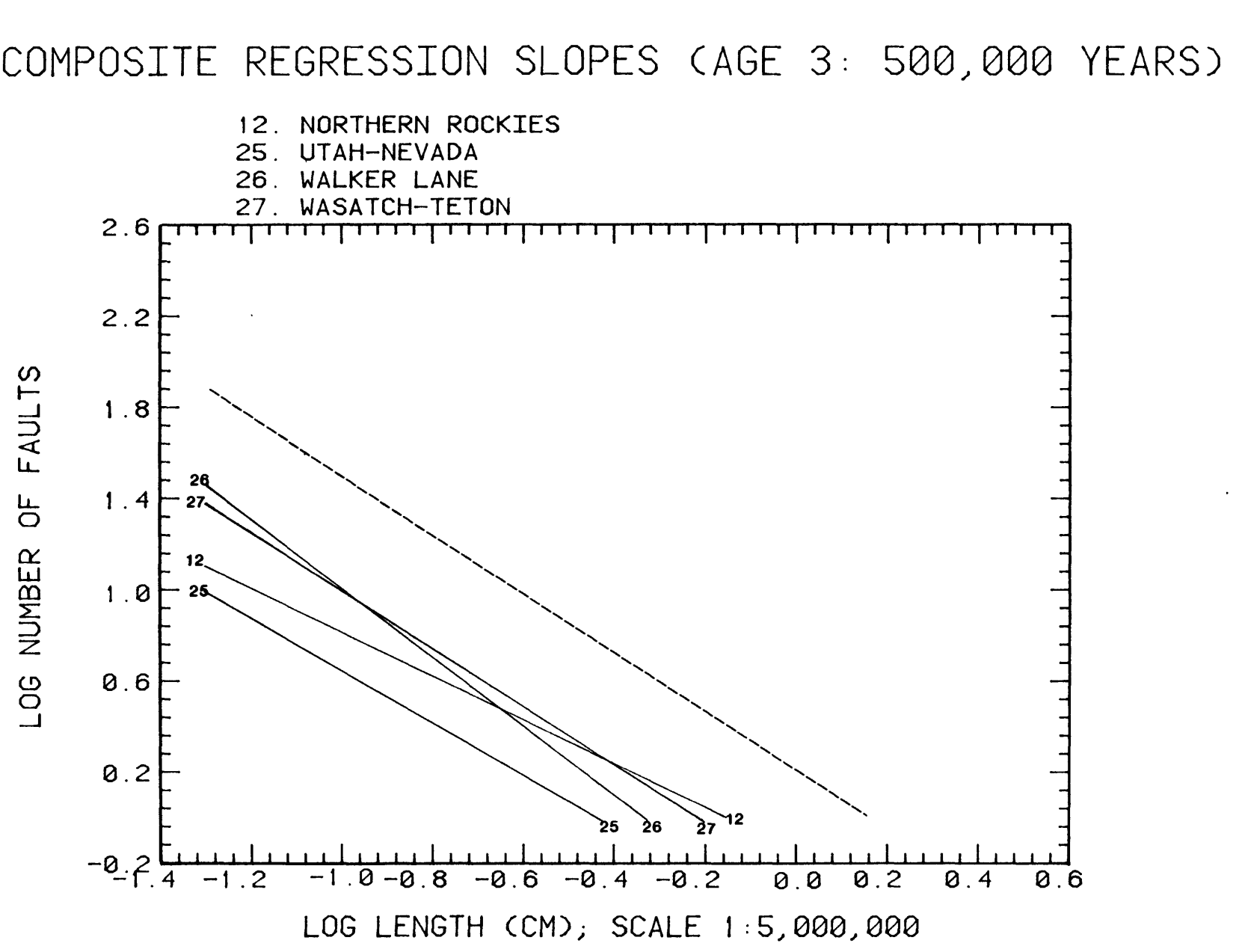

Figure 2.2.2.-10. (B)

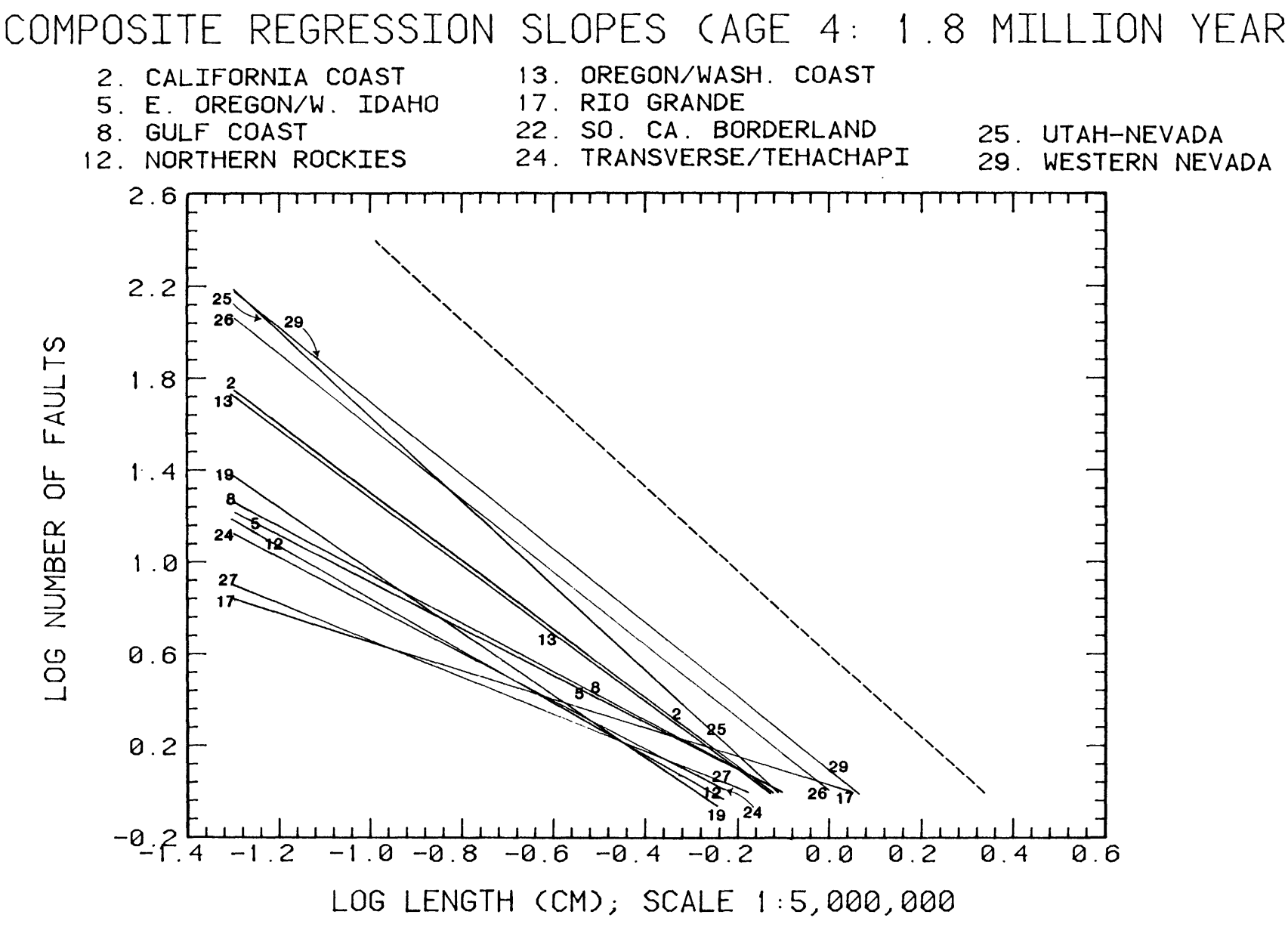

Figure 2.2.2.-10. (C)

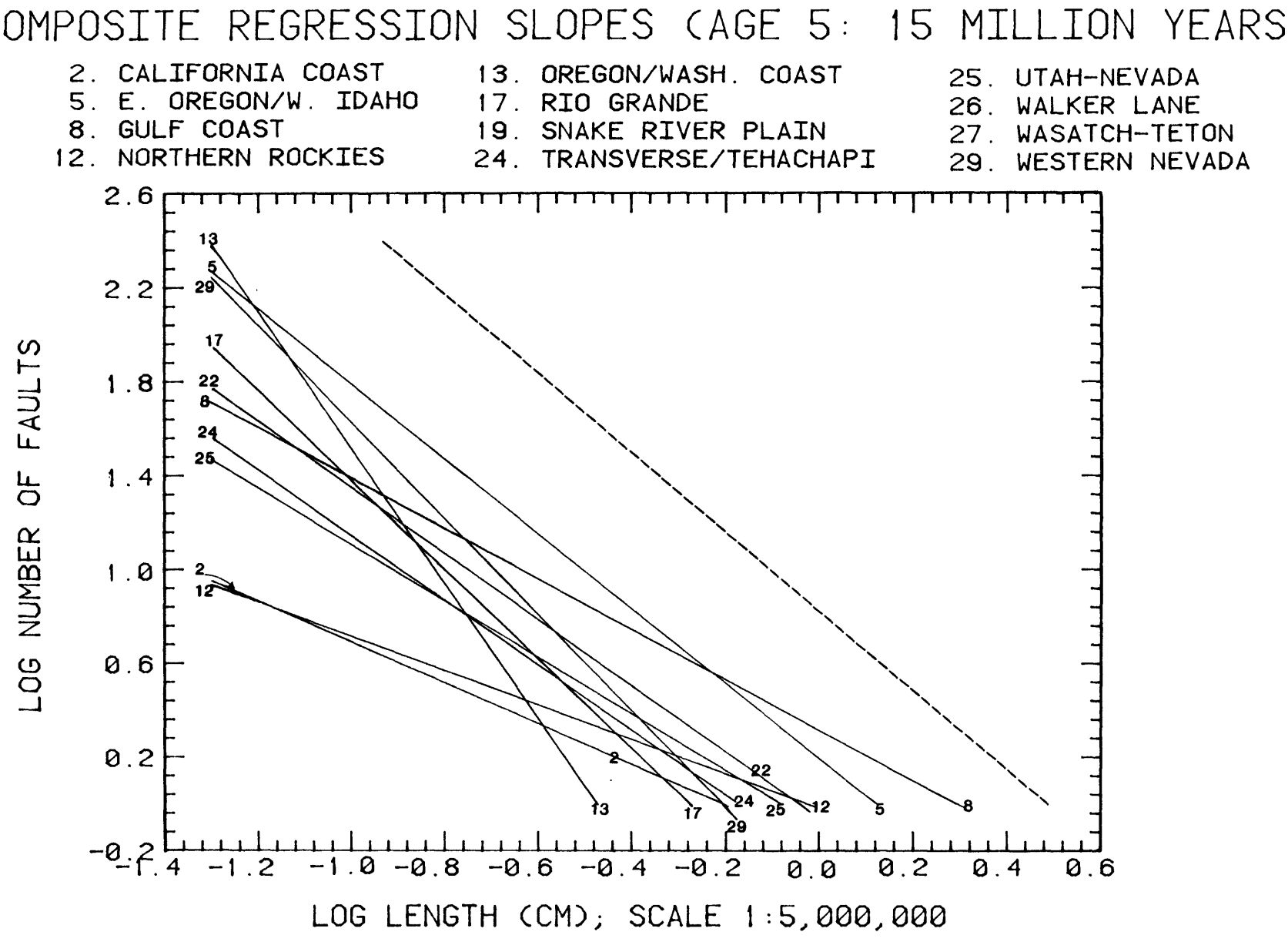

Figure 2.2.2.-10. (D)

COMPOSITE REGRESSION SLOPES (AGE 6: >15 MILLION YEARS)

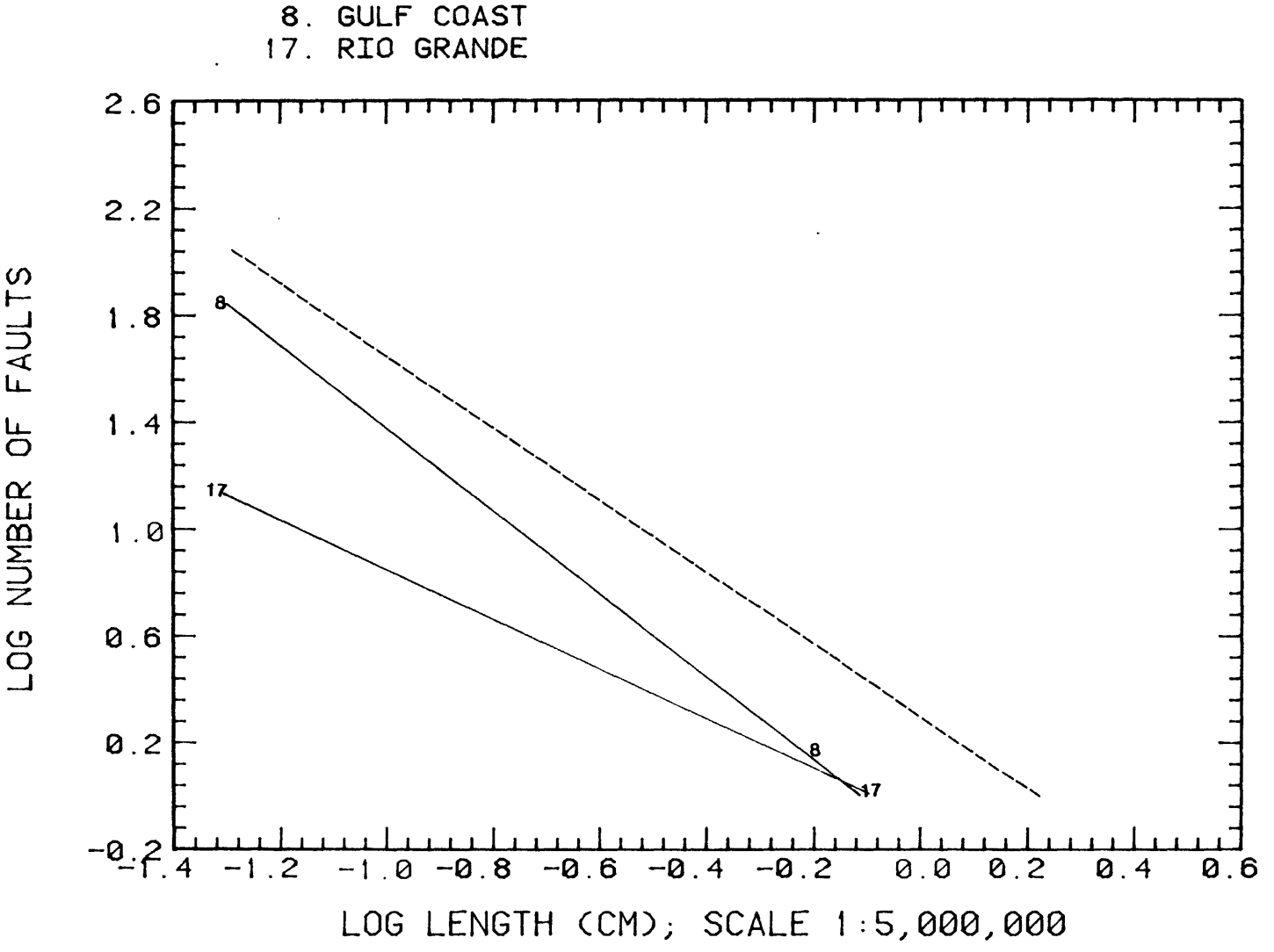

Figure 2.2.2.-10. (E)

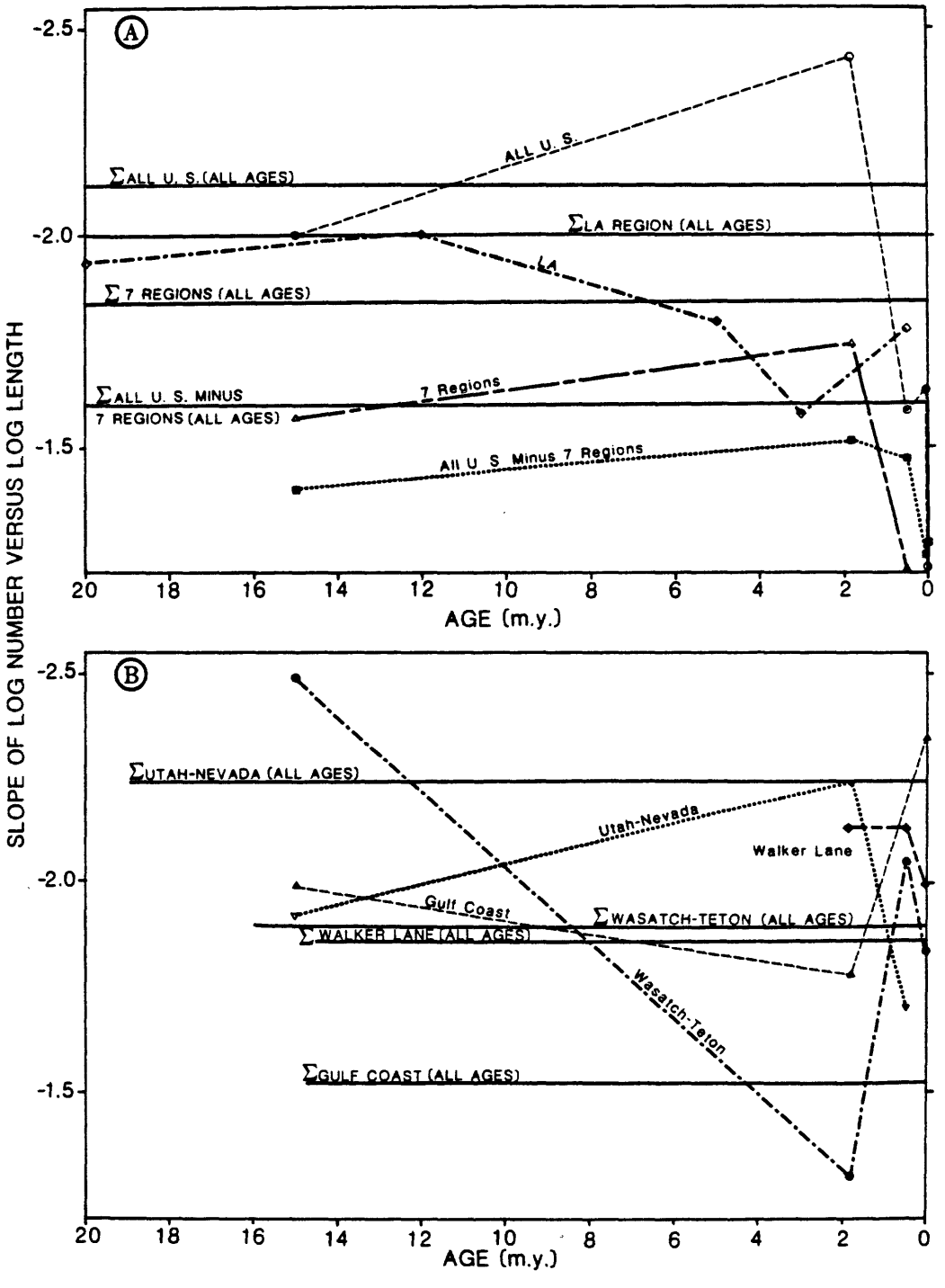

Figure 2.2.2.-11.
Variation of slopes versus age for logarithmic relations between number and fault lengths for selected sets of data.

COMPOSITE REGRESSION SLOPES

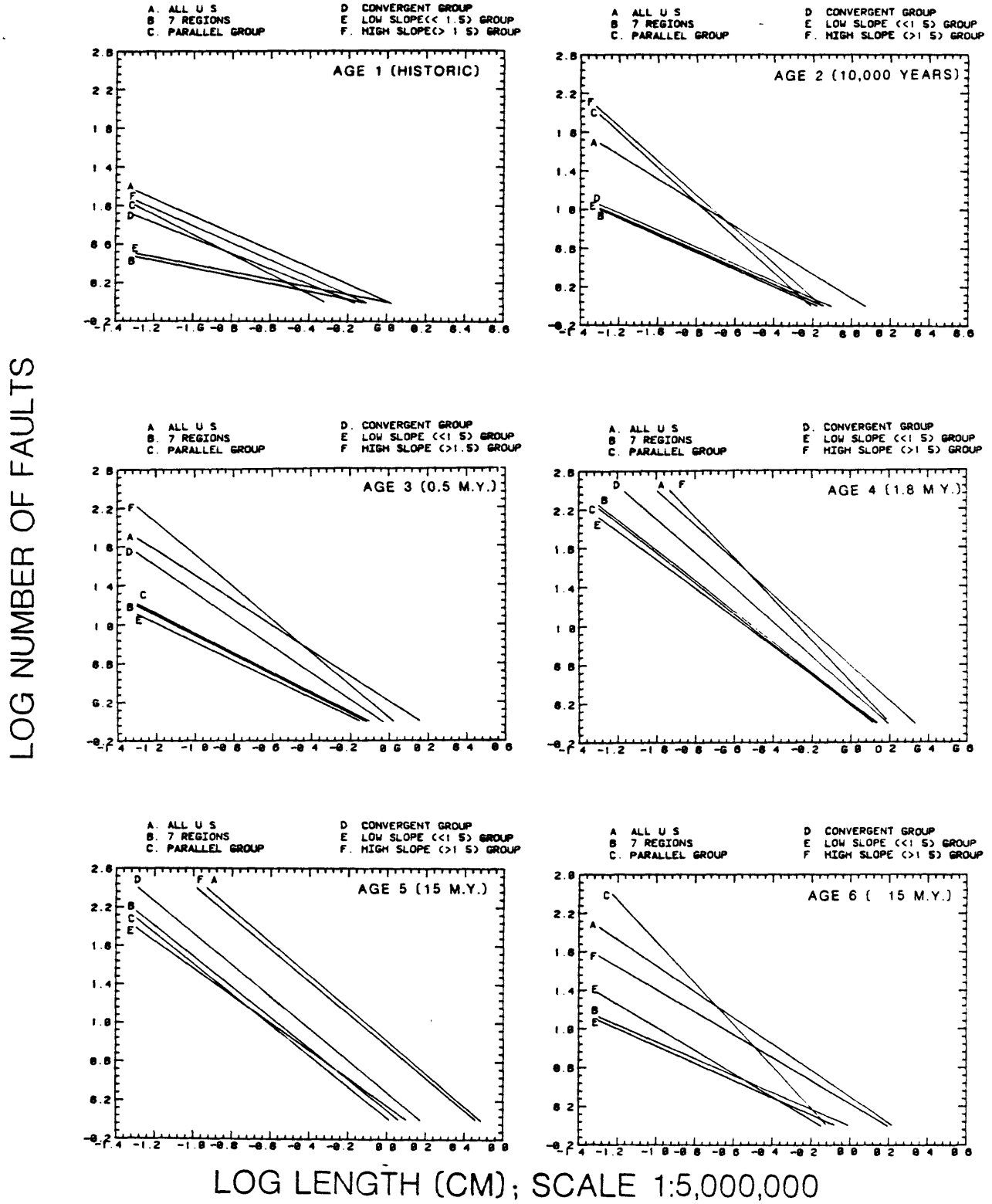

Figure 2.2.2.-12.
Composite diagrams showing comparative trends in regression lines for log number versus log length for various subgroups of regions.

Table 2.2.2.-1 Calculation of subjective slopes for logarithms of length versus frequency by age within groups. Fractions give $\Delta \log n / \Delta \log \ell$.

All U. S. Data:

Age 1: (200 yrs)	$\frac{0 - 1.82}{-0.1 - (1.6)}$	= -1.21
Age 2: (10,000 yrs)	$\frac{0 - 2.52}{-0.06 - (-1.6)}$	= -1.64
Age 3: (0.5 m.y.)	$\frac{0 - 2.76}{+0.14 - (-1.6)}$	= -1.59
Age 4: (1.8 m.y.)	$\frac{0 - 2.8}{+0.12 - (-1.03)}$	= -2.44
Age 5: (15 m.y.)	$\frac{0 - 2.8}{+0.4 - (-1.0)}$	= -2.00
All data:	$\frac{0 - 2.8}{+0.44 - (-0.88)}$	= -2.12

Seven Regions:

Age 3: (0.5 m.y.)	$\frac{0 - 1.81}{-0.10 - (-1.6)}$	= -1.21
Age 4 (1.8 m.y.)	$\frac{0 - 2.76}{+0.08 - (-1.6)}$	= -1.64
Age 5: (15 m.y.)	$\frac{0 - 2.62}{+0.07 - (-1.6)}$	= -1.57
All Data:	$\frac{0 - 2.8}{+0.14 - (-1.38)}$	= -1.84

All U. S. Minus Seven Regions:

Age 1: (200 yrs)	$\frac{0 - 1.74}{-0.13 - (-1.5)}$	= -1.27
Age 2: (10,000 yrs.)	$\frac{0 - 1.9}{+0.03 - (-1.5)}$	= -1.24
Age 3: (0.5 m.y.)	$\frac{0 - 2.3}{+0.06 - (-1.5)}$	= -1.47
Age 4: (1.8 m.y.)	$\frac{0 - 2.5}{+0.42 - (-1.23)}$	= -1.52
Age 5: (15 m.y.)	$\frac{0 - 2.5}{+0.58 - (-1.2)}$	= -1.40
All Data:	$\frac{0 - 2.5}{+0.68 - (-0.88)}$	= -1.60

L.A. Region (Maps 1 and 2)

Age L: (0.5 m.y.)	$\frac{0 - 2.8}{-0.23 - (-1.8)}$	= -1.78
Age Q: (3 m.y.)	$\frac{0 - 2.4}{-0.48 - (-2.0)}$	= -1.58
Age P: (5 m.y.)	$\frac{0 - 2.8}{-0.44 - (-2)}$	= -1.80
Age C: (12 m.y.)	$\frac{0 - 2.8}{-0.35 - (-1.75)}$	= -2.00
Age M: (20 m.y.)	$\frac{0 - 2.8}{-0.48 - (-1.93)}$	= -1.93
All Data: ()	$\frac{0 - 2.8}{-0.32 - (-1.71)}$	= -2.01

Table 2.2.2.-2 Slopes of regression lines by age for selected regions. (Note: These are the regions that have enough data to plot 2 or more age groups)

8. Gulf Coast:

Age 2: (10,000 yrs.)	$\frac{0 - 0.8}{-0.3 - (-0.64)}$	= -2.35
Age 4: (1.8 m.y.)	$\frac{0 - 0.5}{-0.1 - (-0.38)}$	= -1.79
Age 5: (15 m.y.)	$\frac{0 - 1.0}{+0.13 - (-0.37)}$	= -2.00
All Data:	$\frac{0 - 1.2}{+0.37 - (-0.42)}$	= -1.52

12. Northern Rockies[1/]:

*Age 3: (0.5 m.y.)	$\frac{0 - 0.6}{-0.17 - (-0.64)}$	= -1.28
*Age 4: (1.8 m.y.)	$\frac{0 - 0.6}{-0.40 - (-0.73)}$	= -1.82
Age 5: (15 m.y.)	$\frac{0 - 0.8}{-0.08 - (-0.72)}$	= -1.25
All Data:	$\frac{0 - 1.0}{+0.06 - (-0.48)}$	= -1.85

25. Utah-Nevada:

Age 3: (0.5 m.y.)	$\frac{0 - 0.6}{-0.41 - (-0.76)}$	= -1.71
Age 4: (1.8 m.y.)	$\frac{0 - 1.5}{-0.12 - (-0.79)}$	= -2.24
Age 5: (15 m.y.)	$\frac{0 - 1.0}{-0.14 - (-0.66)}$	= -1.92
All Data:	$\frac{0 - 1.5}{-0.03 - (-0.70)}$	= -2.24

26. Walker Lane:

Age 2: (10,000 yrs.)	$\frac{0 - 0.5}{-0.28 - (-0.53)}$	= -2.00
Age 3: (0.5 m.y.)	$\frac{0 - 0.8}{-0.36 - (-0.74)}$	= -2.11
Age 4: (1.8 m.y.)	$\frac{0 - 1.5}{-0.09 - (-0.80)}$	= -2.11
All Data:	$\frac{0 - 1.6}{+0.04 - (-0.82)}$	= -1.86

27. Wasatch-Tetón:

Age 2: (10,000 yrs.)	$\frac{0 - 0.7}{-0.29 - (-0.67)}$	= -1.84
Age 3: (0.5 m.y.)	$\frac{0 - 0.8}{-0.24 - (-0.63)}$	= -2.05
Age 4: (1.8 m.y.)	$\frac{0 - 0.6}{-0.20 - (-0.66)}$	= -1.30
Age 5: (15 m.y.)	$\frac{0 - 0.8}{-0.30 - (-0.61)}$	= -2.58
All Data:	$\frac{0 - 1.2}{-0.04 - (-0.67)}$	= -1.90

29. Western Nevada[1/]:

*Age 2: (10,000 yrs.)	$\frac{0 - 0.5}{-0.2 - (-0.45)}$	= -2.00
Age 4: (1.8 m.y.)	$\frac{0 - 1.5}{+0.13 - (-0.83)}$	= -1.56
*Age 5: (15 m.y.)	$\frac{0 - 0.7}{-0.23 - (-0.51)}$	= -2.50
All Data:	$\frac{0 - 1.6}{+0.04 - (-0.7)}$	= -2.16

[1/] Asterisks indicate regions with sparse data.

SECTION 3.

3. Rates of Fault Activation.

3.1. Cumulative Lengths of Faults Showing Movement Since the Early Miocene; Normalized Activation Lengths versus Age.

Table 3.1.-1 gives additive lengths for faults showing movement in each region and age group together with the total lengths of faults showing movement. The convention about summation raises questions about movement history. Treating the lengths as additive implies either that there was a fault set consisting of the total cumulative length which was progressively activated in time, or that the fault set has grown to its total length during the time from the Miocene to the present. Neither situation is accurate. Many fault movements may be renewed activation along older faults, but new faults also must have been created as the continental crust has evolved. However, we do not need to know the total histories of the faults to discuss activation rates, and, conversely, activation rates may give clues about limits for growth rates of new faults. These clues are also suggested as hypotheses. They concern: (1) the evolution of faulting rates during the total history for growth of the continental crust, (2) fluctuating episodes between high and low faulting rates, and (3) relations between contemporary faulting rates and average earthquake magnitudes and frequencies that may occur within the delineated fault regions.

There are other ways the ages of movement might be treated. One approach might consider that each age category is a unique fault set, the movements of which represent a minimum recurrence frequency for that set. Another viewpoint might hold that all the faults showing younger movements also had older movements. The former assumption is not plausible, and the latter differs only in interpretation of differences in lengths for cumulative movements between age categories. The lengths for all the older age categories would be increased as well as the differences between age categories. The general effect would be to enhance inferred rates of activation between the age categories because the lengths are increased in all categories but the youngest.

Probably the most serious uncertainty concerns faults that may have had movements younger than those recorded but whose younger movements could not be determined because criteria for age brackets were lacking. This also would mean that the total activated length in any age category could be larger by some unknown and variable amount.

We assume in this report that the effects mentioned do not vitiate the patterns observed; they do, however, highlight an issue that needs to be examined in more detail for areas having the most complete records for faulting history. In view of the potential increases in activation lengths mentioned above, our derivations of rates appear, in most instances, to be conservative.

Figure 3.1.-1 compiles graphs showing normalized length versus age based on the data in Table 3.1.-1. As an overview, the graphs include data for various regions compared in each case with the total cumulative curve for the conterminous United States, a curve for the L.A. Area, and a curve that represents a constant activation rate since the early Miocene. The curve for constant rate is an estimate for the overall average in the United States. Figure 3.1.-2 separates out the data set representing the group of regions having the lowest slopes in the Log Frequency distributions. Figure 3.1.-3 shows the "Convergent Group" and Figure 3.1.-4 the "Parallel Group." Figure 3.1.-5 gives normalized curves representing summations of the various subcategories.

The general conclusion we draw from the graphs of normalized lengths versus age is that, analogous to the frequency diagrams, there is a similarity in behavior from region to region and between different categories of regions, though there are numerous differences in detail. Apparent fractional activation rates are given by slopes derived from the curves for normalized length versus age. These are displayed in a parallel series of graphs given in Figures 3.1.-6, 3.1.-7, 3.1.-8, 3.1.-9, and 3.1.-10. Deviation graphs showing differences between the regional and United States rates are given in Figure 3.1.-11.

The graphs for apparent fractional activation rates reveal conspicuous reversals somewhere in the Pleistocene interval, at about one million years B.P. The regions showing this pattern are summarized in Figure 3.1.-12.

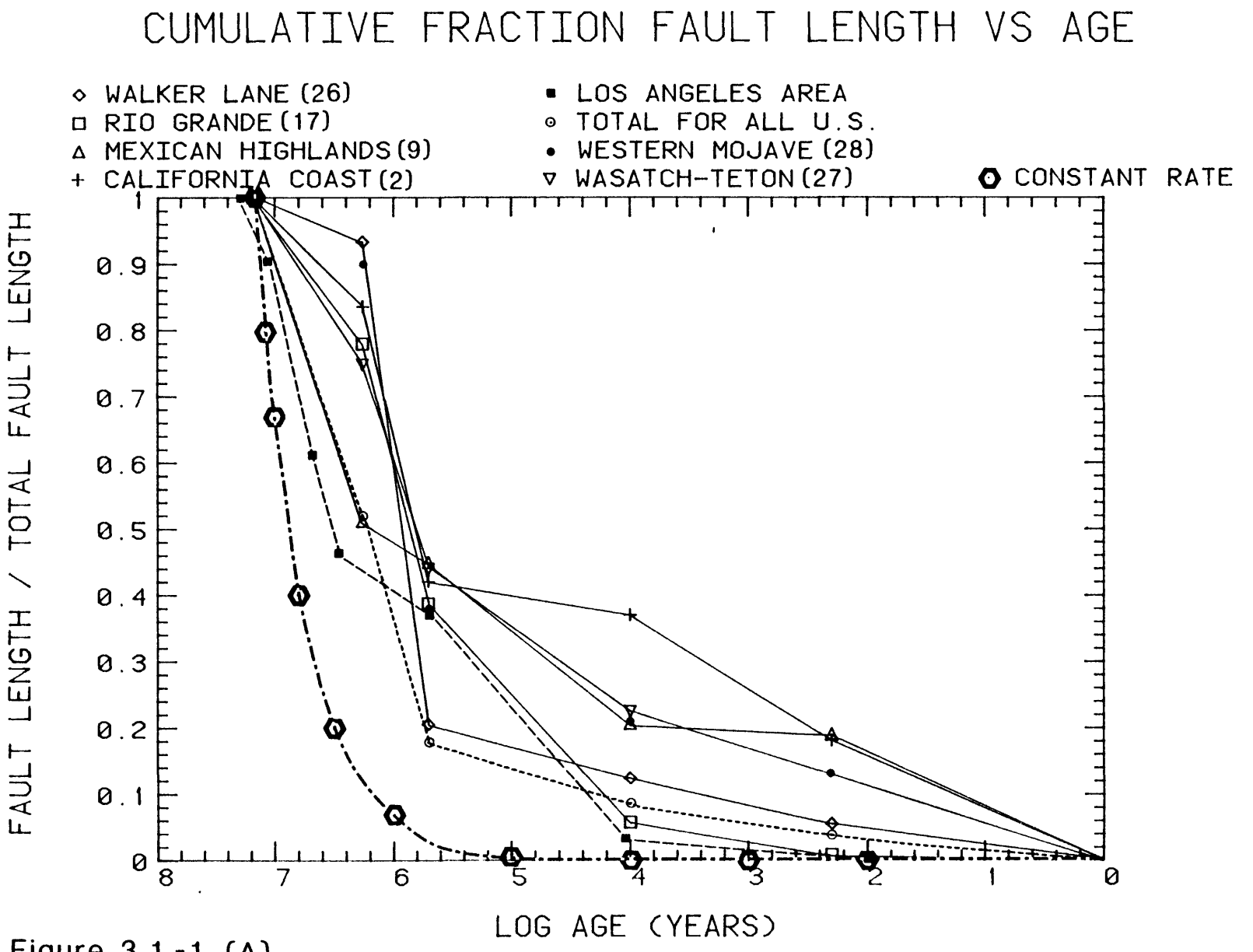

Figure 3.1.-1. (A)
Normalized fault length versus age by region; the normalized length represents the cumulative activated fault length, from youngest to oldest, divided by the total activated length in the latest 15 m.y. Region numbers are given in parentheses.

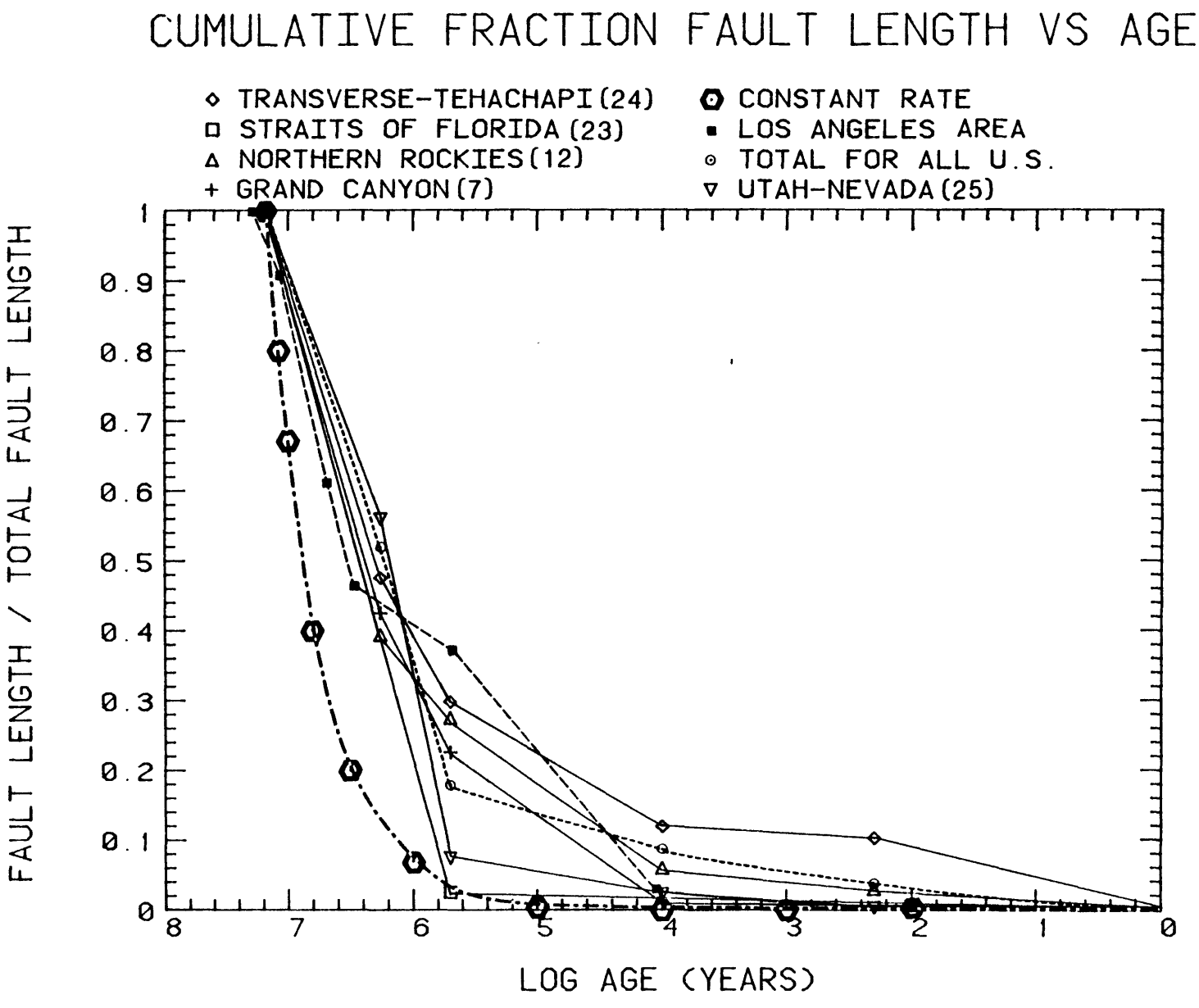
CUMULATIVE FRACTION FAULT LENGTH VS AGE
TRANSVERSE-TEHACHAPI(24)
STRAITS OF FLORIDA(23)
NORTHERN ROCKIES(12)
GRAND CANYON(7)
CONSTANT RATE
LOS ANGELES AREA
TOTAL FOR ALL U.S.
UTAH-NEVADA(25)
FAULT LENGTH / TOTAL FAULT LENGTH
0
0.1
0.2
0.3
0.4
0.5
0.6
0.7
0.8
0.9
1
8
7
6
5
4
3
2
1
0
LOG AGE (YEARS)

Figure 3.1.-1. (B)

SECTION 3.1. FIGURES AND TABLES

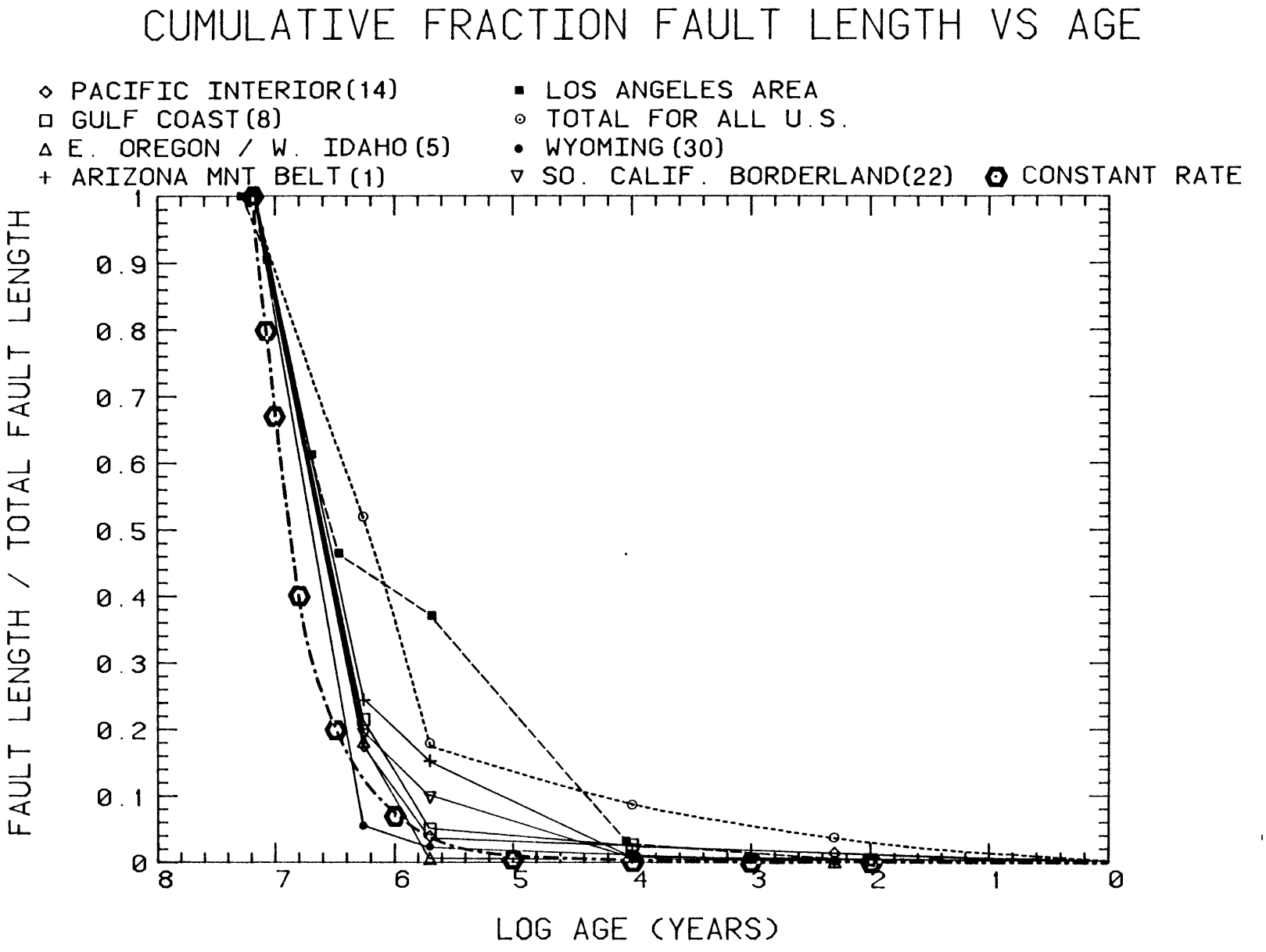
CUMULATIVE FRACTION FAULT LENGTH VS AGE
◇ PACIFIC INTERIOR(14)
□ GULF COAST(8)
△ E. OREGON / W. IDAHO(5)
+ ARIZONA MNT BELT(1)
▪ LOS ANGELES AREA
⊙ TOTAL FOR ALL U.S.
• WYOMING(30)
▽ SO. CALIF. BORDERLAND(22)
CONSTANT RATE
FAULT LENGTH / TOTAL FAULT LENGTH
0
0.1
0.2
0.3
0.4
0.5
0.6
0.7
0.8
0.9
1
8
7
6
5
4
3
2
1
0
LOG AGE (YEARS)

Figure 3.1.-1. (C)

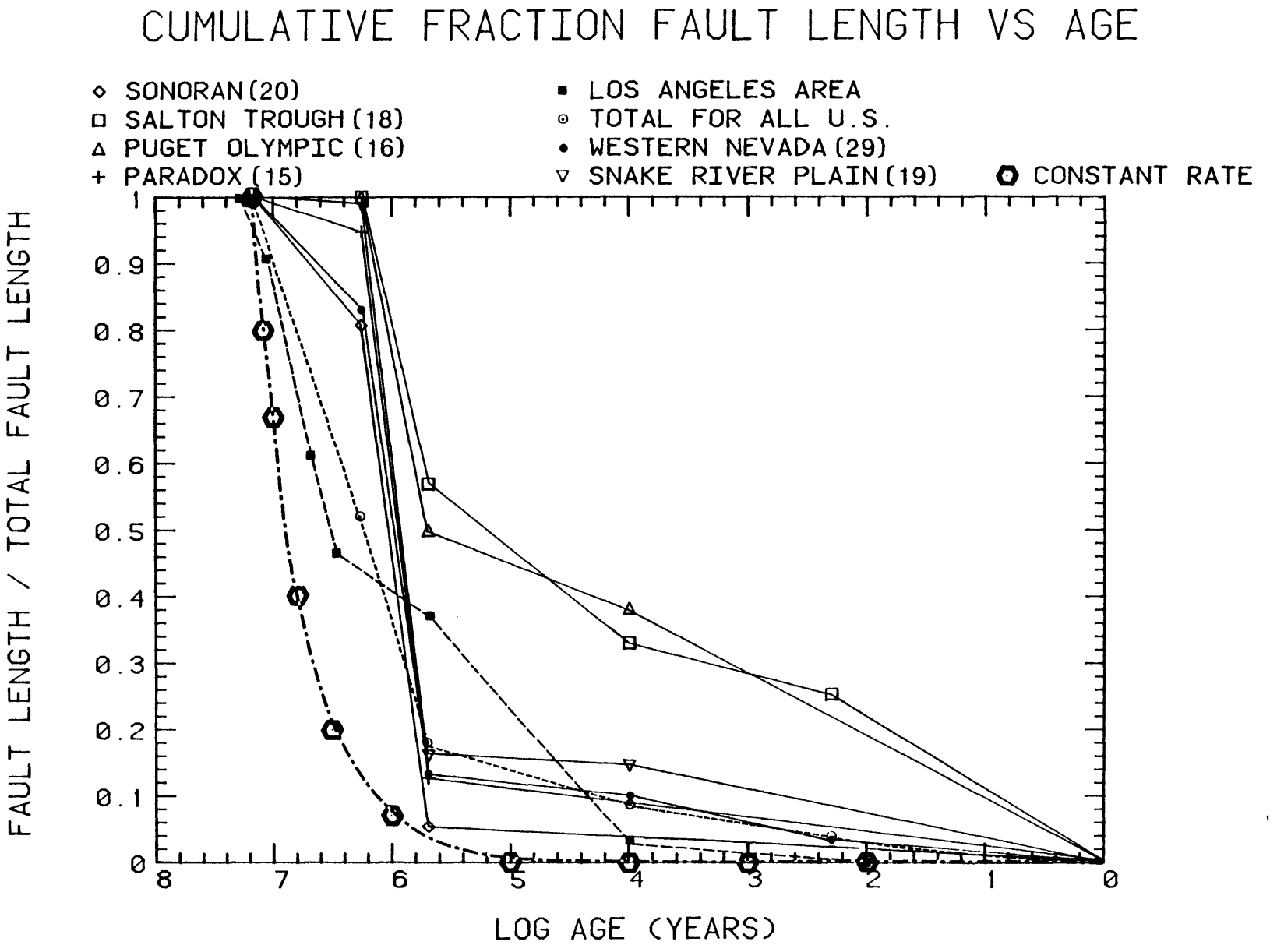
CUMULATIVE FRACTION FAULT LENGTH VS AGE
SONORAN(20)
SALTON TROUGH(18)
PUGET OLYMPIC(16)
PARADOX(15)
LOS ANGELES AREA
TOTAL FOR ALL U.S.
WESTERN NEVADA(29)
SNAKE RIVER PLAIN(19)
CONSTANT RATE
FAULT LENGTH / TOTAL FAULT LENGTH
0
0.1
0.2
0.3
0.4
0.5
0.6
0.7
0.8
0.9
1
8
7
6
5
4
3
2
1
0
LOG AGE (YEARS)

Figure 3.1.-1. (D)

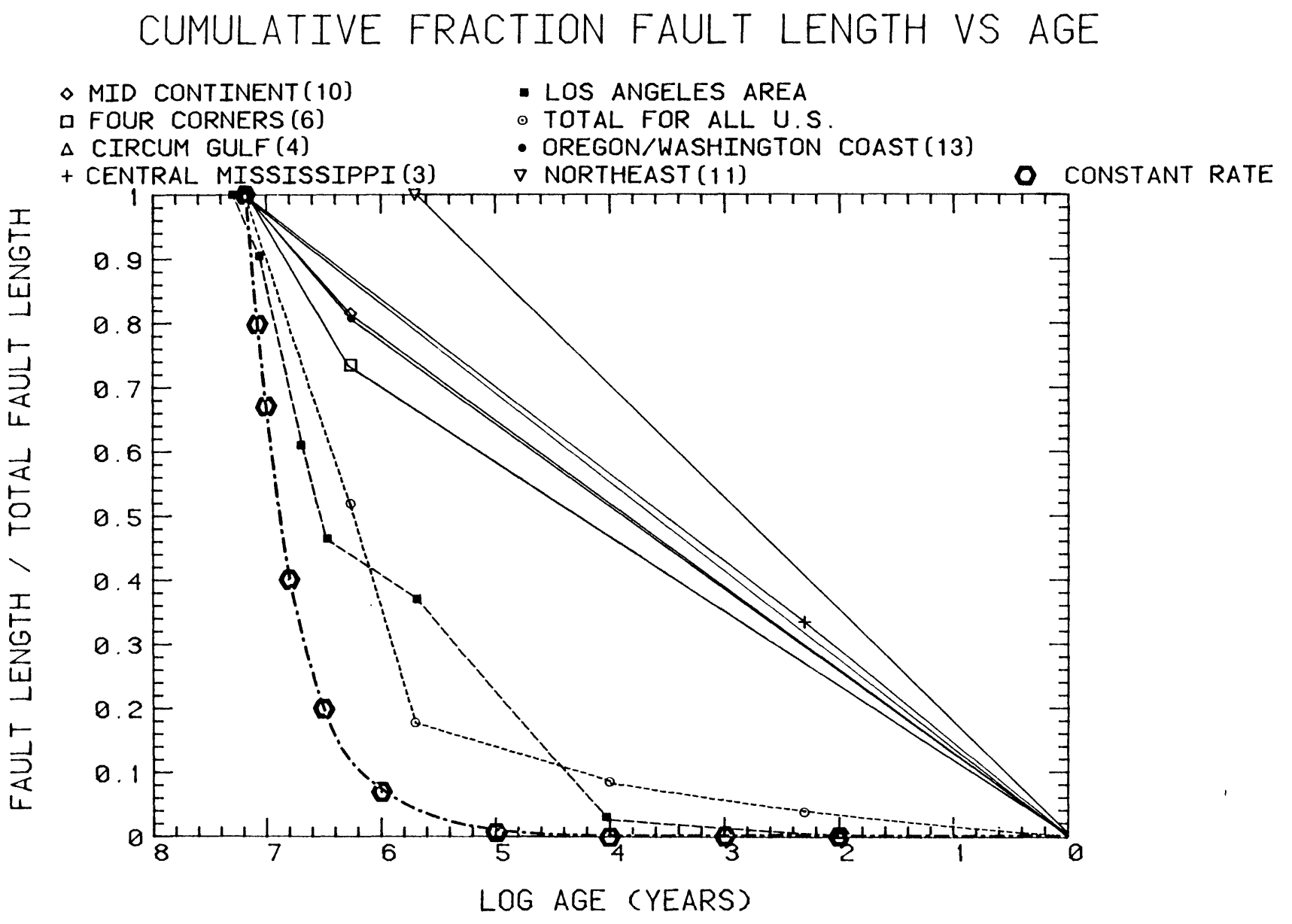
CUMULATIVE FRACTION FAULT LENGTH VS AGE
◇ MID CONTINENT(10)
□ FOUR CORNERS(6)
△ CIRCUM GULF(4)
+ CENTRAL MISSISSIPPI(3)
■ LOS ANGELES AREA
⊙ TOTAL FOR ALL U.S.
• OREGON/WASHINGTON COAST(13)
▽ NORTHEAST(11)
CONSTANT RATE
FAULT LENGTH / TOTAL FAULT LENGTH
1
0.9
0.8
0.7
0.6
0.5
0.4
0.3
0.2
0.1
0
8
7
6
5
4
3
2
1
0
LOG AGE (YEARS)

Figure 3.1.-1. (E)

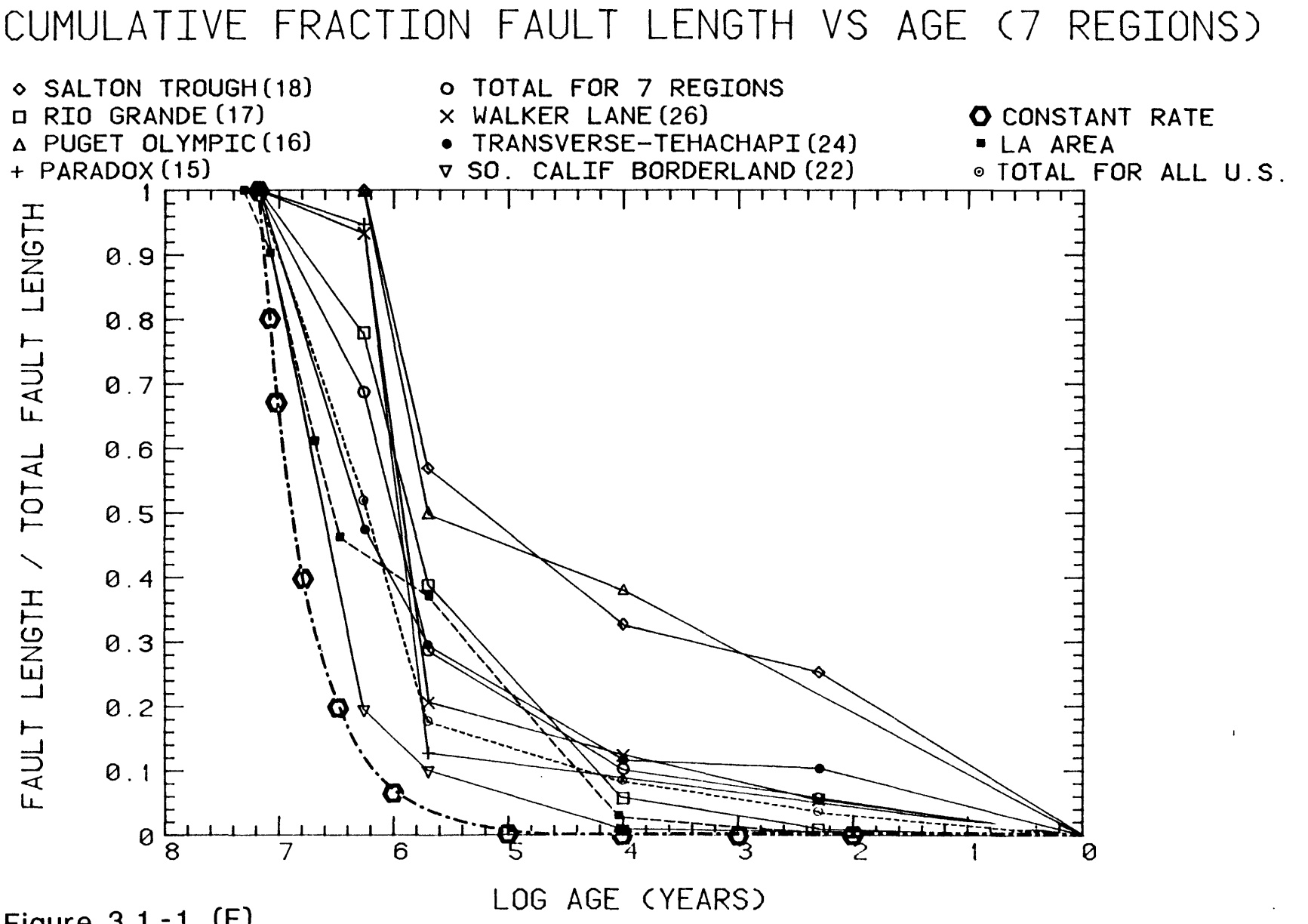
CUMULATIVE FRACTION FAULT LENGTH VS AGE (7 REGIONS)
◇ SALTON TROUGH(18)
□ RIO GRANDE(17)
△ PUGET OLYMPIC(16)
+ PARADOX(15)
o TOTAL FOR 7 REGIONS
× WALKER LANE(26)
• TRANSVERSE-TEHACHAPI(24)
▽ SO. CALIF BORDERLAND(22)
⬡ CONSTANT RATE
▪ LA AREA
⊙ TOTAL FOR ALL U.S.
FAULT LENGTH / TOTAL FAULT LENGTH
0
0.1
0.2
0.3
0.4
0.5
0.6
0.7
0.8
0.9
1
8
7
6
5
4
3
2
1
0
LOG AGE (YEARS)

Figure 3.1.-1. (F)

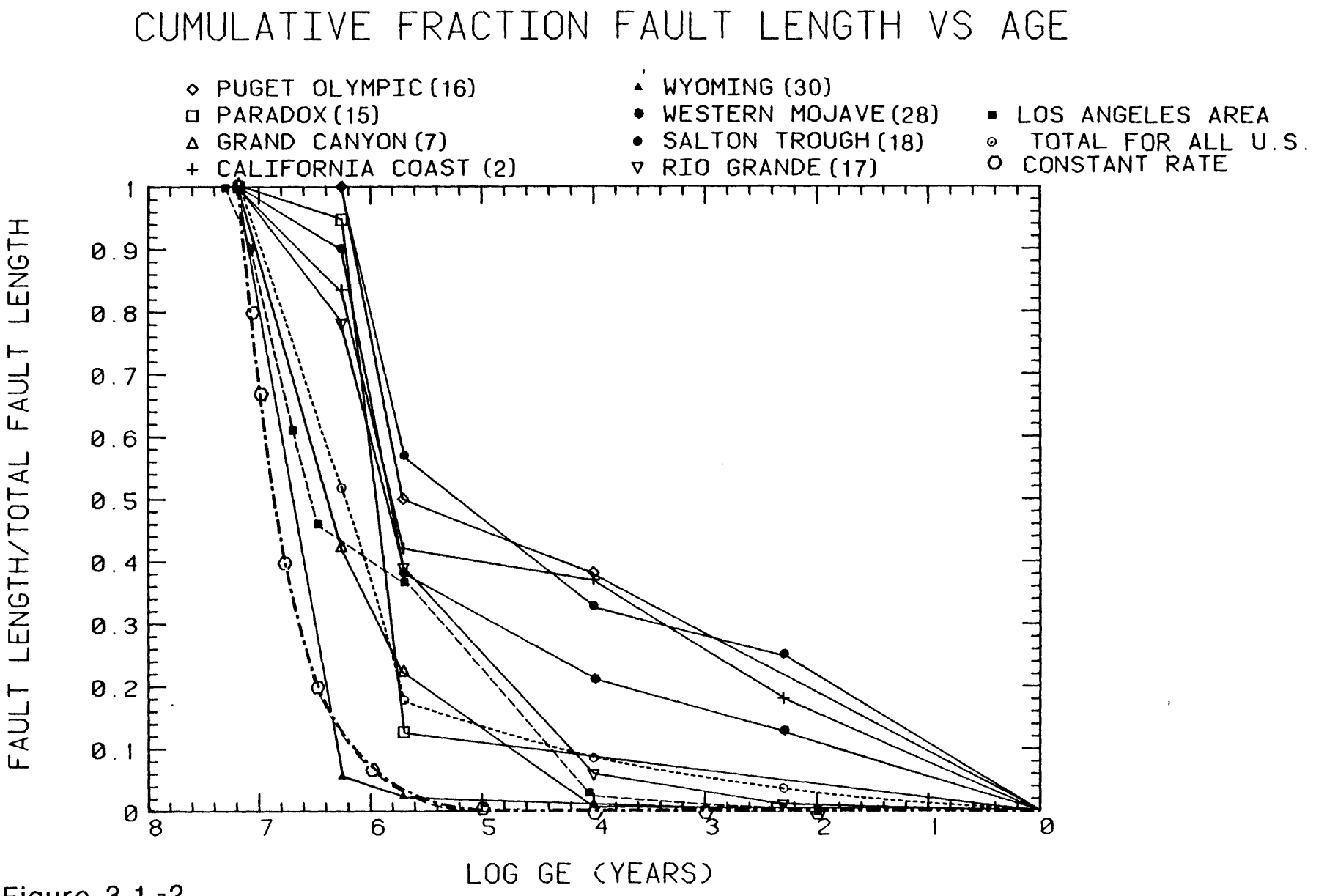

Figure 3.1.-2.
Normalized fault length versus age for the "low slope" group.

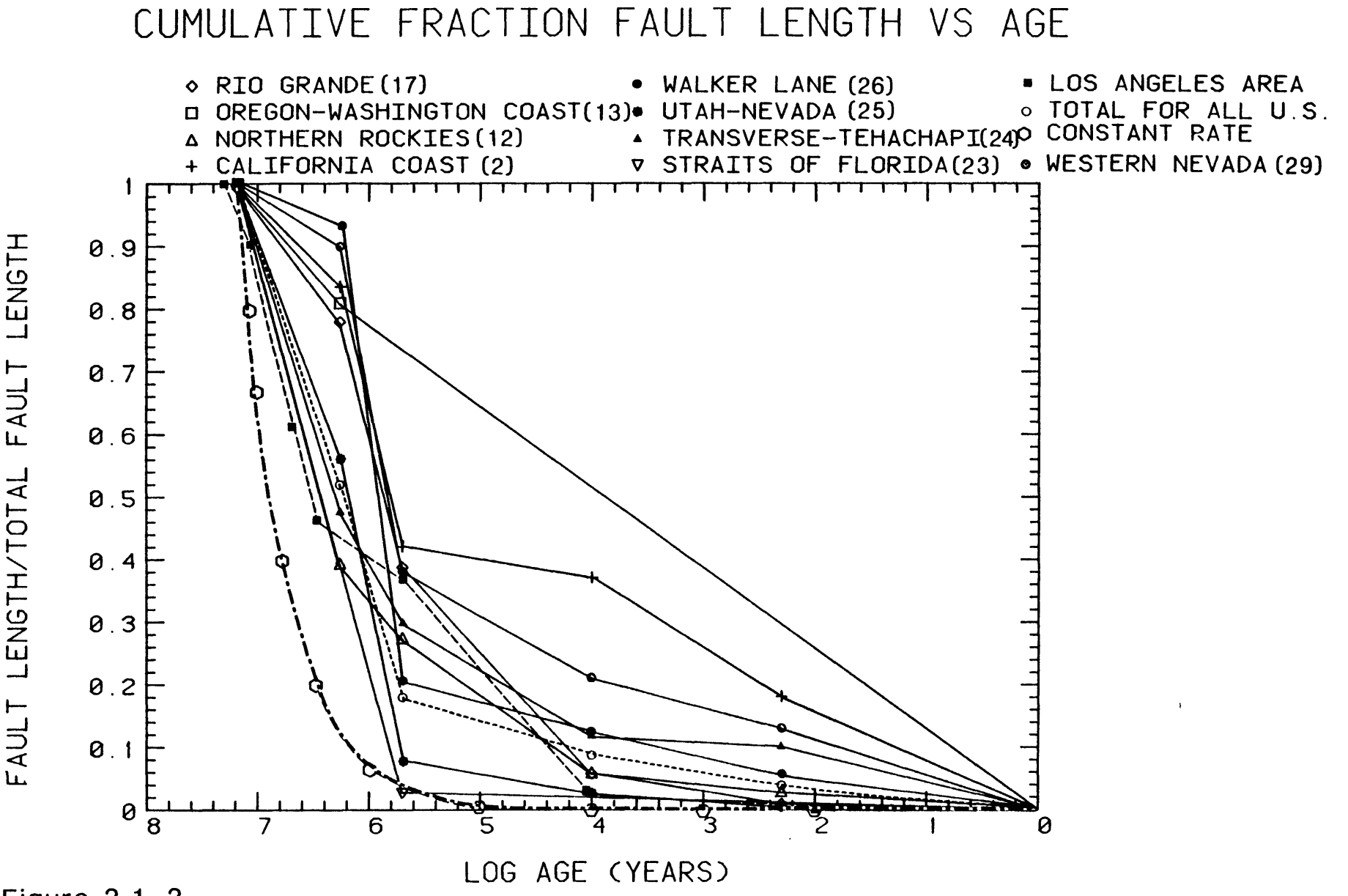

Figure 3.1.-3.
Normalized fault length versus age for the "convergent" group.

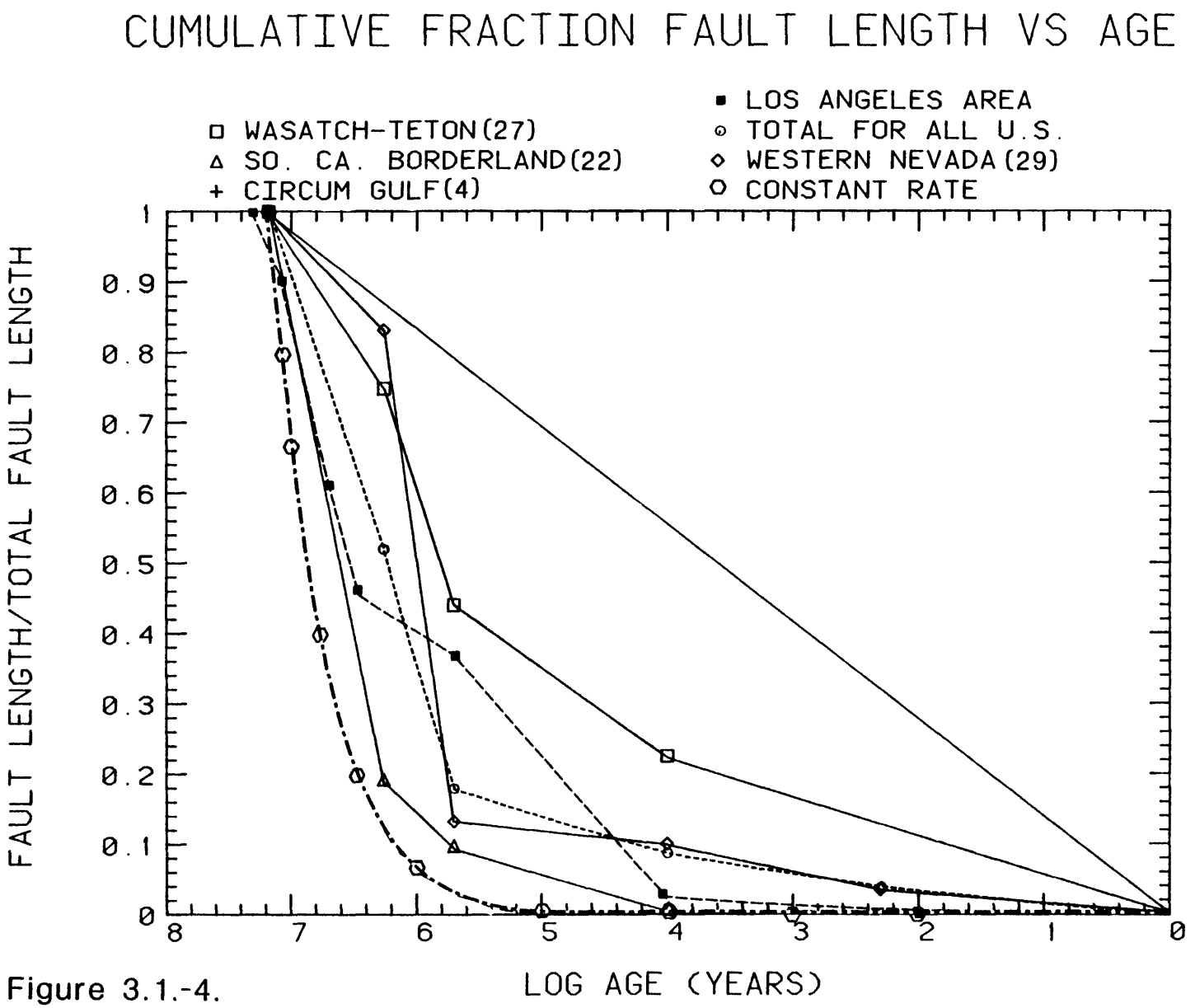

Figure 3.1.-4.
Normalized fault length versus age for the "parallel" group.

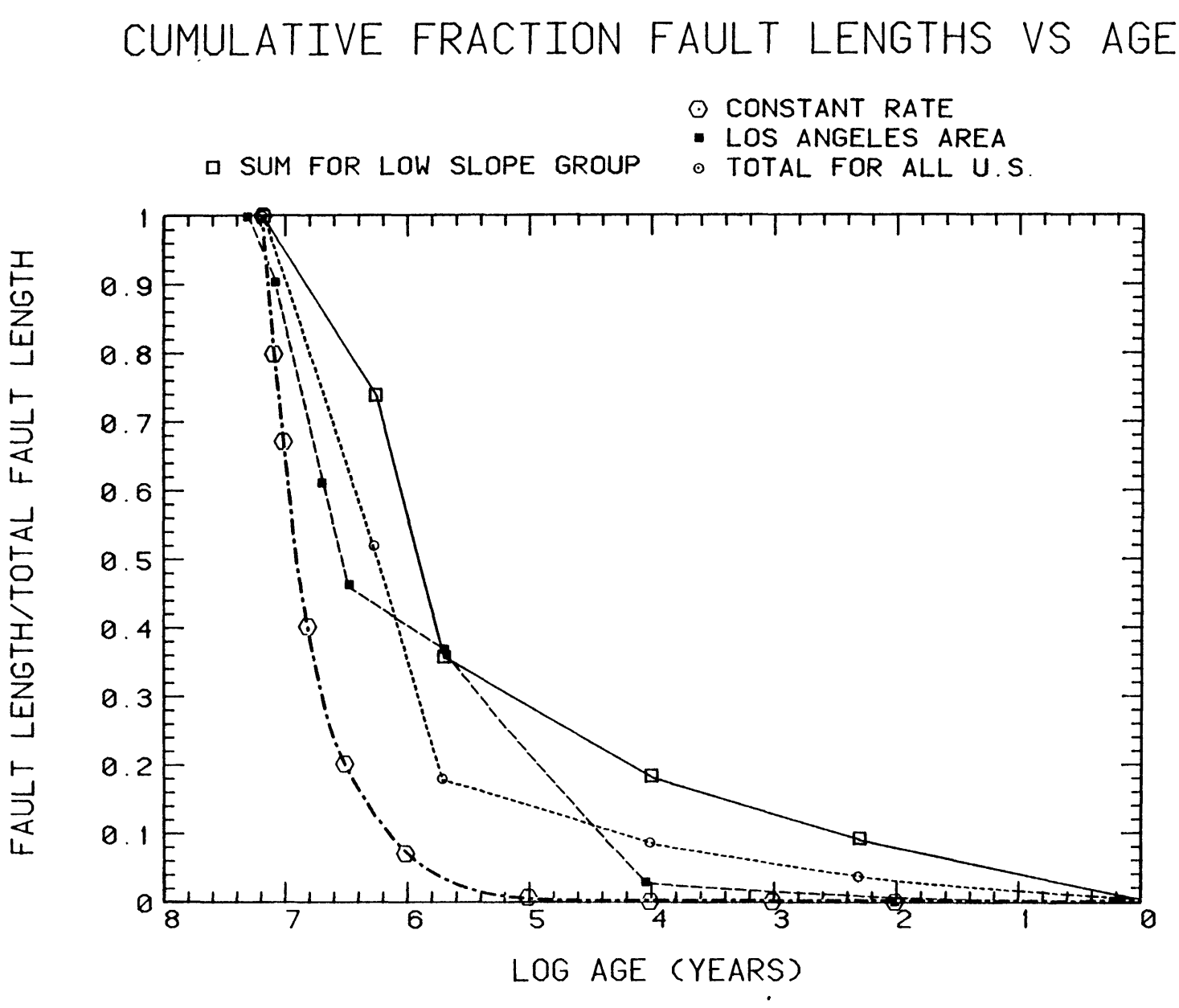

Figure 3.1.-5. (A)
Normalized fault length versus age; summations representing each subgroup.

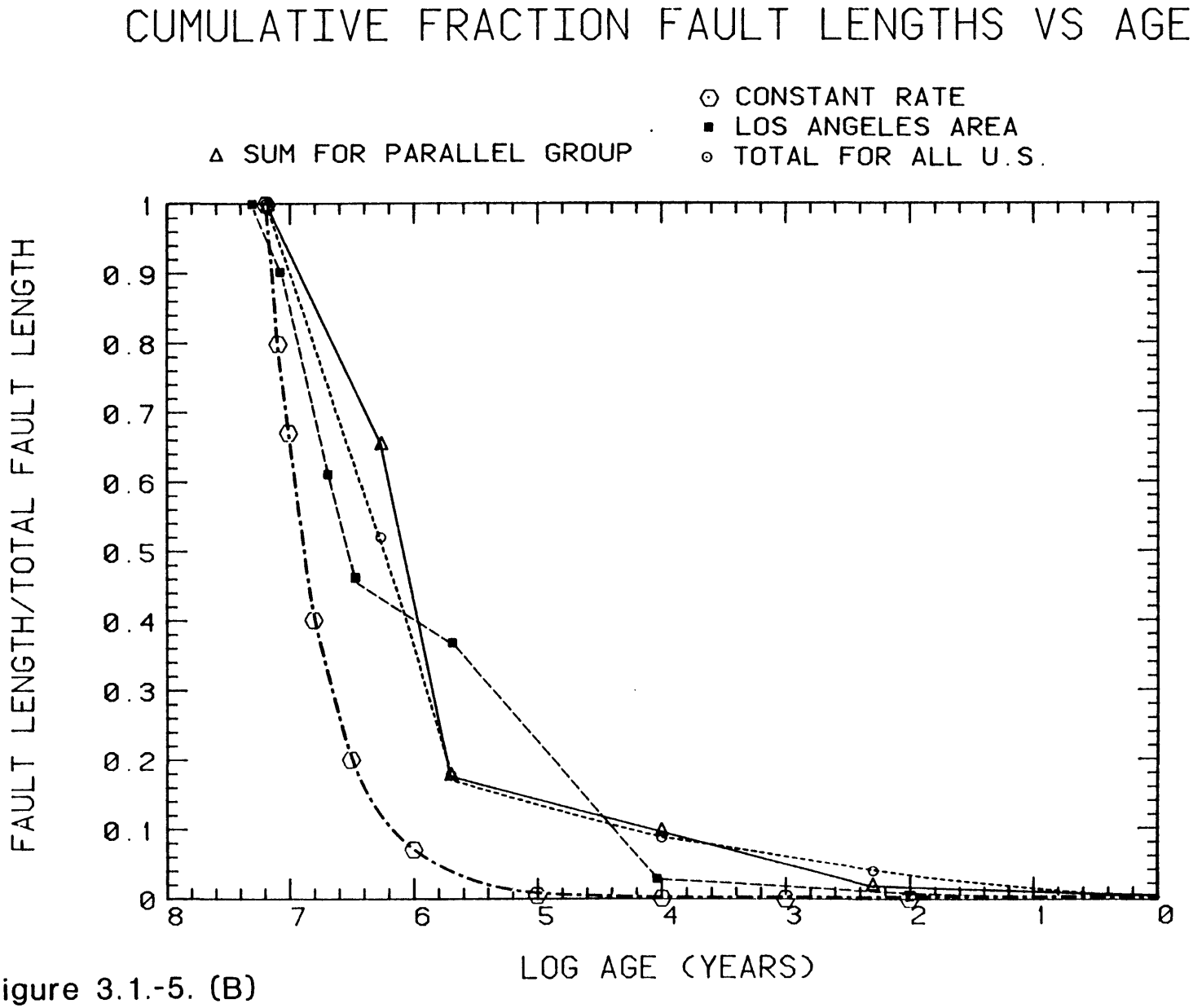
CUMULATIVE FRACTION FAULT LENGTHS VS AGE
CONSTANT RATE
LOS ANGELES AREA
TOTAL FOR ALL U.S.
SUM FOR PARALLEL GROUP
FAULT LENGTH/TOTAL FAULT LENGTH
0
0.1
0.2
0.3
0.4
0.5
0.6
0.7
0.8
0.9
1
8
7
6
5
4
3
2
1
0
LOG AGE (YEARS)

Figure 3.1.-5. (B)

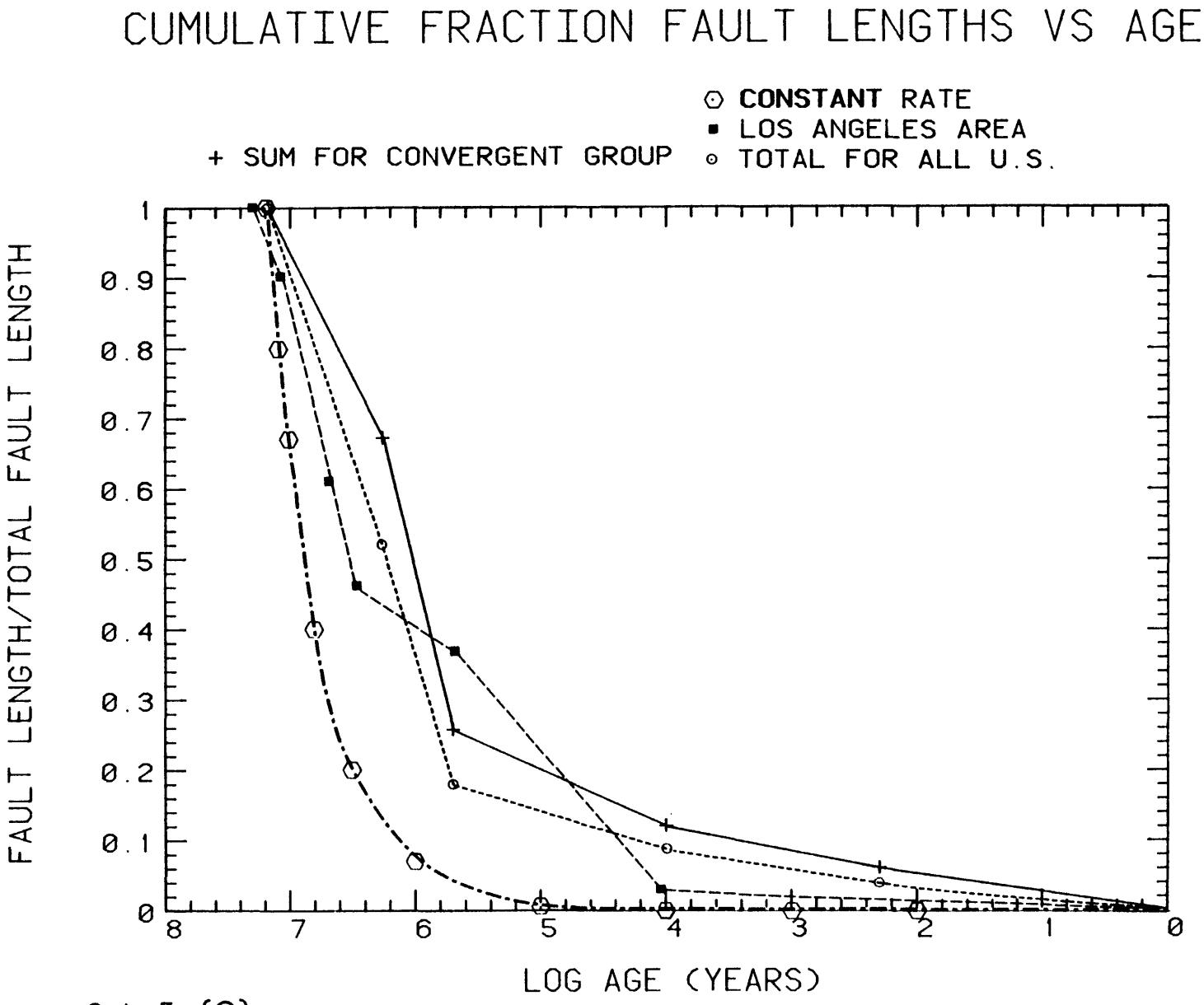
CUMULATIVE FRACTION FAULT LENGTHS VS AGE
⊙ CONSTANT RATE
▪ LOS ANGELES AREA
+ SUM FOR CONVERGENT GROUP
⊙ TOTAL FOR ALL U.S.
FAULT LENGTH/TOTAL FAULT LENGTH
1
0.9
0.8
0.7
0.6
0.5
0.4
0.3
0.2
0.1
0
8
7
6
5
4
3
2
1
0
LOG AGE (YEARS)

Figure 3.1.-5. (C)

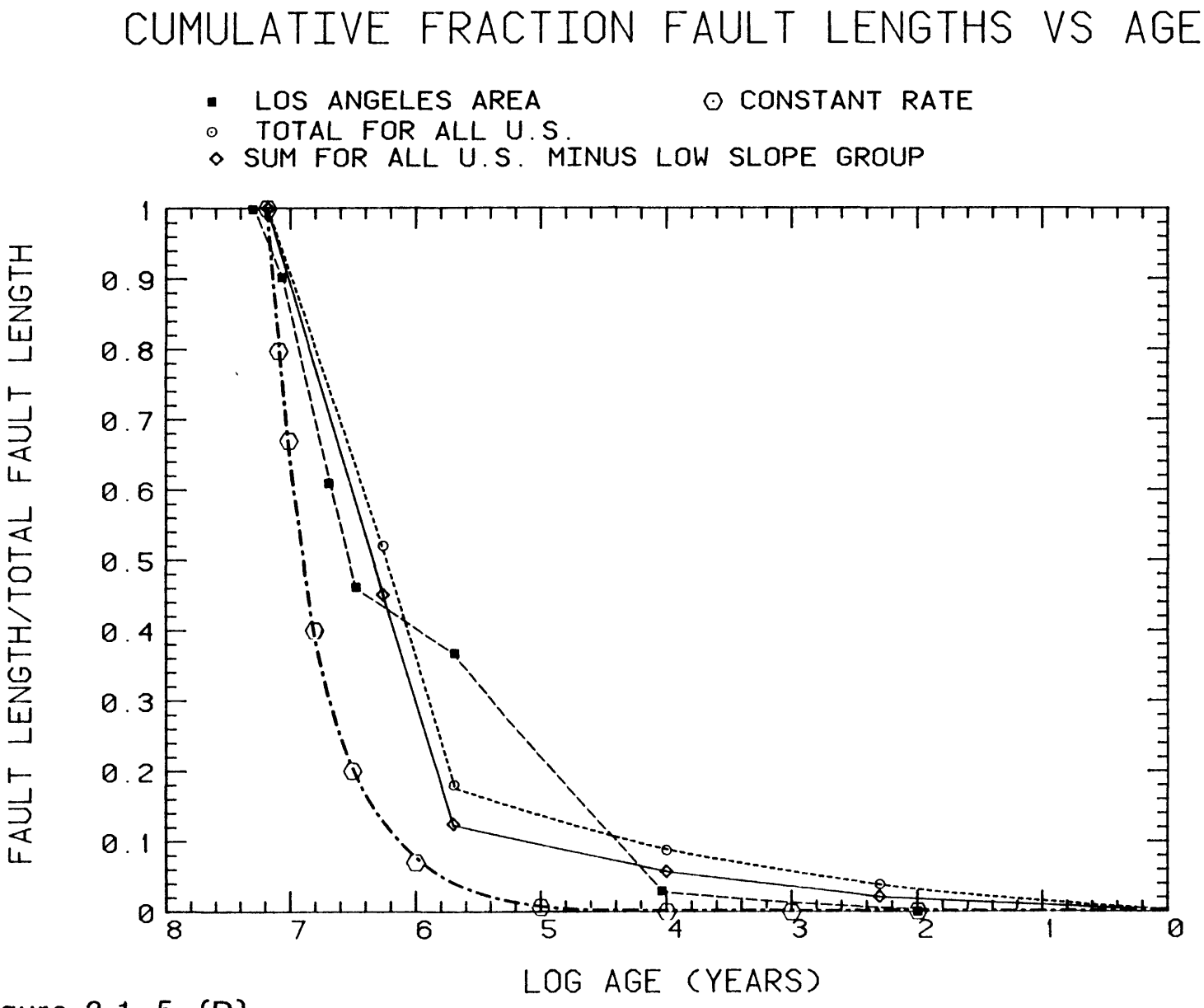
CUMULATIVE FRACTION FAULT LENGTHS VS AGE
LOS ANGELES AREA
CONSTANT RATE
TOTAL FOR ALL U.S.
SUM FOR ALL U.S. MINUS LOW SLOPE GROUP
FAULT LENGTH/TOTAL FAULT LENGTH
1
0.9
0.8
0.7
0.6
0.5
0.4
0.3
0.2
0.1
0
8
7
6
5
4
3
2
1
0
LOG AGE (YEARS)

Figure 3.1.-5. (D)

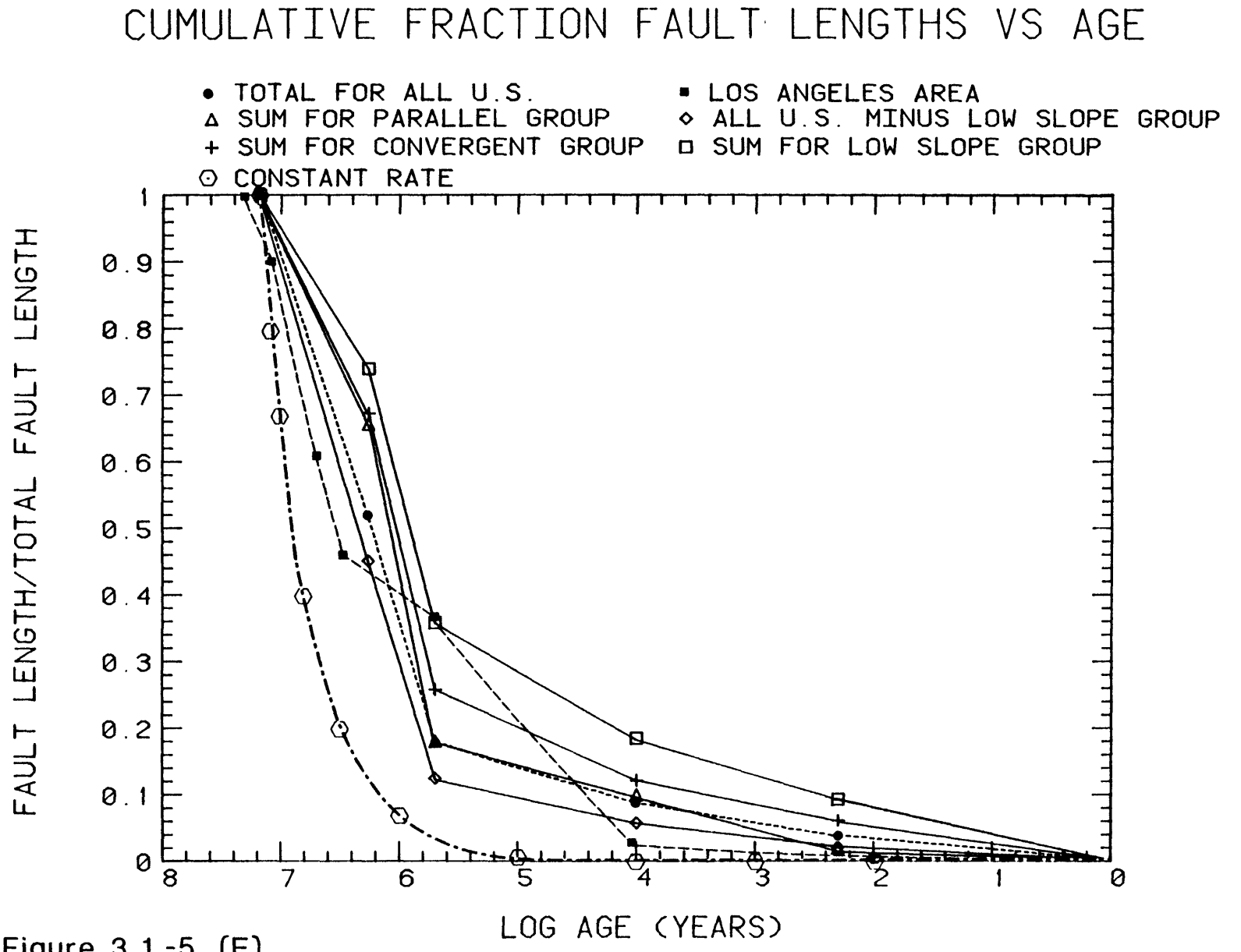
CUMULATIVE FRACTION FAULT LENGTHS VS AGE
• TOTAL FOR ALL U.S.
▪ LOS ANGELES AREA
△ SUM FOR PARALLEL GROUP
◇ ALL U.S. MINUS LOW SLOPE GROUP
+ SUM FOR CONVERGENT GROUP
□ SUM FOR LOW SLOPE GROUP
⊙ CONSTANT RATE
FAULT LENGTH/TOTAL FAULT LENGTH
0
0.1
0.2
0.3
0.4
0.5
0.6
0.7
0.8
0.9
1
8
7
6
5
4
3
2
1
0
LOG AGE (YEARS)

Figure 3.1.-5. (E)

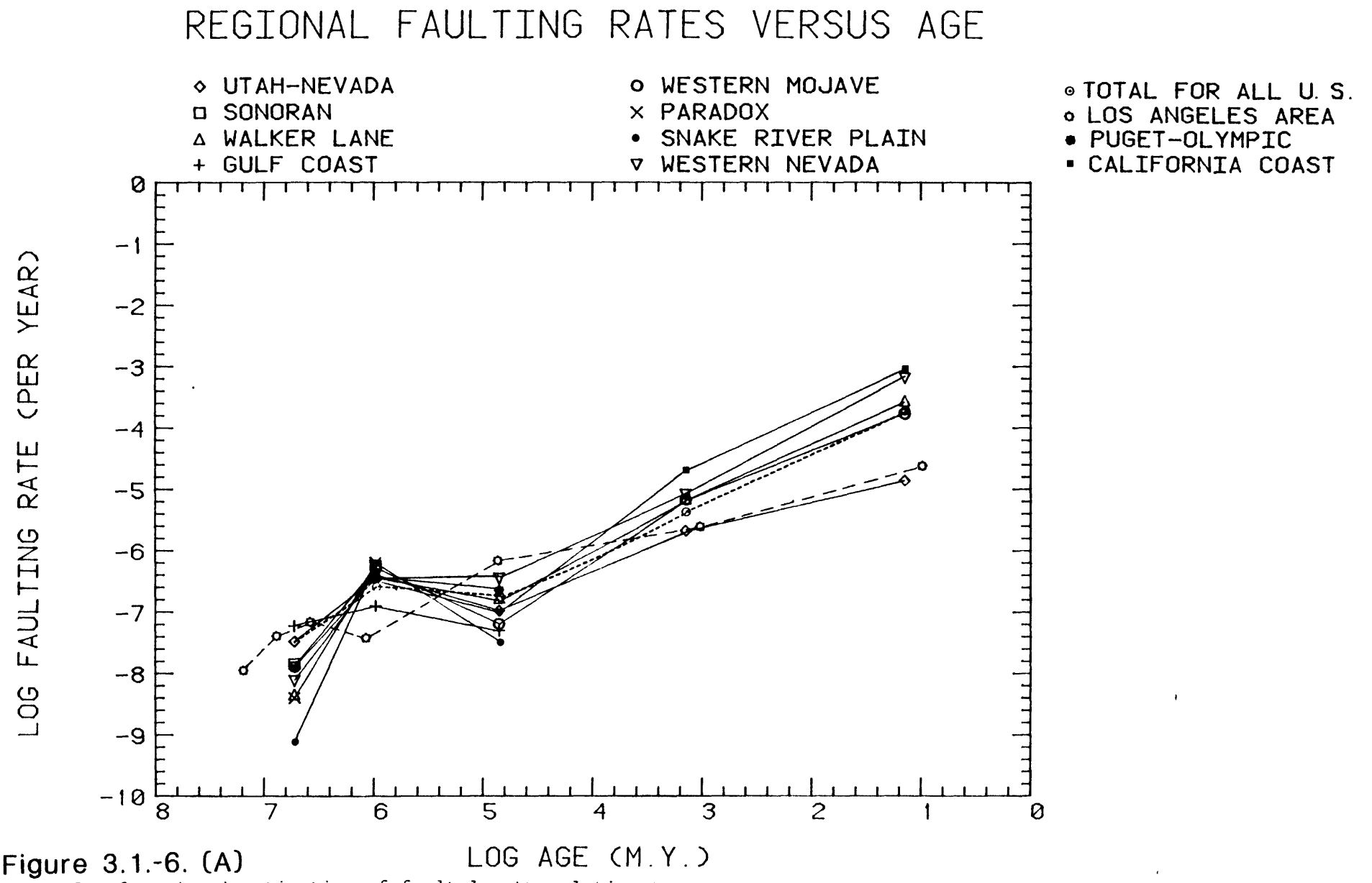

Figure 3.1.-6. (A) Rates for fractional activation of fault length relative to the total activated length in each region.

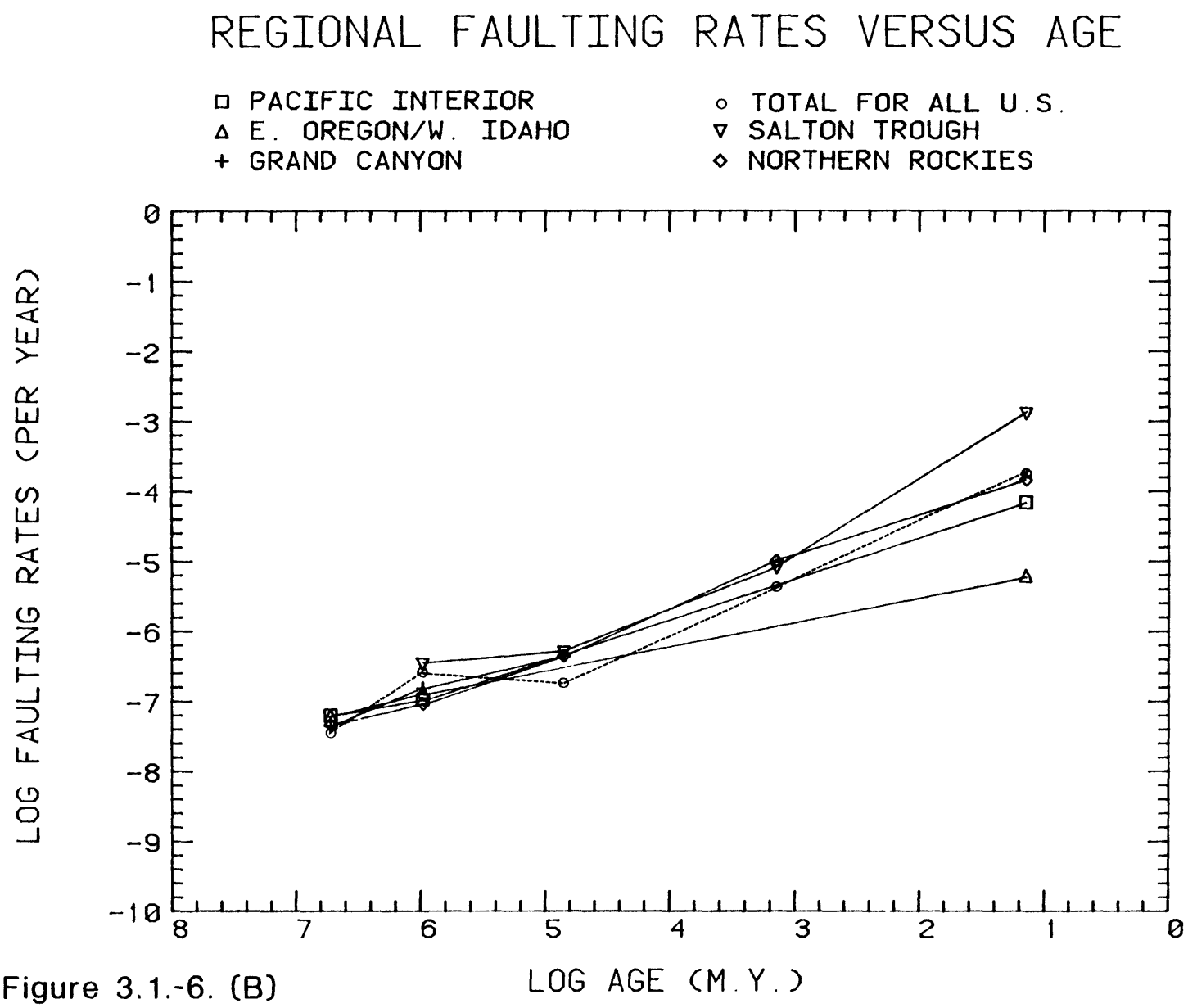
REGIONAL FAULTING RATES VERSUS AGE
□ PACIFIC INTERIOR
△ E. OREGON/W. IDAHO
+ GRAND CANYON
○ TOTAL FOR ALL U.S.
▽ SALTON TROUGH
◇ NORTHERN ROCKIES
LOG FAULTING RATES (PER YEAR)
0
-1
-2
-3
-4
-5
-6
-7
-8
-9
-10
8
7
6
5
4
3
2
1
0
LOG AGE (M.Y.)

Figure 3.1.-6. (B)

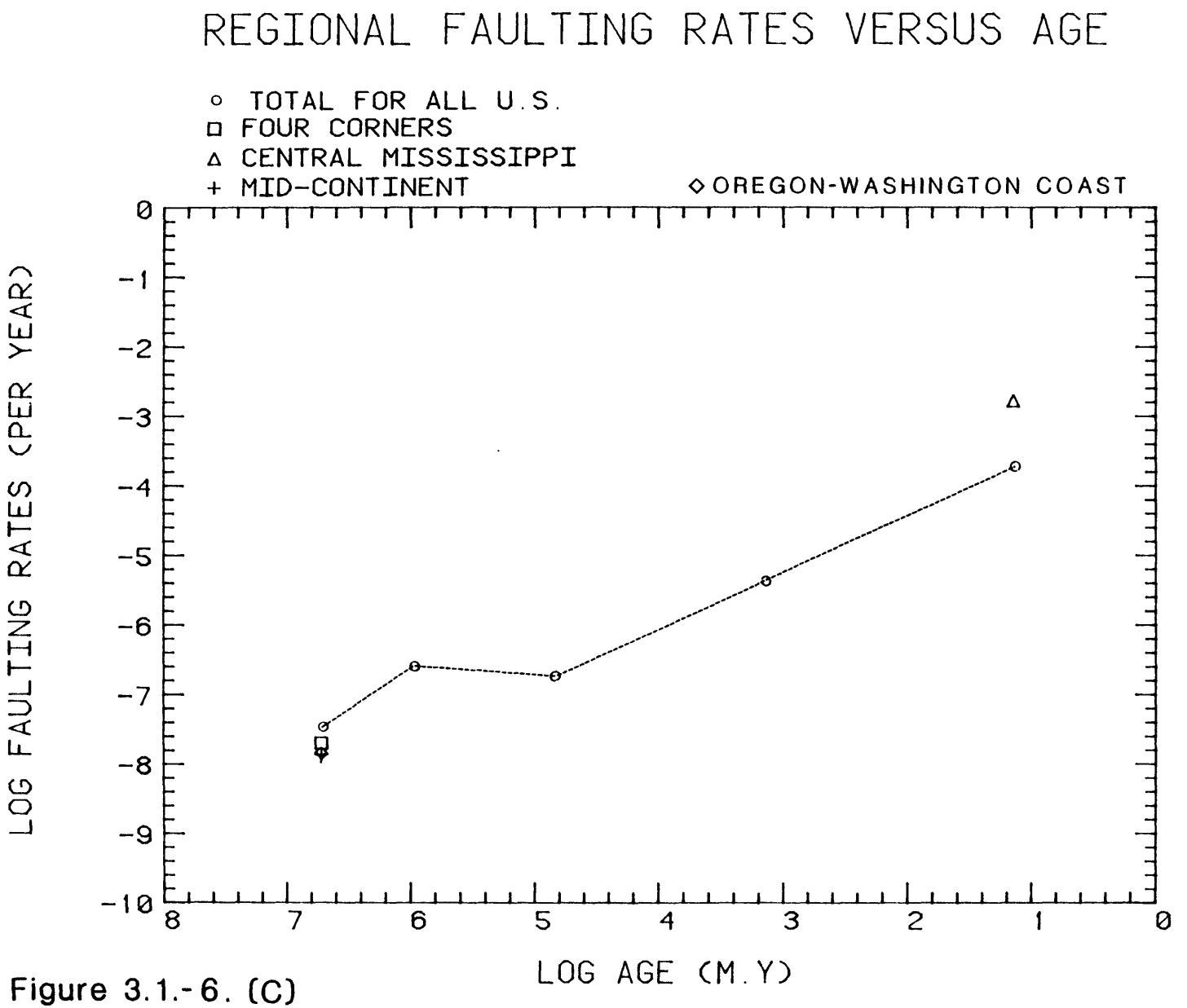
REGIONAL FAULTING RATES VERSUS AGE
○ TOTAL FOR ALL U.S.
□ FOUR CORNERS
△ CENTRAL MISSISSIPPI
+ MID-CONTINENT
◇ OREGON-WASHINGTON COAST
LOG FAULTING RATES (PER YEAR)
0
-1
-2
-3
-4
-5
-6
-7
-8
-9
-10
8
7
6
5
4
3
2
1
0
LOG AGE (M.Y)

Figure 3.1.-6. (C)

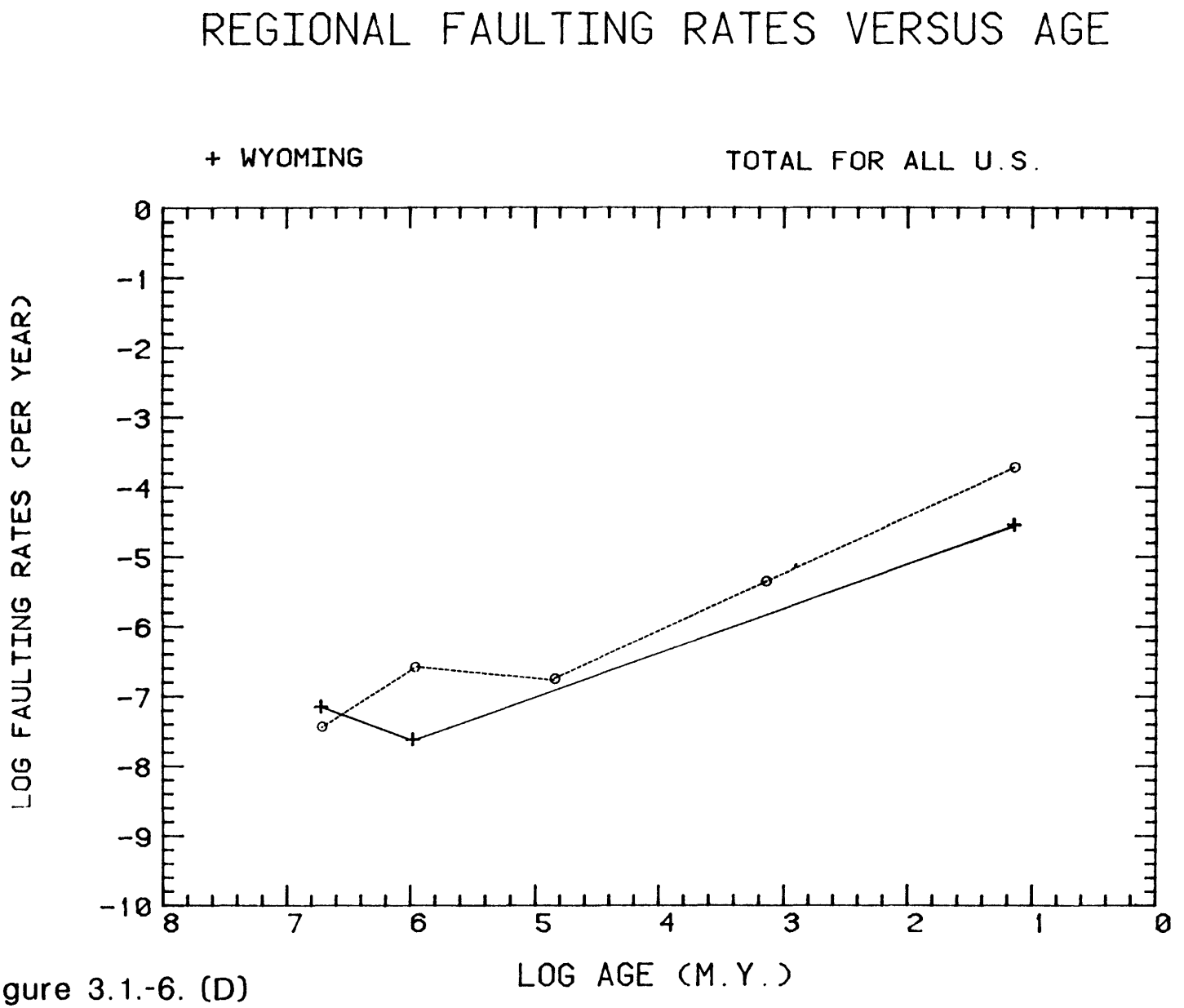
REGIONAL FAULTING RATES VERSUS AGE
+ WYOMING
TOTAL FOR ALL U.S.
LOG FAULTING RATES (PER YEAR)
0
-1
-2
-3
-4
-5
-6
-7
-8
-9
-10
8
7
6
5
4
3
2
1
0
LOG AGE (M.Y.)

Figure 3.1.-6. (D)

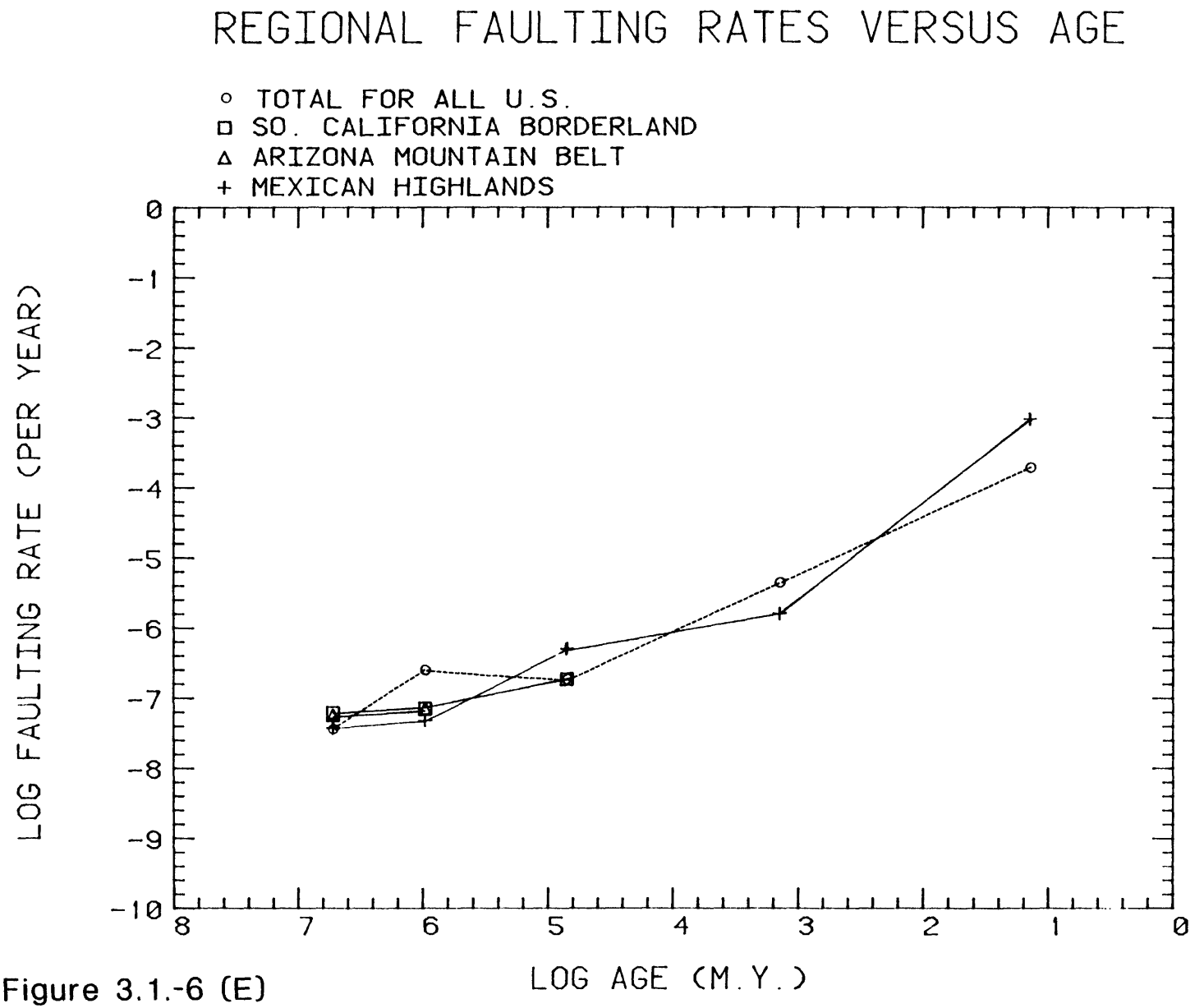
REGIONAL FAULTING RATES VERSUS AGE
TOTAL FOR ALL U.S.
SO. CALIFORNIA BORDERLAND
ARIZONA MOUNTAIN BELT
MEXICAN HIGHLANDS
LOG FAULTING RATE (PER YEAR)
0
-1
-2
-3
-4
-5
-6
-7
-8
-9
-10
8
7
6
5
4
3
2
1
0
LOG AGE (M.Y.)

Figure 3.1.-6 (E)

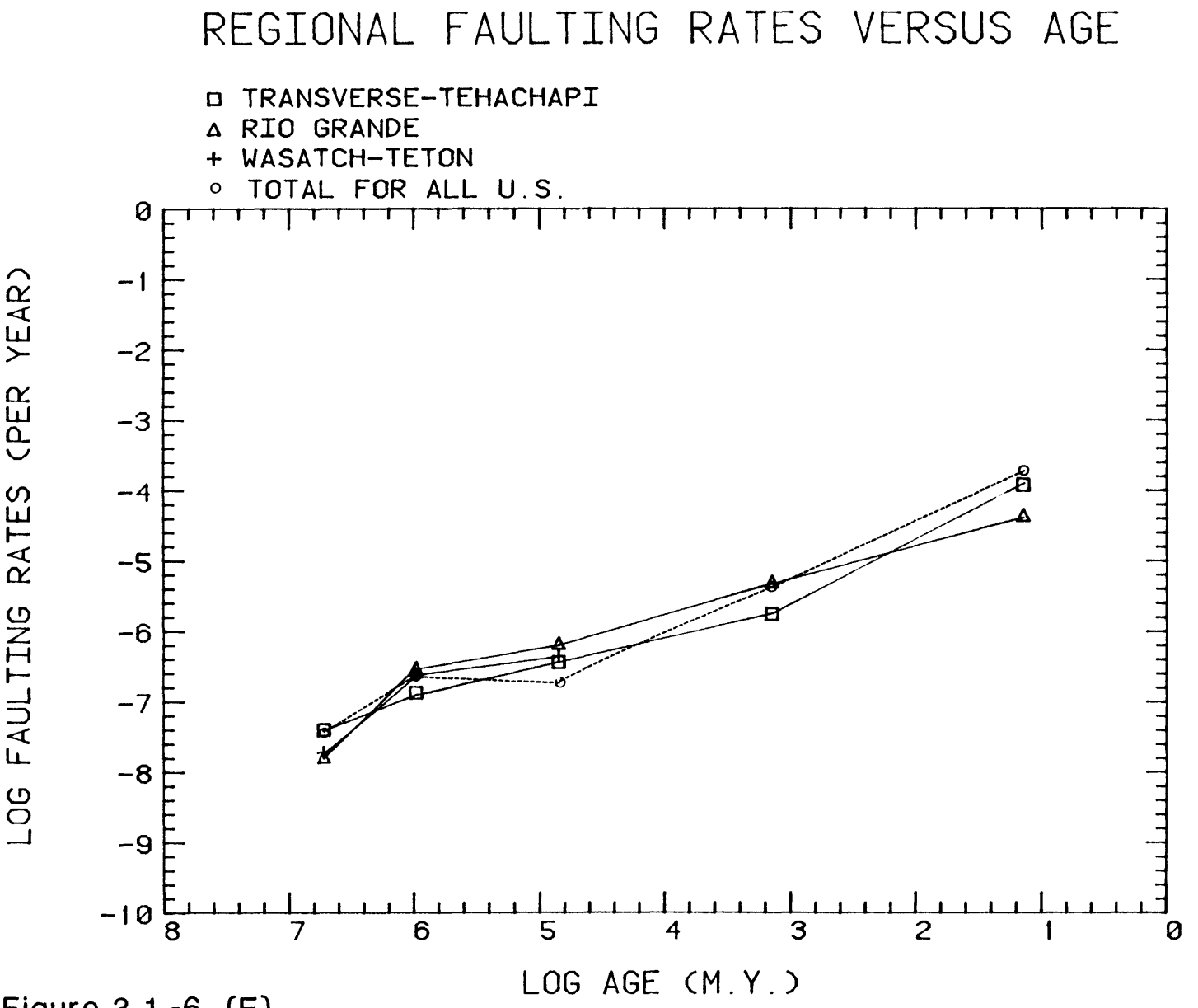
REGIONAL FAULTING RATES VERSUS AGE
TRANSVERSE-TEHACHAPI
RIO GRANDE
WASATCH-TETON
TOTAL FOR ALL U.S.
LOG FAULTING RATES (PER YEAR)
0
-1
-2
-3
-4
-5
-6
-7
-8
-9
-10
8
7
6
5
4
3
2
1
0
LOG AGE (M.Y.)

Figure 3.1.-6. (F)

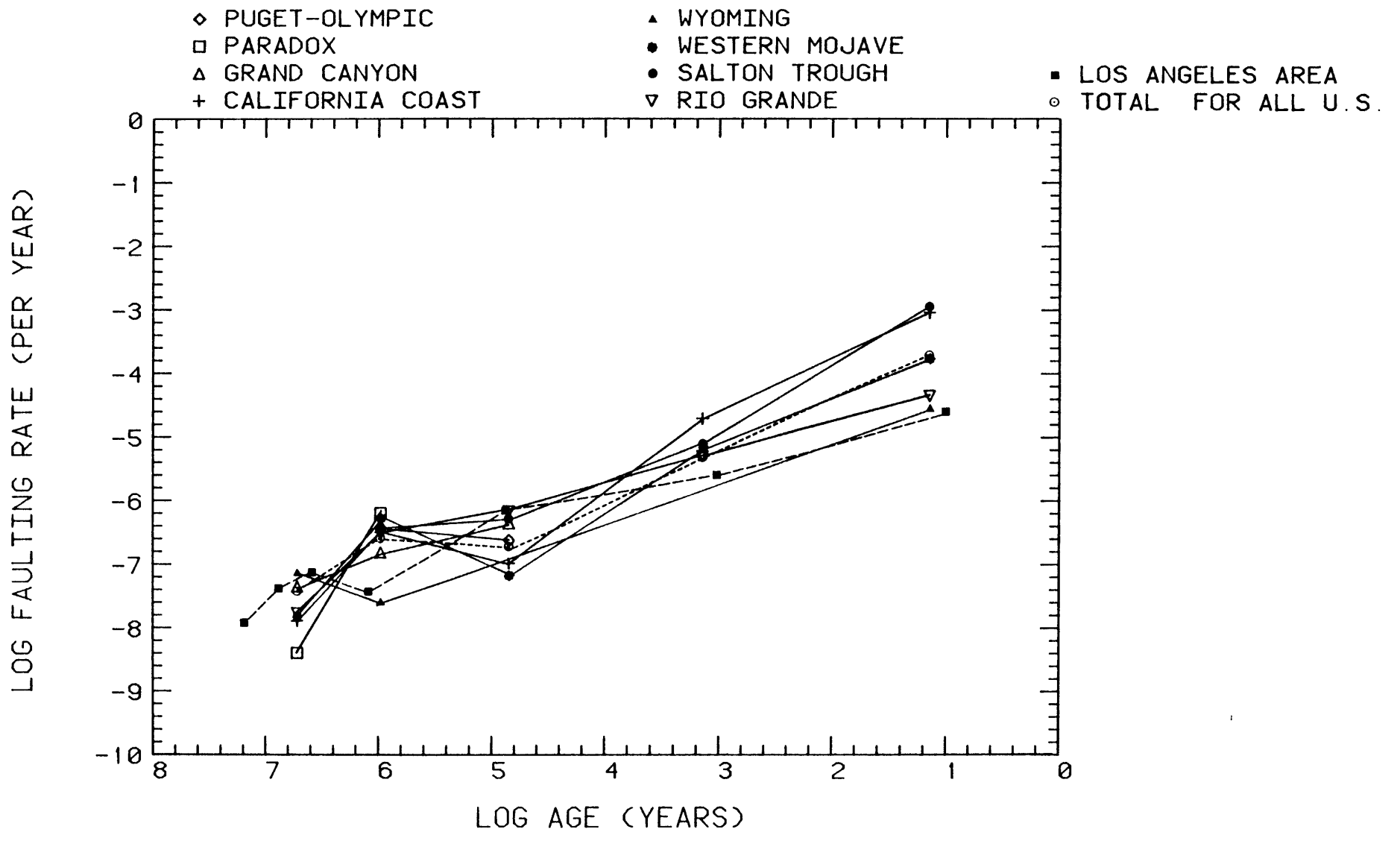

Figure 3.1.-7.

Rates for fractional activation of fault length relative to the total activated length in "low slope" group.

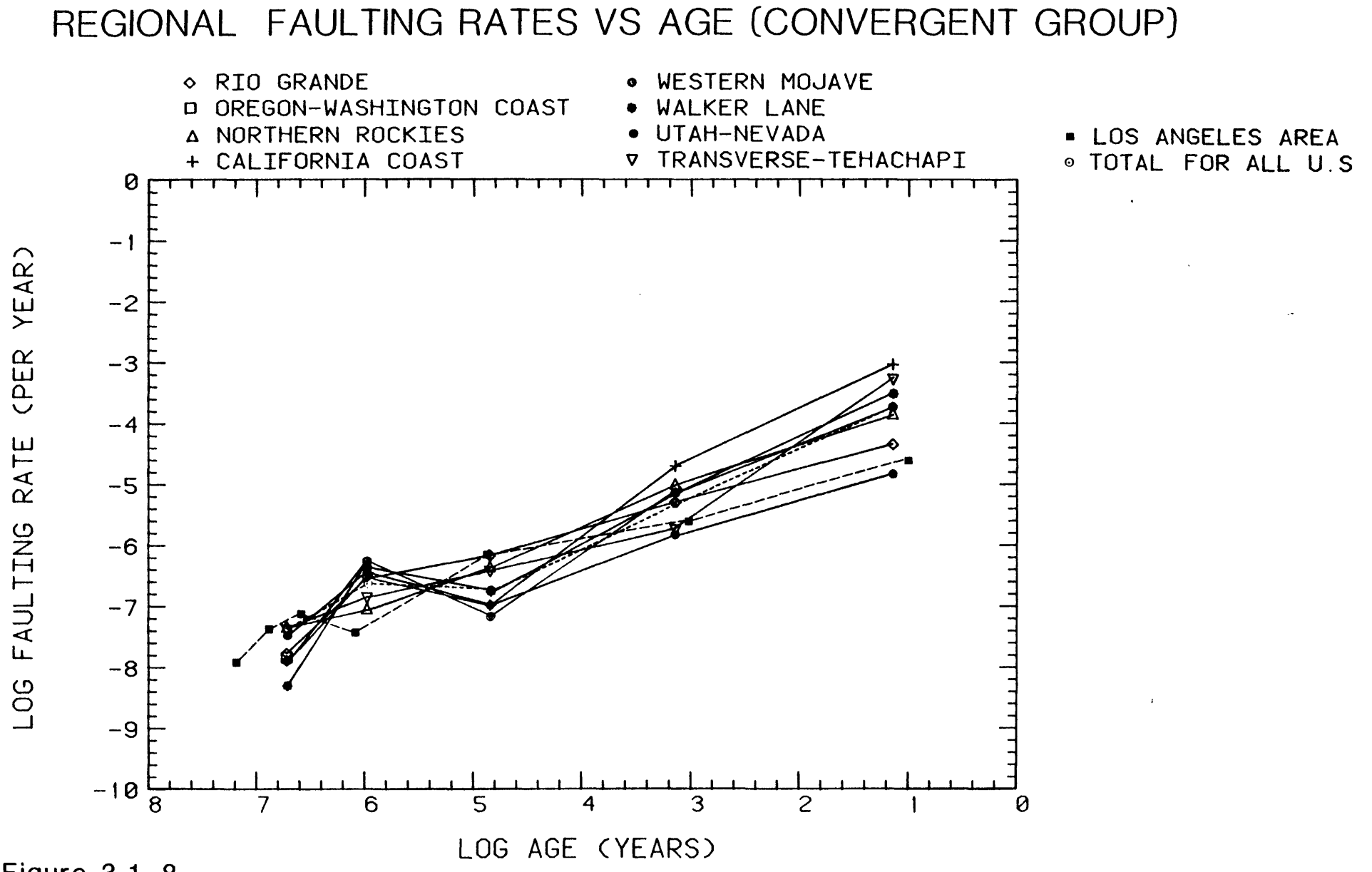

Figure 3.1.-8.
Rates for fractional activation of fault length relative to the total activated length in "convergent" group.

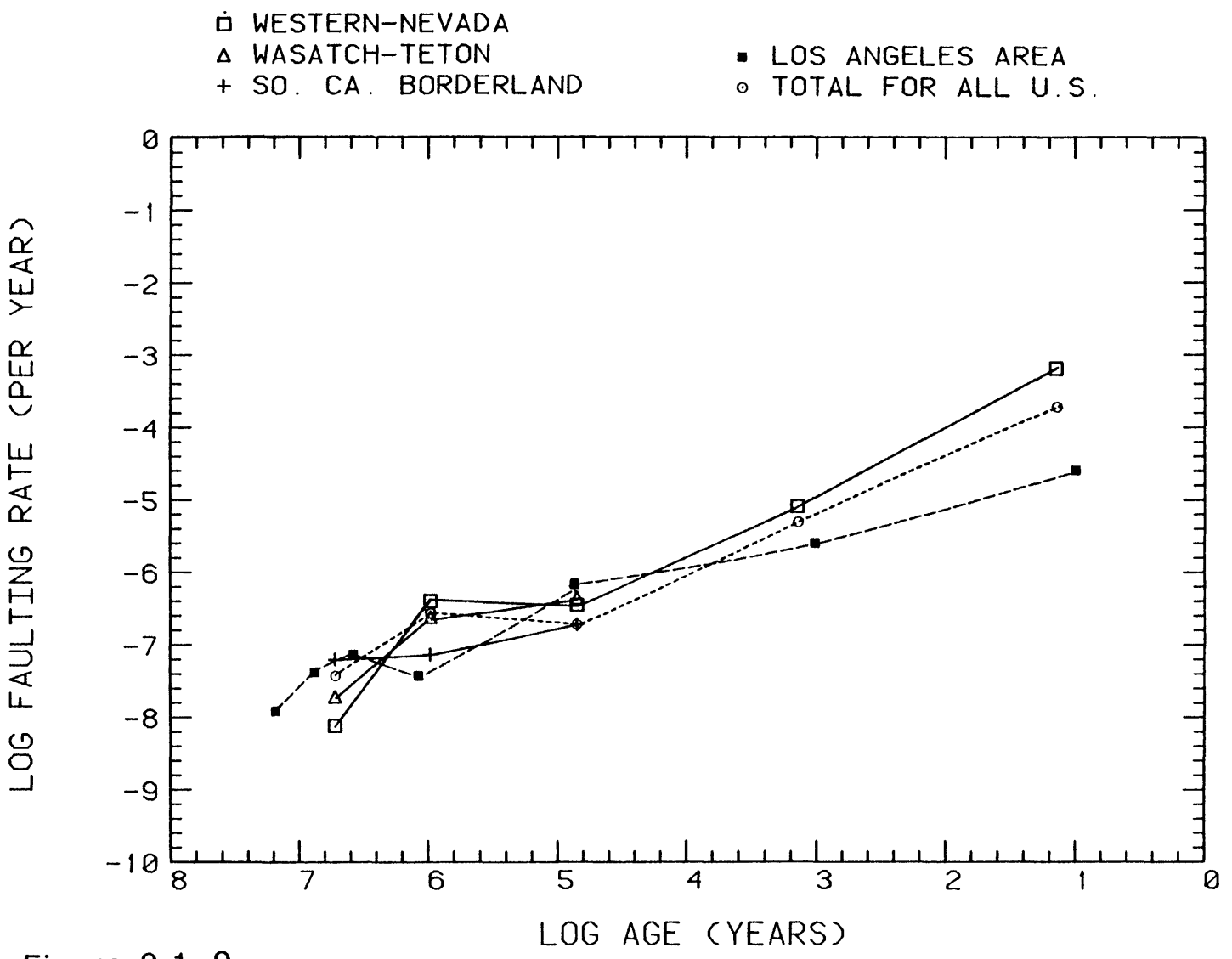

Figure 3.1.-9.
Rates for fractional activation of fault length relative to the total activated length in "parallel" group.

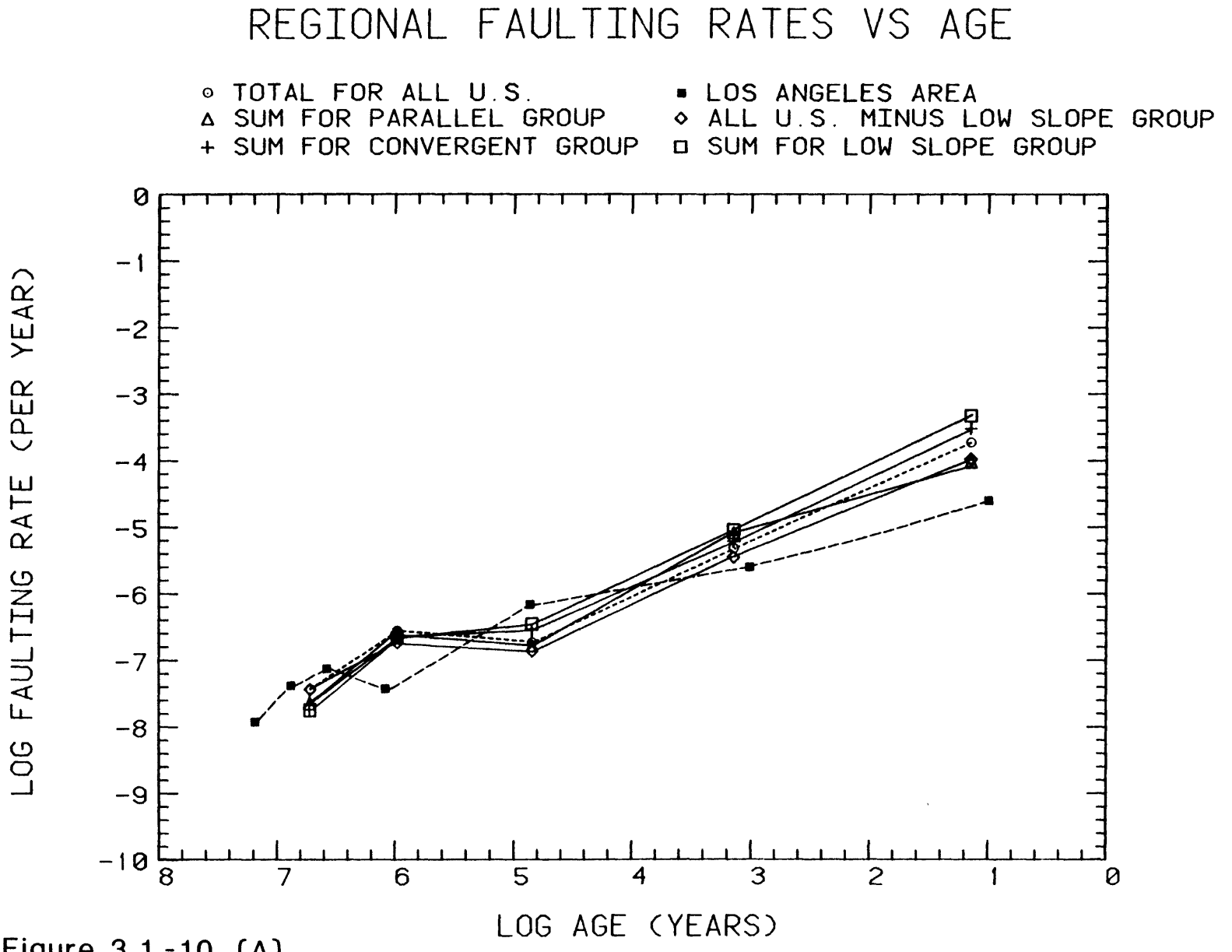

Figure 3.1.-10. (A)
Rates for fractional activation of fault length relative to the total activated length; summations for each subgroup.

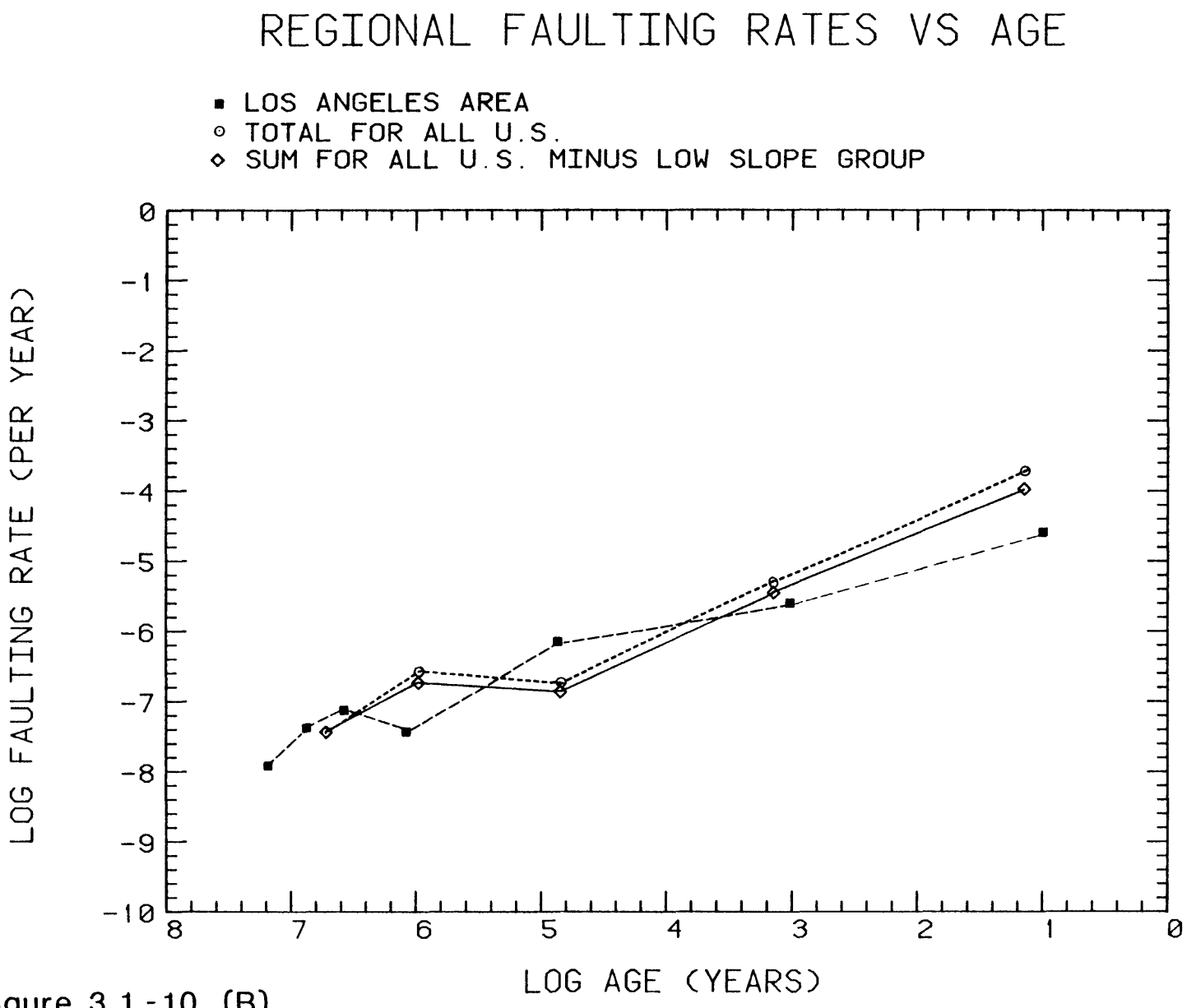

Figure 3.1.-10. (B)

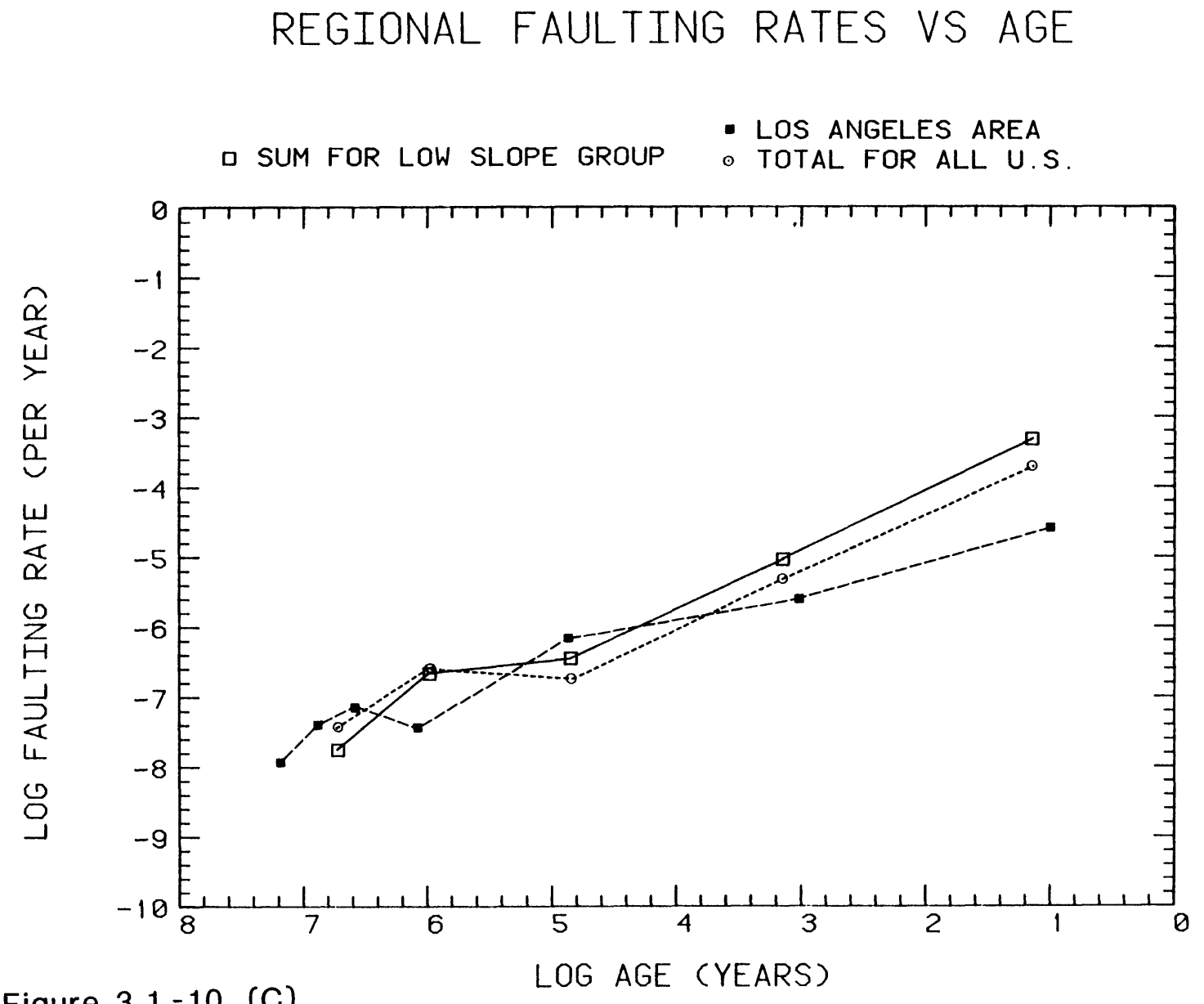

Figure 3.1.-10. (C)

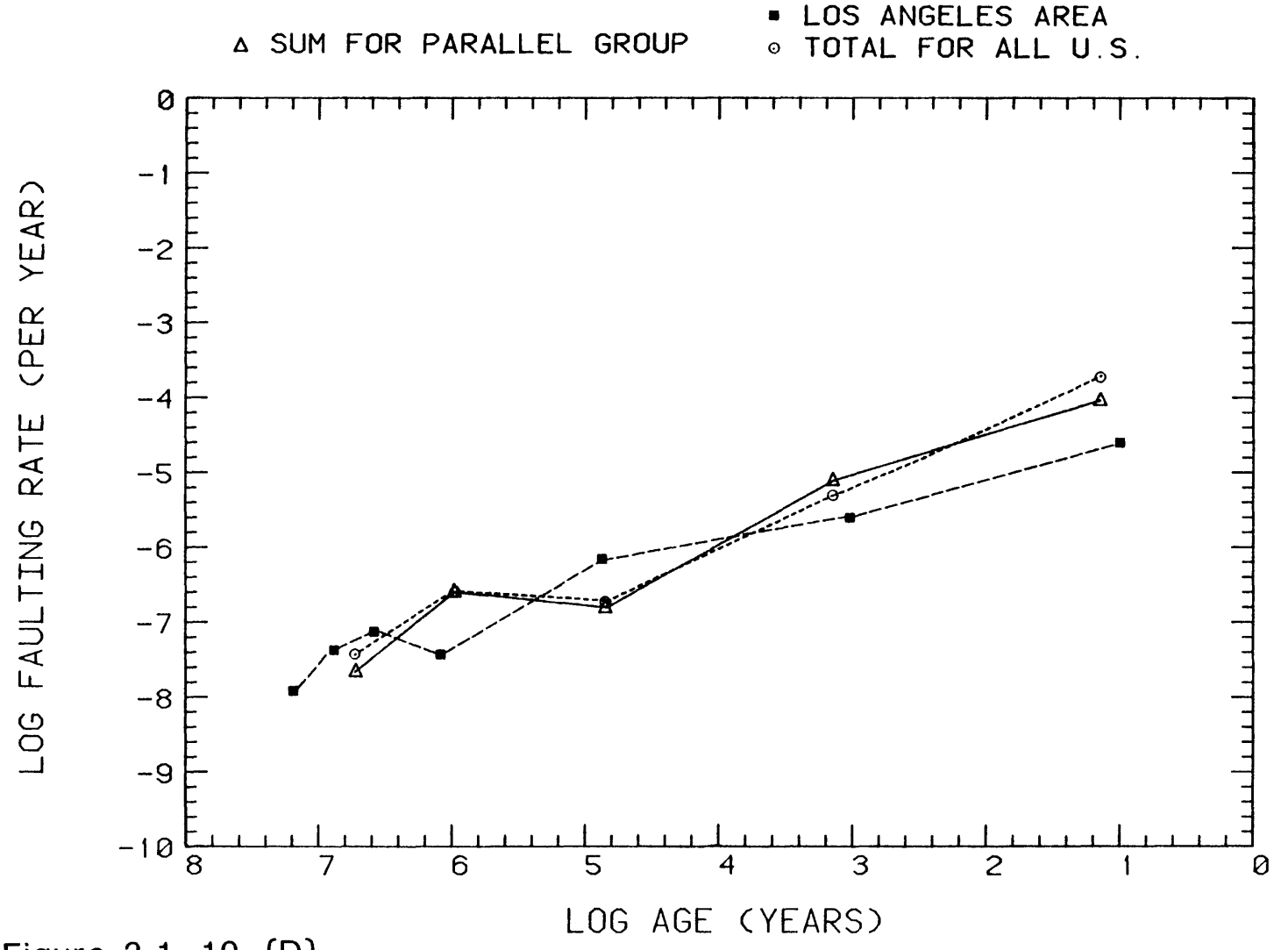

Figure 3.1.-10. (D)

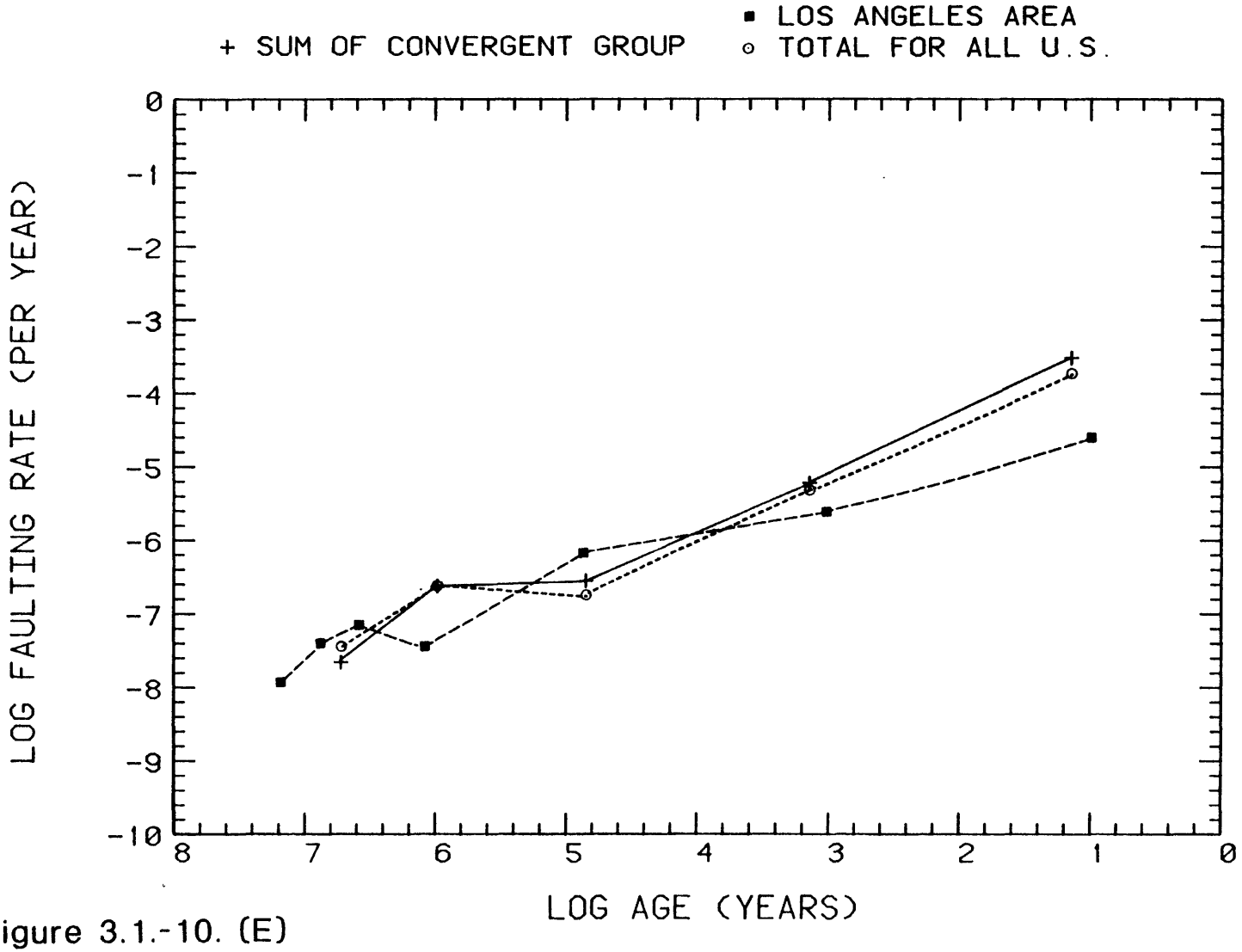

Figure 3.1.-10. (E)

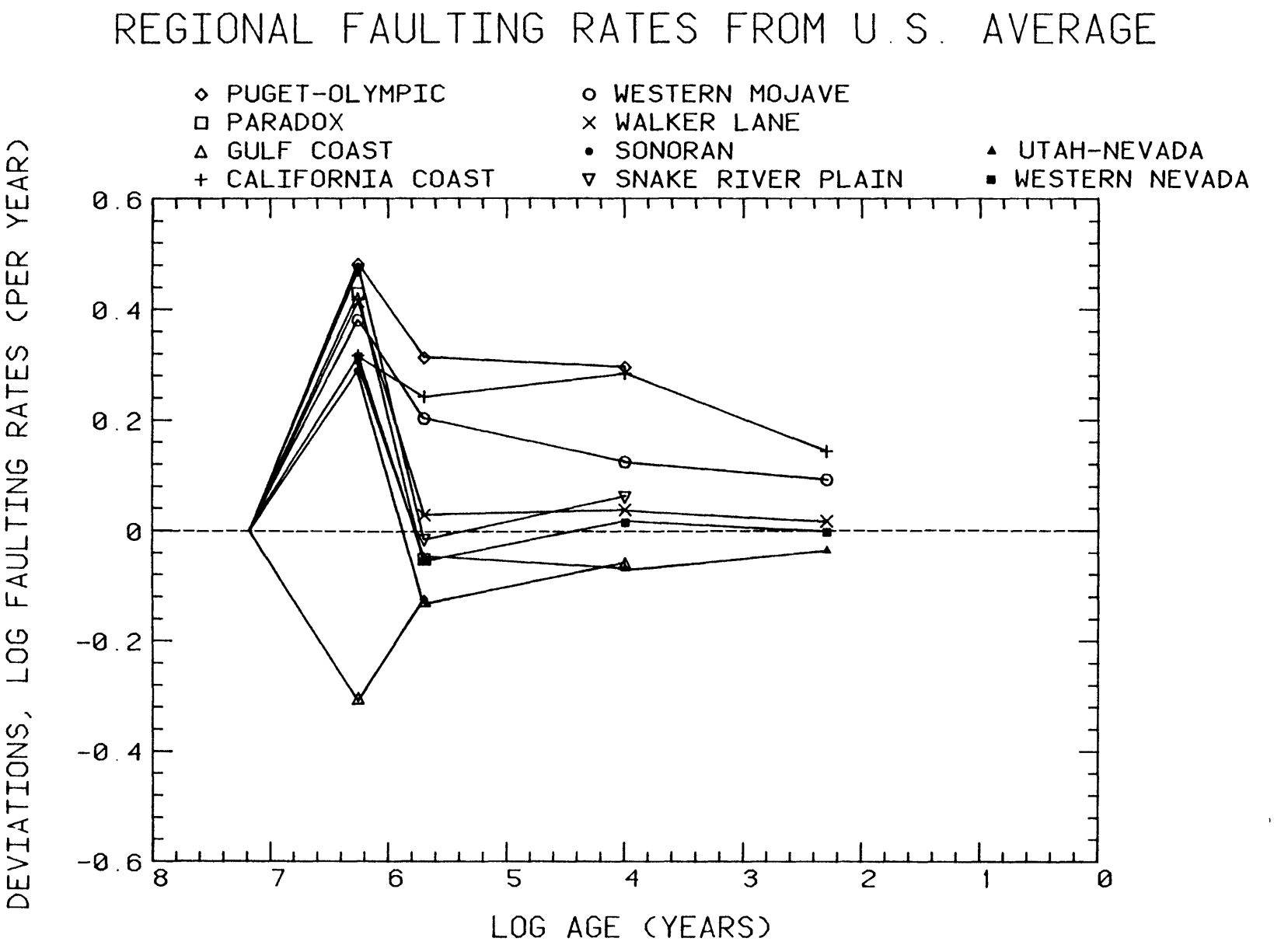

Figure 3.1.-11. (A)
Deviation plots showing the differences between the fractional activation rates by region and the overall fractional activation rates for the conterminous United States.

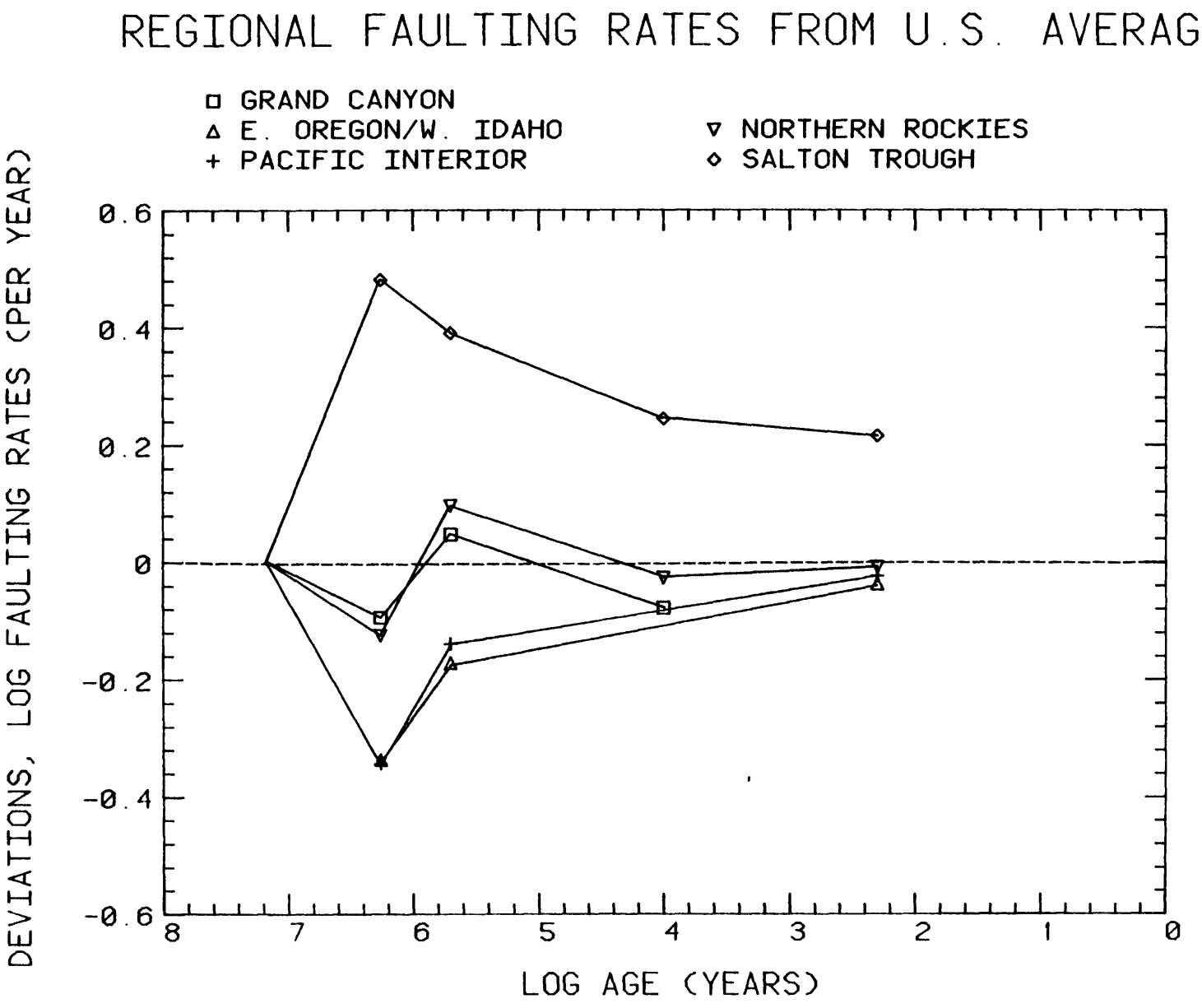

Figure 3.1.-11. (B)

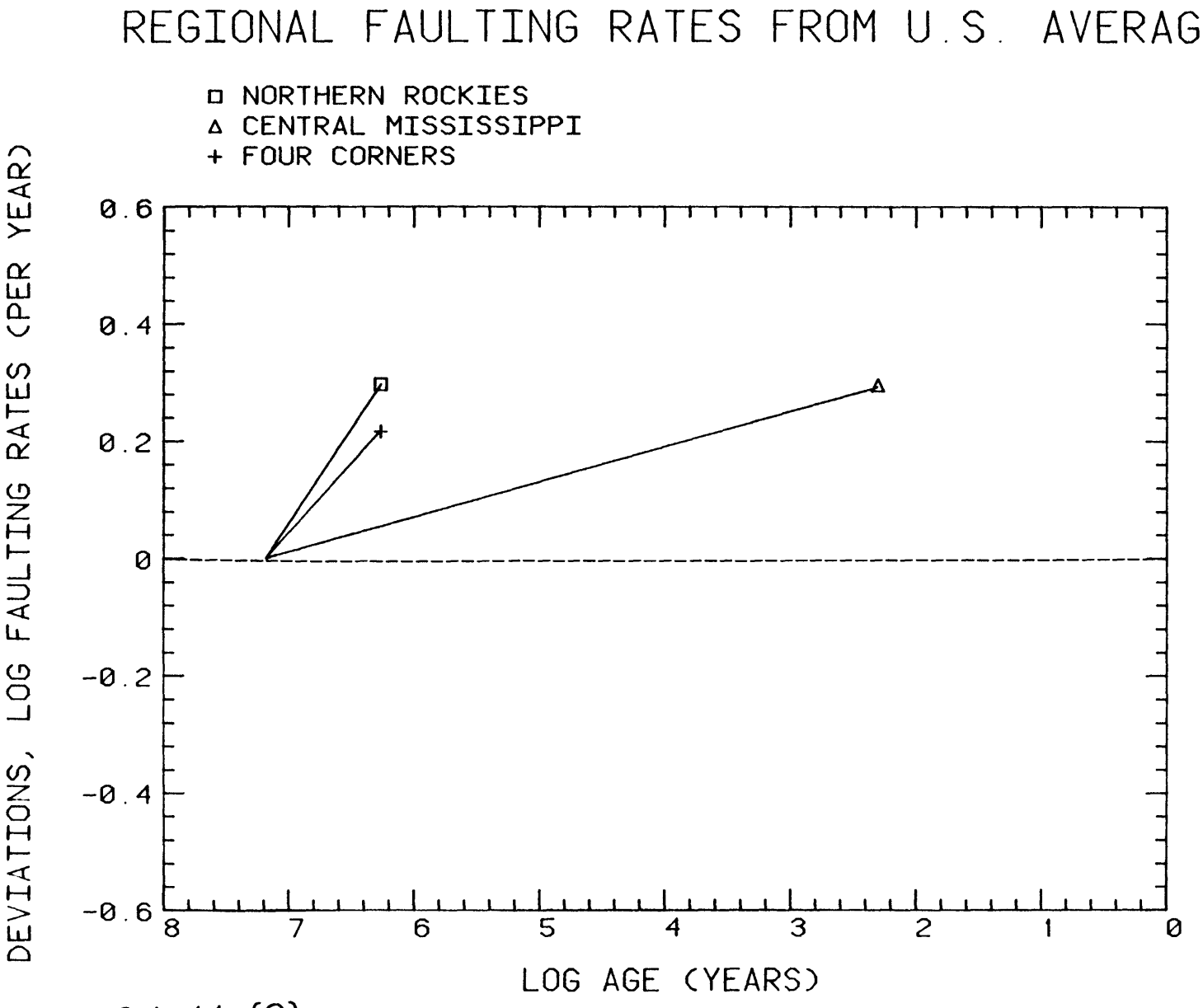

Figure 3.1.-11. (C)

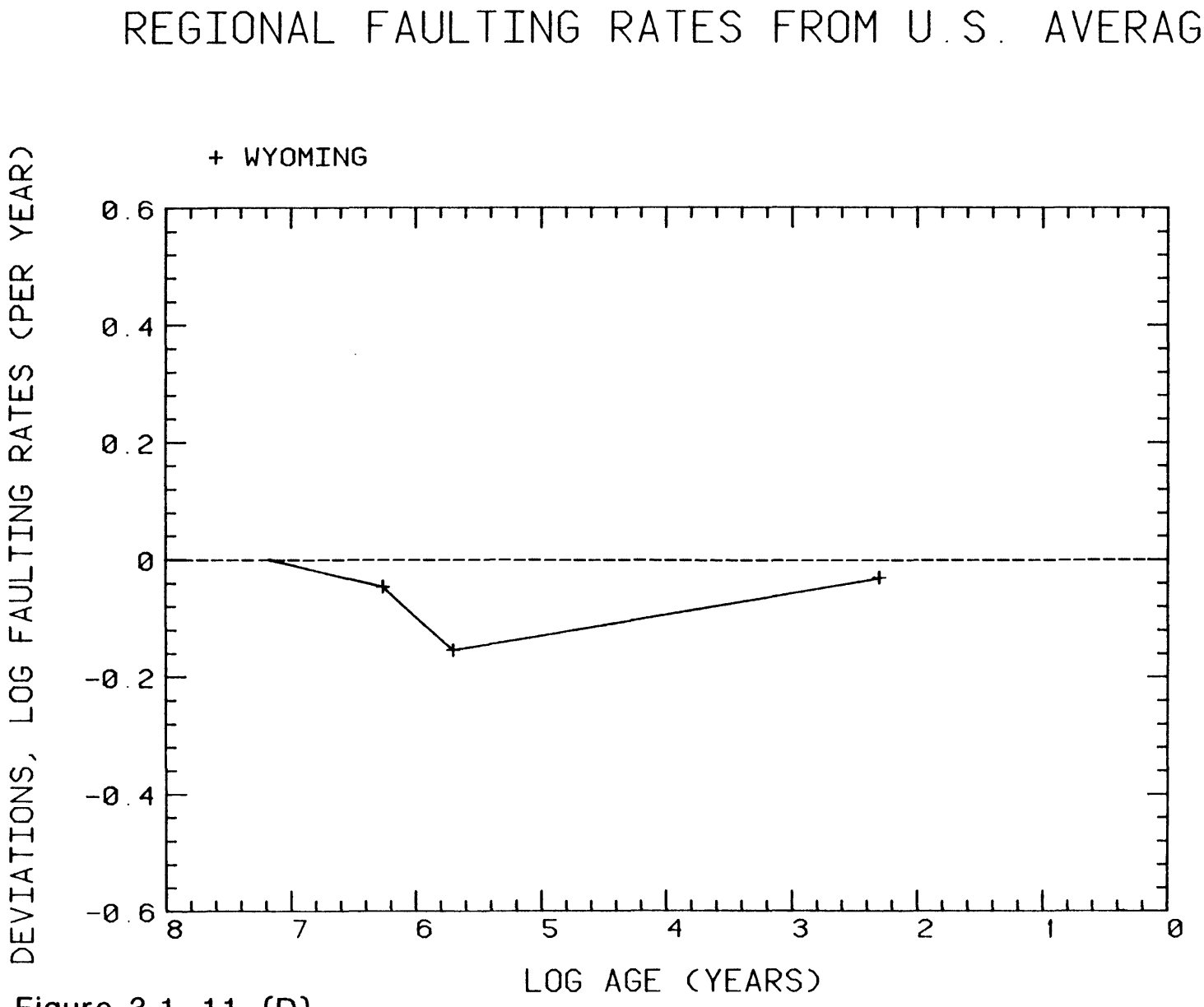

Figure 3.1.-11. (D)

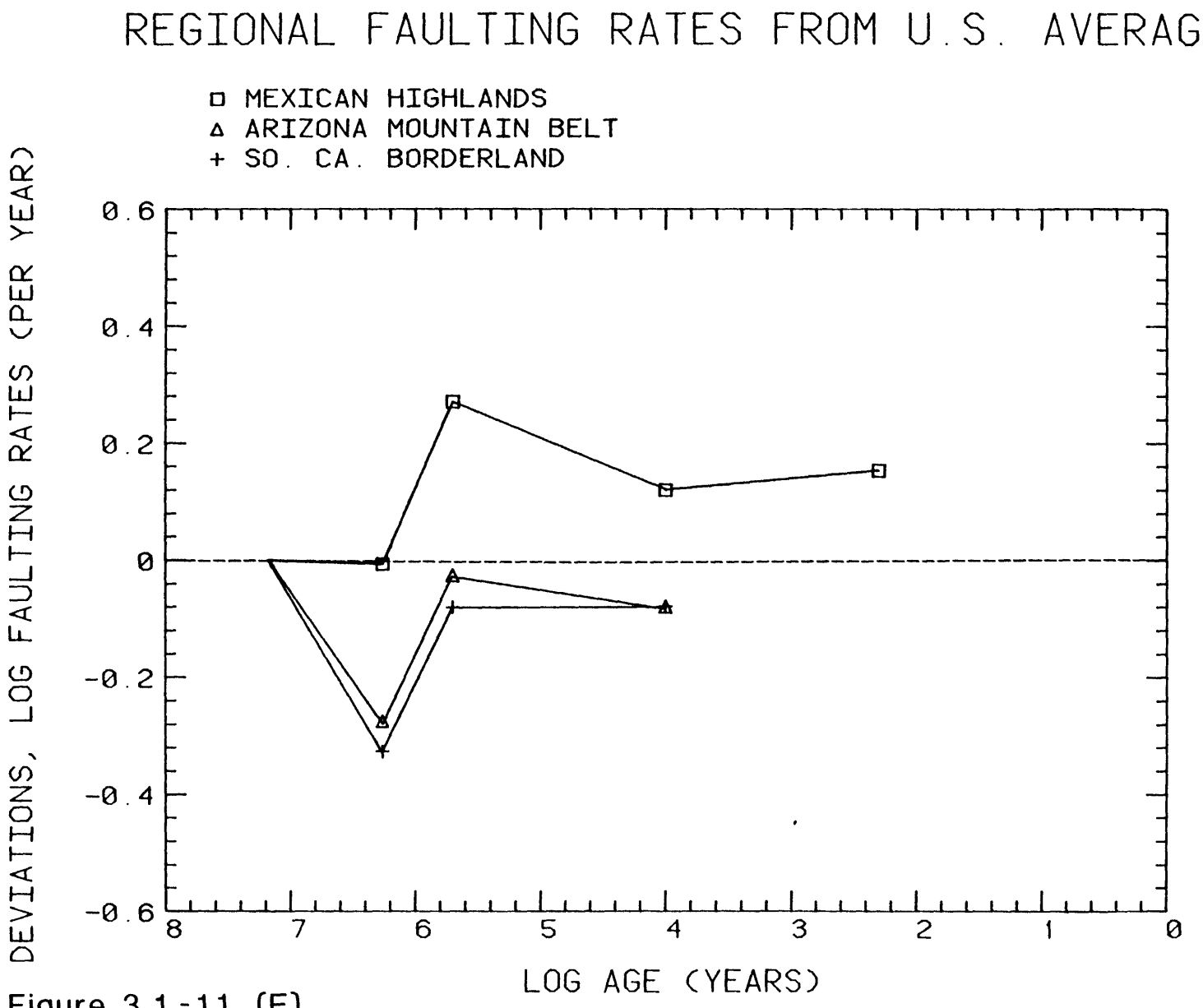

Figure 3.1.-11. (E)

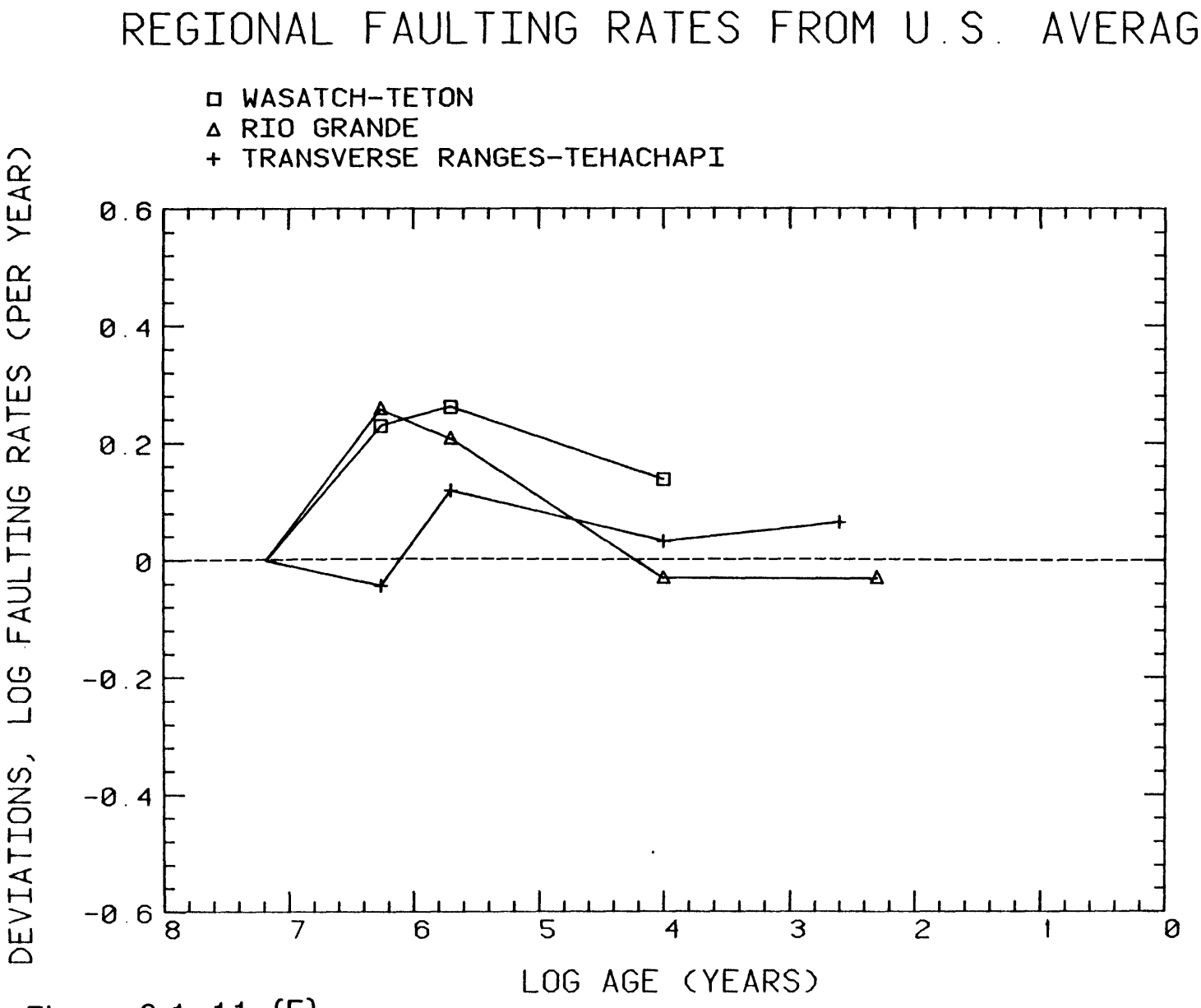

Figure 3.1.-11. (F)

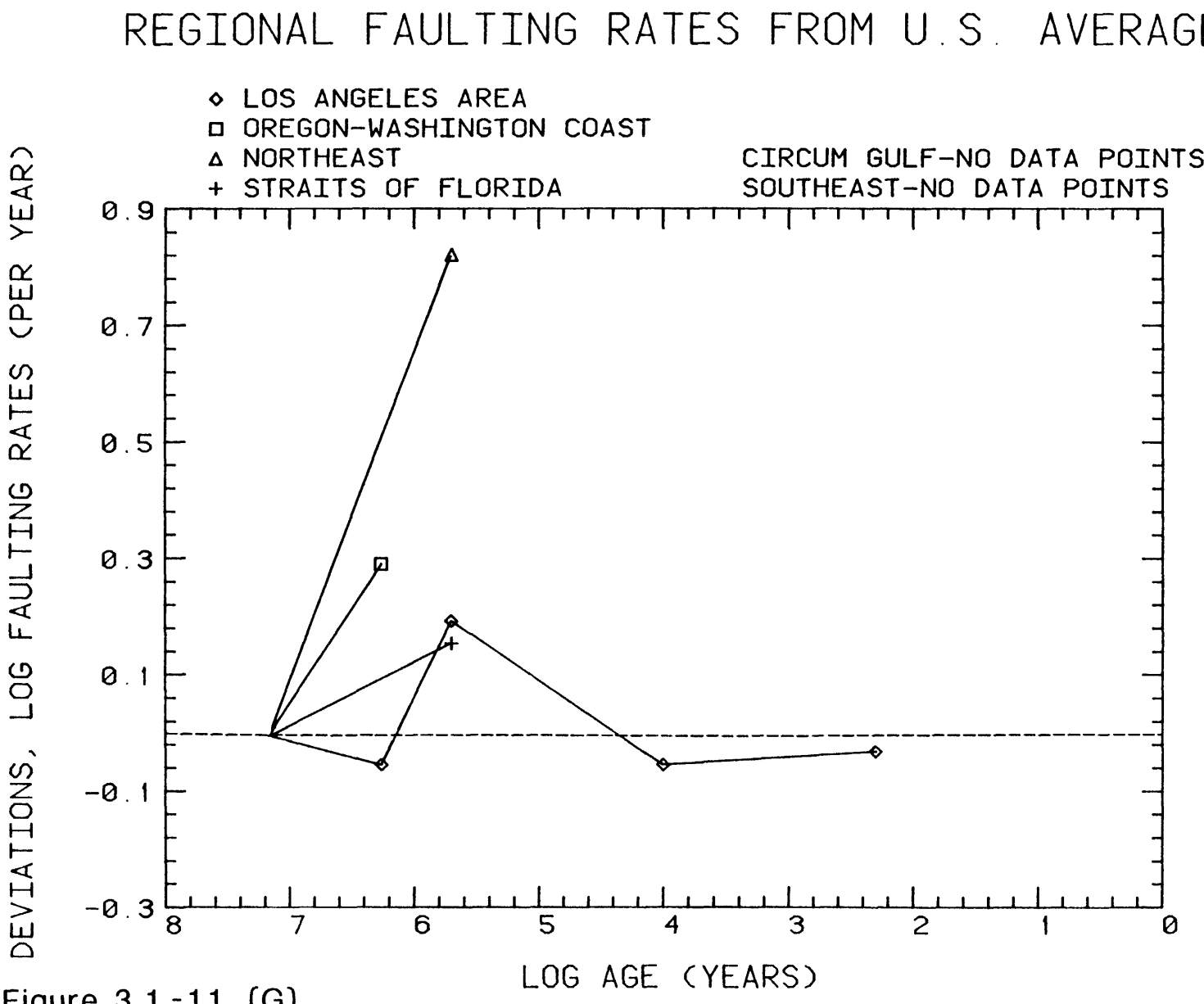

Figure 3.1.-11. (G)

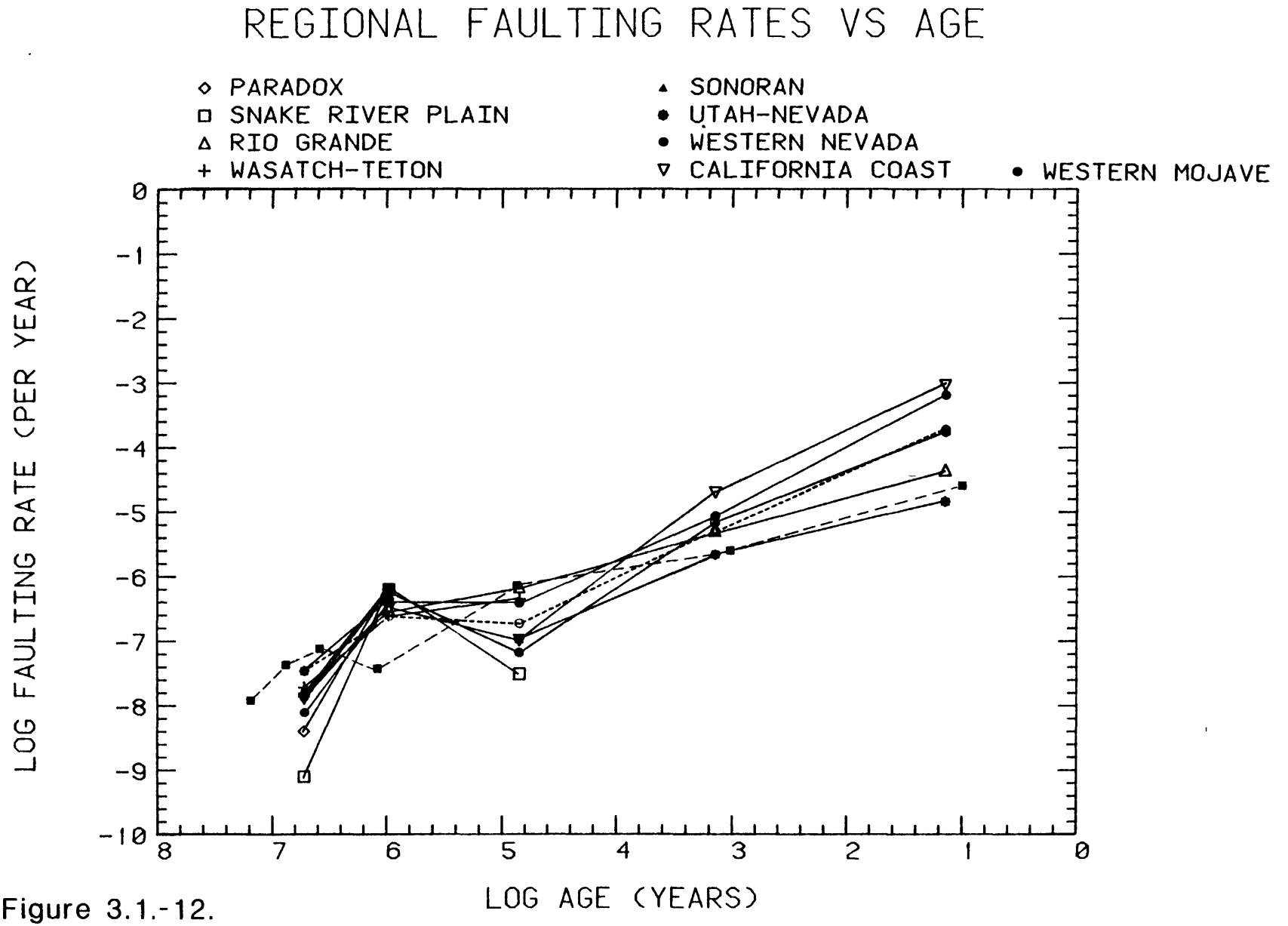

Figure 3.1.-12.
Fractional activation rates compared for those regions having rate reversals at an age of the order 10^6 years.

Table 3.1.-1 Activation lengths per age group[1/] (cm are for map scale 1:5,000,000)

Region no. and name		(200 yr)	(10,000 yr)	(0.5 m.y.)	(1.8 m.y.)	(15 m.y.)	total
1 Arizona Mountain Belt	A[2/]	--	0.18	3.35	2.10	17.41	23.04
	B[3/]	--	23.04	22.86	19.51	17.41	23.04
	C[4/]	--	7.8x10-3	0.15	0.09	0.76	1.01
	D[5/]	--	7.8x10-3	0.15	0.24	1.00	1.00
2 California Coast	A	18.69	19.56	5.24	42.67	17.03	103.19
	B	103.19	84.50	64.94	59.70	17.03	103.19
	C	0.18	0.19	0.05	0.41	0.17	1.00
	D	0.18	0.37	0.42	0.83	1.00	1.00
3 Central Mississippi Valley	A	2.34	--	--	--	4.66	7.00
	B	7.00	--	--	--	4.66	7.00
	C	0.33	--	--	--	0.67	1.00
	D	0.33	--	--	--	1	1.00
4 Circum-Gulf	A	--	--	--	--	0.74	0.74
	B	--	--	--	--	0.74	0.74
	C	--	--	--	--	1.00	1.00
	D	--	--	--	--	1.00	1.00
5 Eastern Oregon-Western Idaho	A	0.20	--	0.88	28.49	132.84	162.41
	B	162.41	--	162.21	161.33	132.84	162.41
	C	1.2x10-3	--	5.4x10-3	0.18	0.82	1.01
	D	1.2x10-3	--	6.7x10-3	0.18	1.0	1.00
6 Four Corners	A	--	--	--	3.22	1.16	4.38
	B	--	--	--	4.38	1.16	4.38
	C	--	--	--	0.74	0.26	1.00
	D	--	--	--	0.74	1.00	1.00
7 Grand Canyon	A	--	0.22	4.93	4.51	13.09	22.75
	B	--	22.75	22.53	17.60	13.09	22.75
	C	--	9.7x10-3	0.22	0.20	0.58	1.01
	D	--	9.7x10-3	0.23	0.43	1.00	1.00
8 Gulf Coast	A	--	6.73	6.2	41.04	197.68	251.65
	B	--	251.65	244.92	238.72	197.68	251.65
	C	--	2.7x10-2	2.5x10-2	0.16	0.79	1.00
	D	--	2.7x10-2	5.1x10-2	0.21	1.00	1.00
9 Mexican Highland	A	1.69	0.14	2.15	0.55	4.31	8.84
	B	8.84	7.15	7.01	4.86	4.31	8.84
	C	0.19	0.02	0.24	0.06	0.49	1.00
	D	0.19	0.20	0.45	0.51	1.00	1.00
10 Mid-continent	A	--	--	--	1.51	0.34	1.85
	B	--	--	--	1.85	0.34	1.85
	C	--	--	--	0.82	0.18	1.00
	D	--	--	--	0.82	1.00	1.00
11 Northeast	A	--	--	0.84	--	--	0.84
	B	--	--	0.84	--	--	0.84
	C	--	--	1.00	--	--	1.00
	D	--	--	1.00	--	--	1.00
12 Northern Rockies	A	2.36	2.45	17.36	9.65	48.86	80.68
	B	80.68	78.32	75.87	58.51	48.86	80.68
	C	0.03	0.03	0.22	0.12	0.61	1.01
	D	0.03	0.06	0.28	0.39	1.00	1.00
13 Oregon-Washington Coast	A	--	--	--	35.95	8.5	44.45
	B	--	--	--	44.45	8.5	44.45
	C	--	--	--	0.81	0.19	1.00
	D	--	--	--	0.81	1.00	1.00
14 Pacific Interior	A	0.38	--	0.71	3.77	22.88	27.74
	B	27.74	--	27.36	26.65	22.88	27.74
	C	0.01	--	0.03	0.14	0.82	1.00
	D	0.01	--	0.04	0.18	1.00	1.00

1/Fault lengths showing movement younger than the indicated age.
2/Length measured on U.S. map at 1:5,000,000 (Howard and others, 1978); to get fault lengths in kilometers, multiply by 50.
3/Cumulative length of faults showing movement, from oldest to youngest age.
4/Fraction of total length in each age group.
5/Cumulative fraction of faults showing movement, from youngest to oldest age.

Region no. and name		(200 yr)	(10,000 yr)	(0.5 m.y.)	(1.8 m.y.)	(15 m.y.)	total
	A[2]	--	--	1.49	9.59	0.62	11.70
15 Paradox	B[3]	--	--	11.70	10.21	0.62	11.70
	C[4]	--	--	0.13	0.82	0.05	1.00
	D[5]	--	--	0.13	0.95	1.00	1.00
	A	--	1.94	0.6	2.54	--	5.08
16 Puget-Olympic	B	--	5.08	3.14	2.54	--	5.08
	C	--	0.38	0.12	0.50	--	1.00
	D	--	0.38	0.50	1.00	--	1.00
	A	0.95	5.27	35.11	41.67	23.62	106.62
17 Rio Grande	B	106.62	105.67	100.40	65.29	23.62	106.62
	C	8.91x10-3	0.05	0.33	0.40	0.22	1.01
	D	8.91x10-3	5.83x10-3	0.39	0.78	1.00	1.00
	A	8.22	2.53	7.74	13.98	--	32.47
18 Salton Trough	B	32.47	24.25	21.72	13.98	--	32.47
	C	0.25	0.08	0.24	0.43	--	1.00
	D	0.25	0.33	0.57	1.00	--	1.00
	A	--	2.38	0.25	13.52	0.18	16.33
19 Snake River Plain	B	--	16.33	13.95	13.70	0.18	16.33
	C	--	0.15	0.01	0.83	0.01	1.00
	D	--	0.15	0.16	0.99	1.00	1.00
	A	--	--	0.15	2.07	0.53	2.75
20 Sonoran	B	--	--	2.75	2.60	0.53	2.75
	C	--	--	0.05	0.75	0.20	1.00
	D	--	--	0.05	0.81	1.00	1.00
	A	--	--	--	--	0.96	0.96
21 Southeast	B	--	--	--	--	0.96	0.96
	C	--	--	--	--	1.00	1.00
	D	--	--	--	--	1.00	1.00
	A	--	-0.42	5.16	5.38	46.08	57.04
22 Southern Calif. Borderland	B	--	57.04	56.62	51.46	46.08	57.04
	C	--	7.40x10-3	9.04x10-2	9.43x10-2	0.81	1.00
	D	--	7.40x10-3	9.80x10-2	0.19	1.00	1.00
	A	--	--	0.81	--	30.94	31.75
23 Straits of Florida	B	--	--	31.75	--	30.94	31.75
	C	--	--	0.03	--	0.97	1.00
	D	--	--	0.03	--	1.00	1.00
	A	8.06	1.33	14.08	14.02	41.37	78.86
24 Transverse Ranges-Tehachapi	B	78.86	70.8	69.47	55.39	41.37	78.86
	C	0.10	0.02	0.18	0.18	0.52	1.00
	D	0.10	0.12	0.30	0.48	1.00	1.00
	A	0.24	1.76	4.53	42.50	38.68	87.71
25 Utah-Nevada	B	87.71	87.47	85.71	81.18	38.68	87.71
	C	2.74x10-3	0.02	0.05	0.48	0.44	0.99
	D	2.74x10-3	2.30x10-2	0.07	0.56	1.00	1.00
	A	5.27	6.67	7.93	70.19	6.49	96.55
26 Walker Lane	B	96.55	91.28	84.61	76.68	6.49	96.55
	C	0.05	0.07	0.08	0.73	0.07	1.00
	D	0.05	0.12	0.21	0.93	1.00	1.00
	A	--	10.00	9.52	13.66	11.15	44.33
27 Wasatch-Tetons	B	--	44.33	34.33	24.81	11.15	44.33
	C	--	0.23	0.21	0.31	0.25	1.00
	D	--	0.23	0.44	0.75	1.00	1.00
	A	5.18	3.19	6.82	20.66	4.05	39.90
28 Western Mojave	B	39.90	34.72	31.53	24.71	4.05	39.90
	C	0.13	0.08	0.17	0.52	0.10	1.00
	D	0.13	0.21	0.38	0.90	1.00	1.00
	A	4.41	8.42	4.10	92.17	22.30	131.40
29 Western Nevada	B	131.40	126.99	118.57	114.47	22.30	131.40
	C	0.03	0.07	0.03	0.70	0.17	1.00
	D	0.03	0.10	0.13	0.83	1.00	1.00
	A	0.21	--	0.69	1.14	35.11	37.15
30 Wyoming	B	37.15	--	36.94	36.25	35.11	37.15
	C	5.70x10-3	--	0.02	0.03	0.95	1.01
	D	5.70x10-3	--	2.42x10-2	5.50x10-2	1.00	1.00

3.2. Fault Activation Rates and Fictive Ages of Origin

Although the graphs based on normalized lengths are useful to show patterns, we have also derived rates on another basis. Figure 3.2.-1 shows the cumulative lengths for fault activation versus latest movement age plotted linearly. Figure 3.2.-2 gives slopes of line segments derived from differences in cumulative lengths for successive age differences extrapolated to an age where there would have been no apparent fault motion. The sets of graphs in these figures accent the apparent accelerative character shown by the data. We have termed the intercepts at zero length in Figure 3.2.-2 the fictive age of origin for a particular length-age interval; e.g., that would be the age activity began on a particular fault set if the cumulative active length involving movement for that set had evolved at that constant rate. We use the term "fictive" because these intercepts have no explicit significance, depending, as they do, on the previous values for cumulative length. The "fictive ages of origin," however, provide another way to classify rates in a way that relates them to geologically available time. They suggest a spectrum in the time periods for episodic fault activity, even though the absolute ages are not significant. We also use the fictive age distribution to suggest limiting rates of fault activity extrapolated backward in earth history and forward to the present time.

Table 3.2.-1 gives rates and fictive origin ages for each region and age interval based on the cumulative lengths in Table 3.1.-1. Figure 3.2.-3 shows the relationship between rates of activation and fictive age. This graph suggests that rates of fault activity oscillate in time and that there has been a systematic shift in rates with time. Figure 3.2.-4 shows regression lines through the data for each fictive time interval (Miocene to Pliocene, etc.), and Figure 3.2.-5 shows the slopes of the regression lines. Figure 3.2.-5 was used as a guide to limit the extrapolated rates at the present time. The trend as drawn in Figure 3.2.-5 suggests that the maximum average activation rate at the present time (dashed line in Figure 3.2.-4) is the order of 1×10^7 cm/yr (100 km/yr) for all faults in the conterminous United States. If the slope continuously approaches a value near zero, shown by the dash-dot line in Figure 3.2.-4, the present average rate is about 3×10^5 cm/yr (3 km/yr). Remember, these are rates for activation of fault length, not movement rates along faults.

Taken literally, Figures 3.2.-4 and 3.2.-5 suggest that fault activity has been accelerating throughout geologic history. Allowances for possible additions of missing data on fault movements do not seem to alter this conclusion and possibly would enhance it. If there were proportionately more older movements, the older rates would be somewhat higher, and the corresponding fictive age intercepts could be either larger or smaller depending on relative adjustments between intervals. Assuming a progressive underestimate of lengths with greater age, the slope intervals in Figures 3.2.-3 and 3.2.-4 would be less steep at the greater ages. It would require at least an order of magnitude increase in the active lengths

for Miocene-Pliocene faults to give a rate approaching that in the Holocene. The uncertainty caused by the inability to document younger movements on older faults would counter that effect.

A slope of minus one on Figures 3.2.-3 and 3.2.-4 represents a hyperbolic distribution, the rate increasing from zero at infinite age to infinite at zero age. The actual rate distribution portrayed represents an accelerating function for which the acceleration rate has been decreasing with time as shown in Figure 3.2.-5. The trend in Figure 3.2.-5 suggests that we are approaching a time when the acceleration will be zero. This could represent an approach to a quasi-steady rate for some time into the future or the culmination of an accelerative episode represented by the behavior during the latest 15 m.y. The backward extrapolation to very low rates at an age equivalent to the age of the earth suggests that the average trend in the rate distribution may represent a general progression for oscillating fault activity during earth history that is approaching its maximum rate around now. This idea is at least qualitatively consistent with concepts for crustal evolution in relation to plate tectonic histories.

Figures 3.2.-6 gives progressions of activation rates for individual regions as derived in Tables 3.2.-1 and 3.2.-2 and as represented by slopes from normalized length versus age relations (Figure 3.1.-1). These graphs provide a check on the extrapolation of rates based on fictive origin ages and also show the reversals in the rate progression during the early Pleistocene seen in the normalized rates given in Figure 3.1.-12. The reversal is sometimes from increasing to transiently decreasing rates and sometimes from transiently decreasing to increasing rates. We suggest that this effect represents a time of transition between different regimes of episodic faulting rates.

SECTION 3.2. FIGURES AND TABLES

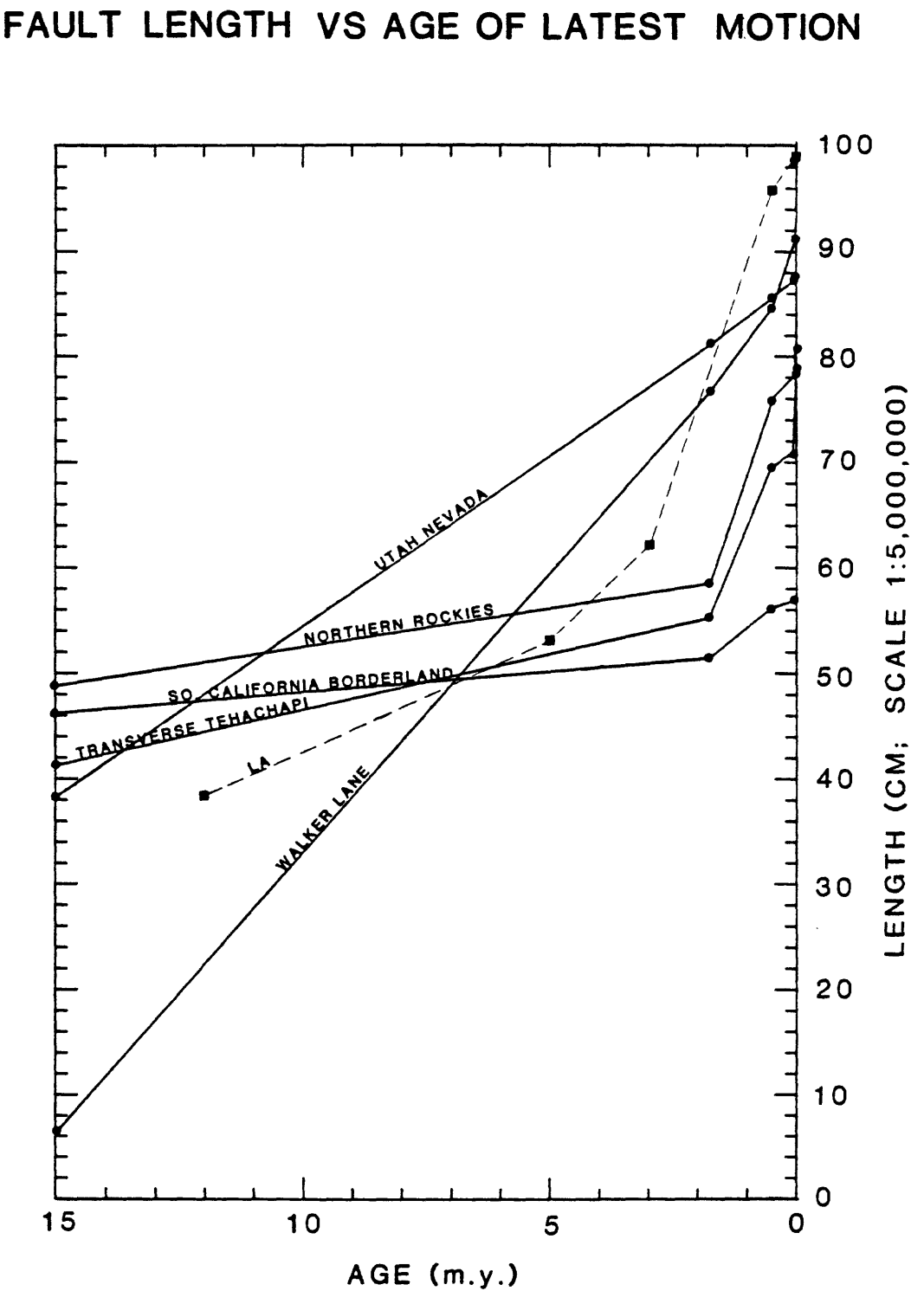

Figure 3.2.-1. (A)
Linear fault activation length versus linear activation age for each fault region including the L.A. Area.

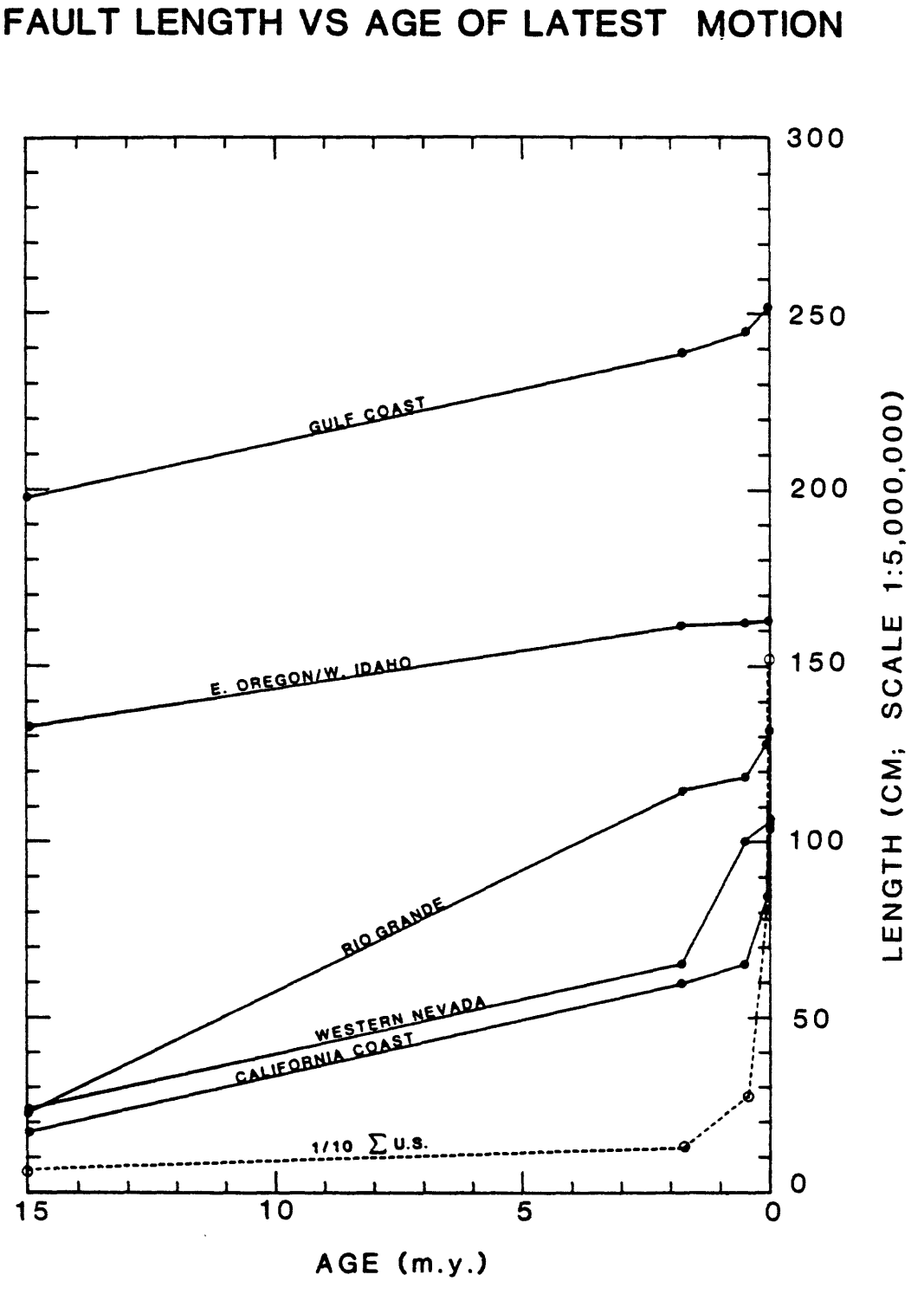
FAULT LENGTH VS AGE OF LATEST MOTION
GULF COAST
E. OREGON/W. IDAHO
RIO GRANDE
WESTERN NEVADA
CALIFORNIA COAST
1/10 Σ U.S.
300
250
200
150
100
50
0
15
10
5
0
AGE (m.y.)
LENGTH (CM; SCALE 1:5,000,000)

Figure 3.2.-1. (B)

FAULT LENGTH VS AGE OF LATEST MOTION

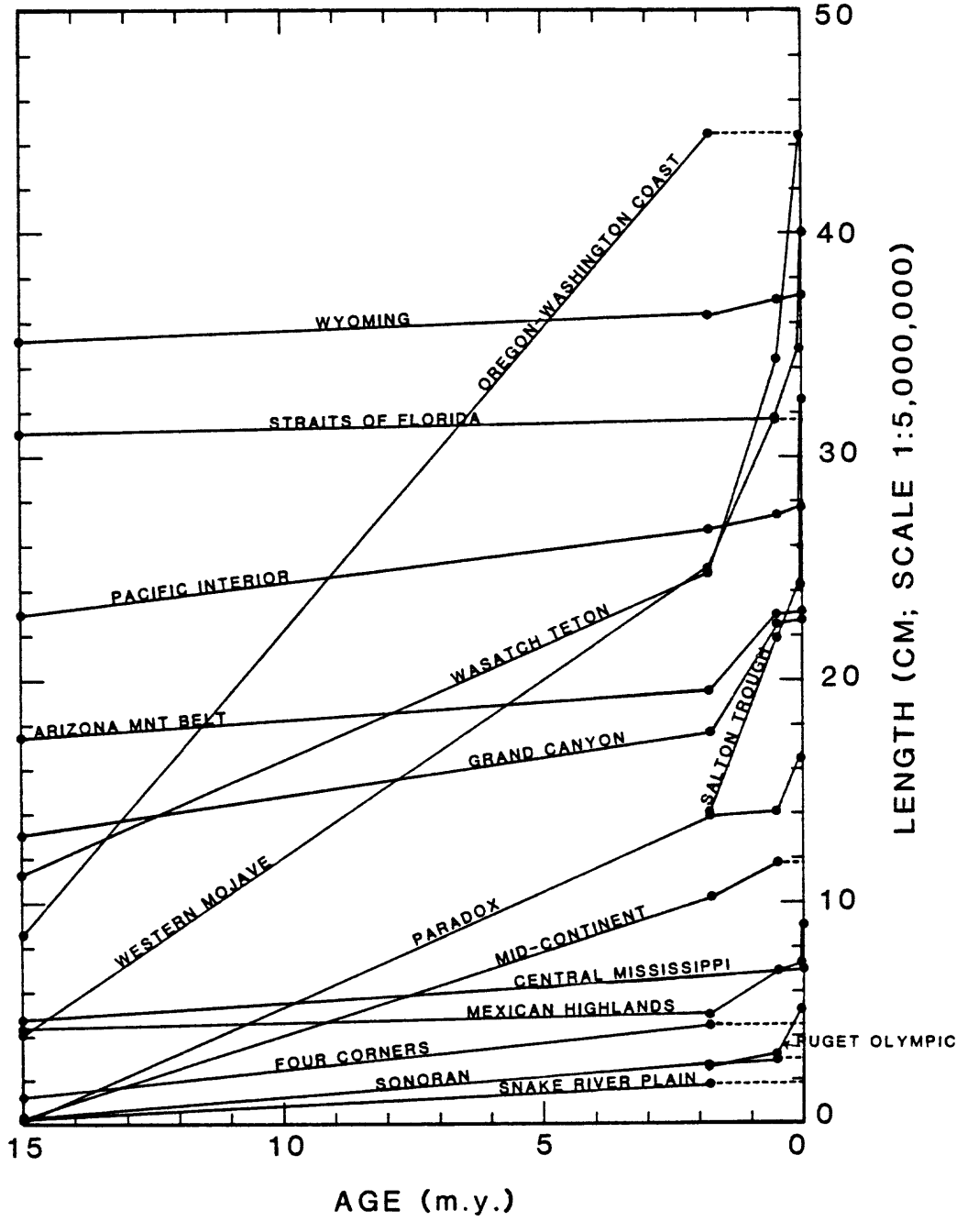

Figure 3.2.-1. (C)

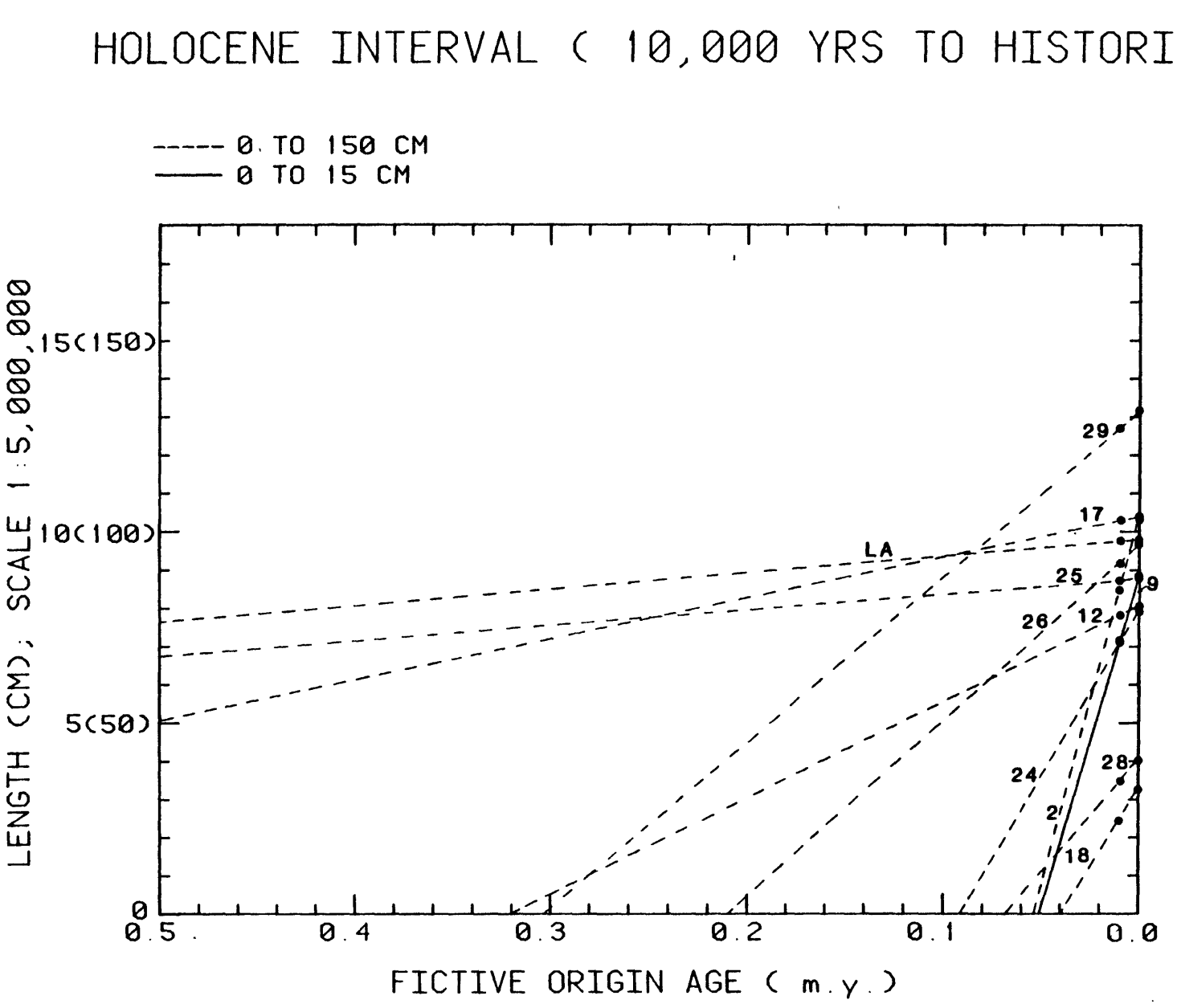

Figure 3.2.-2. (A)
Activation rates and age intercepts determined by extrapolating the linear length-age relations within each age category; the intercept on the age axis at zero length is called the "fictive origin age" for that particular rate interval.

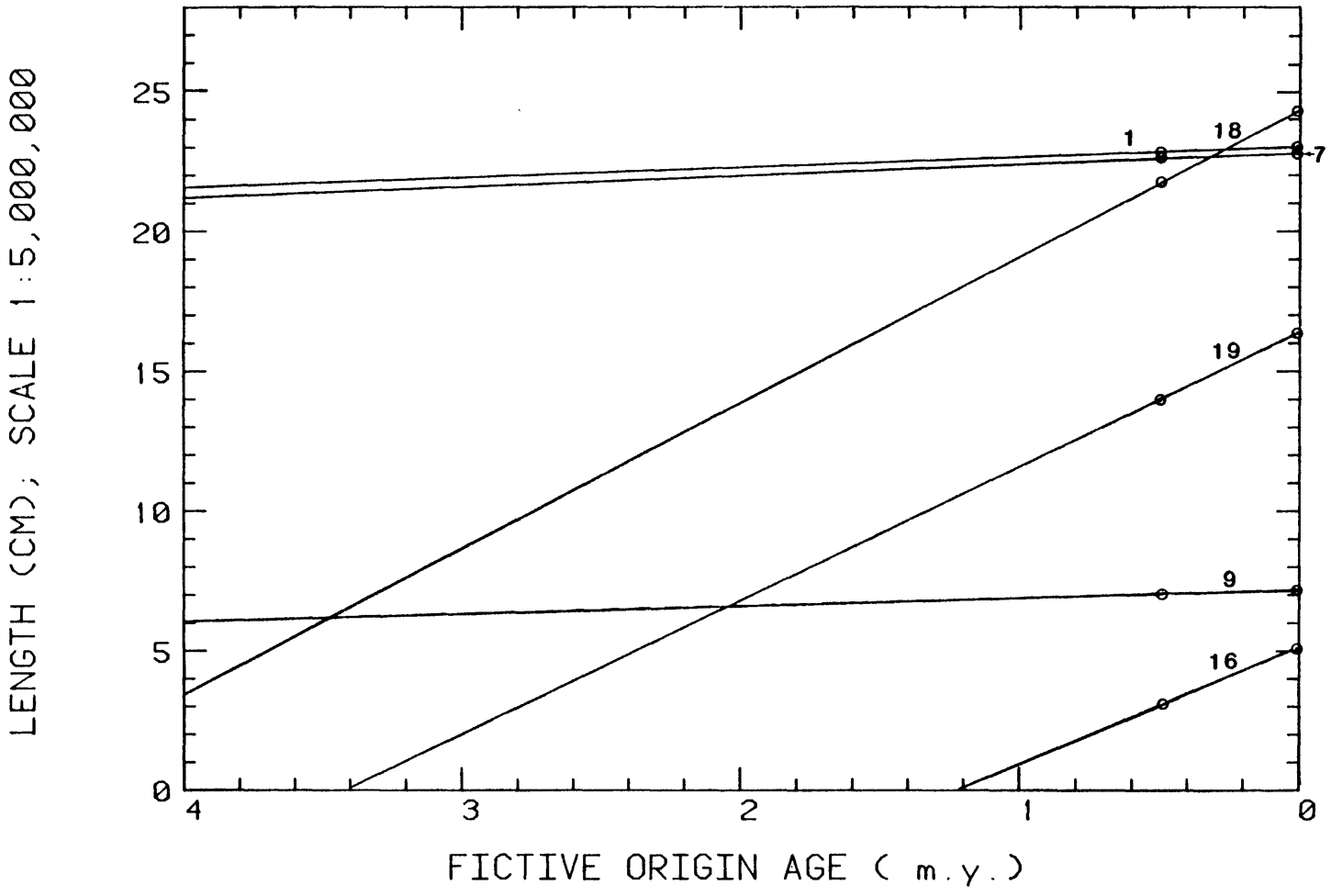
LATE PLEISTOCENE INTERVAL (0.5 TO 0.01 m.y.)
LENGTH (CM); SCALE 1:5,000,000
25
20
15
10
5
0
4
3
2
1
0
FICTIVE ORIGIN AGE (m.y.)
1
18
7
19
9
16

Figure 3.2.-2. (B)

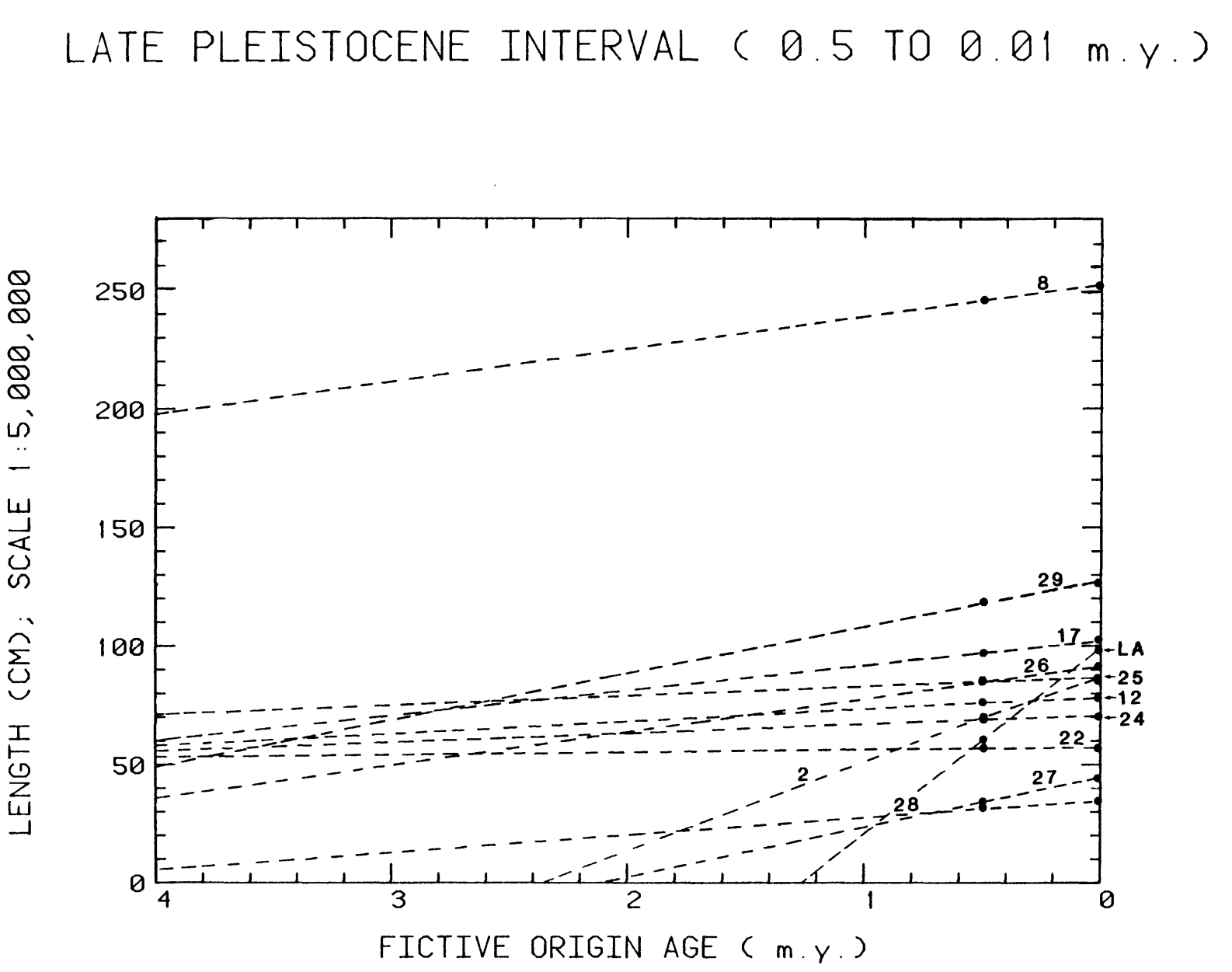
LATE PLEISTOCENE INTERVAL (0.5 TO 0.01 m.y.)
LENGTH (CM); SCALE 1:5,000,000
250
200
150
100
50
0
4
3
2
1
0
FICTIVE ORIGIN AGE (m.y.)
8
29
17
LA
26
25
12
24
22
2
27
28

Figure 3.2.-2. (C)

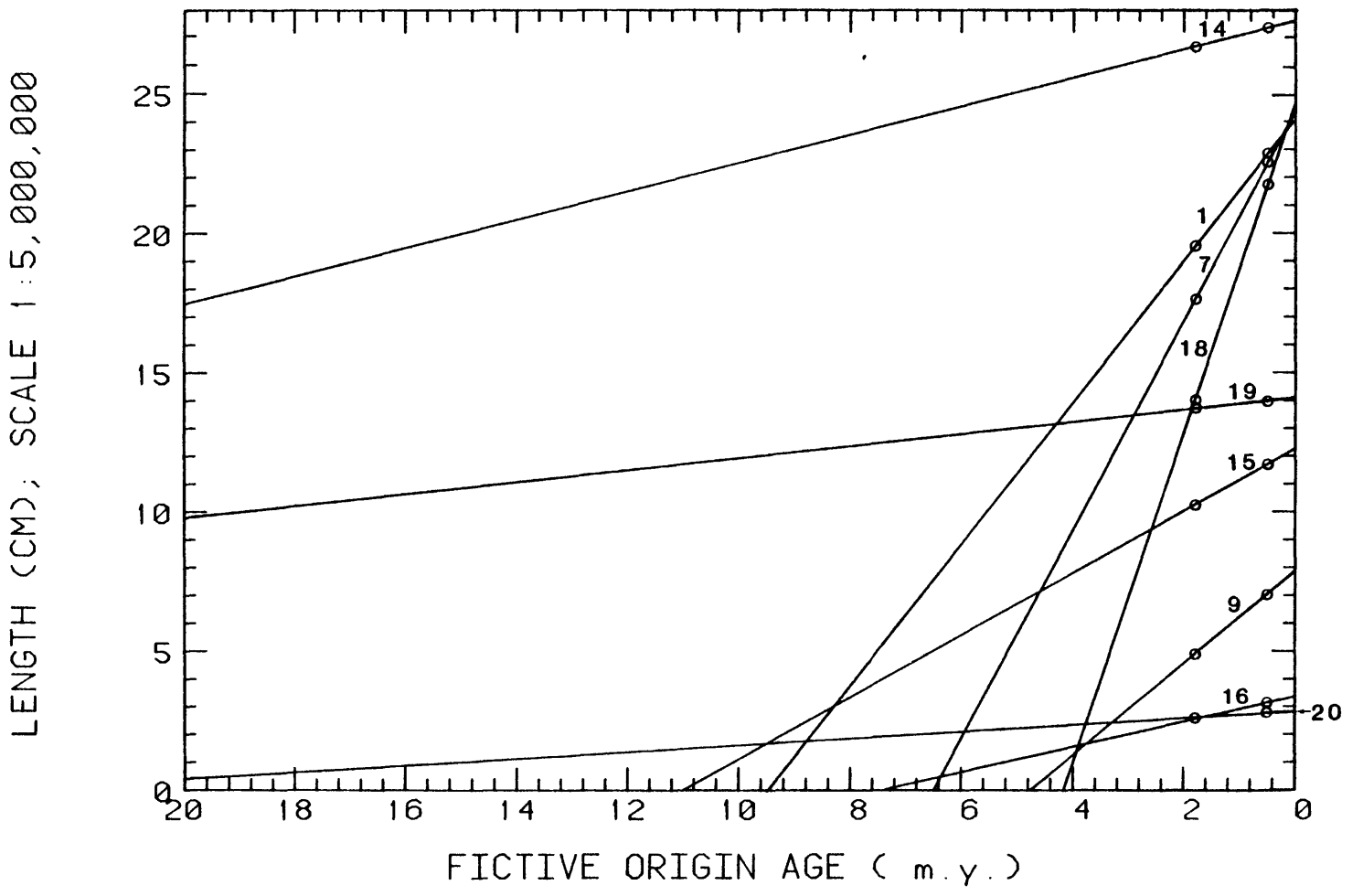
EARLY PLEISTOCENE INTERVAL (1.8 TO 0.5 m.y.)
LENGTH (CM); SCALE 1:5,000,000
FICTIVE ORIGIN AGE (m.y.)
0
5
10
15
20
25
20
18
16
14
12
10
8
6
4
2
0
14
1
7
18
19
15
9
16
20

Figure 3.2.-2. (D)

EARLY PLEISTOCE INTERVAL (1.8 TO 0.5 m.y.)

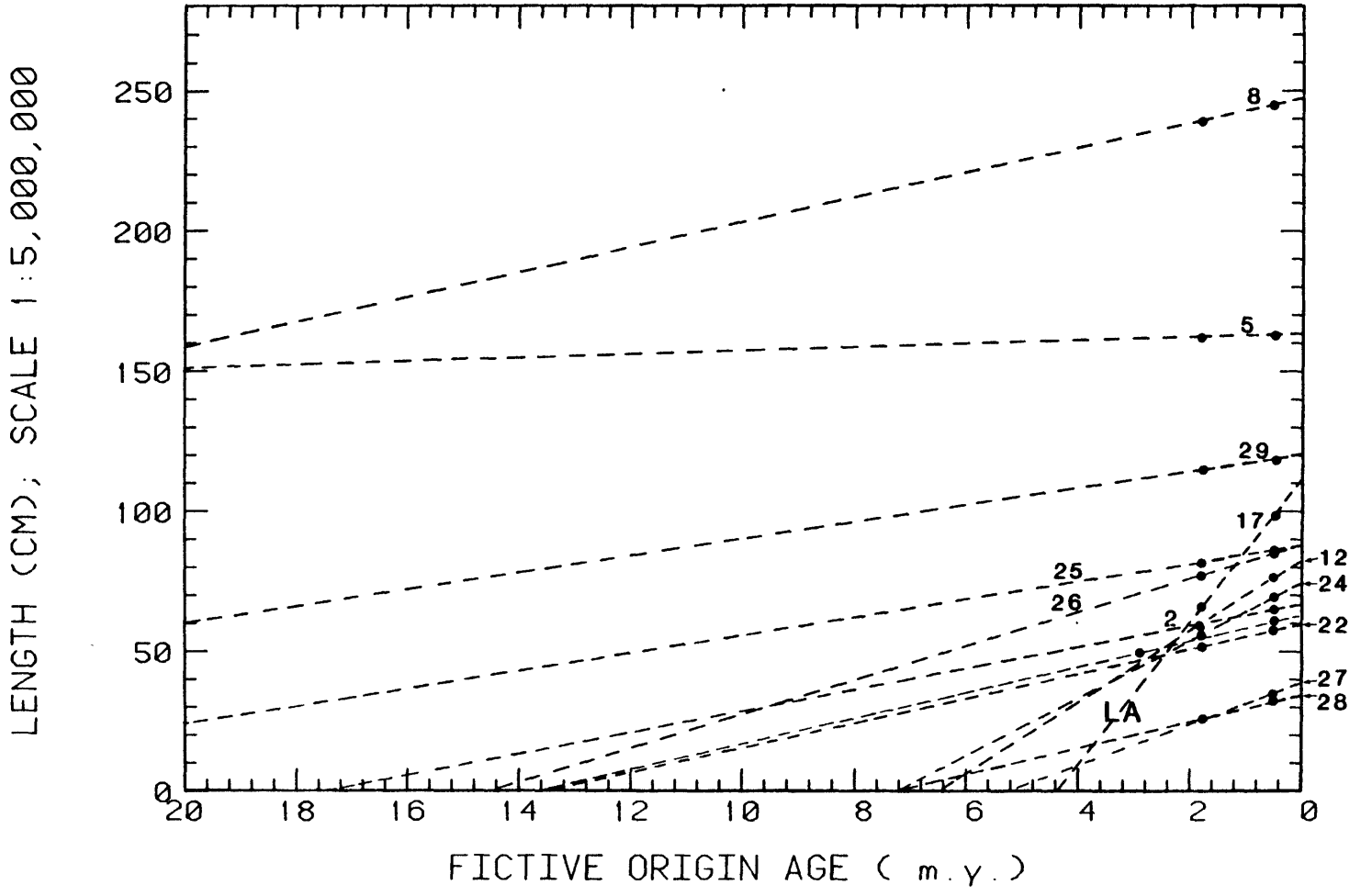

Figure 3.2.-2. (E)

MIOCENE-PLIOCENE INTERVAL (22.5 TO 1.8 m.y.)

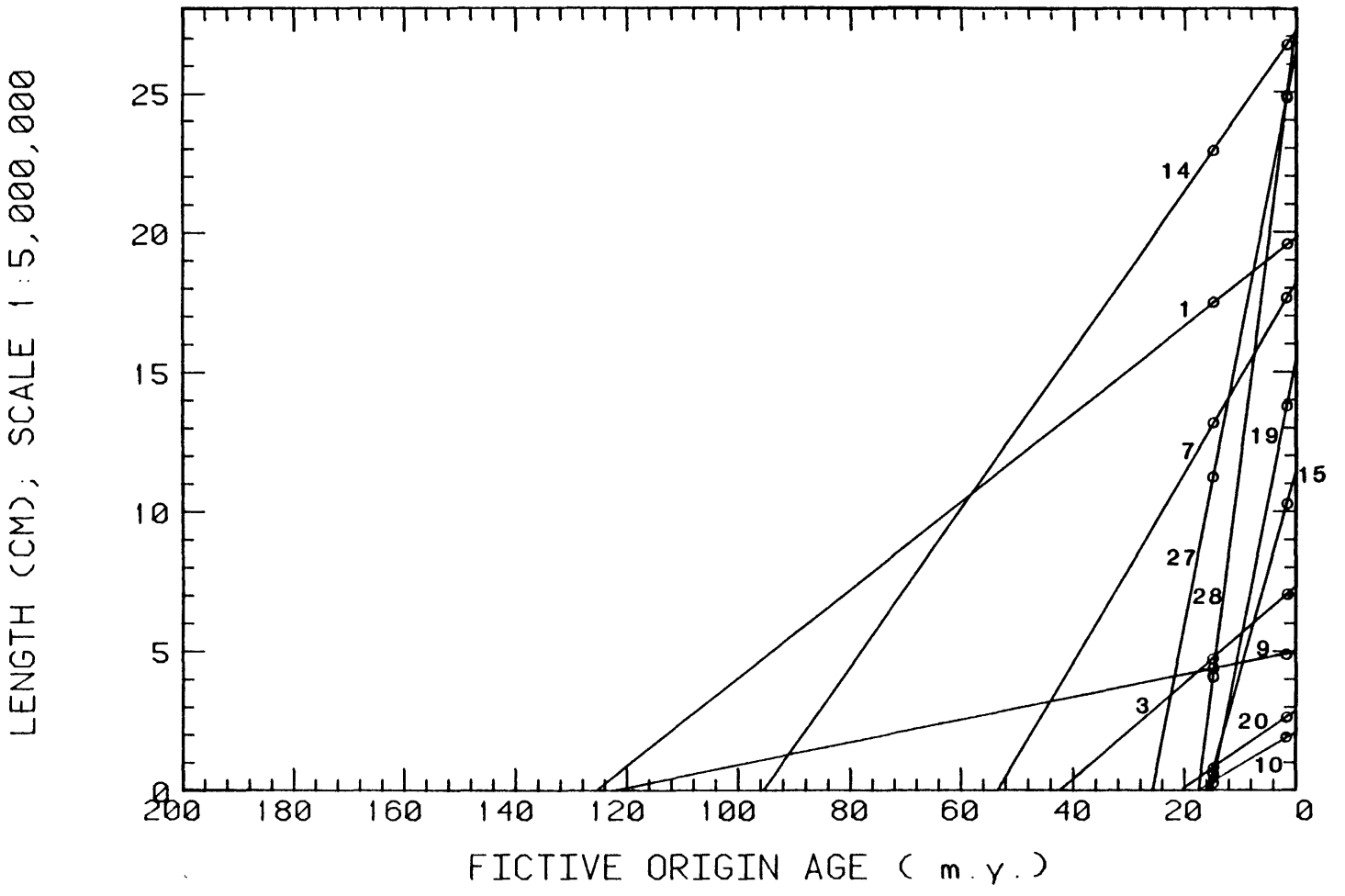

Figure 3.2.-2. (F)

MIOCENE-PLIOCENE INTERVAL (22.5 TO 1.8 m.y.)

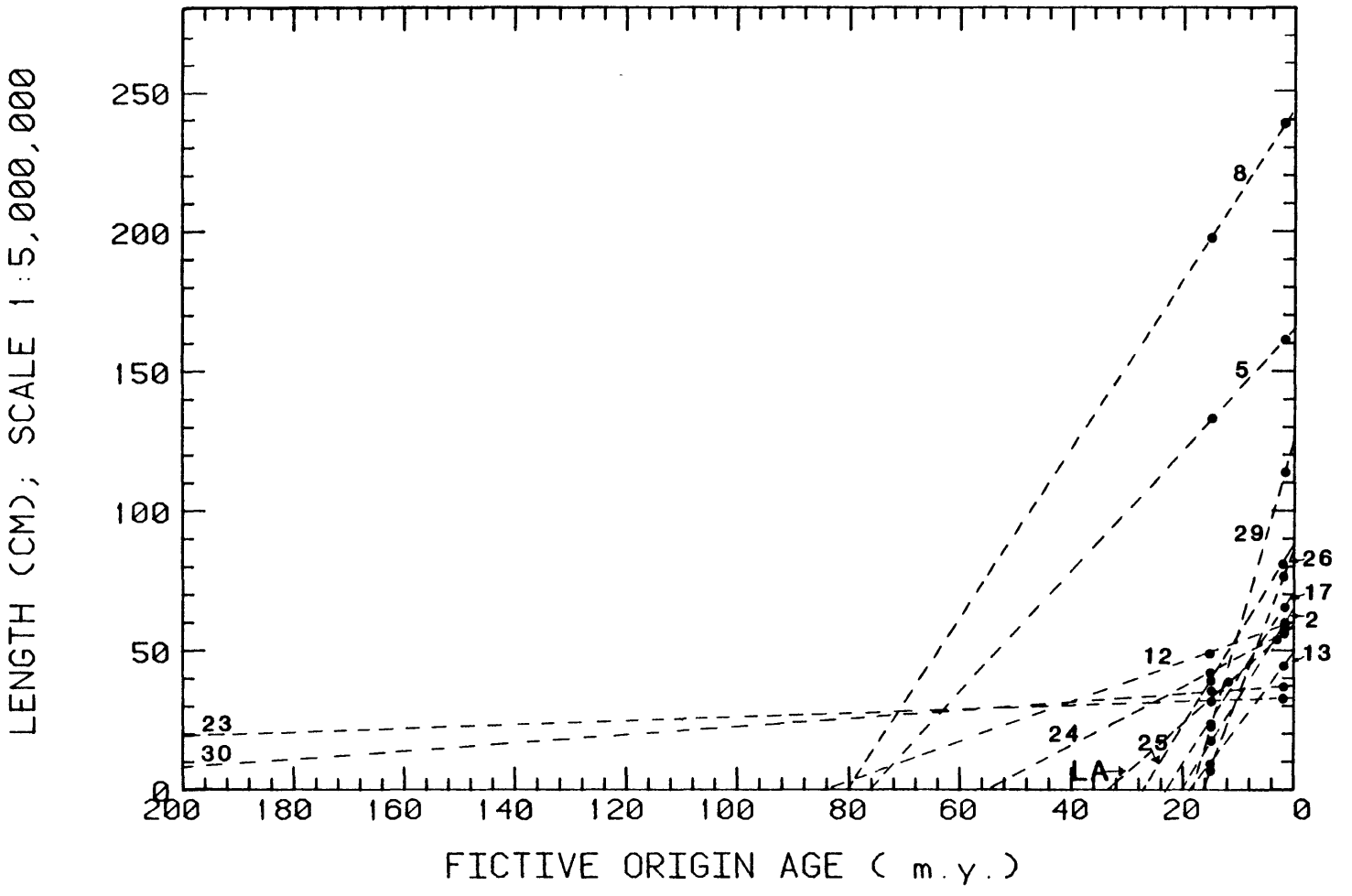

Figure 3.2.-2. (G)

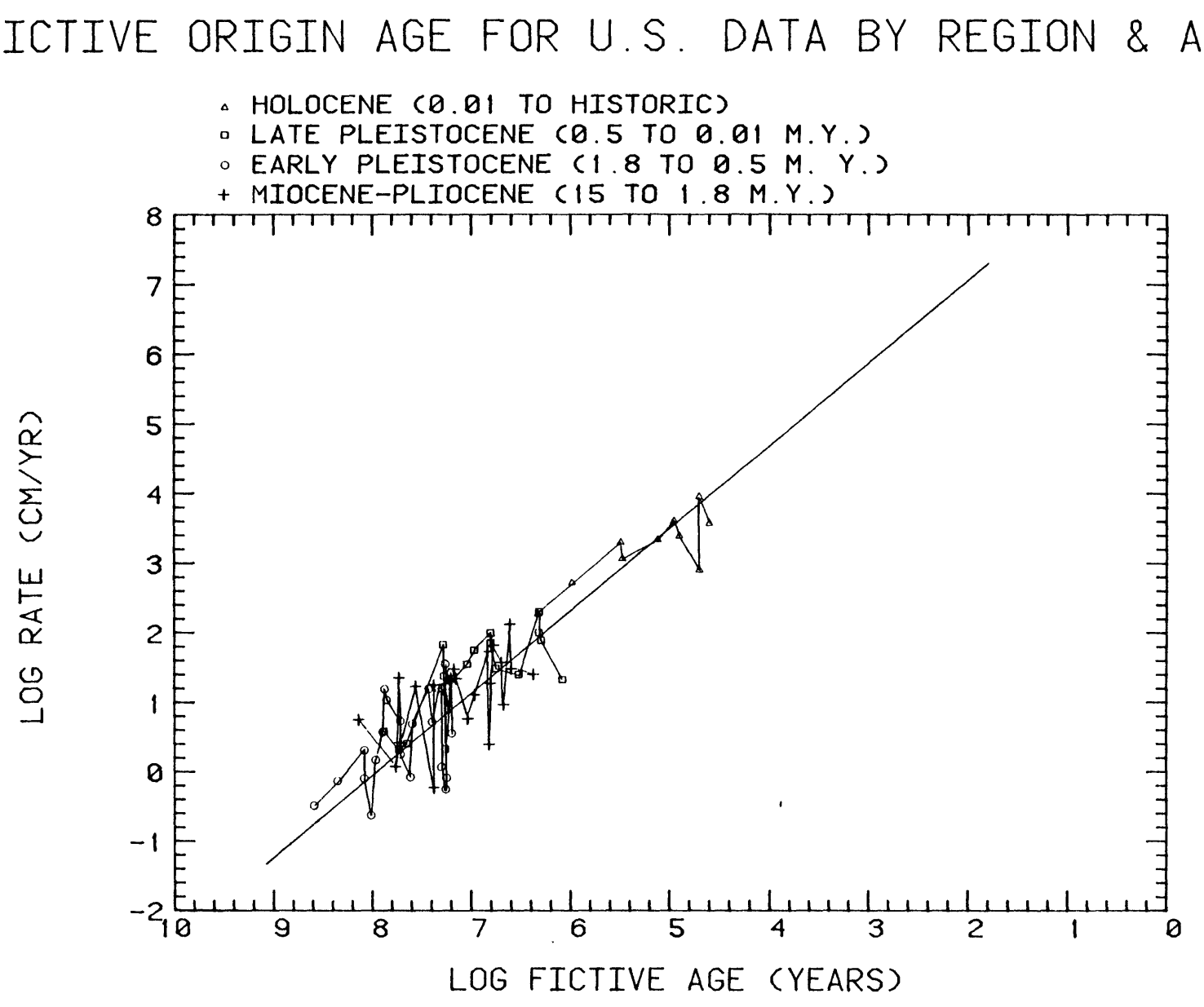

Figure 3.2.-3. (A)
Activation rates versus fictive origin ages for all regions and age categories in the conterminous United States.

FICTIVE ORIGIN AGE FOR U.S. DATA BY REGION & AGE GROUP

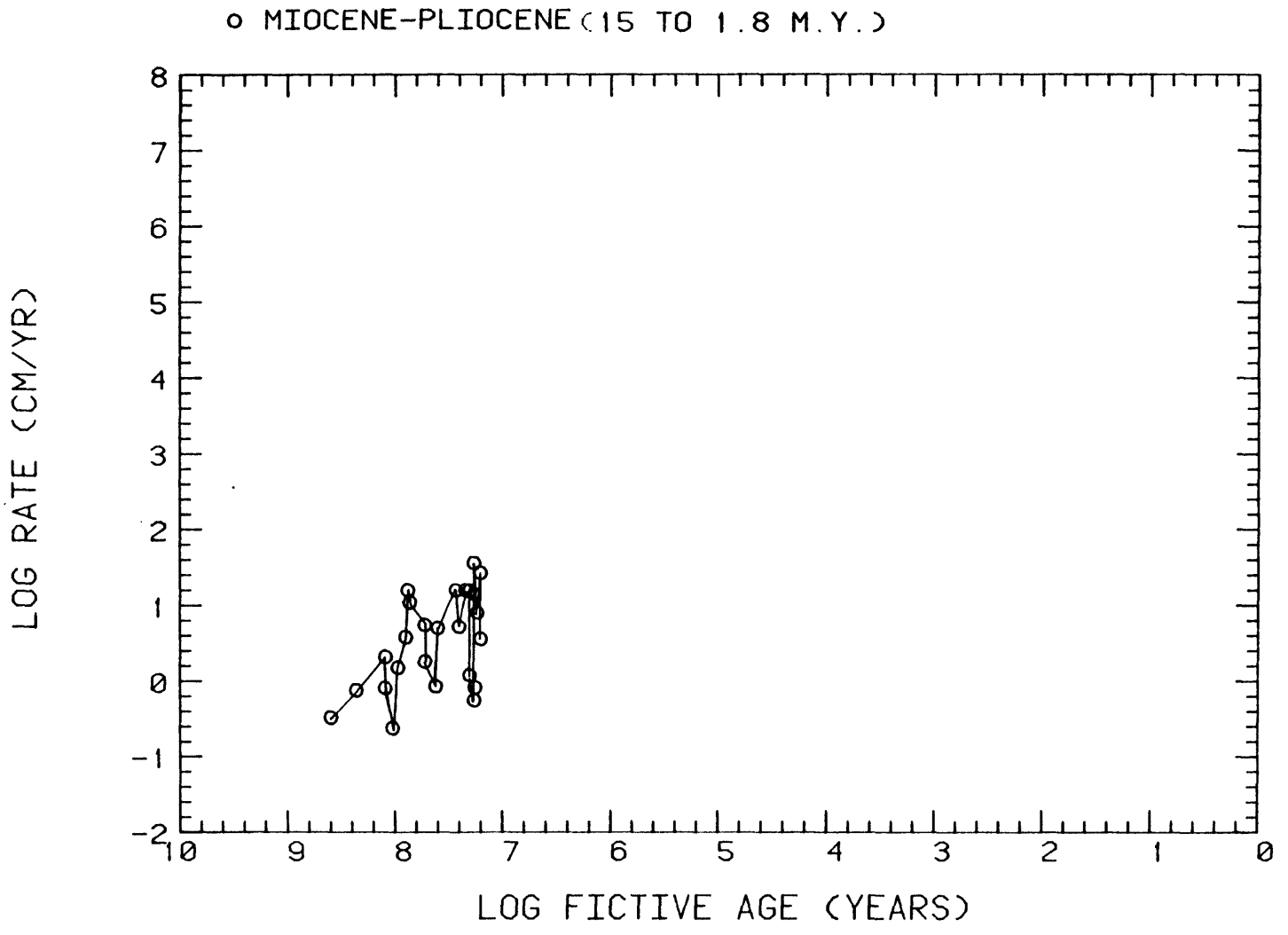

Figure 3.2.-3. (B)

FICTIVE ORIGIN AGE FOR U.S. DATA BY REGION & AGE GROUP

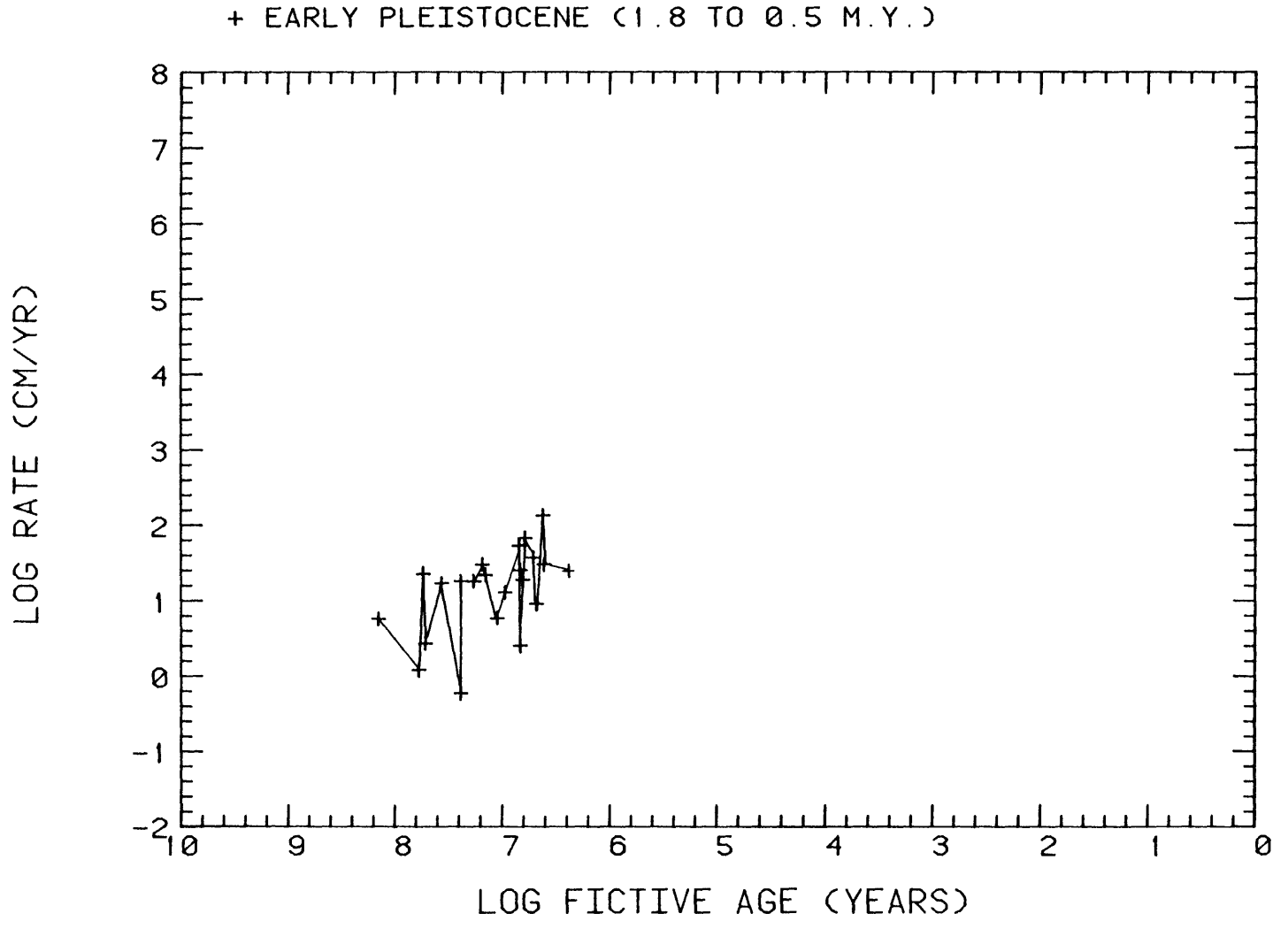

Figure 3.2.-3. (C)

FICTIVE ORIGIN AGE FOR U.S. BY REGION & AGE GROUP

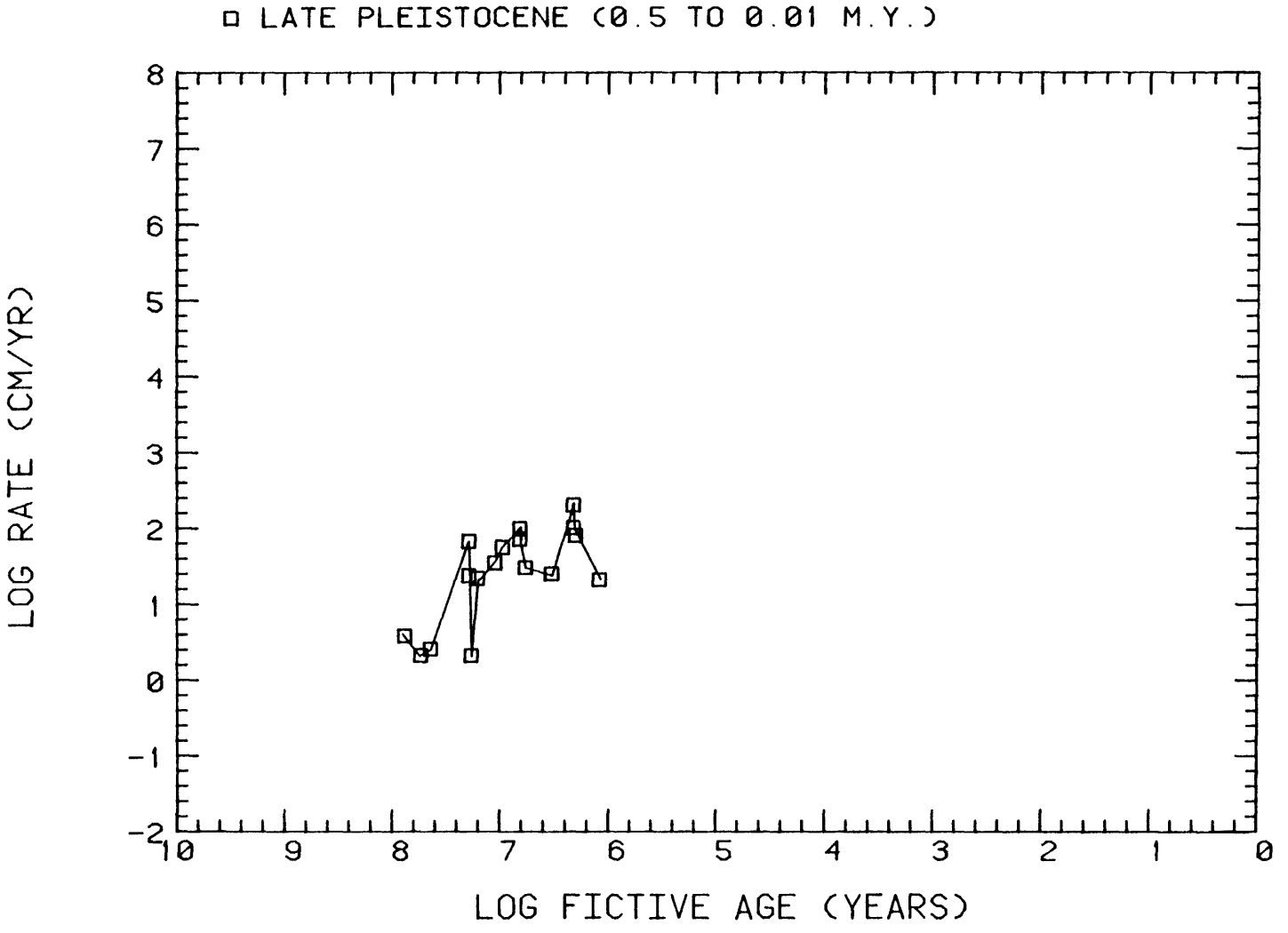

Figure 3.2.-3. (D)

FICTIVE ORIGIN AGE FOR U.S. BY REGION & AGE GROUP

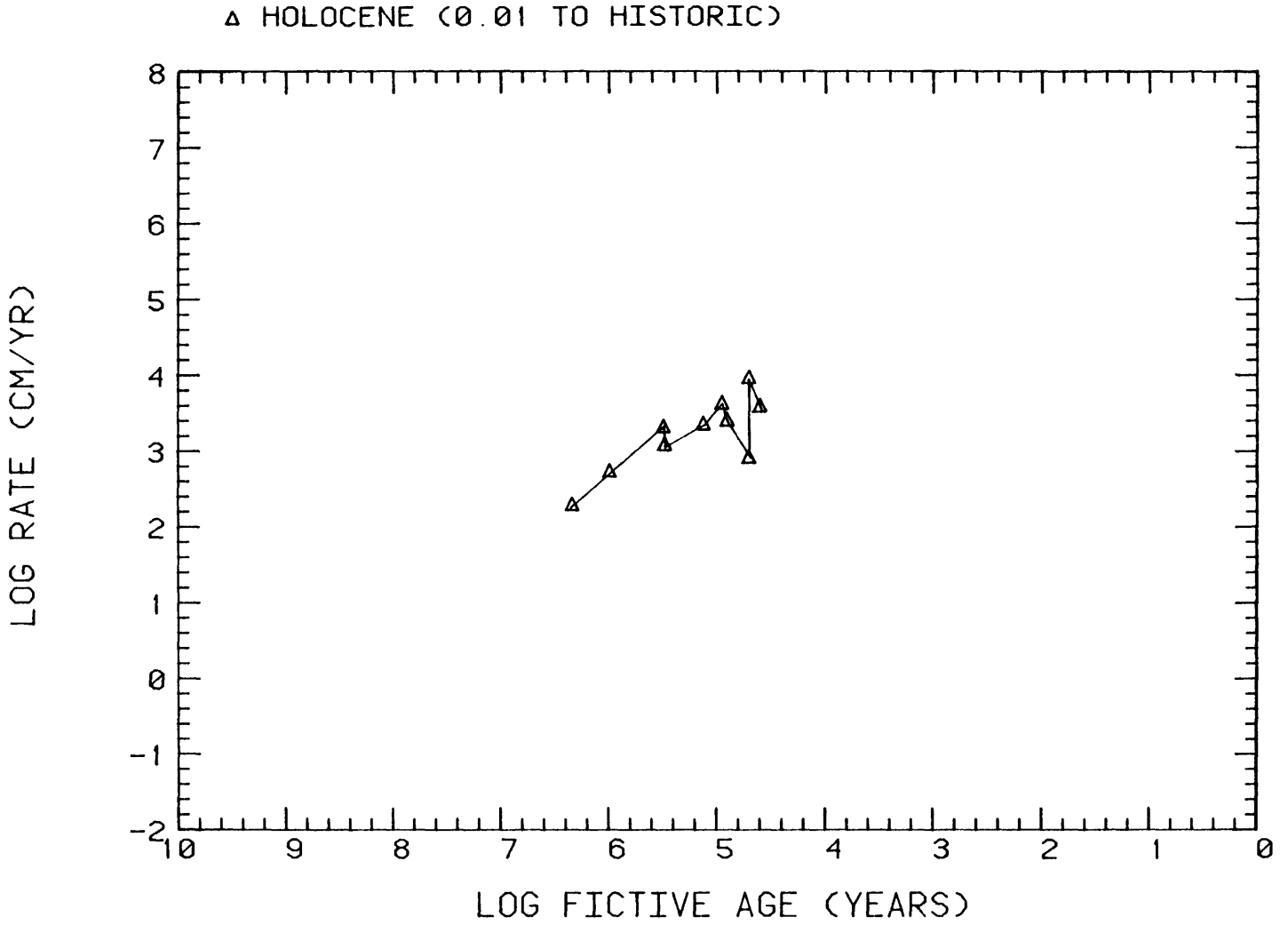

Figure 3.2.-3. (E)

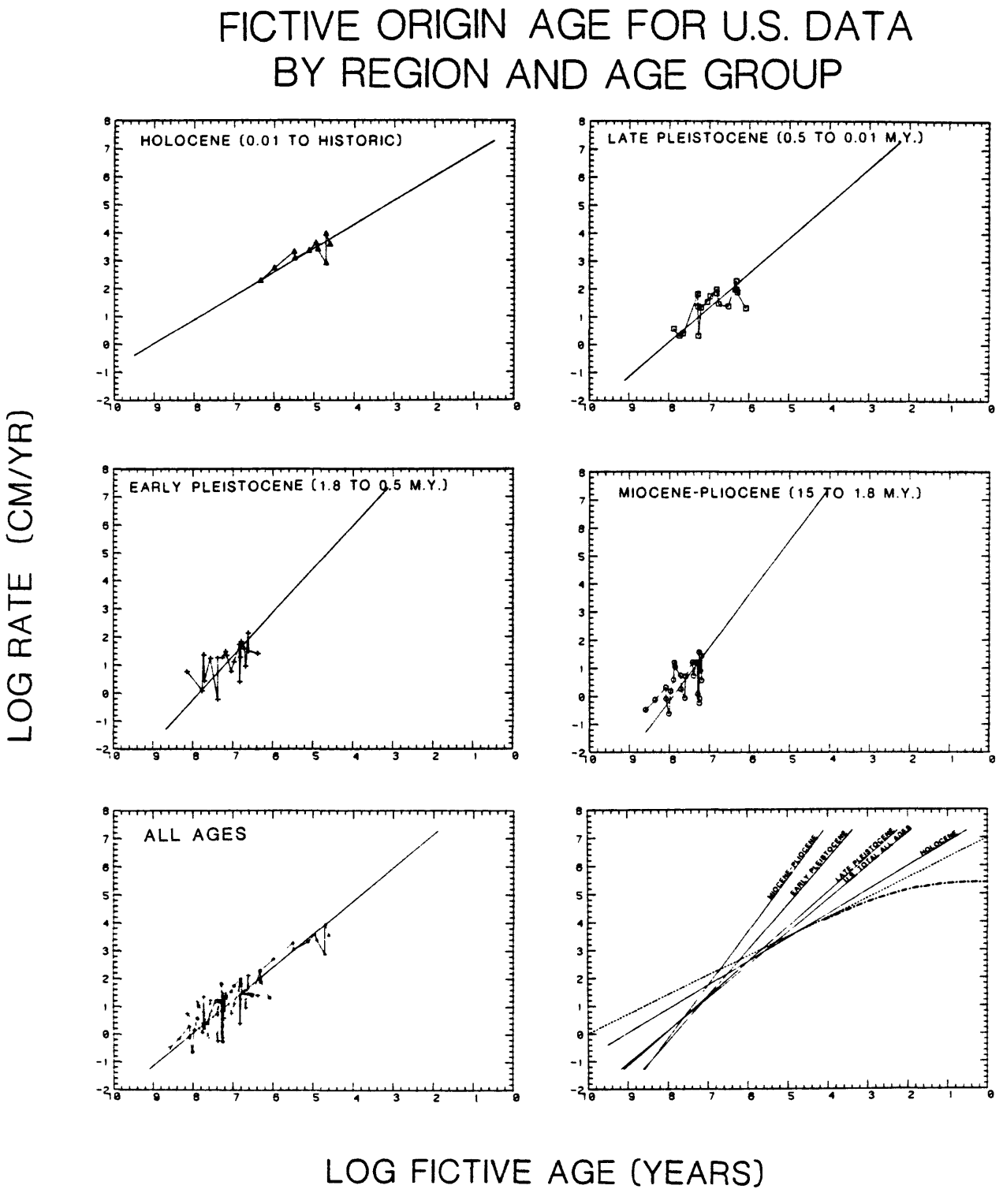

Figure 3.2.-4.
Regression lines and limits for extrapolating fault activation rates backward in time and forward to the overall present day rate in the United States.

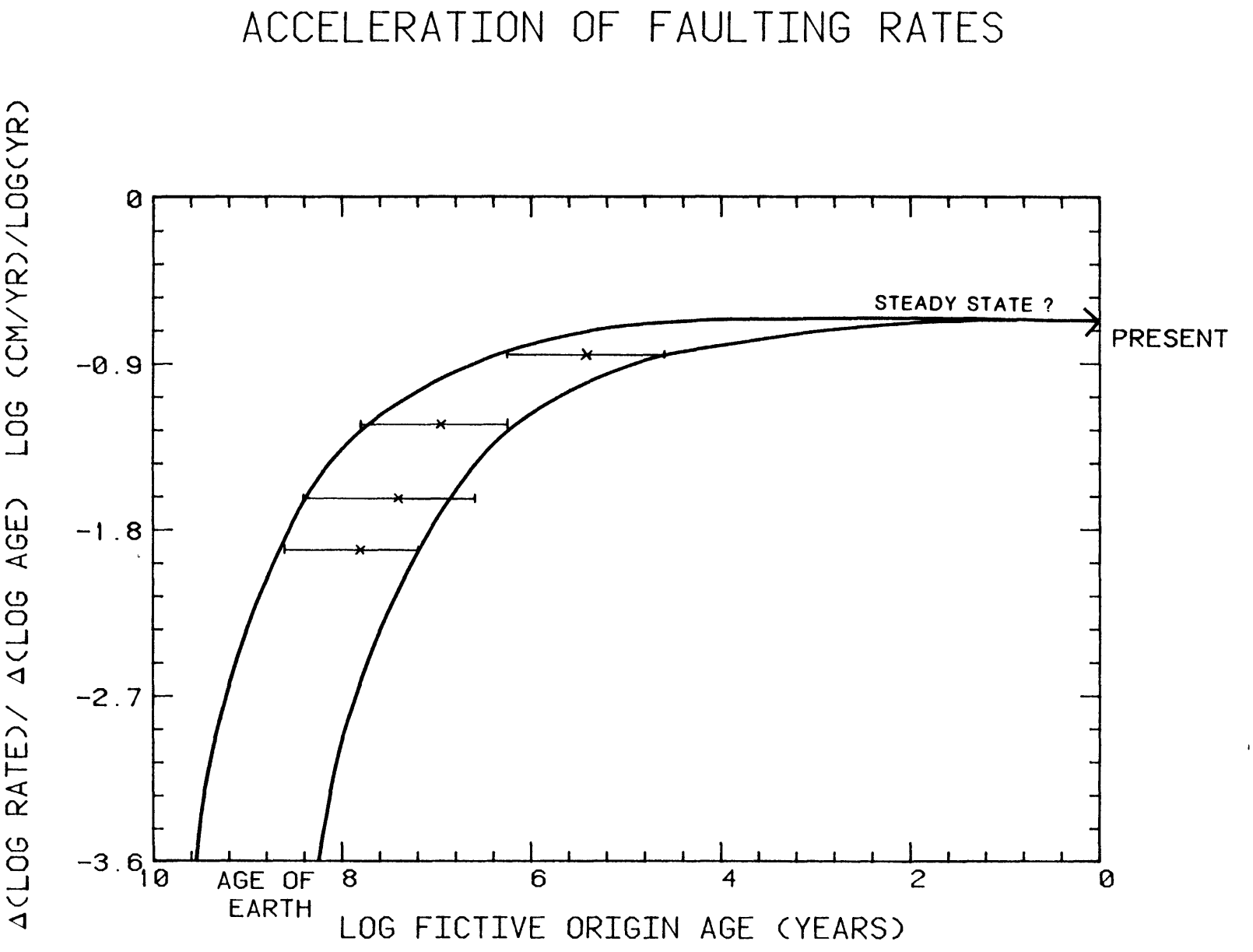

Figure 3.2.-5.
Acceleration of activation rates with decreasing age.

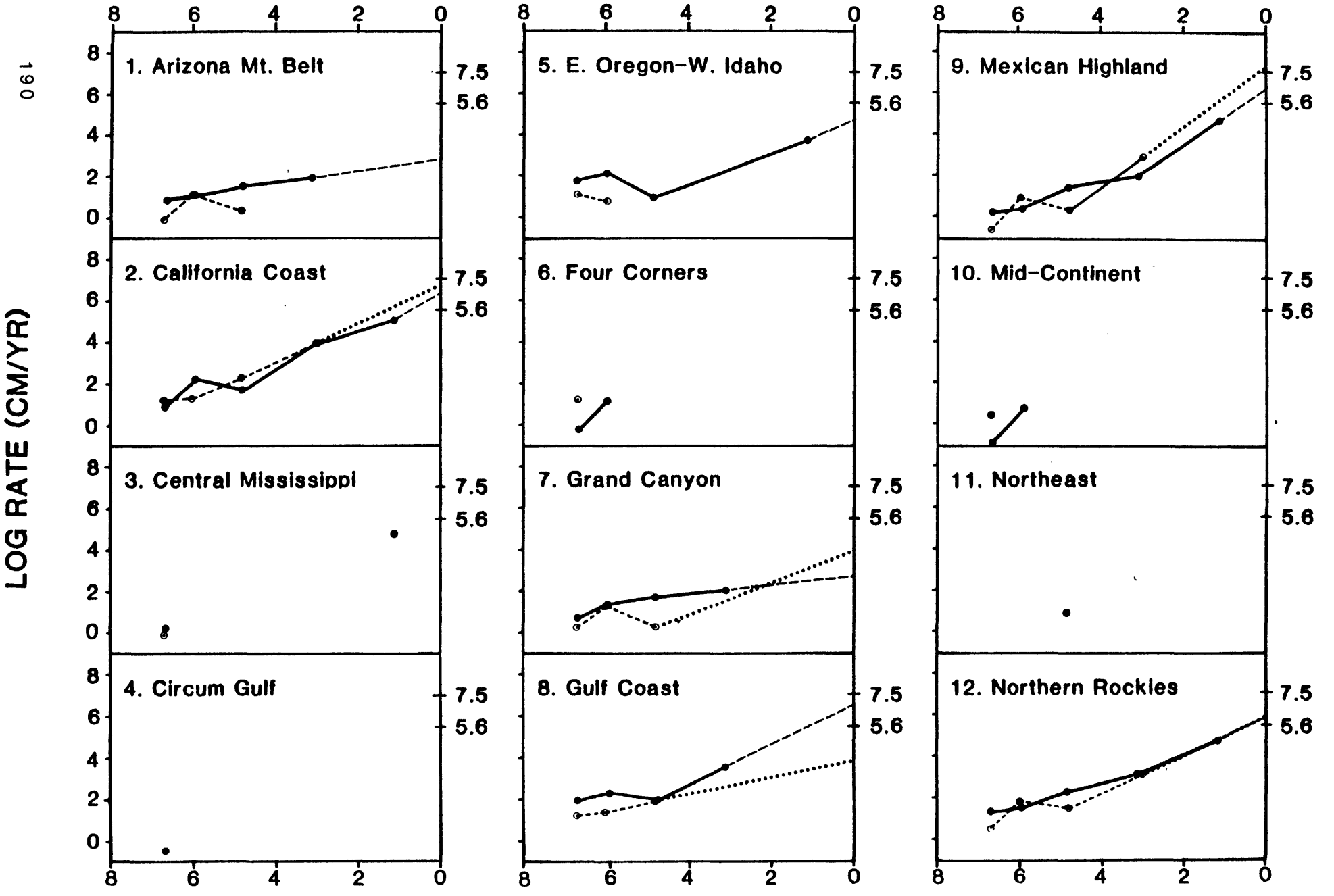

Figure 3.2.-6.

Logarithm of activation rates for each region, including the L. A. Area, versus age calculated in two ways; solid with dashed extension is based on slopes of fractional activation length versus age; light dashed line with dotted extension is based on slopes from the linear diagrams for activation length versus age (see 3.2.-2). Numbers at rightof diagram are a reference scale of magnitude for earthquake events per year at the indicated activation rates.

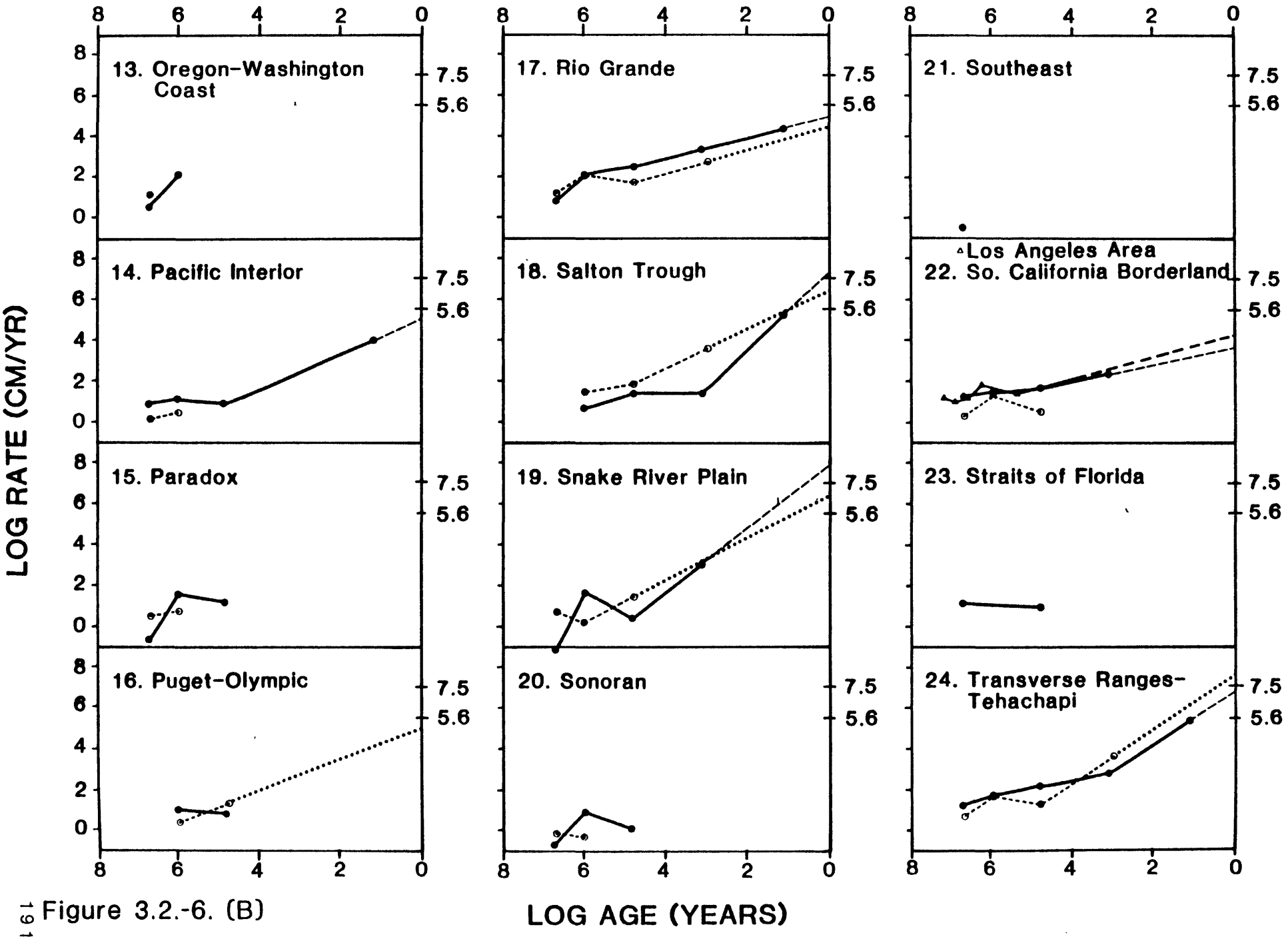
13. Oregon-Washington Coast
14. Pacific Interior
15. Paradox
16. Puget-Olympic
17. Rio Grande
18. Salton Trough
19. Snake River Plain
20. Sonoran
21. Southeast
Los Angeles Area
22. So. California Borderland
23. Straits of Florida
24. Transverse Ranges-Tehachapi
7.5
5.6
8
6
4
2
0
LOG RATE (CM/YR)
LOG AGE (YEARS)

Figure 3.2.-6. (B)

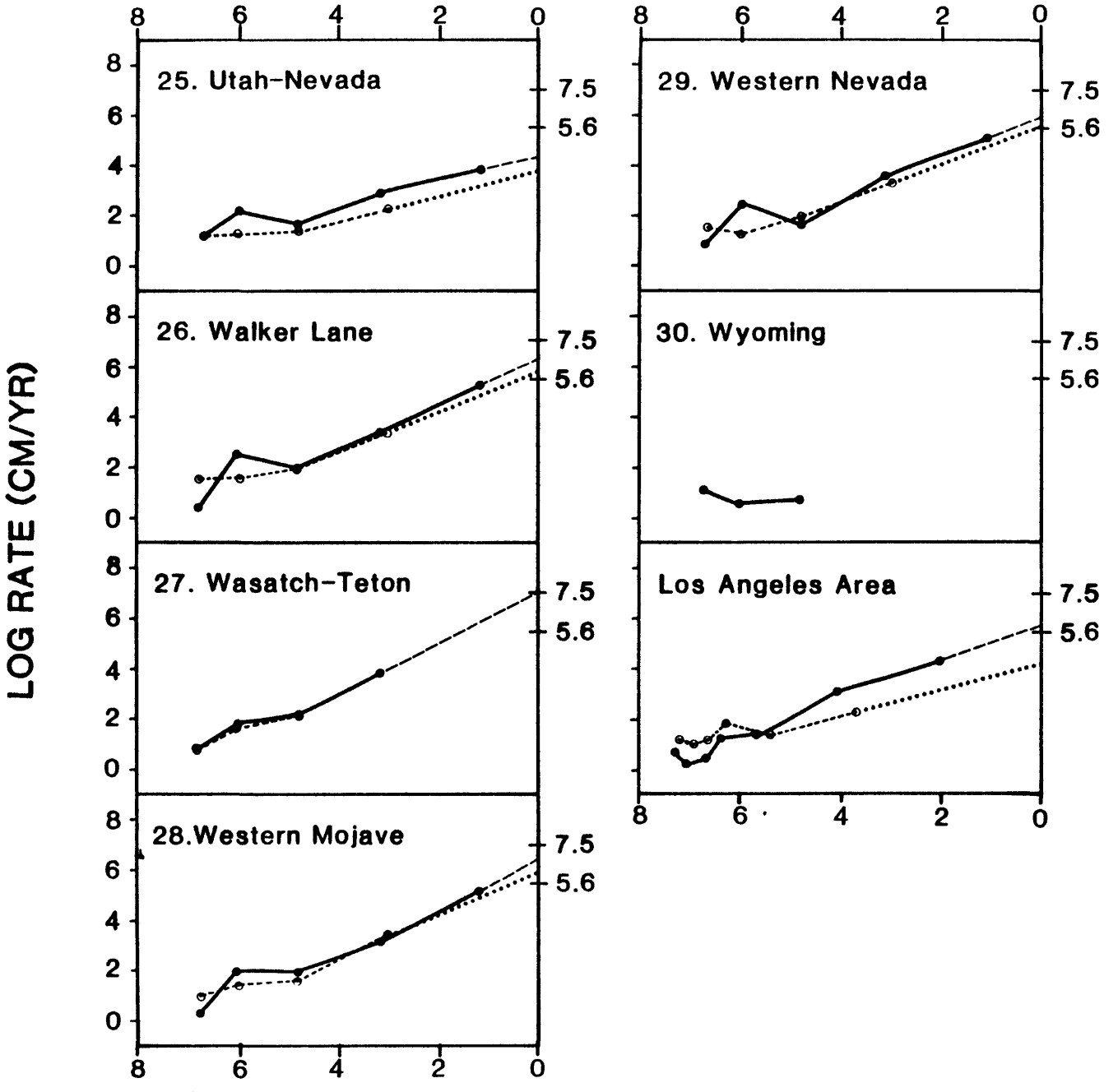
25. Utah-Nevada
26. Walker Lane
27. Wasatch-Teton
28.Western Mojave
29. Western Nevada
30. Wyoming
Los Angeles Area
7.5
5.6
LOG RATE (CM/YR)
LOG AGE (YEARS)

Figure 3.2.-6. (C)

Table 3.2.-1. Fictive origin ages and fault activation rates determined from slopes of age versus cumulative fault activation length (see figure 3.2-2.).

Region		Fictive origin age (m.y.)	Rate (m/yr)
Miocene-Pliocene Interval (15 - 1.8 m.y.):			
23	Straits of Florida	400	3x10-3
30	Wyoming	230	8x10-3
1	Arizona Mountain Belt	122	8x10-3
22	Southern Calif. Borderland	122	2x10-2
9	Mexican Highland	105	2x10-3
14	Pacific Interior	93	2x10-2
12	Northern Rockies	80	4x10-2
8	Gulf Coast	76	0.2
5	Eastern Oregon-Western Idaho	73	0.1
24	Transverse Ranges-Tehachapi	52	6x10-2
7	Grand Canyon	52	2x10-2
3	Central Mississippi Valley	42	1x10-2
25	Utah-Nevada	27	0.2
27	Wasatch-Tetons	25	5x10-2
17	Rio Grande	22	0.2
6	Four Corners	20	6x10-3
2	California Coast	20	0.2
10	Mid-continent	18	6x10-3
20	Sonoran	18	8x10-3
13	Oregon-Washington Coast	18	0.1
29	Western Nevada	18	0.4
28	Western Mojave	17	8x10-2
26	Walker Lane	16	0.3
15	Paradox	16	4x10-2
19	Snake River Plain	16	5x10-2
Late Pleistocene Interval (0.5 to 0.01 m.y.):			
22	Southern Calif. Borderland	76	4x10-2
7	Grand Canyon	54	2x10-2
1	Arizona Mountain Belt	44	3x10-2
8	Gulf Coast	19	0.7
25	Utah-Nevada	19	0.2
9	Mexican Highland	18	2x10-2
	(L.A.)	(17)	(0.3)
24	Transverse Ranges-Tehachapi	16	0.2
12	Northern Rockies	11	0.4
17	Rio Grande	9	0.6
29	Western Nevada	7	1.0
28	Western Mojave	6	0.3
26	Walker Lane	4	0.7
19	Snake River Plain	3	0.3
27	Wasatch-Tetons	2	1.0
2	California Coast	2	2.1
18	Salton Trough	2	0.8
16	Puget-Olympic	1	0.2

Region		Fictive origin age (m.y.)	Rate (m/yr)
Early Pleistocene Interval (1.8 to 0.5 m.y.)			
5	Eastern Oregon-Western Idaho	142	6x10-2
19	Snake River Plain	59	1x10-2
8	Gulf Coast	54	0.2
14	Pacific Interior	51	3x10-2
29	Western Nevada	36	0.2
25	Utah-Nevada	24	0.2
20	Sonoran	24	6x10-3
2	California Coast	18	0.2
26	Walker Lane	15	0.3
22	Southern Calif. Borderland	14	0.2
15	Paradox	11	6x10-2
1	Arizona Mountain Belt	9.3	0.1
24	Transverse Ranges-Tehachapi	7	0.5
16	Puget-Olympic	7	3x10-2
28	Western Mojave	7	3x10-2
7	Grand Canyon	7	0.2
12	Northern Rockies	6	0.7
27	Wasatch-Tetons	5	0.4
9	Mexican Highland	5	9x10-2
17	Rio Grande	4	1.3
18	Salton Trough	4	0.3
Holocene Interval (10,000 - historic):			
26	Walker Lane	3.0	23
25	Utah-Nevada	2.2	2.0
	(L.A.)	(2.1)	(2.4)
17	Rio Grande	0.97	5.5
12	Northern Rockies	0.32	13
29	Western Nevada	0.31	22
24	Transverse Ranges-Tehachapi	0.09	43
28	Western Mojave	0.08	26
2	California Coast	0.05	96
9	Mexican Highland	0.05	8.6
18	Salton Trough	0.04	41

Table 3.2.-2 Fault activation rates for all regions and age intervals determined according to two assumptions: (a) activated fault length for a given age classification is divided by the age difference between that age class and the next younger age class and is plotted at the midpoint of the age range (log scale); (b) activated fault length for a given age classification is divided by the age difference between that age class and the next older age class and is plotted at the midpoint between the two ages (log scale). Assumption (a) is called the "leading" case and (b) the "lagging" case. Assumption (b) is physically as though accumulated strain during a time interval is released at the end of that time interval. Both cases are illustrated in Fig. 3.2.-6. Assumption (a) is considered to be more representative of the geologic assumptions used in classifying activation ages.

Table 3.2.-2

Region no. and name		LEAD				LAG		
		Age	Mean of log age	Rate (cm/yr)	Log rate	Age interval	Rate (cm/yr)	Log rate
1	Arizona Mountain Belt	15 m.y.	6.72	6.57	0.82	Miocene-Pliocene	0.81	-0.09
		1.8 m.y.	5.98	8.06	0.91	Early Pleistocene	13	1.11
		0.5 m.y.	4.85	34.16	1.53	Late Pleistocene	2.6	0.41
		10,000 yrs.	3.15	83.2	1.92	Holocene	--	--
		200 yrs.	1.15	--	--			
2	California Coast	15 m.y.	6.72	6.45	0.81	Miocene-Pliocene	16	1.20
		1.8 m.y.	5.98	164.07	2.22	Early Pleistocene	18	1.26
		0.5 m.y.	4.85	53.50	1.73	Late Pleistocene	206	2.31
		10,000 yrs.	3.15	9000	3.95	Holocene	9630	3.98
		200 yrs.	1.15	4.65×10^5	5.03			
3	Central Mississippi Valley	15 m.y.	6.72	1.77	0.25	Miocene-Pliocene	0.86	-0.07
		1.8 m.y.	5.98	--	--	Early Pleistocene	--	--
		0.5 m.y.	4.85	--	--	Late Pleistocene	--	--
		10,000 yrs.	3.15	--	--	Holocene	--	--
		200 yrs.	1.15	5.85×10^4	4.77			
4	Circum-Gulf	15 m.y.	6.72	0.28	-0.55	Miocene-Pliocene	--	--
		1.8 m.y.	5.98	--	--	Early Pleistocene	--	--
		0.5 m.y.	4.85	--	--	Late Pleistocene	--	--
		10,000 yrs.	3.15	--	--	Holocene	--	--
		200 yrs.	1.15	--	--			
5	Eastern Oregon-Western Idaho	15 m.y.	6.72	50.26	1.70	Miocene-Pliocene	11	1.04
		1.8 m.y.	5.98	109.58	2.04	Early Pleistocene	5.8	0.76
		0.5 m.y.	4.85	8.99	0.95	Late Pleistocene	--	--
		10,000 yrs.	3.15	--	--	Holocene	--	--
		200 yrs.	1.15	5000	3.70			
6	Four Corners	15 m.y.	6.72	0.44	-0.36	Miocene-Pliocene	1.2	0.08
		1.8 m.y.	5.98	12.38	1.09	Early Pleistocene	--	--
		0.5 m.y.	4.85	--	--	Late Pleistocene	--	--
		10,000 yrs.	3.15	--	--	Holocene	--	--
		200 yrs.	1.15	--	--			
7	Grand Canyon	15 m.y.	6.72	4.96	0.69	Miocene-Pliocene	1.8	0.26
		1.8 m.y.	5.98	17.33	1.24	Early Pleistocene	19	1.28
		0.5 m.y.	4.85	50.48	1.70	Late Pleistocene	2.1	0.32
		10,000 yrs.	3.15	101.85	2.01	Holocene	--	--
		200 yrs.	1.15	--	--			
8	Gulf Coast	15 m.y.	6.72	74.83	1.87	Miocene-Pliocene	16	1.20
		1.8 m.y.	5.98	157.85	2.20	Early Pleistocene	23	1.36
		0.5 m.y.	4.85	63.39	1.80	Late Pleistocene	68	1.83
		10,000 yrs.	3.15	3115.74	3.49	Holocene	--	--
		200 yrs.	1.15	--	--			
9	Mexican Highland	15 m.y.	6.72	1.63	0.21	Miocene-Pliocene	0.24	-0.62
		1.8 m.y.	5.98	2.11	0.32	Early Pleistocene	9.2	0.96
		0.5 m.y.	4.85	2.20	1.34	Late Pleistocene	2.1	0.32
		10,000 yrs.	3.15	65.5	1.82	Holocene	856	2.93
		200 yrs.	1.15	4.22×10^4	4.63			
10	Mid-continent	15 m.y.	6.72	0.13	-0.89	Miocene-Pliocene	0.56	0.25
		1.8 m.y.	5.98	5.81	0.76	Early Pleistocene	--	--
		0.5 m.y.	4.85	--	--	Late Pleistocene	--	--
		10,000 yrs.	3.15	--	--	Holocene	--	--
		200 yrs.	1.15	--	--			

Table 3.2.-2

Region no. and name		LEAD Age	Mean of log age	Rate (cm/yr)	Log rate	LAG Age interval	Rate (cm/yr)	Log rate
		15 m.y.	6.72	--	--	Miocene-Pliocene	--	--
11	Northeast	1.8 m.y.	5.98	--	--	Early Pleistocene	--	--
		0.5 m.y.	4.85	8.59	0.93	Late Pleistocene	--	--
		10,000 yrs.	3.15	--	--	Holocene	--	--
		200 yrs.	1.15	--	--			
		15 m.y.	6.72	18.5	1.27	Miocene-Pliocene	3.8	0.58
12	Northern Rockies	1.8 m.y.	5.98	37.1	1.57	Early Pleistocene	67	1.83
		0.5 m.y.	4.85	1.77×10^2	2.25	Late Pleistocene	35	1.54
		10,000 yrs.	3.15	1.13×10^3	3.05	Holocene	1265	3.10
		200 yrs.	1.15	5.85×10^4	4.77			
		15 m.y.	6.72	3.22	0.51	Miocene-Pliocene	14	1.15
13	Oregon-Washington Coast	1.8 m.y.	5.98	1.38×10^2	2.14	Early Pleistocene	--	--
		0.5 m.y.	4.85	--	--	Late Pleistocene	--	--
		10,000 yrs.	3.15	--	--	Holocene	--	--
		200 yrs.	1.15	--	--			
		15 m.y.	6.72	8.67	0.94	Miocene-Pliocene	1.5	0.18
14	Pacific Interior	1.8 m.y.	5.98	14.5	1.16	Early Pleistocene	2.7	0.43
		0.5 m.y.	4.85	7.26	0.86	Late Pleistocene	--	--
		10,000 yrs.	3.15	--	--	Holocene	--	--
		200 yrs.	1.15	9.71×10^3	3.99			
		15 m.y.	6.72	0.23	-0.63	Miocene-Pliocene	3.6	0.56
15	Paradox	1.8 m.y.	5.98	36.9	1.57	Early Pleistocene	5.9	0.77
		0.5 m.y.	4.85	15.2	1.18	Late Pleistocene	--	--
		10,000 yrs.	3.15	--	--	Holocene	--	--
		200 yrs	1.15	--	--			
		15 m.y.	6.72	--	--	Miocene-Pliocene	--	--
16	Puget-Olympic	1.8 m.y.	5.98	9.77	0.99	Early Pleistocene	2.5	0.40
		0.5 m.y.	4.85	6.13	0.79	Late Pleistocene	21	1.32
		10,000 yrs.	3.15	8.98×10^2	2.95	Holocene	--	--
		200 yrs	1.15	--	--			
		15 m.y.	6.72	8.95	0.95	Miocene-Pliocene	16	1.2
17	Rio Grande	1.8 m.y.	5.98	1.60×10^2	2.20	Early Pleistocene	134	2.13
		0.5 m.y.	4.85	3.59×10^2	2.56	Late Pleistocene	56	1.75
		10,000 yrs.	3.15	2.44×10^3	3.39	Holocene	550	2.74
		200 yrs	1.15	2.38×10^4	4.38			
		15 m.y.	6.72	--	--	Miocene-Pliocene	--	--
18	Salton Trough	1.8 m.y.	5.98	5.3	0.72	Early Pleistocene	30	1.48
		0.5 m.y.	4.85	29.8	1.47	Late Pleistocene	81	1.91
		10,000 yrs.	3.15	25.9	1.42	Holocene	4062	3.61
		200 yrs	1.15	206×10^5	5.32			
		15 m.y.	6.72	0.07	-1.17	Miocene-Pliocene	5.0	0.70
19	Snake River Plain	1.8 m.y.	5.98	52.0	1.72	Early Pleistocene	1.2	0.08
		0.5 m.y.	4.85	--	--	Late Pleistocene	25	1.40
		10,000 yrs.	3.15	2.51	0.40	Holocene	--	--
		200 yrs	1.15	11.3	3.04			
		15 m.y.	6.72	0.2	-0.7	Miocene-Pliocene	0.83	-0.08
20	Sonoran	1.8 m.y.	5.98	7.96	0.9	Early Pleistocene	0.59	-0.23
		0.5 m.y.	4.85	--	--	Late Pleistocene	--	--
		10,000 yrs.	3.15	1.55	0.19	Holocene	--	--
		200 yrs	1.15	--	--			

Table 3.2.-2

Region no. and name		LEAD Age	Mean of log age	Rate (cm/yr)	Log rate	LAG Age interval	Rate (cm/yr)	Log rate
		15 m.y.	6.72	0.37	-0.44	Miocene-Pliocene	--	--
21	Southeast	1.8 m.y.	5.98	--	--	Early Pleistocene	--	--
		0.5 m.y.	4.85	--	--	Late Pleistocene	--	--
		10,000 yrs.	3.15	--	--	Holocene	--	--
		200 yrs	1.15	--	--			
		15 m.y.	6.72	17.5	1.24	Miocene-Pliocene	2.1	0.32
22	Southern Calif. Borderland	1.8 m.y.	5.98	20.7	1.32	Early Pleistocene	22	1.34
		0.5 m.y.	4.85	52.8	1.72	Late Pleistocene	3.8	0.58
		10,000 yrs.	3.15	1.94×10^2	2.29	Holocene	--	--
		200 yrs	1.15					
		15 m.y.	6.72	11.7	1.07	Miocene-Pliocene	0.33	-0.48
23	Straits of Florida	1.8 m.y.	5.98	--	--	Early Pleistocene	--	--
		0.5 m.y.	4.85	8.28	0.92	Late Pleistocene	--	--
		10,000 yrs.	3.15	--	--	Holocene	--	--
		200 yrs	1.15	--	--			
		15 m.y.	6.72	15.7	1.20	Miocene-Pliocene	5.5	0.74
24	Transverse Ranges-Tehachapi	1.8 m.y.	5.98	53.9	1.73	Early Pleistocene	54	1.73
		0.5 m.y.	4.85	1.44×10^2	2.16	Late Pleistocene	22	1.34
		10,000 yrs.	3.15	6.16×10^2	2.79	Holocene	4340	3.64
		200 yrs	1.15	2.02×10^5	5.3			
		15 m.y.	6.72	14.7	1.17	Miocene-Pliocene	16	1.20
25	Utah-Nevada	1.8 m.y.	5.98	1.63×10^2	2.21	Early Pleistocene	18	1.26
		0.5 m.y.	4.85	46.3	1.67	Late Pleistocene	24	1.38
		10,000 yrs.	3.15	8.15×10^2	2.91	Holocene	198	2.30
		200 yrs	1.15	6.0×10^3	3.79			
		15 m.y.	6.72	2.46	0.39	Miocene-Pliocene	27	1.43
26	Walker Lane	1.8 m.y.	5.98	2.69×10^2	2.43	Early Pleistocene	30	1.48
		0.5 m.y.	4.85	80.9	1.90	Late Pleistocene	71.6	1.86
		10,000 yrs.	3.15	3.09×10^3	3.49	Holocene	2322	3.37
		200 yrs	1.15	1.32×10^5	5.12			
		15 m.y.	6.72	4.22	0.63	Miocene-Pliocene	5.3	0.72
27	Wasatch-Tetons	1.8 m.y.	5.98	52.5	1.72	Early Pleistocene	37	1.57
		0.5 m.y.	4.85	97.3	1.99	Late Pleistocene	103	2.01
		10,000 yrs.	3.15	4.63×10^3	3.67	Holocene	--	--
		200 yrs	1.15	--	--			
		15 m.y.	6.72	1.53	0.19	Miocene-Pliocene	8.2	0.91
28	Western Mojave	1.8 m.y.	5.98	79.5	1.90	Early Pleistocene	2.5	1.40
		0.5 m.y.	4.85	69.7	1.85	Late Pleistocene	30	1.48
		10,000 yrs.	3.15	1.48×10^3	3.17	Holocene	2631	3.42
		200 yrs	1.15	1.29×10^5	5.11			
		15 m.y.	6.72	8.45	0.93	Miocene-Pliocene	36	1.56
29	Western Nevada	1.8 m.y.	5.98	3.55×10^2	2.55	Early Pleistocene	17	1.23
		0.5 m.y.	4.85	41.9	1.62	Late Pleistocene	98	1.99
		10,000 yrs.	3.15	3.9×10^3	3.59	Holocene	2155	3.33
		200 yrs	1.15	1.12×10^5	5.05			
		15 m.y.	6.72	13.3	1.72	Miocene-Pliocene	0.76	-0.12
30	Wyoming	1.8 m.y.	5.98	4.58	0.64	Early Pleistocene	--	--
		0.5 m.y.	4.85	5.7	0.72	Late Pleistocene	--	--
		10,000 yrs.	3.15	--	--	Holocene	--	--
		200 yrs	1.15	5.57×10^3	3.75			

3.3. Rates of Fault Activation and Regional Earthquake Activity.

Mark (1977) has discussed empirical correlations between fault lengths involved in earthquakes and the corresponding earthquake magnitudes. Because the present data represent fault lengths showing movement, the activation rates reflect the average lengths of fault traces that could experience movement each year. Therefore, we examine the implicit or potential level in earthquake activity associated with those movements using Mark's correlation as a numerical guide. For this purpose we used the equation he suggested for correlating magnitude with length (Mark, 1977, Figure 3, curve BB') reproduced here as Figure 3.3.-1:1/

$\overline{MM} = 1.235 + 1.243 \text{ Log}(\ell)$, ℓ is activated length in meters2/

Here we call $\overline{MM}$ the "Mark Magnitude;" it refers to the mean value for earthquake magnitude implied by our data as calculated from Mark's equation; the equation represents a magnitude for which half the earthquakes could be larger. Similarly a length calculated from Mark's equation for a given magnitude is a "Mark Length". Using this correlation we have shown an earthquake magnitude scale on the graphs of activation rates in Figure 3.2.-6. The scale represents a guide to the implied magnitude for an earthquake if all movement each year produced a single earthquake that year. This correlation also suggests possible recurrence intervals for assumed levels in earthquake activity. If the implied activation rate has been operating 10 years without an earthquake, the potential magnitude of a single quake is roughly an order of magnitude larger, and so on.

We offer these comparisons as suggestions for work on earthquake occurrences related to regional faulting patterns. The levels in earthquake activity implied by patterns for activation rates are grossly consistent with earthquake records. Later we derive relations between numbers and lengths of faults, activation rates, and earthquake magnitude-frequency correlations in the United States.

1/ The symbol $\overline{MM}$ is not to be confused with the modified Mercalli convention for magnitudes. Modified Mercalli magnitudes are nowhere used in this report to represent earthquake data.

2/ This correlation is for strike-slip faults; however, it resembles other correlations for world-wide data at the larger magnitudes. We use the equation as a standard of comparison and not as the best representation of the data. Correlation schemes for data subdivided by style and regional scope are given by Mark and Bonilla (1977).

SECTION 3.3. FIGURES AND TABLES

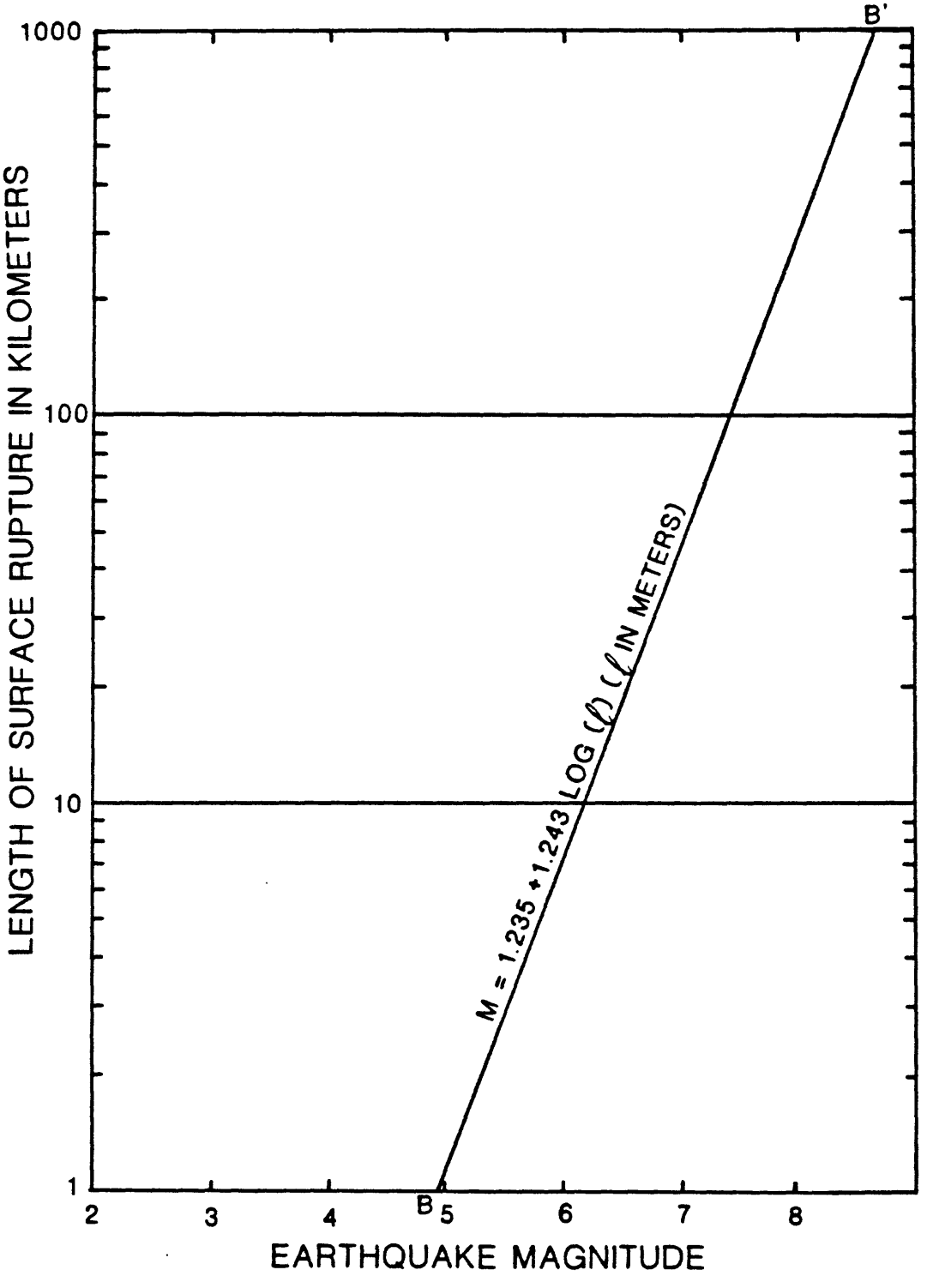

Figure 3.3.-1.
Relation between fault rupture length and earthquake magnitude according to Mark (1977, Fig. 3, line BB'). This correlation is for strike-slip faults. We used it because the discussion clarifies differences between regressions on length and magnitude. Correlations for different styles and geographic scope are give by Mark and Bonilla (1977).

3.4. Map Patterns for Fault Activation Rates.

Figure 3.4.-1 shows the patterns for calculated activation rates in the 30 regions of the conterminous United States for each age interval from Miocene to Holocene. Figure 3.4.-2 shows the regions having the most accelerative increases in activation rates since the Pleistocene. Figure 3.4.-3 shows the map distribution having positive or negative rate changes in the Plio-Pleistocene interval, and regions with continuously increasing rates during that interval. Figure 3.4.-4 shows the distributions for recorded earthquakes in the conterminous United States. Figure 3.4.-5 shows contours for seismic risk in the United States and Figure 3.4.-6 shows patterns of seismic energy release.

The maps are mostly self-evident and can be compared with length frequency distributions in Figures 2.2.1.7 and 2.2.1.-8; we defer discussion to later sections where we present relations between magnitude, earthquake frequency, fault length, length frequency (numbers of length segments), and activation rates for faults having given segment lengths.

SECTION 3.4. FIGURES AND TABLES

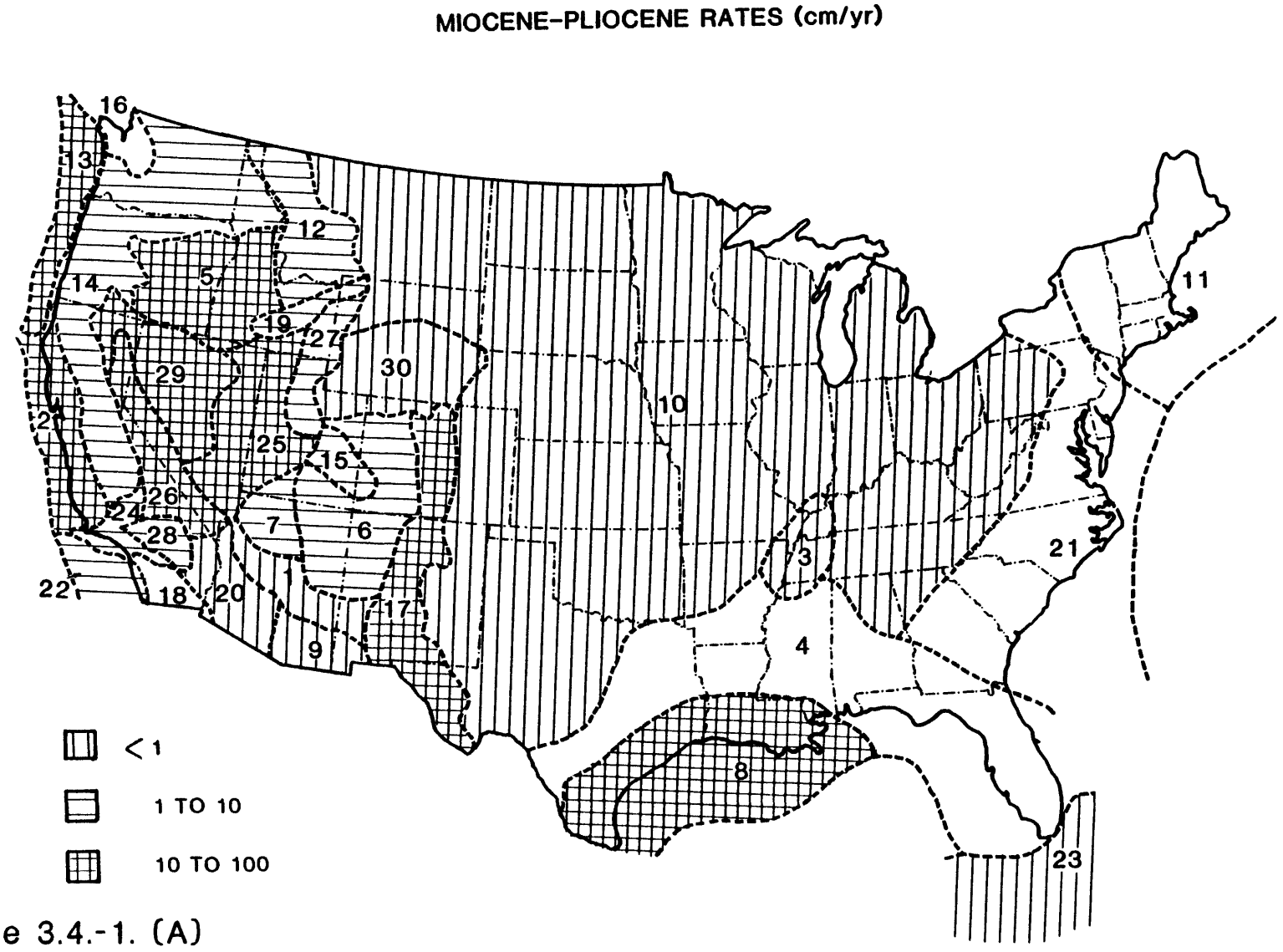

Figure 3.4.-1. (A)

Map distributions for regional fault activation rates. Rates in cm/yr represent the actual ground rupture length, not the map scale length. Blank areas on the map represent regions with insufficient data to derive rates.

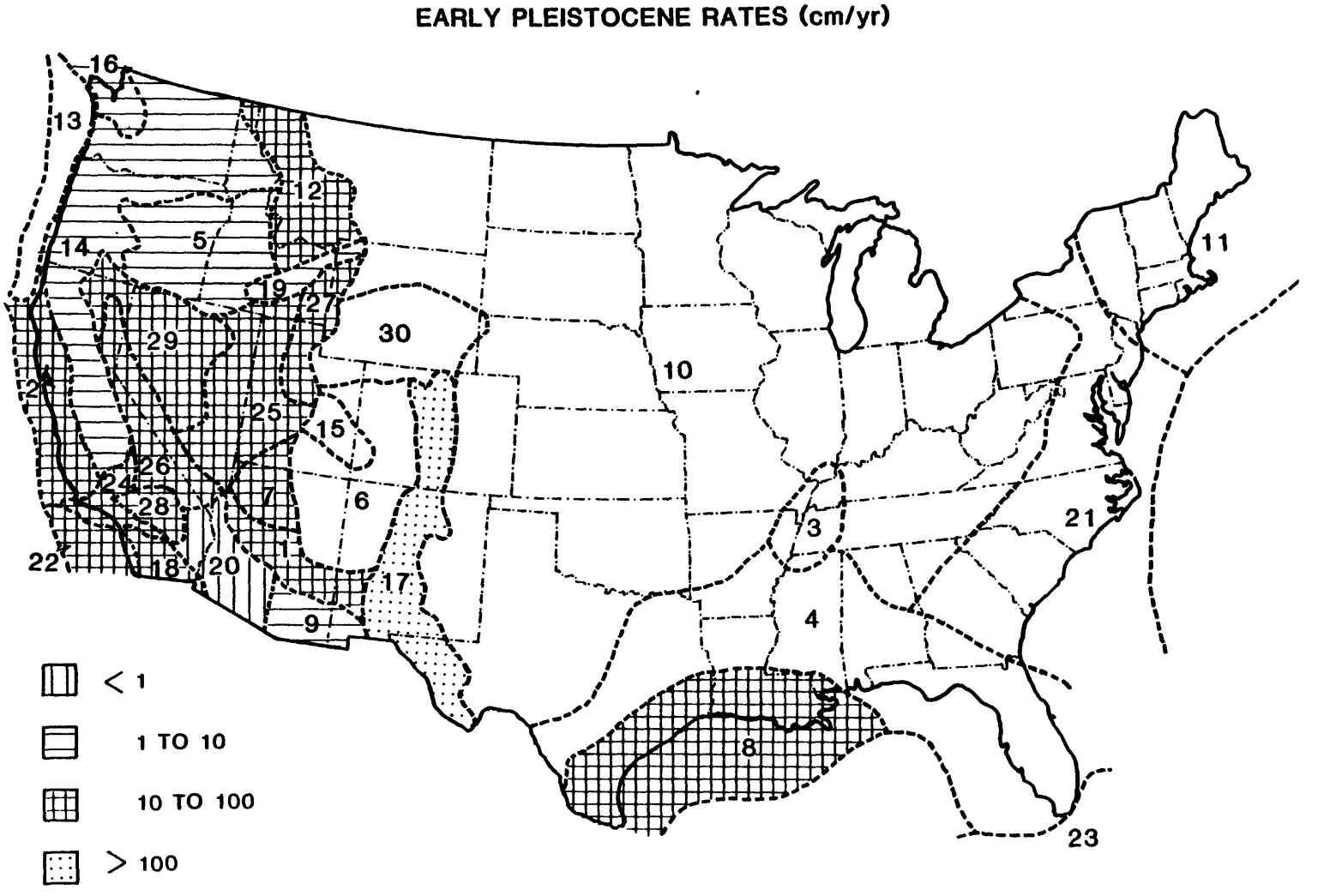
EARLY PLEISTOCENE RATES (cm/yr)
16
13
12
5
14
19
27
30
29
10
11
2
25
15
26
24
28
7
6
3
21
22
18
20
1
17
4
9
8
23
< 1
1 TO 10
10 TO 100
> 100

Figure 3.4.-1. (B)

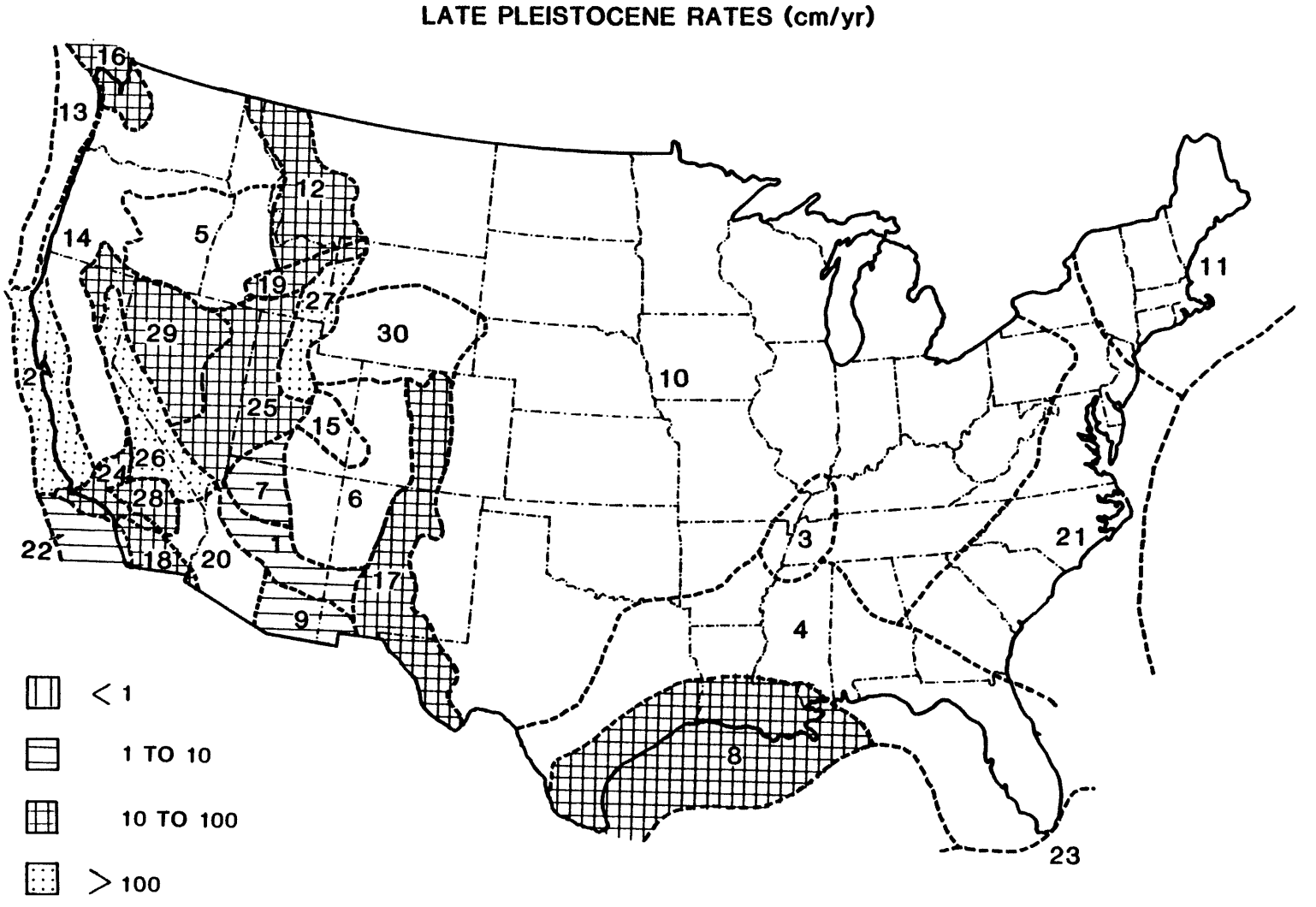
LATE PLEISTOCENE RATES (cm/yr)
16
13
12
14
5
19
27
29
30
2
10
25
15
26
24
28
7
6
22
18
20
1
17
9
3
21
4
8
23
11
< 1
1 TO 10
10 TO 100
> 100

Figure 3.4.-1. (C)

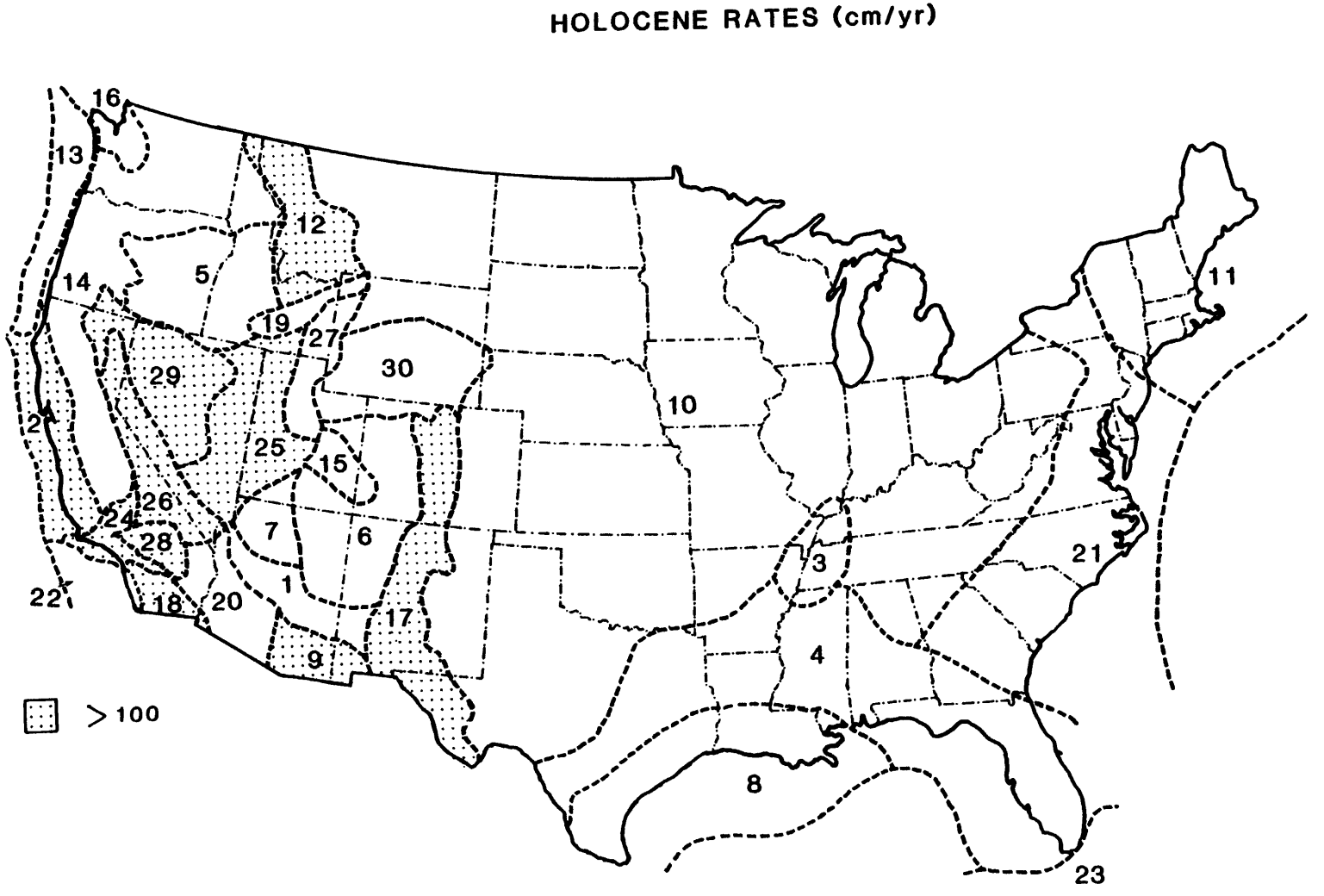
HOLOCENE RATES (cm/yr)
16
13
12
5
14
19
27
30
29
10
11
2
25
15
26
24
28
7
6
3
21
22
1
18
20
17
9
4
>100
8
23

Figure 3.4.-1. (D)

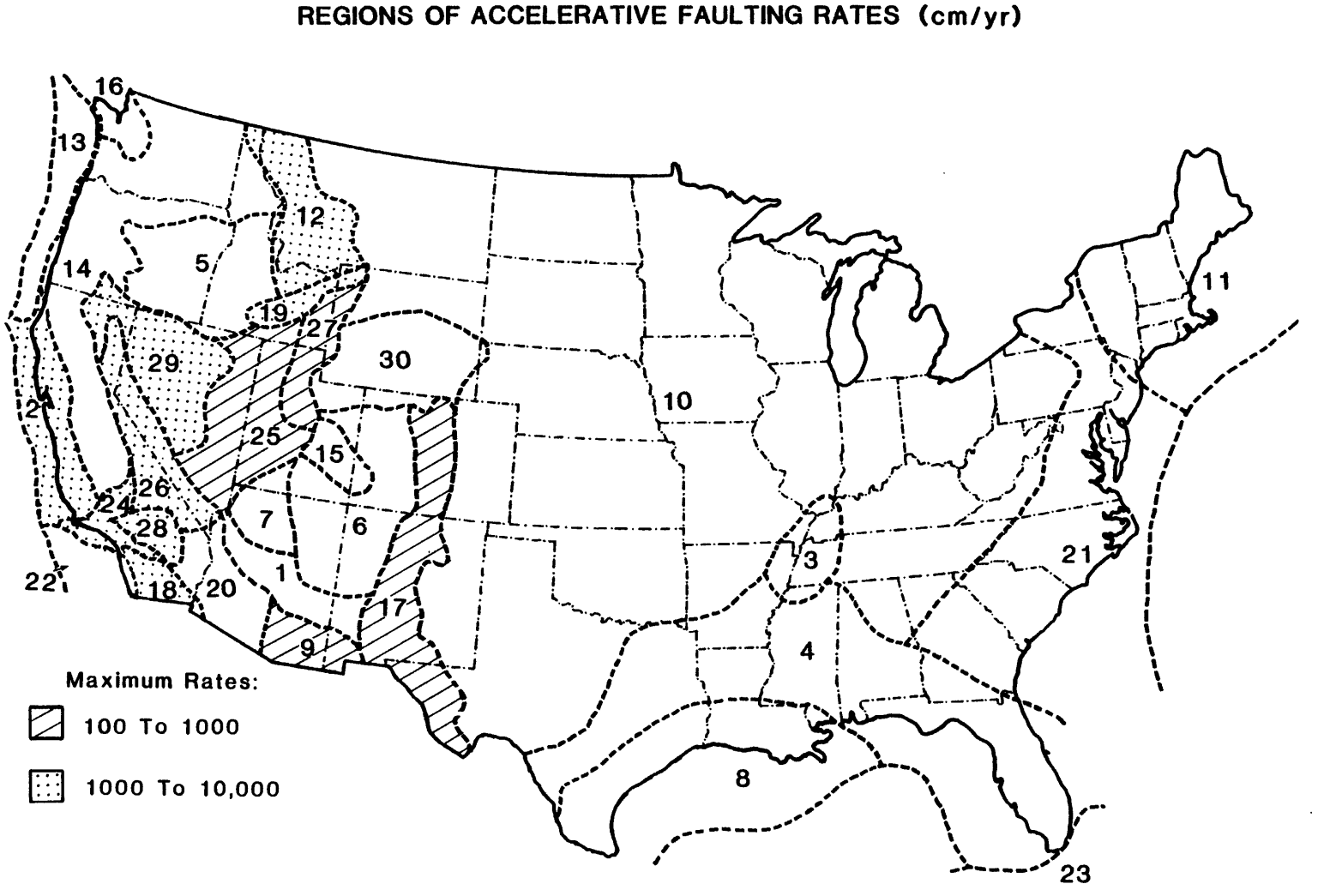

Figure 3.4.-2.

Map distribution for regions showing accelerative fault activation rates.

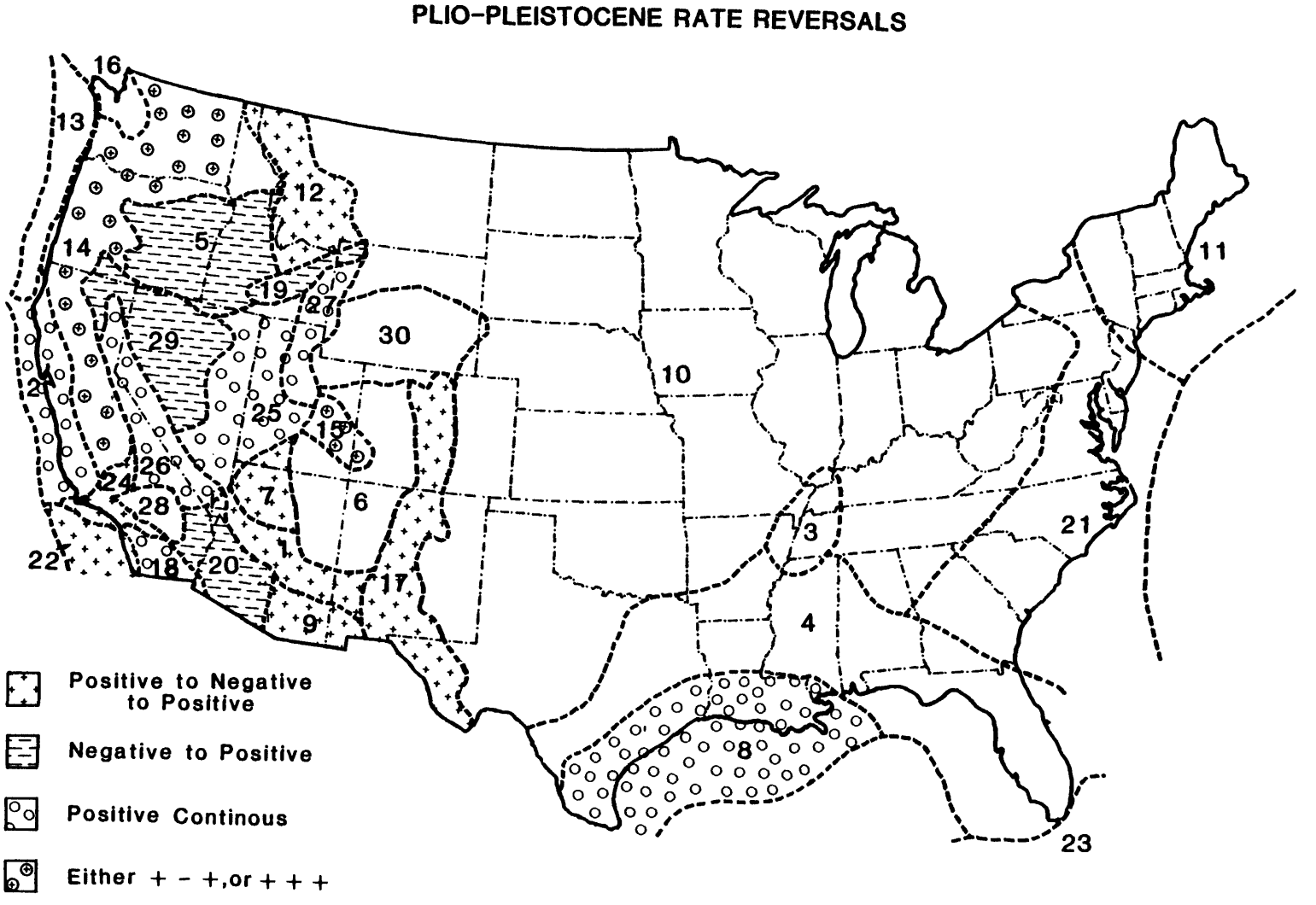

Figure 3.4.-3. (A)

Map showing regions that have reversals in fault activation rates at an age around 10^6 years B.P., based on convention (a) for activation rates in table 3.2.-2 (solid lines in Figure 3.2.-6). Areas identified by horizontal lines have only partial curve forms; blank areas represent regions lacking sufficient rate data to identify any progression.

REGIONS GROUPED ACCORDING TO SIMILAR CURVE FORMS FOR REGIONAL FAULTING RATES VS AGE

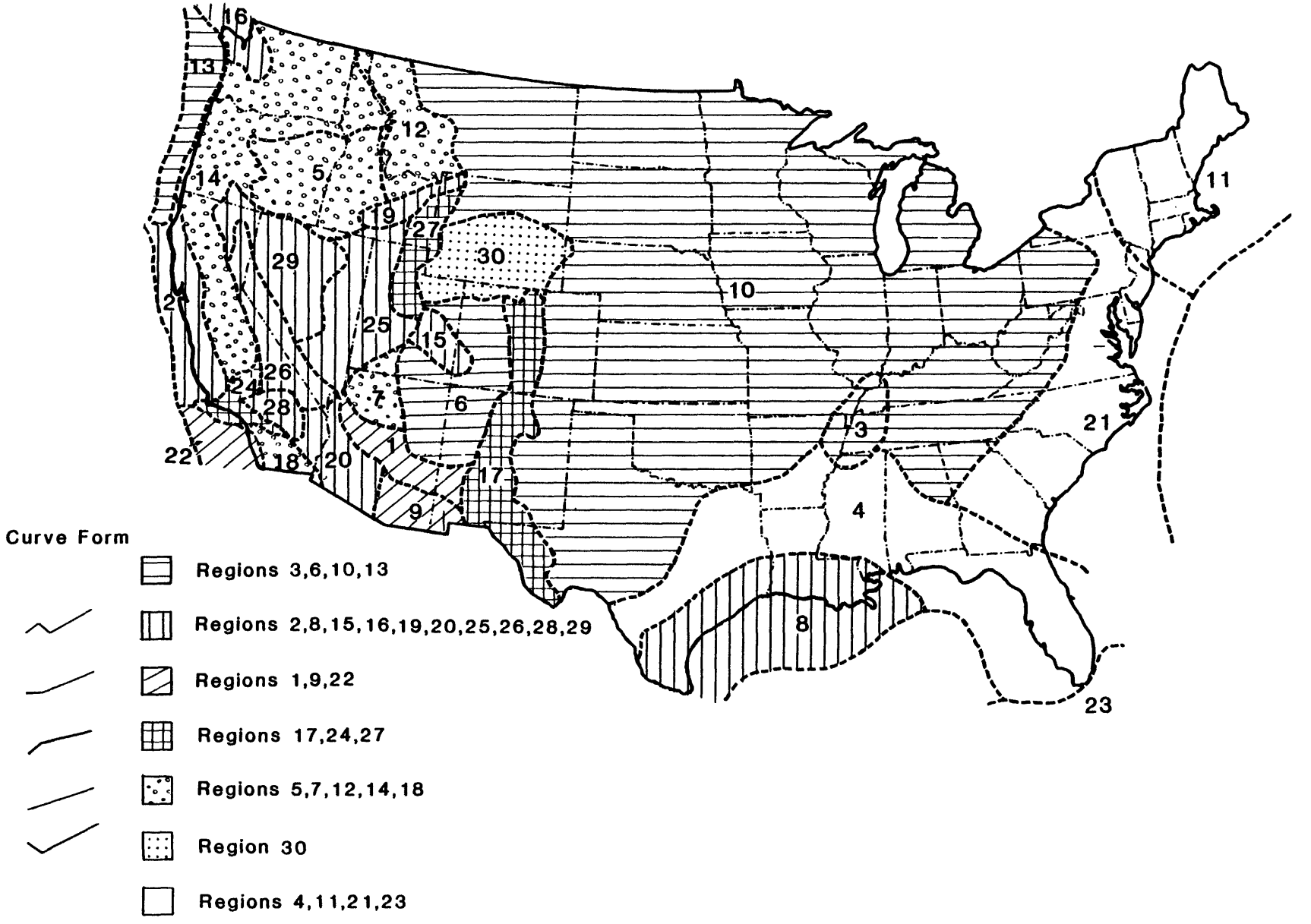

Figure 3.4.-3. (B)

REGIONS GROUPED ACCORDING TO SIMILAR CURVE FORMS
FOR CUMULATIVE FRACTION OF FAULT LENGTHS VS AGE

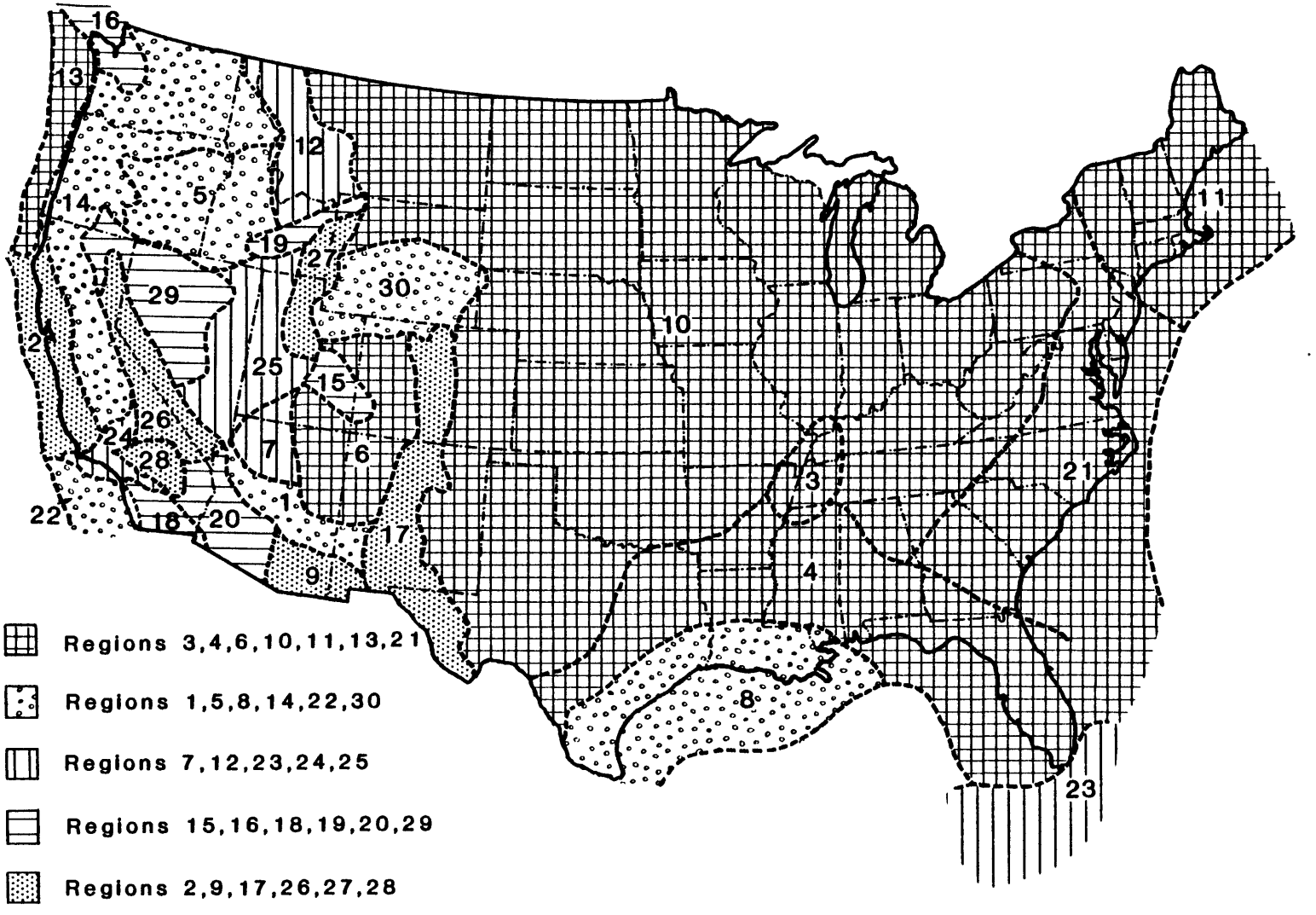

Figure 3.4.-.3. (C)

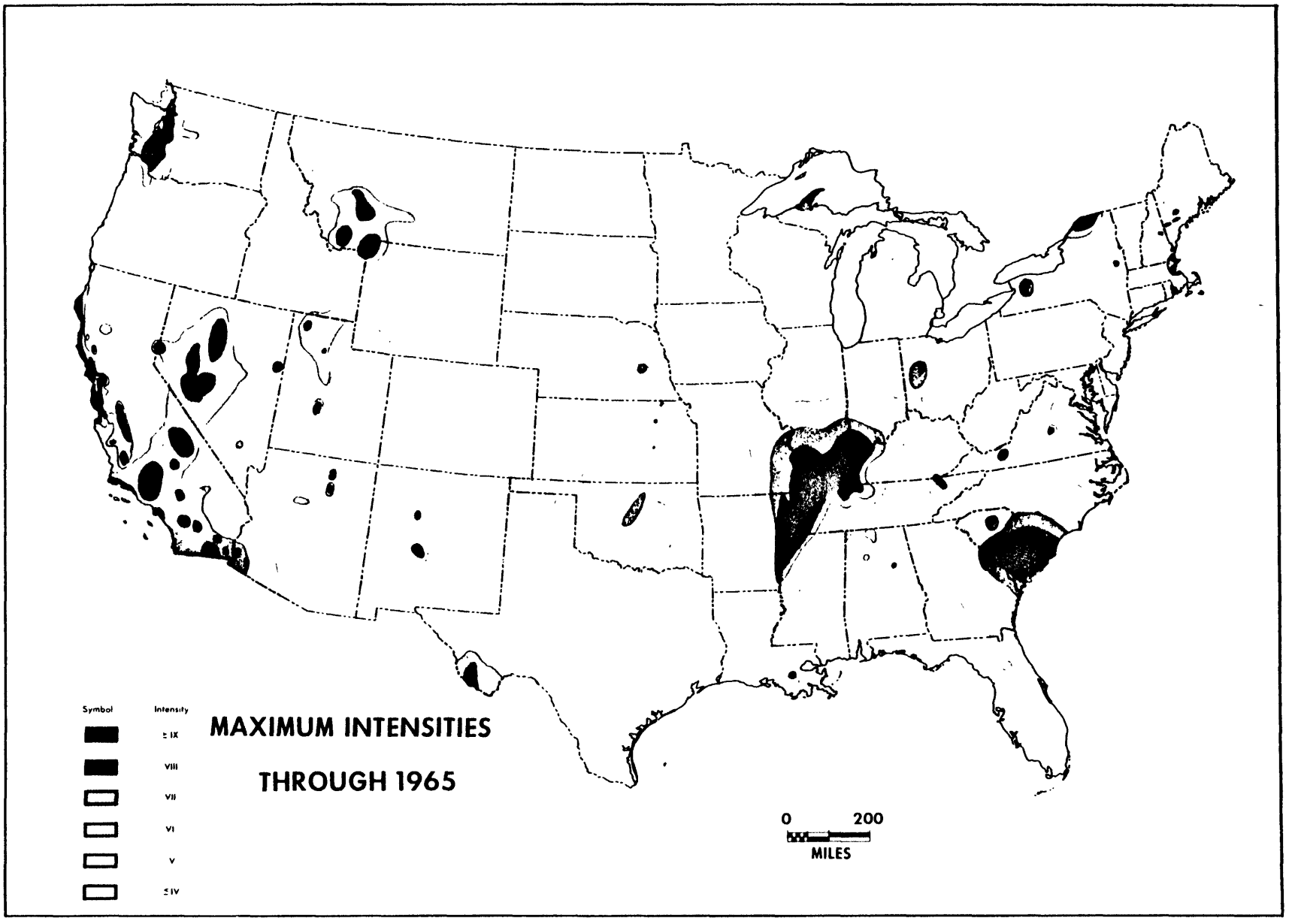

Figure 3.4.-4.

Map showing the general distribution for earthquake epicenters in the United States during recorded history to 1965; for details see Algermissen (1969). Note: Accurate reproduction of the shaded regions was not possible, and enlarged maps were not available from the author.

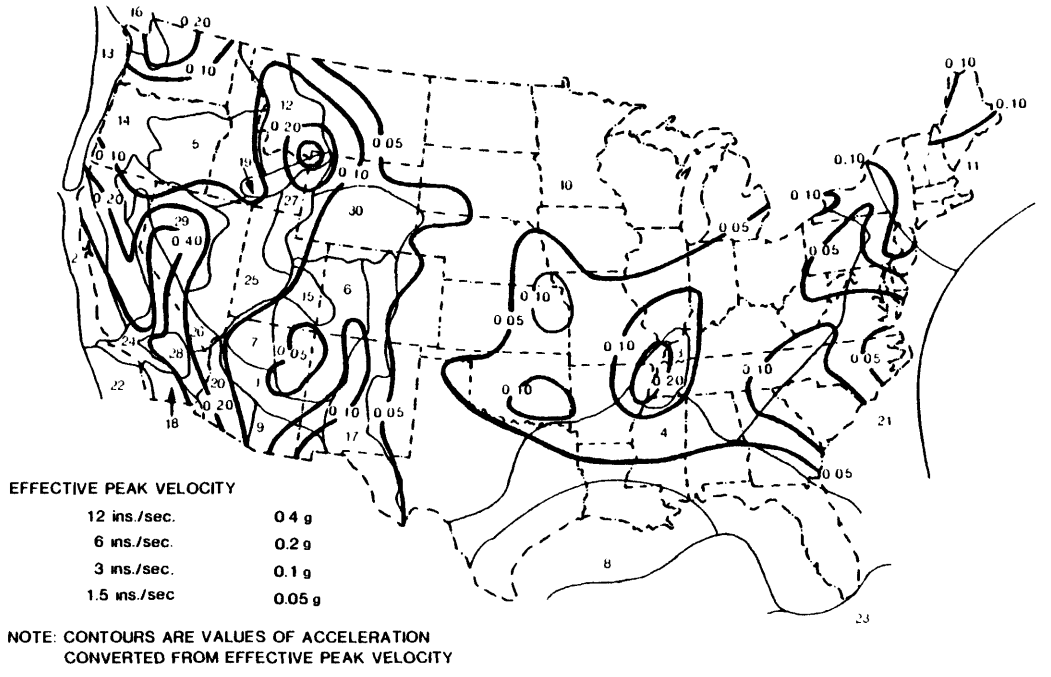

Figure 3.4.-5.
Contour map showing seismic risk distribution (from Donovan and others, 1978).

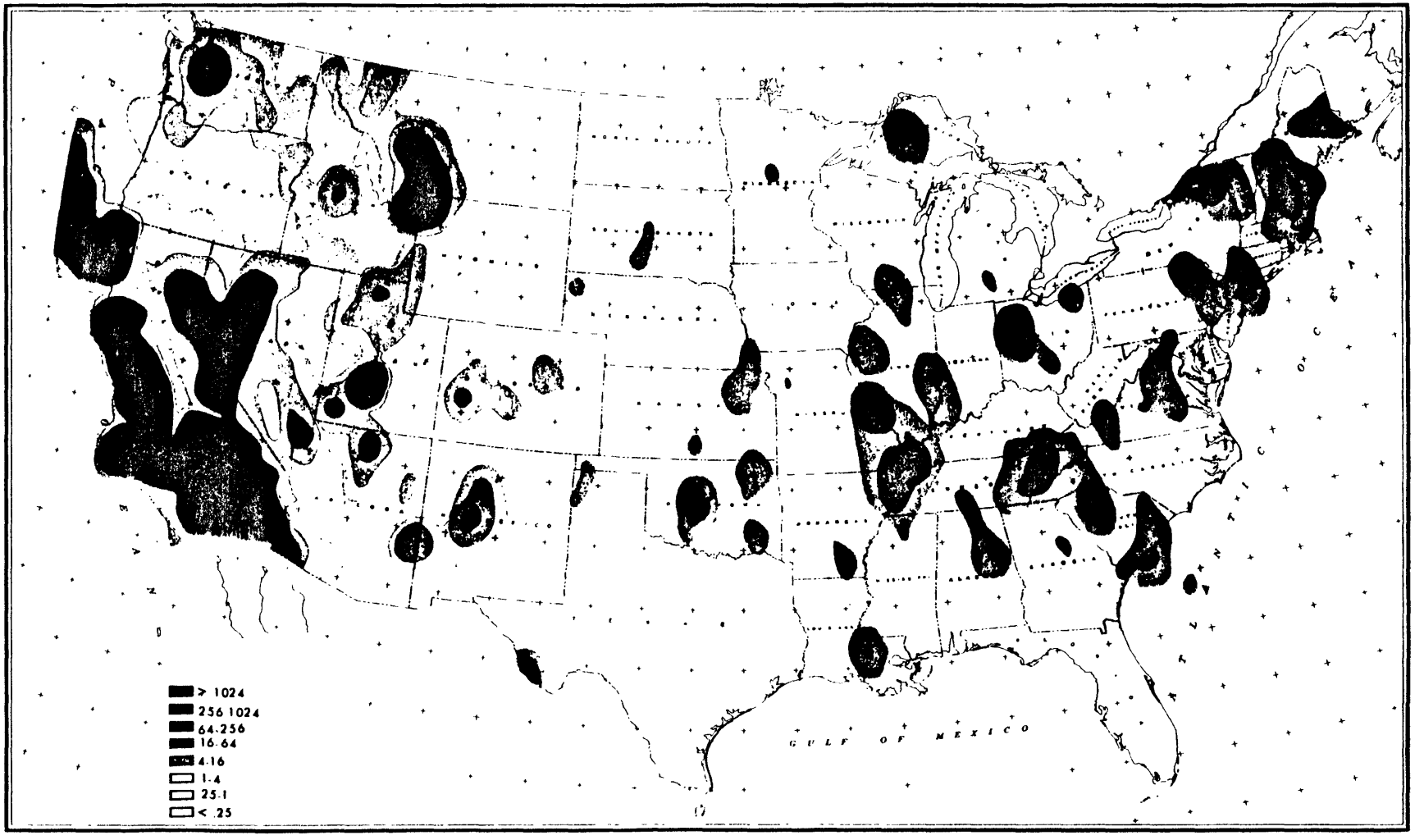

Figure 3.4.-6.

Generalized map pattern representing seismic energy dissipation in the conterminous United States; for details see Algermissen (1969). Note: Accurate reproduction of the shaded regions was not possible, and enlarged maps were not available from the author.

SECTION 4.

4. Frequency Distributions and Fault Branching.

So far we have displayed the data in ways that have emphasized their statistical variations. We now generalize the distributions in order to discuss the different possible forms of representation and the question of whether or not the data support the existence of some systematic law for fault length distributions.

4.1 Cumulative Frequency Distributions Based on Linearly Equal Increments of Length.

4.1.1 Fault Data.

Figure 4.1.1.-1 gives the total numbers of faults, for the United States data, greater than a given length, plotted in three different ways to bring out scale effects and shapes in the distributions. Figure 4.1.1.-1(1) shows the numbers represented by faults greater than a given length. Figure 4.1.1.-1(2) gives the same data plotted as logarithms for fractions of faults greater than a given length; e.g. about 10 percent of the United States data represent faults greater than 50 km. Figure 4.1.1.-1(3) shows the linear fraction versus the logarithmic length.

Figure 4.1.1.-2 gives the same sets of plots for the L. A. Area. In this case, 10 percent of the faults have lengths greater than about 10 km but less than 50 km, reflecting the finer measurement scale and curtailment for data beyond a length at about 40 km because of the scale.

In both data sets, the logarithmic scale for lengths shows a maximum density for points at intermediate lengths, reflecting the way measurements at equal length intervals affect the distribution. To give added insight about the size scale effects and sampling intervals we determined analogous distributions for other contrasting data types and have explored various types of graphical representation.

The problem with the cumulative distributions as shown in Figures 4.1.1.-1 and 4.1.1.-2 is that the central body of the data is compressed, and sampling peculiarities at very short and very long lengths are emphasized. In some instances, these kinds of plots are revealing, particularly for comparative shapes in different sets of data. An example is given in Figure 4.1.1.-3 where cumulative frequencies are plotted together for sets of data representing microfracture, faulting on two map scales and septa lengths for bubble walls in soap films obtained from a photograph of a froth (original data are referenced in the next section). The plots emphasize the frequency cutoff where data are not represented at short lengths and the length cutoff where the data approach the system size. The froth data, particularly, are biased by a restricted length range.

SECTION 4.1.1. FIGURES AND TABLES

CUMULATIVE NUMBER VERSUS FAULT LENGTH ALL U. S.

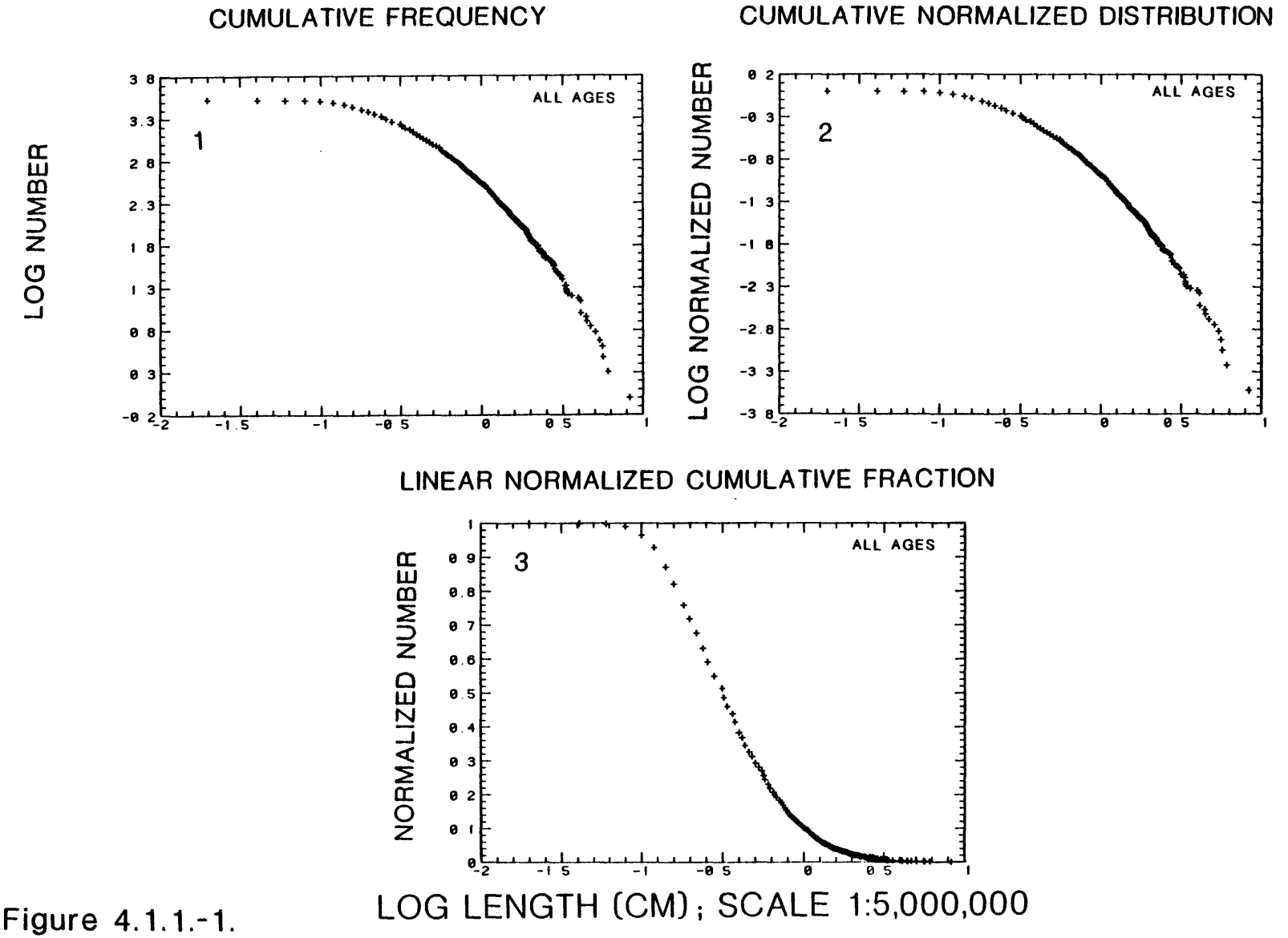

Figure 4.1.1.-1.

Cumulative number versus fault length relations for the United States: (1) log of actual cumulative number versus log fault length; (2) log of normalized cumulative fraction versus log fault length; (3) linear normalized cumulative fraction versus log fault length.

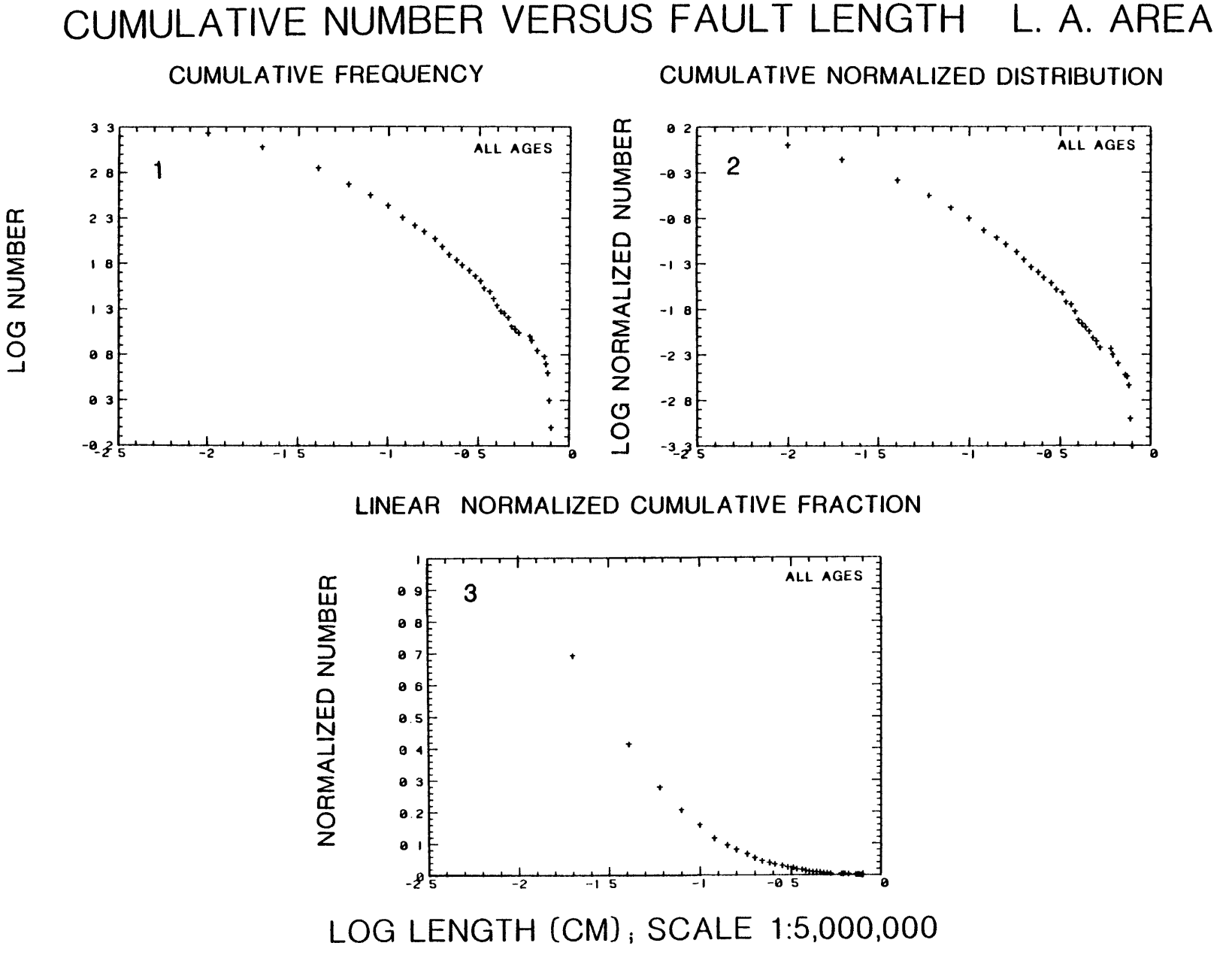

Figure 4.1.1.-2.
Cumulative number versus fault length relations for L.A. area.

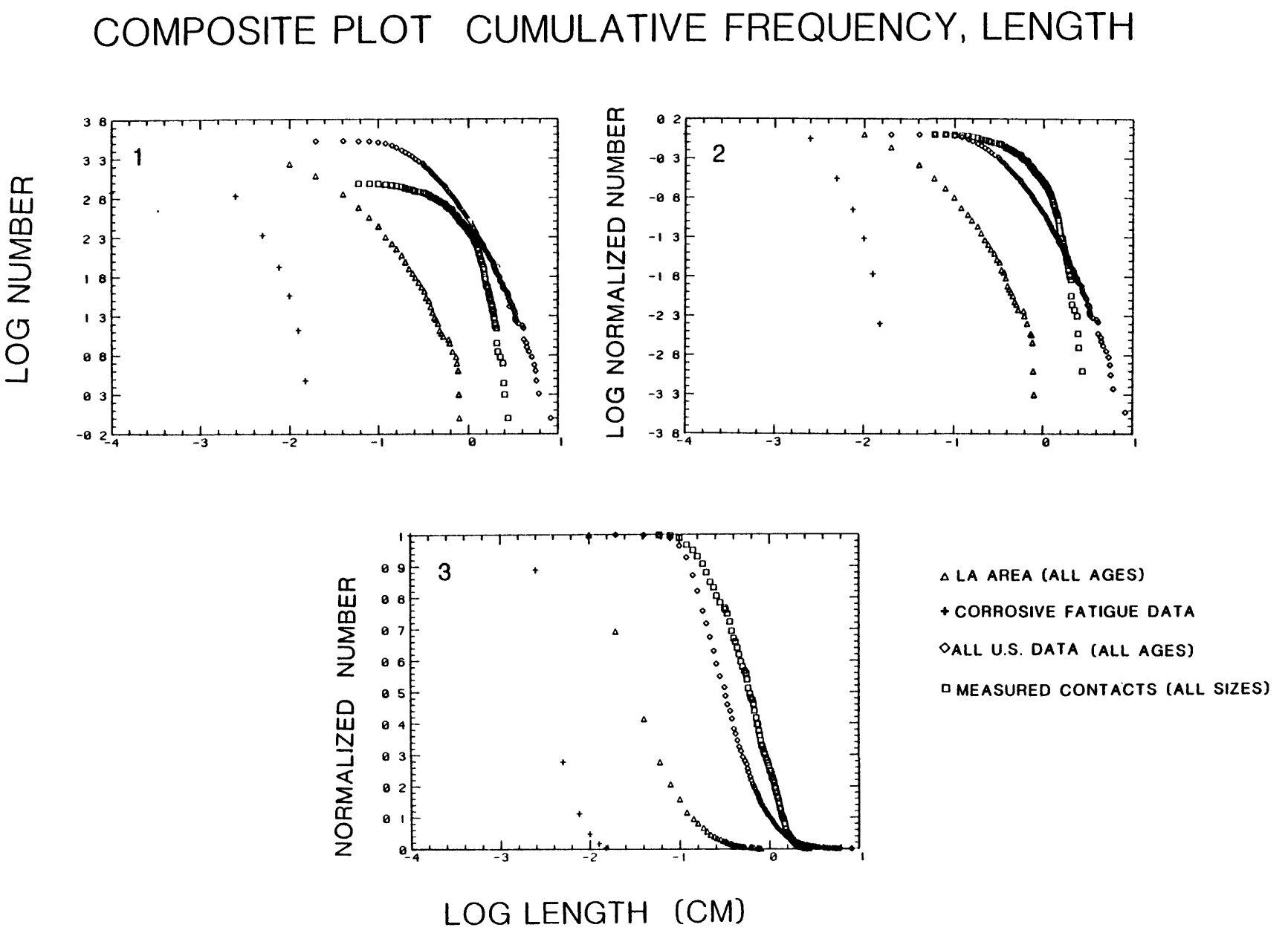

Figure 4.1.1.-3.
Cumulative number versus length relations for different data sets compared (soap films, microfractures, etc.).

4.1.2. Other Types of Length Distributions

When we noticed that the fault length distributions suggested constant frequency ratios over different portions and length ranges, we began to look for other phenomena with similar behavior. As it has turned out, we didn't have to search far to find data for many different classes of phenomena that show similar branching patterns. Many examples for branching patterns are illustrated by Thompson (1942) and Stevens (1974) and there have been several quantitative studies demonstrating branching distributions in stream systems. The most conspicuous studies we have found are those by Horton (1945), Strahler (1950), Leopold and Langbein (1962), Shreve (1966) and Woldenberg (1969). In particular, Woldenberg (1966, 1967, 1968a and b, 1969; Woldenberg and Berry, 1967) and coworkers have systematically explored analogous laws for hierarchical orders in many systems, including rivers, glaciers, trees, internal organs in animals, cities, and human economic systems. So far we have not encountered any analogous studies for fracture and faulting, except for the stochastic model of branching proposed by Vere-Jones (1976). Parallel relations portraying cratering sizes and distribution densities on planetary surfaces are reviewed by Hartmann (1977).

In a sense the problem of hierarchical order in faulting can be visualized as being a bit like measuring branch lengths in a dismembered tree, where the pieces have been scattered around over some more or less localized area. Obvious limits in this pictorial analogy involve the fact that fault distributions change with time and may involve displacements between different parts in the system over long distances of separation--conceivably amounting to hundreds of kilometers in 15 m.y. However, the fact that branches hundreds of kilometers in length are included in the distributions can actually give clues to either related or unrelated branching patterns if the areal scale of observation is sufficiently large and fault patterns can be mapped.

We have chosen to illustrate branching patterns for different scales and types of systems by comparing data for faulting with data for microfracturing, with data for lengths of septa between bubble walls in a froth and with stream lengths in a drainage basin.

Figure 4.1.2.-1 gives data obtained by Kitagawa and Suzuki (1975) for fracture in a metal test specimen. Microcracks were measured at different deformation stages until the specimen failed. They observed that fractures with intermediate lengths apparently coalesced to form the final through-going fracture representing failure. The slopes for the distributions are steeper than those in the fault data, and this may relate to both the finite specimen size and the high deformation rates. The other diagrams in Figure 4.1.2.-1 are plotted for a systematic length interval to be explained.

Figure 4.1.2.-2 gives the analogous distribution for septa lengths in the photograph of a froth shown in Figure 4.1.2.-3. The distribution in this instance is clearly biased by the limited size range relative to the field of view. Like the case of microfractures in the laboratory specimen, the slopes from the regressions (log frequency versus log length) are steeper in this artificially bounded sample.

Figure 4.1.2.-4 gives data for numbers and lengths (by both Horton and Strahler conventions) representing stream segments using Horton's (1945) drainage basin for the example (Figure 4.1.2.-5), as figured by Shreve (1966). In this instance the distribution and slopes from the regressions are virtually indistinguishable from samples for fault distributions. Analogously, Figure 4.1.2.-6 represents the same drainage basin according to Strahler's (1950) ordering system as shown in Figure 4.1.2.-5 for the Horton system. The difference between the Horton and Strahler systems relates to different choices for the junctions representing bifurcation between stream segments with different magnitudes. Therefore, there are somewhat different numbers of stream segments in the two conventions. The distinction is analogous to choosing which is the main branch in an imbricate or bifurcating fault system.

In the case of stream ordering, the numbers of drainage basins corresponding to stream order give additional clues to ordering systems; see Woldenberg (1969) for systematic ways to represent order in hierarchical systems. Analogous relations may also exist to aid the process describing order in fault systems.

SECTION 4.1.2. FIGURES AND TABLES

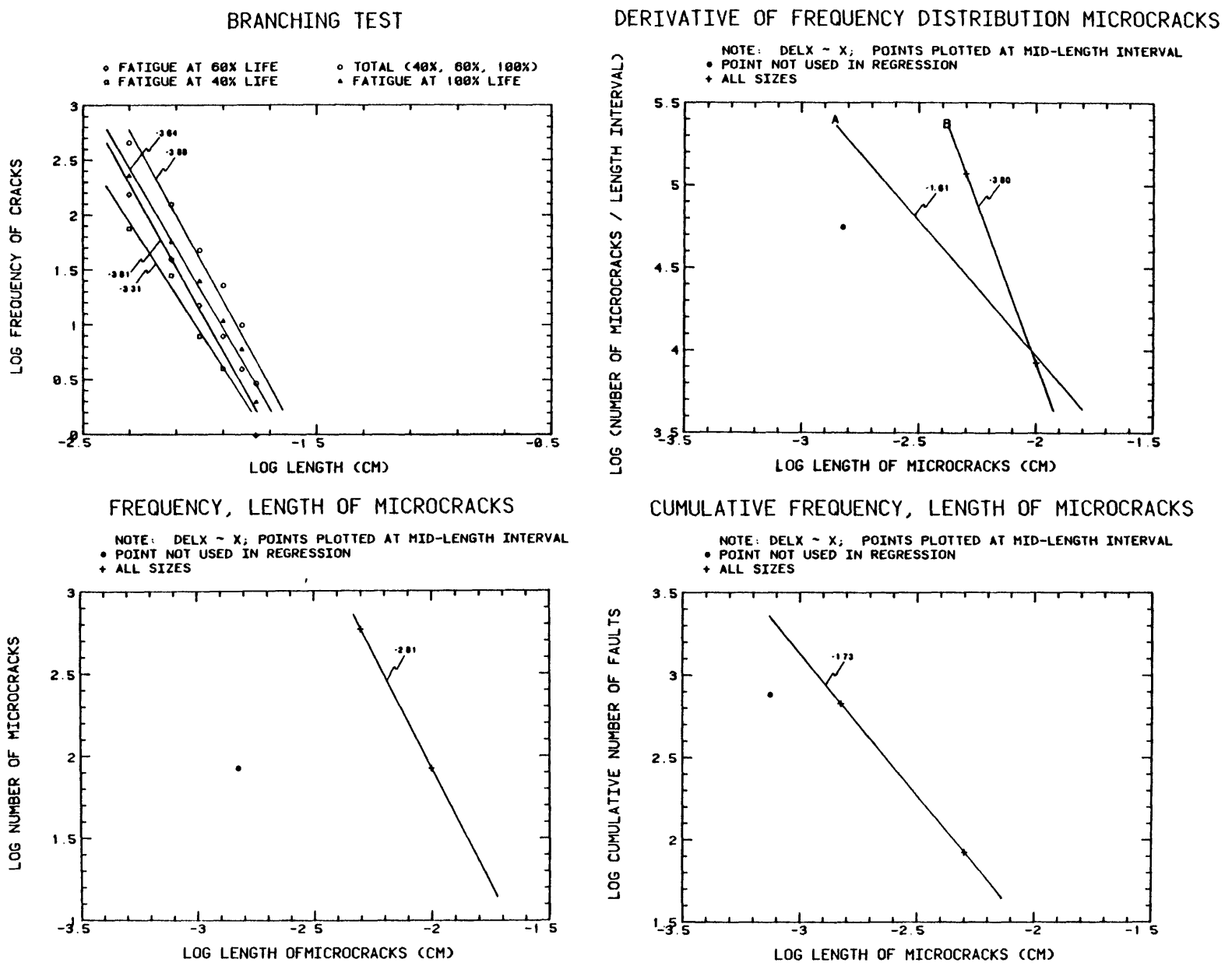

Figure 4.1.2.-1.
Experimental metal fracture; number versus fracture length based on data in Kitagawa and Suzuki (1975).

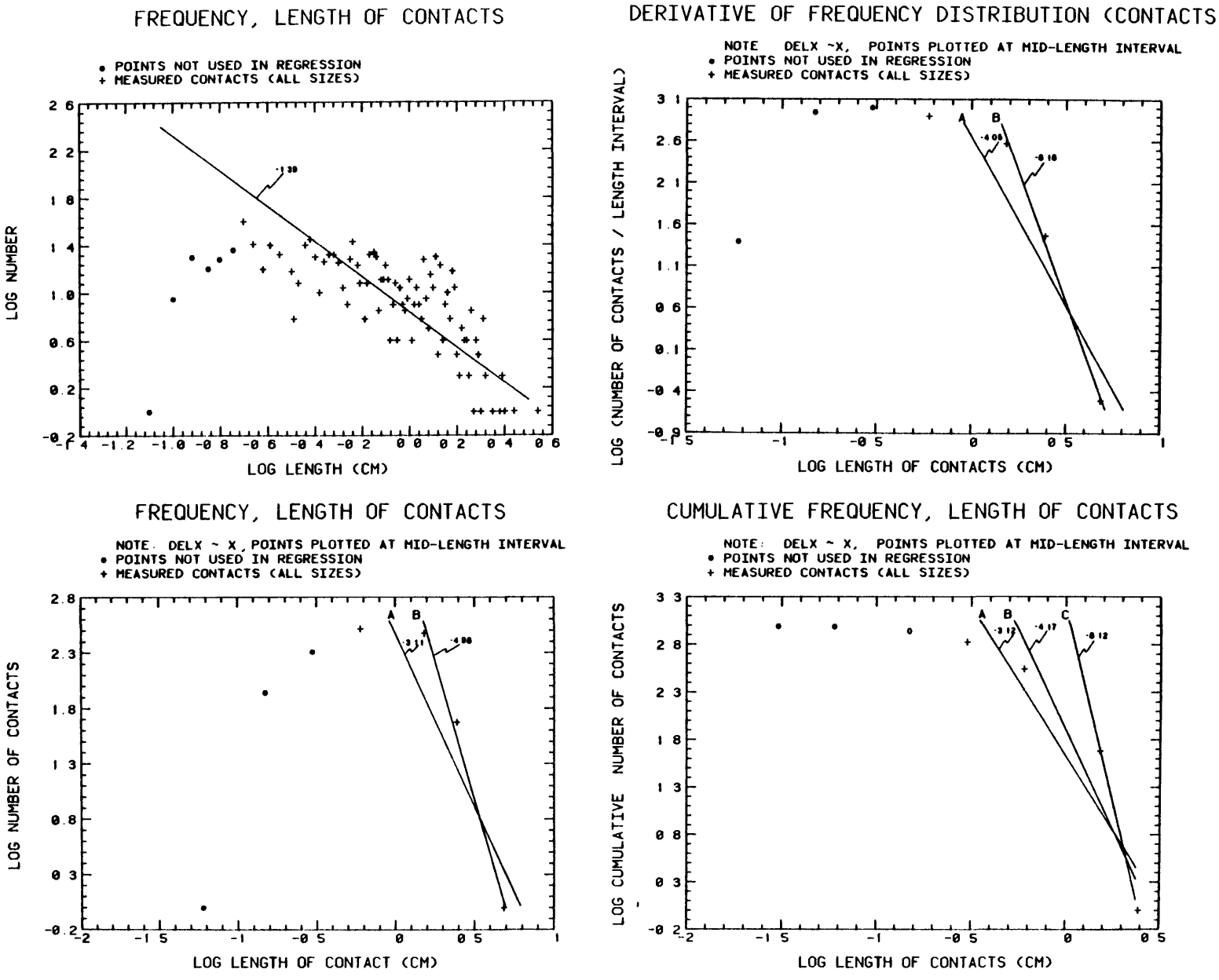

Figure 4.1.2.-2.
Numbers versus septa lengths for soap films.

MEASURED LENGTHS OF CONTACTS
(ALL SIZES)

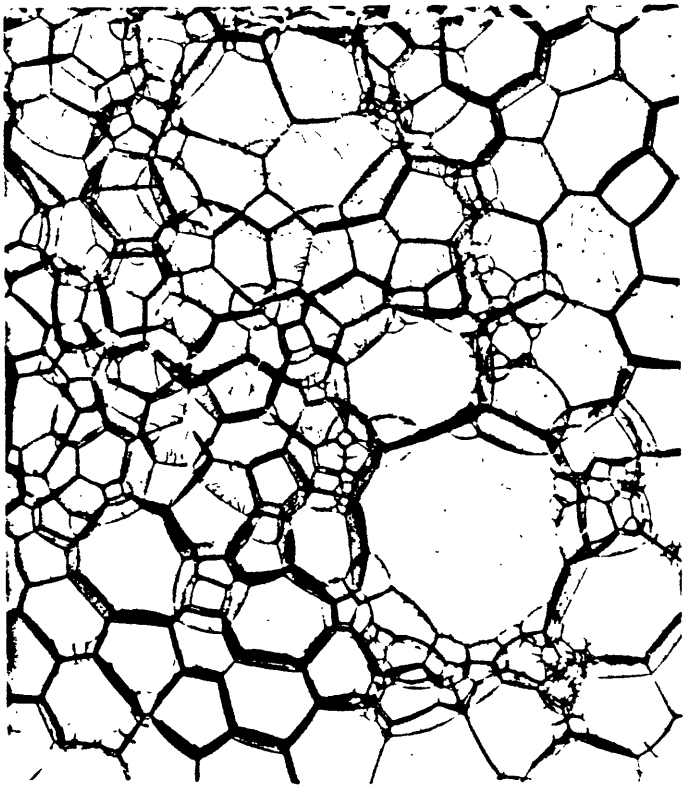

Figure 4.1.2.-3.
Photograph of froth (reduced 56 percent from scale used in numerical work; from Miller, 1977).

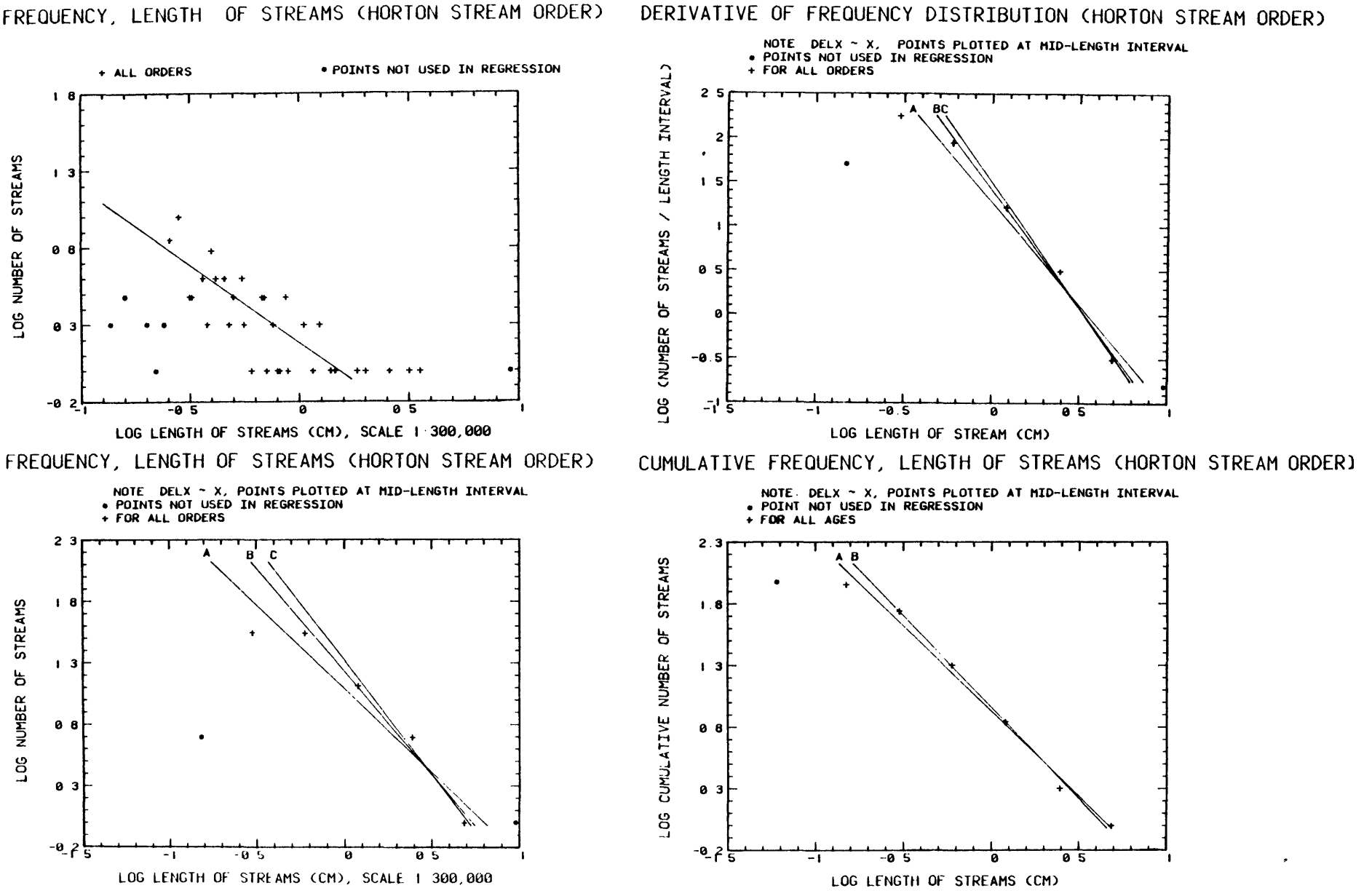

Figure 4.1.2.-4. (A)

Logarithms of number versus length for stream data from Horton (after Shreve, 1966).
Regression equations are given in Table 4.2.1.-1.

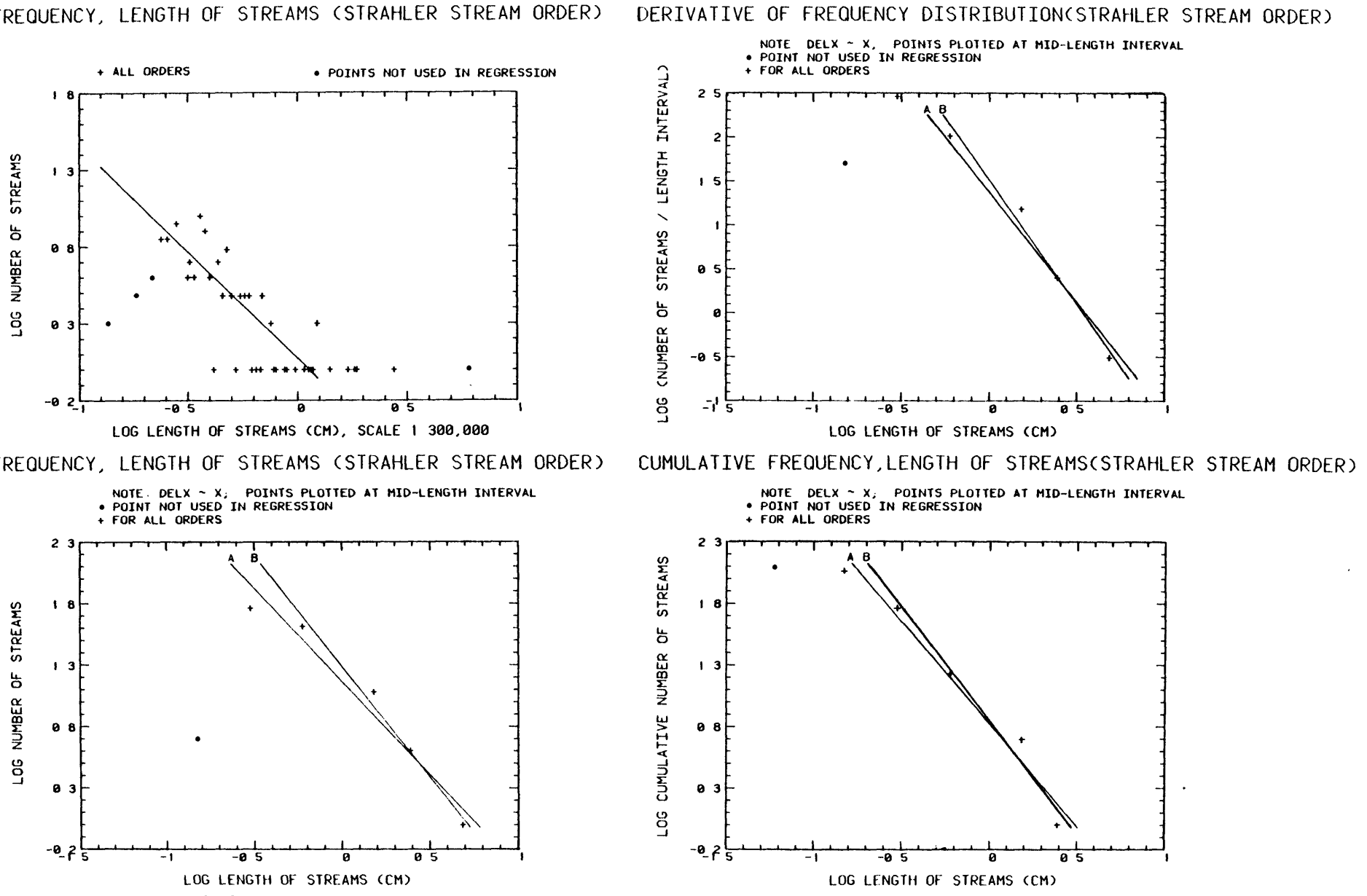

Figure 4.1.2.-4. (B)

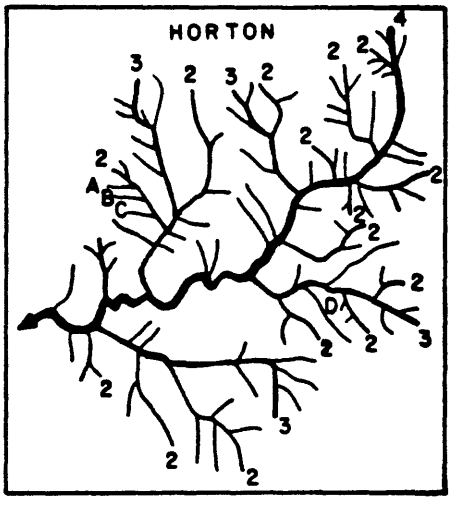

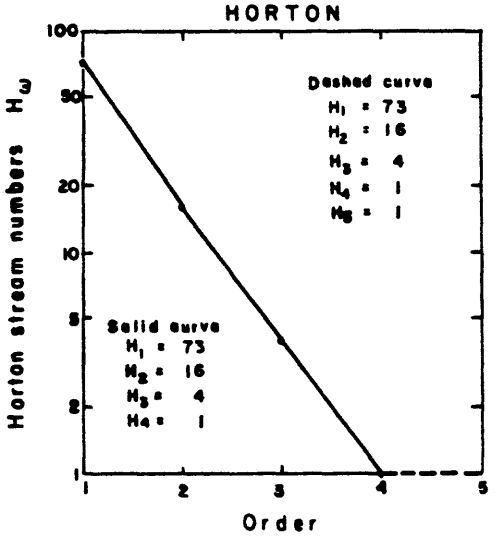

Figure 4.1.2.-5.
Map showing stream drainage patterns for stream orders according to Horton (1945); map modified from Shreve (1966).

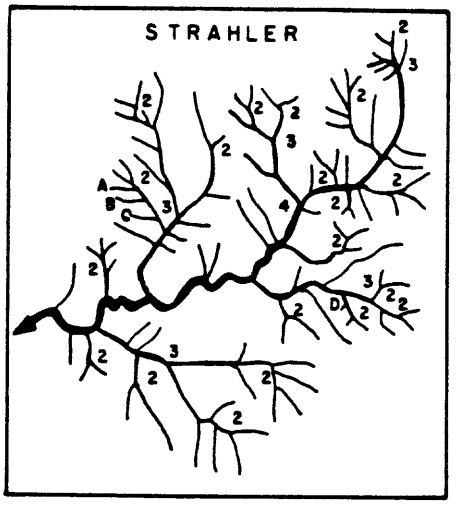

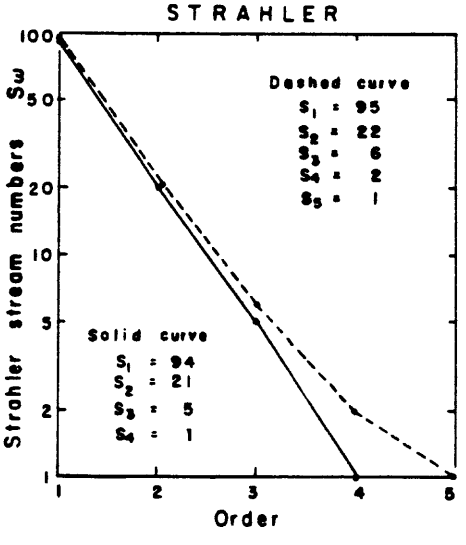

Figure 4.1.2.-6.
Map showing stream drainage patterns for stream orders according to Strahler (1952); map modified from Shreve (1966).

4.2. Frequency Distributions Based on Concepts of Branching Order.

In considering power law models for fault length distributions we had a problem with what to do about gaps in the data representing equal length increments. For example, the general form of the relation between number and length is represented by

$$n = n_1 - s \qquad \text{(eq. 4.2.-1)}$$

where n_1 is the mean value for numbers of faults at unit length, and s is the absolute value for slope in a log-log plot representing number versus length.

Because the histogram for lengths represents discontinuous data we can not simply integrate the regression curve to obtain an analytic expression for the cumulative distribution. In fact the raw distributions so far portrayed are akin to derivatives of eq. 4.2.-1 because they represent how many faults are within a given length increment.

4.2.1 Expanding Length Intervals, DELX ~ X.

In order to represent the large data set in a manageable way, and to derive systematic analytic functions, we adopted a modified convention for varying the length interval. Following hints from analyses for stream order we looked at distributions as functions involving geometrical progressions in length. The simplest one that includes all data without gaps is to use a length interval approximately equal to the chosen length. Physically this represents grouping the data into orders for length magnitudes in which the ranges in lengths for that order is given by the mean length. We refer to data expressed this way by the symbol DELX ~ X. We also looked at geometrical progressions to the bases 2 and 3. Generally speaking the distributions are similar.

Histograms for equal length increments compared with data for DELX ~ X are given in Figure 4.2.1.-1 (A and C). The scatter is, of course, reduced and the overall simplicity of the distribution is sharpened.

Figure 4.2.1.-2 gives a series of four-part diagrams representing the various logarithmic relations between numbers and lengths. Part (a) gives the ordinary distribution for linearly equal increments; part (b) gives the analogous plot for DELX ~ X; part (c) gives a log-log diagram for $\log(\Delta n/\Delta \ell)$ vs $\log(\ell)$ and part (d) gives the observed cumulative distribution.[1] Table 4.2.1.-1 gives the coefficients in regression equations. Regressions are given for several combinations among the data points shown. Generally speaking, the points greater than a certain length are arranged linearly on log-log paper, and these are taken to define the most appropriate analytic regression equation. The regressions exclude points at successively greater lengths until a fit of comparatively constant slope is obtained.

Although rigorous statistical tests are unknown to use for these interdependent distributions, the comparisons of regression equations with analytic functions gives some hints about internal consistency. For example, the absolute slope for the cumulative curve should be (S-1) if S is taken to be the slope for the derivative function.

---

[1]/Distribution (c), $\log(\Delta n/\Delta \ell)$ versus $\log(\ell)$, is termed the DERIVATIVE in Figure 4.2.1.-2 and Table 4.2.1.-1 for brevity even though it is a difference function obtained directly from the ratio between the number of faults in a given length interval divided by the length difference in that interval. Distribution (d), the cumulative frequency, is obtained by summing all faults with lengths greater than a given length and plotting this value at the midpoint of the next larger length interval. This was done for uniformity of plotting and leads to a slight weighting of the longer faults in the cumulative distribution.

SECTION 4.2.1. FIGURES AND TABLES

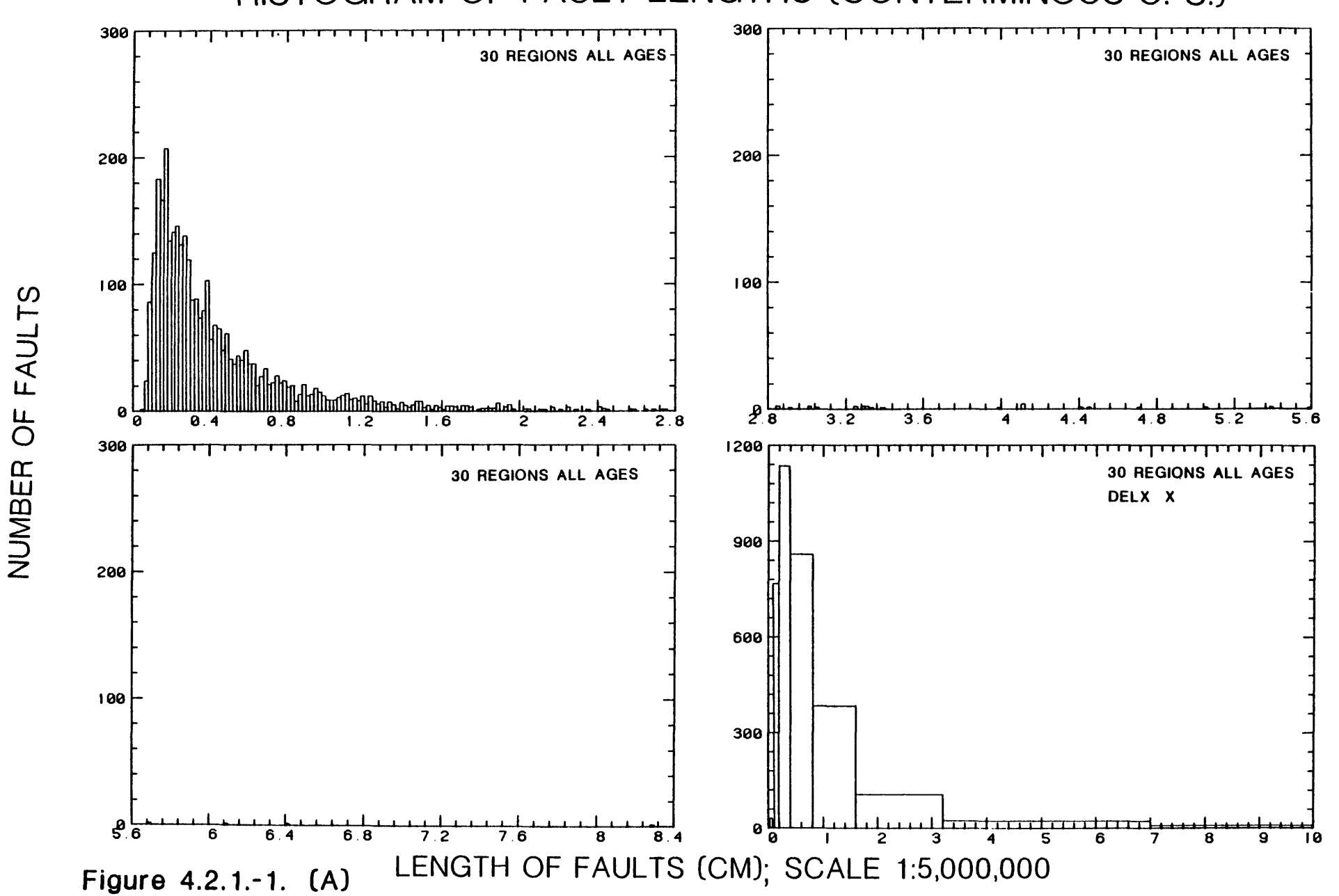

Figure 4.2.1.-1. (A)

Comparison of frequencies based on constant length intervals with frequencies based on length intervals approximately equal to mean length (convention labeled DELX~X); A and B compare conventions for all U.S.; C and D compare conventions for L. A. area.

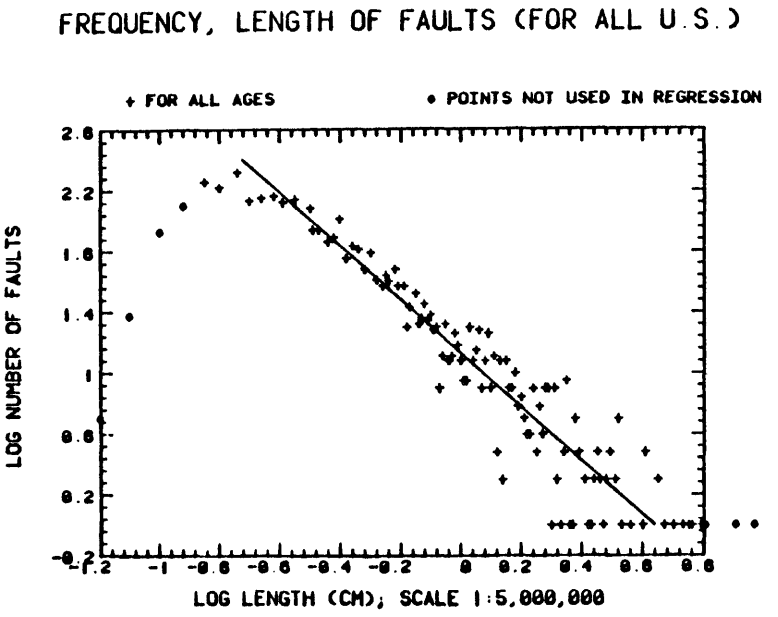

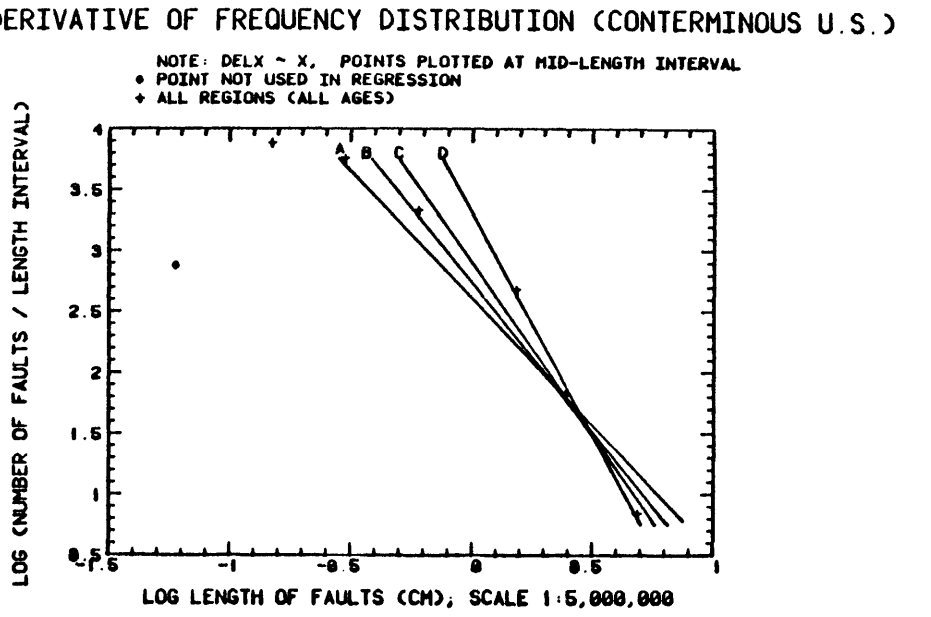

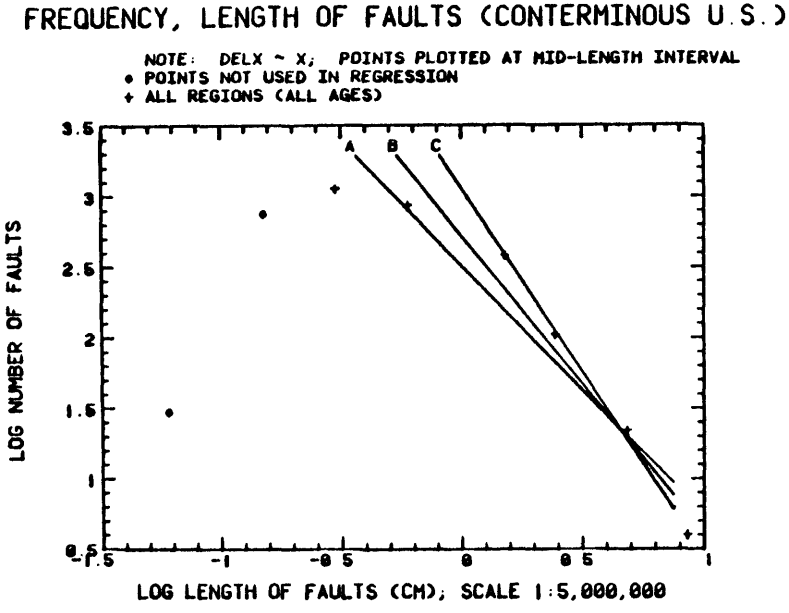

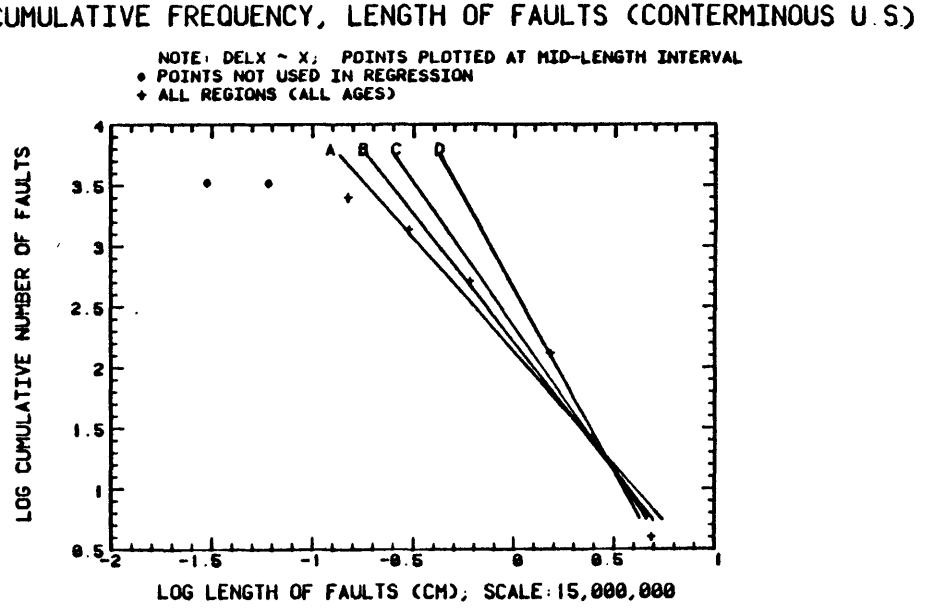

Figure 4.2.1.-1. (B)

See Table 4.2.1.-1. for coefficients in regression equations.

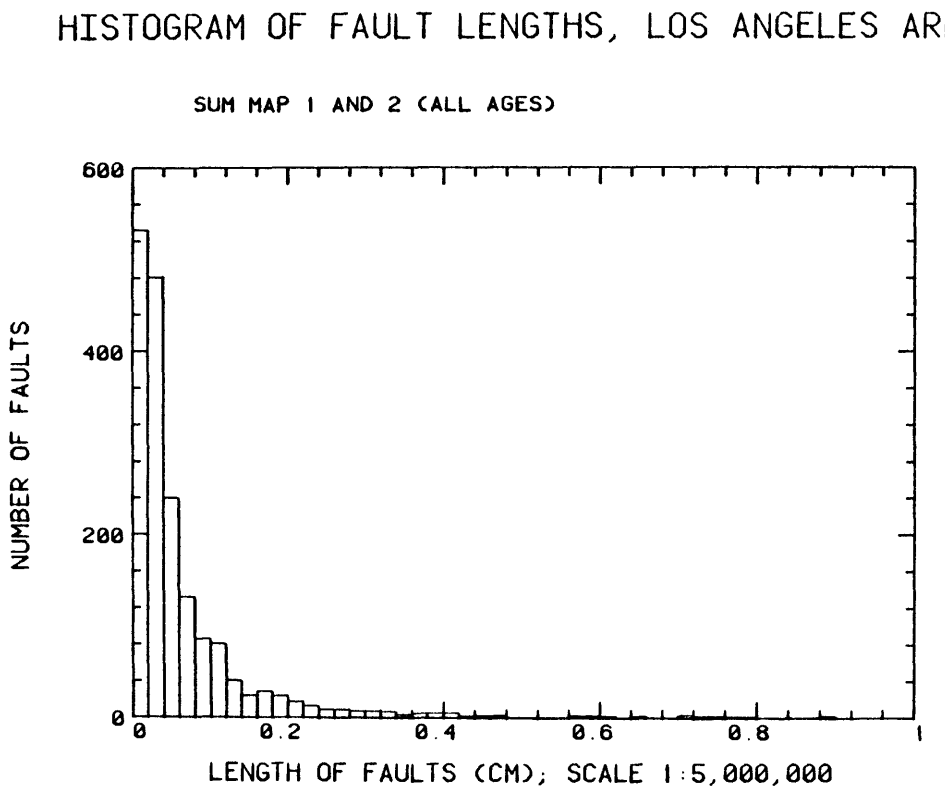

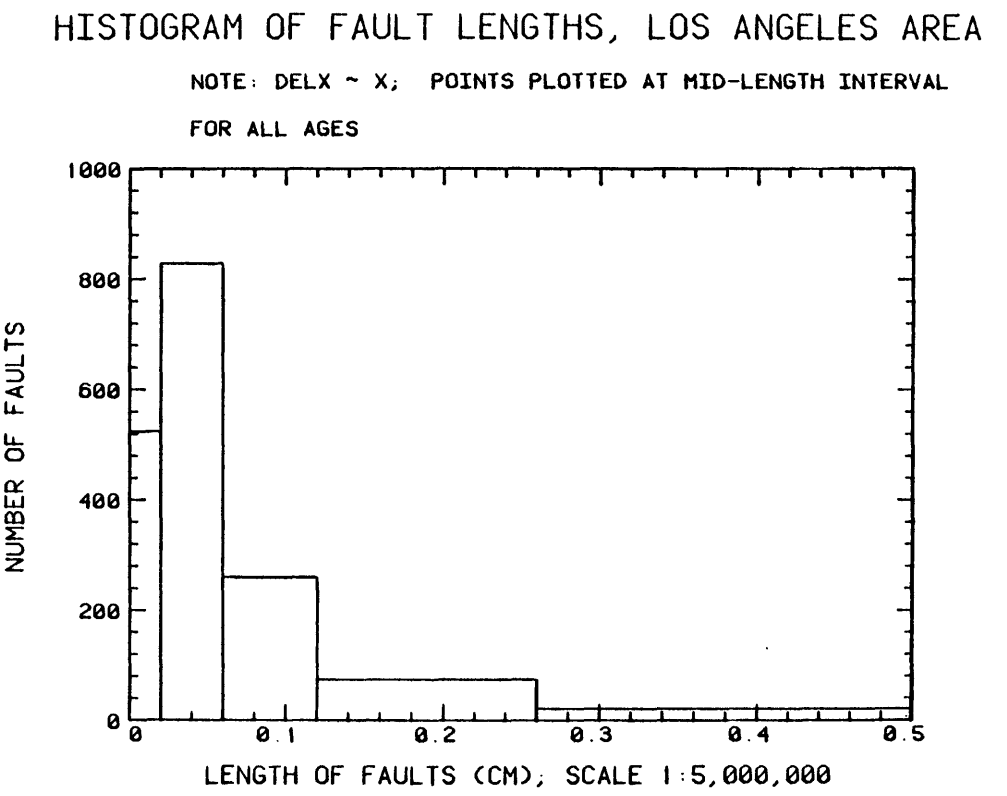

Figure 4.2.1.-1. (C)

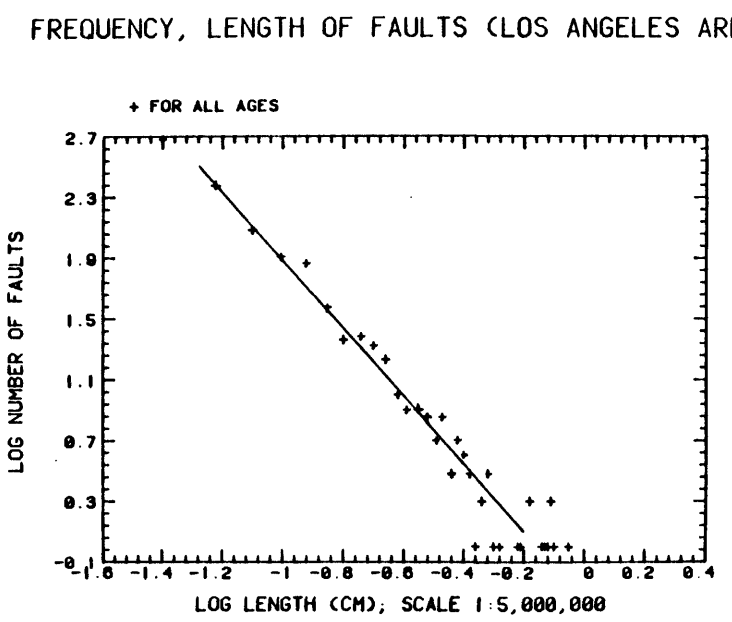

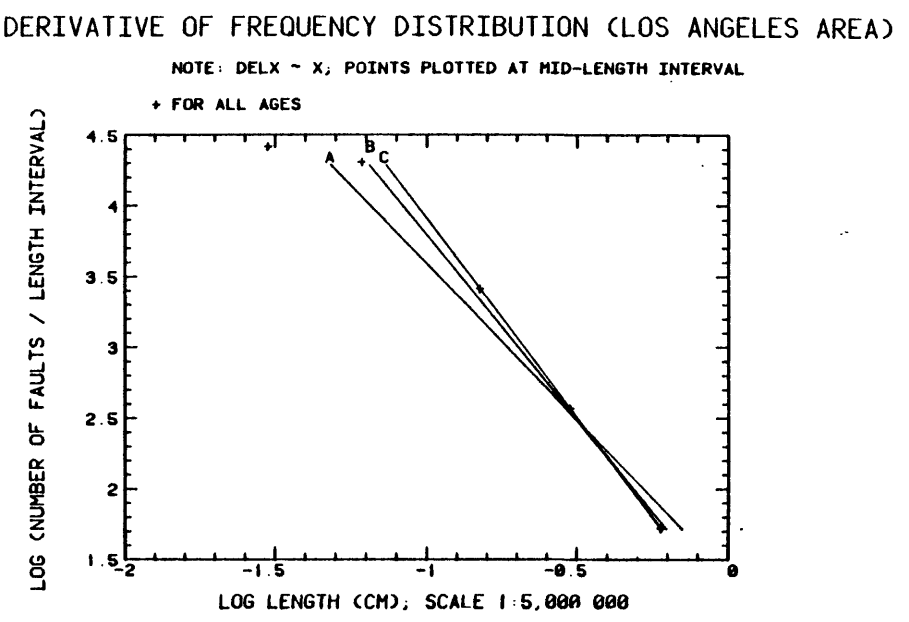

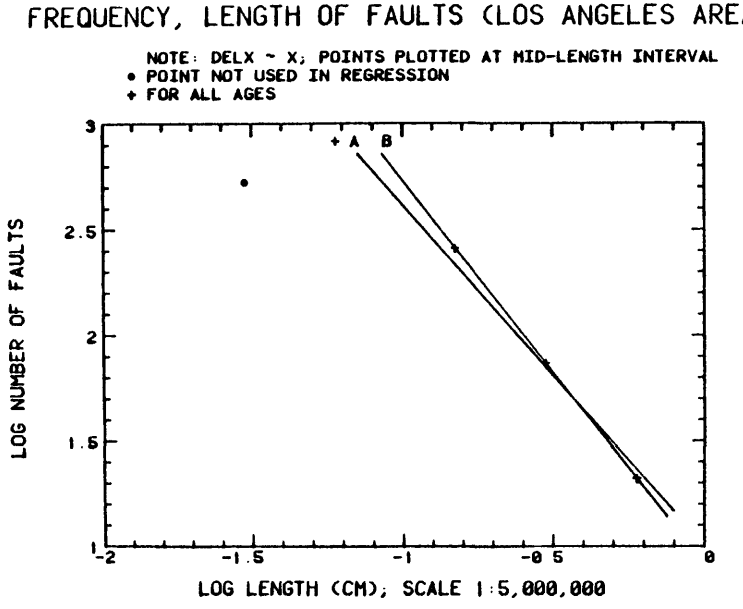

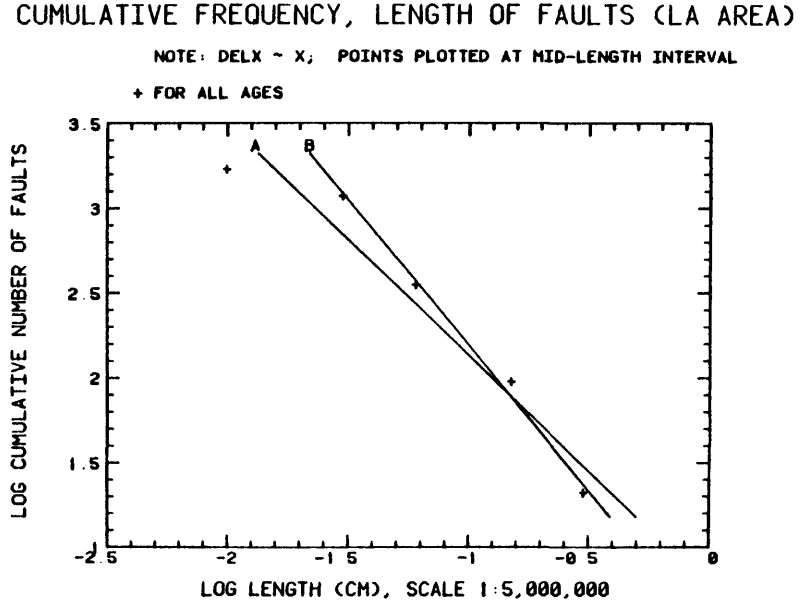

Figure 4.2.1.-1. (D)

See Table 4.2.1.-1. for coefficients in regression equations.

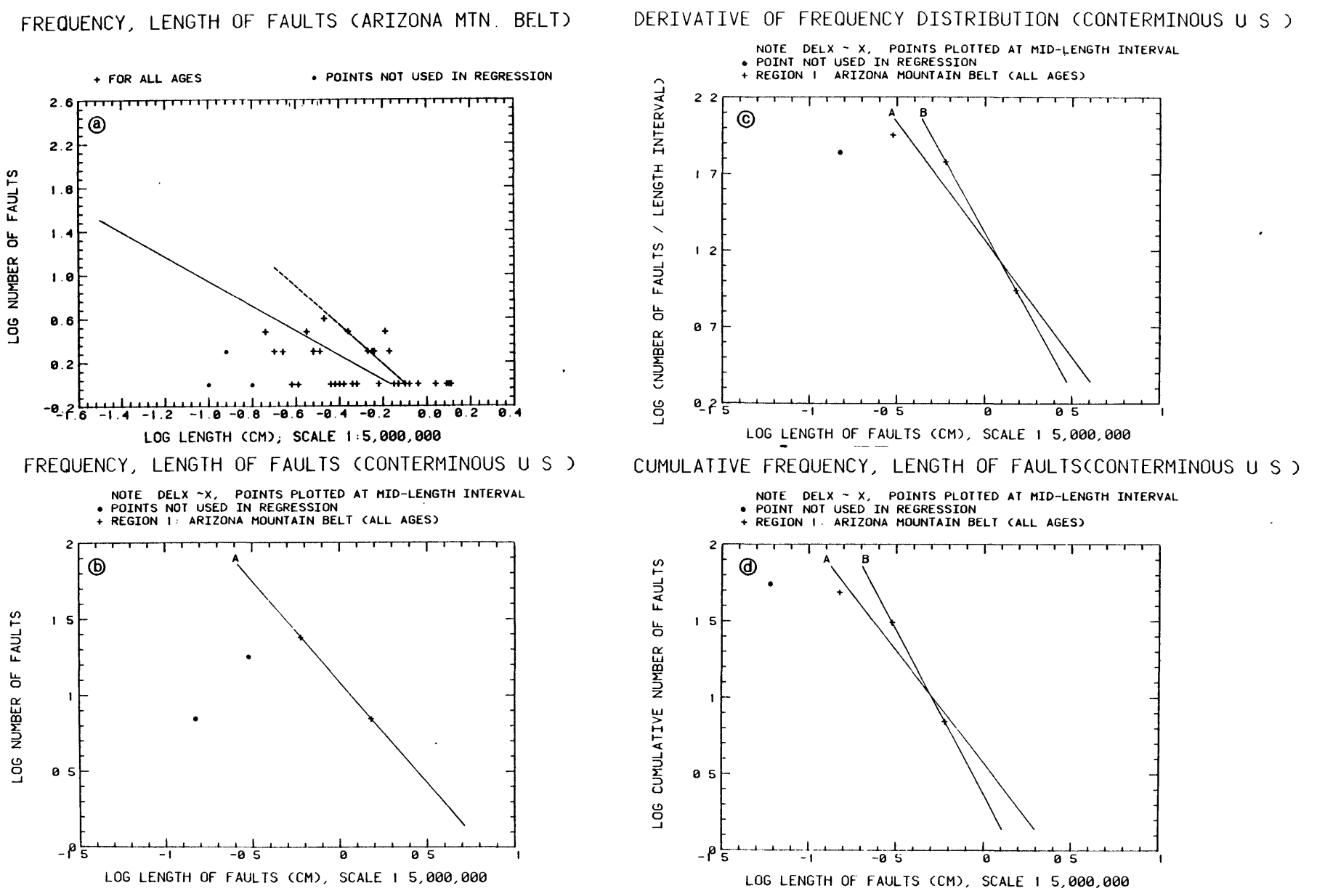

Figure 4.2.1.-2. (1)

Logarithmic diagrams illustrating four different ways of representing relations between fault numbers and lengths: (a) log number versus log length based on constant length interval, (b) log number versus log length for DELX~X, (c) log cumulative number versus log length for DELX~X, (d) log derivative of number versus length for DELX~X. Regression equations are given in Table 4.2.1.-1.

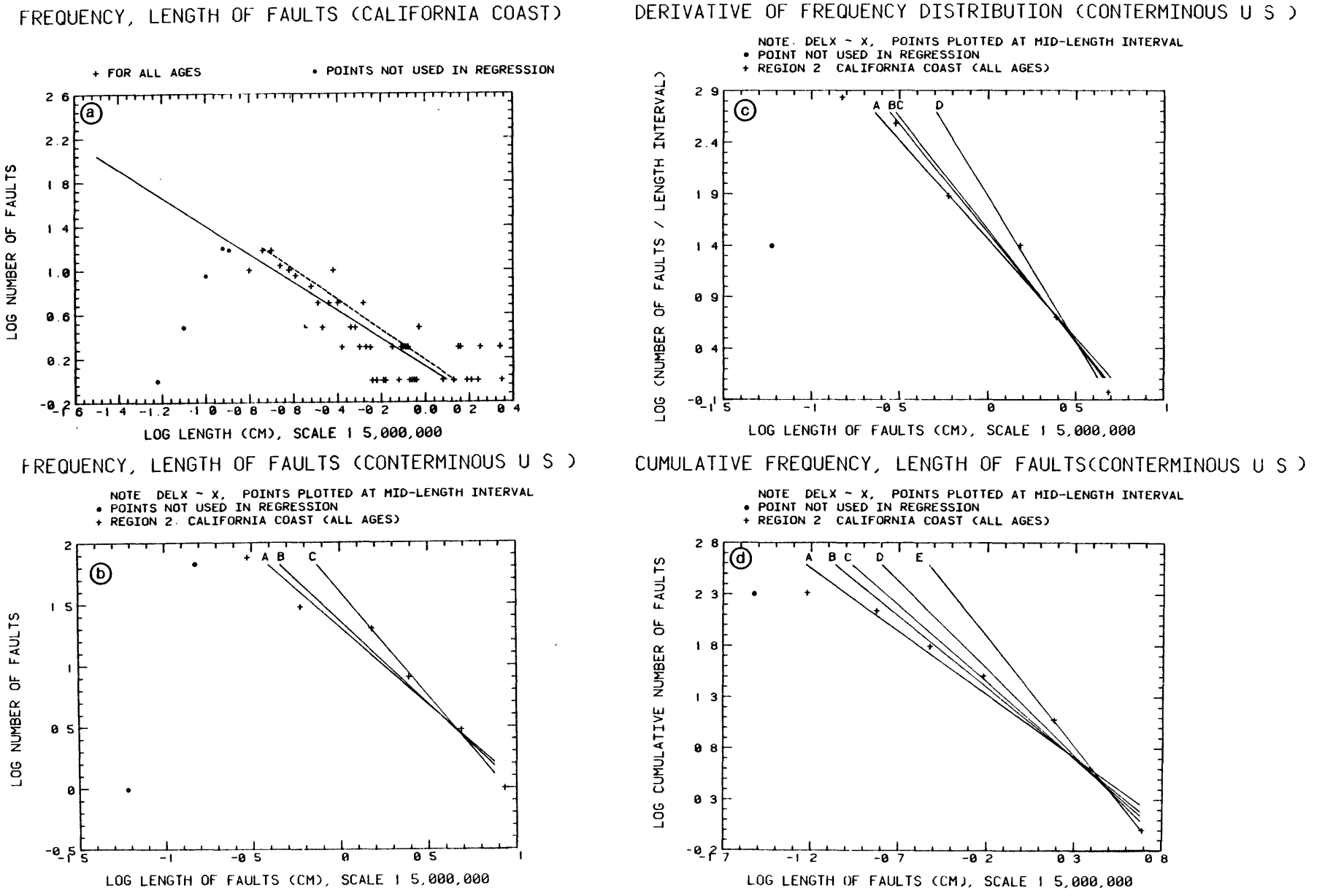

Figure 4.2.1.-2. (2)

FREQUENCY, LENGTH OF FAULTS (CENTRAL MISSISSIPPI)

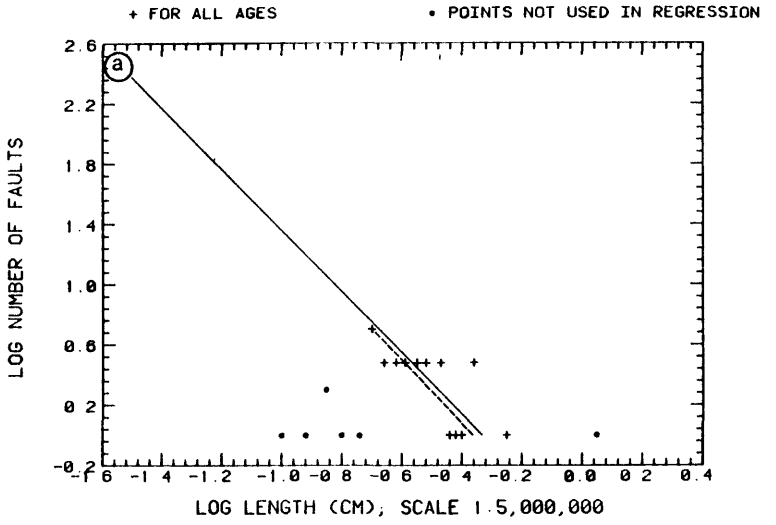

DERIVATIVE OF FREQUENCY DISTRIBUTION (CONTERMINOUS U S)

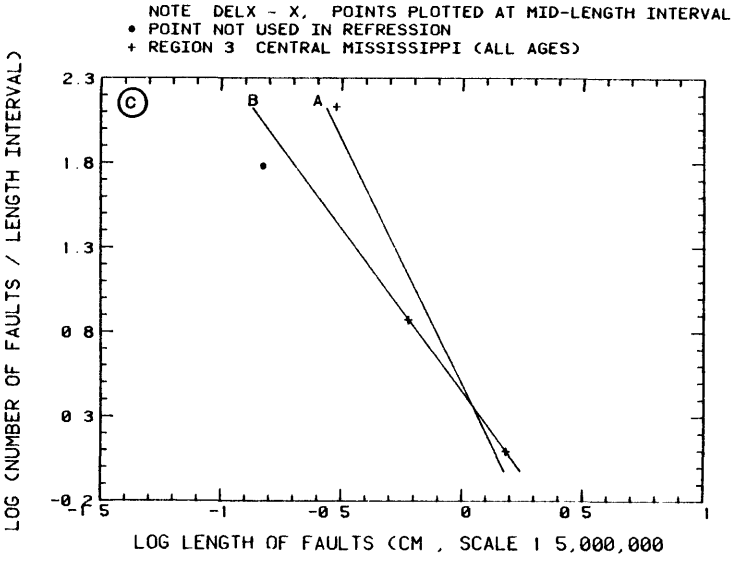

FREQUENCY, LENGTH OF FAULTS (CONTERMINOUS U S)

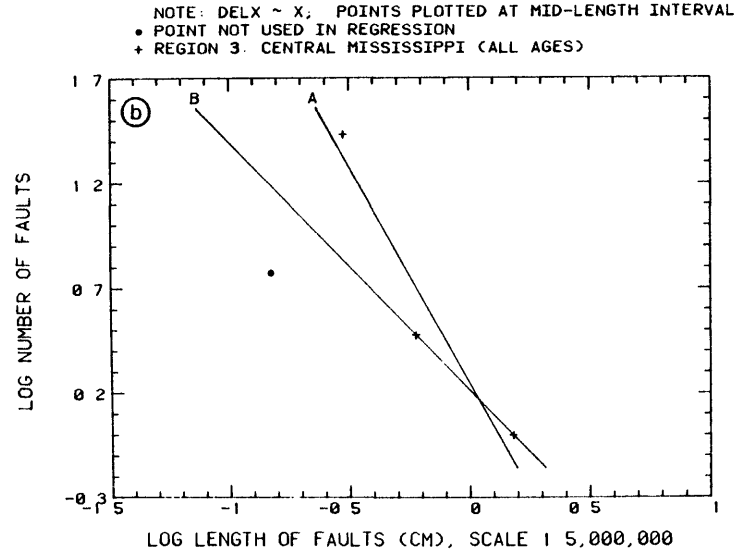

CUMULATIVE FREQUENCY, LENGTH OF FAULTS(CONTERMINOUS U S)

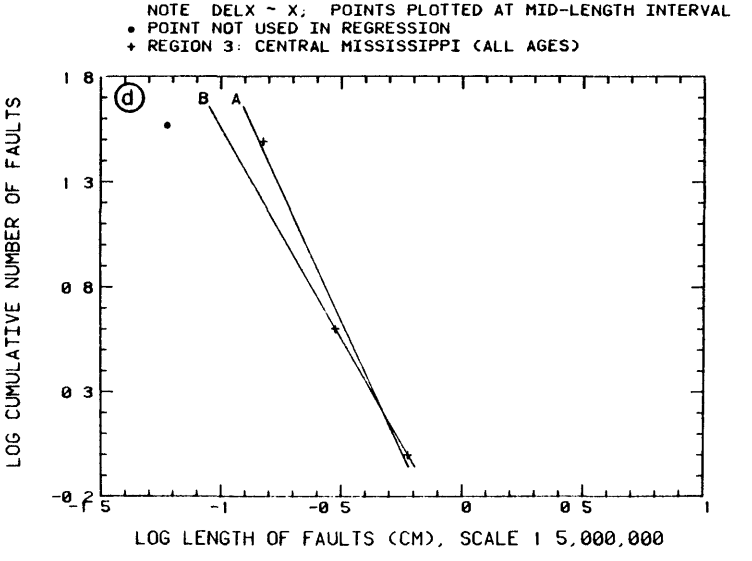

Figure 4.2.1.-2. (3)

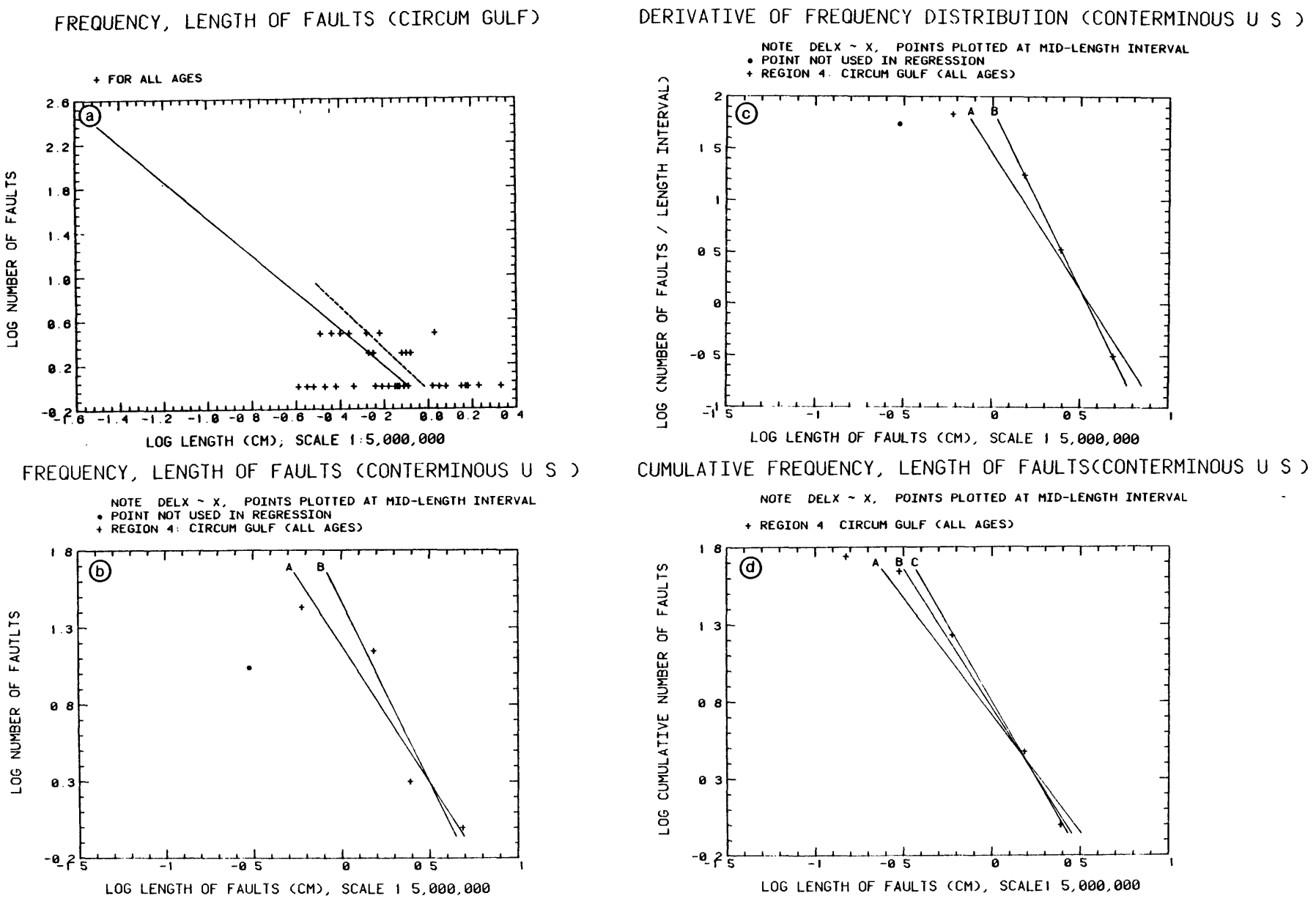

Figure 4.2.1.-2. (4)

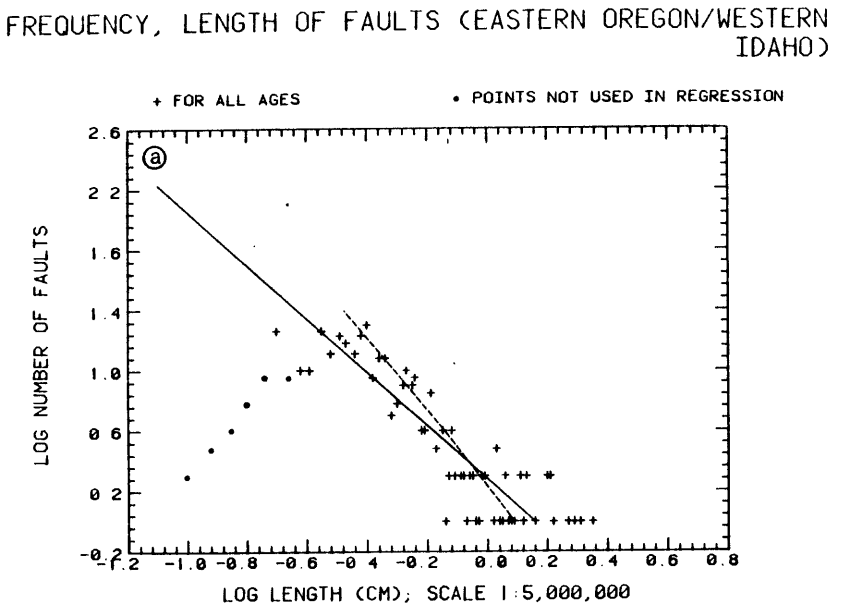

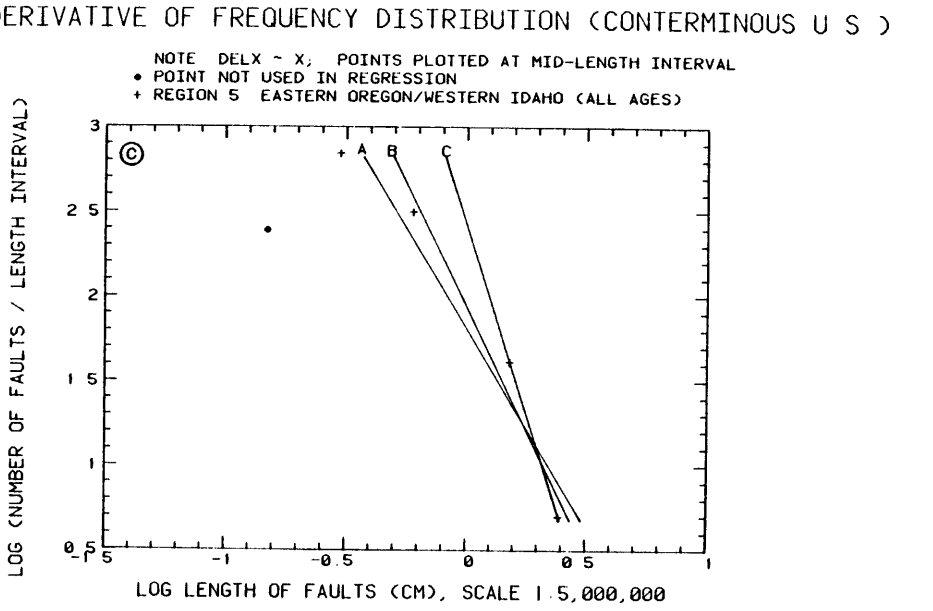

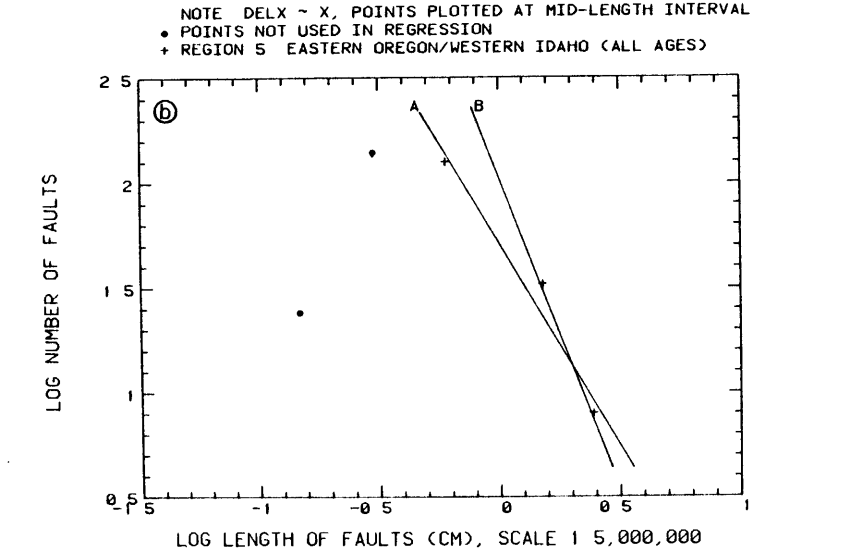

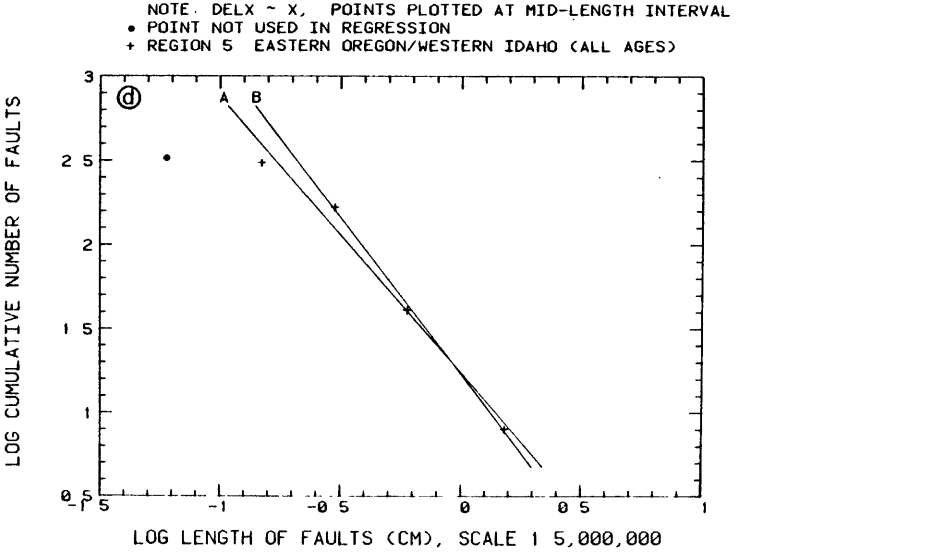

Figure 4.2.1.-2. (5)

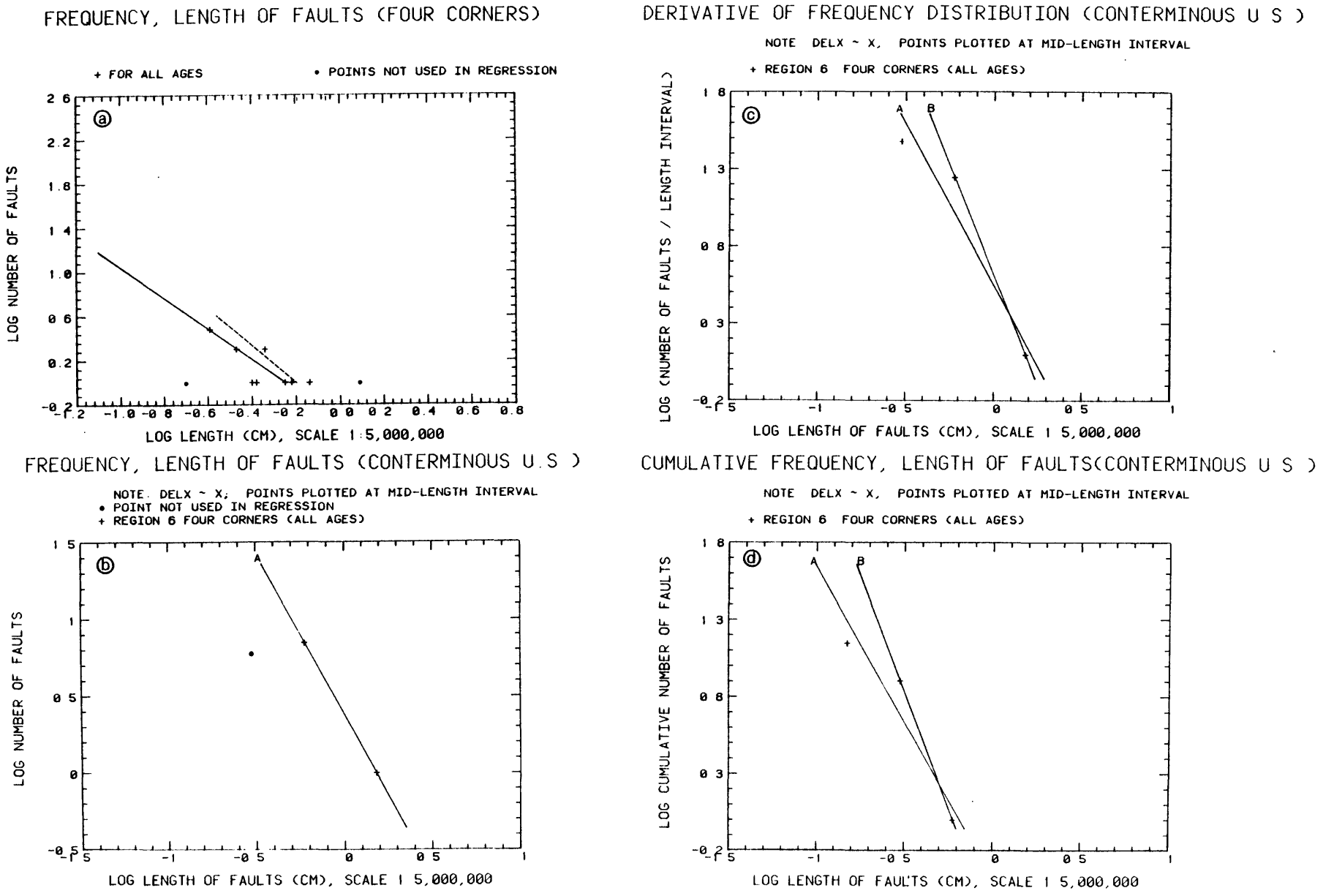

Figure 4.2.1.-2. (6)

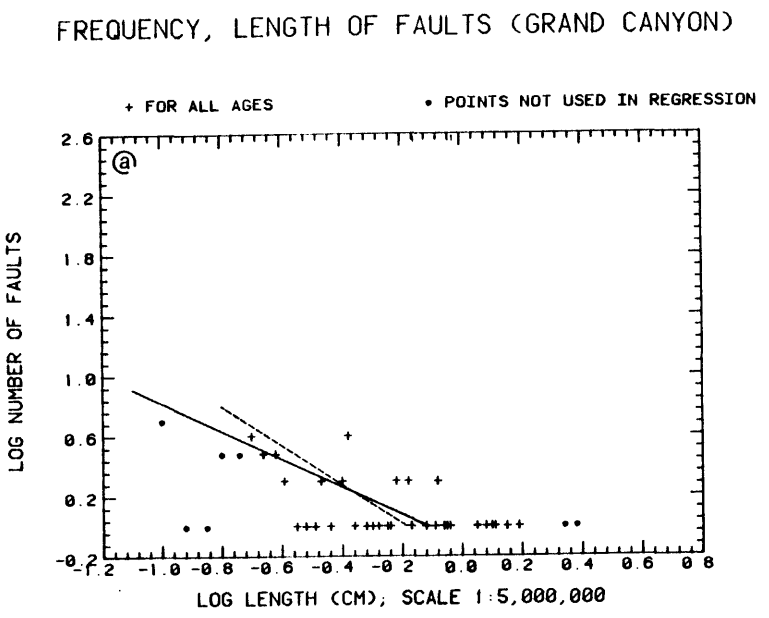

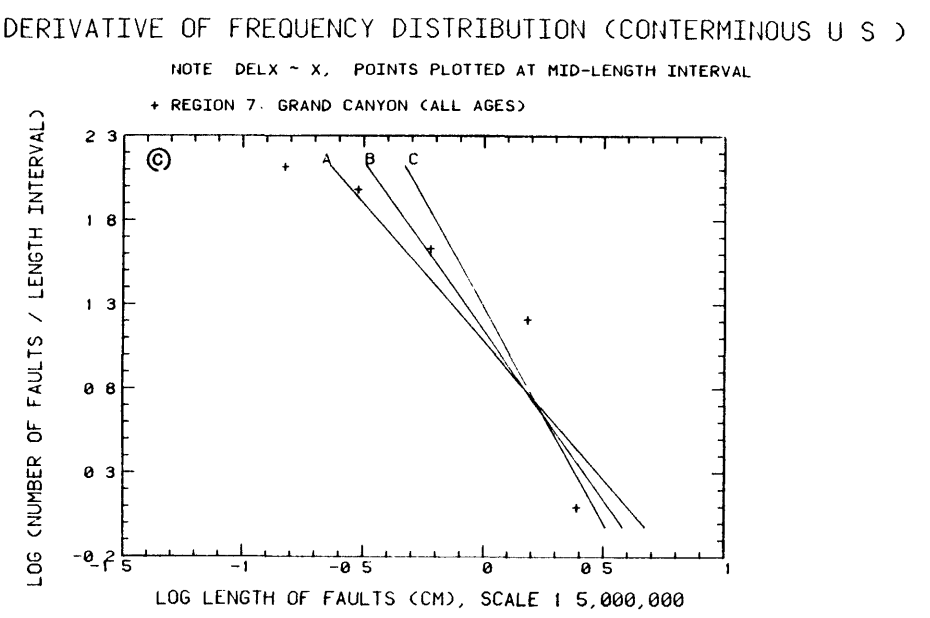

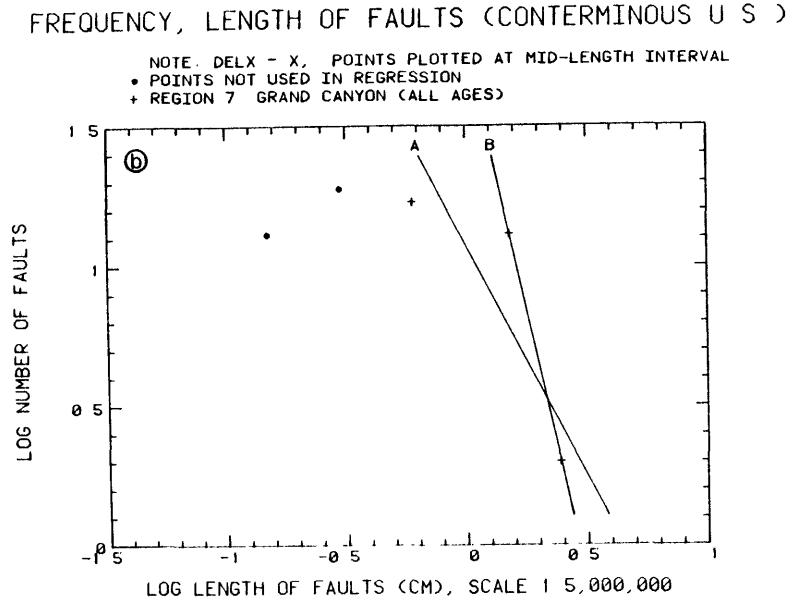

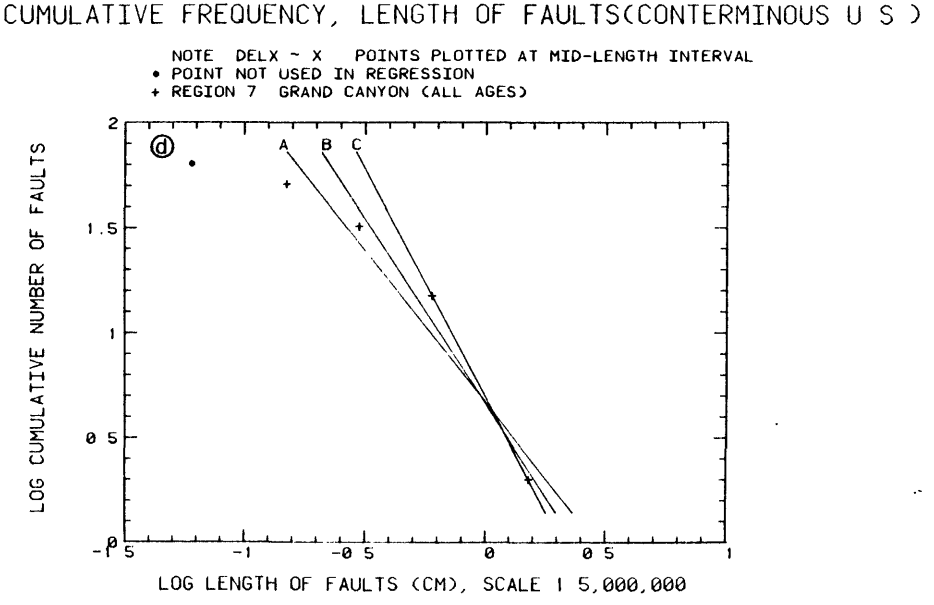

Figure 4.2.1.-2. (7)

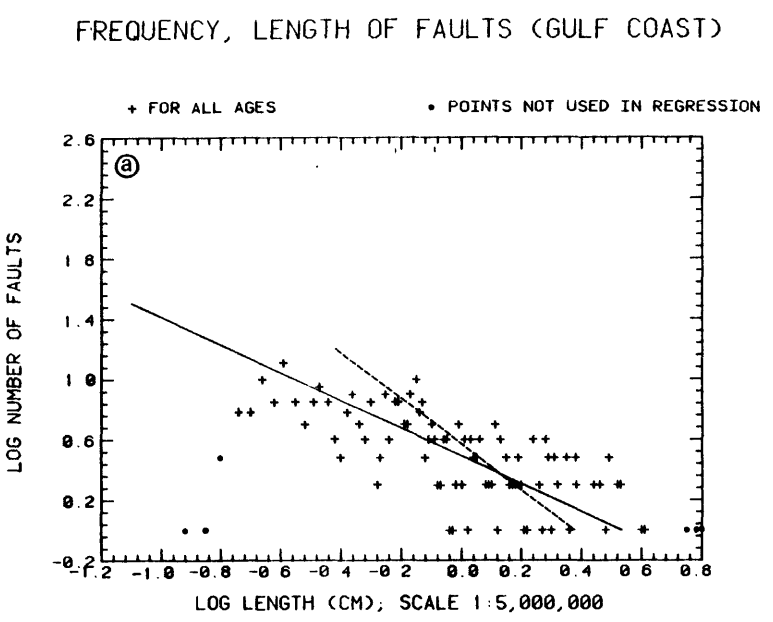

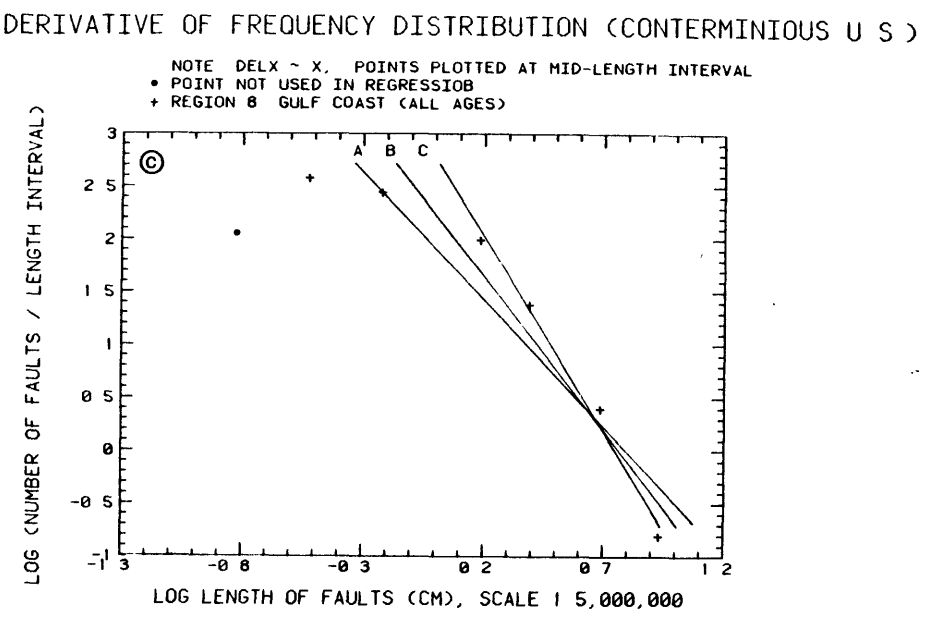

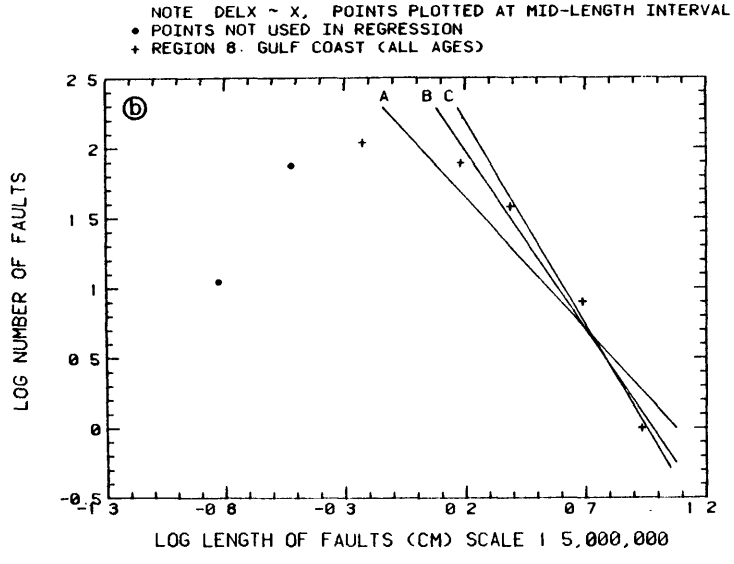

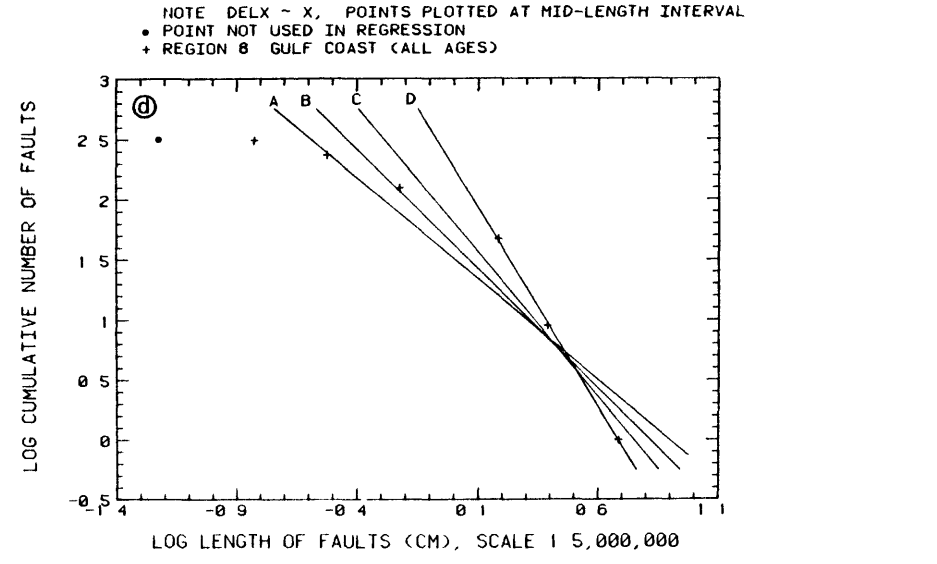

Figure 4.2.1.-2. (8)

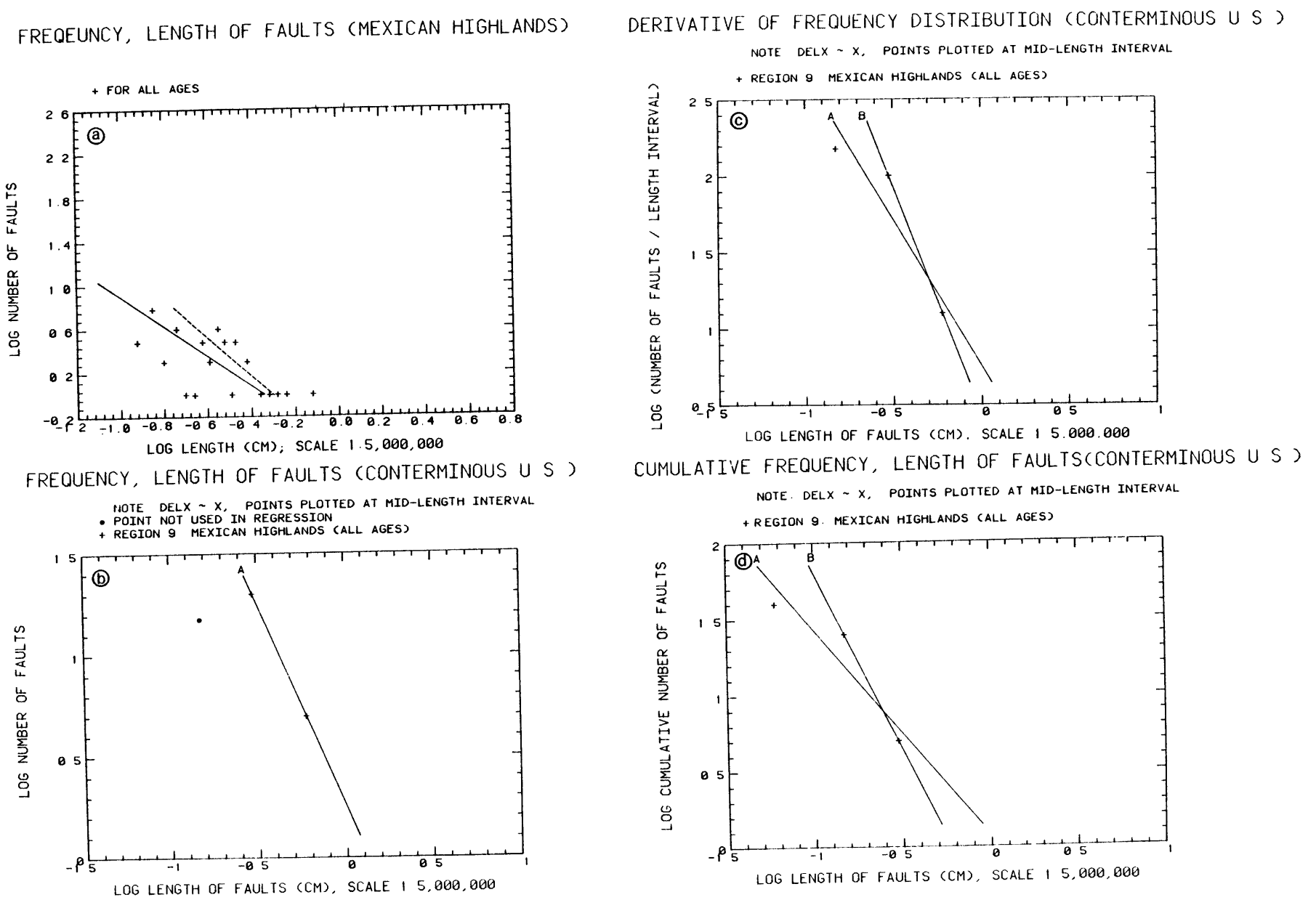

Figure 4.2.1.-2. (9)

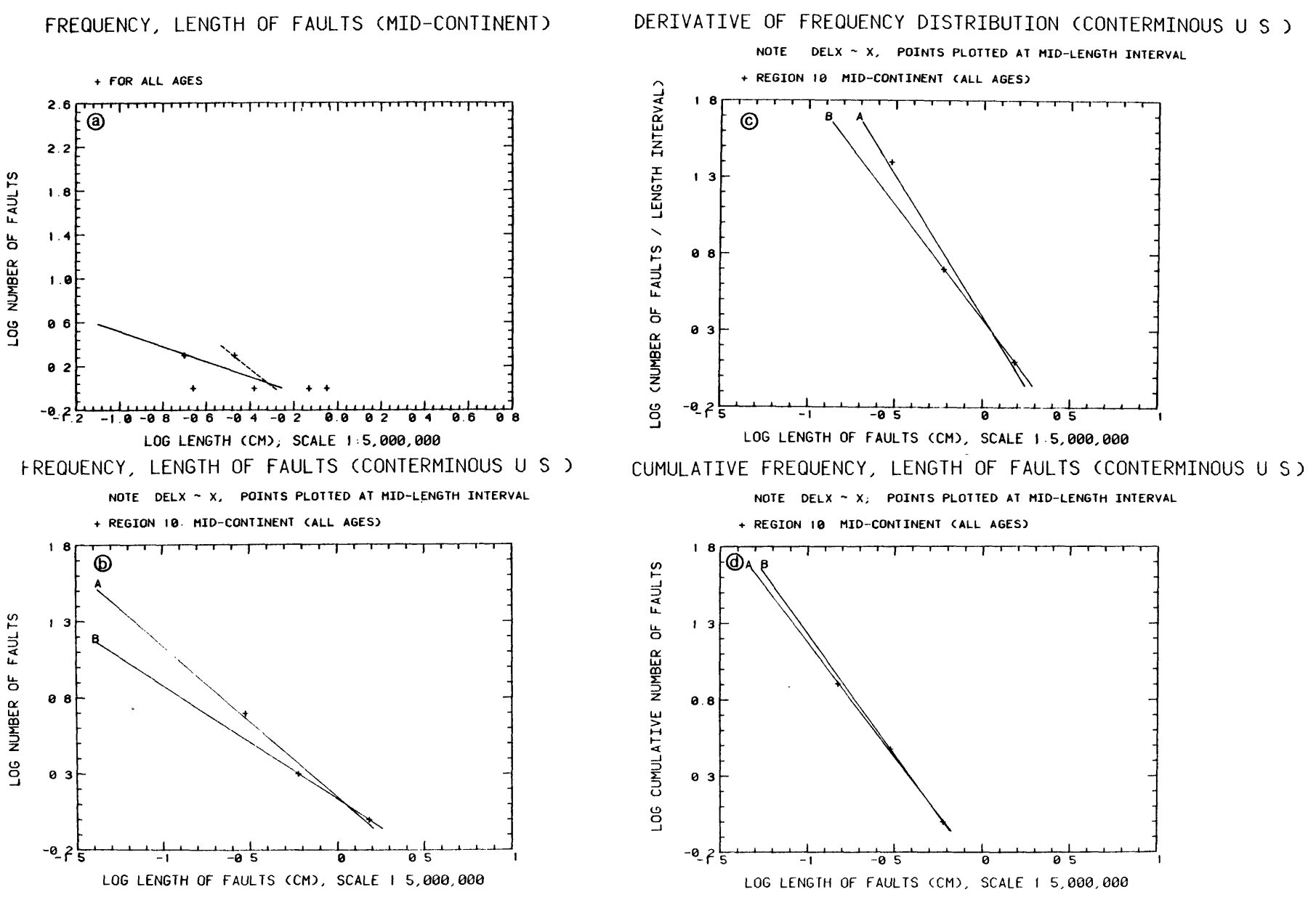

Figure 4.2.1.-2. (10)

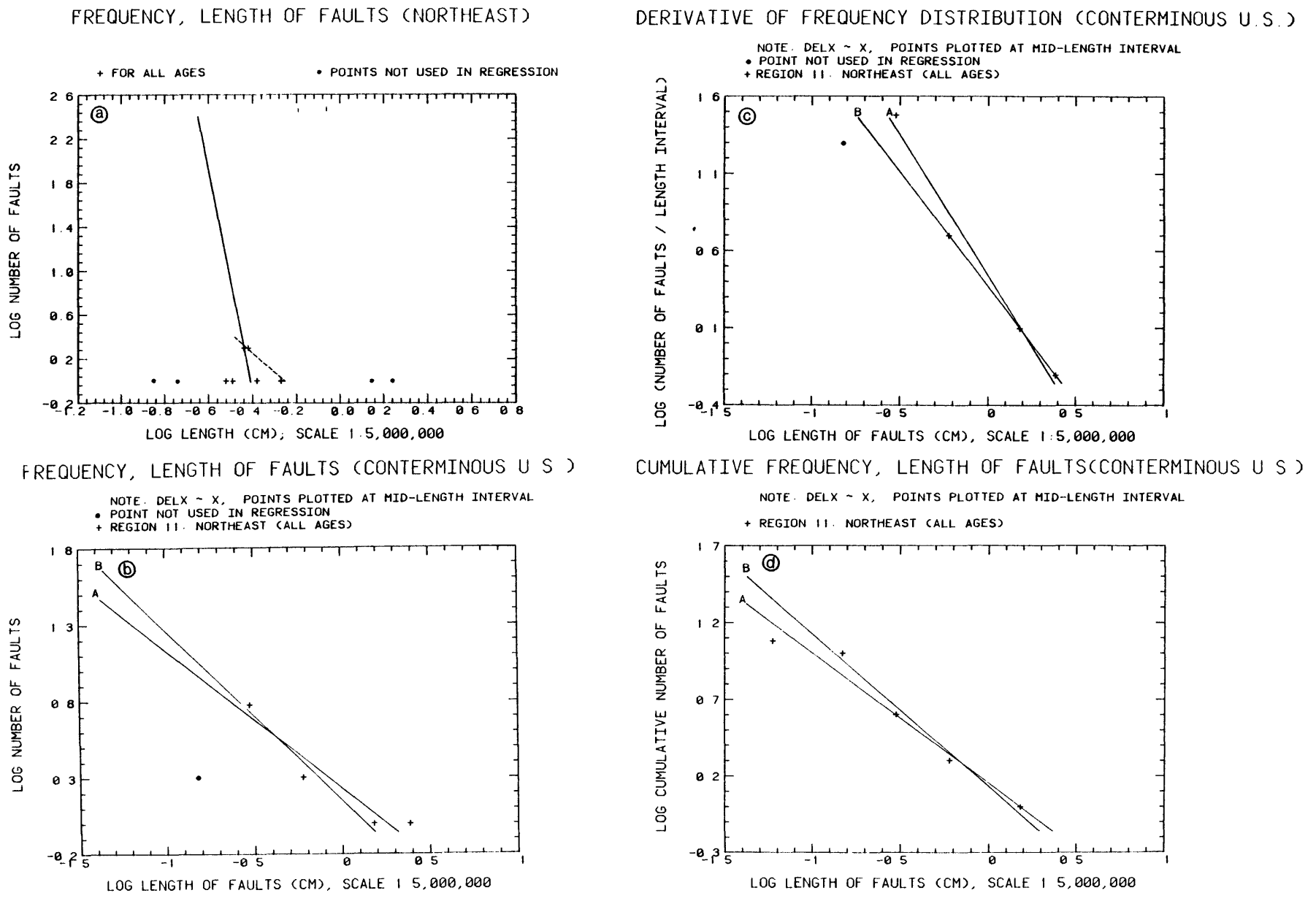

Figure 4.2.1.-2. (11)

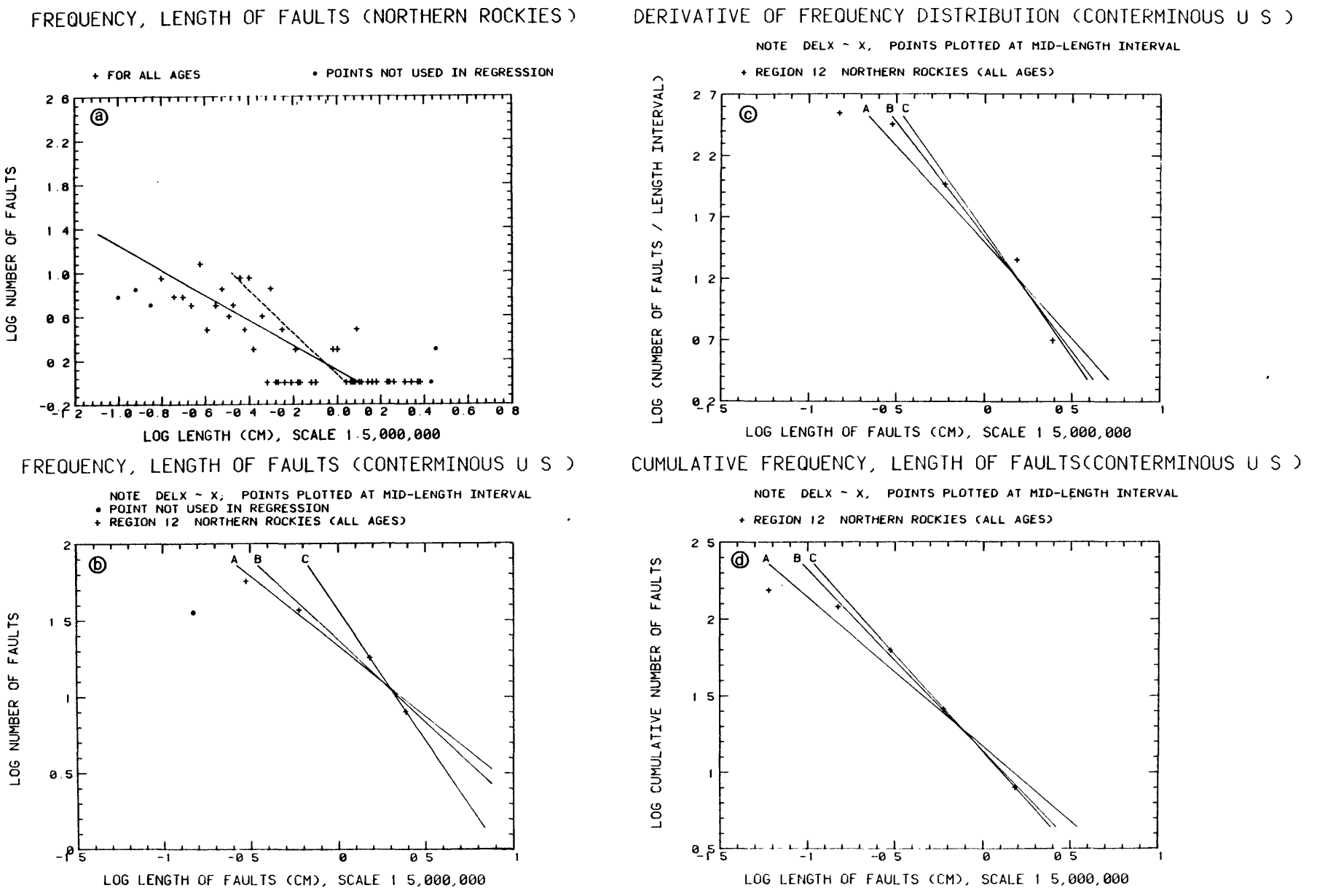

Figure 4.2.1.-2. (12)

FREQUENCY, LENGTH OF FAULTS (OREGON/WASHINGTON COAST)

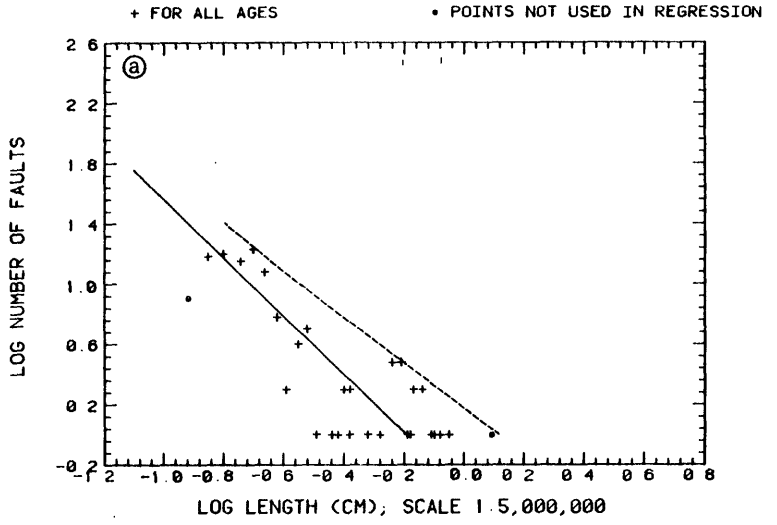

DERIVATIVE OF FREQUENCY DISTRIBUTION (CONTERMINOUS U S)

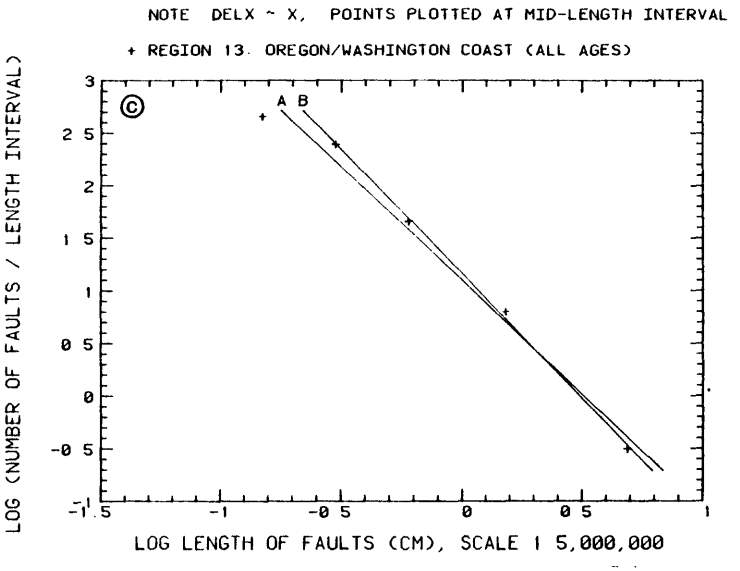

FREQUENCY, LENGTH OF FAULTS (CONTERMINOUS U S)

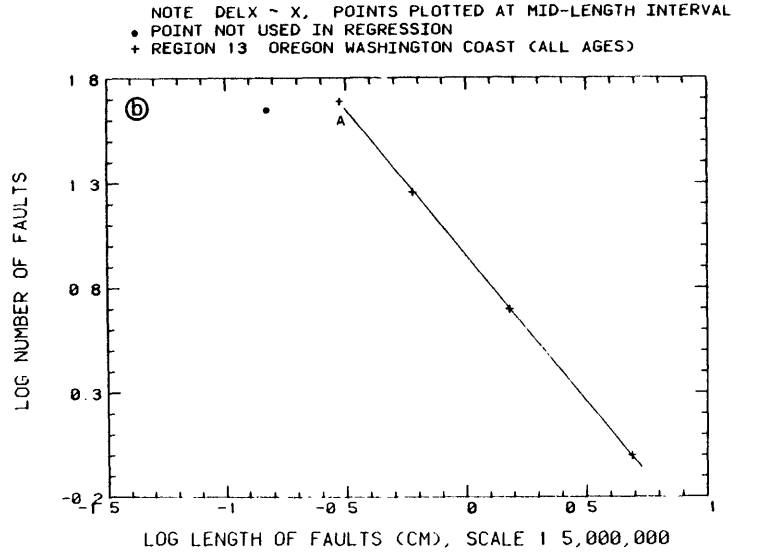

CUMULATIVE FREQUENCY, LENGTH OF FAULTS(CONTERMINOUS U S.)

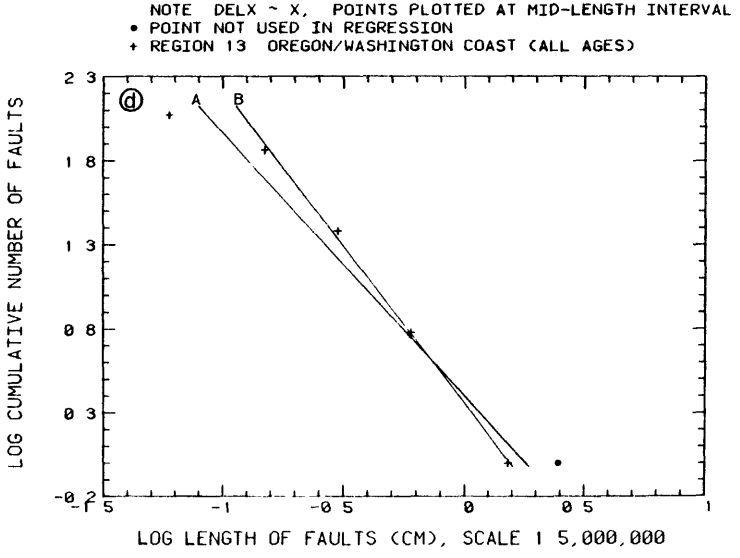

Figure 4.2.1-3 (13)

FREQUENCY, LENGTH OF FAULT (PACIFIC INTERIOR)

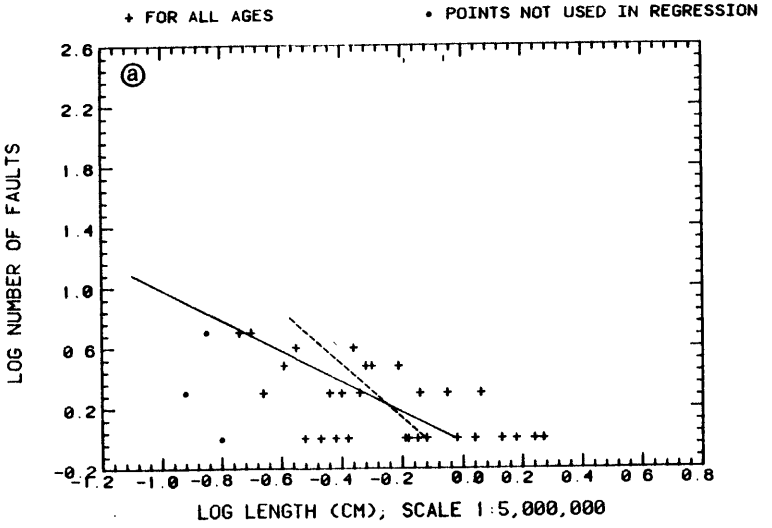

DERIVATIVE OF FREQUENCY DISTRIBUTION (CONTERMINOUS U S)

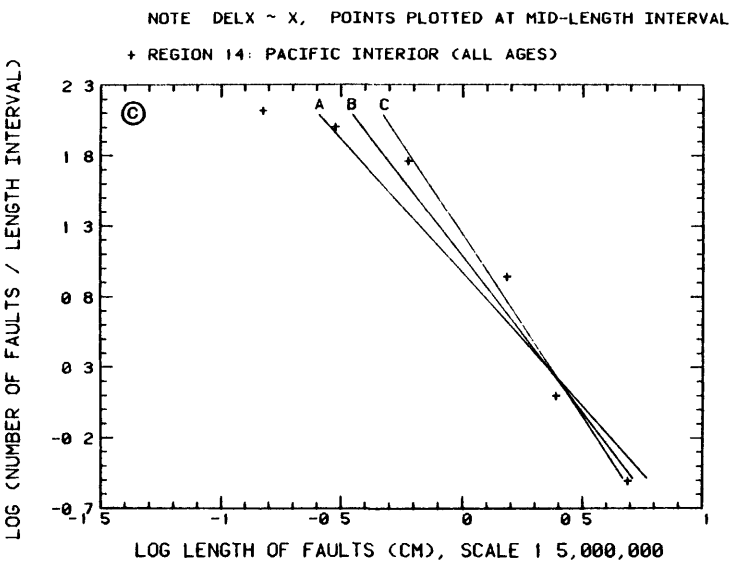

FREQUENCY, LENGTH OF FAULTS (CONTERMINOUS U S)

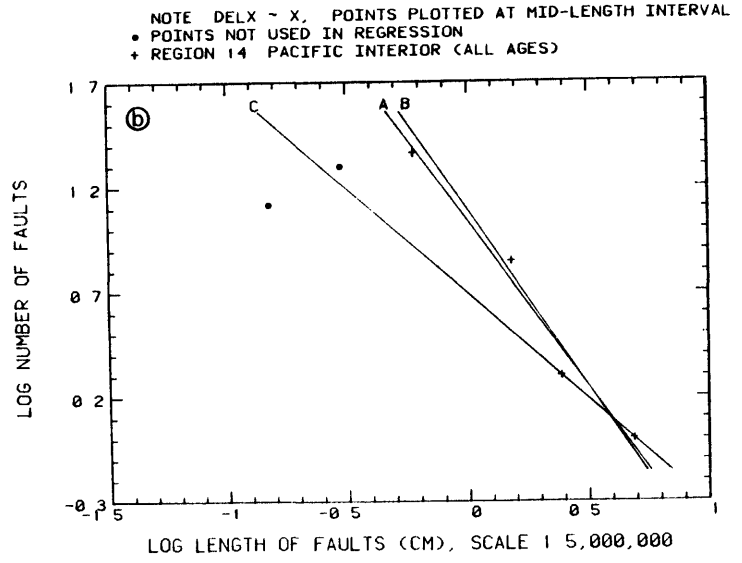

CUMULATIVE FREQUENCY, LENGTH OF FAULTS(CONTERMINOUS U S)

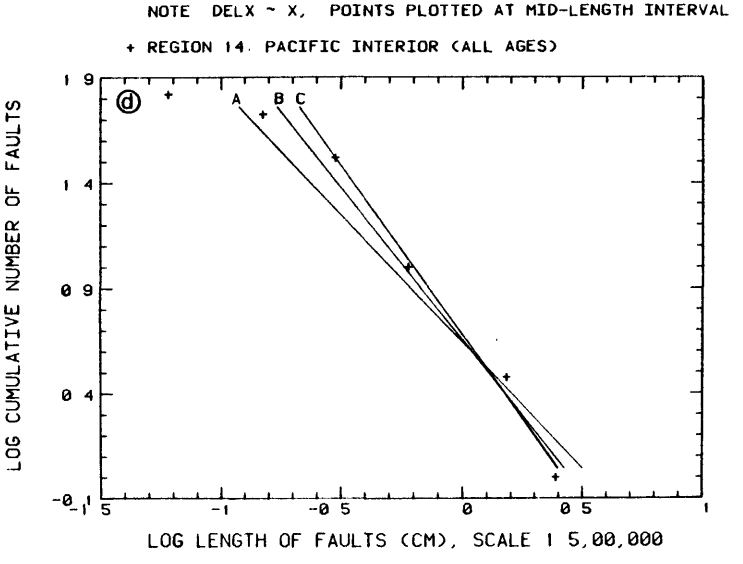

Figure 4.2.1.-2. (14)

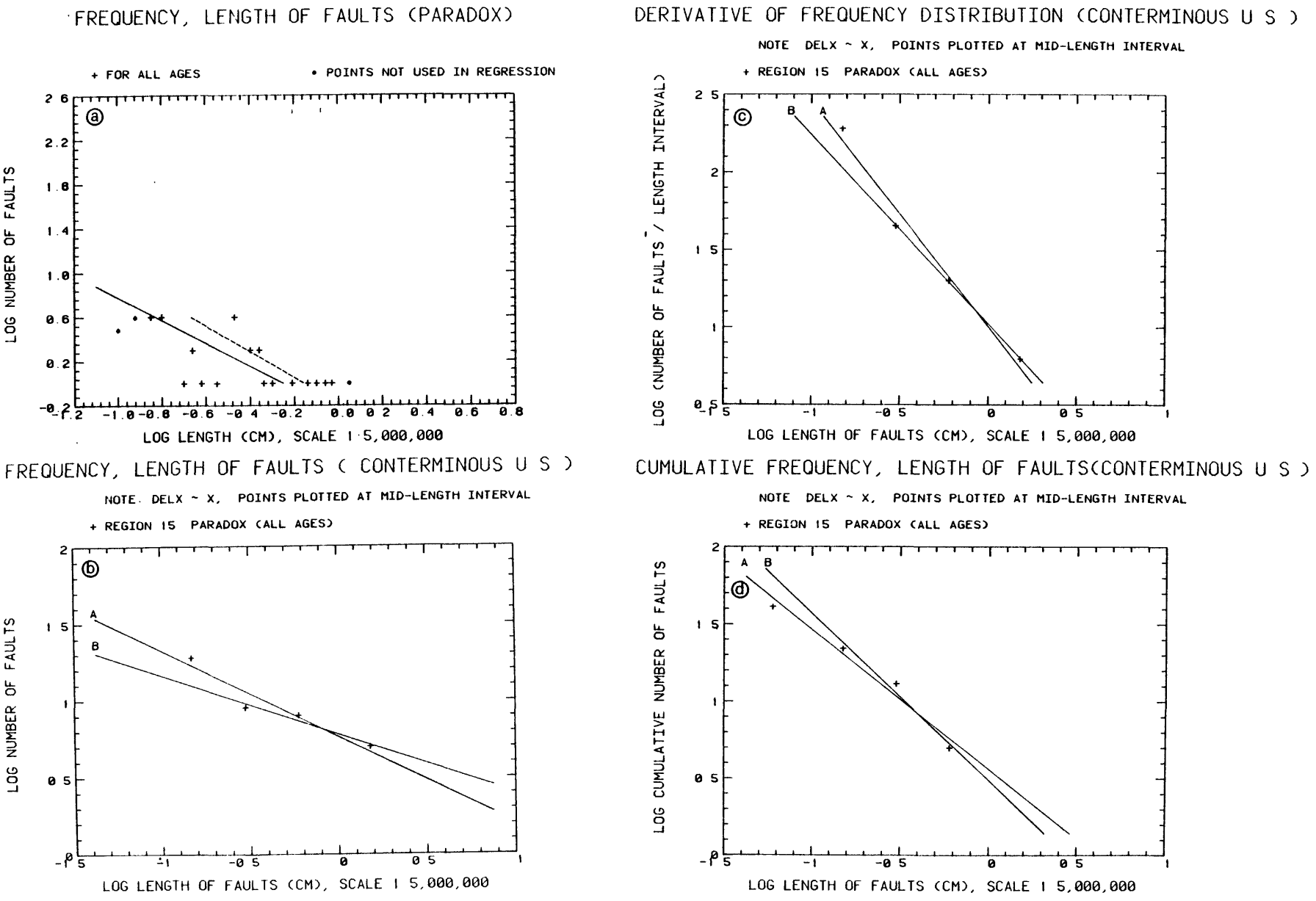

Figure 4.2.1.-2. (15)

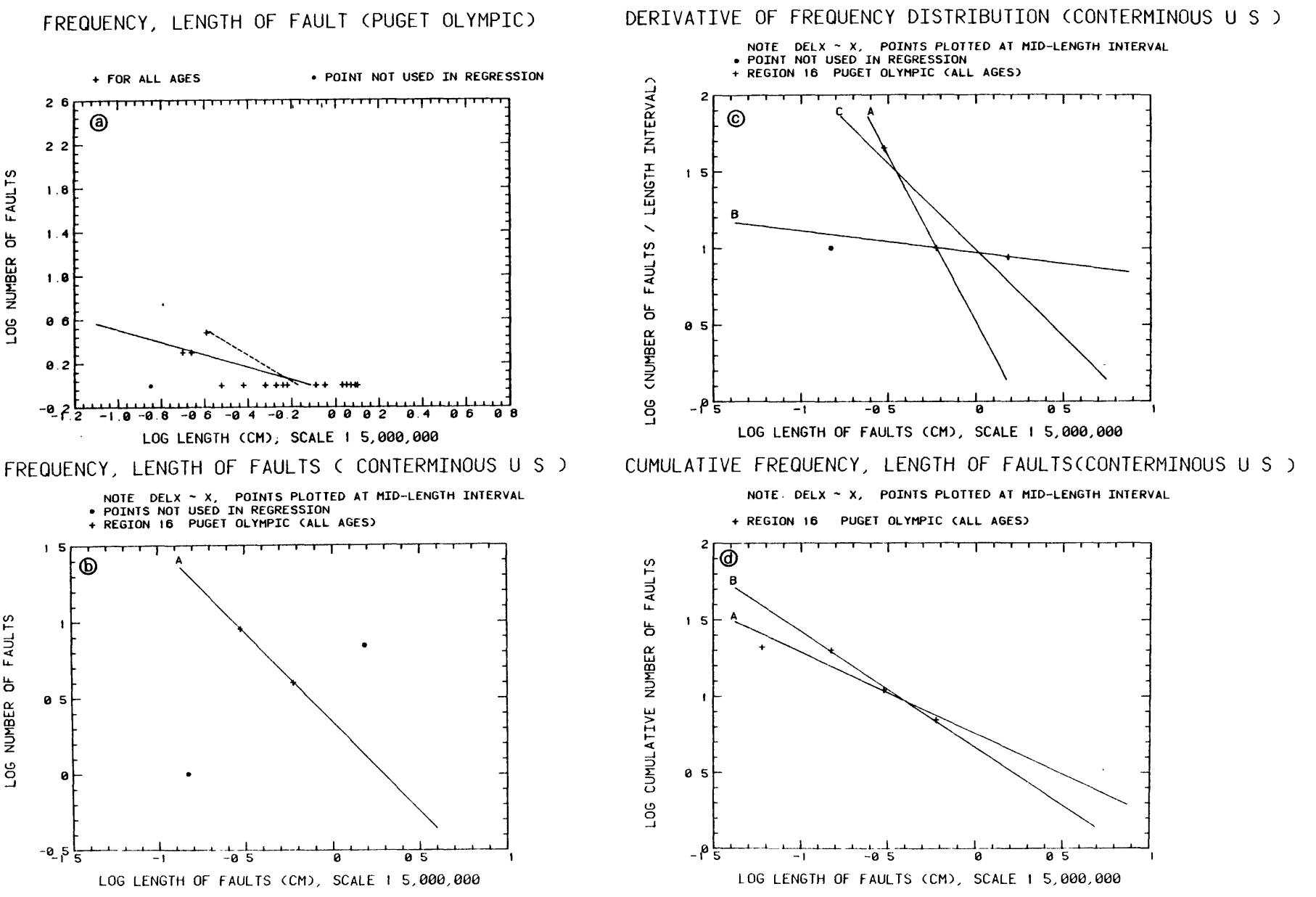

Figure 4.2.1.-2. (16)

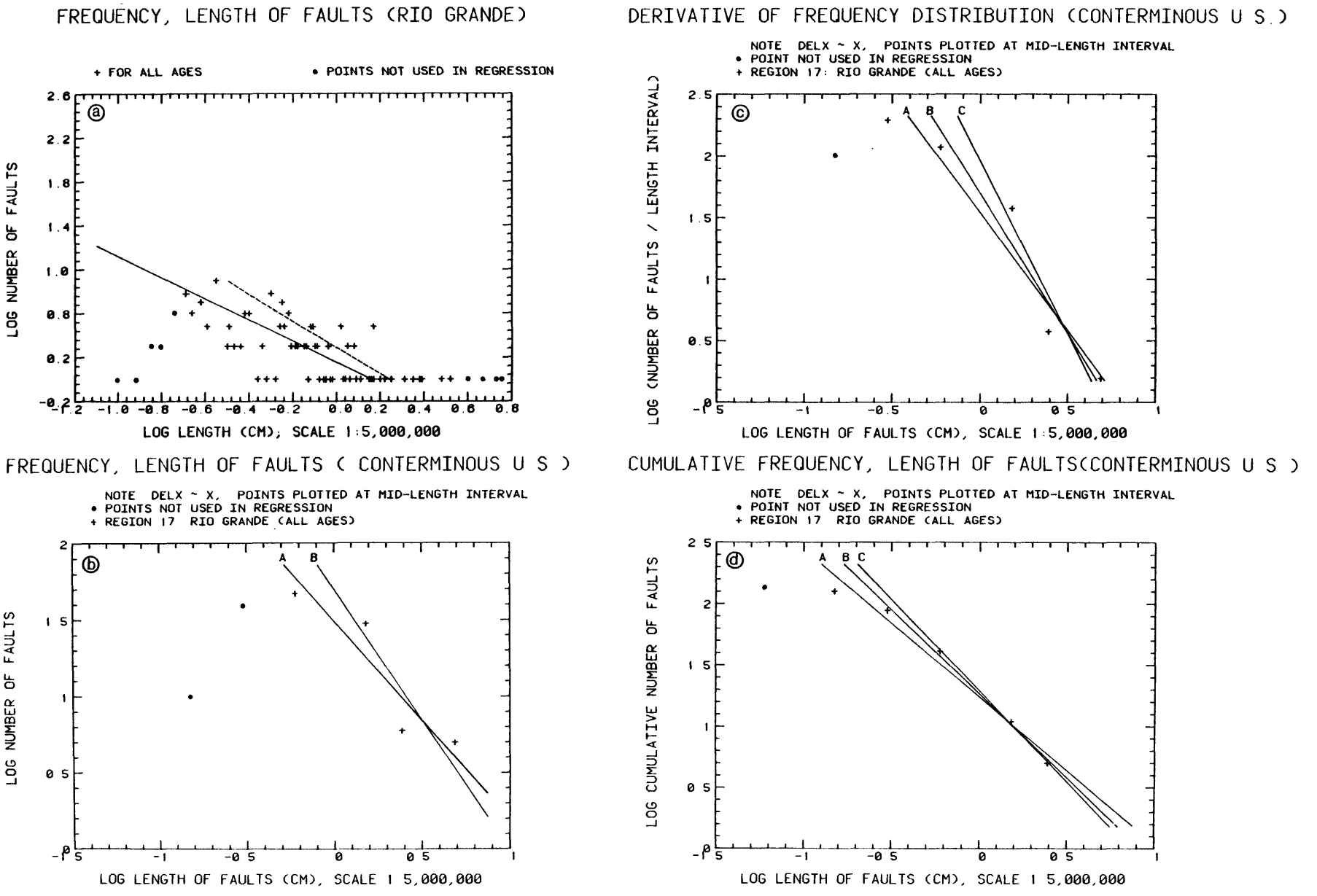

Figure 4.2.1.-2. (17)

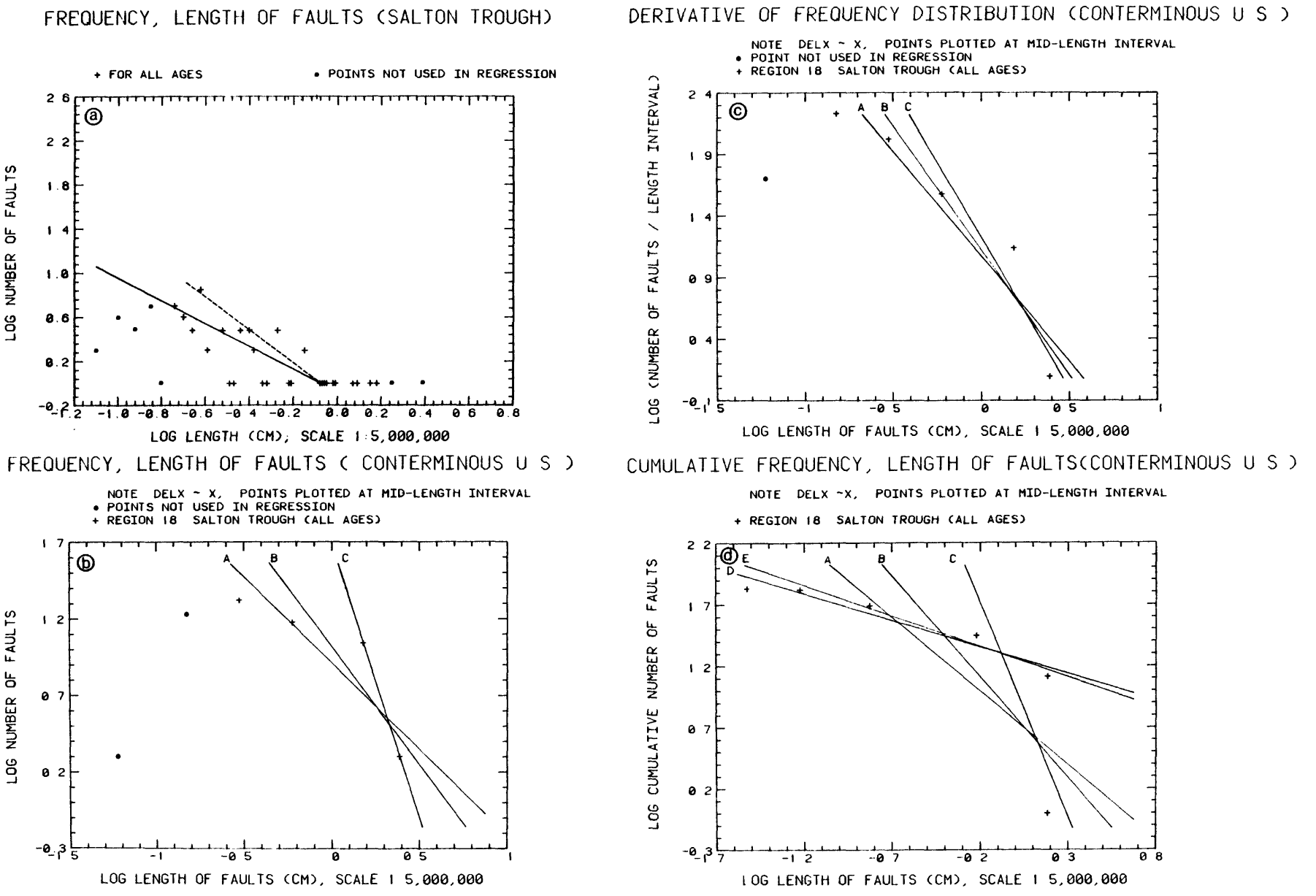

Figure 4.2.1.-2. (18)

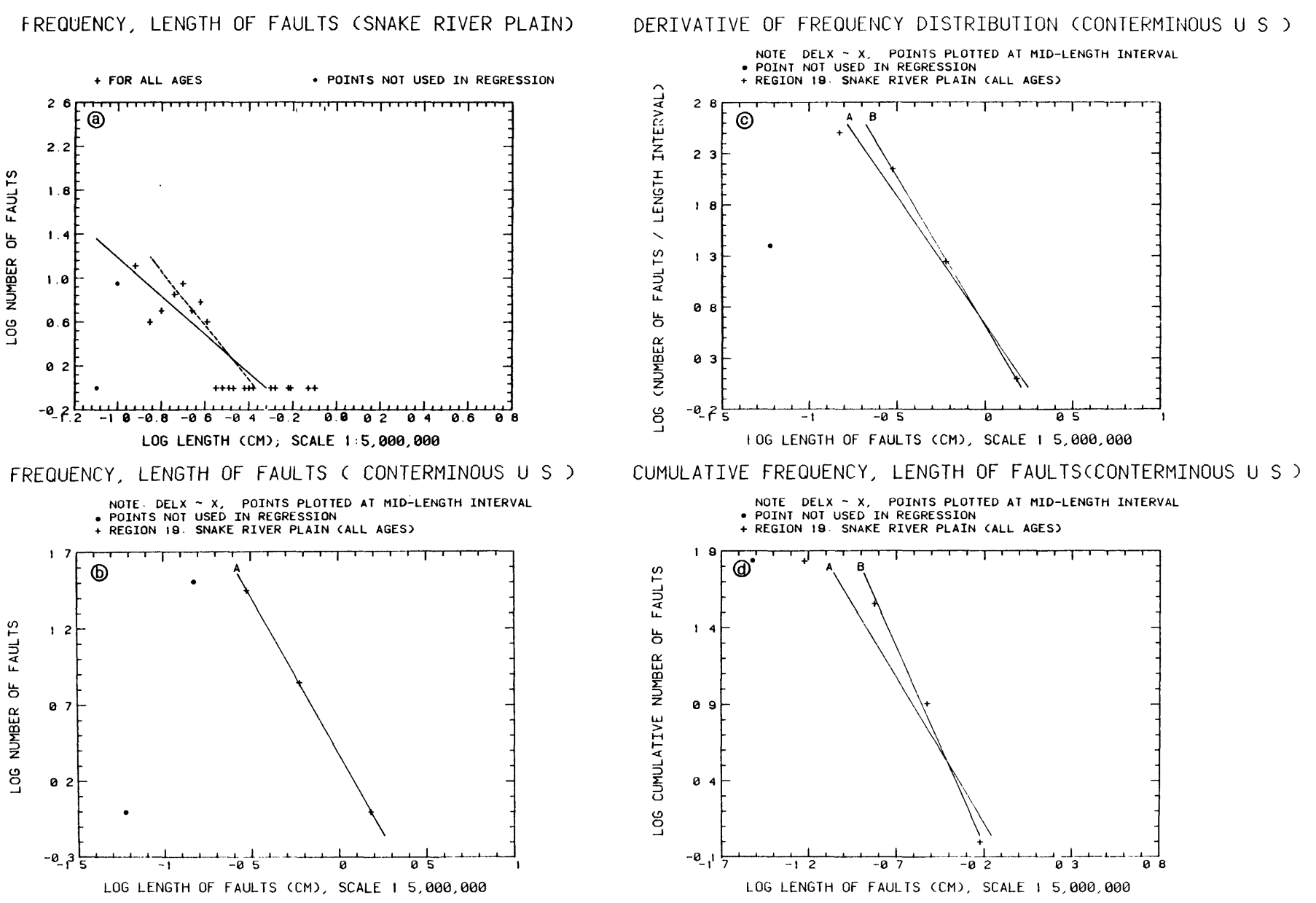

Figure 4.2.1.-2. (19)

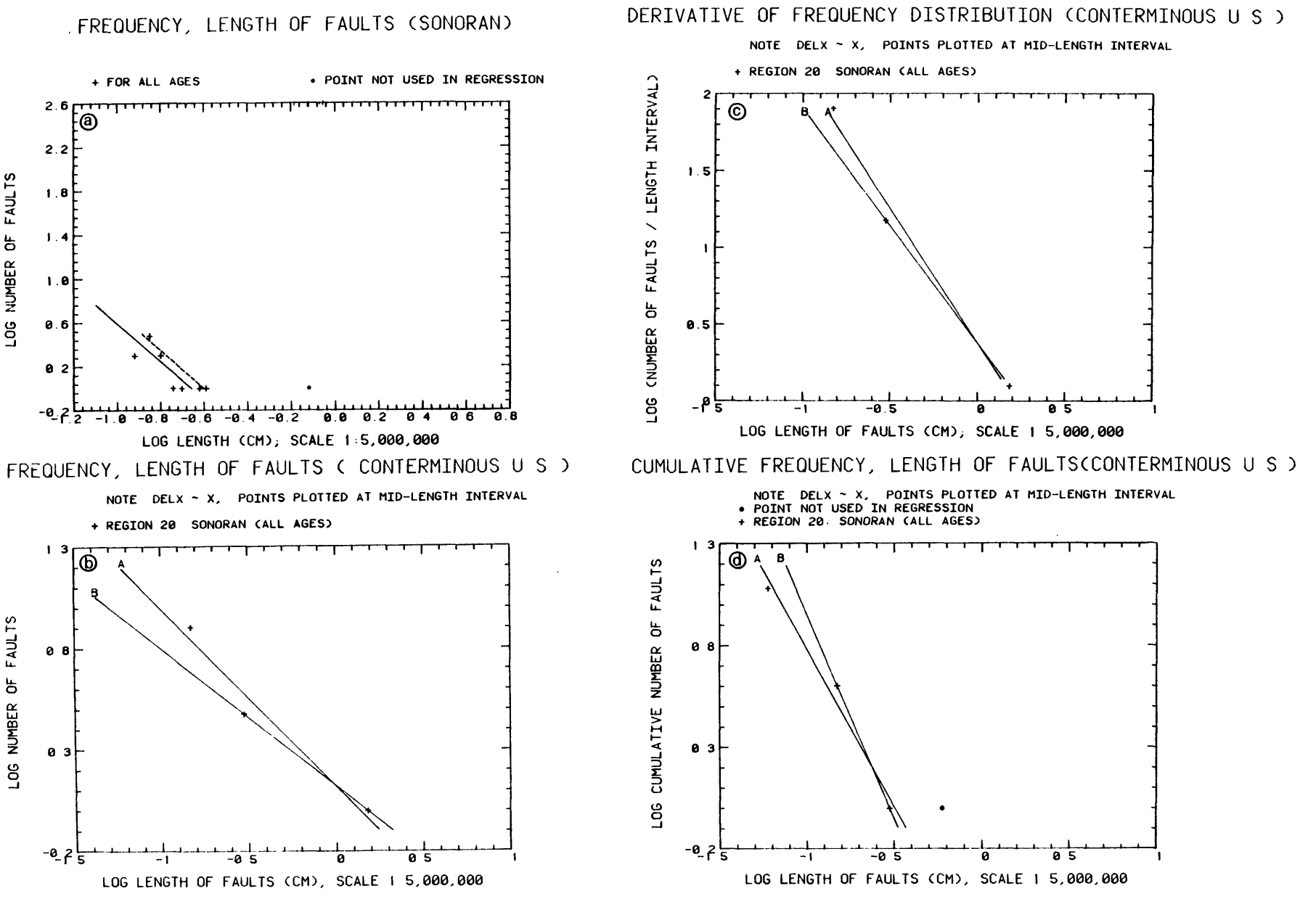

Figure 4.2.1.-2. (20)

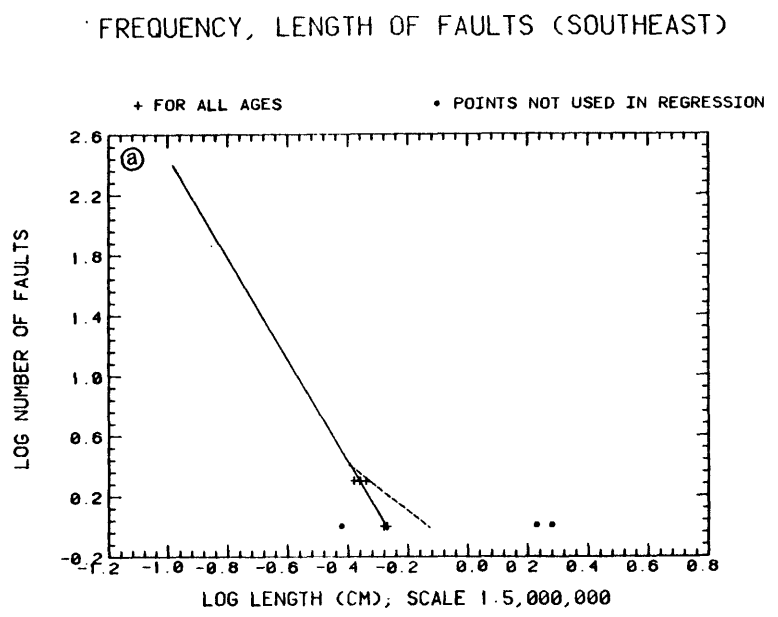

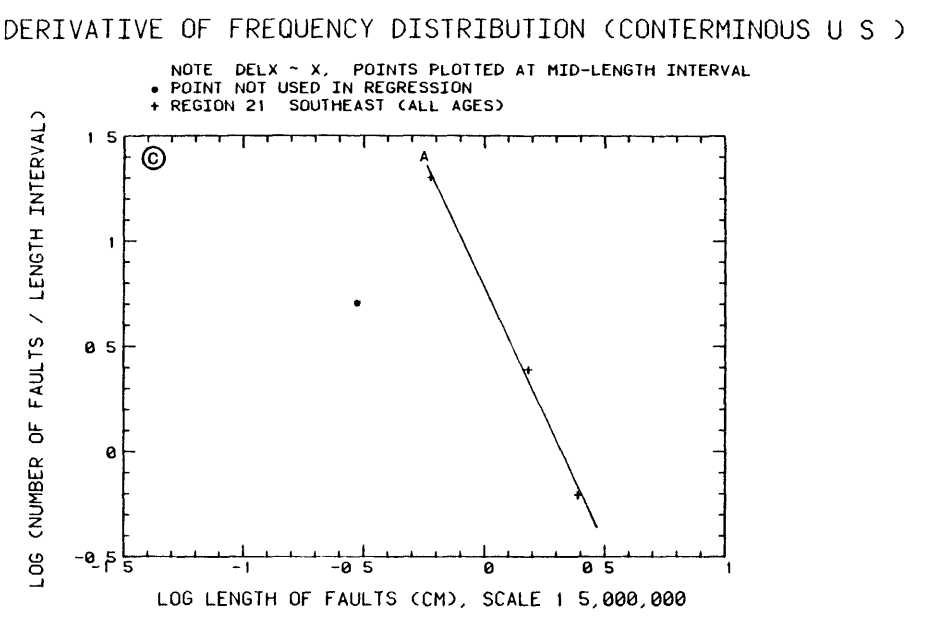

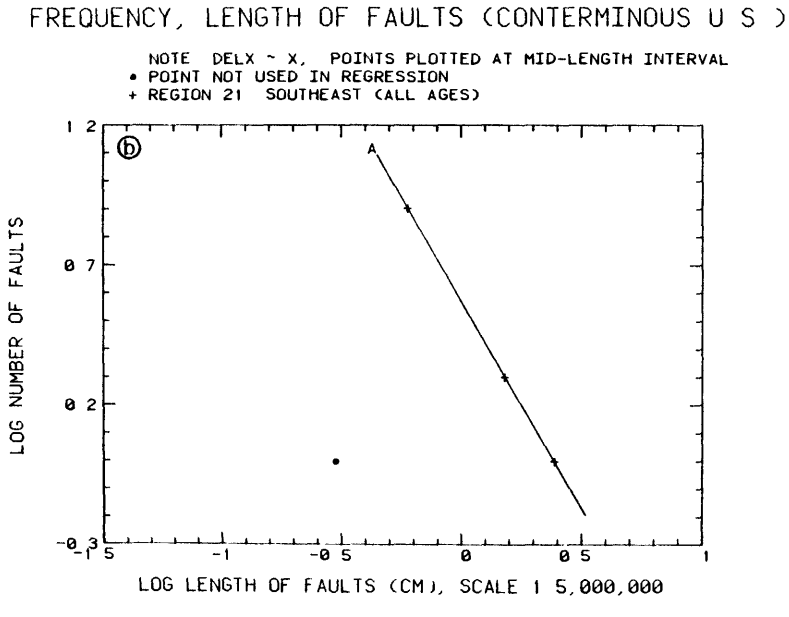

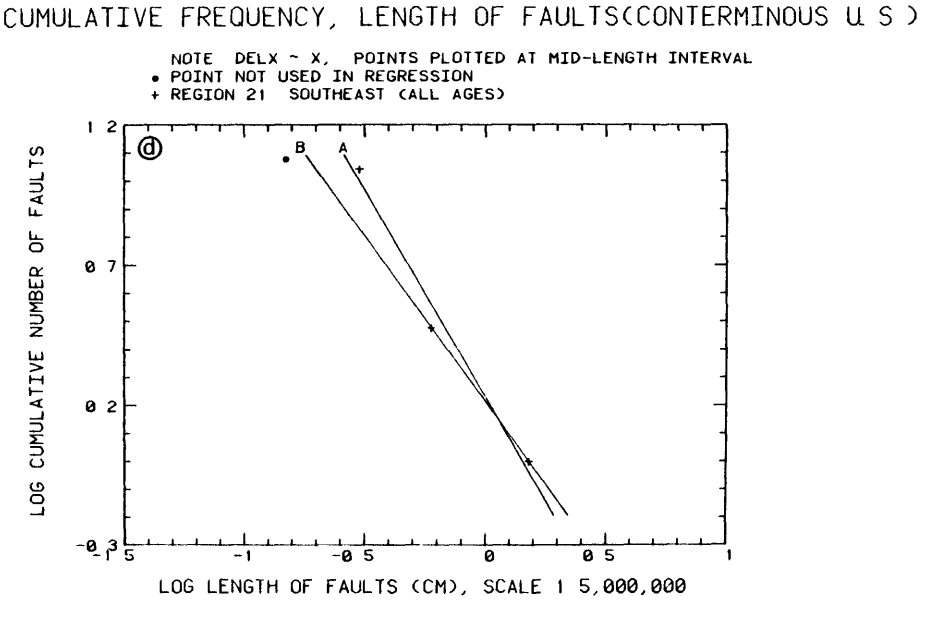

Figure 4.2.1.-2. (21)

FREQUENCY, LENGTH OF FAULTS (SOUTHERN CA. BORDERLAND)

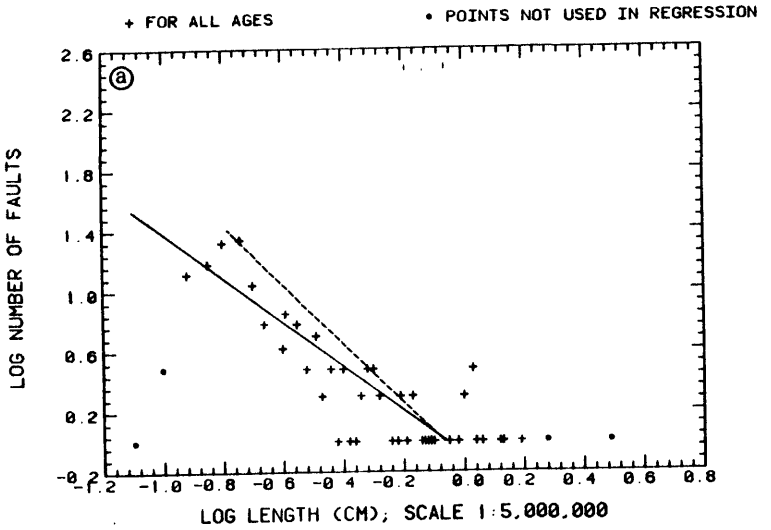

DERIVATIVE OF FREQUENCY DISTRIBUTION (CONTERMINOUS U.S.)

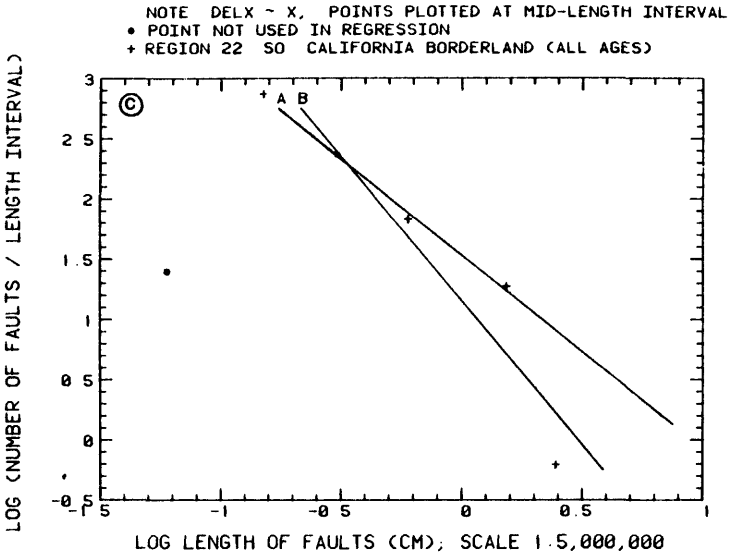

FREQUENCY, LENGTH OF FAULTS (CONTERMINOUS U S)

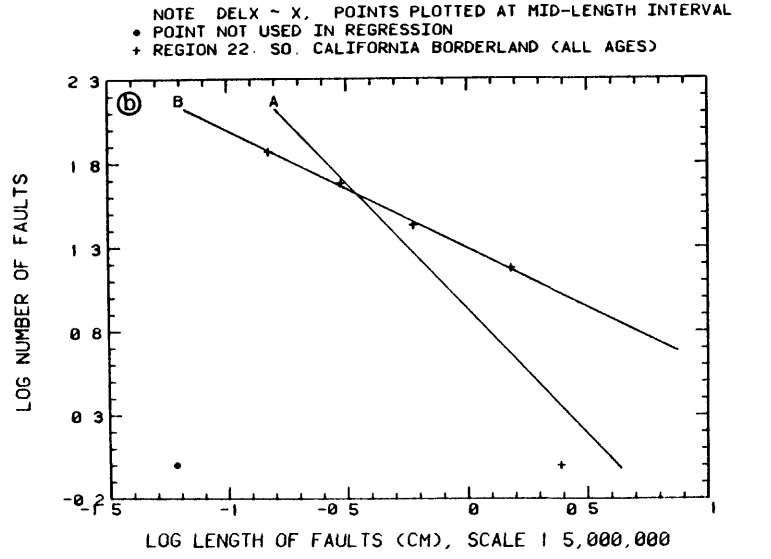

CUMULATIVE FREQUENCY, LENGTH OF FAULTS(CONTERMINOUS U S)

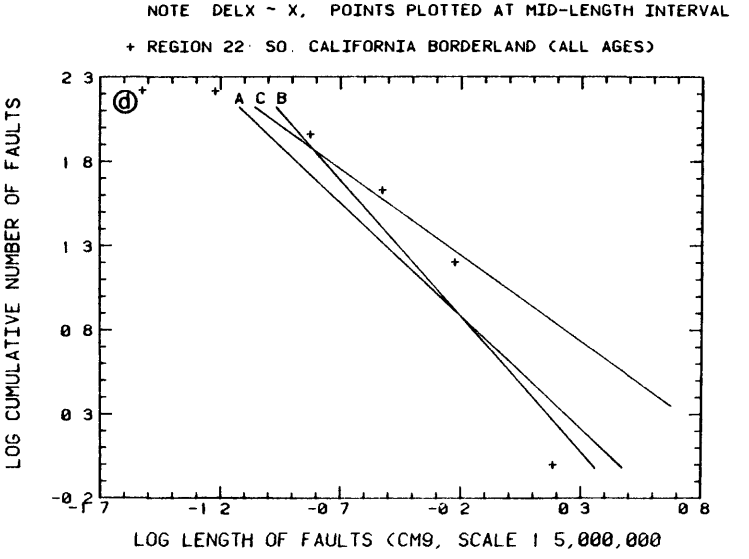

Figure 4.2.1.-2. (22)

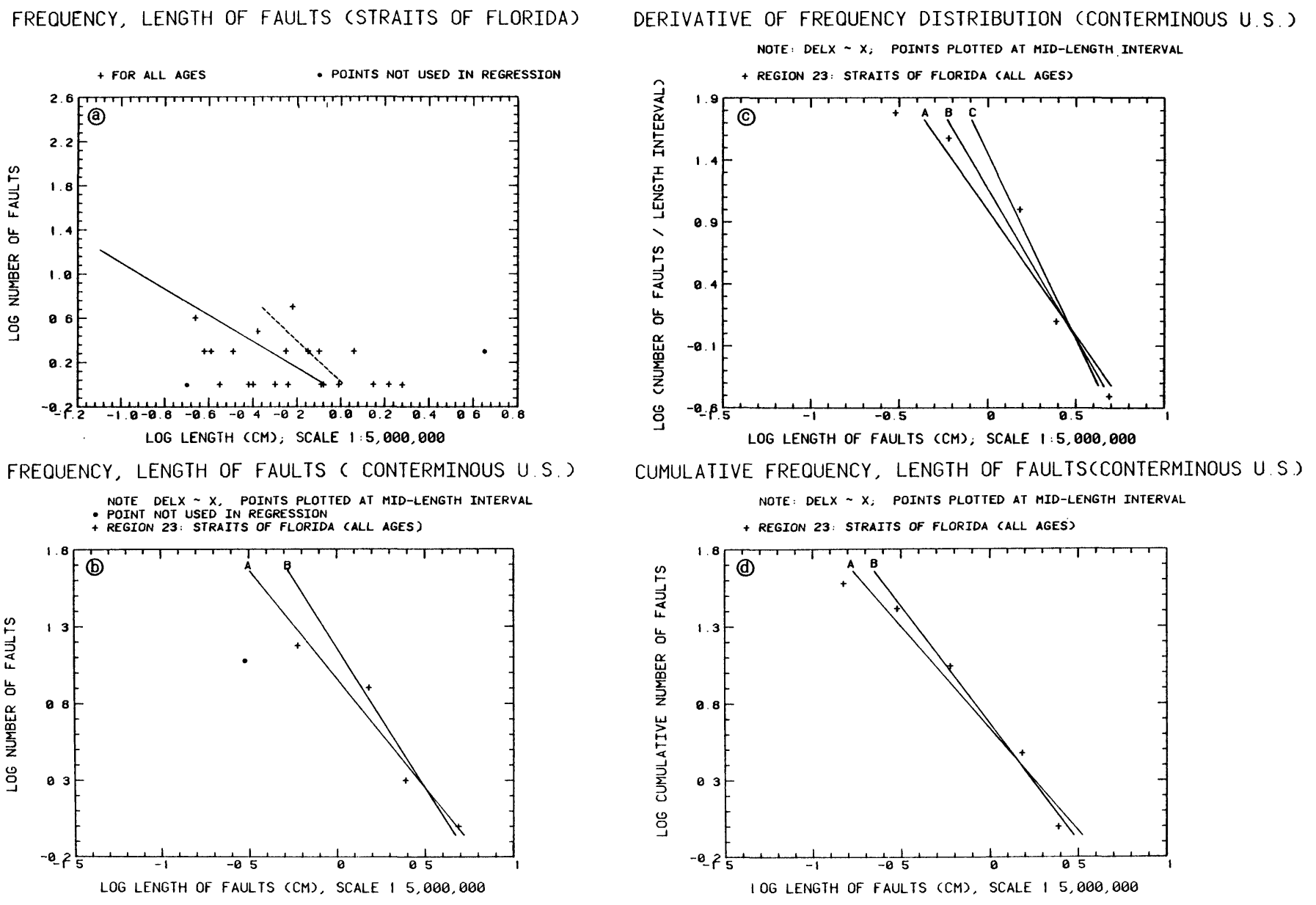

Figure 4.2.1.-2. (23)

FREQUENCY, LENGTH OF FAULTS (TRANSVERSE-TEHACHAPI)

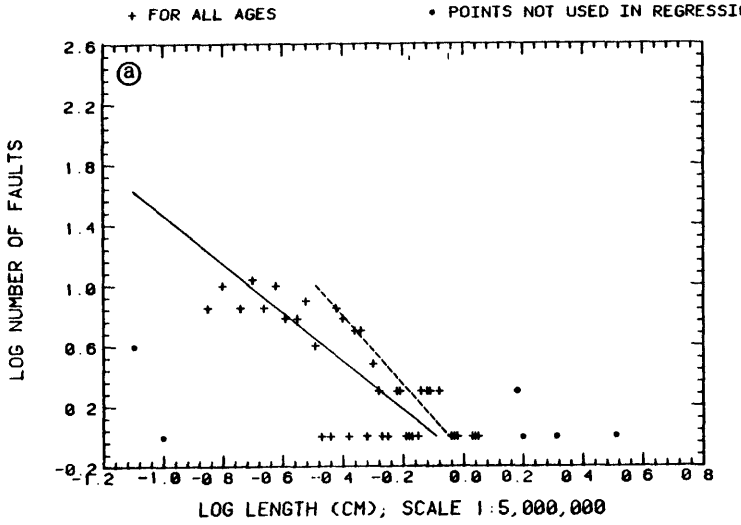

DERIVATIVE OF FREQUENCY DISTRIBUTION (CONTERMINOUS U.S.)

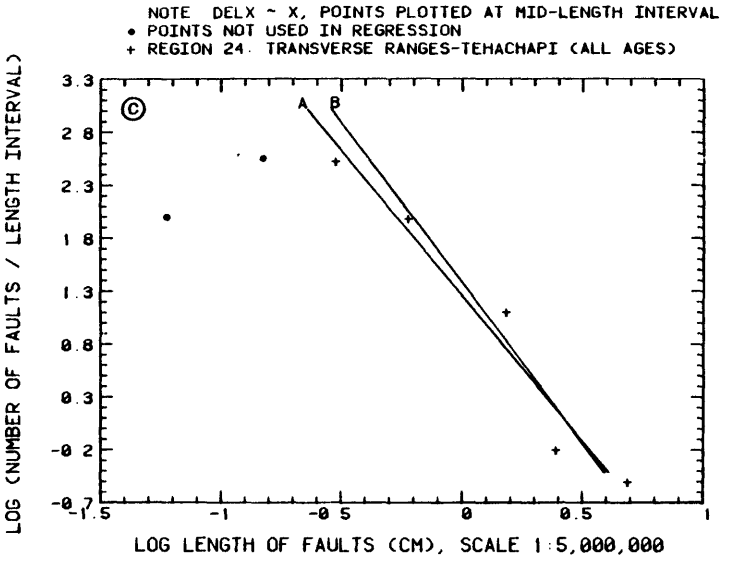

FREQUENCY, LENGTH OF FAULTS (CONTERMINOUS U S)

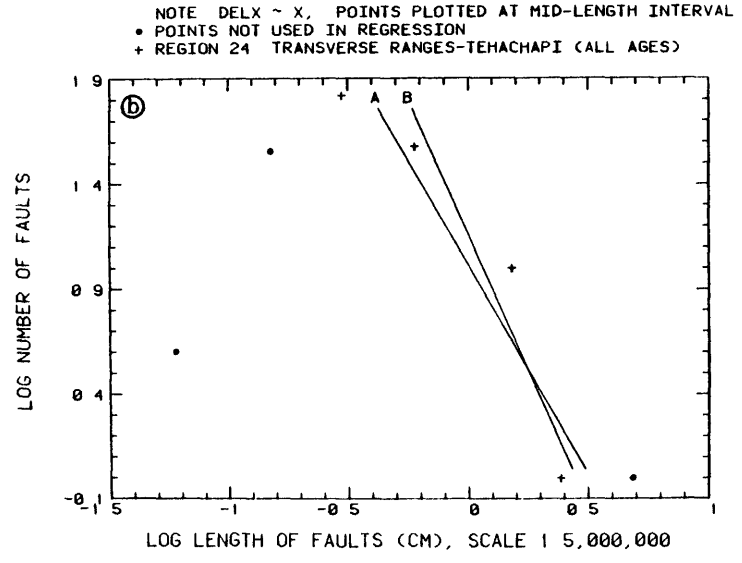

CUMULATIVE FREQUENCY, LENGTH OF FAULTS(CONTERMINOUS U S)

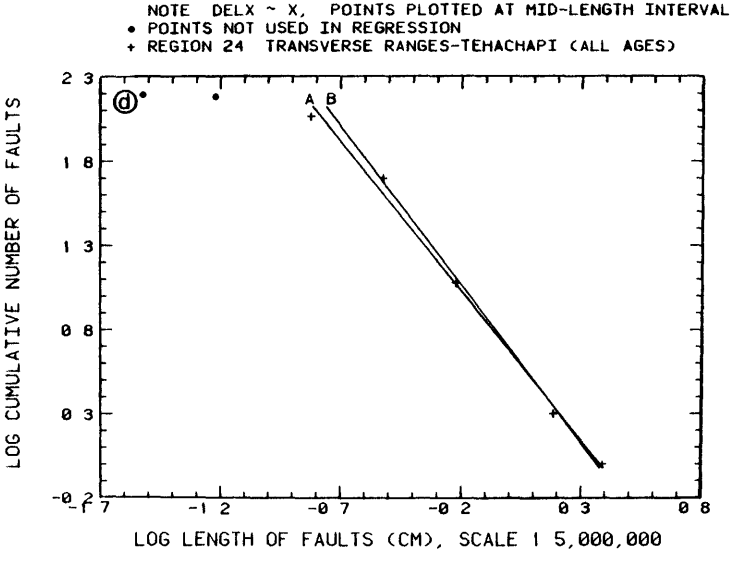

Figure 4.2.1.-2. (24)

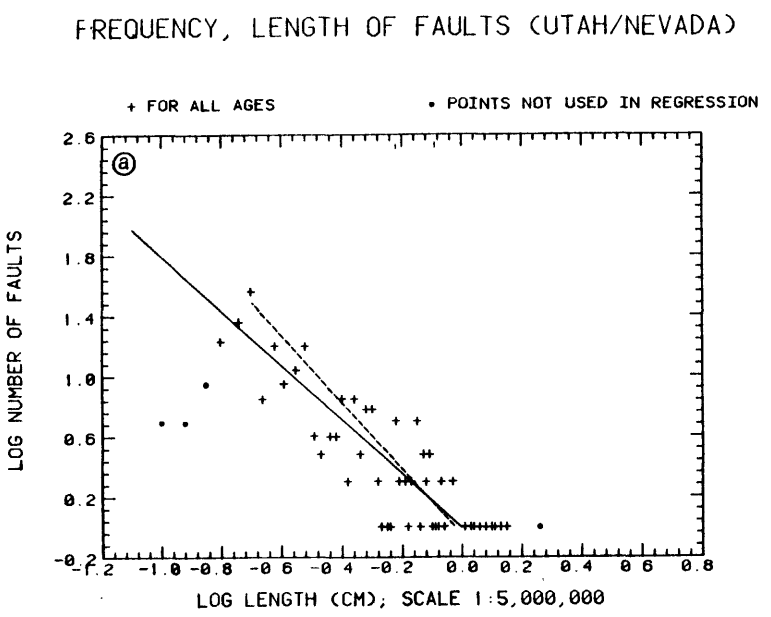

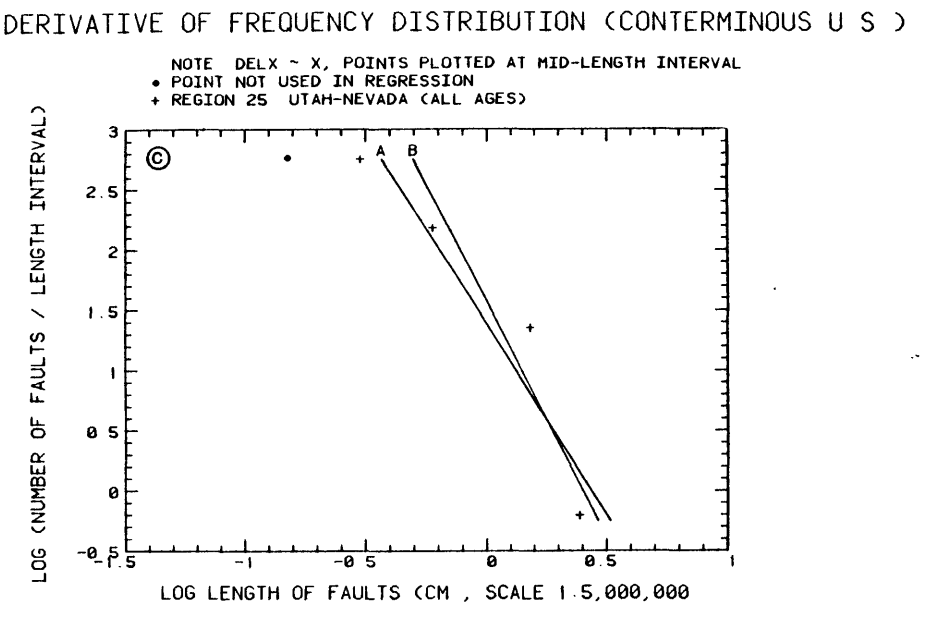

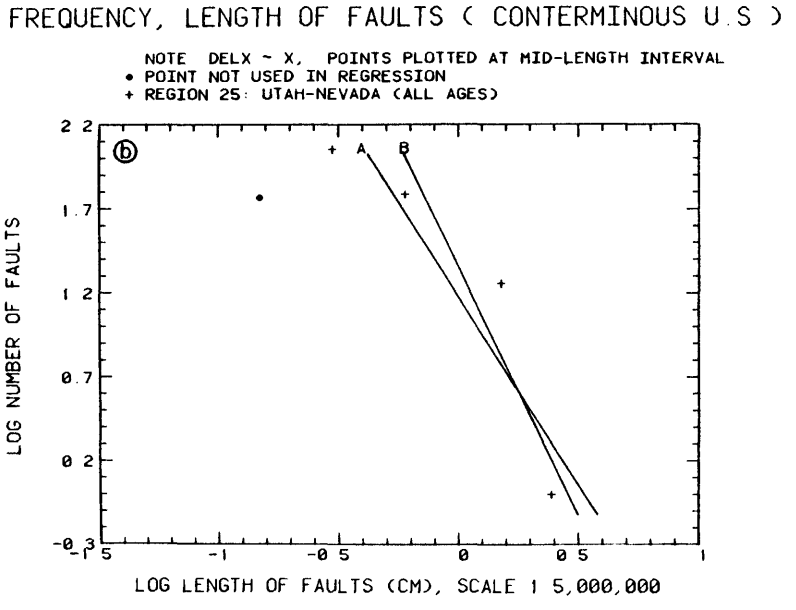

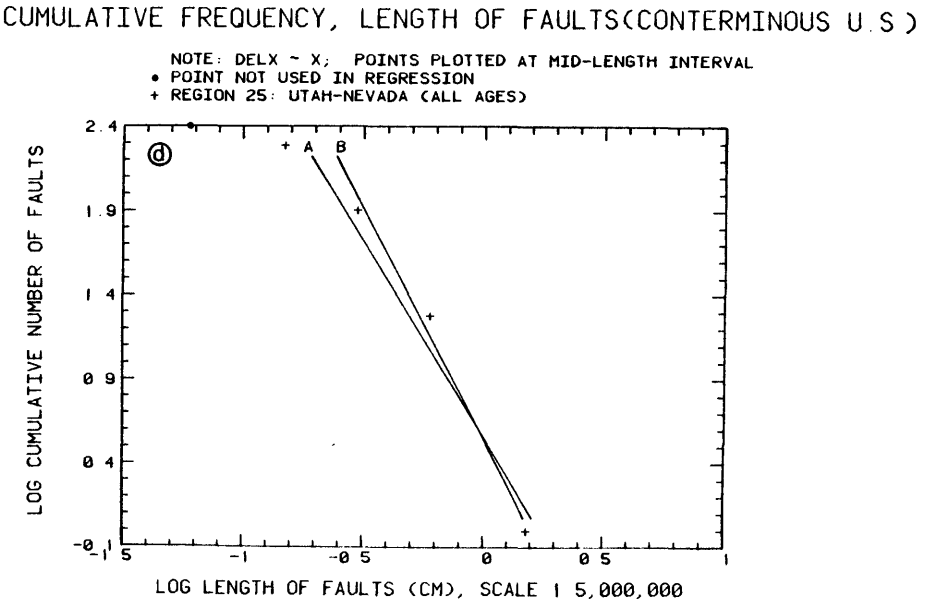

Figure 4.2.1.-2. (25)

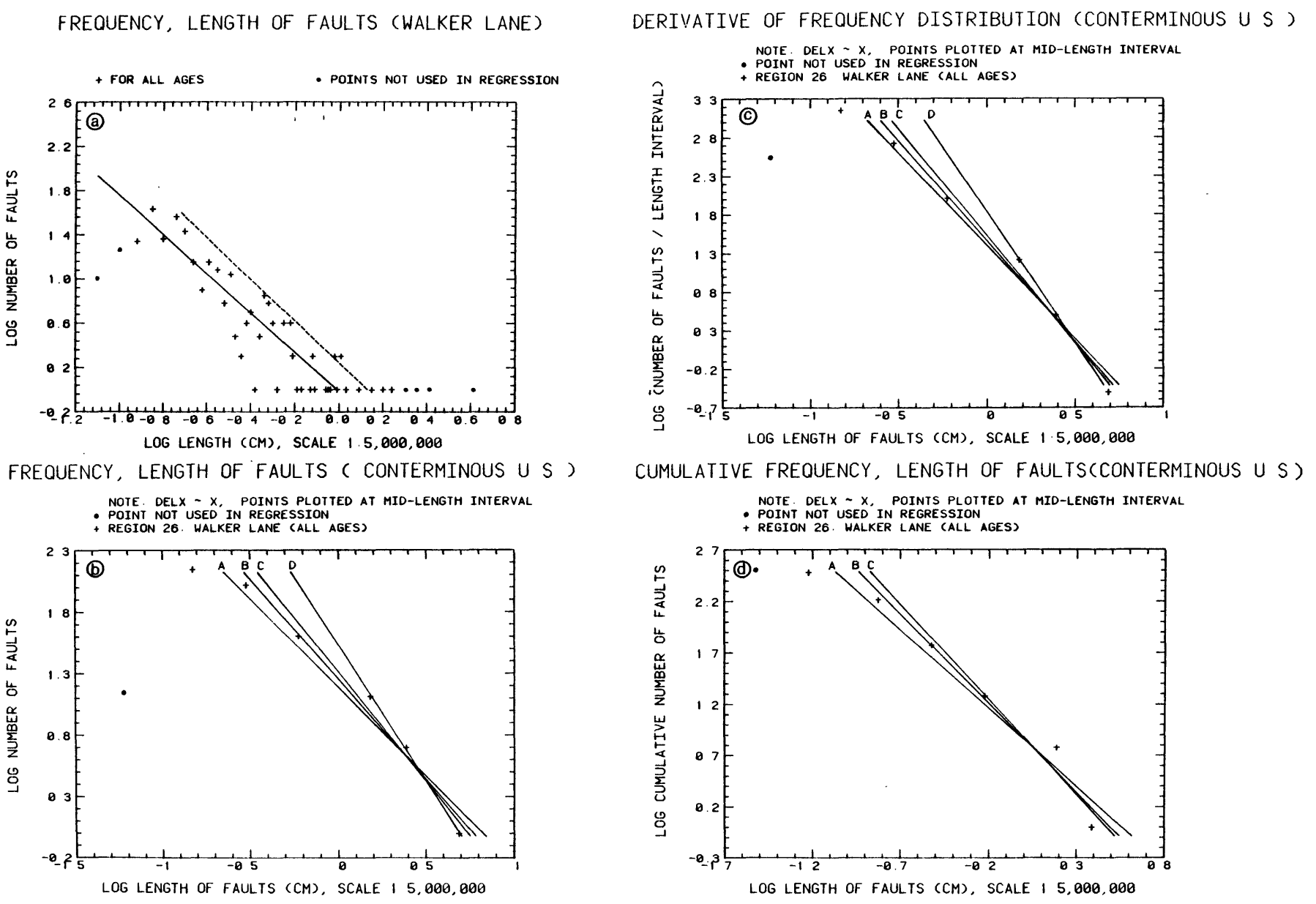

Figure 4.2.1.-2. (26)

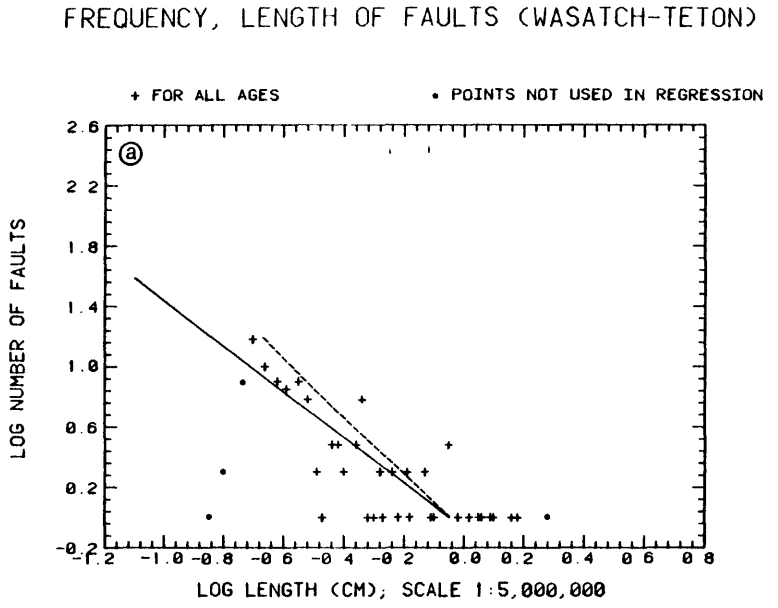

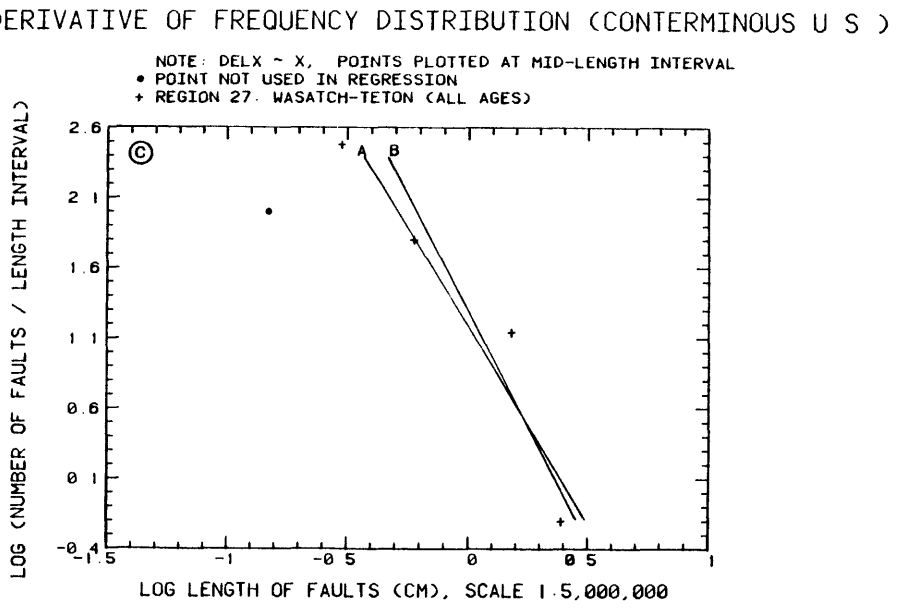

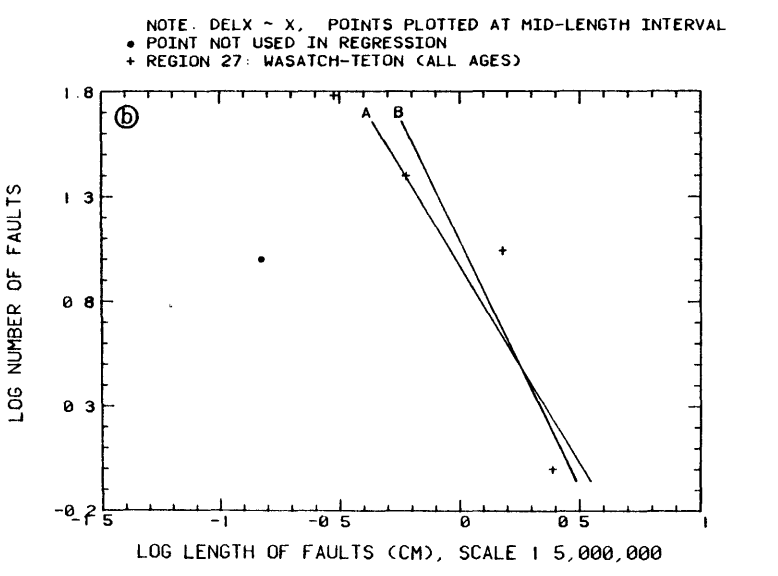

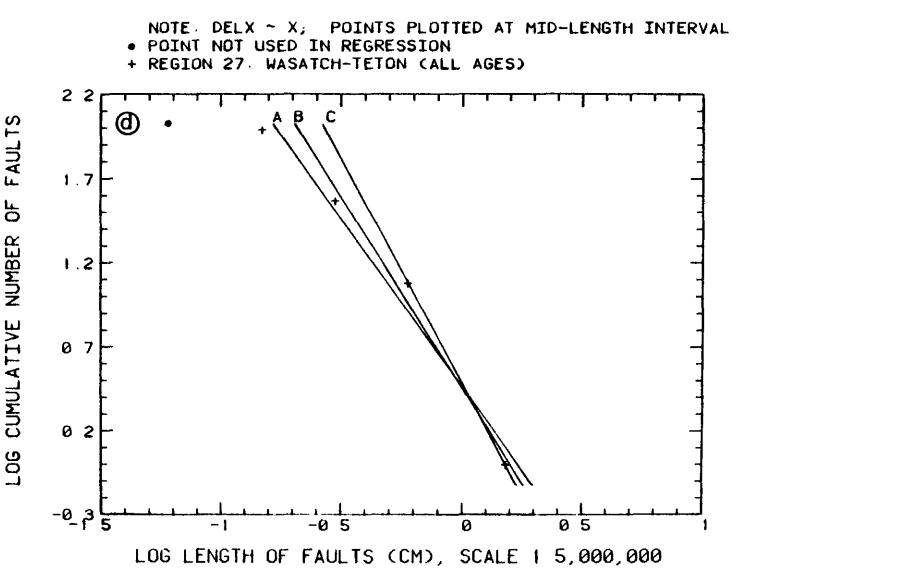

Figure 4.2.1.-2. (27)

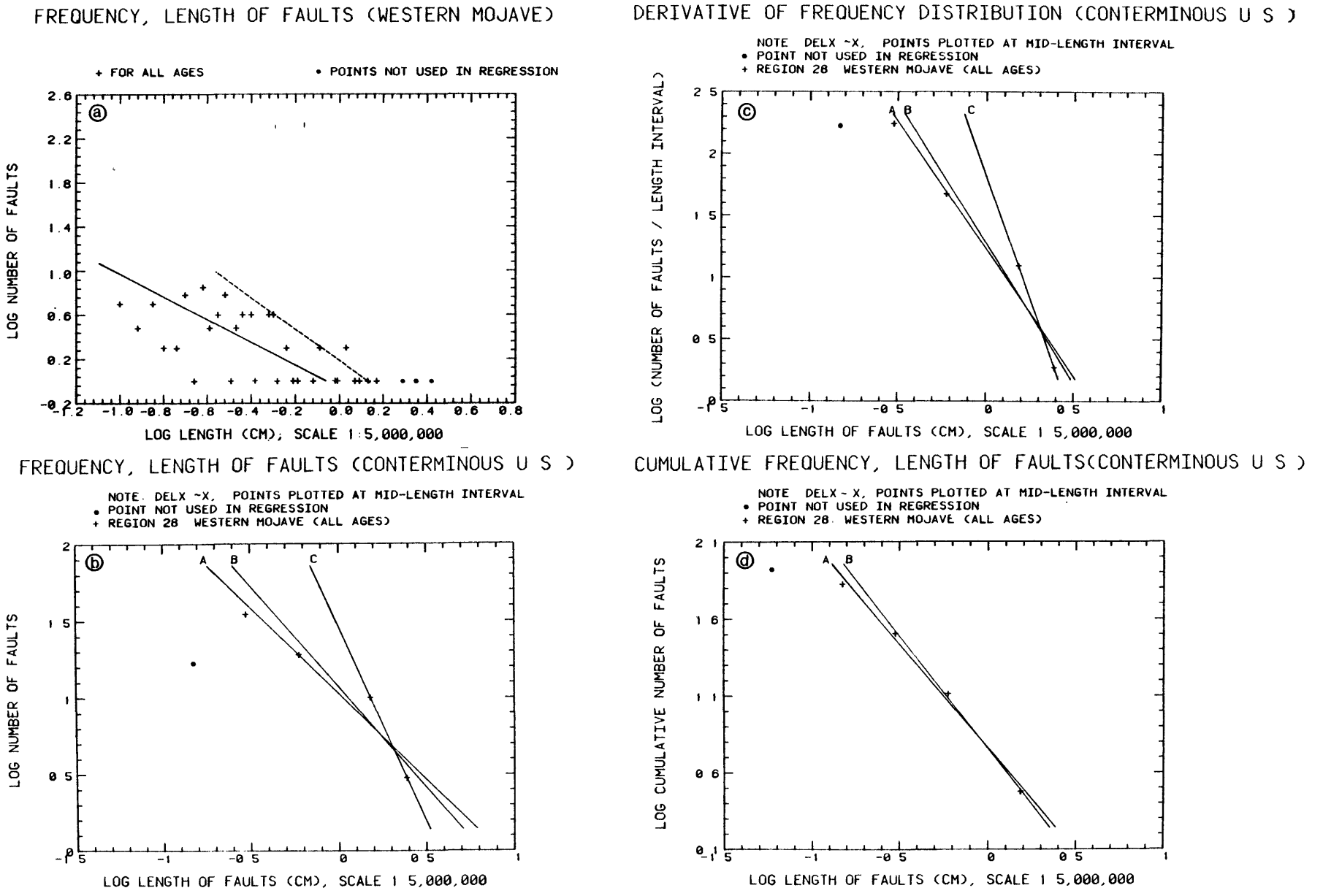

Figure 4.2.1.-2. (28)

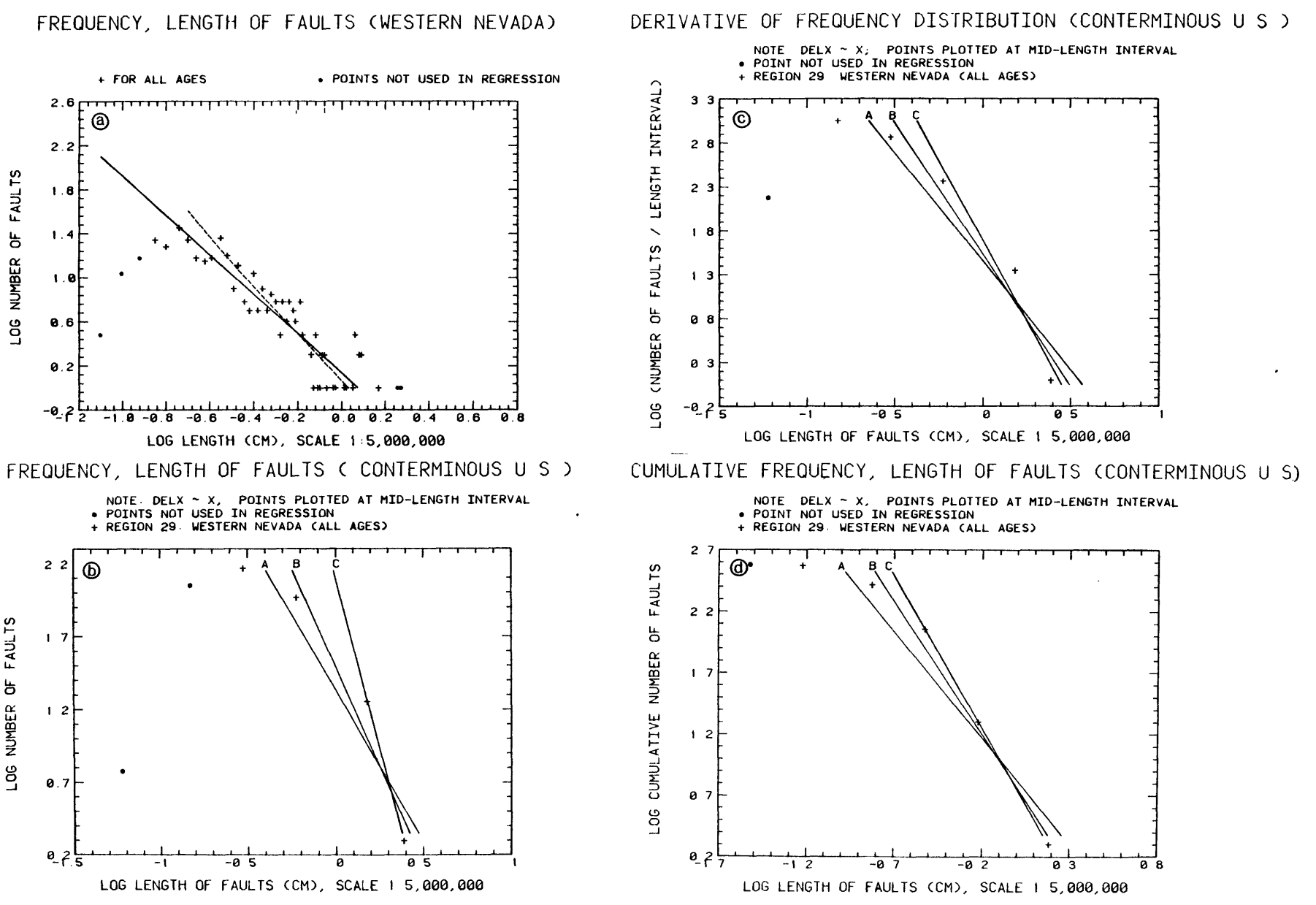

Figure 4.2.1.-2. (29)

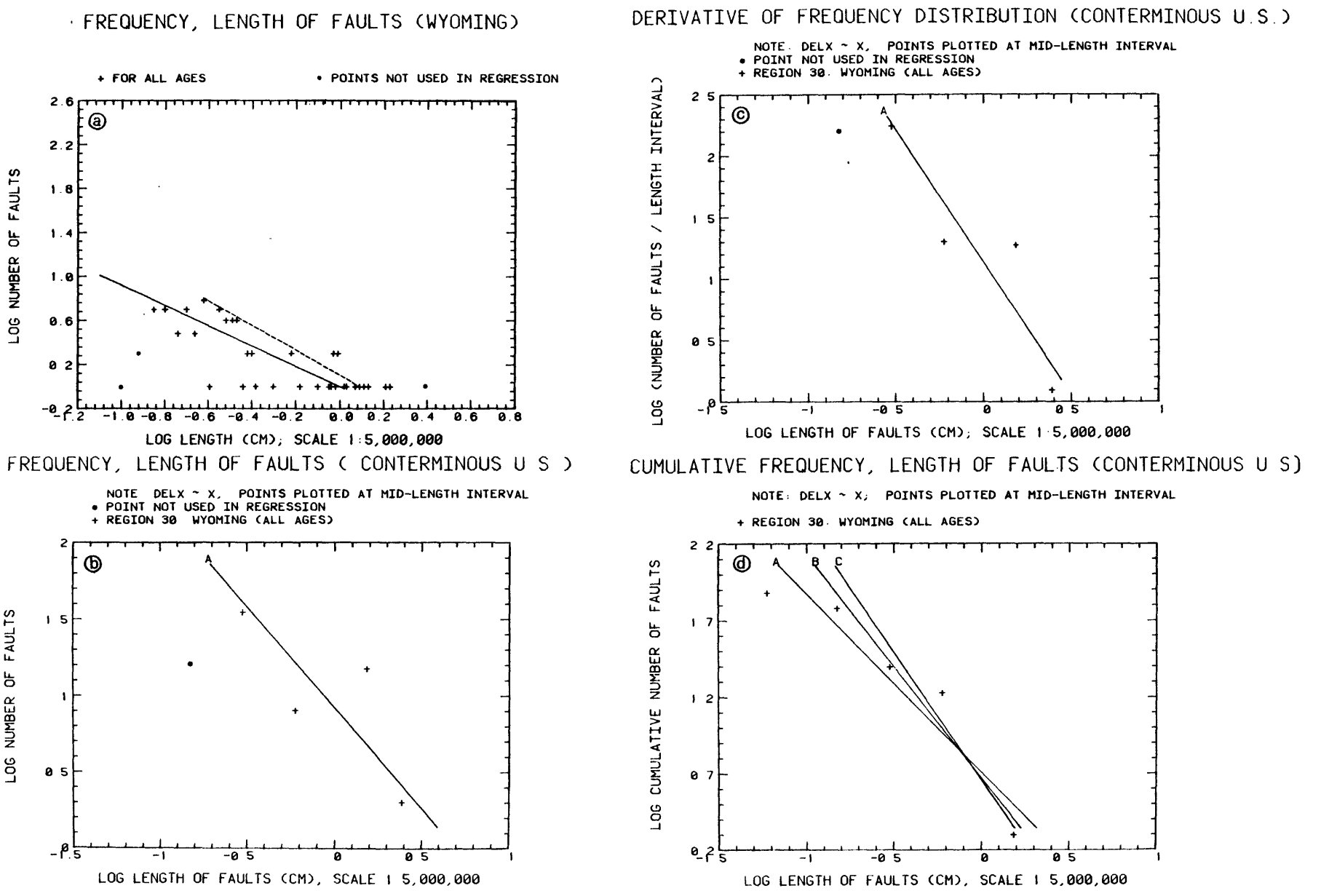

Figure 4.2.1.-2. (30)

Table 4.2.1.-1. Coefficients in Regression Equations.

Legend: Equation form: $\log n = -s \log \ell + c$ (ℓ, map cm). Equation sequences in table: (i) log n vs log ℓ in constant Δ ; (ii) log n vs log ℓ for DELX ~ X; (iii) log ($\Delta n/\Delta \ell$) vs log ℓ for derivative DELX ~ X; (iv) log Σn vs log ℓ for cumulative DELX ~ X. Regression sets per graph are labeled A,B,C, etc.

Microcrack Data (Figure 4.1.2.-1)

		S	C
(i)	A	3.31	-5.67
	B	3.81	-6.48
	C	3.64	-5.94
	D	3.88	-6.16
(ii)		2.81	-3.69
(iii)	A	1.61	0.71
	B	3.80	-3.68
(iv)		1.73	-2.05

Measured Bubble Contacts (Figure 4.1.2-2.)

(i)		1.48	0.84
(ii)	A	3.11	2.47
	B	4.98	3.47
(iii)	A	4.05	2.65
	B	6.16	3.76
(iv)	A	3.12	1.62
	B	4.17	1.89
	C	8.12	3.16

Horton Stream Order (Figure 4.1.2-4.(A))

(i)		0.99	0.19
(ii)	A	1.32	1.10
	B	1.69	1.27
	C	2.21	1.53
(iii)	A	2.32	1.31
	B	2.74	0.49
	C	3.41	1.82
(iv)	A	1.36	0.95
	B	1.48	0.99

Strahler Stream Order (Figure 4.1.2.-4.(B))

		S	C
(i)		1.39	0.07
(ii)	A	1.51	1.16
	B	1.79	1.29
(iii)	A	2.49	1.36
	B	2.82	1.50
(iv)	A	1.84	0.84
	B	1.66	0.81

All U.S. Data (Figure 4.2.1-1.(B))

(i)		1.76	1.12
(ii)	A	1.76	2.51
	B	2.10	2.72
	C	2.59	3.06
(iii)	A	2.09	2.61
	B	2.44	2.73
	C	2.83	2.90
	D	3.62	3.30
(iv)	A	1.87	2.13
	B	2.10	2.21
	C	2.38	2.23
	D	2.99	2.63

Los Angeles Area (Figure 4.2.1.-1.(D)

(i)		2.23	-0.34
(ii)	A	1.61	1.01
	B	1.81	0.92
(iii)	A	2.21	1.38
	B	2.61	1.18
	C	2.81	1.09
(iv)	A	1.36	0.77
	B	1.71	0.47

30 faulting regions (Figure 4.2.1.-2 (1-30). Equation form: $\log n = -s \log \ell + c$ (ℓ, map cm).

1. Arizona Mtn. Belt

		S	C
(i)		1.28	-0.19
(ii)	A	1.32	1.09
(iii)	A	1.53	1.27
	B	2.07	1.32
(iv)	A	1.47	0.57
	B	2.15	0.37

2. California Coast

		S	C
(i)		1.28	0.13
(ii)	A	1.26	1.31
	B	1.35	1.36
	C	1.70	1.60
(iii)	A	1.93	1.46
	B	2.11	1.52
	C	2.18	1.55
	D	2.81	1.87
(iv)	A	1.23	1.08
	B	1.38	1.11
	C	1.49	1.15
	D	1.70	1.24
	E	2.13	1.46

3. Central Mississippi Valley

		S	C
(i)		2.03	-0.33
(ii)	A	2.06	0.25
	B	1.18	0.22
(iii)	A	2.90	0.49
	B	1.93	0.45
(iv)	A	2.49	-0.61
	B	2.00	-0.44

4. Circum-Gulf

		S	C
(i)		1.68	-0.15
(ii)	A	1.78	1.18
	B	2.35	1.47
(iii)	A	2.64	1.46
	B	3.47	1.87
(iv)	A	1.52	0.71
	B	1.81	0.76
	C	1.99	0.80

5. Eastern Oregon-Western Idaho

		S	C
(i)		1.77	0.28
(ii)	A	1.93	1.73
	B	2.98	2.06
(iii)	A	2.35	1.81
	B	2.89	1.94
	C	4.43	2.42
(iv)	A	1.64	1.24
	B	1.87	1.23

6. Four Corners

		S	C
(i)		1.39	-0.35
(ii)		2.09	0.38
(iii)	A	2.09	0.55
	B	2.84	0.61
(iv)	A	2.01	-0.37
	B	3.00	-0.67

7. Grand Canyon

		S	C
(i)		0.93	-0.11
(ii)	A	1.66	1.07
	B	3.93	1.83
(iii)	A	1.64	1.08
	B	2.01	1.41
	C	2.56	1.28
(iv)	A	1.45	0.67
	B	1.76	0.66
	C	2.17	0.70

8. Gulf Coast

		S	C
(i)		0.92	0.49
(ii)	A	1.88	2.02
	B	2.54	2.49
	C	2.91	2.78
(iii)	A	2.41	1.91
	B	2.92	2.23
	C	3.71	2.77
	D		
(iv)	A	1.68	1.51
	B	1.99	1.62
	C	2.41	1.80
	D	3.31	2.26

9. Mexican Highland

		S	C
(i)		1.37	-0.47
(ii)	A	2.06	0.26
(iii)	A	1.93	0.75
	B	3.00	0.43
(iv)	A	1.36	0.07
	B	2.32	-0.52

10. Mid-Continent

		S	C
(i)		0.69	-0.18
(ii)	A	0.99	0.15
	B	0.75	0.14
(iii)	A	1.84	0.39
	B	1.49	0.37
(iv)	A	1.50	-0.33
	B	1.59	-0.35

11. Northeast

		S	C
(i)		10.08	-4.13
(ii)	A	0.90	0.23
	B	1.11	0.15
(iii)	A	1.82	0.44
	B	1.48	0.37
(iv)	A	0.85	0.15
	B	0.99	0.13

12. Northern Rockies

		S	C
(i)		1.15	0.11
(ii)	A	0.92	1.33
	B	1.07	1.37
	C	1.71	1.56
(iii)	A	1.57	1.49
	B	1.86	1.54
	C	2.04	1.58
(iv)	A	0.98	1.17
	B	1.19	1.14
	C	1.27	1.13

13. Oregon-Washington Coast

		S	C
(i)		1.94	-0.38
(ii)	A	1.39	0.96
	B		
(iii)	A	2.16	1.09
	B	2.37	1.16
(iv)	A	1.56	0.40
	B	1.87	0.36

14. Pacific Interior

		S	C
(i)		1.01	-0.03
(ii)	A	1.57	1.04
	B	1.68	1.09
	C	1.00	0.69
(iii)	A	1.89	0.97
	B	2.22	1.09
	C	2.58	1.24
(iv)	A	1.20	0.64
	B	1.44	0.66
	C	1.61	0.68

15. Paradox

		S	C
(i)		1.04	-0.26
(ii)	A	0.56	0.77
	B	0.38	0.78
(iii)	A	1.45	1.00
	B	1.22	1.03
(iv)	A	0.91	0.56
	B	1.08	0.48

16. Puget-Olympic

		S	C
(i)		0.57	-0.07
(ii)	A	1.17	0.34
(iii)	A	1.13	0.99
	B	0.14	0.97
	C	2.16	0.52
(iv)	A	0.53	0.76
	B	0.76	0.67

17. Rio Grande

		S	C
(i)		0.97	0.15
(ii)	A	1.29	1.49
	B	1.70	1.70
(iii)	A	1.91	1.54
	B	2.27	1.69
	C	2.80	1.96
(iv)	A	1.20	1.24
	B	1.37	1.27
	C	1.49	1.29

18. Salton Trough

		S	C
(i)		1.03	-0.08
(ii)	A	1.13	0.91
	B	1.54	1.02
	C	3.57	1.69
(iii)	A	1.71	1.07
	B	2.02	1.12
	C	2.45	1.22
(iv)	A	1.20	0.76
	B	1.64	0.78
	C	3.49	1.02
	D	0.43	1.27
	E	0.49	1.26

19. Snake River Plain

		S	C
(i)		1.75	-0.56
(ii)		2.06	0.38
(iii)	A	2.50	0.63
	B	2.90	0.62
(iv)	A	1.91	-0.26
	B	2.59	-0.54

20. Sonoran

		S	C
(i)		1.71	-1.12
(ii)	A	0.88	0.12
	B	0.68	0.12
(iii)	A	1.76	0.38
	B	1.53	0.38
(iv)	A	1.54	-0.76
	B	2.00	-1.05

21. Southeast

		S	C
(i)		3.37	-0.92
(ii)	A	1.48	0.57
(iii)	A	2.44	0.78
(iv)	A	1.48	0.23
	B	1.18	0.22

22. Southern Calif. Borderland

		S	C
(i)		1.47	-0.09
(ii)	A	1.49	0.93
	B	0.70	1.85
(iii)	A	2.39	1.15
	B	1.61	1.53
(iv)	A	1.34	0.61
	B	1.61	0.56
	C	1.62	1.04

23. Straits of Florida

		S	C
(i)		1.19	-0.09
(ii)	A	1.41	0.96
	B	1.81	1.16
(iii)	A	2.02	0.99
	B	2.42	1.17
	C	2.97	1.45
(iv)	A	1.33	0.64
	B	1.52	0.67

24. Transverse Ranges-Tehachapi

		S	C
(i)		1.61	-0.15
(ii)	A	1.99	1.01
	B	2.58	1.16
(iii)	A	2.74	1.26
	B	3.02	1.38
(iv)	A	1.78	0.67
	B	1.88	0.37

25. Utah-Nevada

		S	C
(i)		1.81	-0.01
(ii)	A	2.24	1.18
	B	2.96	1.36
(iii)	A	3.15	1.38
	B	3.91	1.57
(iv)	A	2.33	0.56
	B	2.74	0.55

26. Walker Lane

		S	C
(i)		1.77	-0.02
(ii)	A	1.44	1.19
	B	1.63	1.25
	C	1.77	1.31
	D	2.21	1.53
(iii)	A	1.44	1.19
	B	1.63	1.25
	C	1.77	1.31
	D	2.21	1.53
(iv)	A	1.53	0.86
	B	1.74	0.86
	C	1.85	0.88
	D		

27. Wasatch-Tetons

		S	C
(i)		1.51	-0.07
(ii)	A	1.88	0.97
	B	2.35	1.09
(iii)	A	2.80	1.18
	B	3.29	1.29
(iv)	A	1.99	0.47
	B	2.27	0.46
	C	2.67	0.18

28. Western Mojave

		S	C
(i)		1.03	-0.66
(ii)	A	1.12	1.03
	B	1.31	1.07
	C	2.53	1.46
(iii)	A	2.06	1.23
	B	2.27	1.28
	C	3.98	1.82
(iv)	A	1.35	0.76
	B	1.47	0.76

29. Western Nevada

		S	C
(i)		1.63	0.18
(ii)	A	2.07	1.33
	B	2.69	1.49
	C	4.61	2.09
(iii)	A	2.47	1.45
	B	2.99	1.54
	C	3.66	1.70
(iv)	A	1.74	0.82
	B	2.17	0.76
	C	2.48	0.75

30. Wyoming

		S	C
(i)		0.92	-0.00
(ii)	A	1.32	0.92
(iii)	A	2.16	1.13
(iv)	A	1.17	0.71
	B	1.46	0.67
	C	1.67	0.66

4.3 Distributions of Earthquake Frequencies and Magnitudes Based on Fault Distributions.

Given information about the fault numbers for different lengths and the total activation rate for faults in a specified tectonic region, the possible ranges of earthquake activity can be defined for that region. Conversely, information on earthquake magnitude-frequency relations gives information on the possible distribution of faults. This information, however, is not very specific unless there are auxilliary relationships to identify correlations between given faults and given earthquakes. This section considers the calculations for earthquake distributions from given fault distributions to lay the groundwork for general relations that may be applicable to regions where data on faulting are sparse, or where the only information is a history of earthquake activity.

Figure 4.3.-1 illustrates the construction of magnitude-frequency relations from data on fault lengths and activation rates obtained from the statistical data. Three different assumptions were made to draw the primary control lines from which isoactivity lines are connected to give a nomogram for relations among fault length, number, rupture length, rupture length rate, earthquake magnitude, and earthquake frequency. We will describe the assumptions by going stepwise through an illustrative calculation, and then we will discuss some of the more obvious physical relations among the permutations comprised by the six variables mentioned.

4.3.1 Model Calculation of Earthquake Magnitudes and Frequencies from Fault Activation Data and the Rupture-Length vs. Magnitude Relation from Mark (1977, Figure 3, Curve BB').

4.3.1.1 Number vs. Length Model; All United States Data, DELX ~ X (Equation from Figure 4.2.1.-1 (B), (C), regression line C)

$$\log n = -2.60 \log \ell + 3.06$$

n	log n	log ℓ (map, cm)	ℓ (km)	nℓ (km)	$X = \frac{n\ell}{\Sigma n\ell}$
1	0	1.177	751	751	0.011
10	1	0.792	310	3,100	0.045
100	2	0.408	128	12,800	0.185
1000	3	0.023	52.7	52,700	0.760
				$\Sigma n\ell$ = 69,351	1.001

Text Note: Use of these relations is approximate, as is seen by inspecting Figure 4.3.-1. Derivatives of the cumulative curves (Figure 4.2.1.-2) theoretically should be used, but the regressions themselves have large uncertainties and the above relation between number and length is used to describe the method. The basis for Figure 4.3.-1 is given in the following subsections of section 4.3.1.

SECTION 4.3. FIGURES AND TABLES

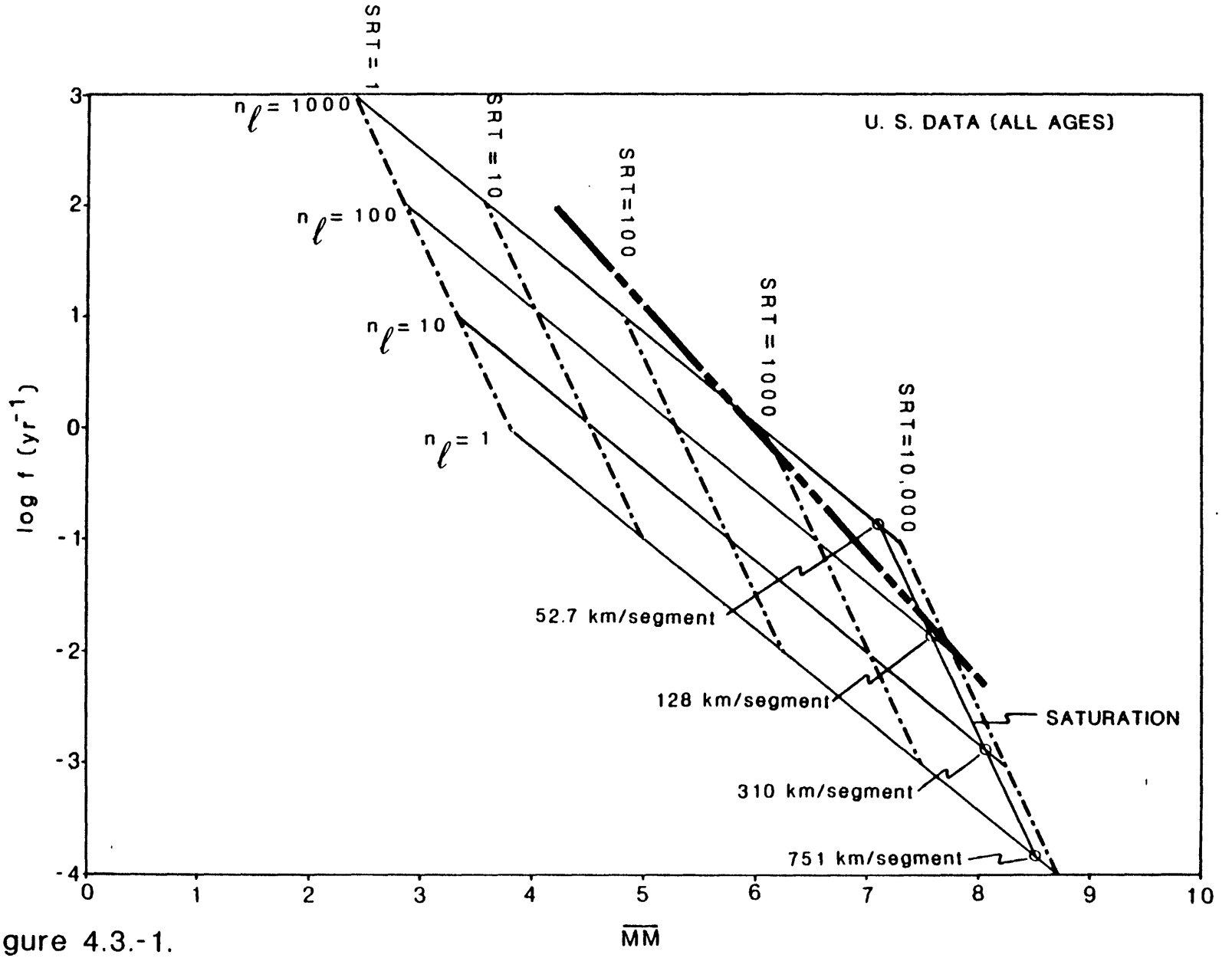

Figure 4.3.-1.

Construction of magnitude-frequency diagram representing the range of options derived from calculations based on fault lengths, numbers and activation rates using relation between magnitude and length from Mark (1977, Figure 3, BB'); this report refers to the resulting area as the paleoseismic parallelogram. (see text pg. 273)

4.3.1.2 Rupture Length Rate (R.L.R.); Total for United States

We base this estimate on a conservative extrapolation of the plot showing fictive age versus apparent rupture rate, Figure 3.2.-4. Inspection of this diagram and the distribution in rates for individual regions (Figure 3.2.-6), suggests that the likely total rate for the United States is between 10 and 100 km for newly activated fault length each year. This represents all faults and all lengths; judging from the rate progressions, the shorter lengths accommodate most movements if the length distribution is constant with time. We use R.L.R. = 10 km/year in the example calculation for the conterminous United States. The model calculations also assume that fault distributions maintain a steady overall rate (10,000 year time frame) and a steady distribution in the fault lengths versus time (equations for log n vs log ℓ also remain constant).

4.3.1.3 Distributed Model (All U.S. data).

Rupture is distributed equally over all fault segments at all lengths so that the number versus length relation remains constant with time; i.e. this is the uniformly steady state model.

For a Rupture Length Rate, R.L.R. = 10 km/yr, and for the fractional rupture length rate per segment, F.R.L.R., the calculated earthquake magnitudes are given, respectively, by the following equations:

$$F.R.L.R. = X \cdot R.L.R.$$

(Rupture Length per Length Order per Year)

$$\overline{MM} = 1.235 + 1.243 \log (F.R.L.R./n)$$ (SEE FOOTNOTE PAGE 197)

(Magnitude Calculated from Mark's Eq.; Length in Meters).

Using these relations, we calculate the following example:

$n = 1$, $f = n / S.R.T.$

(S.R.T. = Segment Recurrence Time)

$F.R.L.R./n = (0.011)(10^4)/1 = 110$ m/yr

$\overline{MM} = 1.235 + 1.243 \log (110) = 3.77$

Chart: Calculated $\overline{MM}$ for Assumed ℓ and S.R.T.:

f(year^{-1})	n=1(751)	10(310)	100(128)	1000(52.7)	S.R.T. (years)
10^3				2.33(0.01)	1
10^2			2.81(0.02)	3.57(0.08)	10
10^1		3.29(0.05)	4.05(0.19)	4.82(0.76)	100
1	3.79(0.1)	4.53(0.45)	5.30(1.85)	6.06(7.6)	1000
10^{-1}	5.02(1.1)	5.78(4.5)	6.54(18.5)	7.30(76)	10,000
10^{-2}	6.26(11)	7.05(45)	7.80(185)		
10^{-3}	7.50(110)	8.26(450)			
10^{-4}	8.74(1100)				

The heavy solid line is the cutoff, or saturation, where all faults of all orders have had movement over their total lengths. Numbers in parentheses are the calculated rupture lengths; total segment lengths (km)are given at top for each number order from 1 to 1000.

4.3.1.4 Transition Models

Rupture is concentrated on a single fault in each length order with potential slip accumulating at a rate given by the rupture length rate (R.L.R.) times the segment fraction (X) :

$$(F.R.L.R.) = (R.L.R.) \cdot (X)$$

The event rupture length (E.R.L) per segment is given by:

$$(E.R.L.) = (F.R.L.R.) \cdot (S.R.T.)$$

The frequency at each length is, of course, given by:

$$f = 1/(S.R.T.)$$

The results for various combinations are tabulated as follows:

Chart: Calculated $\overline{MM}$ for assumed n and S.R.T.:

f(year^{-1})	1(751)	10(310)	100(128)	1000(53)	S.R.T (years)
1	3.78(0.1)	4.53(0.5)	5.30(1.9)	6.06(7.6)	1
10^{-1}	5.02(1)	5.78(4.5)	6.54(19)	7.30(76)	10
10^{-2}	6.26(11)	7.02(45)	7.78(185)	8.55(770)	100
10^{-3}	7.50(110)	8.26(450)	9.03(1850)	9.79(7700)	1000
10^{-4}	8.74(1100)	9.50(4500)	10.27(18,500)	11.03(77,000)	10,000

The heavy solid line shows the cutoff for earthquakes occurring on single segments in each order; the maximum magnitude for the steady state model is bracketed by values on opposite sides of the dashed line. At higher recurrence times single events are only possible by segments coalescing, hence with consequent modifications in the length distributions (i.e. shorter lengths decrease in numbers, and the exponent for absolute slope in the number versus length distribution decreases).

4.3.1.5 Total Rupture Along Total Segment Lengths for Each Order in Single Events

Strain accumulates until a fault segment ruptures along its total length. The recurrence time is given by the segment length divided by the fractional rupture length rate

$$S.R.T. = \ell/F.R.L.R.$$

This is the recurrence time for a single event on a single segment of length ℓ or for the same magnitude events on all segments of that length. If every segment has a total rupture event, then the fractional rupture length rate is reduced by the number of segments, meaning that the segment recurrence time is increased by the factor n. However, there are n segments that rupture in the steady state, during the modified recurrence time, so that time is reduced, on the average, by the factor n. Hence, the average result is the same for steady state models whether there is one or more segments per order totally activated. Any other assumption results in deviations from the steady state and will lead to either an increase or decrease in slope of the number versus length relation.

Thus the magnitude-frequency relation is obtained as follows:

n =1;
ℓ = 751 km; R.L.R. = 10^4 m/yr; X = 0.011
(S.R.T.) = $\ell/(R.L.R.)(X)$
= $7.51 \times 10^5 / 1.1 \times 10^2$ = 6827 years
$\underline{f}$ = 1.46×10^{-4} year^{-1} (log f = -3.84)
$\overline{MM}$ = 1.235 + 1.243 log (ℓ) = 8.54

n =10;
ℓ = 310 km; R.L.R. = 10^4 m/yr; X = 0.045
(S.R.T.) = $\ell/(R.L.R.)(X)$
= $3.10 \times 10^5 / 4.5 \times 10^2$ = 689 years
$\underline{f}$ = 1.45×10^{-3} year^{-1} (log f = -2.84)
$\overline{MM}$ = 1.235 + 1.243 log (ℓ) = 8.06

n =100;
ℓ = 128 km; R.L.R. = 10^4 m/yr; X = 0.185
(S.R.T.) = $\ell/(R.L.R.)(X)$
= $1.28 \times 10^5 / 1.85 \times 10^3$ = 69 years
$\underline{f}$ = 0.014 (log f = -1.85)
$\overline{MM}$ = 1.235 + 1.243 log (ℓ) = 7.58

n =1000;
ℓ = 52.7 km; R.L.R. = 10^4 m/yr; X = 0.760
(S.R.T.) = $\ell/(R.L.R.)(X)$
= $5.27 \times 10^4 / 7.6 \times 10^3$ = 6.93 years
$\underline{f}$ = 0.144 (log f = -0.84)
$\overline{MM}$ = 1.235 + 1.243 log (ℓ) = 7.10

4.3.2 Relations Among f, M_c, n, ℓ, $\overline{MM}$, X, and R.L.R.

4.3.2.1 The Paleoseismic Parallelogram.

The numerical results in the above calculations were used to construct Figure 4.3.-1. We term the area outlined by such calculations, a paleoseismic parallelogram, because the bounding values are determined from geologic mapping and geochronologic data. It is useful as a guide to various different assumptions about faulting activity associated with observed ranges in earthquake activity, as well as the assumptions about deviations from the steady state.

The seismic parallelogram outlines an area that gives the earthquake frequencies and magnitudes corresponding to the three assumptions:

(a) the geologically deduced value for rupture length rate (R.L.R.) is simultaneously and equally distributed over all faulting orders, with some constant assumed recurrence time (S.R.T.) for each fault segment;

(b) each number order, from 1 to 1000 segments, has all slip on a single fault segment in that order, and in a given recurrence time, according to the length fraction (X) in that order; and

(c) the total segment length for given faults in each order, whether considered to occur individually or on all faults simultaneously, is completely activated along its entire length at the time an earthquake event happens.

In Figure 4.3.-1 lines are drawn according to assumption (a) for a series of segment recurrence times labeled S.R.T. = 1 year to S.R.T. = 10,000 years; lines for assumption (b) are parallel to the abscissa at any chosen frequency between 100/year and 10^{-4}/year (one every 10,000 years). Assumption (c) has only the one line marked SATURATION. Saturation refers to the assumption that each fault has to be activated along its total length for an earthquake to occur; the same line applies whether each event on each number and length scale always happens along the same fault or on different faults in each subsequent event until all possible faults are sampled. This is so because though it takes longer to activate more faults at the same overall rupture length rate (R.L.R.), there are proportionately more events averaged over the total time required to activate them. The total time to run sequentially through the repertoire of lengths, if it were to happen that way, is given roughly by the recurrence time for the longest fault length (n =1, ℓ=751 km, and S.R.T.~7,000 years in Figure 4.3.-1).

Incidentally, the value ℓ=751 km for the conterminous United States does not mean that this is the longest actual fault mapped (see table of actual lengths); it is the longest length consistent with the steady state

model and with the statistical distribution of fault orders according to the model DELX ~ X (adopted to insure that there are no gaps in the data and because it is roughly consistent with the resemblance of fault branching order to stream branching order). Notice that, for a given relation between fault length and number, there is a unique saturation line corresponding to a given rupture length rate. This line, however, is not always at the same relative position in the paleoseismic parallelogram arbitrarily delimited in Figure 4.3.-1, as will be seen in subsequent examples for specific fault regions.

The location for the paleoseismic parallelogram and the saturation line in the frequency-magnitude plane depends on knowledge of activation rates, R.L.R., lacking complete data on actual earthquake histories for the whole range of recurrence times (the order of at least 10,000 years). Conversely, given the earthquake histories, deducing the activation rates requires knowledge about the fractional distribution of fault lengths and numbers.

Lines representing constant fractional rupture length rate (F.R.L.R.) in Figure 4.3.-1 are identified on the left by the number order (n =1 to 1000) and on the right by the length order (ℓ=751 km to 52.7 km). The connecting solid line represents the range for partial activation on faults having that length and number (e.g., one fault 751 km long activated along its length over different length and time intervals).

Rupture length rates (R.L.R.) are drawn as a nomogram in Figure 4.3.2.1.-1 to be used as locator, and as an overlay to interpret subsequent paleoseismic diagrams. The range in rates from 0.1 to 1000 km/yr encompasses the rates we will discuss from either the fractional or overall viewpoints. The rate curves themselves are the same, being given by the length value associated with a magnitude value ($\overline{MM}$ from Mark's equation) times the frequency: (see authors note, Table 4.3.2.2.-3.)

$$\log (R.L.R.) = [(\overline{MM}-1.235)/(1.243)] + \log f.$$

The question is how to locate and interpret paleoseismic parallelograms relative to this rate spectrum.

SECTION 4.3.2.1. FIGURES AND TABLES

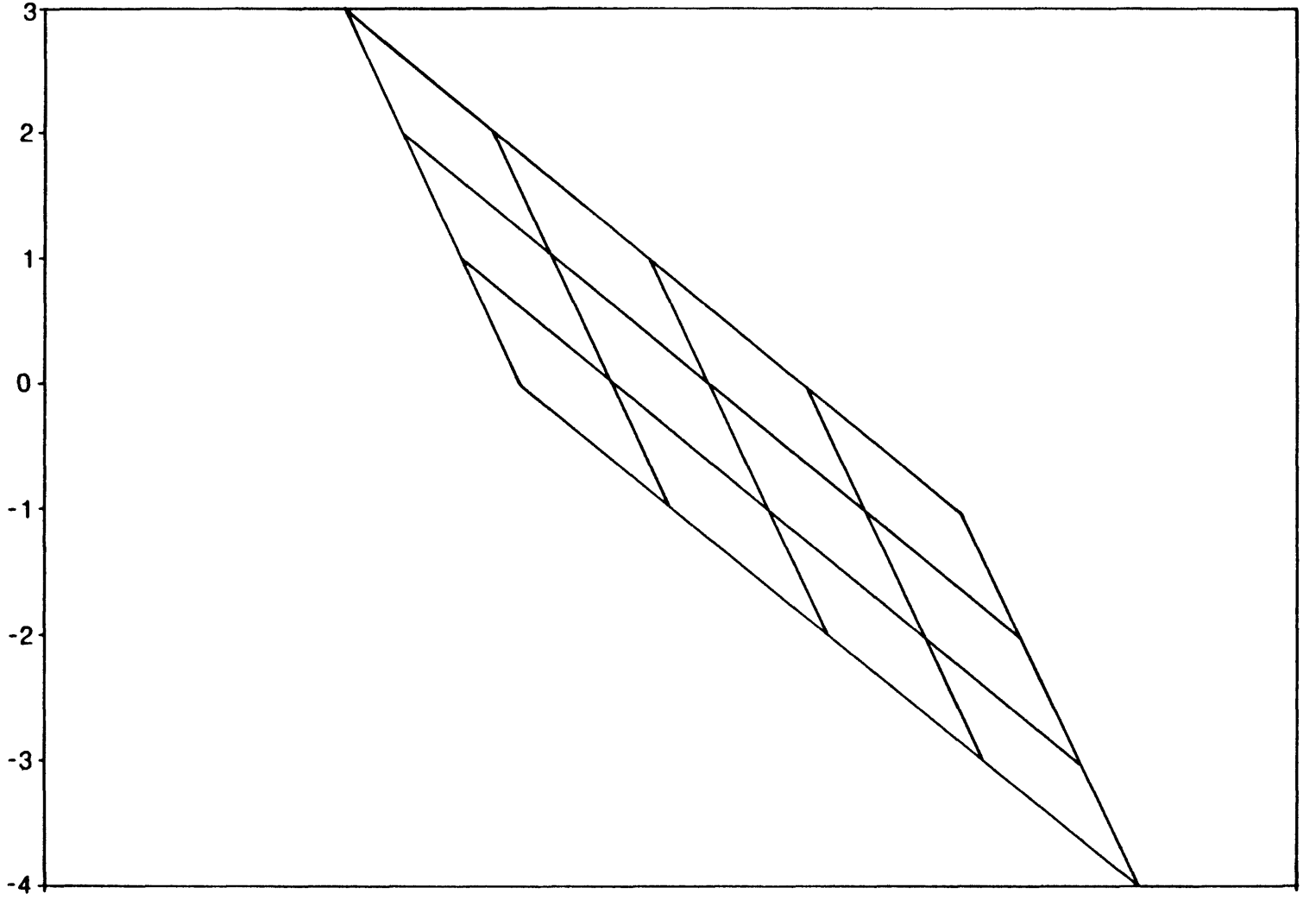

Figure 4.3.2.1.-1.
Reference nomogram for paleoseismic parallelogram.

4.3.2.2 Graphical Comparisons Between Paleoseismic and Seismic Data.

In Figure 4.3.-1, the heavy dashed line represents the frequency-magnitude relation given by Algermissen (1969) for all available earthquake data in the conterminous United States. We comment later on its location and slope relative to the parallelogram after illustrating patterns with the more restricted faulting regions.

We use the parallelogram in Figure 4.3.2.1.-1 as an approximate guide for this discussion; to be totally consistent with the faulting statistics, a parallelogram should be calculated for each regression equation representing log n vs log , because the length fractions and the slopes of the S.R.T. and SATURATION lines will correspondingly vary somewhat. Except for extreme variations from the average, the relative area outlined in Figure 4.3.-1 suffices to describe the situation. Note, however, that the parallelogram can shift along the magnitude axis relative to either R.L.R. or the position of the SATURATION line. These limits and shifts relative to the observed frequency-magnitude regressions on earthquake data (Algermissen and Perkins 1976, Table 1) are instructive concerning correlating earthquakes with fault regions, steady state models, and maximum activated fault lengths beyond the statistical averages.

Figure 4.3.2.2.-1 shows nomograms from Figure 4.3.2.1.-1 for each faulting region on which is plotted a paleoseismic parallelogram wherever we have an estimate for R.L.R. On each of these diagrams we have also plotted curves for log frequency f vs. magnitude identified by numbered Seismic Source Area from Table 1 in Algermissen and Perkins (1976); the limits on frequency and magnitude ranges are given here as Table 4.3.2.2.-1. Evidently most log frequency f versus magnitude regression lines are nearly parallel to the rate curves for R.L.R., suggesting that they identify domains of constant R.L.R. In all there are 71 numbered Seismic Source Areas, some of which are areally discontinuous (see map Figure 2 in Algermissen and Perkins, 1976, reproduced here in reduced form as Figure 4.3.2.2.-2 overlay). We plotted data from those Seismic Source Areas on Figure 4.3.2.2.-1 that either fall within or seem most closely associated with the larger and less detailed Faulting Regions. For this reason Seismic Source Area numbers sometimes occur on more than one nomogram in Figure 4.3.2.2.-1. The distribution of seismic areas relative to faulting regions are listed in Table 4.3.2.2.-2.

For those regions where there is both an estimate for R.L.R. and abundant seismic data it is possible to calculate two parallelograms, one based on fault data, the other on earthquake data. Figure 4.3.2.2.-3 shows an example with parallelograms derived on each basis.

Constructing parallelograms from earthquake data is ambiguous but the possible ranges are limited. For example, using the largest magnitude from seismic area 9 (Figure 4.3.2.2.-3), we calculate the apparent fault length as 230 km. Combining the length and frequency we obtain the apparent

fractional rupture length rate, F.R.L.R. = 1.7 km/year (which could be read from the nomogram, if there were calibration lines at closer intervals). At this stage, some judgement is required to complete the estimate. We note that the length is intermediate relative to typical ranges, suggesting that the length fraction is probably more than 0.1 and less than 0.2. We also note that relative to our overall estimate for R.L.R. in the conterminous United States, the local value should be less than 10 km/year (conservative estimate) and certainly less than 100 km/yr. If the fraction is closer to 0.5, the overall estimate for R.L.R. is near 10 km/yr which agrees with the geologic estimate for region 29 (western Nevada). These large rates indicated for seismic area 9, and region 29 suggest that we need to check other areas and see if the cumulative total exceeds 10 km/yr (see Table 4.3.2.2.-2). For this illustration, the comparison is roughly consistent, except that the SATURATION line calculated from the earthquake data is at greater magnitudes, suggesting a maximum potential fault length greater than 1000 km with a recurrence interval between 10,000 and 100,000 years.

Figure 4.3.2.2.-4 shows the series of Fault Regions with seismic parallelograms estimated from the earthquake data. It is possible to identify a general parallelogram even where the log f vs. Mc curve represents limited data, because evaluating R.L.R. fixes the left side at n =1 and f=1 year^{-1}; the maximum value for S.R.T. and the SATURATION line are not uniquely determined without other data. In principle, however, it might be possible to solve a set of simultaneous equations to obtain a position on the saturation curve. That approach, however, is not attempted in this report. Table 4.3.2.2.-3 lists the calculations for rupture length rates and compares sums for the earthquake and faulting data.

Although considerable leeway exists for plotting the areas, the correspondences between Figures 4.3.2.2.-1 and 4.3.2.2.-4 are encouraging from the standpoint of either interpreting seismic data in terms of fault length distributions, or conversely proposing fault distributions to match the earthquake data (where geologic data are sparse for reasons of exposure, incomplete mapping, depth of faulting, etc.). One of the more obvious applications is to check for inconsistencies between Seismic Source Areas and Faulting Regions, and to promote more detailed breakdowns of corresponding domains. For example, the diagram for Fault Region 18 (Salton Trough) in Figure 4.3.2.2.-1 shows positions for regression lines from Seismic Source Areas 17, 18, and 19. Inspection of the map, Figure 4.3.2.2.-2., shows that Areas 17 and 19 are consistent with the tectonic setting appropriate to the Salton Trough and Area 18 is marginal on the west coast. In the diagram it is noted that the lines for areas 17 and 19 are mostly within the parallelogram defined by fault data, whereas the line for area 18 is at much lower frequencies. The spread between lines 18 and 19 is too large to fit a parallelogram based on the same steady state model. Clearly the opportunity is indicated for much more explicit comparisons.

We can also say something about possible, or likely, deviations from steady state conditions. Where frequency-magnitude regression lines parallel the lines for R.L.R., the time variations must affect all fault lengths uniformly and proportionately. In some instances, it also appears that in order to explain activation rates for longer faults, it is necessary that groups of shorter faults must coalesce. For the conterminous United States, overall, the deviation from parallelism with R.L.R. lines indicates that, relative to the parallelogram, there are more activations in the shorter rather than the longer faults. This suggests that presently the overall frequency distribution is out of balance even though local regions are approximately in balance. If the Algermissen (1969) regression is representative, we can expect a trend toward either a reduction in activations on the shorter faults or an increase in the activations on longer faults, overall. The difference has major importance for whether the trend is toward more and larger earthquakes or toward fewer smaller earthquakes and about the same frequencies for large earthquakes. The trend for the overall curve representing R.L.R. versus age (Figure 3.2.-3) suggests the former interpretation, but it is always possible that the comtemporary trend reflects the end of a preceding accelerative episode.

Whichever is the preferred interpretation, there seems to be a strong indication that there is currently a flow from activations on shorter faults to activations on longer faults. This observation is consistent with the idea that the longer faults are themselves created by coalescence of shorter faults.

SECTION 4.3.2.2. FIGURES AND TABLES

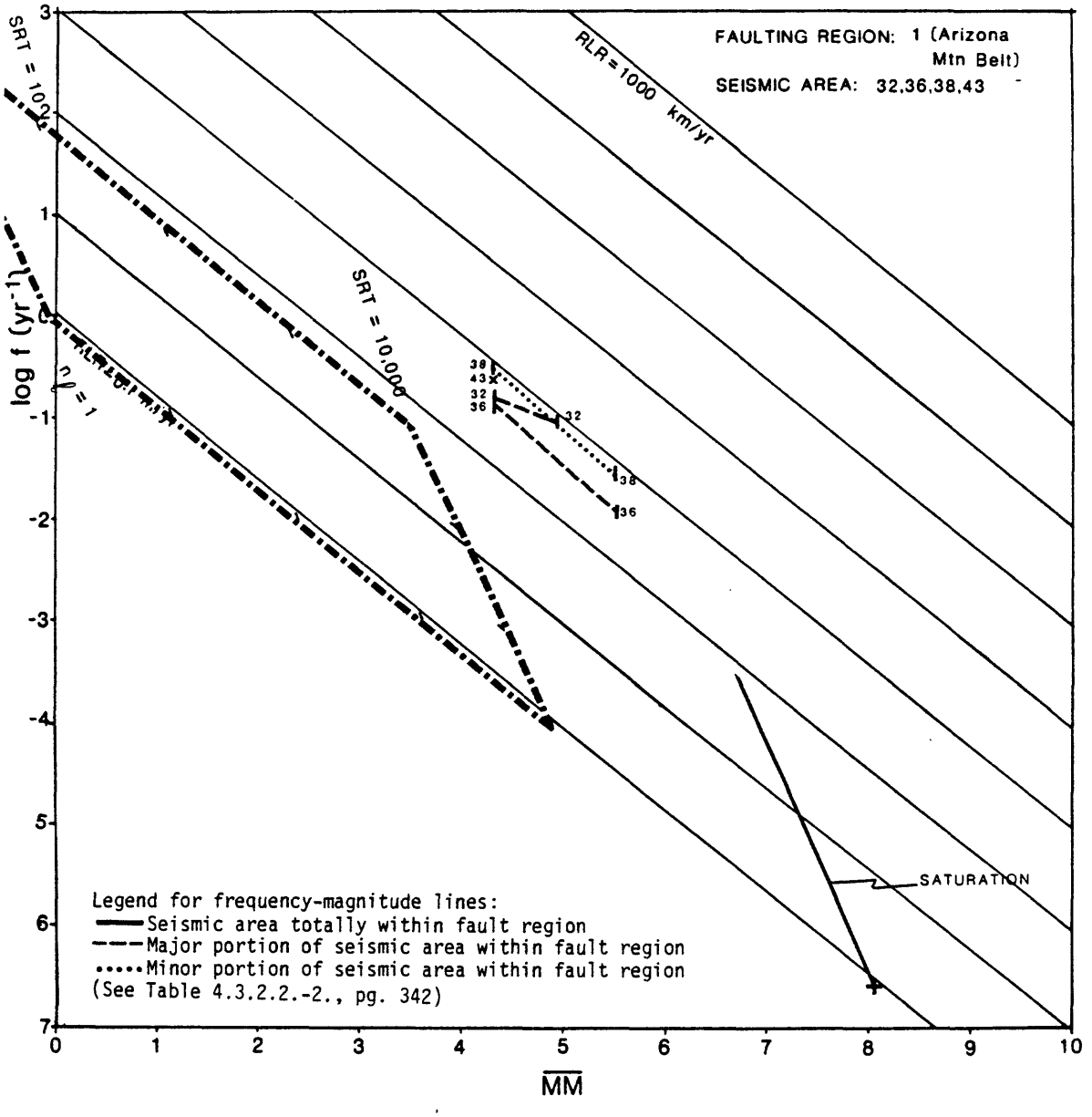

Figure 4.3.2.2.-1. (1)

Paleoseismic parallelograms based on number, length, and faulting rate data for the thirty faulting regions. This graph attempts to answer the question: what ranges of frequency versus magnitude would be predicted from the observed fault distributions and activation rates? The plotted frequency-magnitude lines are drawn for comparisons of predicted and observed earthquakes.

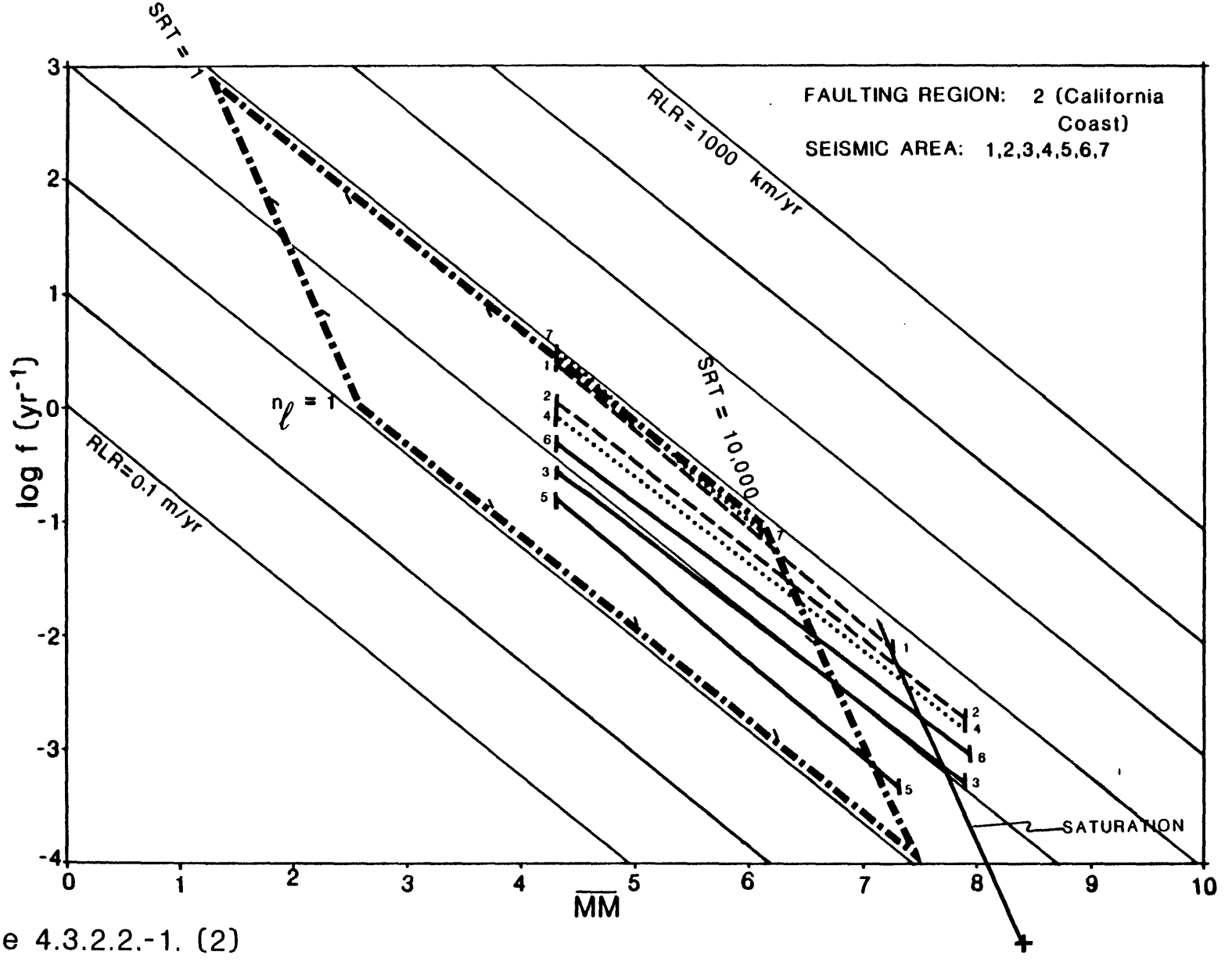

Figure 4.3.2.2.-1. (2)

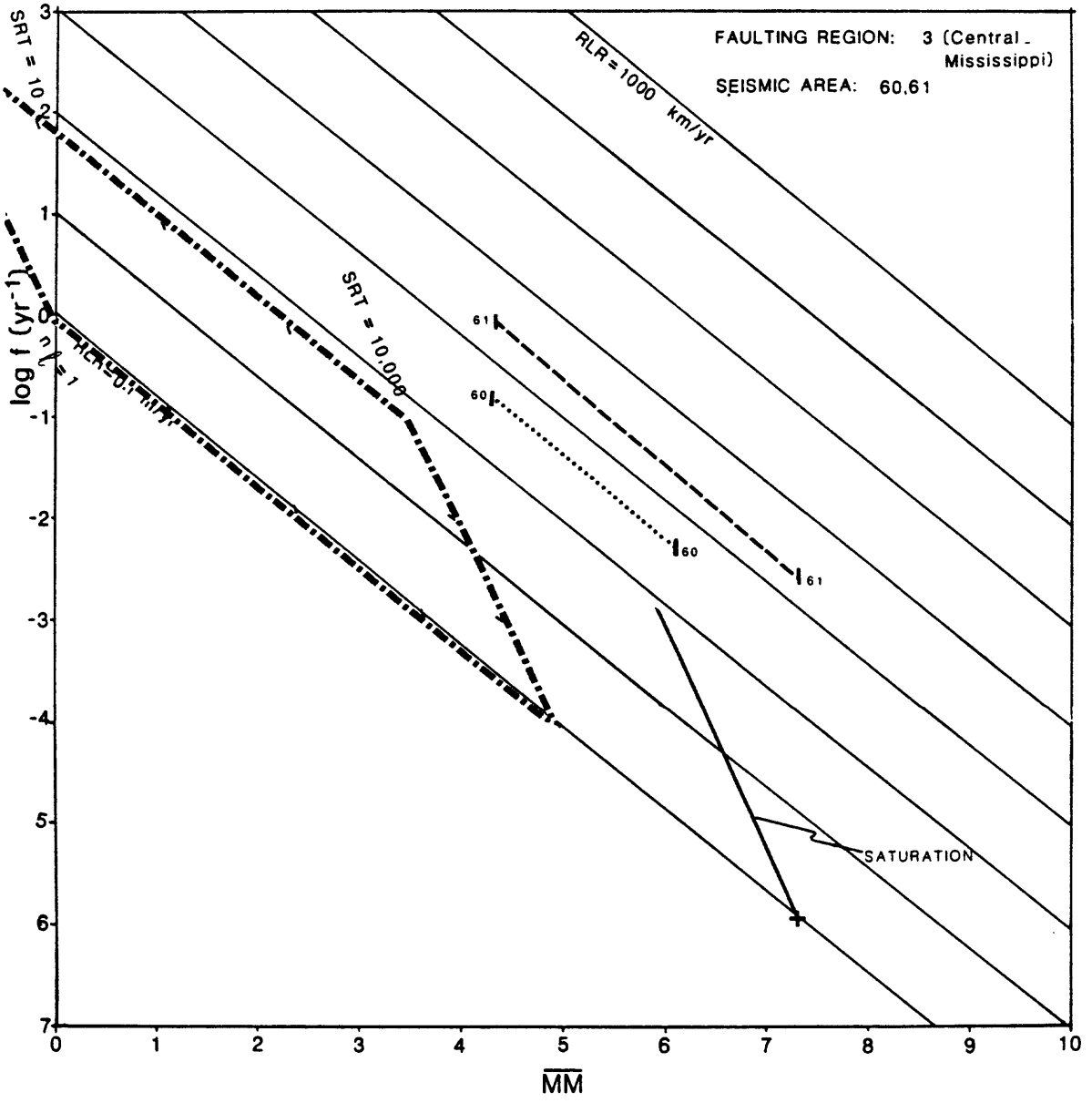

Figure 4.3.2.2.-1. (3)

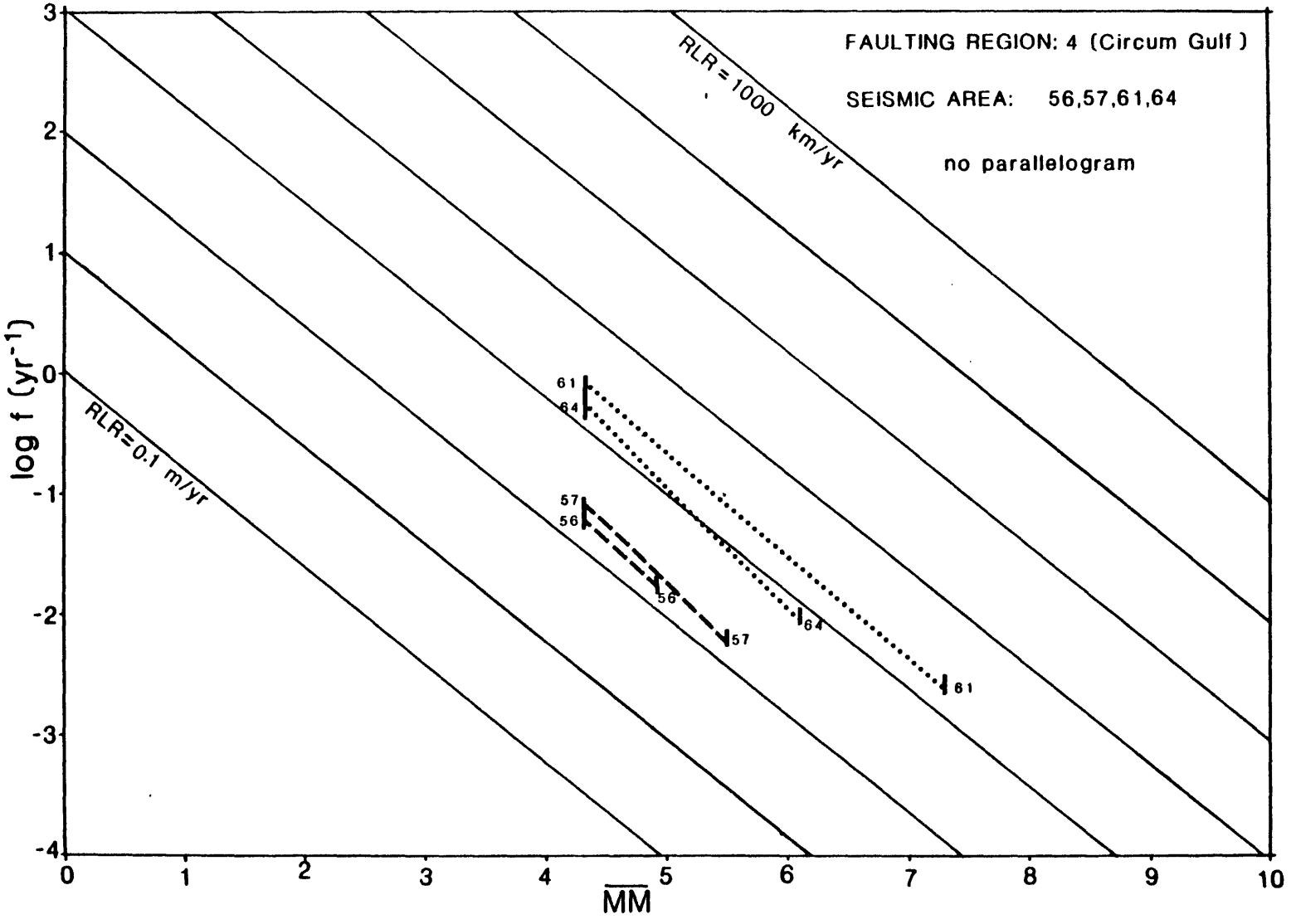

Figure 4.3.2.2.-1. (4)

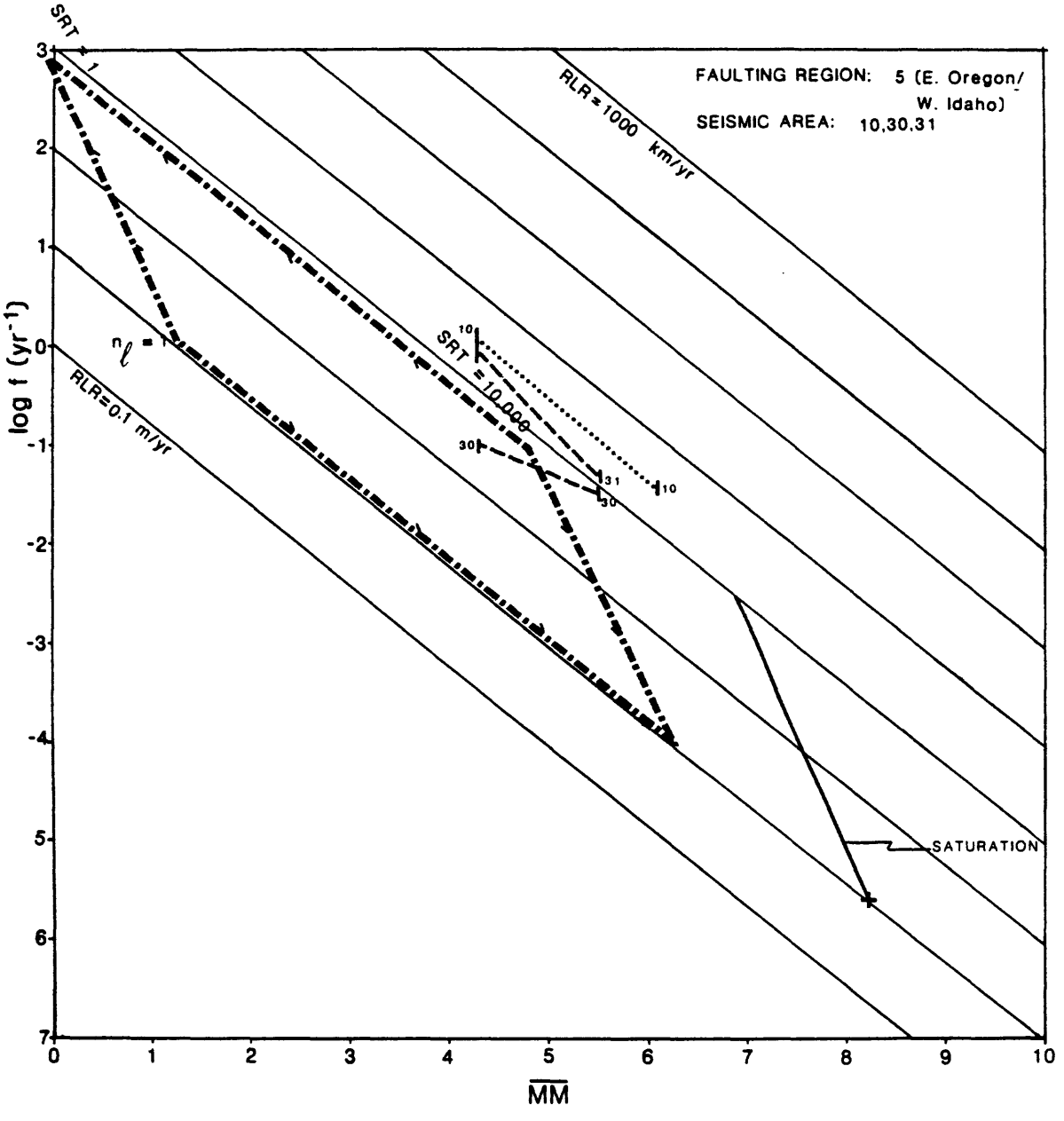

Figure 4.3.2.2.-1. (5)

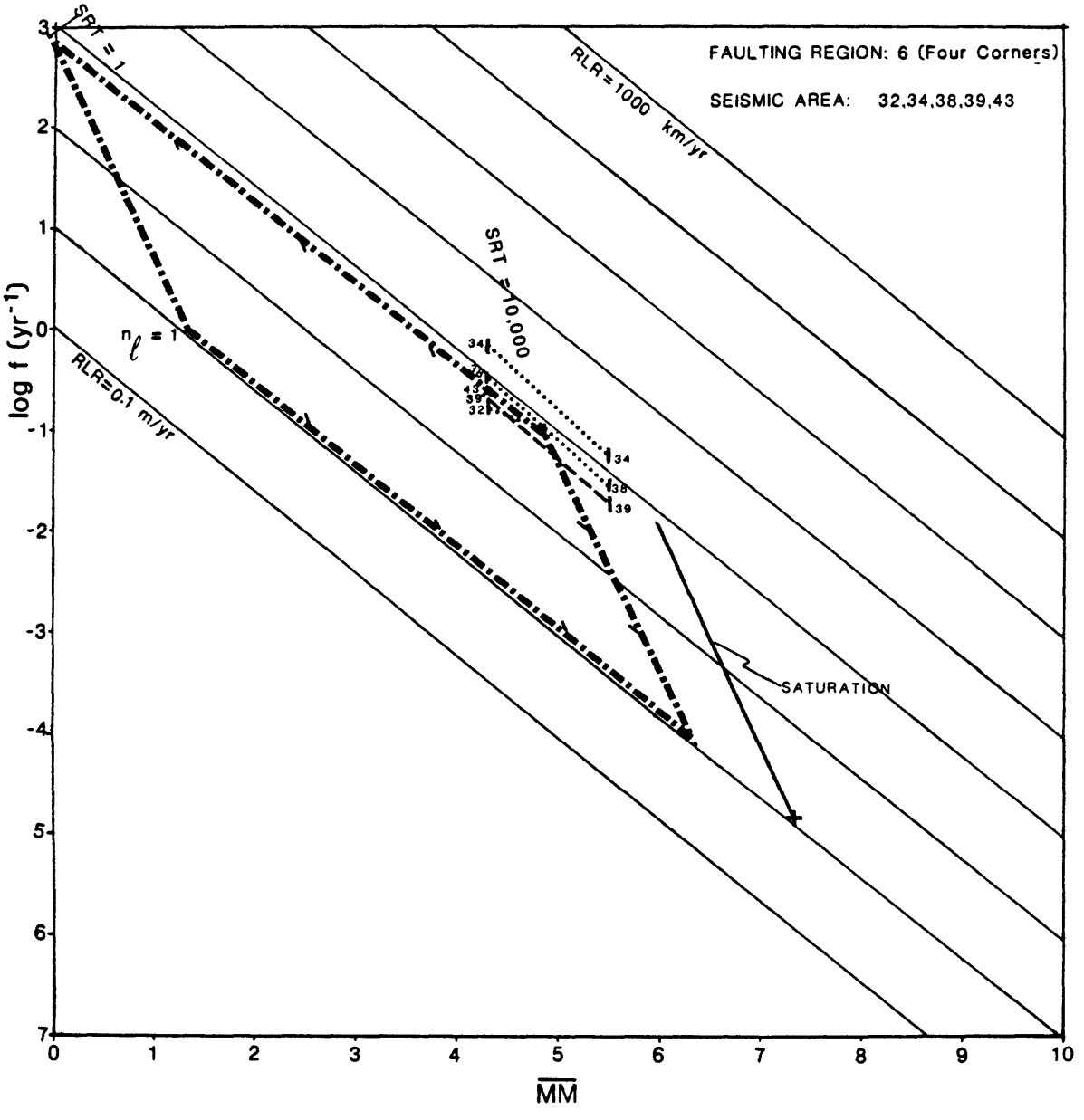

Figure 4.3.2.2.-1. (6)

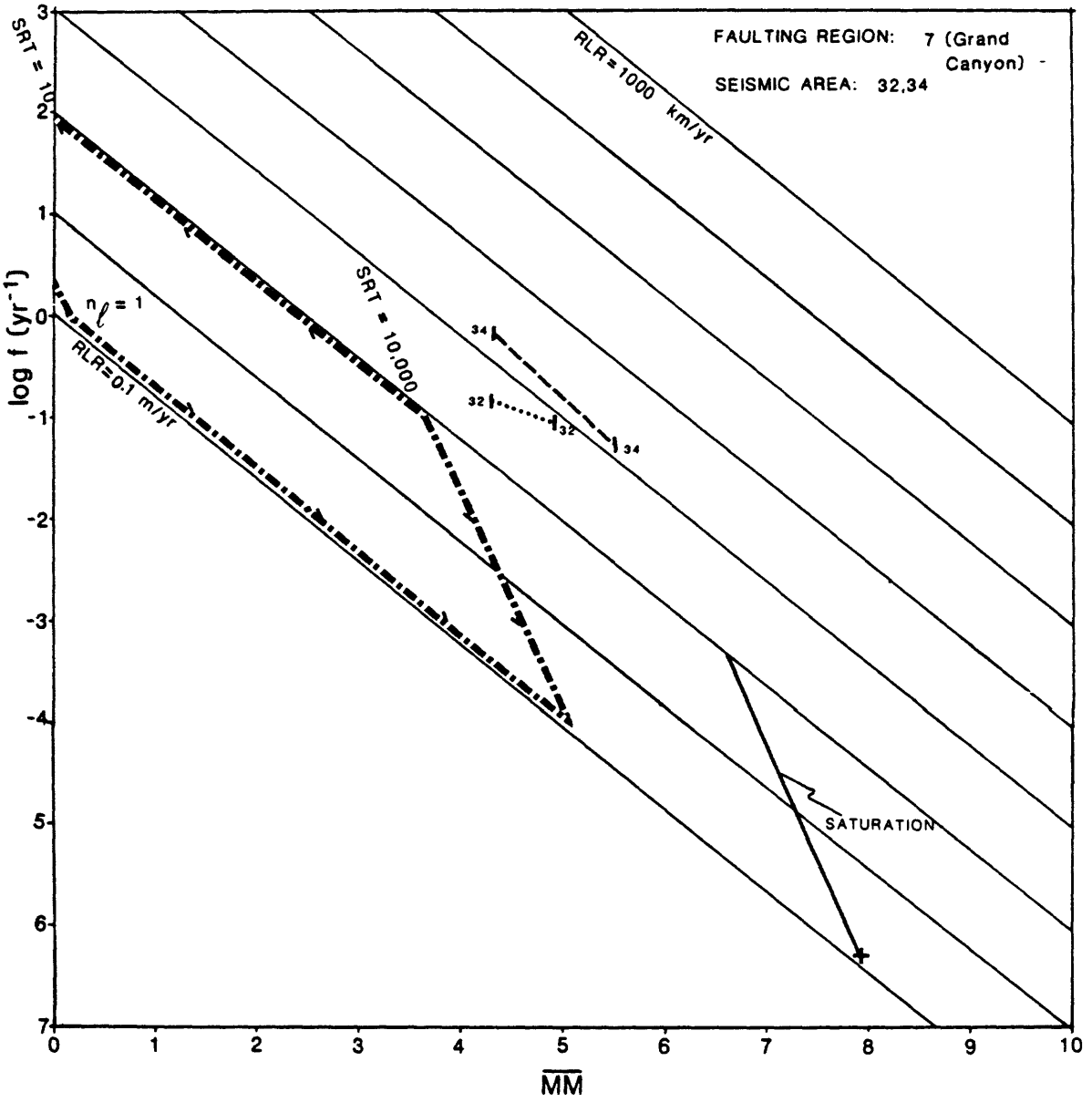

Figure 4.3.2.2.-1. (7)

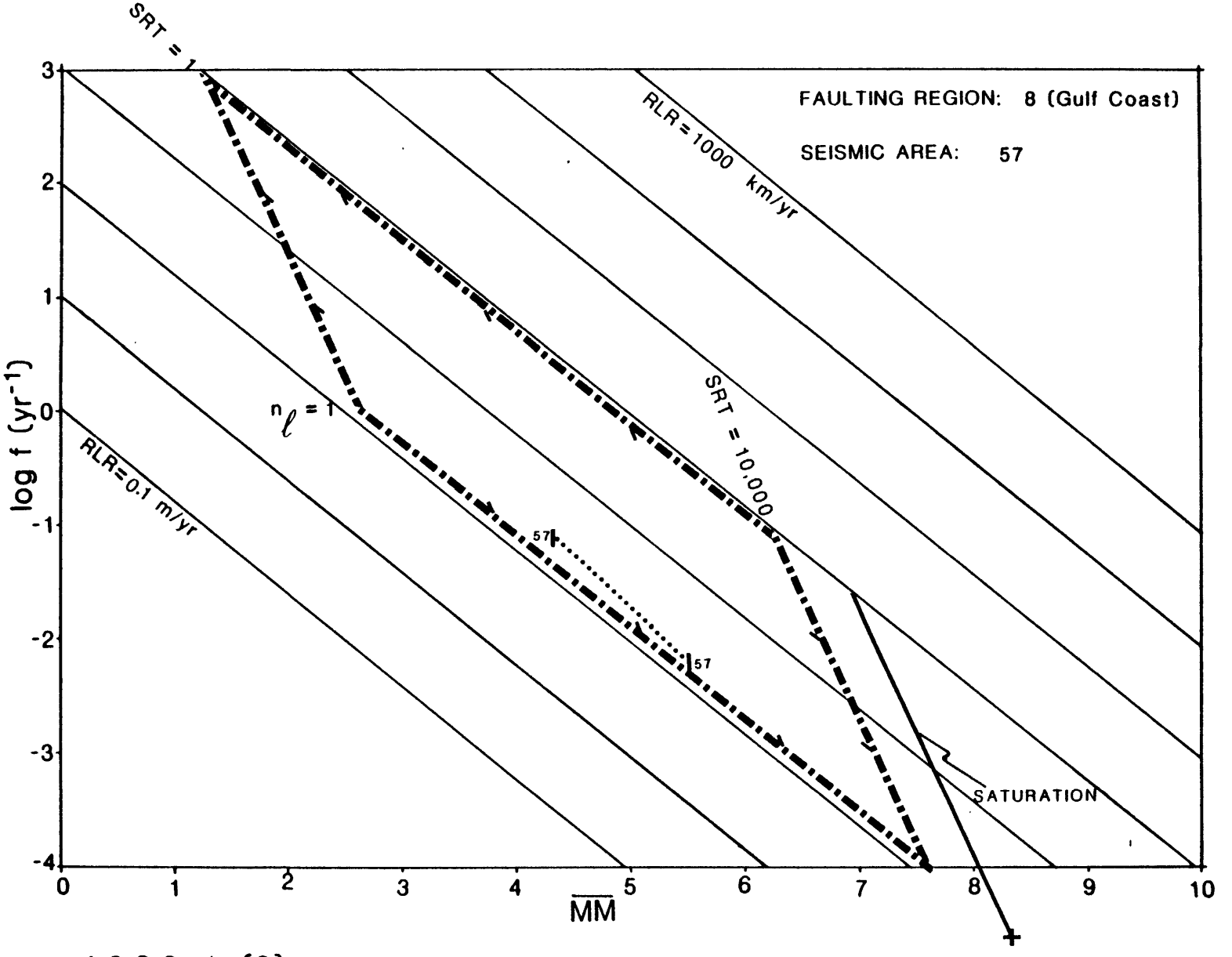

Figure 4.3.2.2.-1. (8)

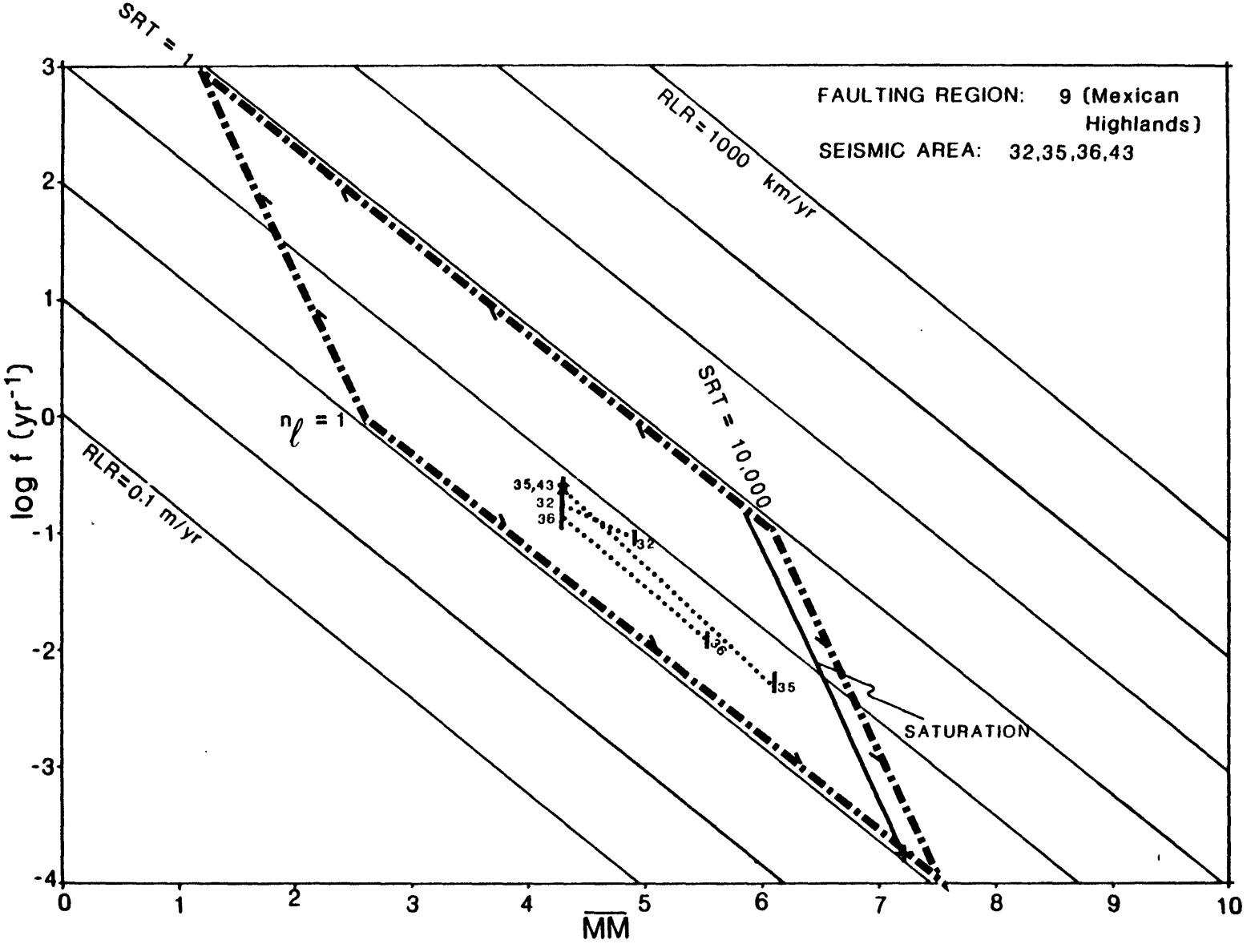

Figure 4.3.2.2.-1. (9)

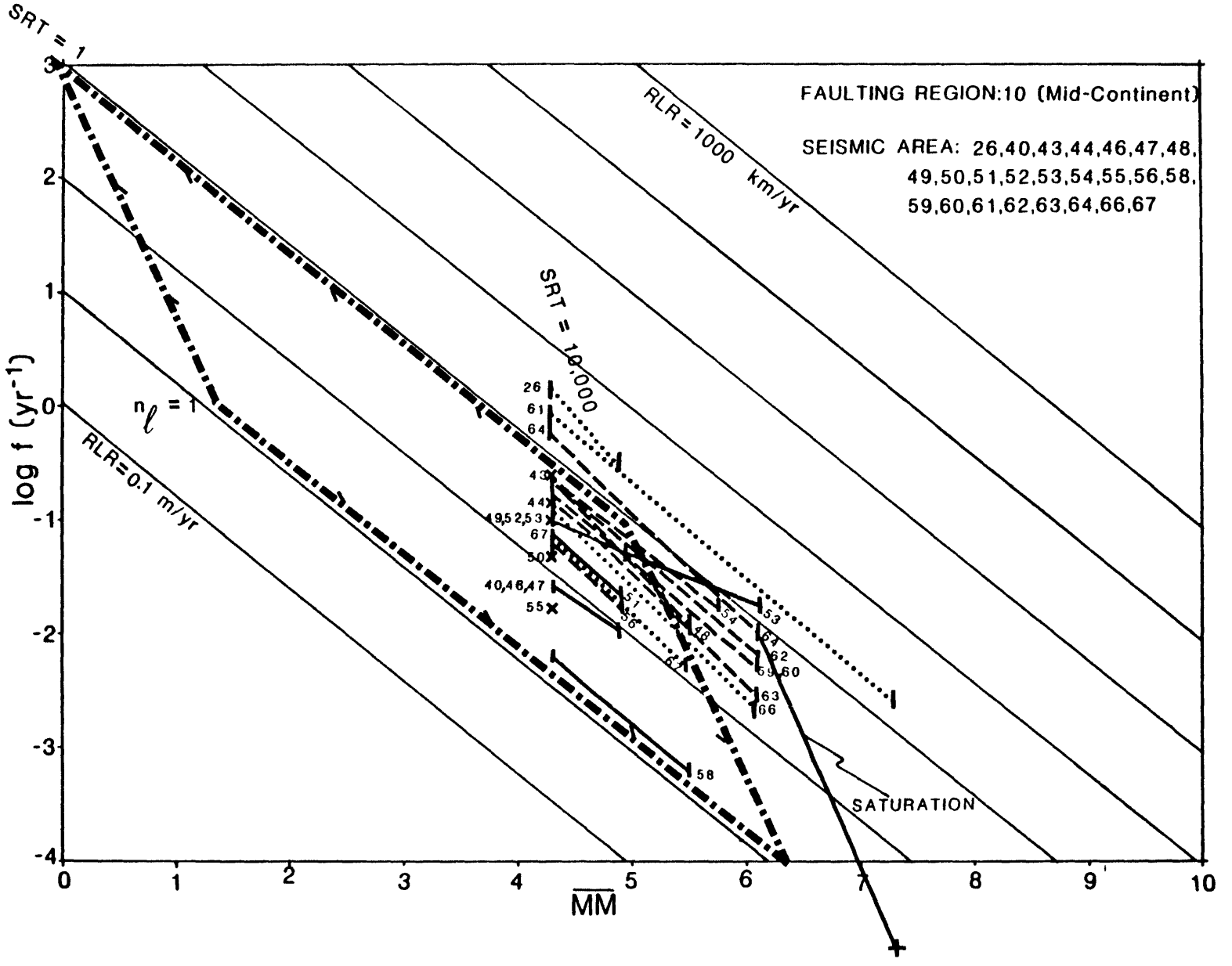

Figure 4.3.2.2.-1. (10)

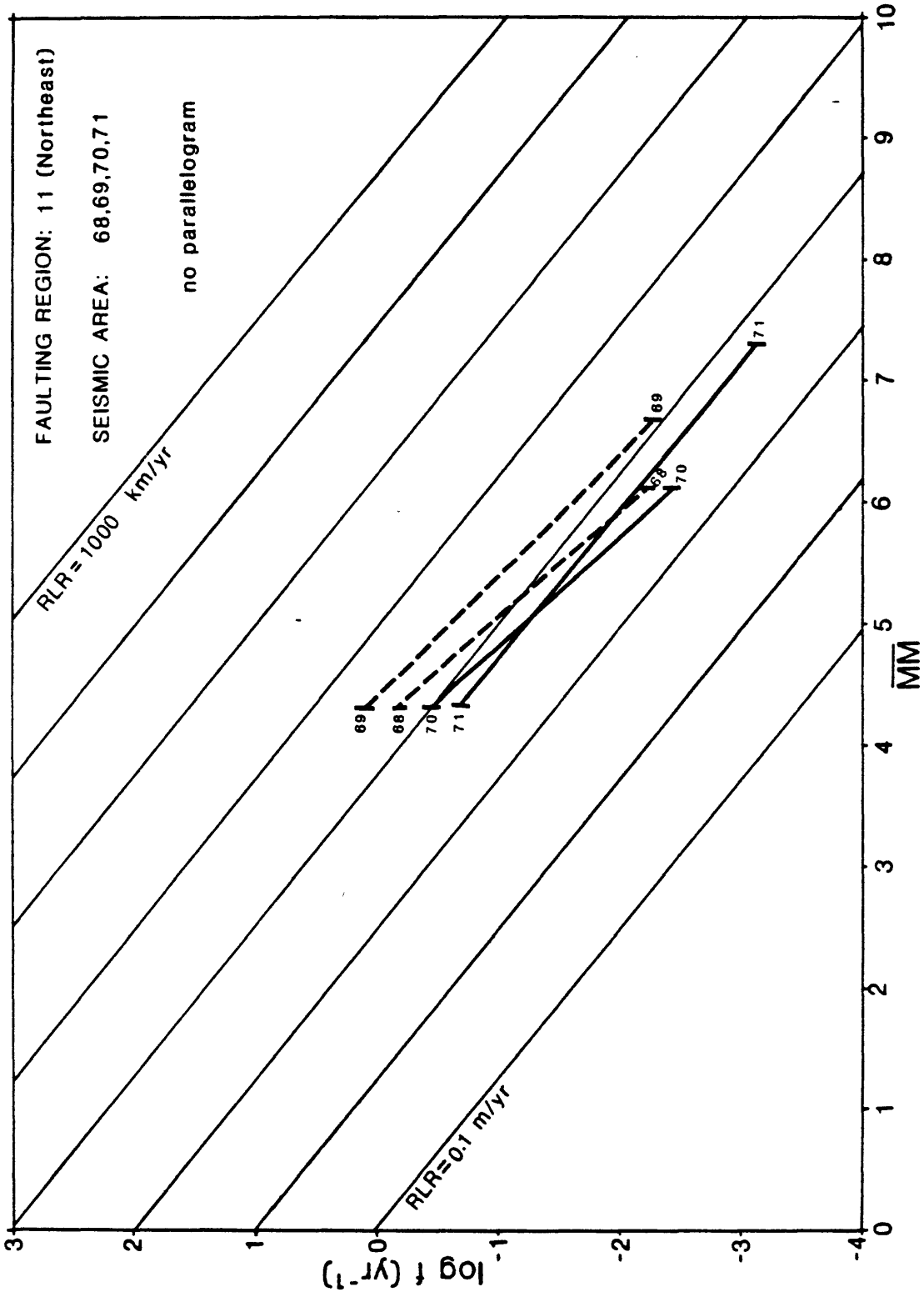

Figure 4.3.2.2.-1. (11)

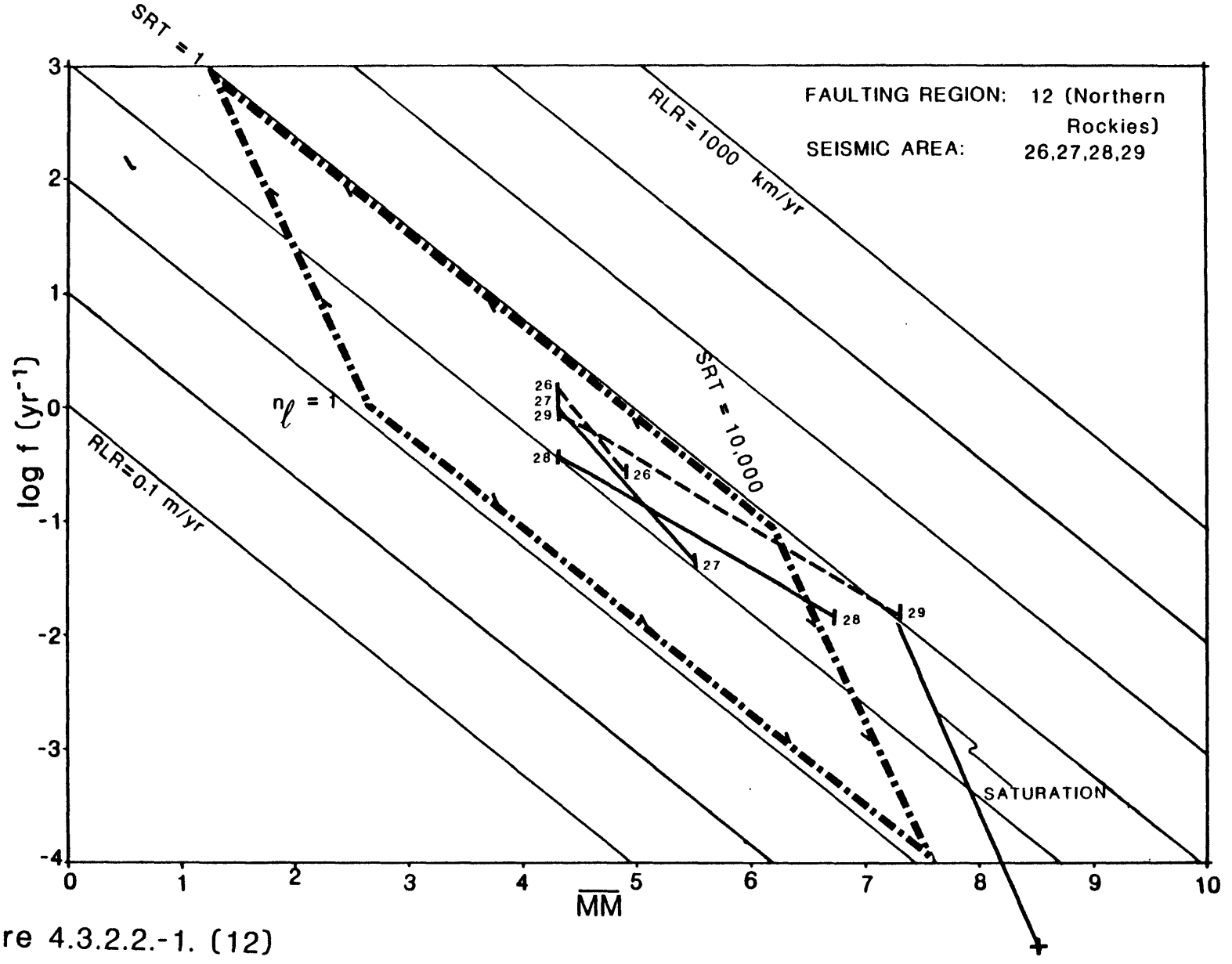

Figure 4.3.2.2.-1. (12)

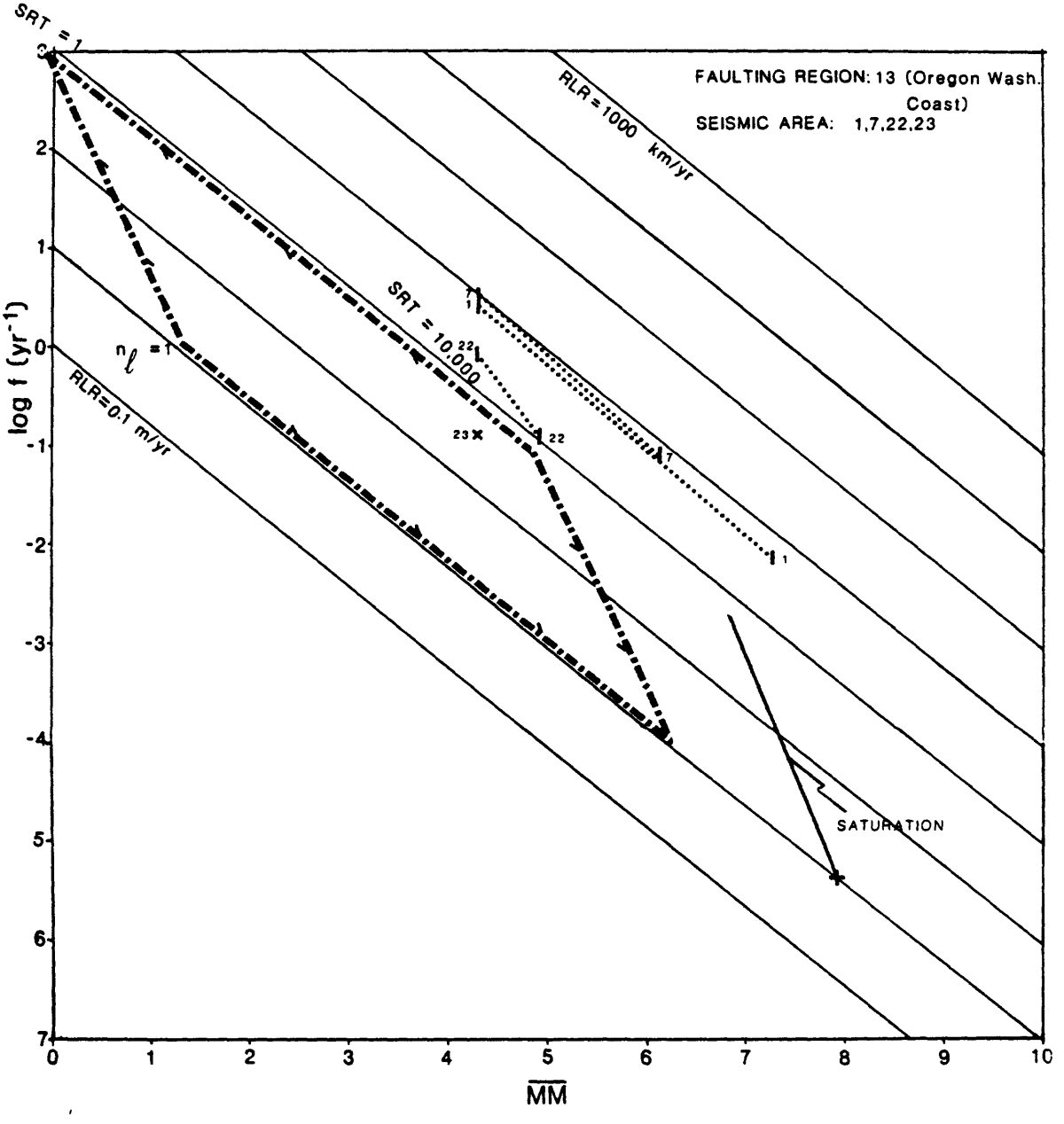

Figure 4.3.2.2.-1. (13)

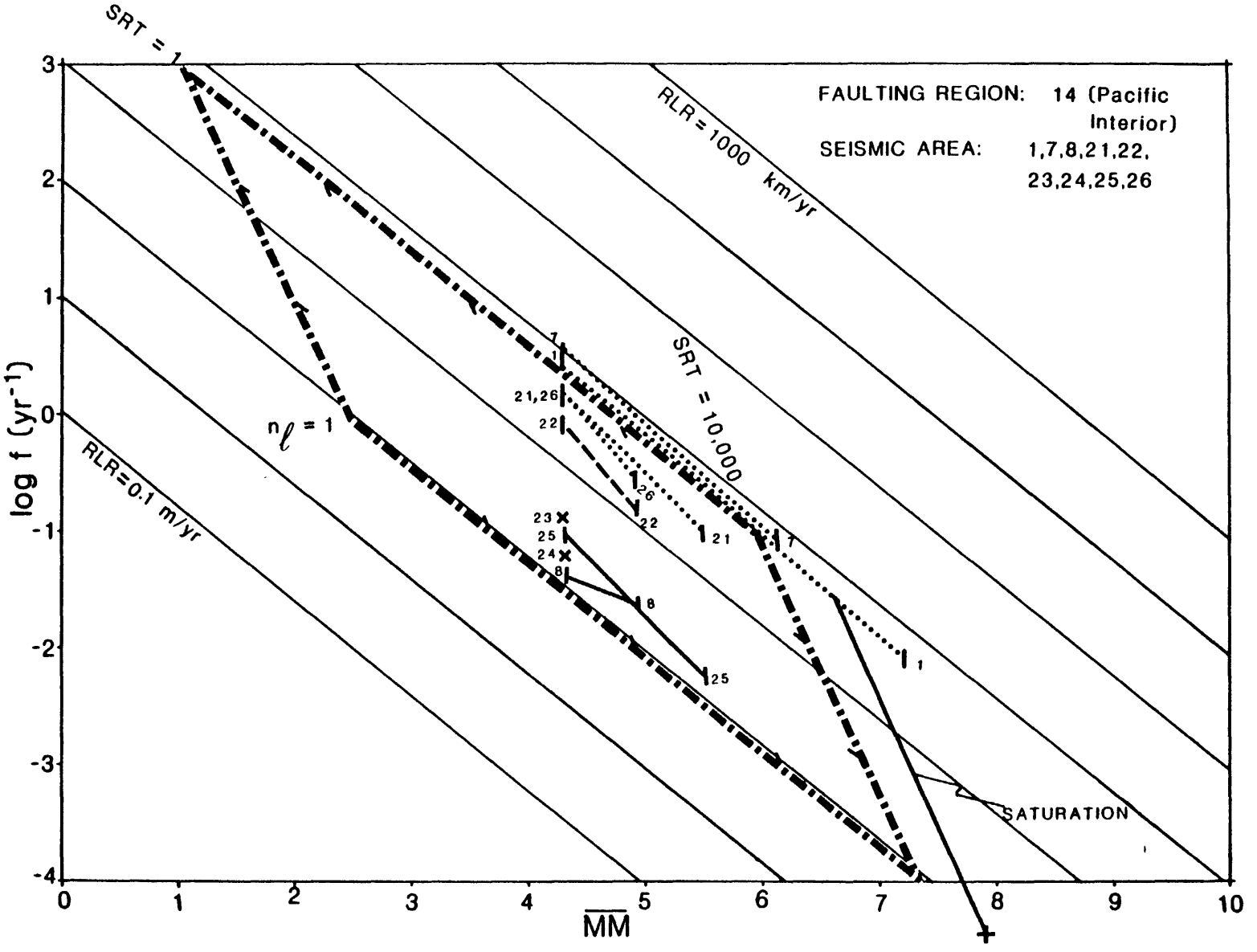

Figure 4.3.2.2.-1. (14)

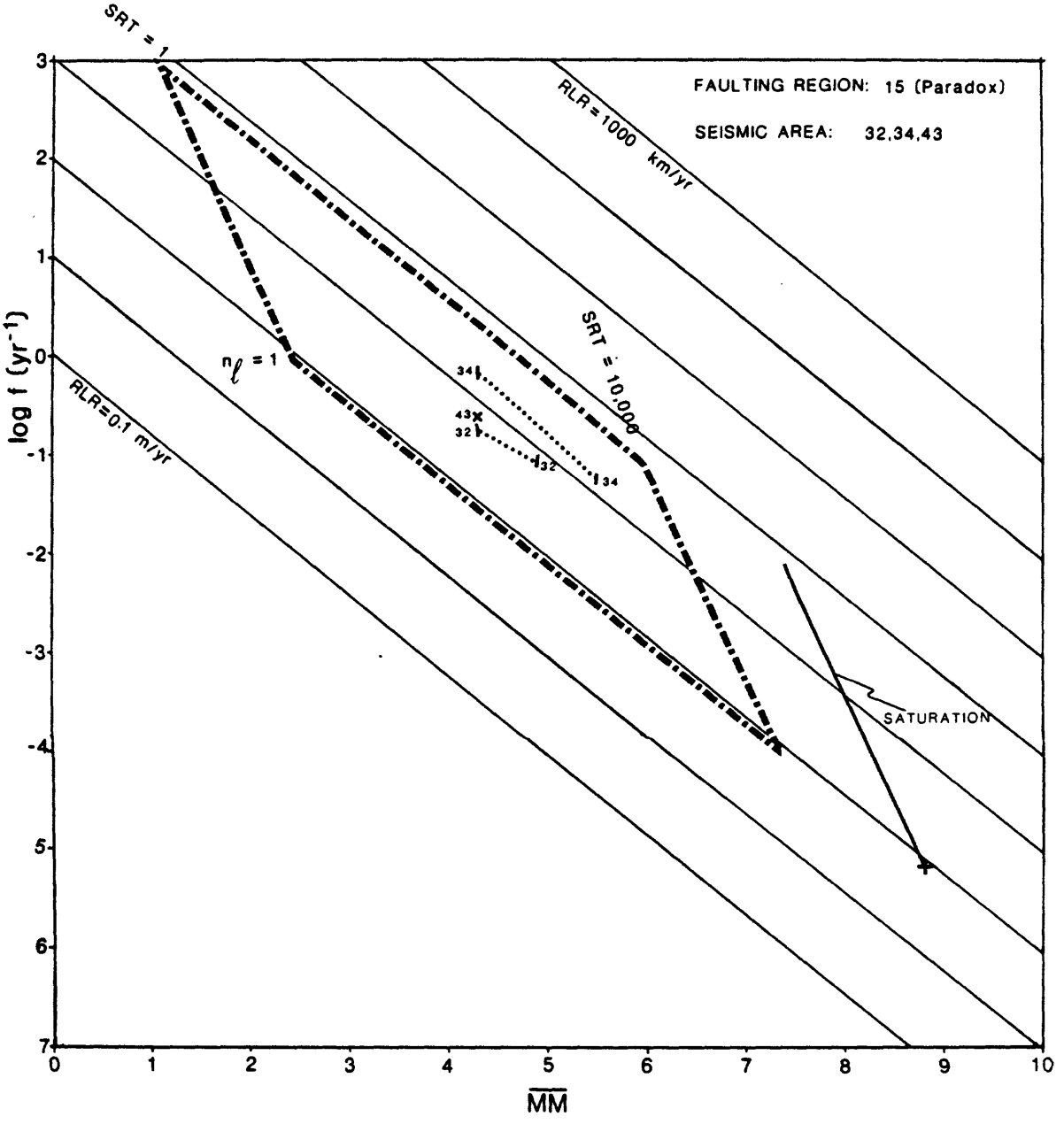

Figure 4.3.2.2.-1. (15)

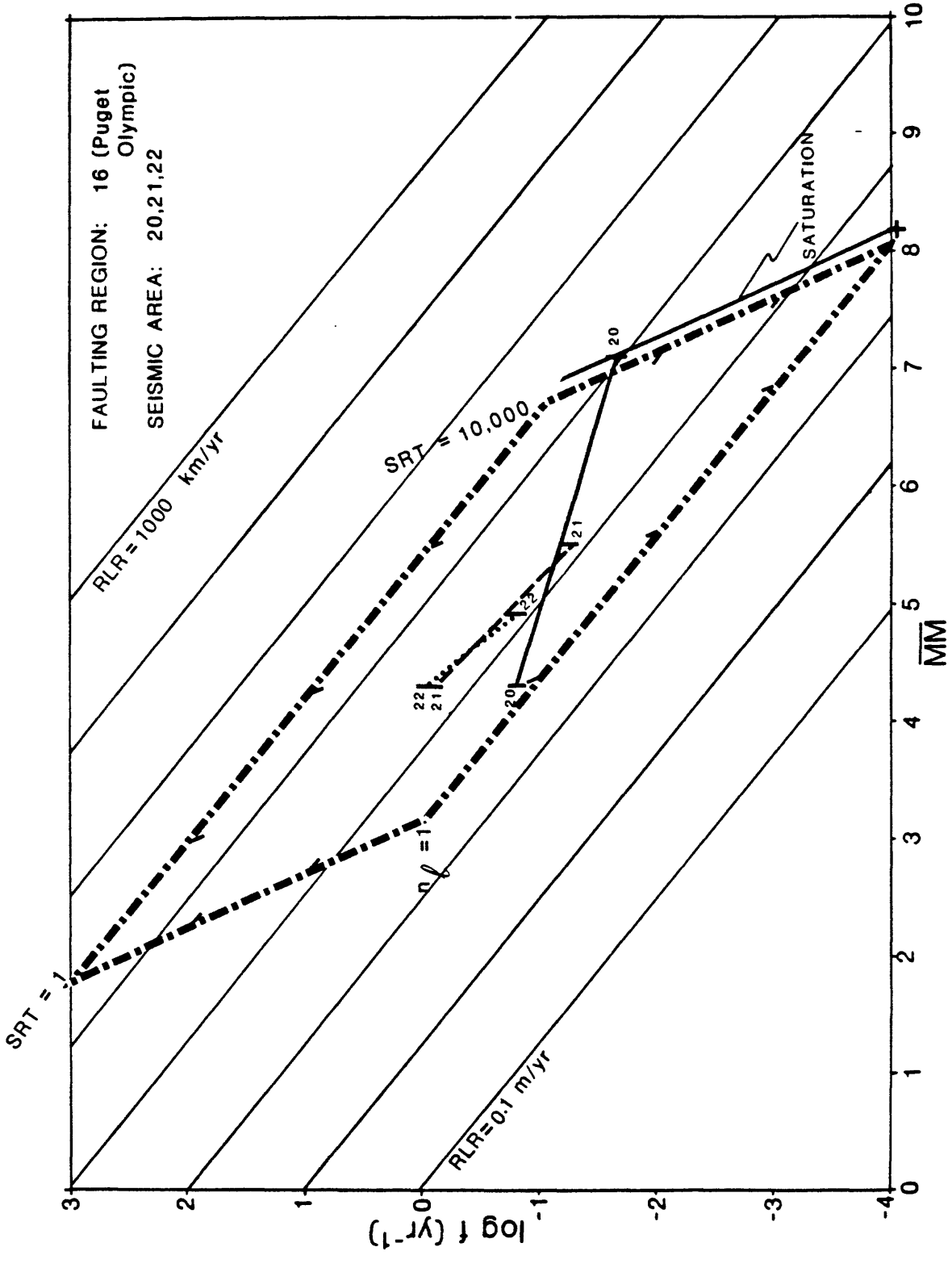

Figure 4.3.2.2.-1. (16)

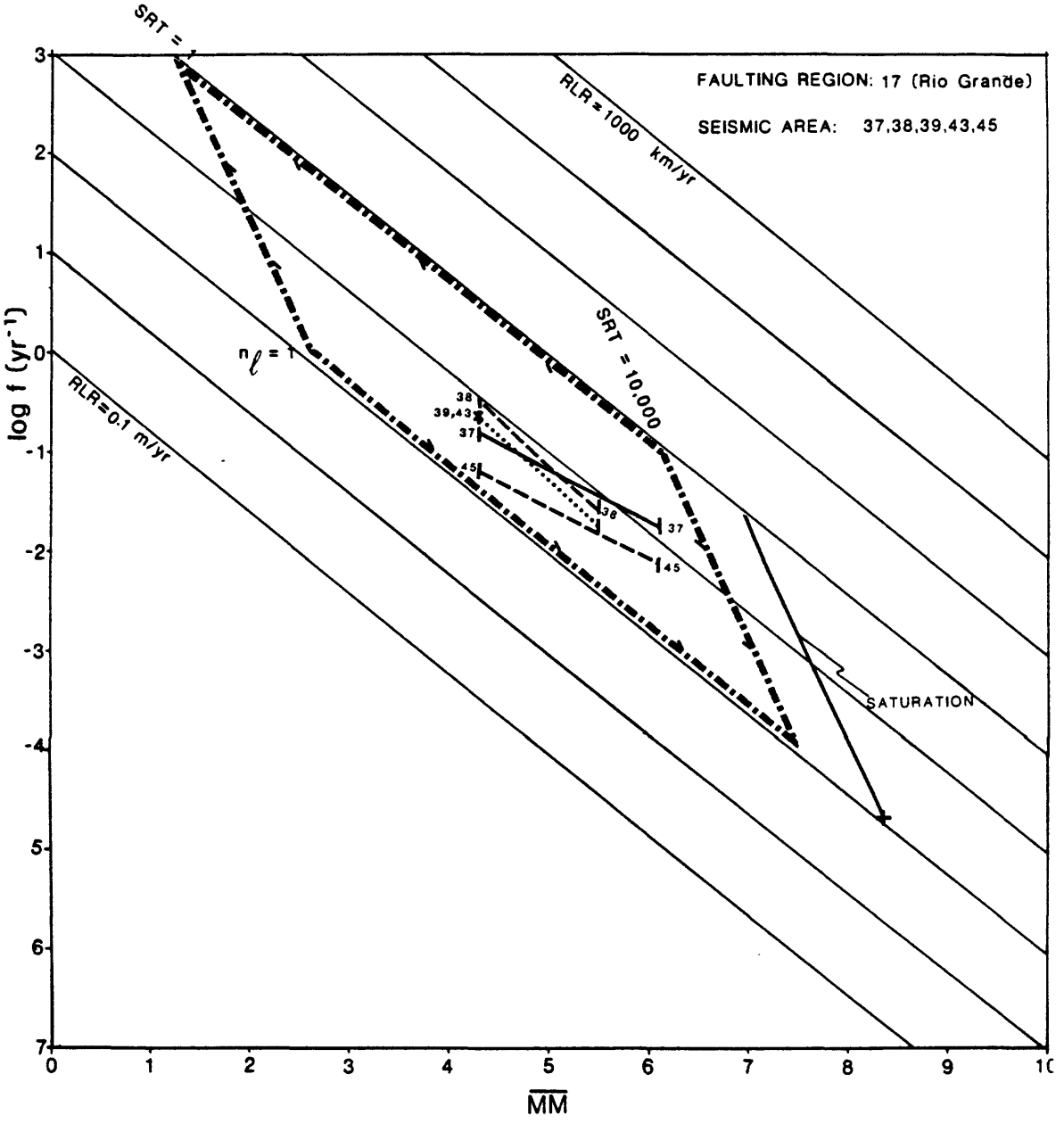

Figure 4.3.2.2.-1. (17)

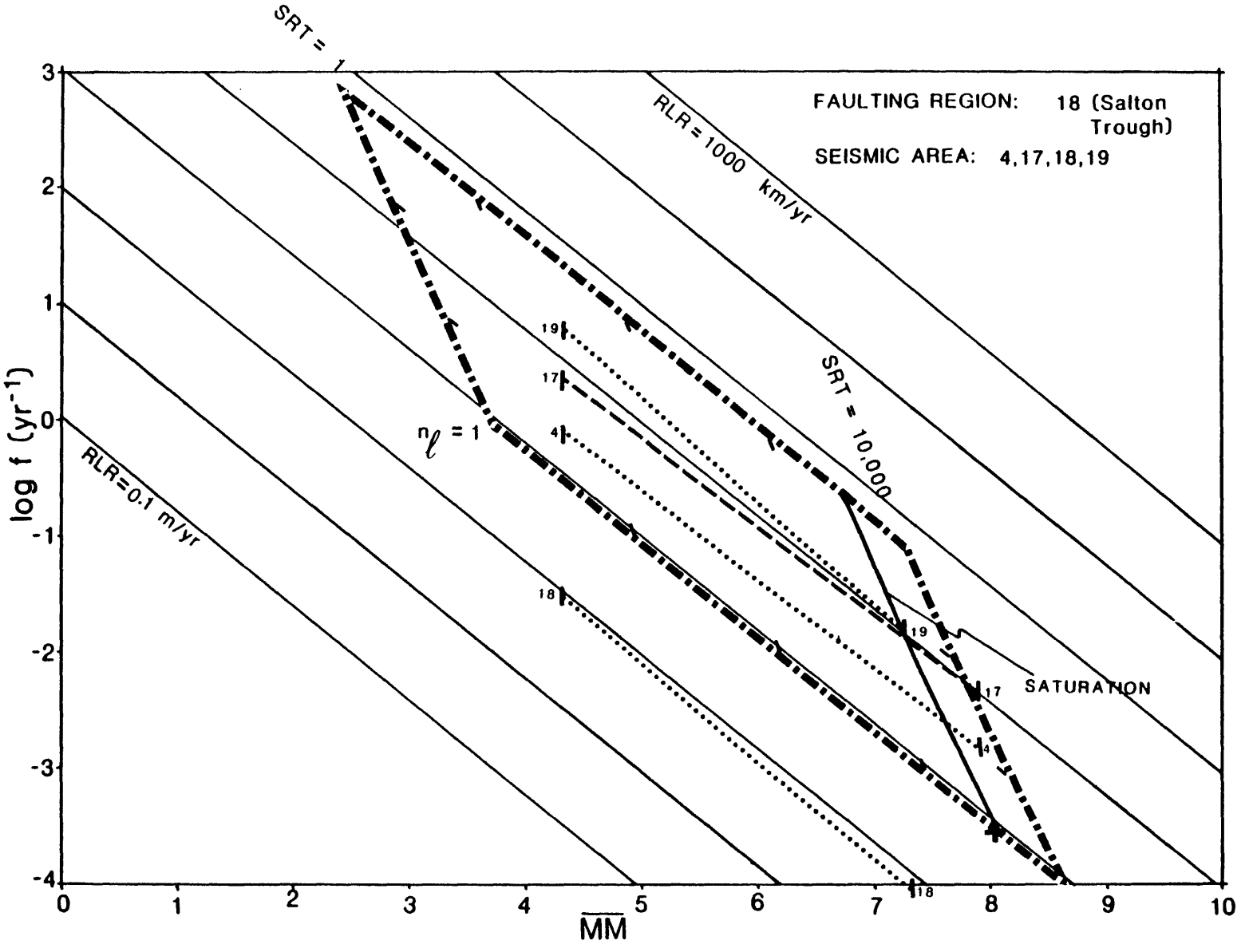

Figure 4.3.2.2.-1. (18)

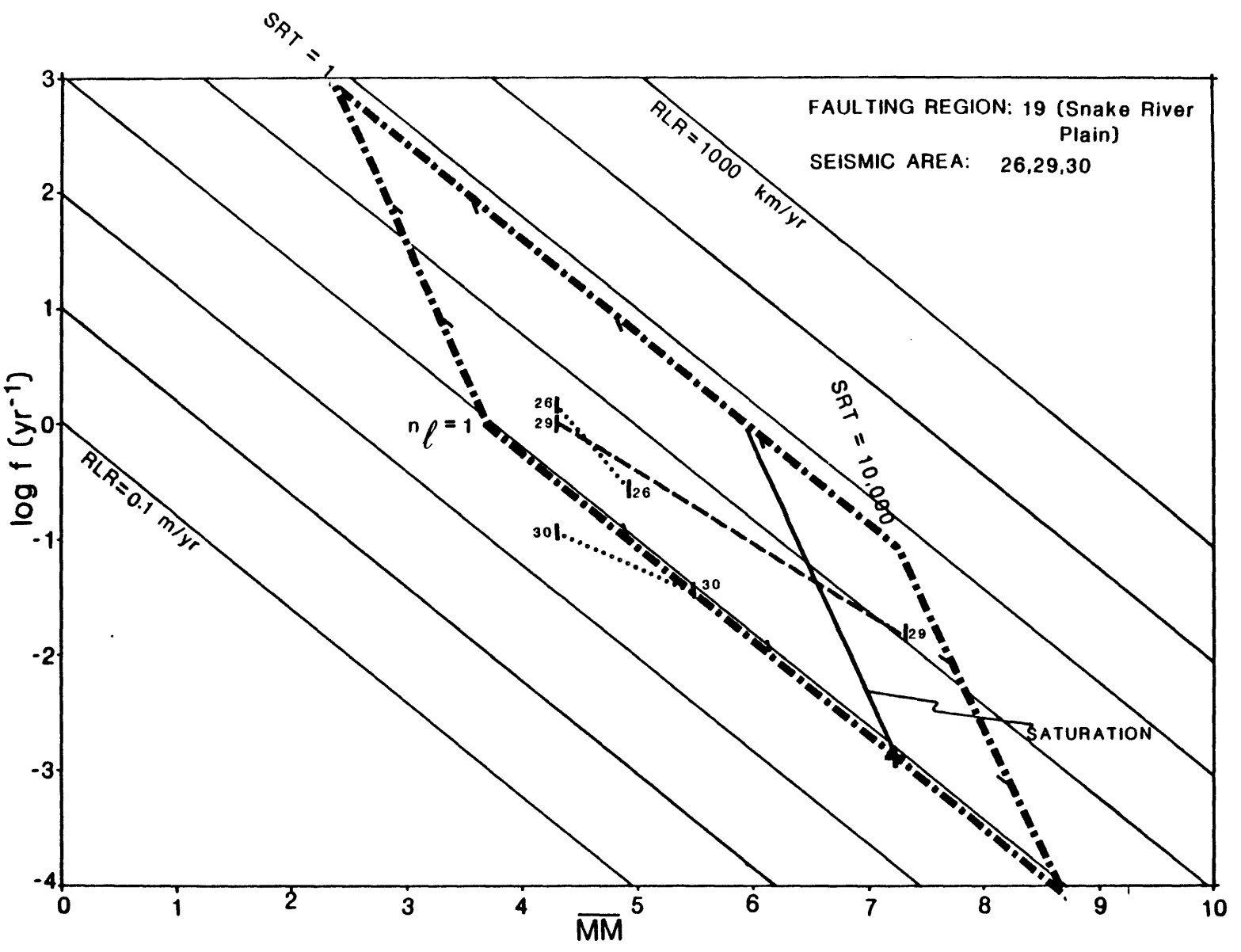

Figure 4.3.2.2.-1. (19)

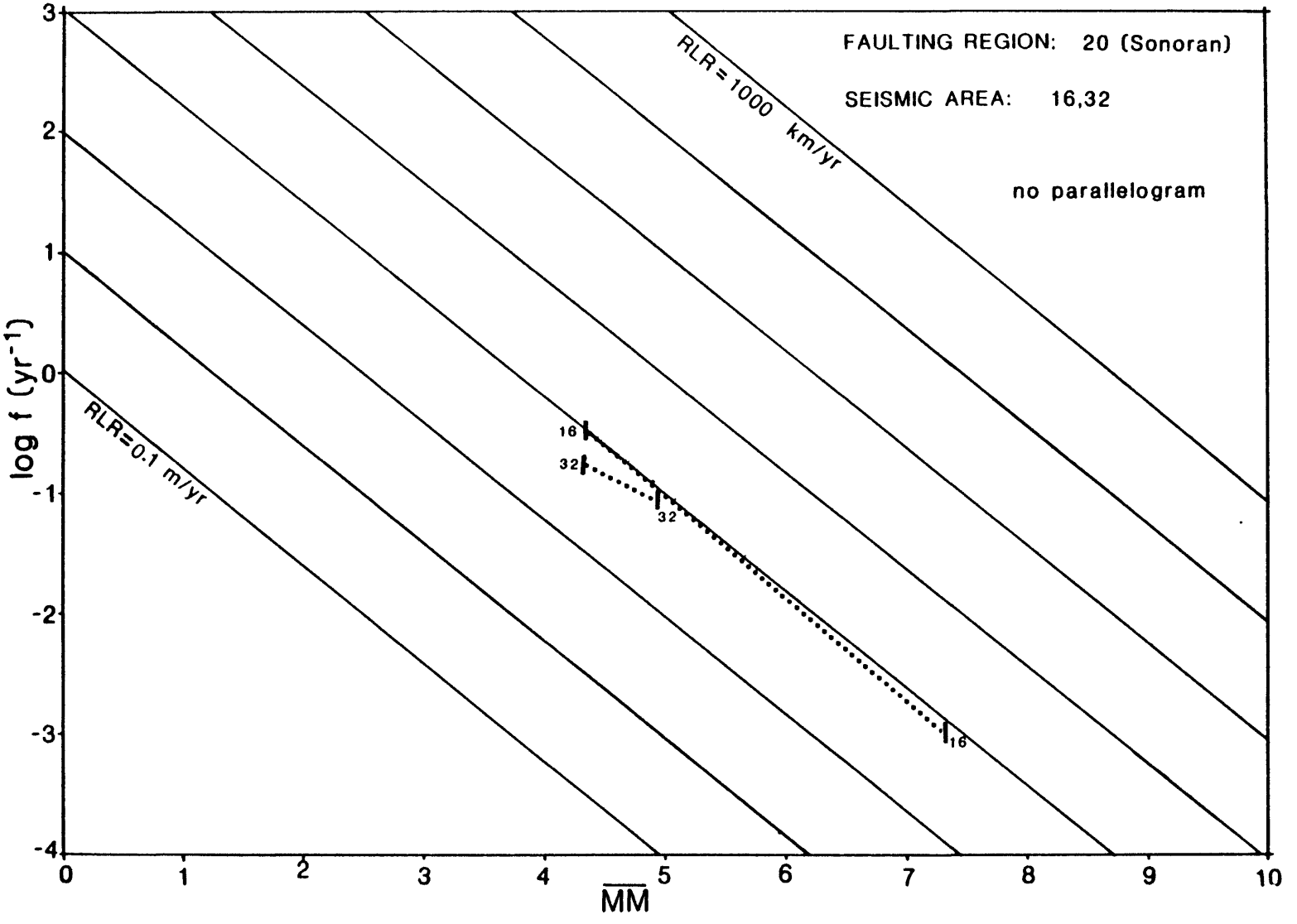

Figure 4.3.2.2.-1. (20)

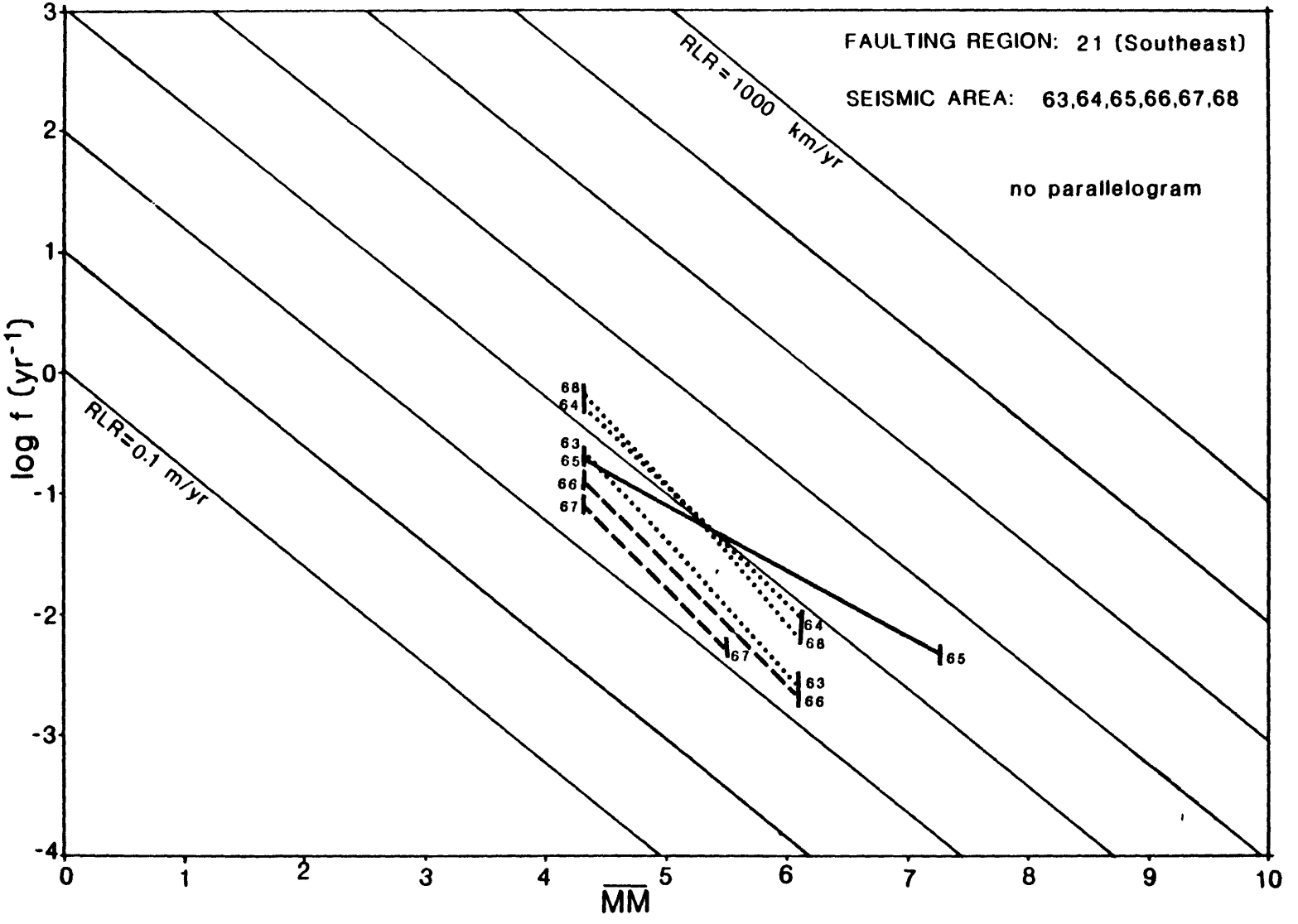

Figure 4.3.2.2.-1. (21)

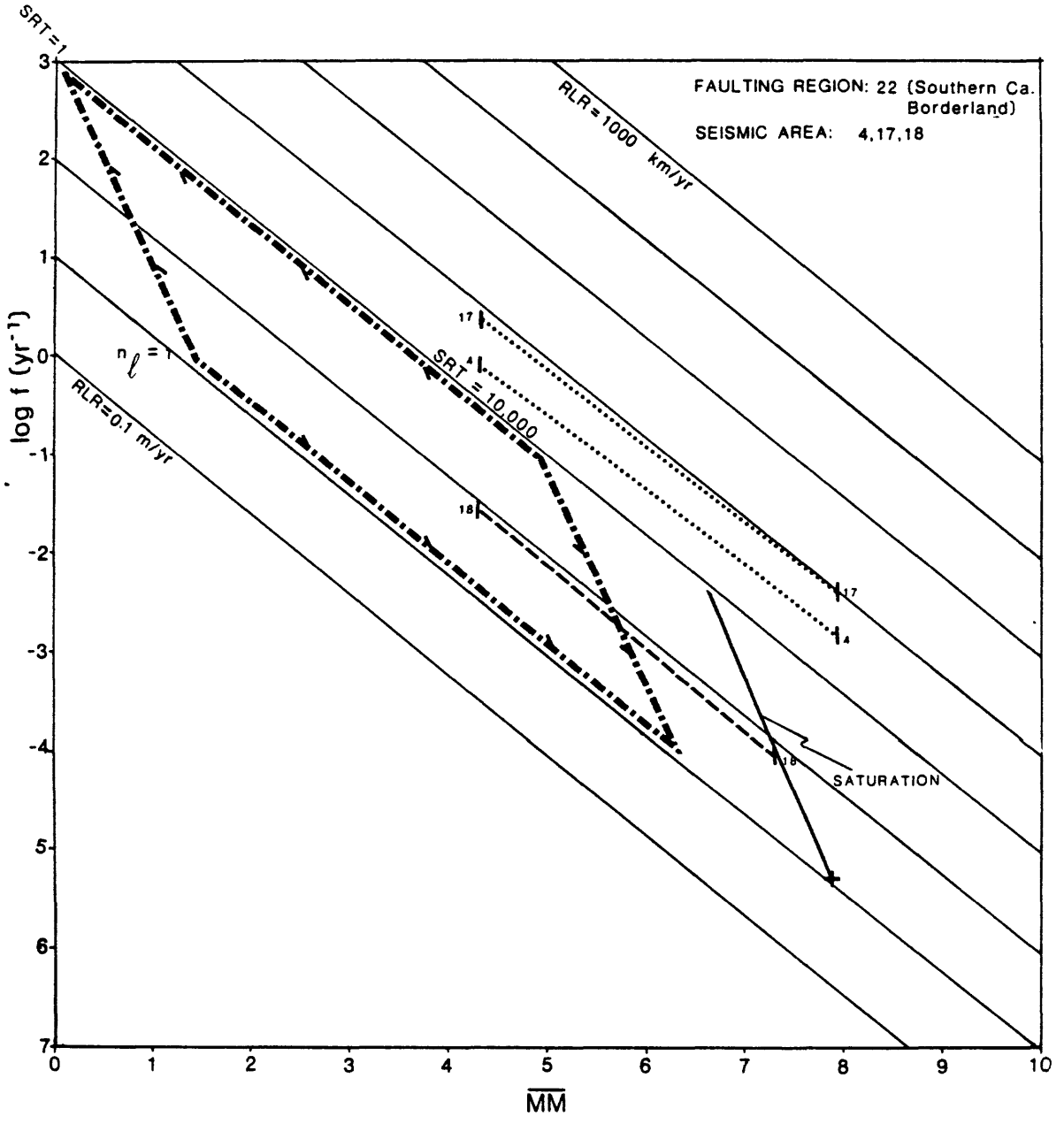

Figure 4.3.2.2.-1. (22)

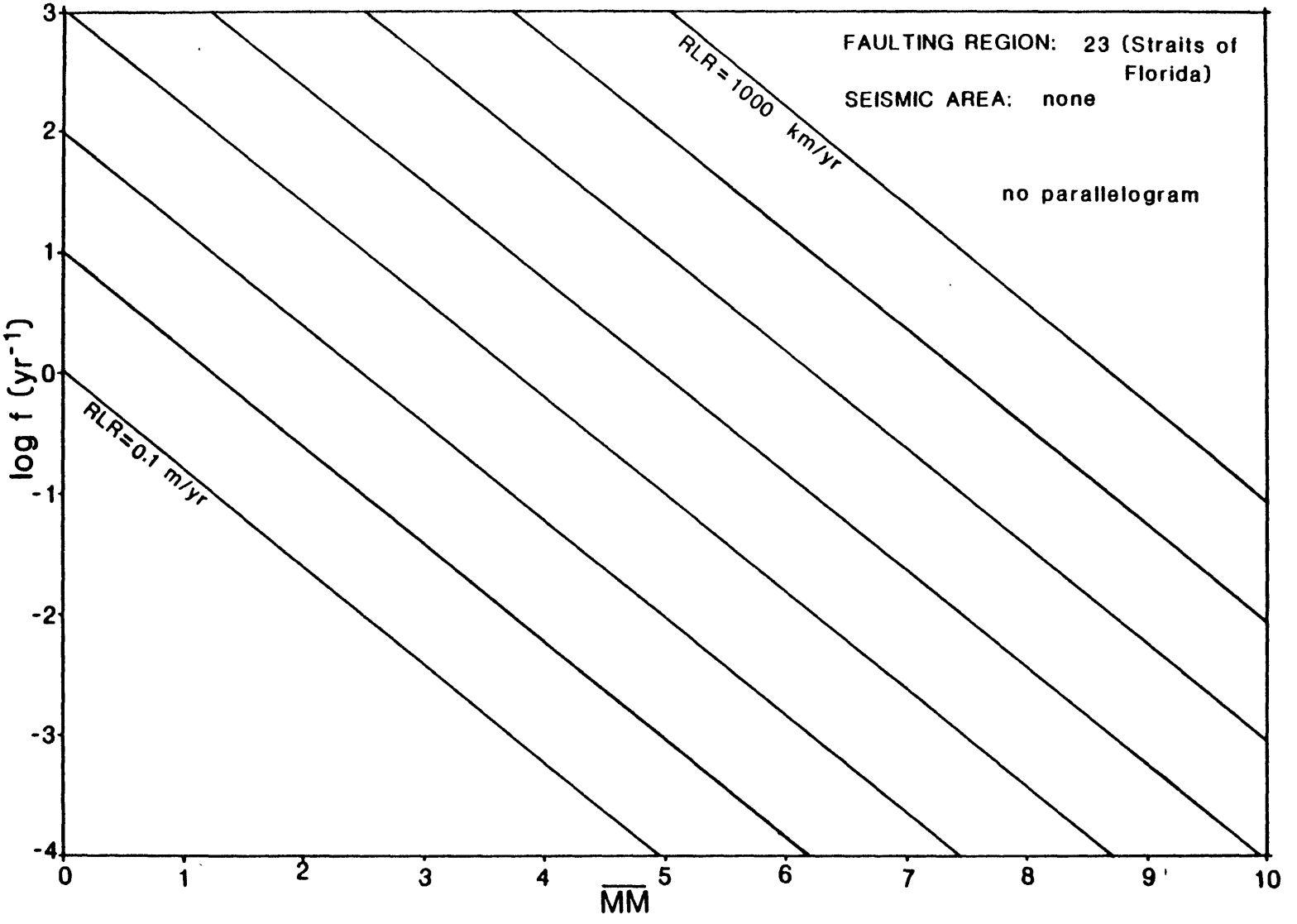

Figure 4.3.2.2.-1. (23)

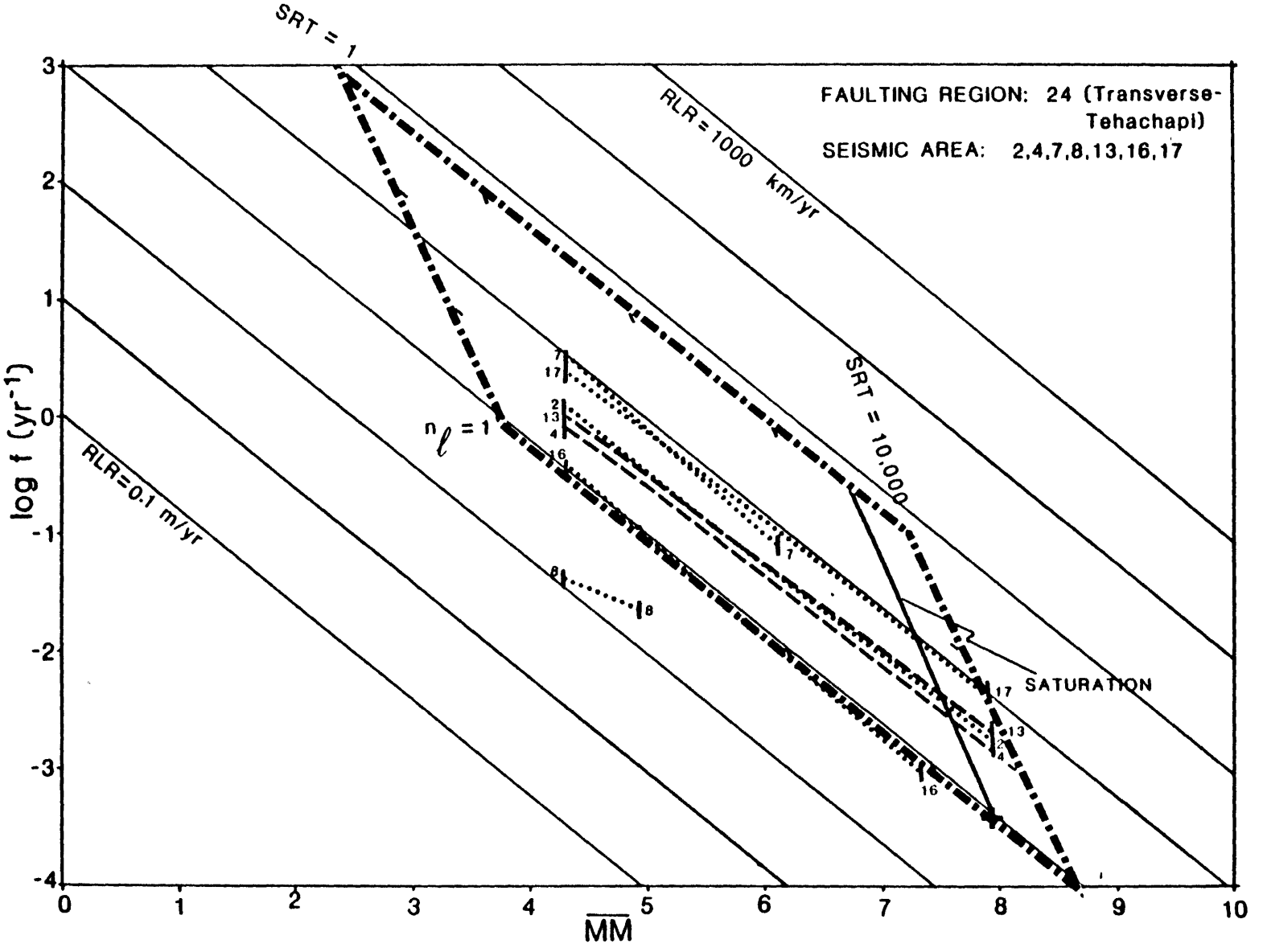

Figure 4.3.2.2.-1. (24)

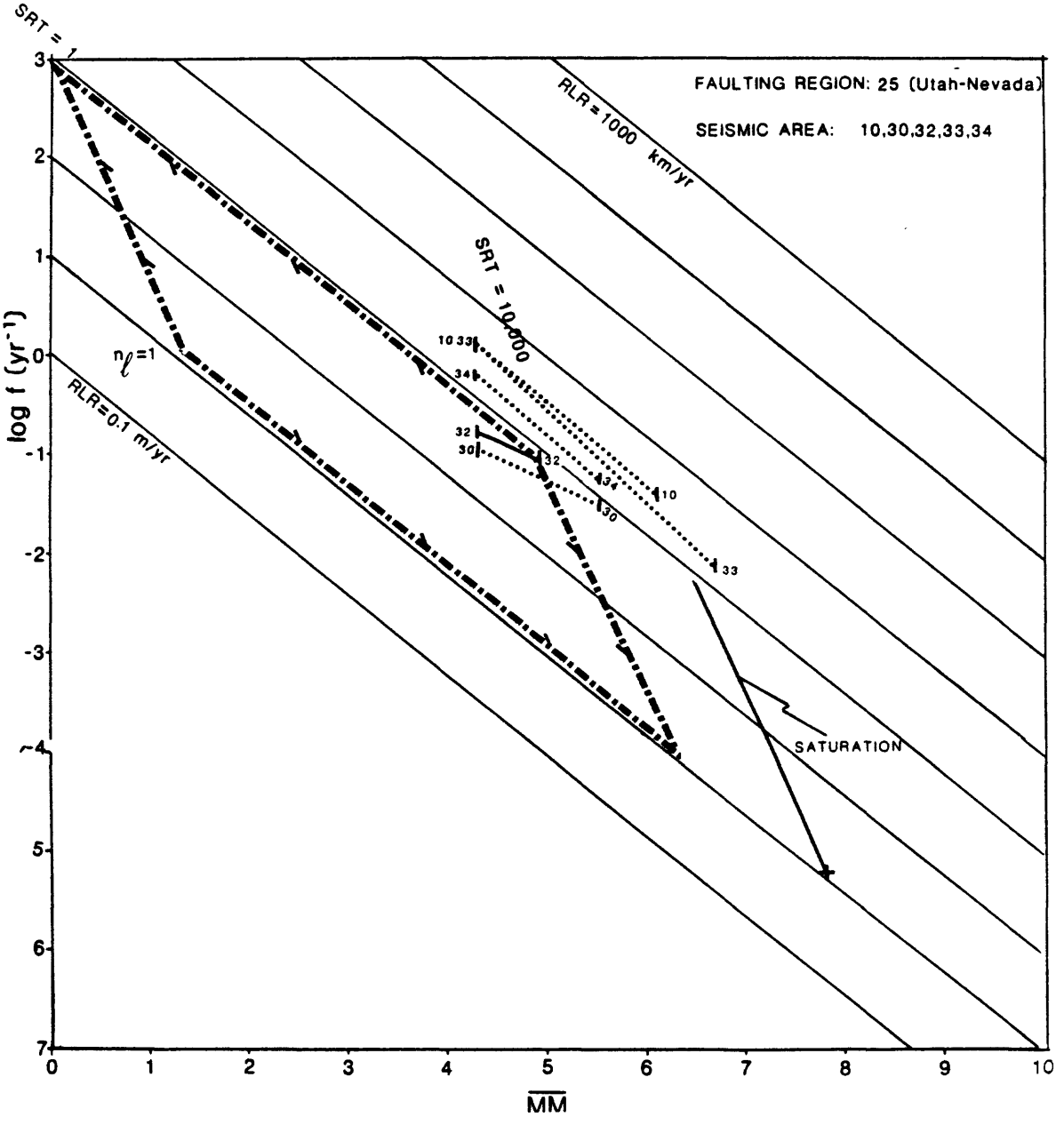

Figure 4.3.2.2.-1. (25)

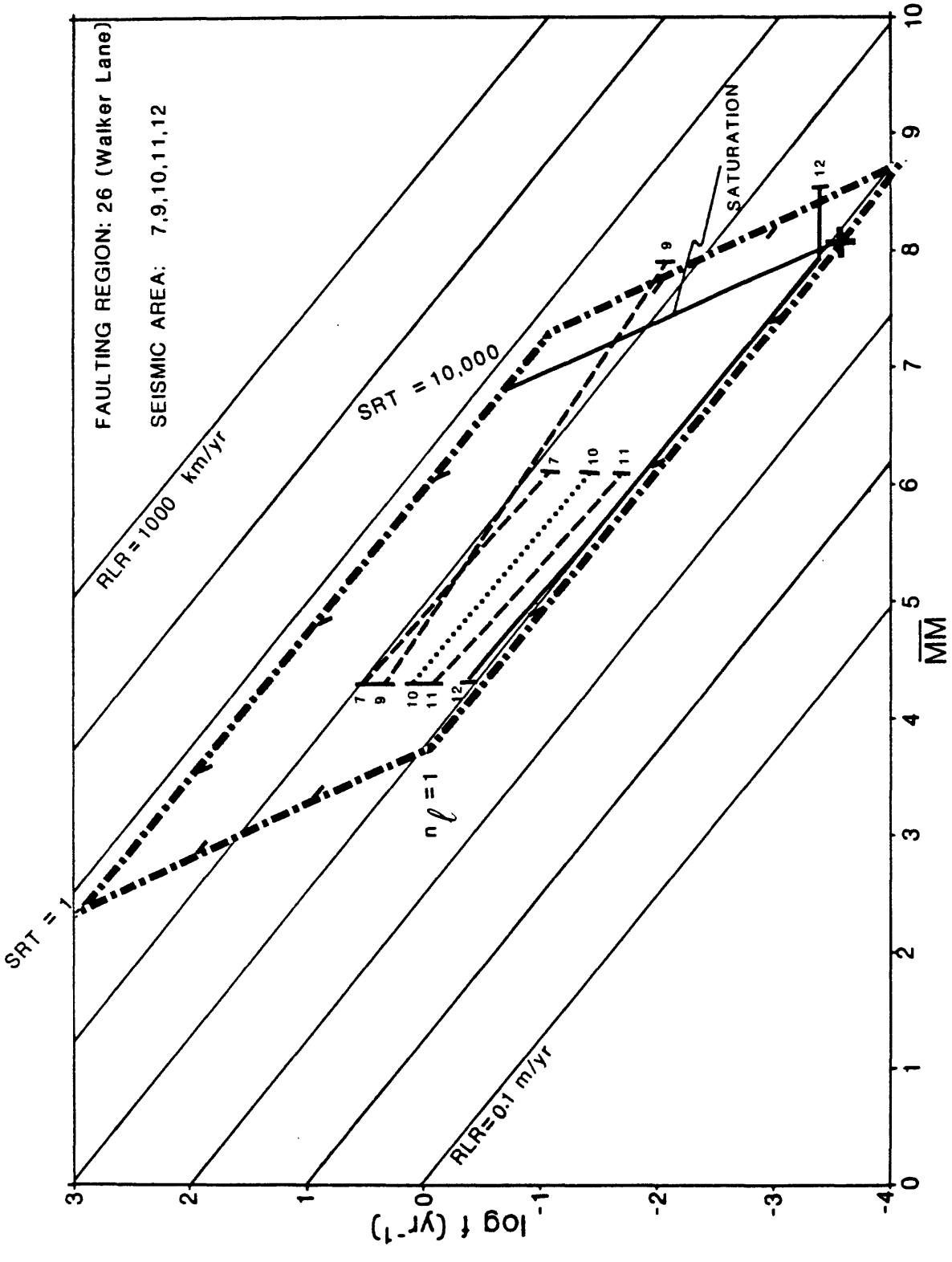

Figure 4.3.2.2.-1. (26)

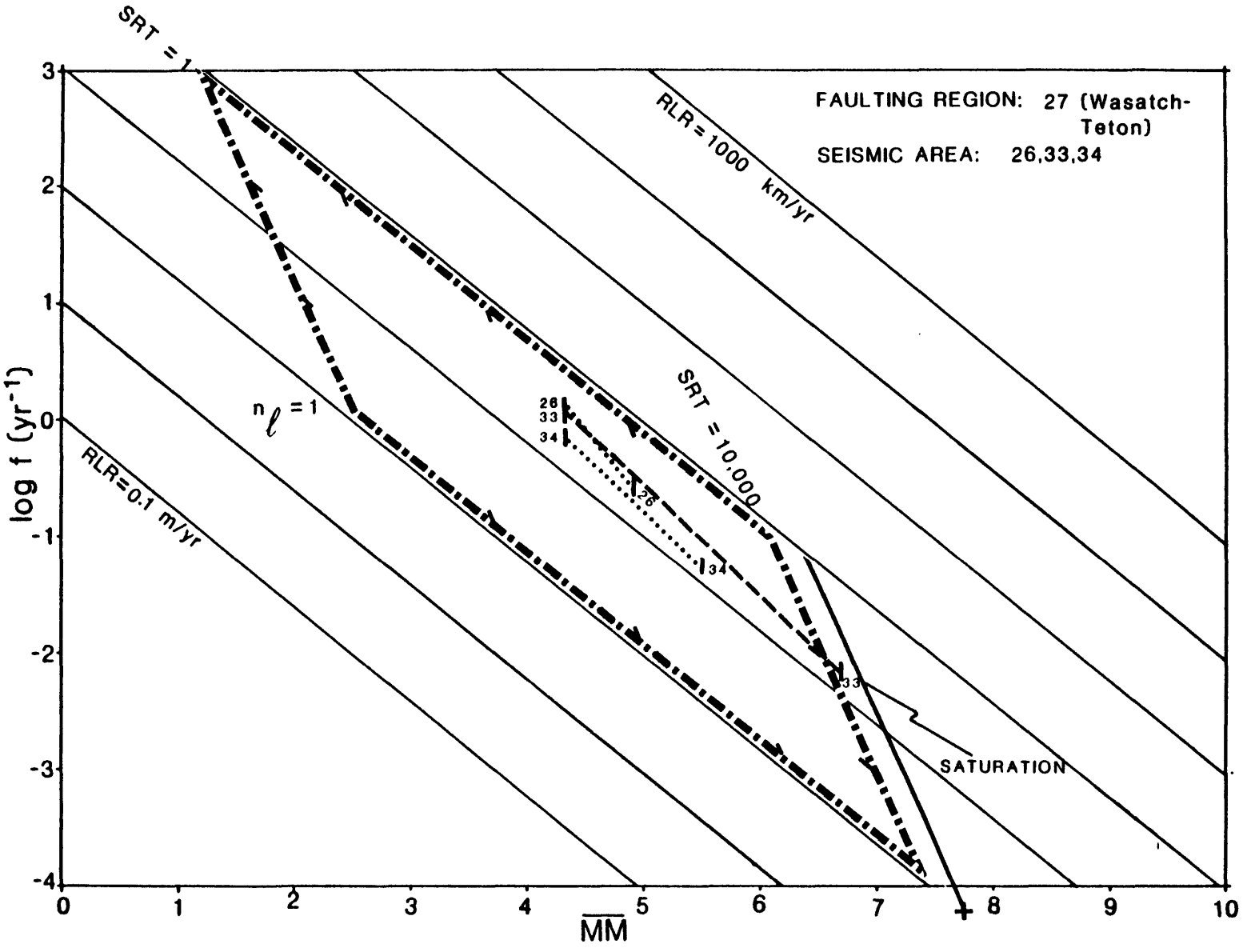

Figure 4.3.2.2.-1.(27)

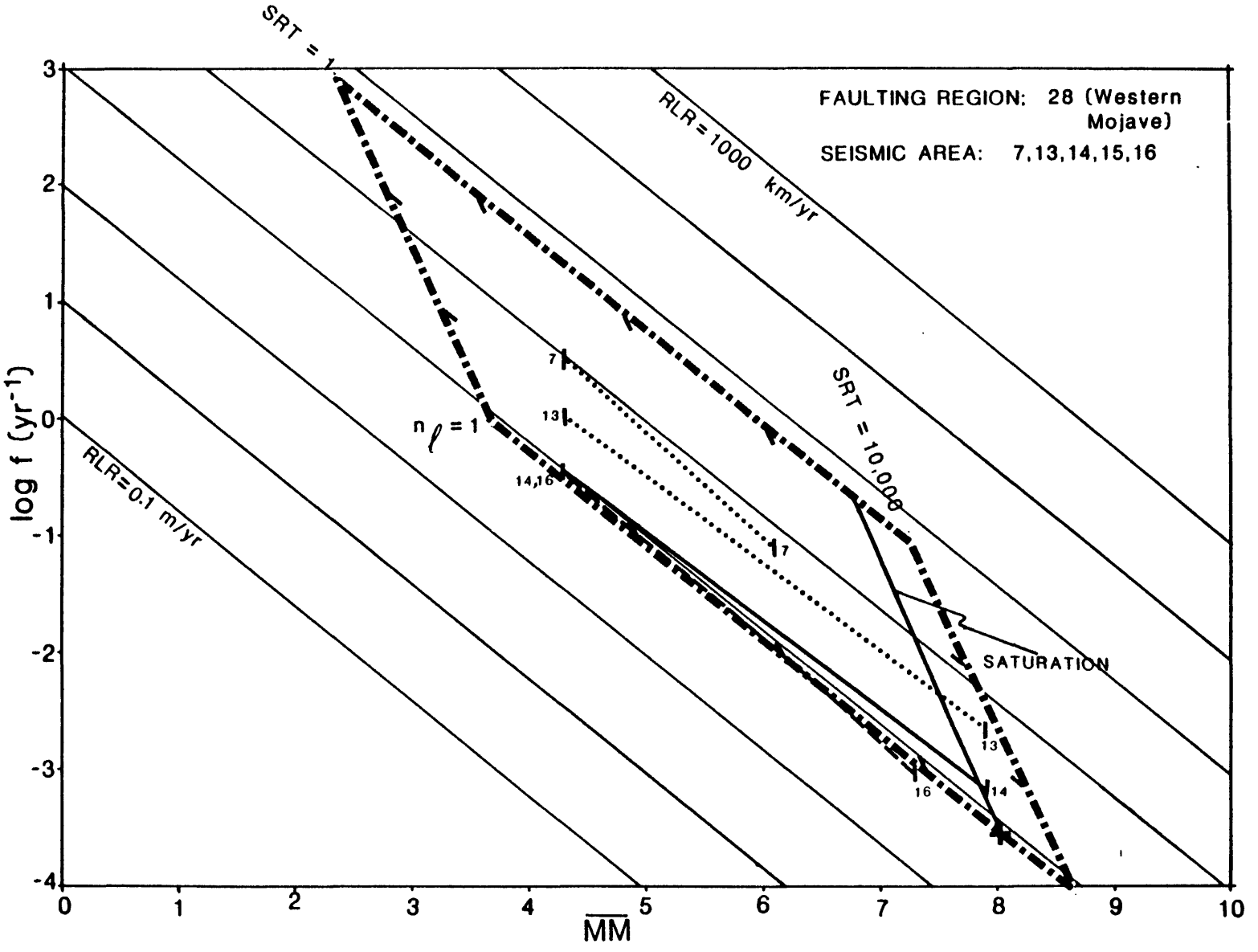

Figure 4.3.2.2.-1. (28)

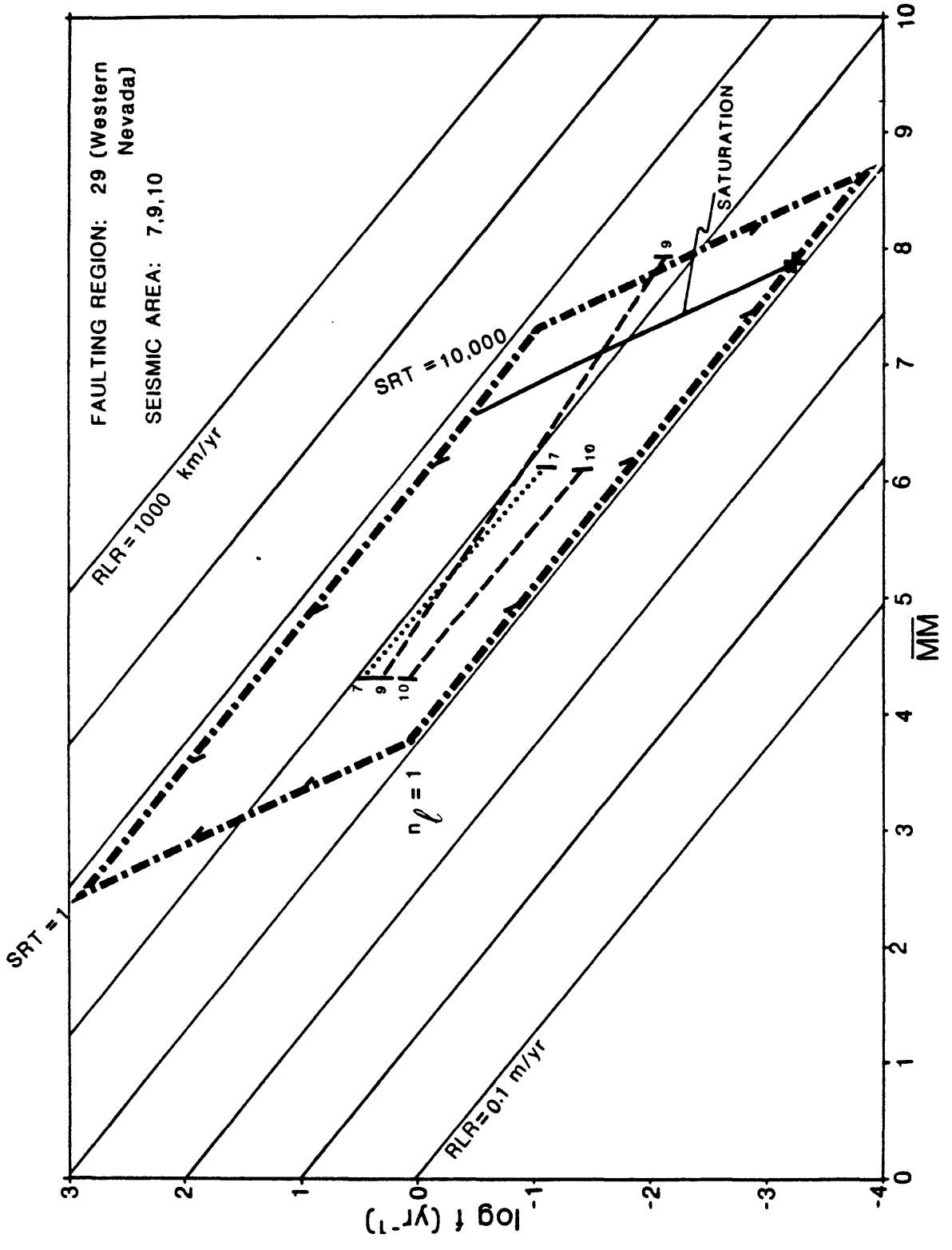

Figure 4.3.2.2.-1. (29)

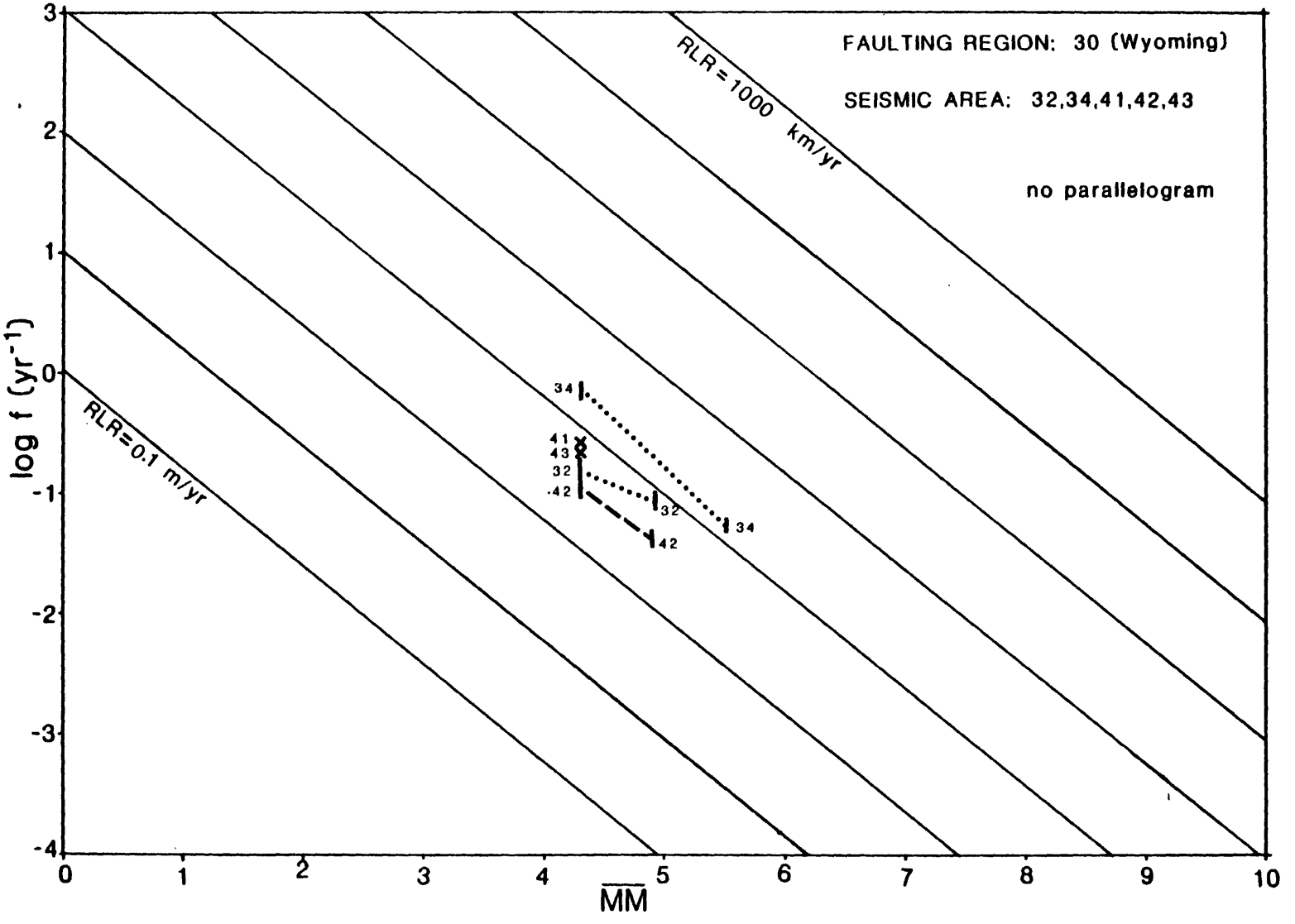

Figure 4.3.2.2.-1. (30)

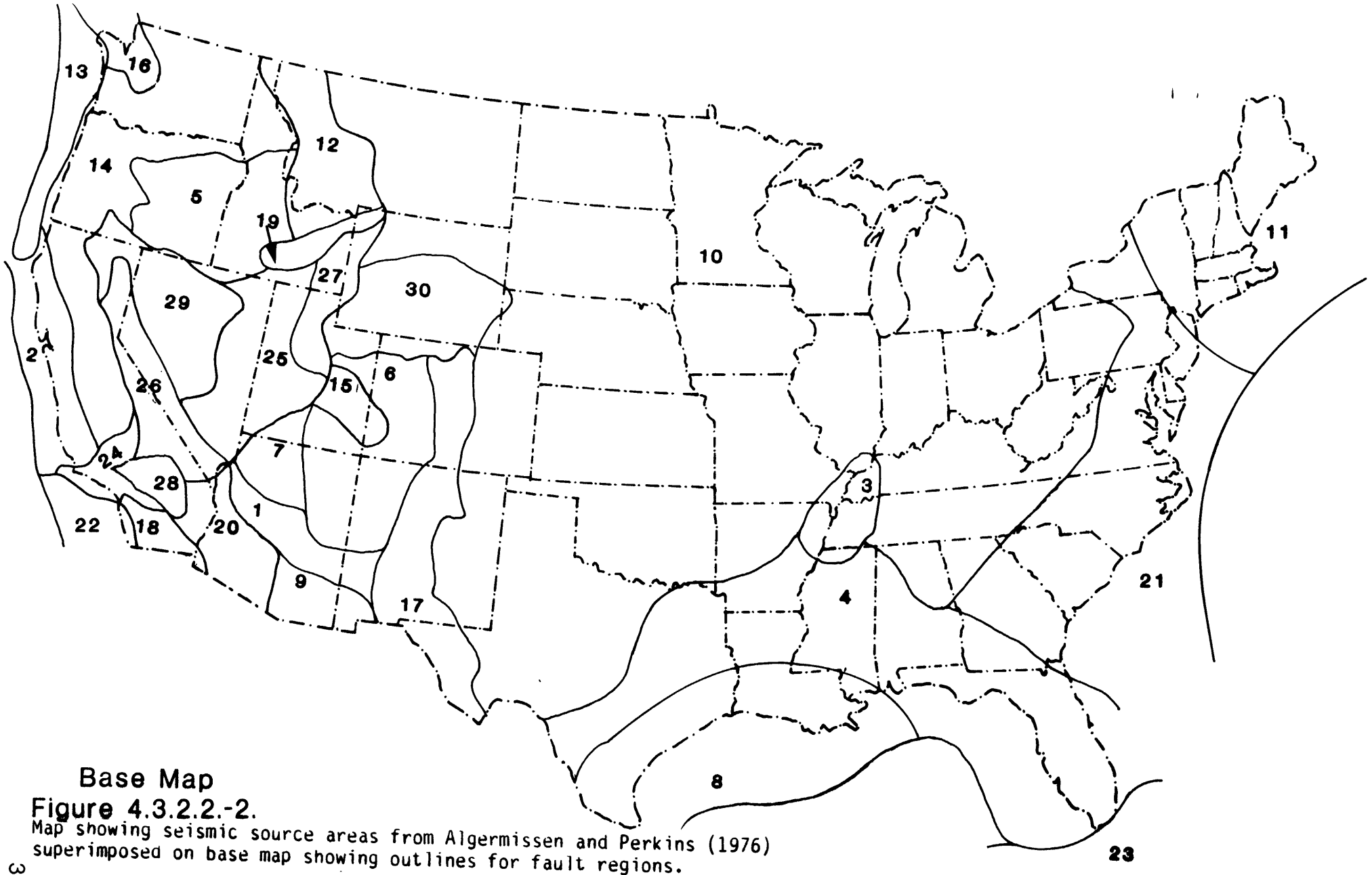

Base Map

Figure 4.3.2.2.-2.
Map showing seismic source areas from Algermissen and Perkins (1976) superimposed on base map showing outlines for fault regions.

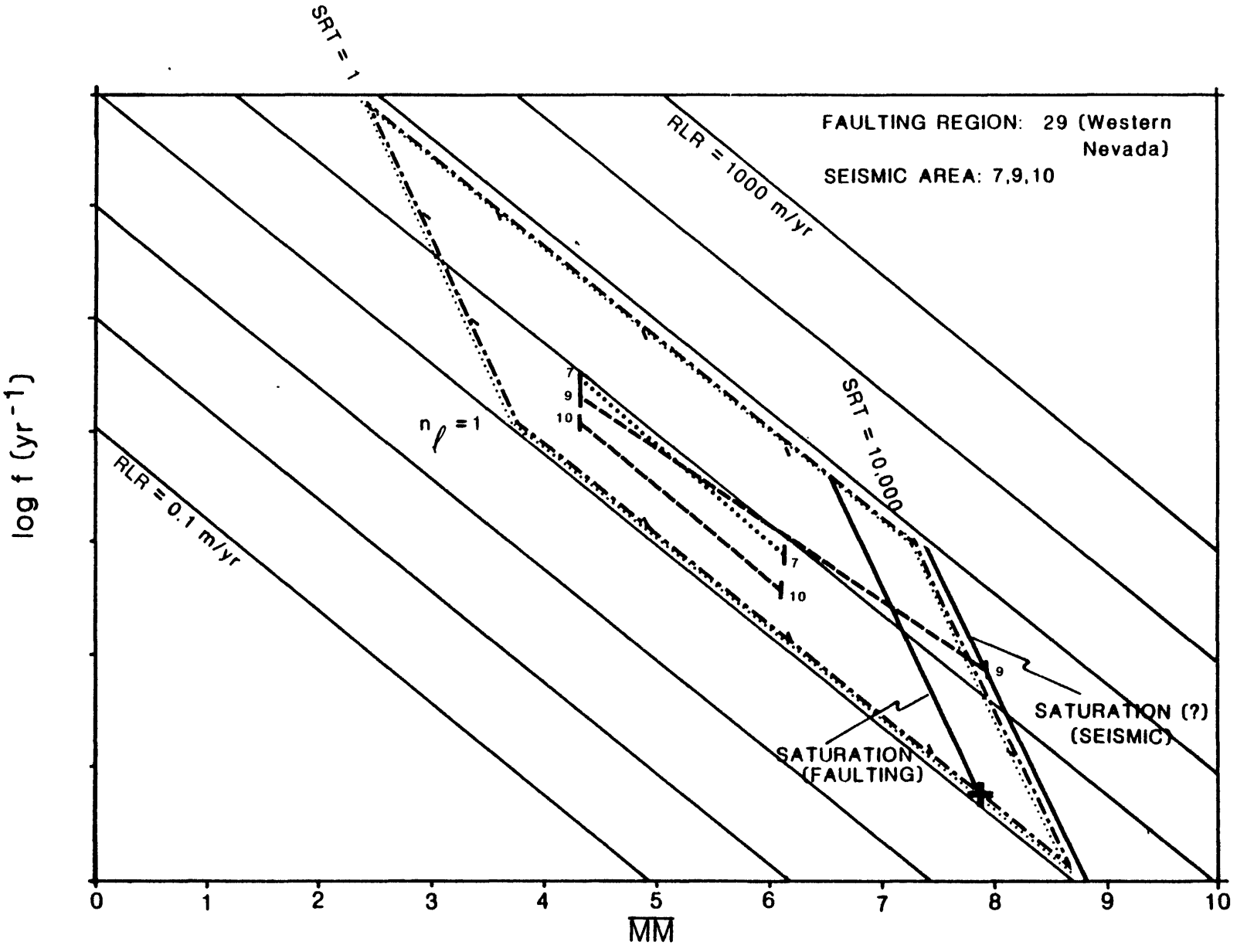

Figure 4.3.2.2.-3.
Comparison of alternative constructions for paleoseismic parallelograms derived, respectively, from fault data (heavy dot-dash lines) and from earthquake data (light dotted lines).

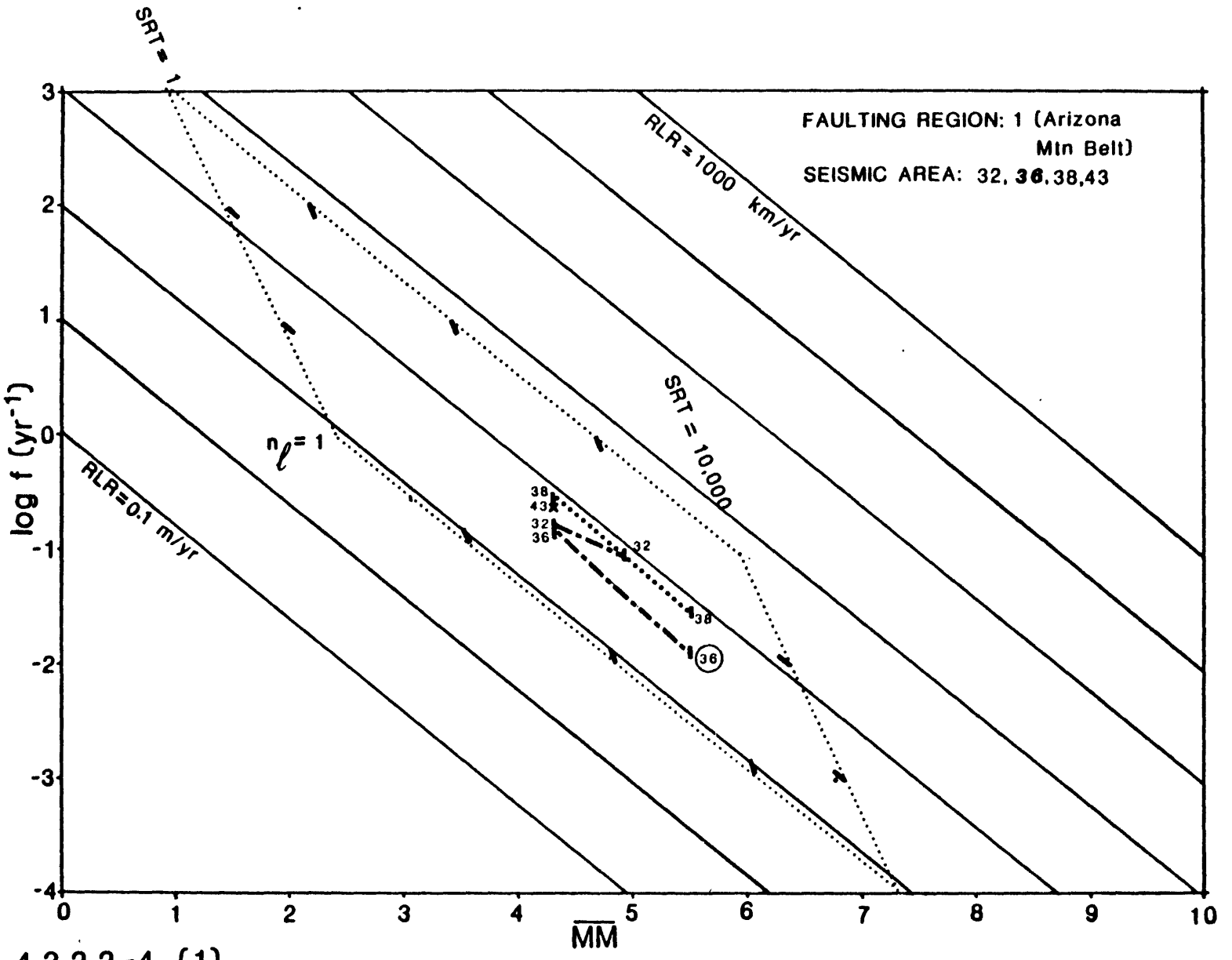

Figure 4.3.2.2.-4. (1)

Paleoseismic parallelograms based on seismic data from each of the thirty fault regions The construction represents a tentative answer to the questions: What are the possible fault sets and activation rates that would produce the observed earthquakes if actual data existed for such faults. This plot essentially represents an adjustment to the parallelogram in Figure 4.3.2.2.-1 required to bring them into better agreement with earthquake data. Figure 5.1.-1 shows the implied shift in faulting rates required for improved agreement.

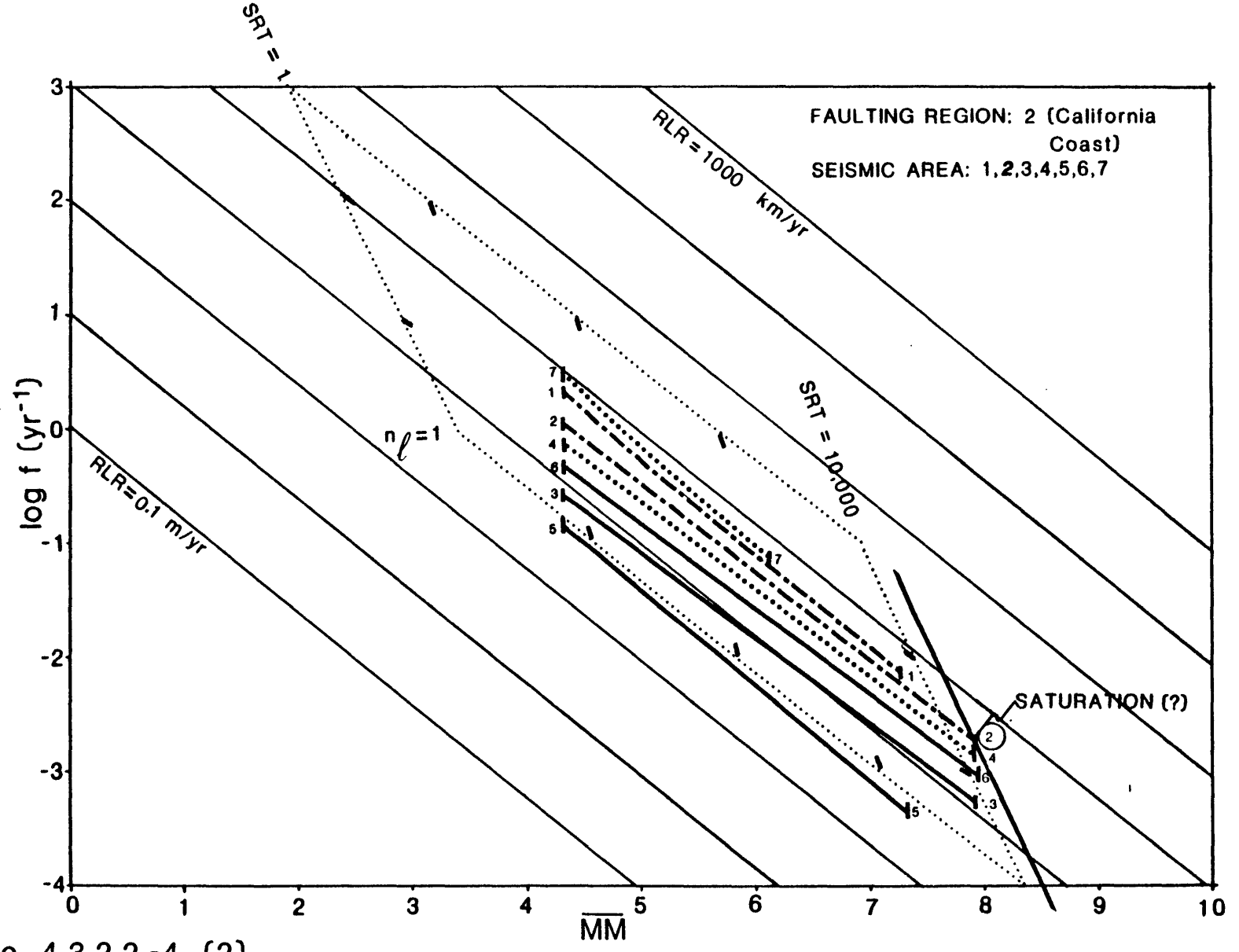

Figure 4.3.2.2.-4. (2)

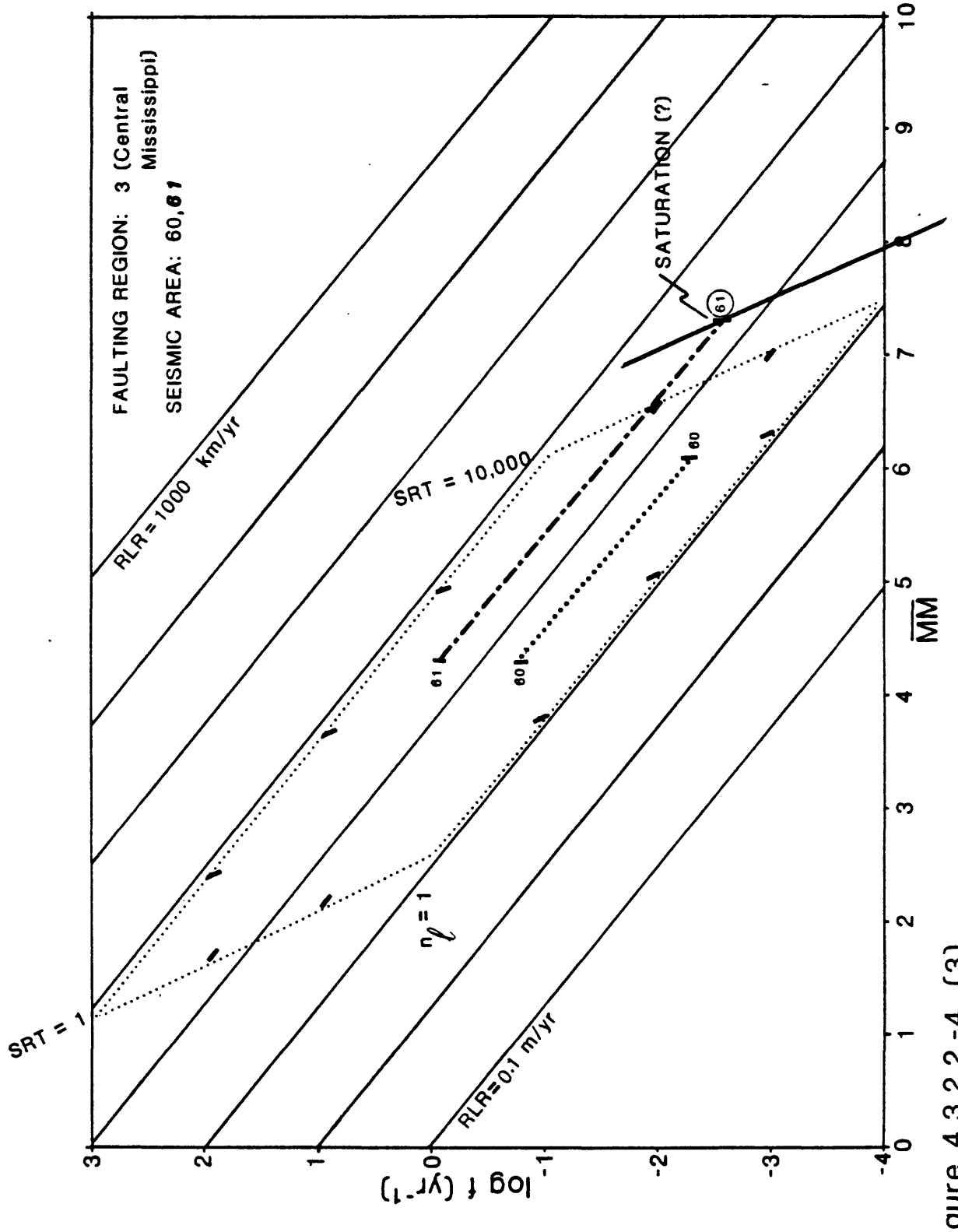

Figure 4.3.2.2.-4. (3)

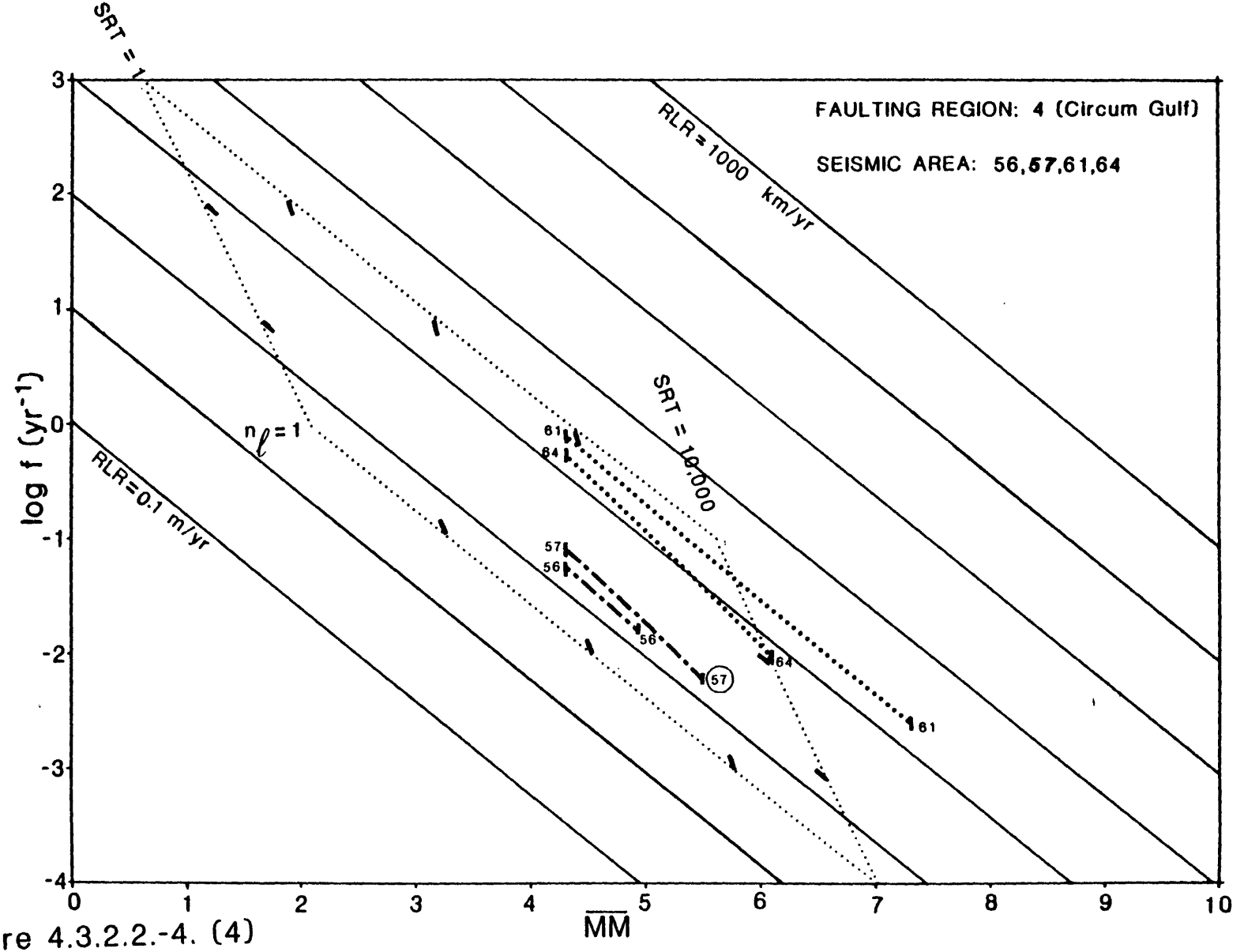

Figure 4.3.2.2.-4. (4)

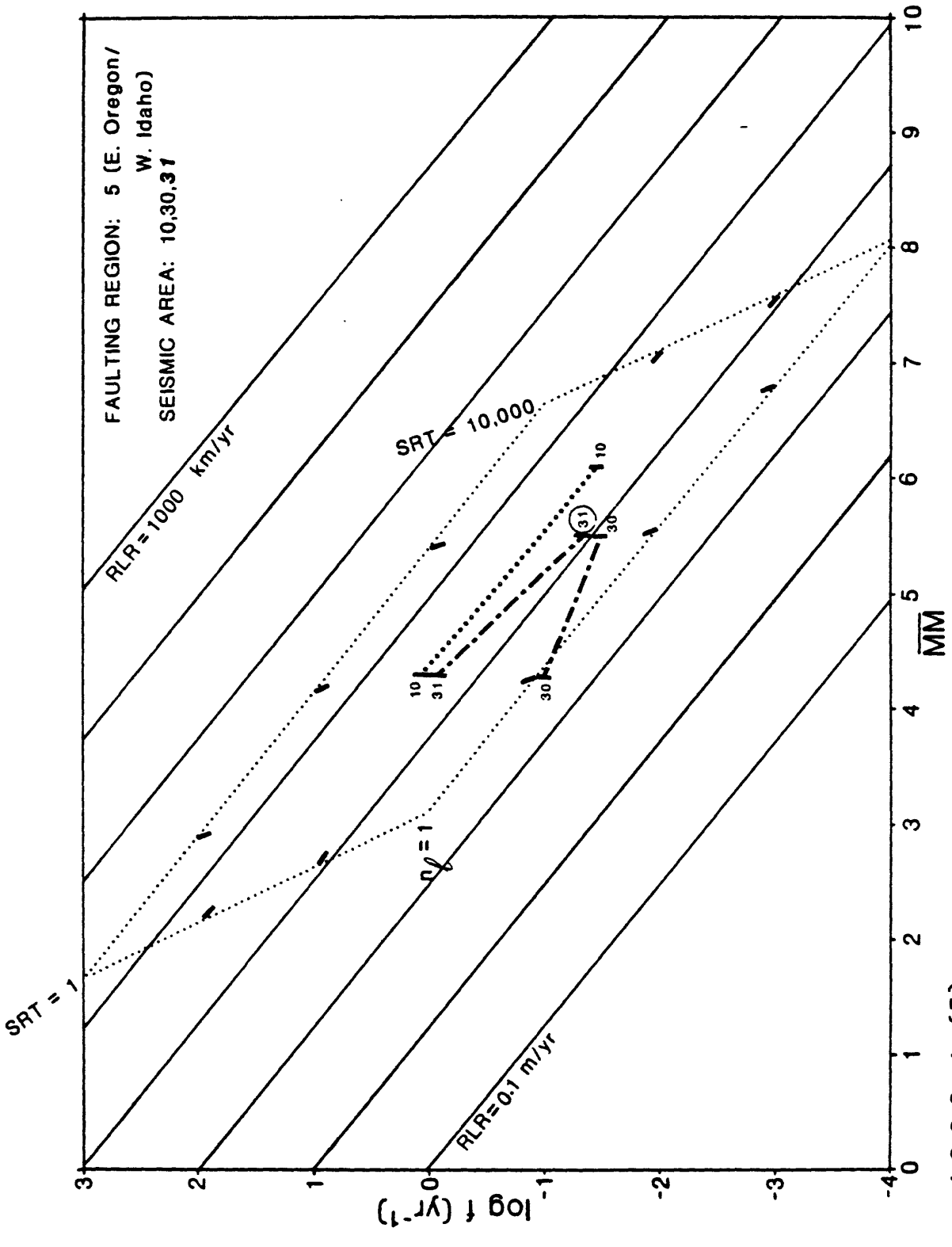

Figure 4.3.2.2.-4. (5)

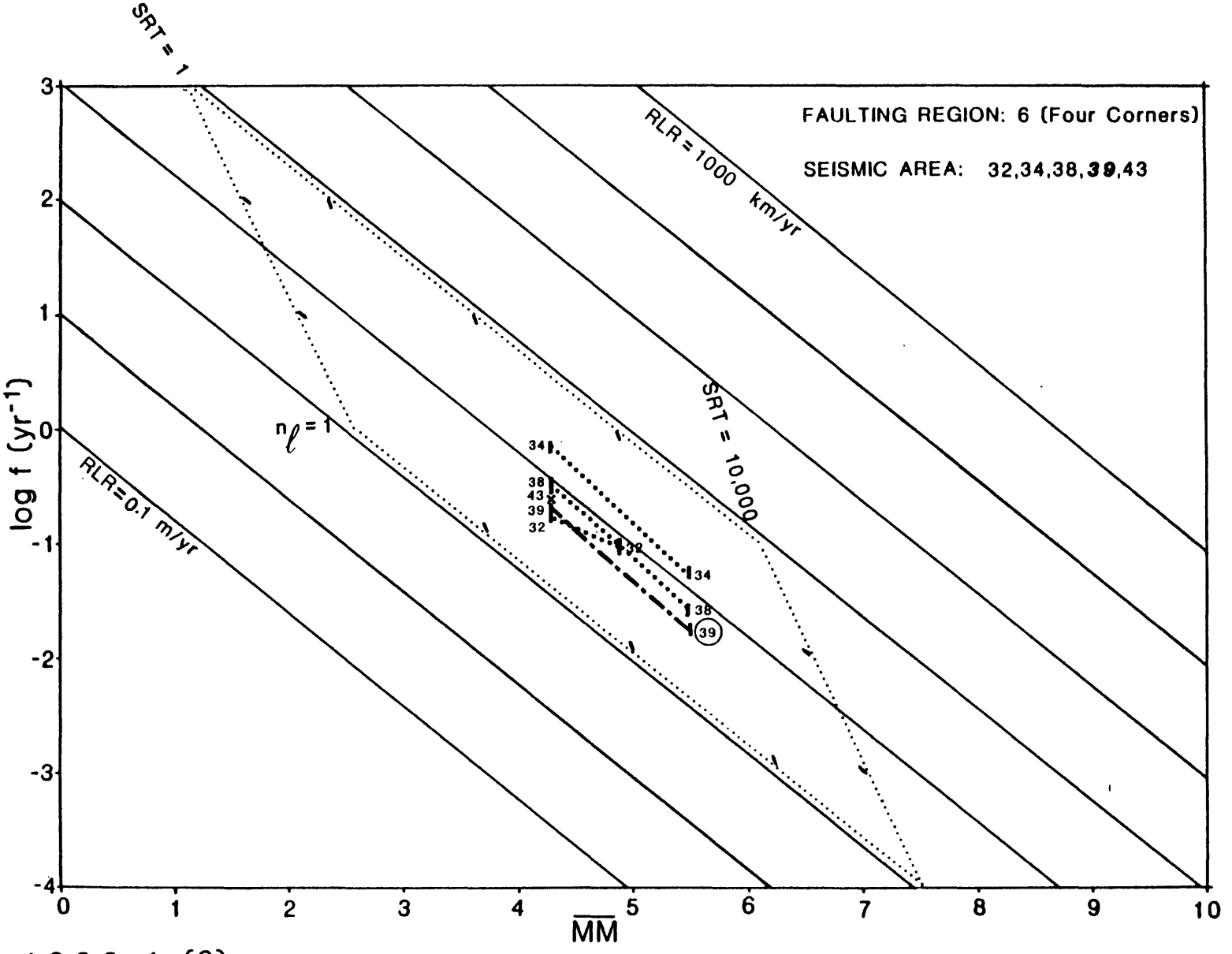

Figure 4.3.2.2.-4. (6)

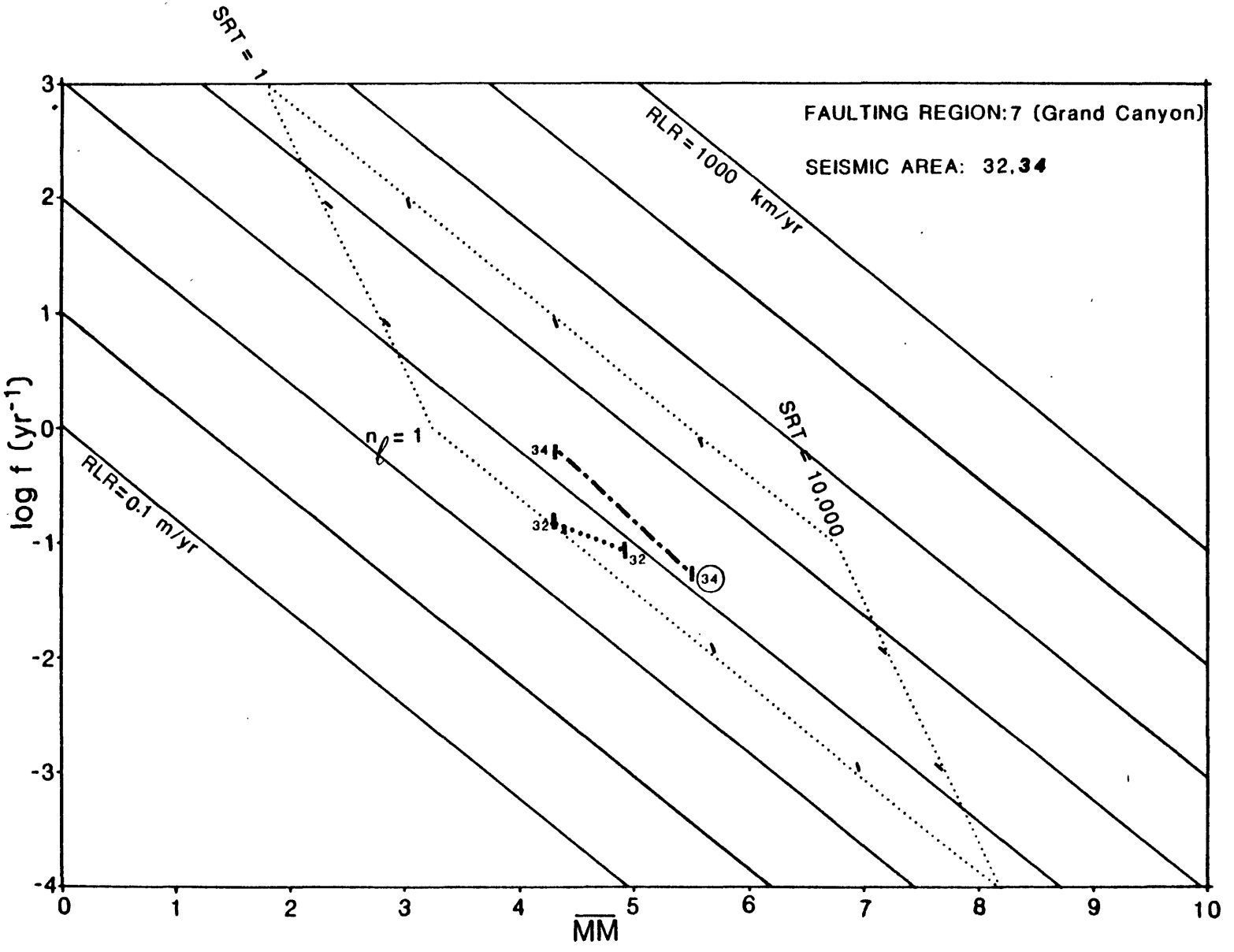

Figure 4.3.2.2.-4. (7)

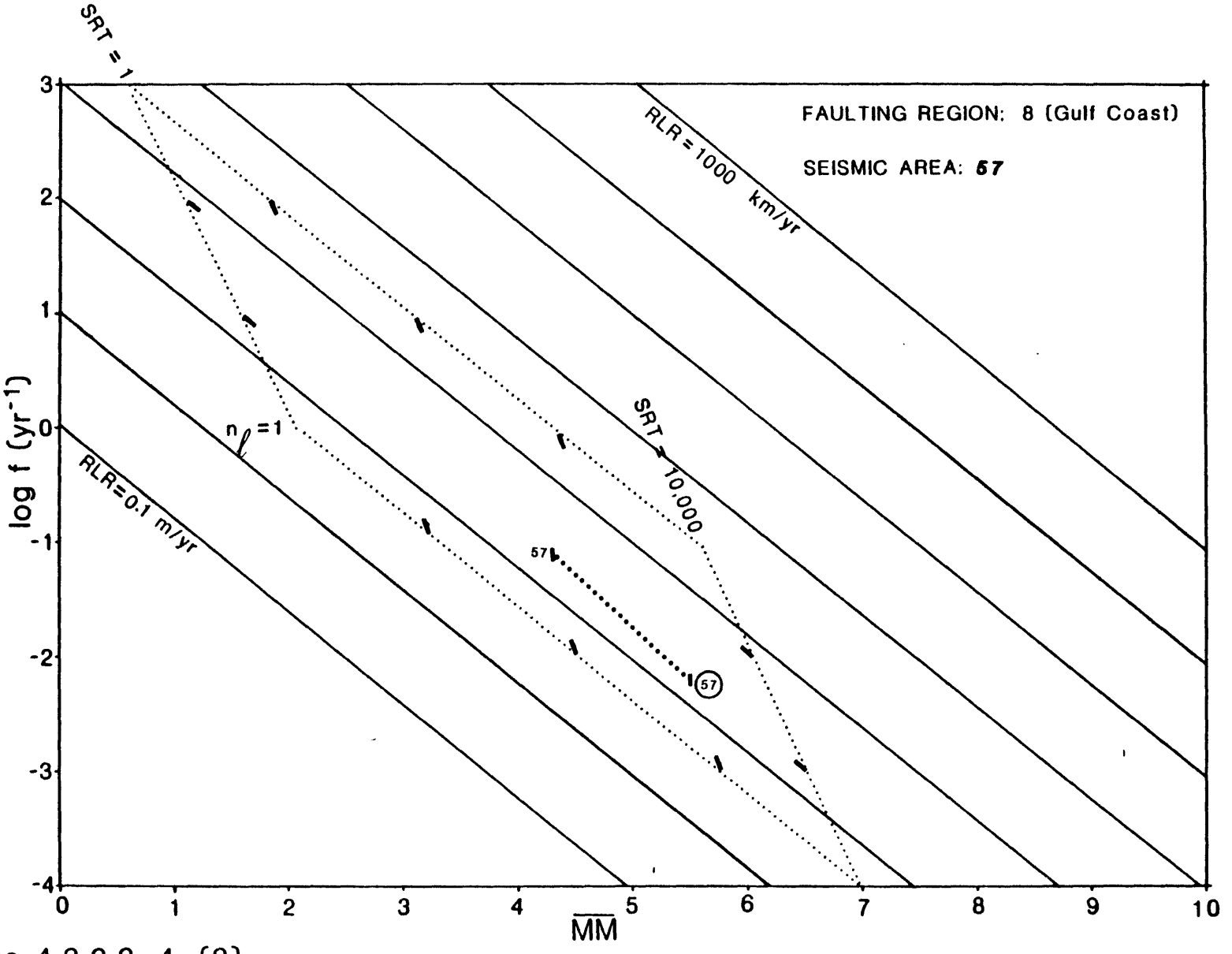

Figure 4.3.2.2.-4. (8)

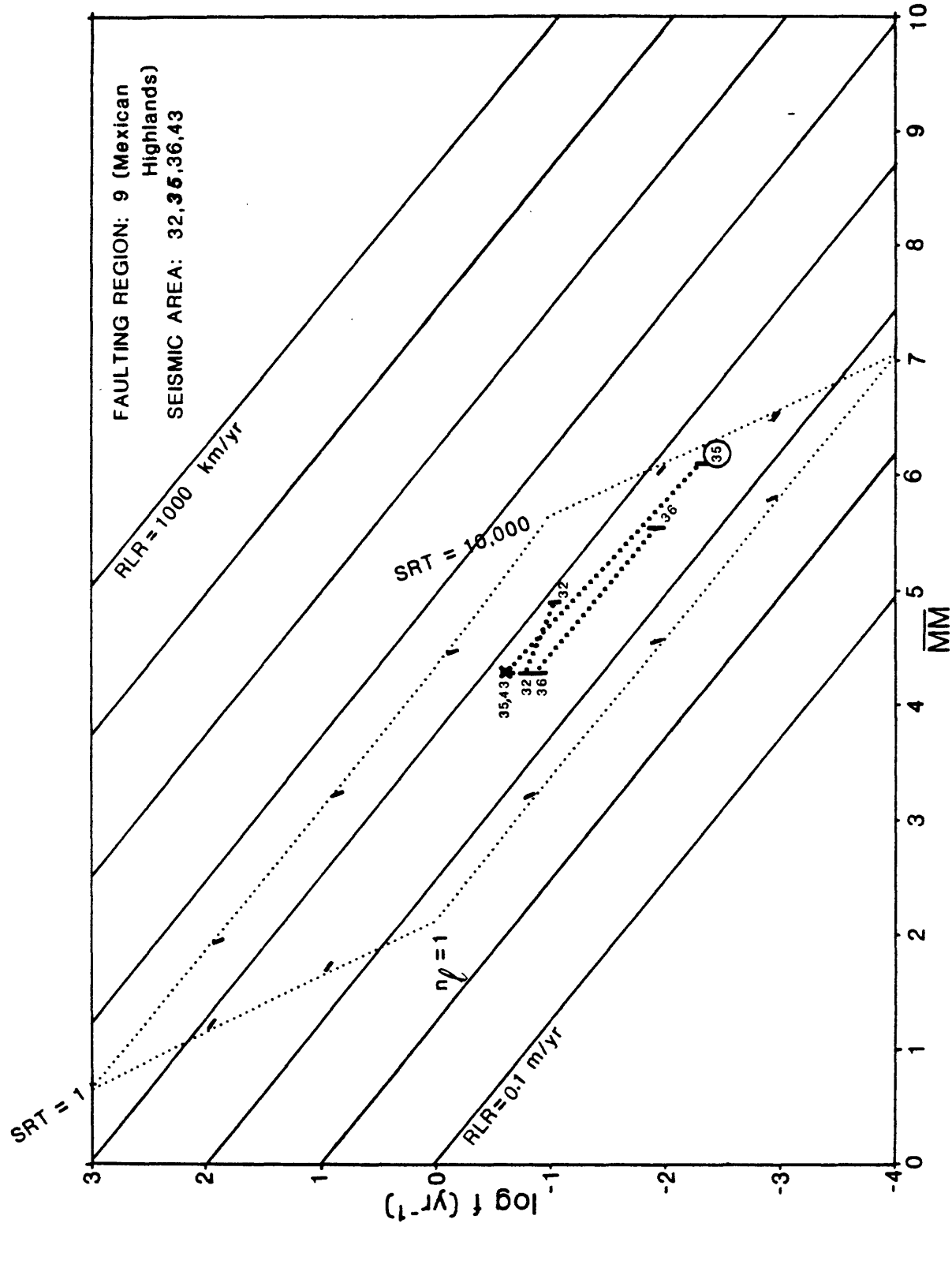

Figure 4.3.2.2.-4. (9)

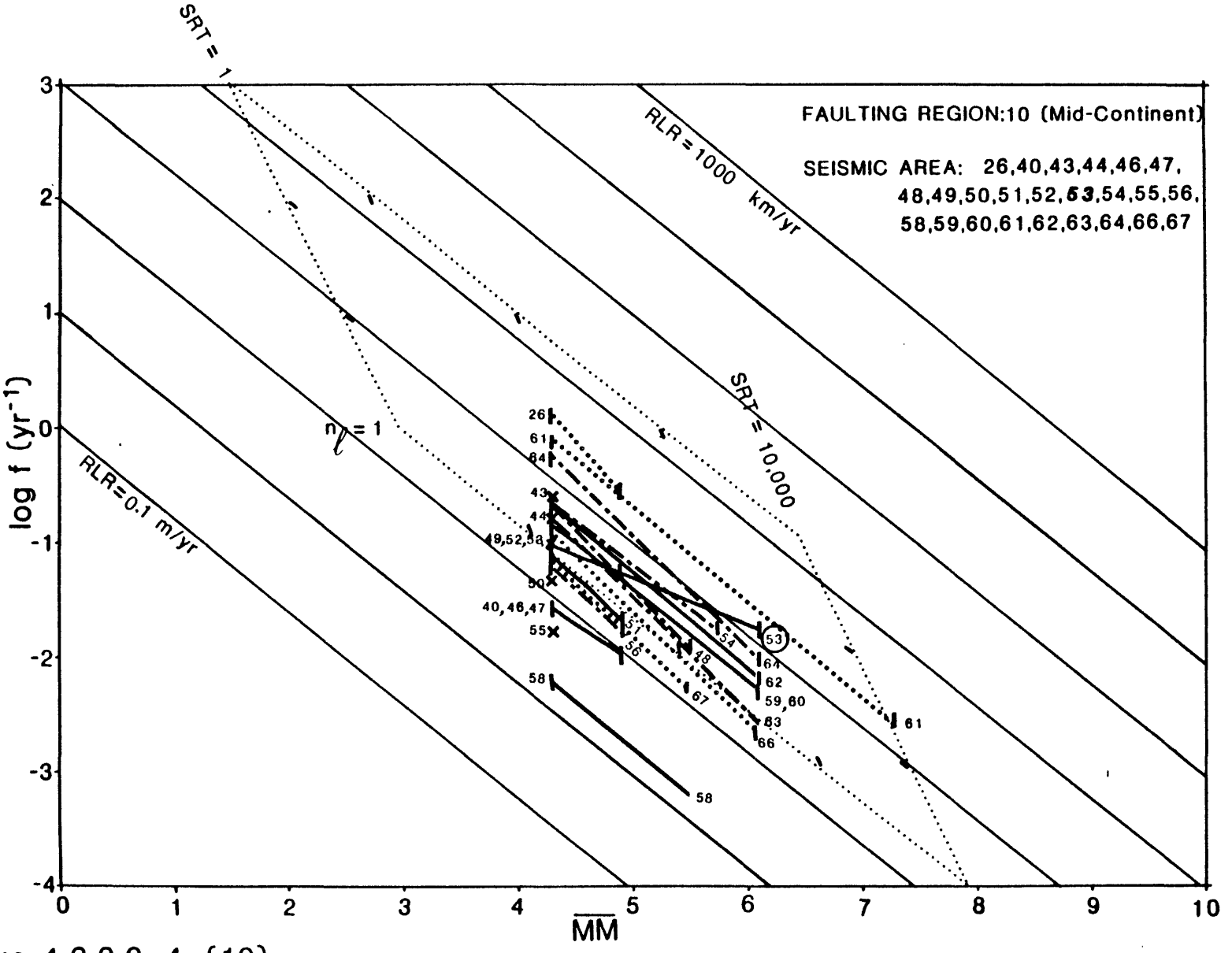

Figure 4.3.2.2.-4. (10)

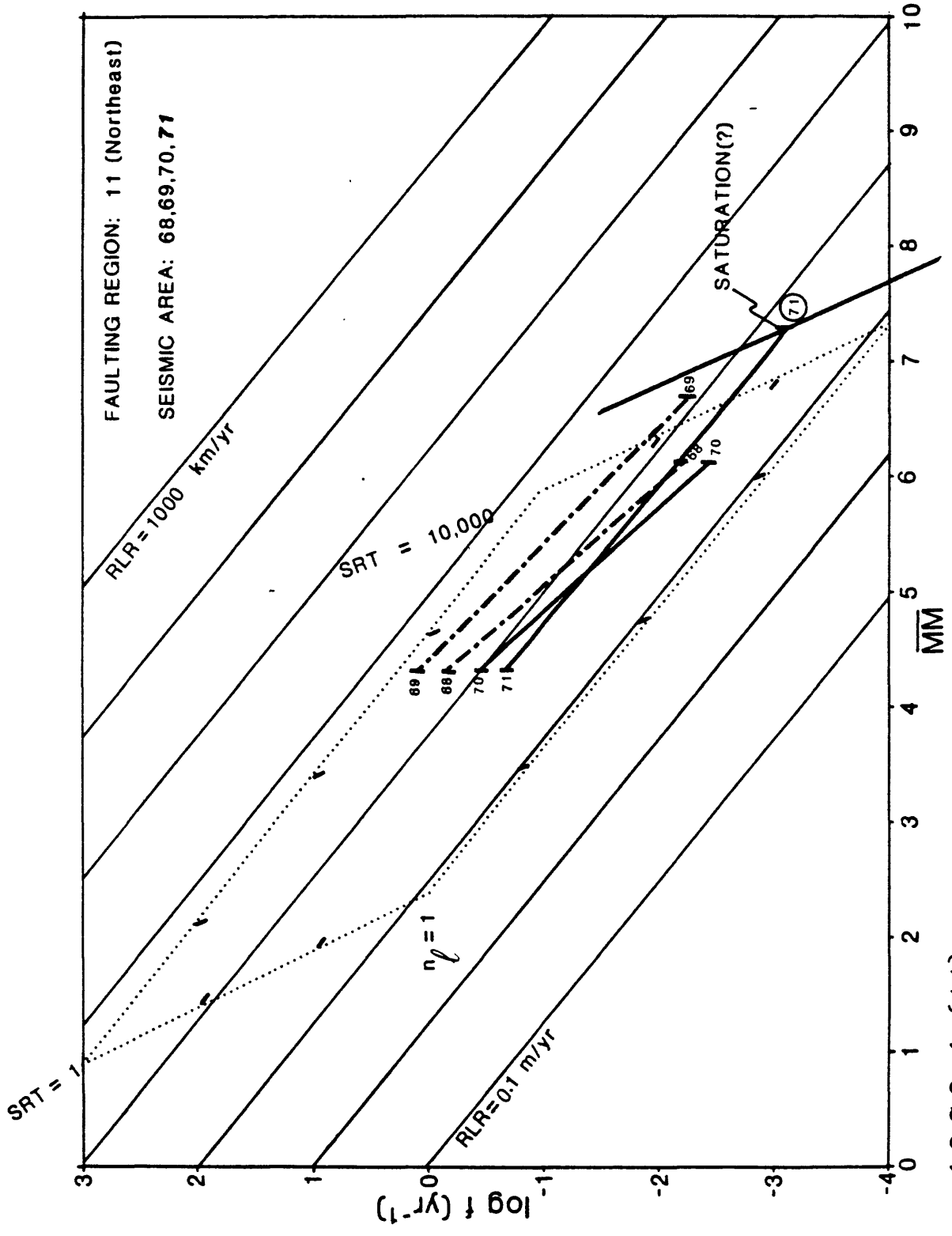

Figure 4.3.2.2.-4. (11)

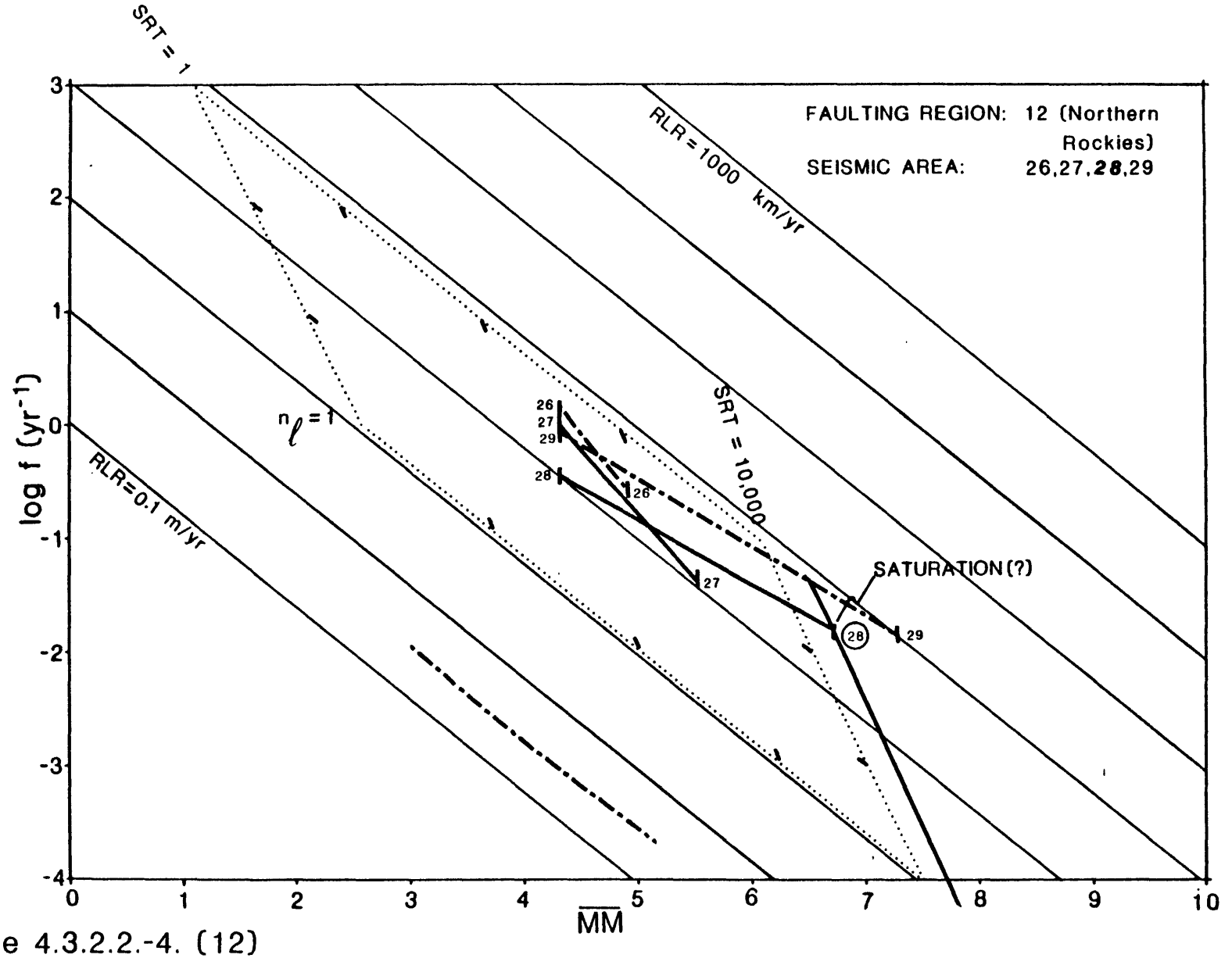

Figure 4.3.2.2.-4. (12)

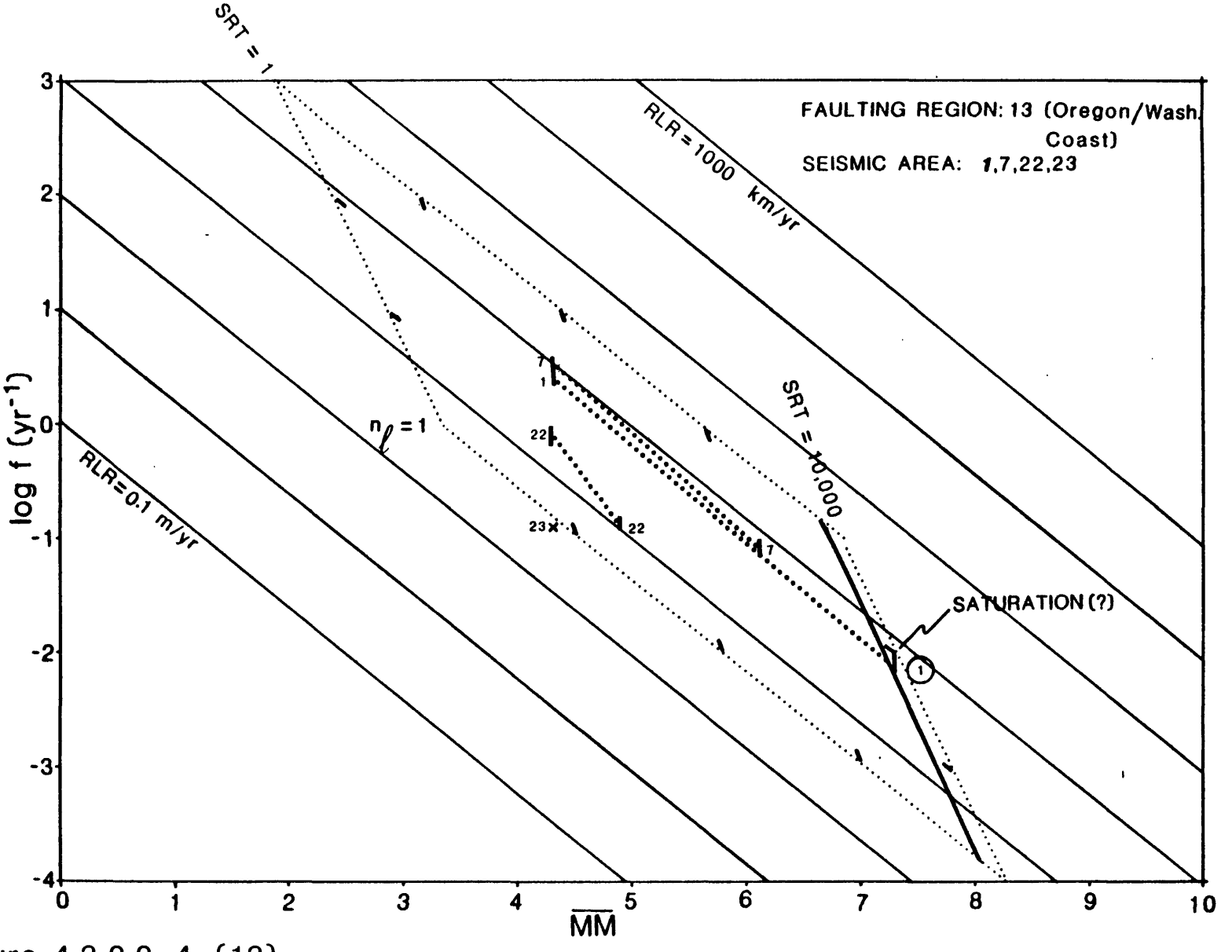

Figure 4.3.2.2.-4. (13)

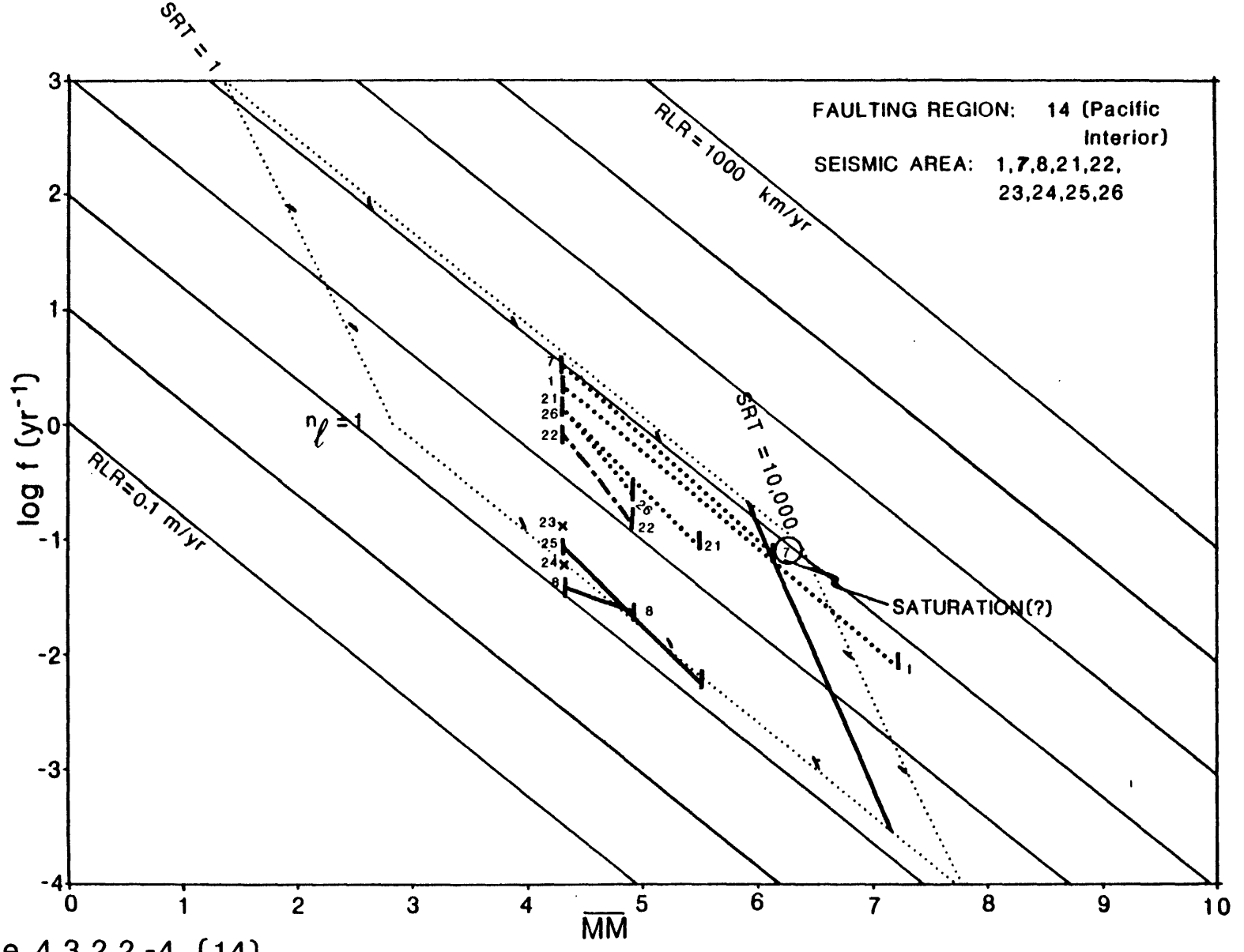

Figure 4.3.2.2.-4. (14)

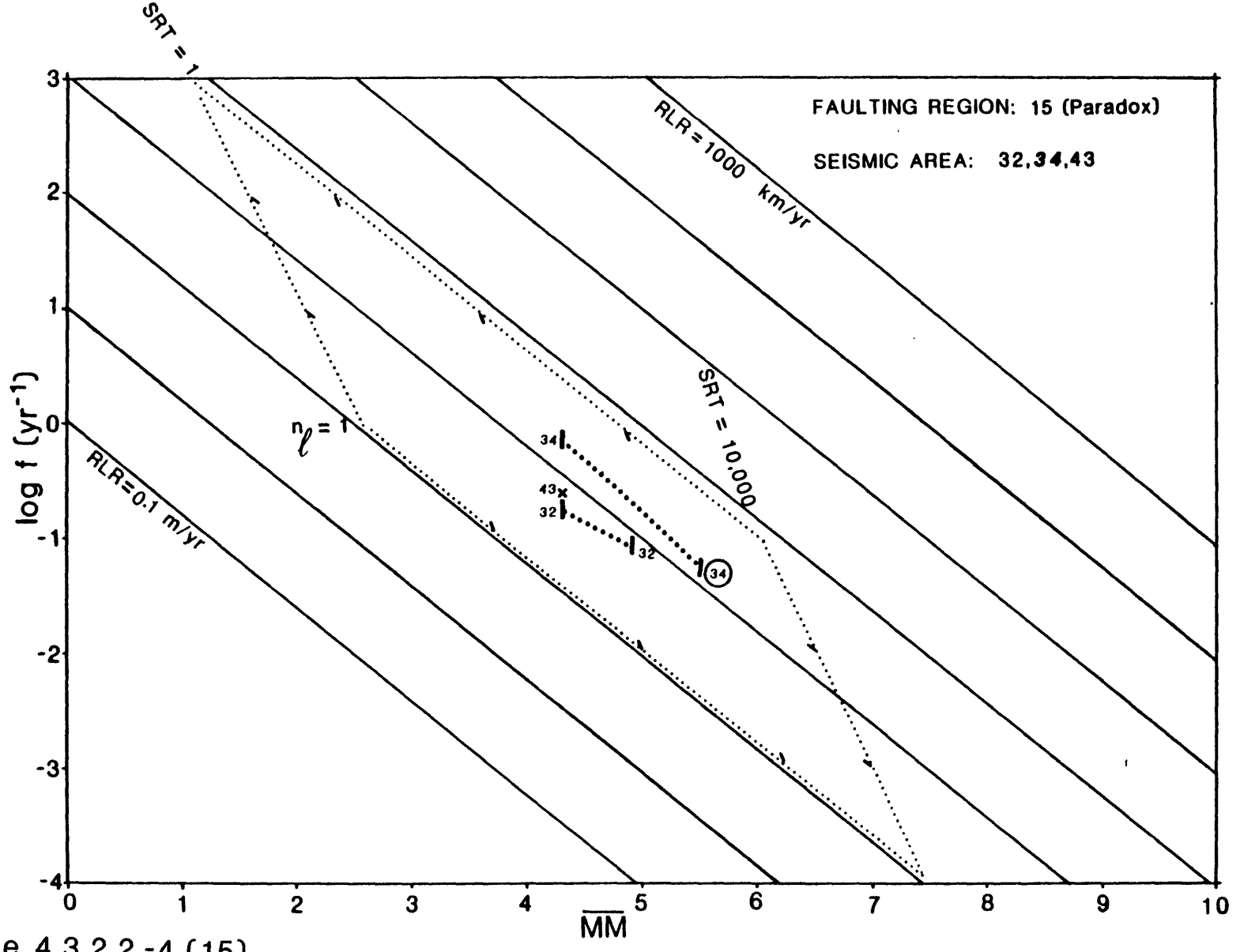

Figure 4.3.2.2.-4.(15)

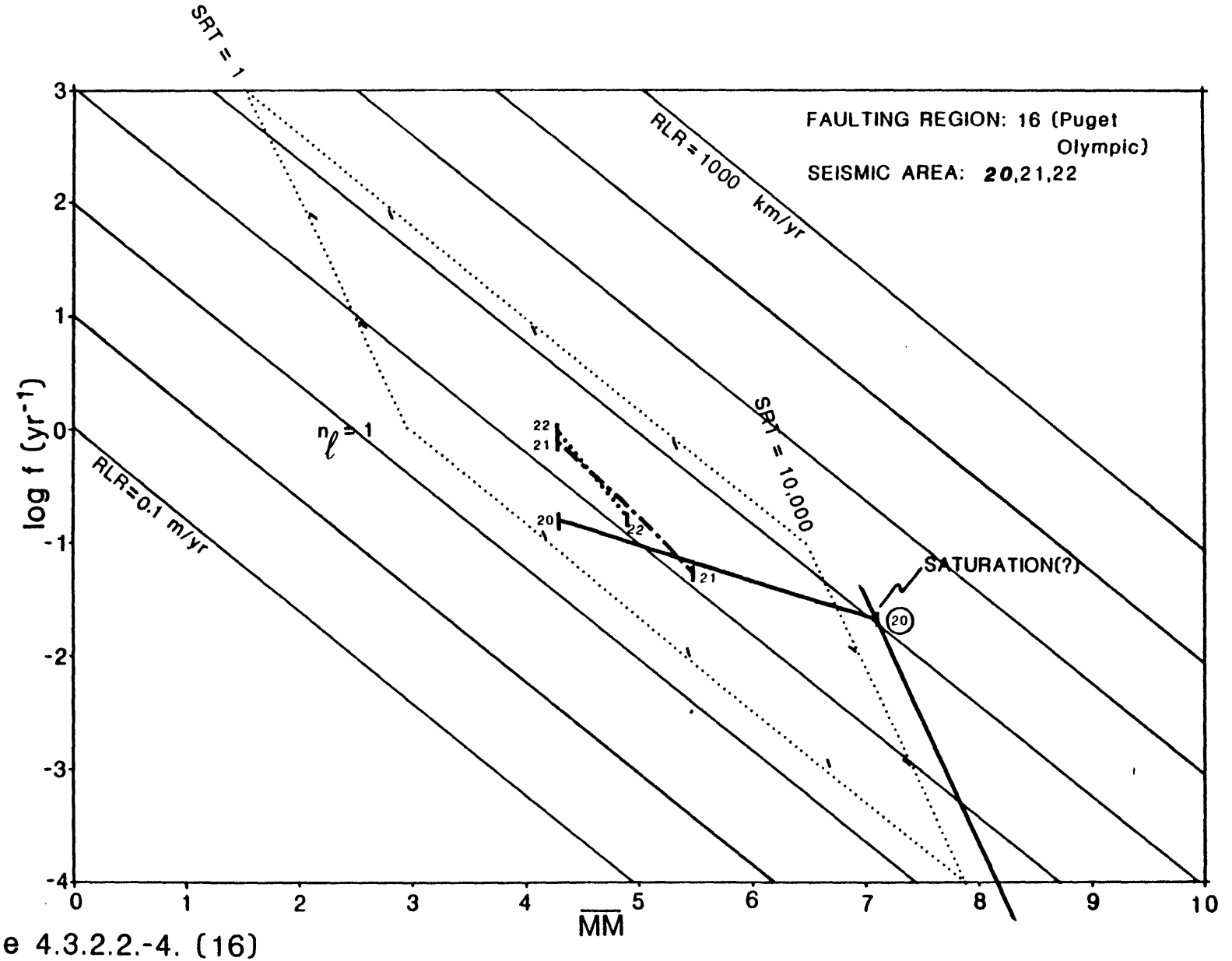

Figure 4.3.2.2.-4. (16)

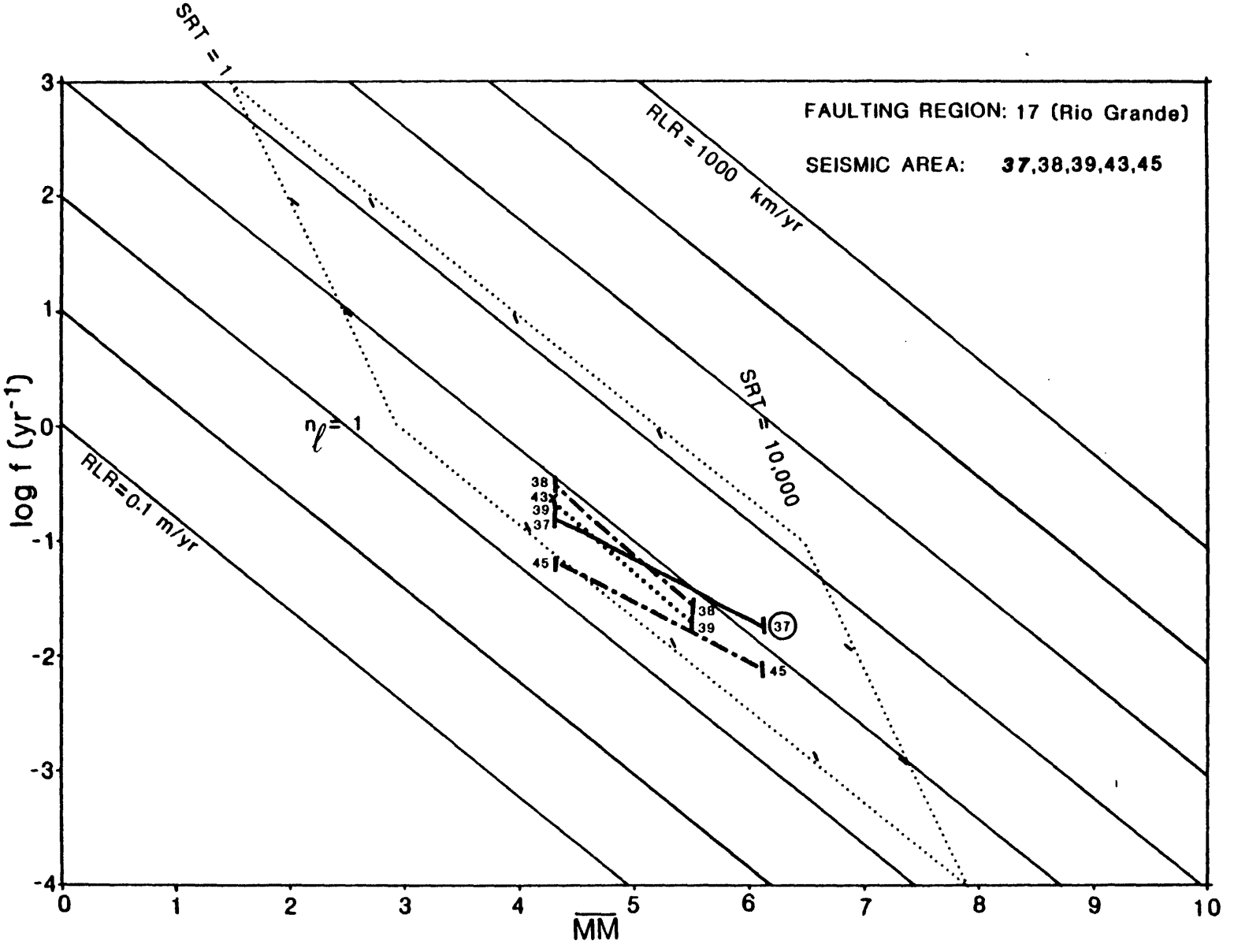

Figure 4.3.2.2.-4. (17)

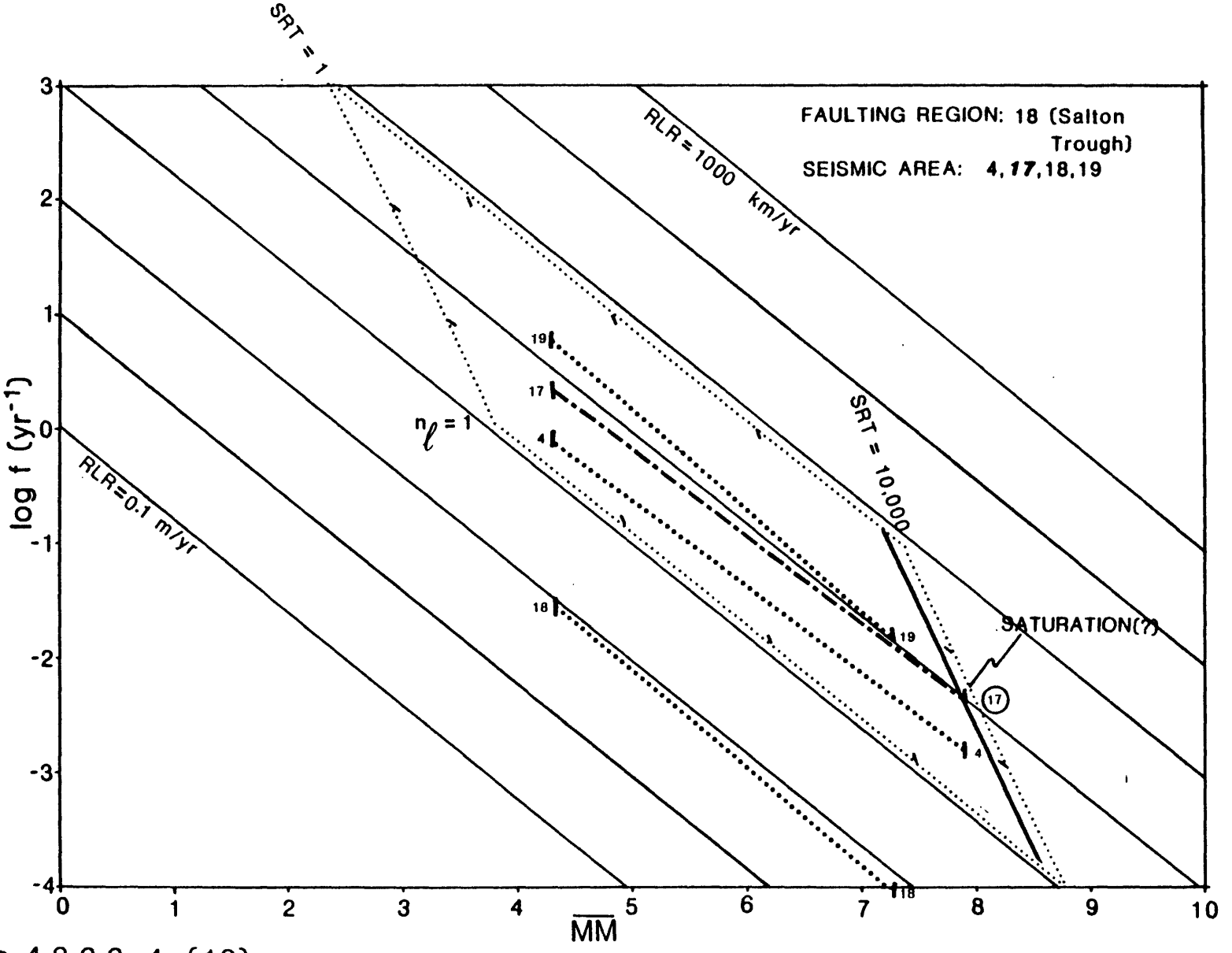

Figure 4.3.2.2.-4. (18)

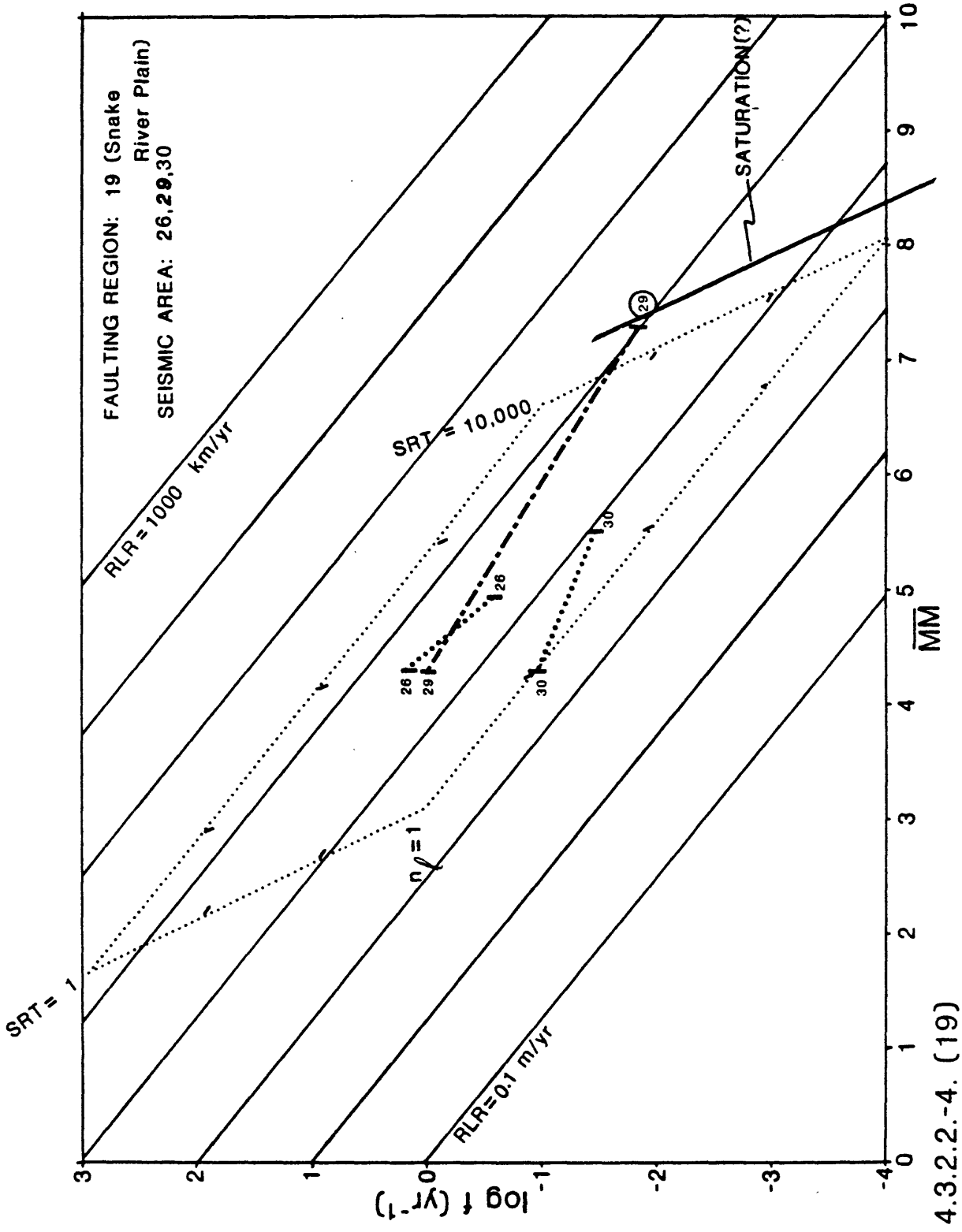

Figure 4.3.2.2-4. (19)

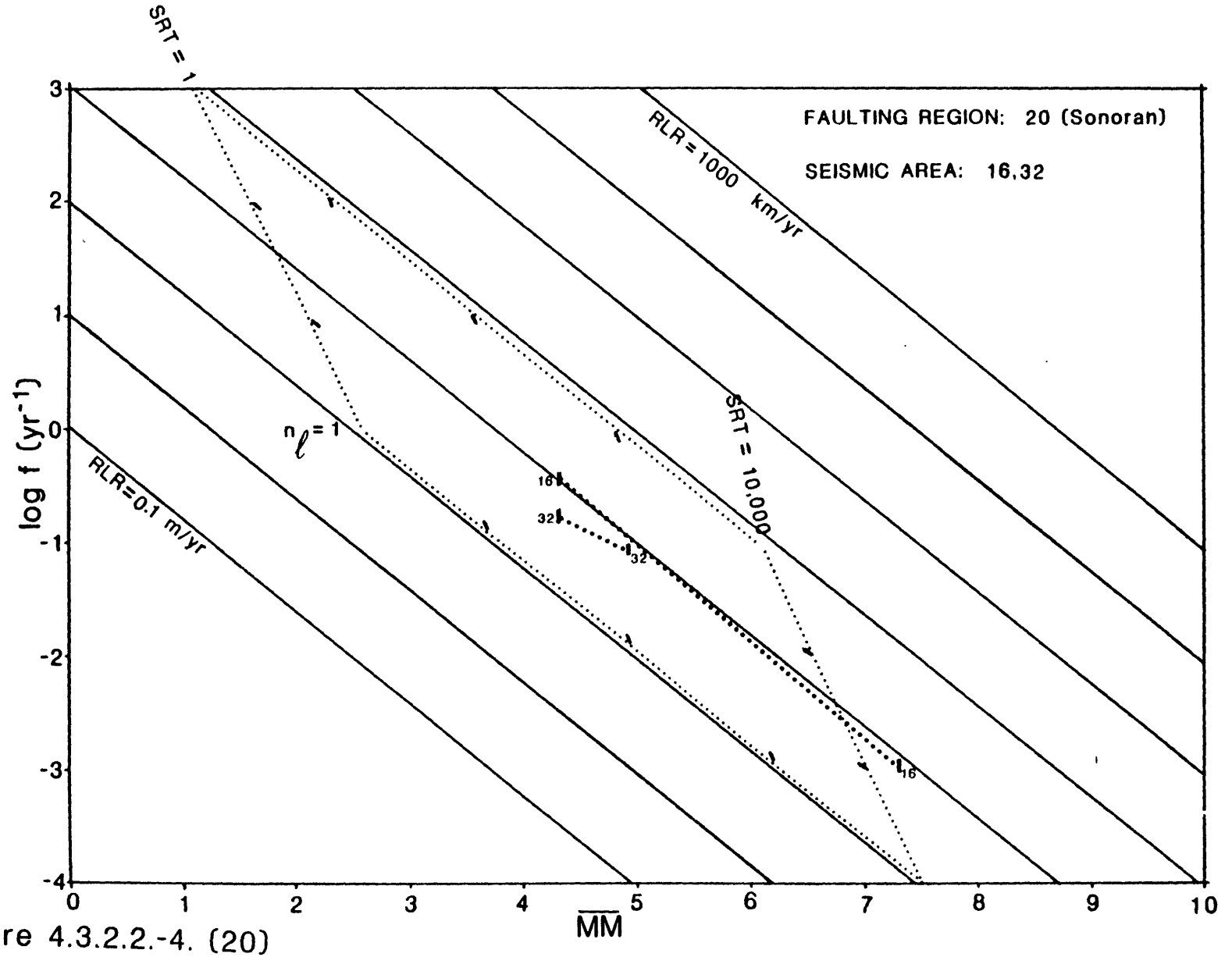

Figure 4.3.2.2.-4. (20)

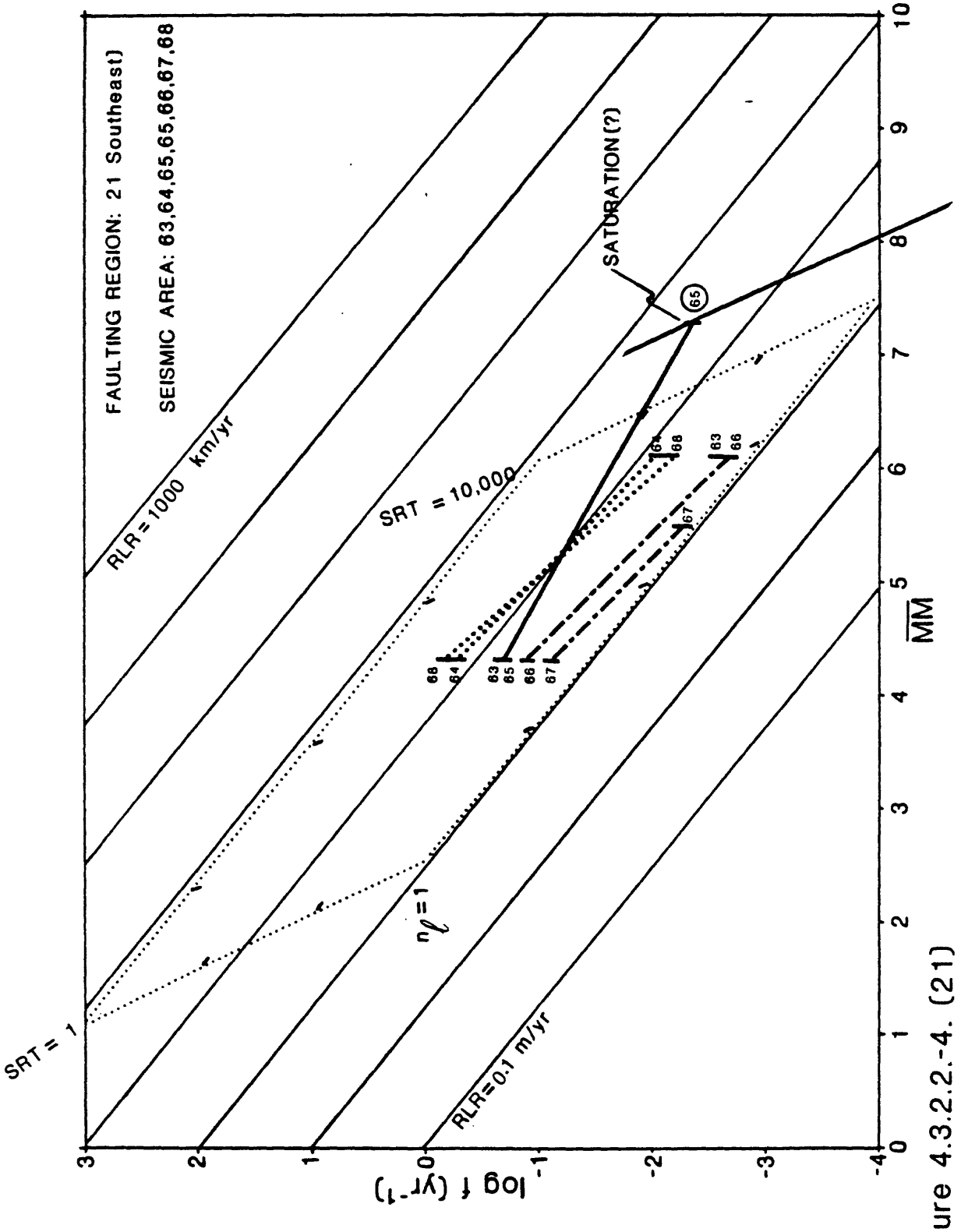

Figure 4.3.2.2.-4. (21)

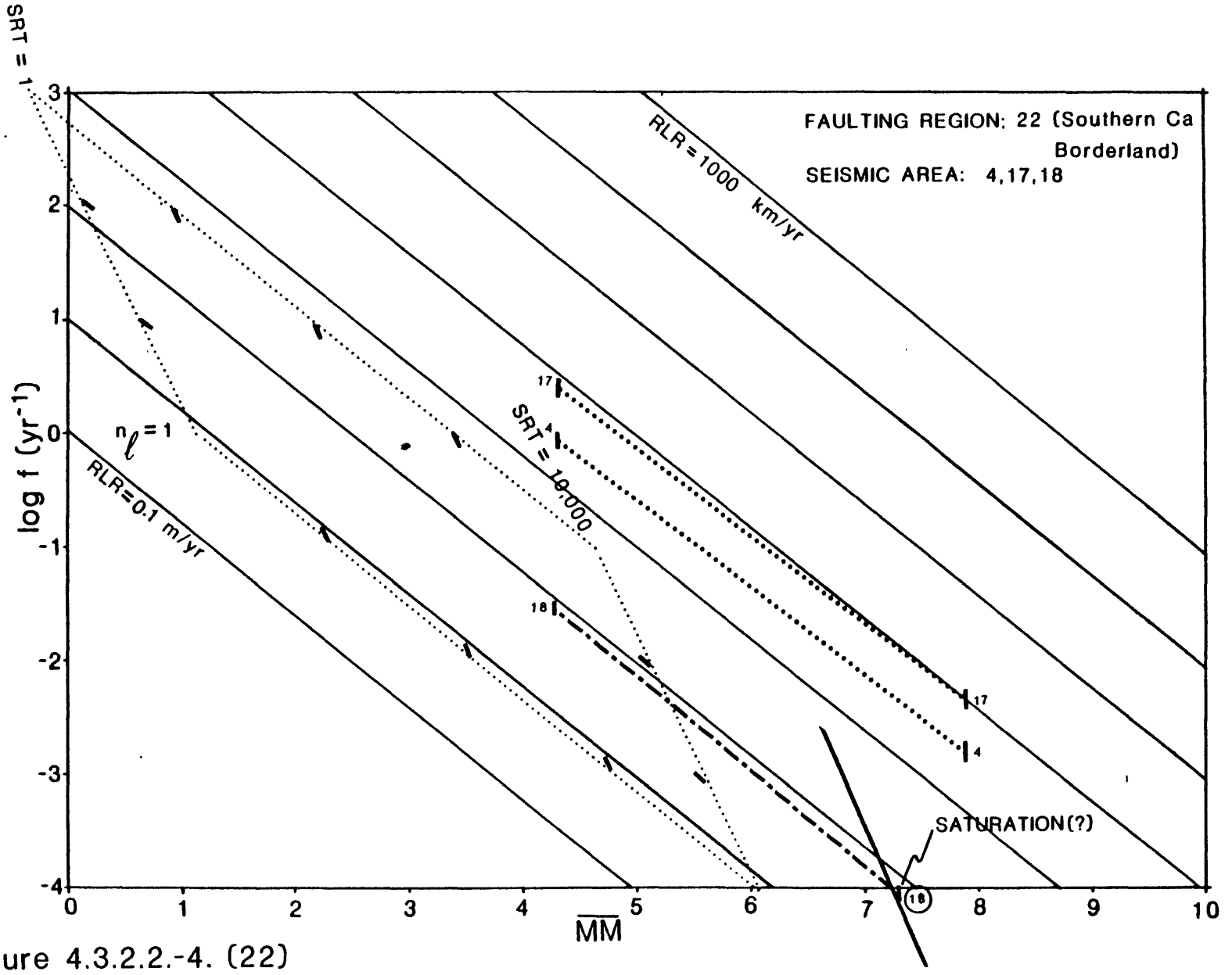

Figure 4.3.2.2.-4. (22)

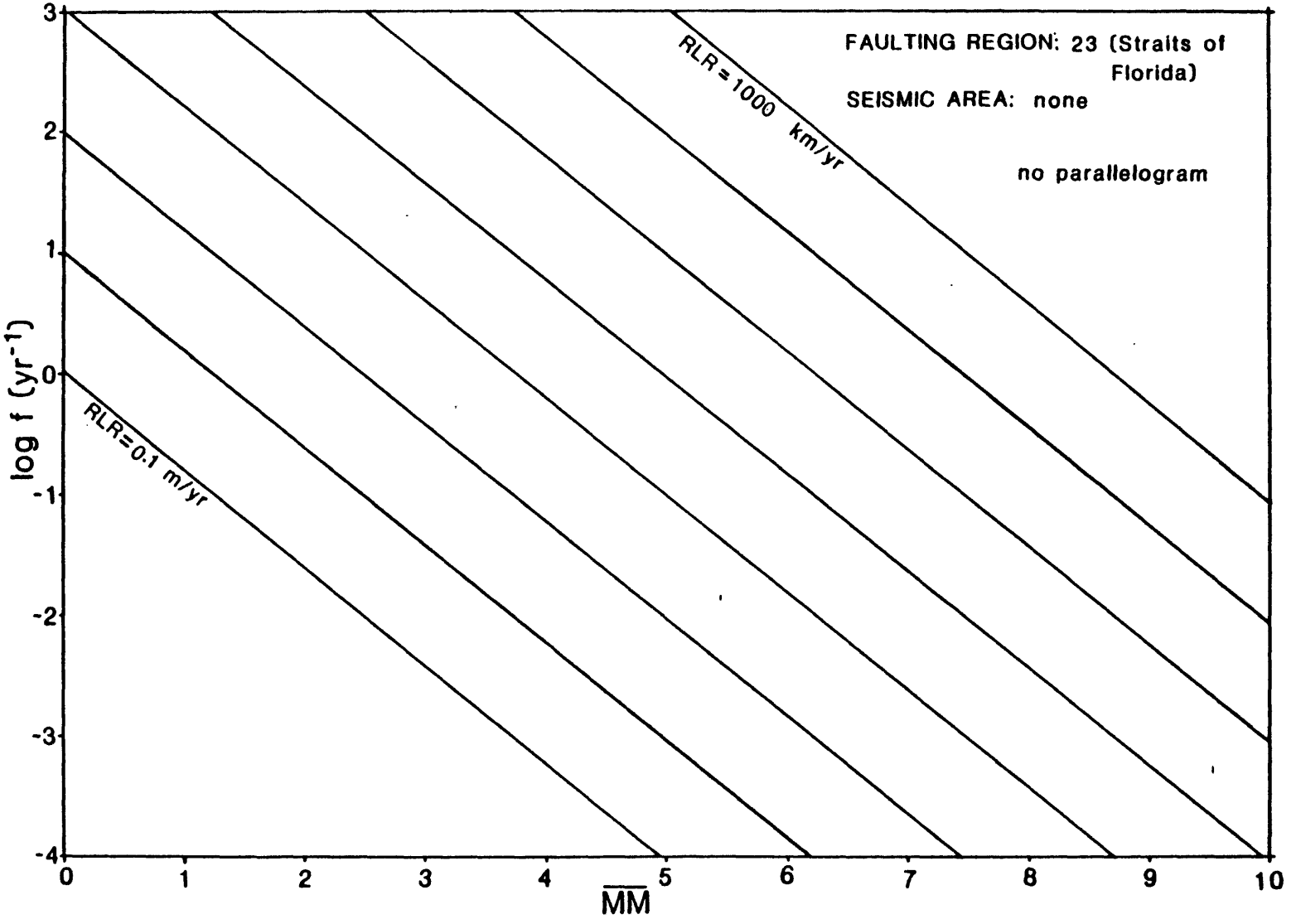

Figure 4.3.2.2.-4. (23)

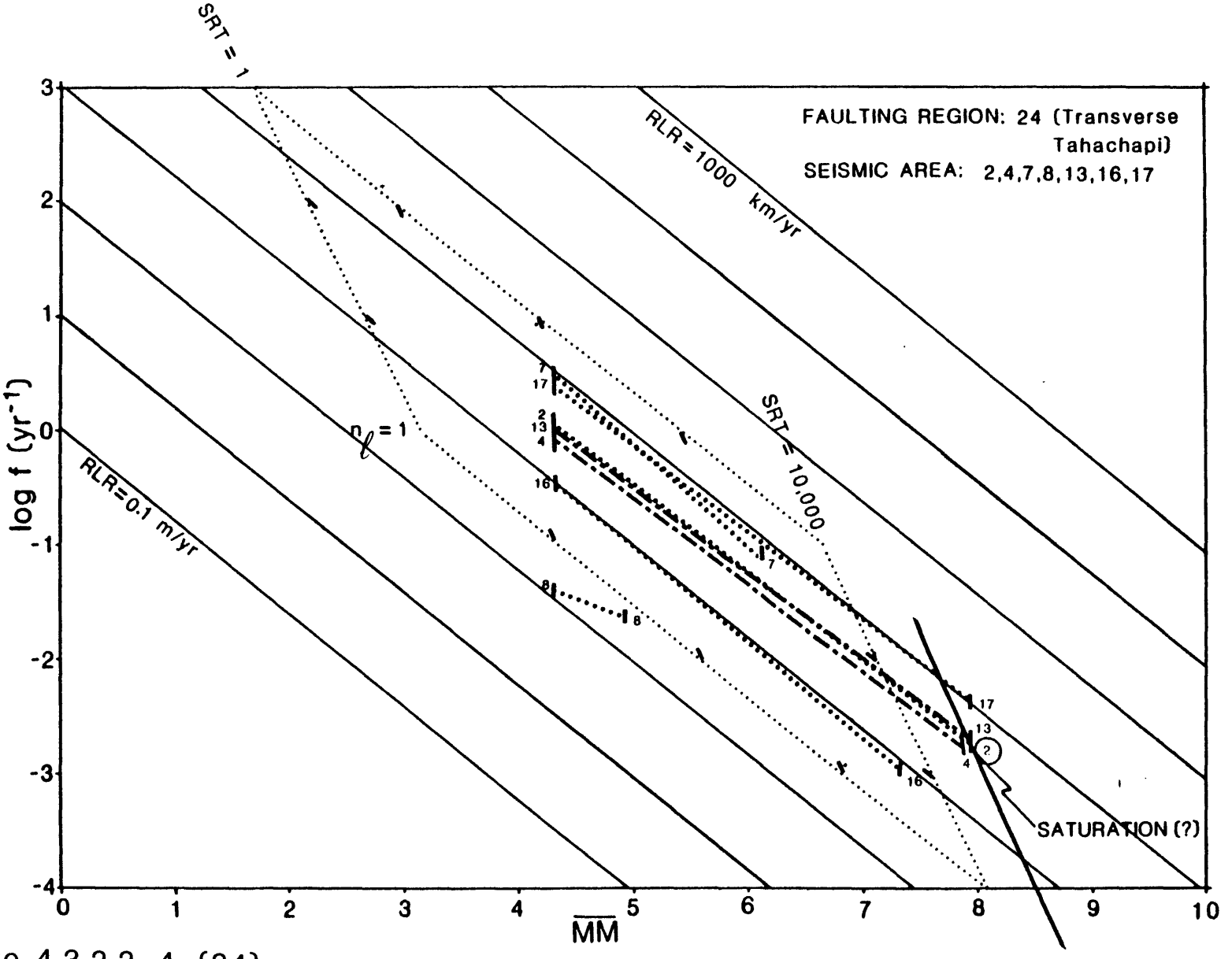

Figure 4.3.2.2.-4. (24)

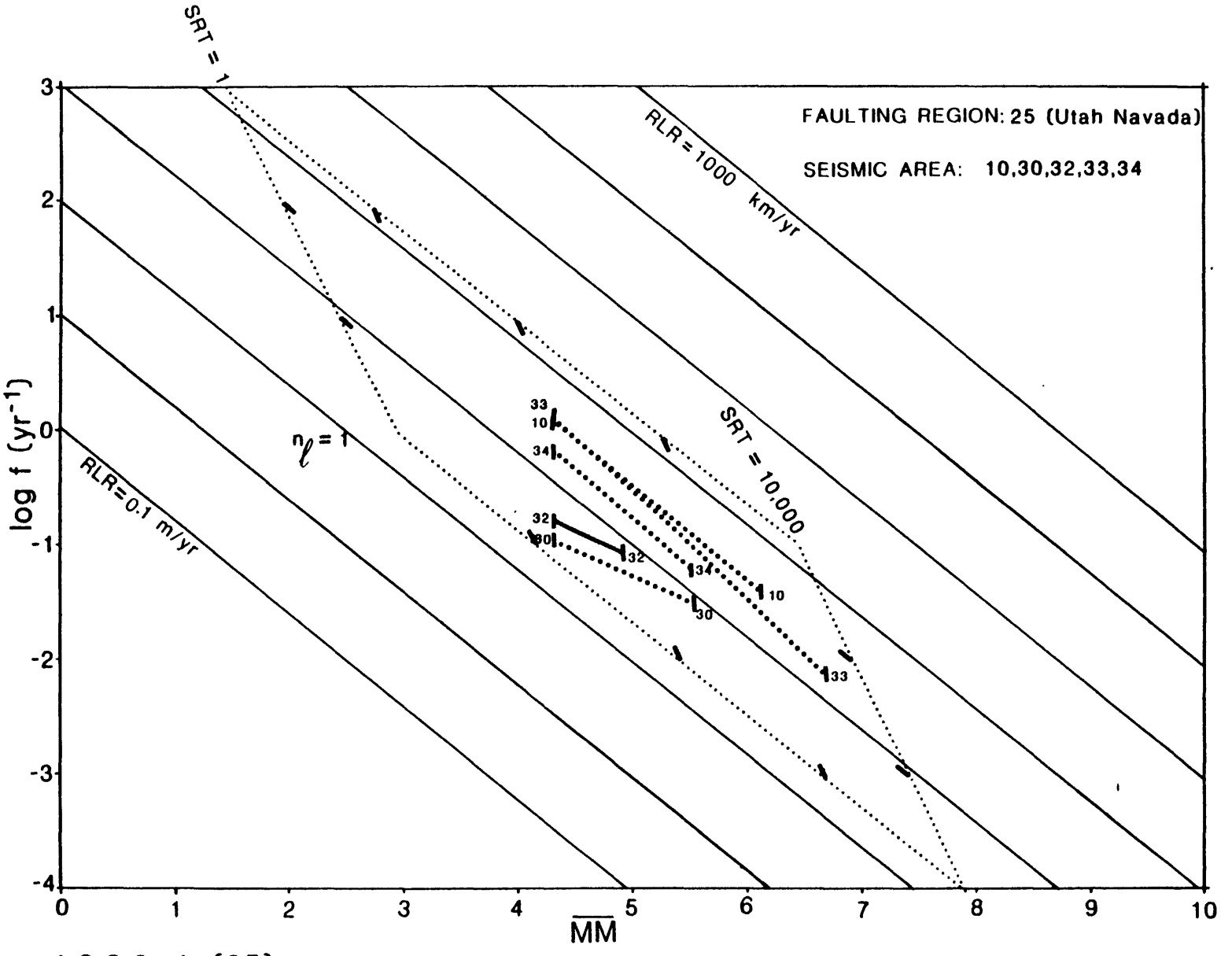

Figure 4.3.2.2.-4. (25)

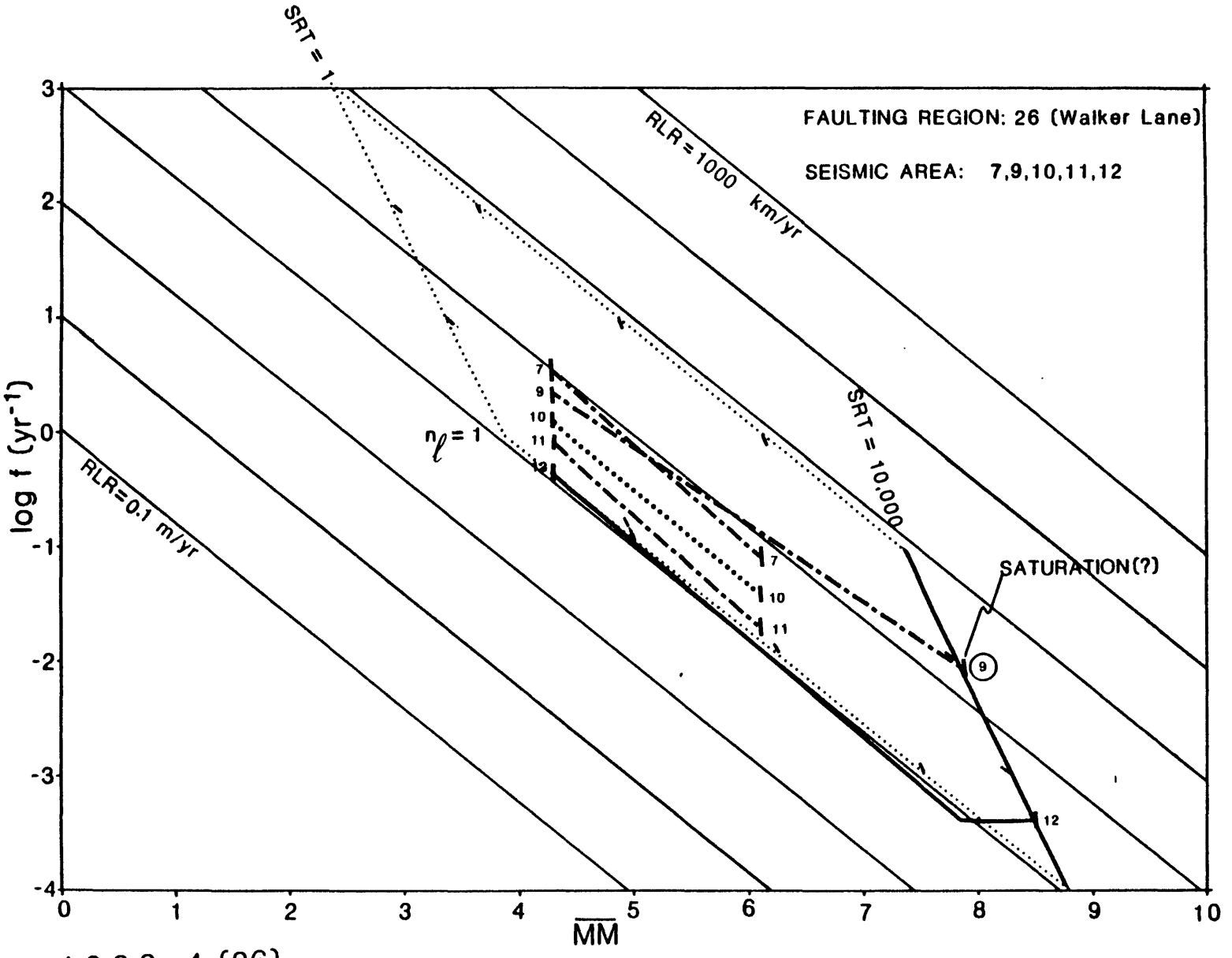

Figure 4.3.2.2.- 4. (26)

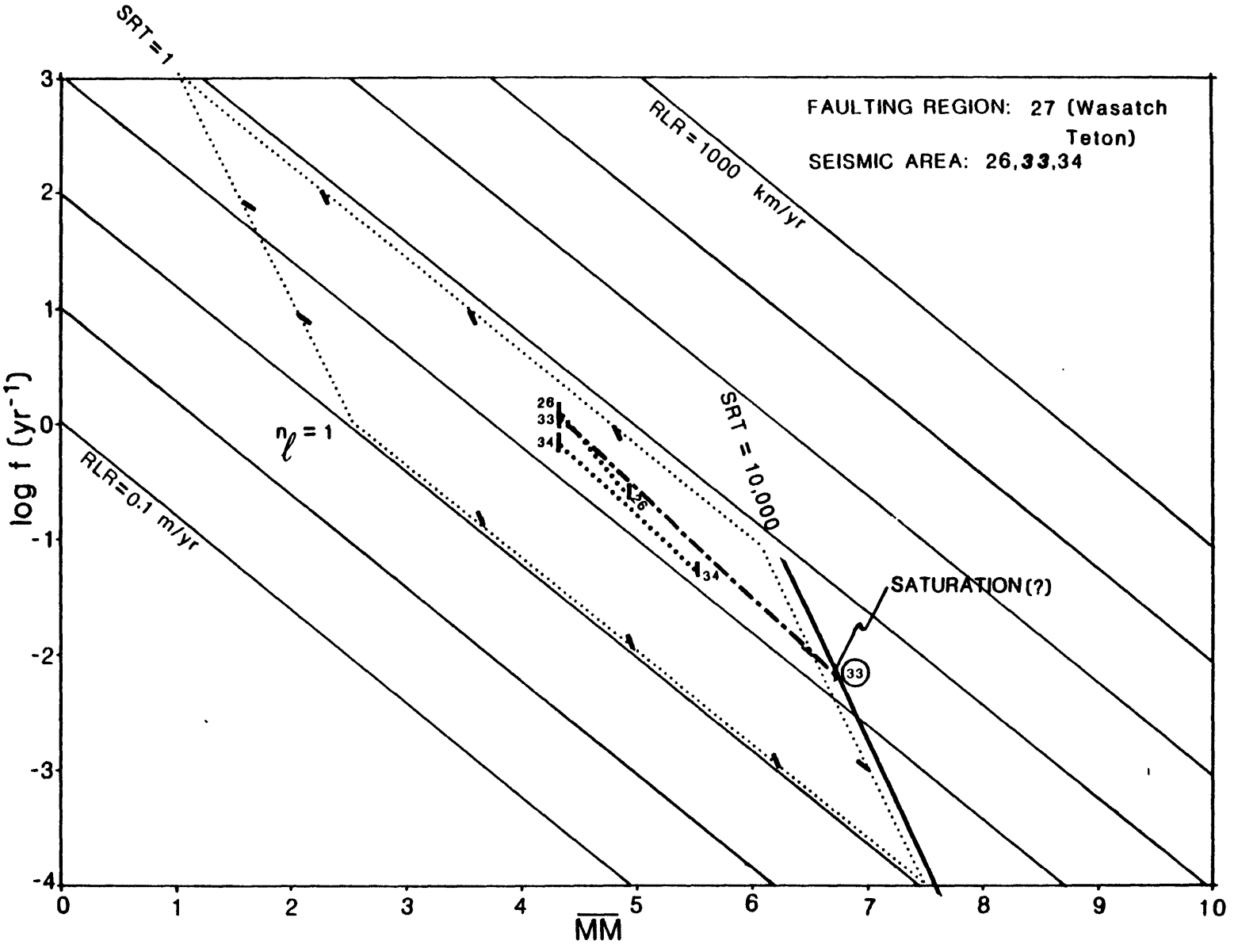

Figure 4.3.2.2.-4. (27)

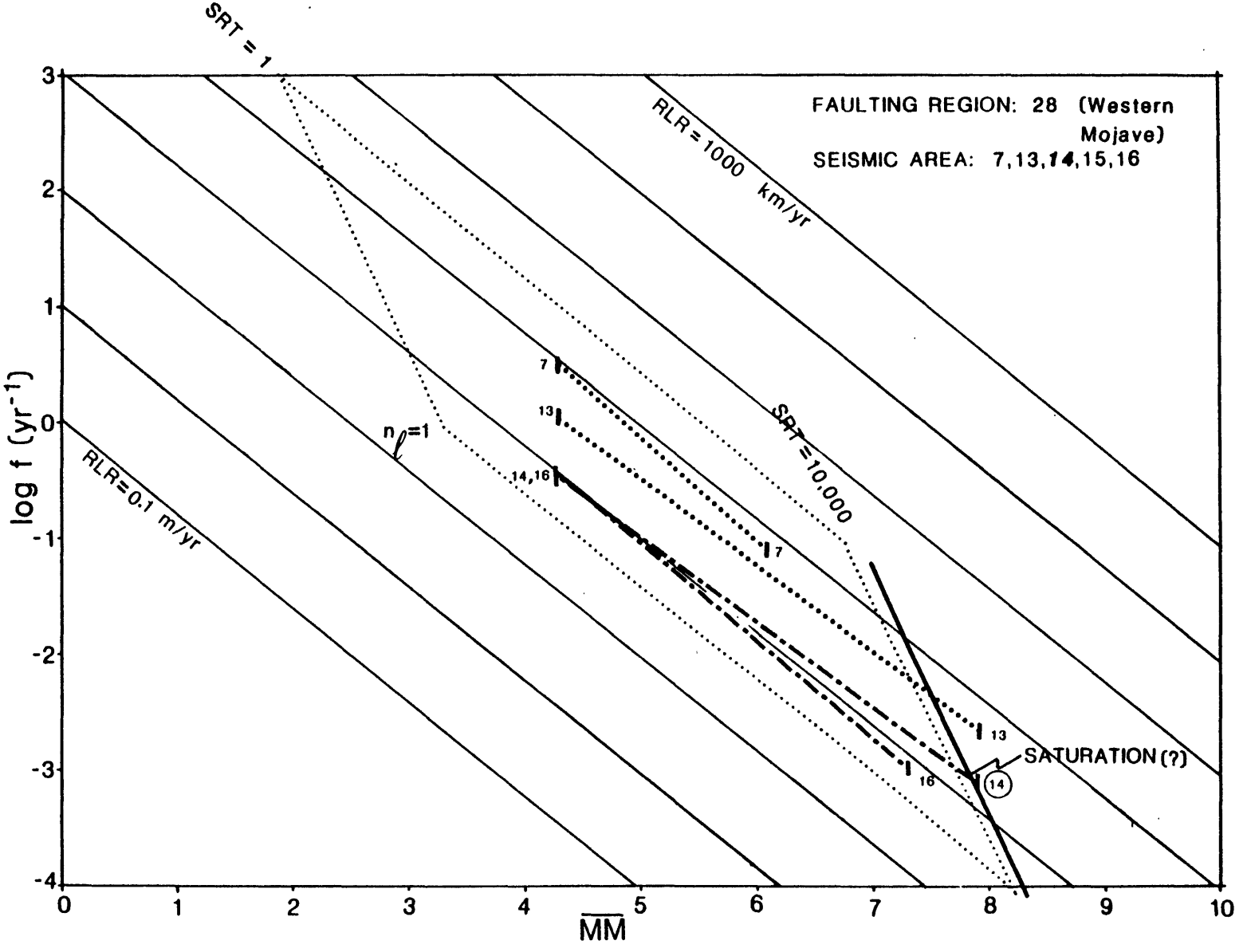

Figure 4.3.2.2.-4. (28)

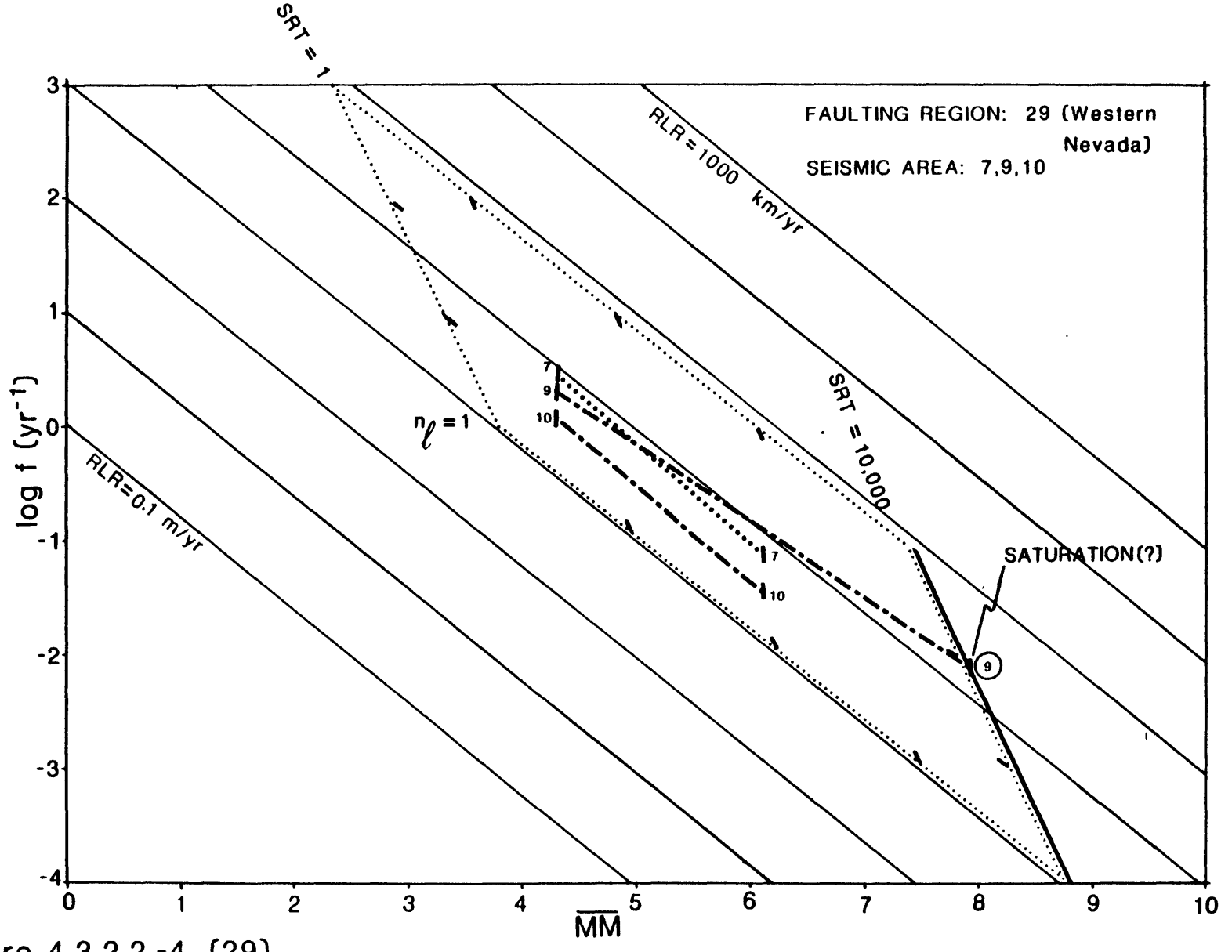

Figure 4.3.2.2.-4. (29)

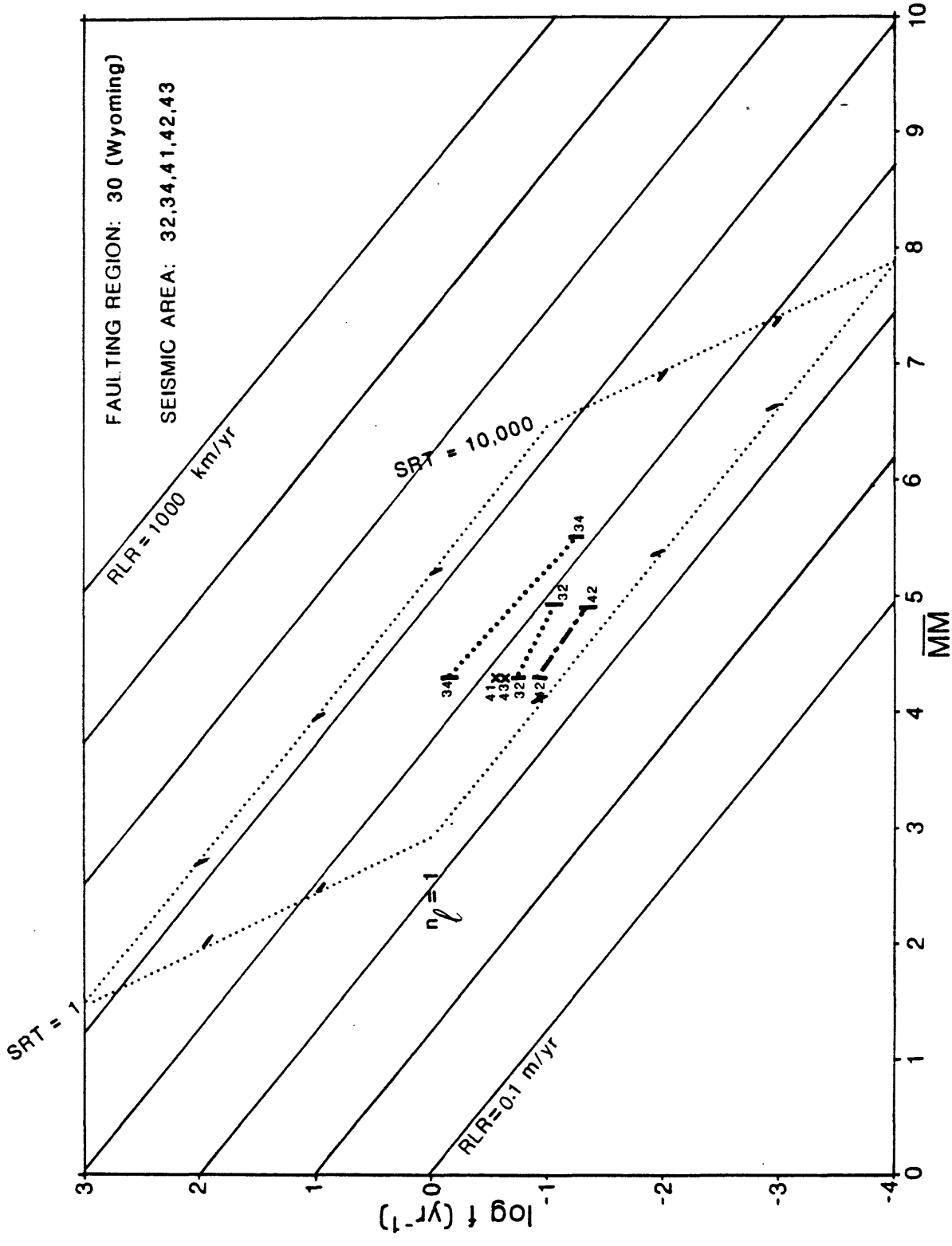

Figure 4.3.2.2.-4. (30)

Table 4.3.2.2.-1. Limits for magnitude-frequency relations calculated from Algermissen and Perkins (1976, Table 1)

Seismic source area[1]	$N_V(yr^{-1})$[2]	log N_V[3]	No. of Max.$I_o(yr^{-1})$	log $N_{Max.I_o}$	Maximum M_C[6]
1	2.45	+0.39	7.8x10-3	-2.11	7.3
2	1.10	+0.04	1.7x10-3	-2.76	8.5
3	0.27	-0.57	5.0x10-4	-3.27	7.9
4	0.75	-0.12	1.5x10-3	-2.82	7.9
5	0.15	-0.83	5.0x10-4	-3.33	7.3
6	0.44	-0.35	9.0x10-4	-3.05	7.9
7	2.99	+0.48	7.8x10-2	-1.11	6.1
8	0.07	-1.14	2.3x10-2	-1.63	4.9
9	2.08	+0.32	8.3x10-3	-2.08	7.9
10	1.25	+0.10	3.7x10-2	-1.43	6.1
11	0.80	-0.10	2.0x10-2	-1.69	6.1
12	0.43	-0.37	4.0x10-4	-3.38	8.5
13	0.99	-0.01	1.9x10-3	-2.70	7.9
14	0.35	-0.46	7.0x10-4	-3.16	7.9
15	0.00	--	--	--	6.1
16	0.34	-0.47	1.1x10-3	-2.97	7.3
17	2.23	+0.43	4.4x10-3	-2.36	7.9
18	0.03	-1.55	9.0x10-5	-4.05	7.3
19	6.14	+0.79	1.5x10-3	-1.81	7.3
20	0.15	-0.83	2.0x10-3	-1.70	7.1
21	0.79	-0.10	5.3x10-2	-1.28	5.5
22	0.80	-0.10	13.8x10-2	-0.86	4.9
23	0.13	-0.90	--	--	4.3
24	0.06	-1.22	--	--	4.3
25	0.08	-1.07	5.6x10-3	-2.25	5.5
26	1.37	+0.14	26.3x10-2	-0.58	4.9
27	0.99	-0.01	4.6x10-2	-1.34	5.5
28	0.35	-0.45	18.6x10-2	-1.73	6.7
29	0.90	-0.04	1.4x10-2	-1.84	7.3
30	0.10	-0.98	3.2x10-2	-1.50	5.5
31	0.85	-0.07	4.7x10-2	-1.33	5.5
32	0.17	-0.77	8.7x10-2	-1.06	4.9
33	1.27	0.10	7.2x10-3	-2.14	6.7
34	0.71	-0.15	5.4x10-2	-1.27	5.5
35	0.23	-0.64	4.8x10-3	-2.32	6.1
36	0.15	-0.82	1.3x10-2	-1.90	5.5
37	0.16	-0.81	1.8x10-2	-1.74	6.1
38	0.31	-0.51	2.6x10-2	-1.59	5.5
39	0.22	-0.67	1.8x10-2	-1.75	5.5
40	0.03	-1.57	1.1x10-2	-1.97	4.9
41	0.28	-0.56	--	--	4.9
42	0.11	-0.95	4.5x10-2	-1.35	4.9
43	0.23	-0.64	--	--	4.3
44	0.14	-0.86	--	--	4.3
45	0.07	-1.17	7.9x10-3	-2.10	6.1
46	0.03	-1.57	1.1x10-2	-1.97	4.9
47	0.03	-1.57	1.1x10-2	-1.97	4.9
48	0.15	-0.83	1.2x10-2	-1.91	5.5
49	0.10	-0.99	--	--	4.3
50	0.05	-1.34	--	--	4.3
51	0.07	-1.13	2.2x10-2	-1.66	4.9
52	0.13	-0.89	5.1x10-2	-1.29	4.9
53	0.09	-1.03	1.8x10-2	-1.75	6.1
54	0.21	-0.67	1.7x10-2	-1.77	5.5
55	0.02	-1.77	--	--	4.3
56	0.06	-1.24	1.7x10-2	-1.77	4.9
57	0.08	-1.11	6.2x10-3	-2.21	5.5
58	0.01	-1.78	6.0x10-4	-3.22	5.5
59	0.16	-0.80	5.0x10-3	-2.30	6.1
60	0.16	-0.80	5.0x10-3	-2.30	6.1
61	0.85	-0.07	2.7x10-3	-2.57	7.3
62	0.22	-0.66	6.9x10-3	-2.16	6.1
63	0.22	-0.66	2.6x10-3	-2.58	6.1
64	0.54	-0.26	9.3x10-3	-2.03	6.1
65	0.20	-0.70	4.5x10-3	-2.35	7.3
66	0.13	-0.89	2.2x10-3	-2.66	6.1
67	0.07	-1.11	5.1x10-3	-2.29	5.5
68	0.69	-0.16	6.8x10-3	-2.17	6.1
69	1.17	+0.07	5.1x10-3	-2.29	6.7
70	0.34	-0.47	3.8x10-3	-2.42	6.1
71	0.22	-0.66	8.0x10-4	-3.11	7.3

1/ The zones are shown in Figure 4.3.2.2-2.
2/ Number of modified Mercalli maximum intensity v's/yr.
3/ Log of number of modified Mercalli maximum intensity V's/yr.; the M_C equivalent of Mercalli V has been calculated as 4.3.
4/ Number of Max I_o earthquakes in one year.
5/ Log number of maximum I_o/yr from equation log N = a+b$_I$+I_o.
6/ M_C for log N max I_o. Note: M_C is the "corresponding magnitude" calculated from the modified Mercalli magnitude from the relation (Algermissen and Perkins 1976, p. 16) $M_C = 1.3 + 0.6\ I_o$

Table 4.3.2.2.-2 Relationship of seismic source areas and 30 faulting regions

	Region	Seismic source areas inside fault region[1/] Total portion	Major portion	Minor portion
1	Arizona Mountain Belt		32,36	38,43
2	California Coast	3,5,6	1,2	4,7
3	Central Mississippi Valley		61	60
4	Circum-Gulf		56,57	61,64
5	Eastern Oregon-Western Idaho		30,31	10
6	Four Corners		39	32,34,38,43
7	Grand Canyon		34	32
8	Gulf Coast			57
9	Mexican Highland			32,35,36,43
10	Mid-continent	40,44,46,47,49,50 51,52,53,55,58,59,62	48,54,56,60,63,64	61,66,67
11	Northeast	70,71	68,69	
12	Northern Rockies	27,28	26,29	
13	Oregon-Washington Coast			1,7,22,23
14	Pacific Interior	8,25	22,23,24	1,7,21,26
15	Paradox			32,34,43
16	Puget-Olympic	20	21	22
17	Rio Grande	37	38,43,45	39
18	Salton Trough		17	4,18,19
19	Snake River Plain		29	26,30
20	Sonoran			16,32
21	Southeast	65	66,67	63,64,68
22	Southern Calif. Borderland		18	4,17
23	Straits of Florida			
24	Transverse Ranges-Tehachapi		4,13	2,7,8,16,17
25	Utah-Nevada	32		10,30,33,34
26	Walker Lane	12	7,9,11	10
27	Wasatch-Tetons		33	26,34
28	Western Mojave	14,15	16	7,13
29	Western Nevada		9,10	7
30	Wyoming		41,42,43	32,34

1/ from Algermissin and Perkins (1976, Table 1).
Total portion is represented as solid line on parallelograms.
Major portion is represented as dashed line on parallelograms.
Minor portion is represented as dotted line on parallelograms.

Table 4.3.2.2.-3 Rupture length rates inferred from seismic data compared with faulting rates; frequency versus magnitude data from Algermissen and Perkins (1976). See author's note at bottom of table.

Fault Region	Seismic Source Area [1]	M_c [2]	log f (year^{-1})	L(calc.) [3] km	F.R.L.R. [4] (m/yr)	X_L [5]	R.L.R. [6] (m/yr) Seismic (inferred)	R.L.R. [6] (m/yr) Faulting (observed)
1	36	5.5	-1.90	2.7	35	0.05	700	10
2	2	7.9	-2.76	230	400	0.1	4000	1000
3	61	7.3	-2.57	76	204	0.2	800	10
4	57	5.5	-2.21	2.7	17	0.05	330	--
5	31	5.5	-1.33	2.7	125	0.05	2500	~100
6	39	5.5	-1.75	2.7	45	.05	900	~100
7	34	5.5	-1.27	2.7	145	0.1	1450	10
8	57	5.5	-2.21	2.7	17	0.05	330	1000
9	35	6.1	-2.32	8.2	40	0.1	400	1000
10	53	6.1	-1.75	8.2	145	0.1	1450	100
11	71	7.3	-3.11	76	60	0.1	600	--
12	28	6.7	-1.73	25	460	0.5	920	~1000
13	1	7.3	-2.11	76	600	0.2	3000	>100
14	7	6.1	-1.11	8.2	630	0.5	1260	1000
15	34	5.5	-1.27	2.7	145	0.2	720	~1000
16	20	7.1	-1.70	52	1000	0.6	1700	~3000
17	37	6.1	-1.74	8.2	150	0.1	1480	~1000
18	17	7.9	-2.3	230	900	0.1	9000	~10,000
19	29	7.3	-1.84	74	1000	0.5	2000	~10,000
20	32	4.9	-1.06	0.9	80	0.1	800	--
21	65	7.3	-2.25	76	430	0.5	860	--
22	18	7.3	-4.05	76	7	0.1	70	~100
23	--	--	--	--	--	--	--	--
24	13	7.9	-2.70	230	460	0.2	2300	~10,000
25	10	6.1	-1.43	8.2	300	0.2	1500	~100
26	9	7.9	-2.08	230	1900	0.2	9500	~10,000
27	33	6.7	-2.14	25	180	0.3	600	~1000
28	14	7.8	-3.16	190	132	0.05	2640	~10,000
29	9	7.9	-2.08	230	1900	0.2	9500	~10,000
30	34	5.5	-1.27	2.7	145	0.1	1450	--
						Sum	62,760	71,630

1/ From Algermissen and Perkins (1976, Figure 2); the indicated Seismic Source Areas were chosen generally to maximize rupture length and rupture length rate.
2/ Maximum magnitude from Algermissen and Perkins (1976, Table 1).
3/ Length calculated from M_c according to Mark (1977, Figure 3, BB).
4/ Fractional rupture length rate; event length times frequency.
5/ Length fraction estimated from ranges of lengths and rates.
6/ Rupture length rate; F.R.L.F./X_L for seismic data; estimates for projected faulting rates are listed for comparison.

Author's note: The length is calculated from Figure 3, curve BB' in Mark (1977) rather than his curve AA' because we wish to determine the lengths that would give the magnitude data assuming that those length data existed. In other words we are using the regression for magnitude on length throughout because we are comparing data sets as though length is the independent variable of interest. If we wish to determine the best estimate for actual rupture rates, a correlation of length on magnitude should be used (see Mark and Bonilla, 1977).

SECTION 5.

5. Summary of Earthquake and Faulting Relations.

Figure 5.-1 compares parallelograms derived, respectively, from faulting data and earthquake data. In many instances the fault-based paleoseismic parallelogram is at lower frequencies or at lower magnitudes than the seismic-derived parallelograms. On the other hand, the summations for rupture length rates, in the respective categories, are approximately equal (Table 4.3.2.2.-3). The conclusions we can draw from the comparison include the following points:

(a) Some fault regions do not have faulting rates representing the level of seismic activity going on in those regions, and some regions that have no mapped young active faults have significant seismicity. In view of the overwhelming agreement between faulting rates and seismicity levels in other regions, we must conclude that undetected fault movements are occurring in those regions as well. The regions that appear to have nonrepresentatively low indications for faulting activity are the following: 1, 3, 5, 6, 7, 10, 13, and 25; and regions having no indicated young fault movements but significant seismicity are: 4, 11, 20, 21, and 30. Region 23, Straits of Florida, has no indications for either significant faulting rates or seismicity at the present time. Thus, more than half the faulting regions are matched fairly well in the faulting rates inferred, respectively, from faulting statistics and earthquake magnitude-frequency relations. That level of correspondence is strong confirmation for the statistical significance in the geologic faulting data.

(b) Faulting regions and seismic source areas obviously do not closely correspond geographically. Thus, the numerical correspondences in Table 4.3.2.2.-3 may be poor in specific instances because faulting regions are areally less selective than seismic source areas. The correspondence between total activation rates, however, suggests that there is an overall balance between quasisteady faulting rates and earthquake frequencies in the continent as a whole.

(c) The lines marked SATURATION in the parallelograms derived from faulting rates give an indication for maximum expectable earthquakes because they are based on the longest probable lengths of fault activation in each region. This is so even though the frequencies may be in error owing to underestimated rupture length rates. Generally speaking, these SATURATION lines agree fairly well with the observed distributions for maximum earthquakes. It seems likely in a number of faulting regions, however, that larger earthquakes can be expected than have been recorded. Conspicuous examples are the Rio Grande region (17), Paradox region (15), Pacific Interior (14), Mid-Continent (10), Mexican Highlands (9), Gulf Coast (8), Grand Canyon (7), Eastern Oregon-Western Idaho (6), and the Arizona Mountain Belt (1).

(d) Regions for which there is a seismic parallelogram but no faulting rate data are inferred to have branching fault systems analogous to other regions. Therefore, the seismic parallelogram can be used to infer a general model for the length distribution in hidden faults.

There are numerous implications beyond these broad generalizations. The most conspicuous concerns the need to sharpen the geographic correspondences between faulting regions and seismic source areas. Sequels to this study should take more specific areas having consistent seismic data and focus more sharply on the corresponding fault patterns and faulting rates. Each of these more specific regions should be examined in more detail for agreements between fault length distributions, branching model and earthquake frequencies. As we said earlier, the seismic parallelograms we have used for illustration are approximations to the more rigorous comparisons available among specific power law models.

Another point that catches the eye in the comparison between parallelograms and frequency-magnitude lines in Figures 4.3.2.2.-1, 4.3.2.2.-4 and 5.-1 is the band width for the spectrum of lines relative to the parallelogram width. That is, assuming that a given branching model is totally activated, the steady state distribution for earthquakes probably should cover the whole parallelogram. If the observed earthquakes represented selective fault activations there would be some specific and non-steady consequences. For example, if all earthquakes represented total activations along all faults, the frequency-magnitude line should parallel the SATURATION lines. Or, if all earthquakes represented movements along partial segments of the longest fault, the frequency-magnitude line should parallel the lower side at n=1, and so on.

The observed distributions suggest that earthquakes occur both partially and totally on faults of all lengths and in an approximately steady balance over time. Deviations from the steady state show up as frequency-magnitude lines at sharp angles to the rupture rate lines and as incomplete sets of lines. The limits for the relevant seismic parallelogram then suggest what fault lengths and numbers can be expected to be eventually activated, or what changes in time can be expected to restore a quasi-steady state balance. For example, in the Puget-Olympic region (16) we might expect a great deal of activity in partial movements along the short faults and eventually more incidents having both partial and total activation along the longer fault branches. Larger earthquakes can eventually be expected but at much longer recurrence intervals than are presently recorded. The Arizona Mountain Belt (1), by similarity, might be expected to have increasing numbers of larger earthquakes for some period before analogous compensations involving movements on all branches takes place.

In some diagrams the band width representing frequency-magnitude data exceeds the seismic parallelogram width. Barring a length distribution that is grossly different from an average model, this situation indicates a

nonhomogeneous region or data set. For examples, the Mid-Continent region (10) obviously requires more subregions to make the comparisons more specific. The Salton Trough region (18) clearly involves more than one fault branching distribution.

By and large, however, the frequency-magnitude bands fall within and have similar widths as the seismic parallelograms. We conclude from this correspondence that the branching concepts are generally operative and that an average power law model with an exponent-2 gives a remarkably accurate indication for expected variations in earthquake magnitudes and frequencies over the continental U.S.

SECTION 5.1. FIGURES AND TABLES

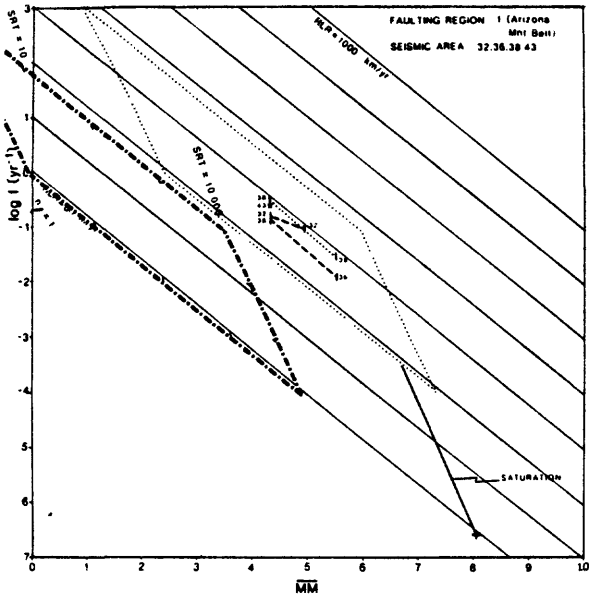

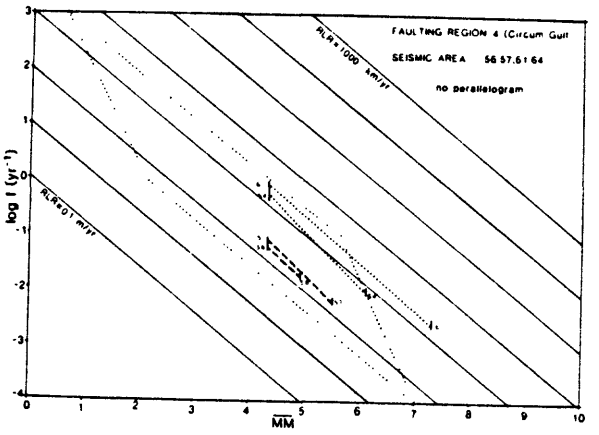

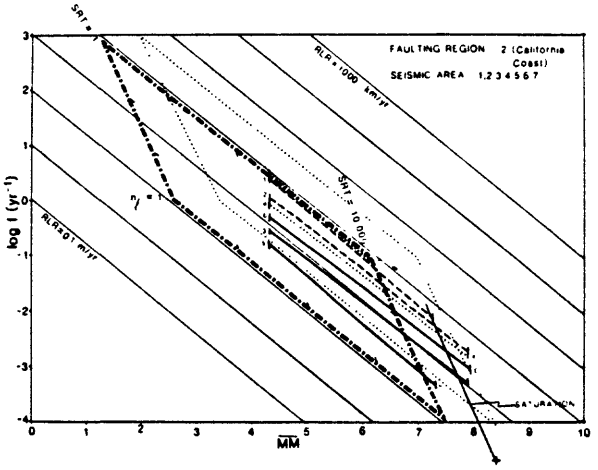

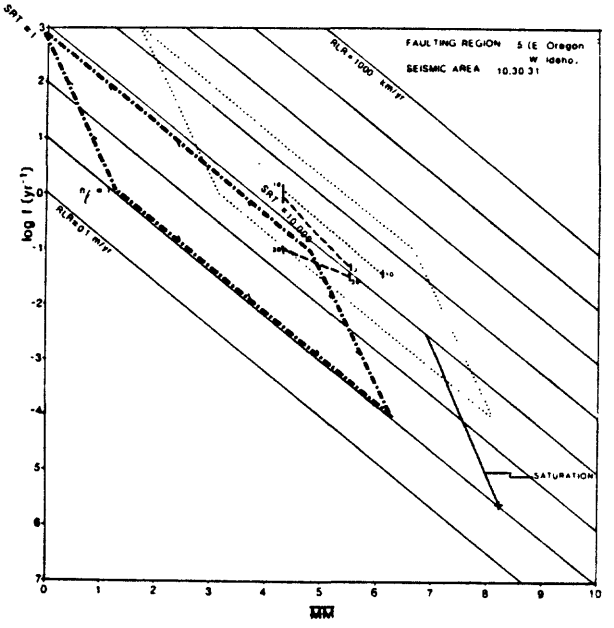

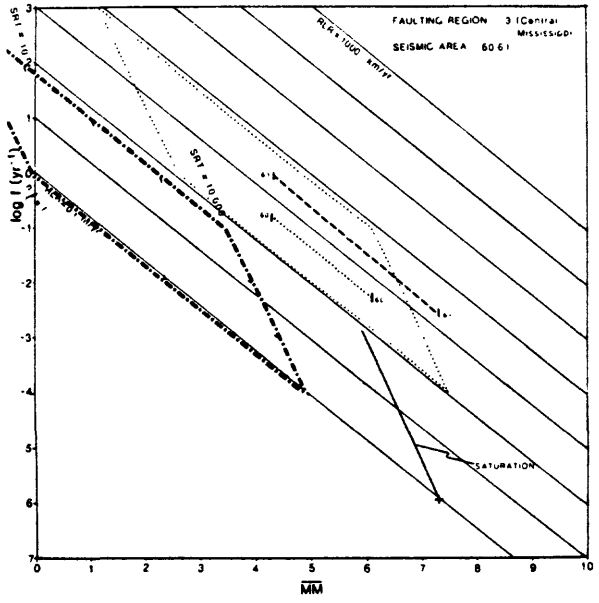

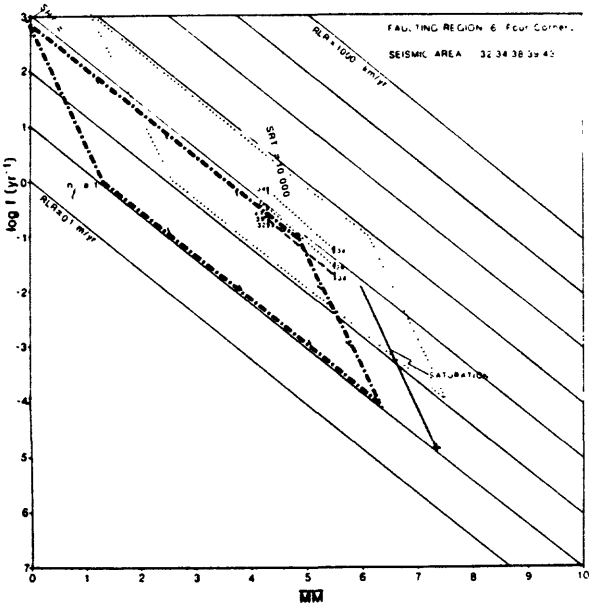

Figure 5.1.-1 (A)

Direct comparisons of paleoseismic parallelograms derived, respectively, from faulting data and from earthquake magnitude and frequency records (i.e., these are composite diagrams comparing the graphs in Figs. 4.3.2.2..-3 and 4.3.2.2.-4).

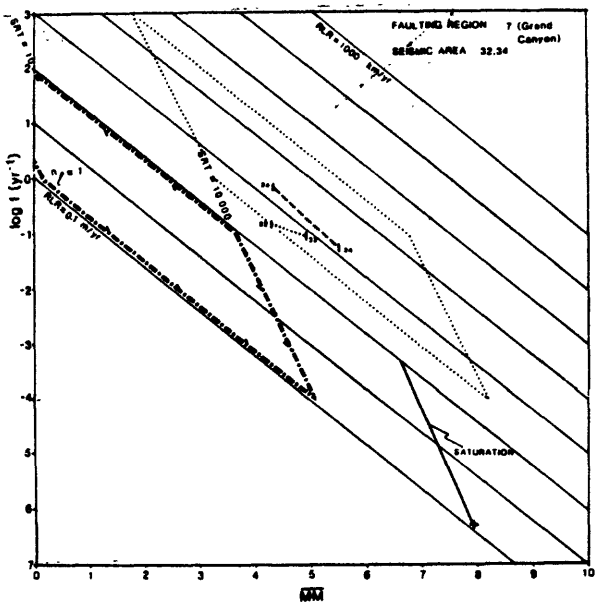
FAULTING REGION 7 (Grand Canyon)
SEISMIC AREA 32,34
RLR = 1000 km/yr
SRT = 10 000
RLR = 0.1 m/yr
SATURATION
log I (yr⁻¹)
MM

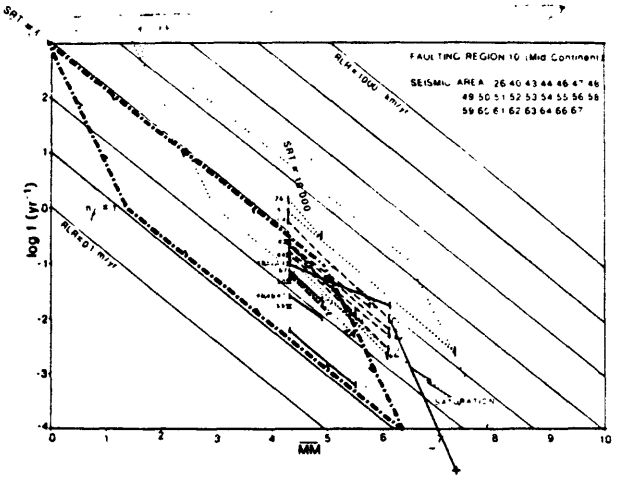
FAULTING REGION 10 (Mid Continent)
SEISMIC AREA 26 40 43 44 46 47 48
49 50 51 52 53 54 55 56 58
59 60 61 62 63 64 66 67
RLR = 1000 km/yr
SRT = 10 000
RLR = 0.1 m/yr
SATURATION
log I (yr⁻¹)
MM

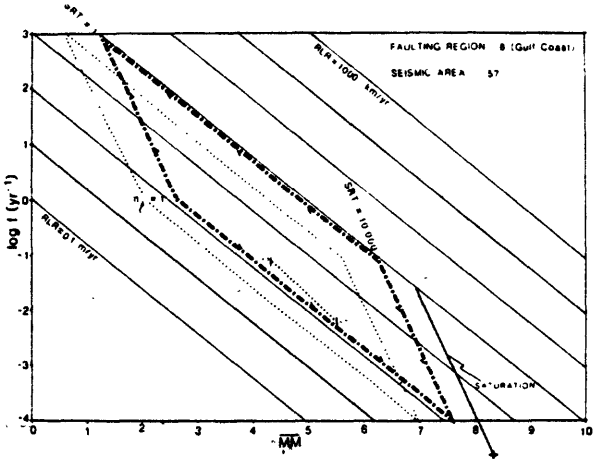
FAULTING REGION 8 (Gulf Coast)
SEISMIC AREA 57
RLR = 1000 km/yr
SRT = 10 000
RLR = 0.1 m/yr
SATURATION
log I (yr⁻¹)
MM

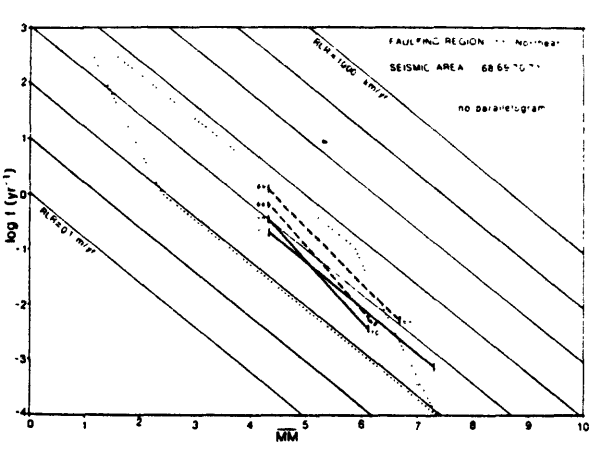
FAULTING REGION
SEISMIC AREA
no parallelogram
RLR = 1000 km/yr
RLR = 0.1 m/yr
log I (yr⁻¹)
MM

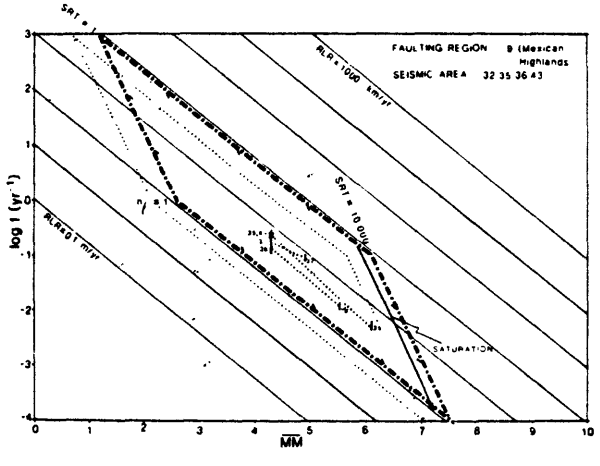
FAULTING REGION 9 (Mexican Highlands)
SEISMIC AREA 32 35 36 43
RLR = 1000 km/yr
SRT = 10 000
RLR = 0.1 m/yr
SATURATION
log I (yr⁻¹)
MM

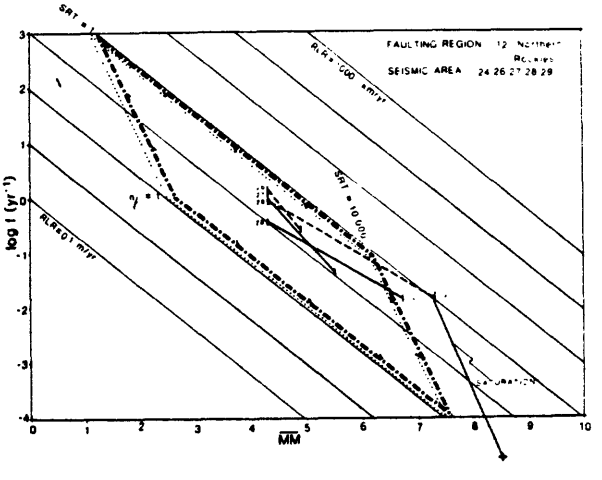
FAULTING REGION 12
SEISMIC AREA 24 26 27 28 29
RLR = 1000 km/yr
SRT = 10 000
RLR = 0.1 m/yr
SATURATION
log I (yr⁻¹)
MM

Figure 5.1.-1. (B)

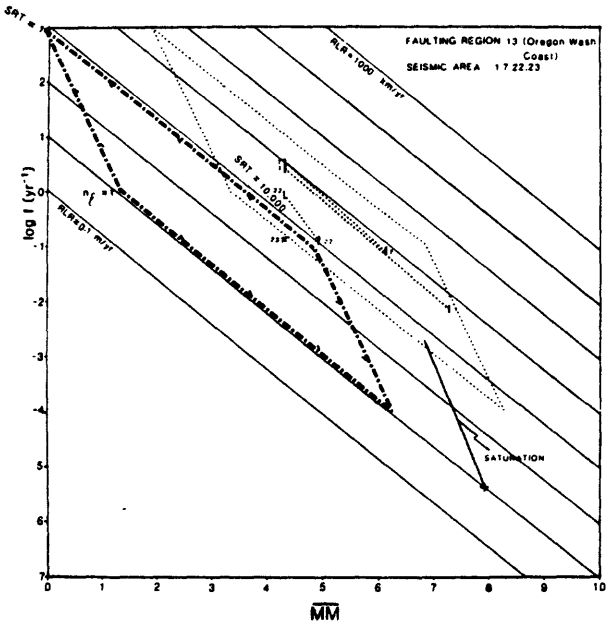
FAULTING REGION 13 (Oregon Wash Coast)
SEISMIC AREA 17 22 23
RLR = 1000 km/yr
RLR = 0.1 m/yr
SRT = 10,000
SATURATION
log f (yr⁻¹)
MM

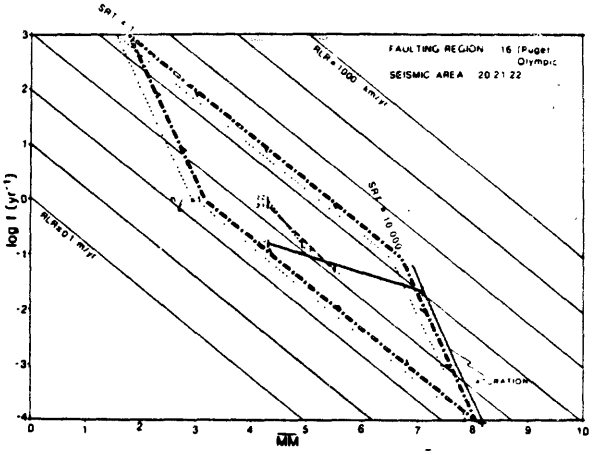
FAULTING REGION 16 (Puget Olympic
SEISMIC AREA 20 21 22
RLR = 1000 km/yr
RLR = 0.1 m/yr
SRT = 10,000
SATURATION
log f (yr⁻¹)
MM

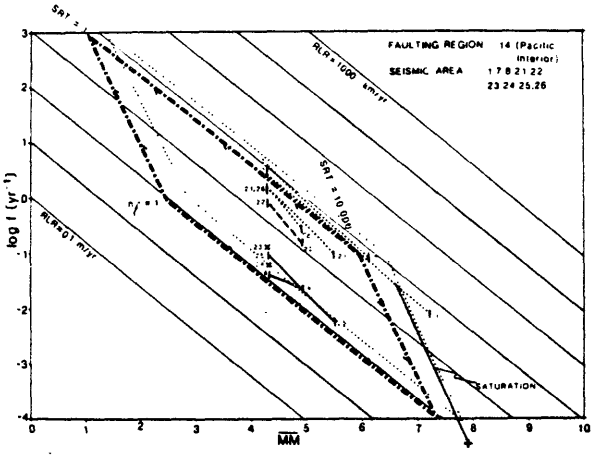
FAULTING REGION 14 (Pacific Interior)
SEISMIC AREA 17 18 21 22 23 24 25 26
RLR = 1000 km/yr
RLR = 0.1 m/yr
SRT = 10,000
SATURATION
log f (yr⁻¹)
MM

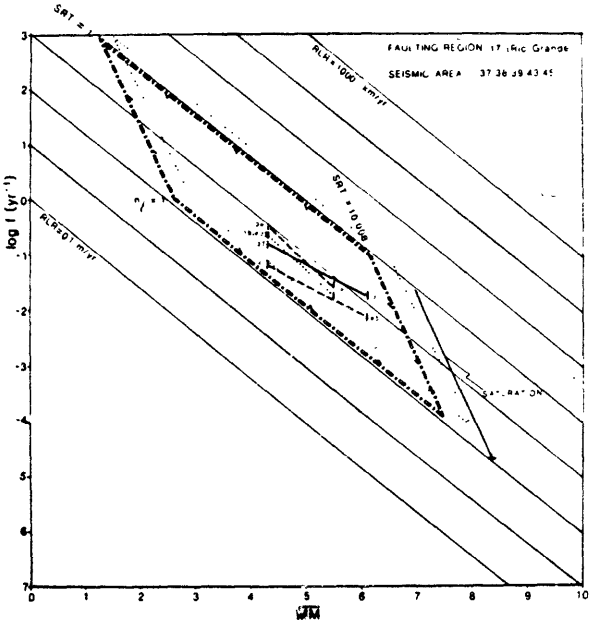
FAULTING REGION 17 (Rio Grande
SEISMIC AREA 37 38 39 43 45
RLR = 1000 km/yr
RLR = 0.1 m/yr
SRT = 10,000
SATURATION
log f (yr⁻¹)
MM

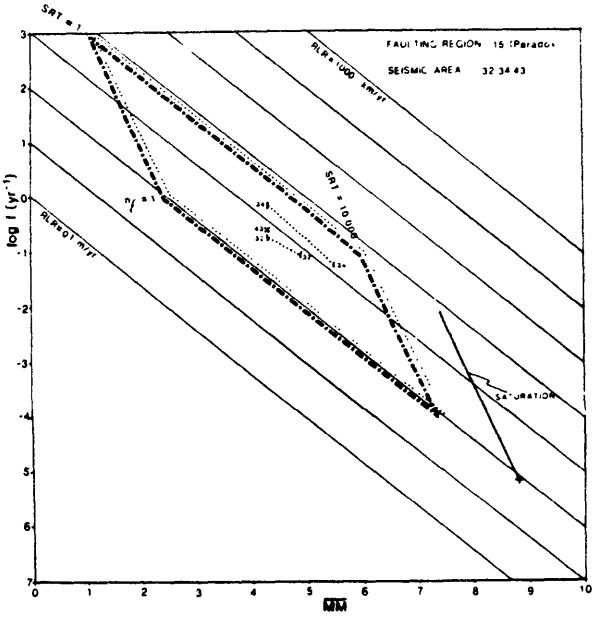
FAULTING REGION 15 (Paradox
SEISMIC AREA 32 34 43
RLR = 1000 km/yr
RLR = 0.1 m/yr
SRT = 10,000
SATURATION
log f (yr⁻¹)
MM

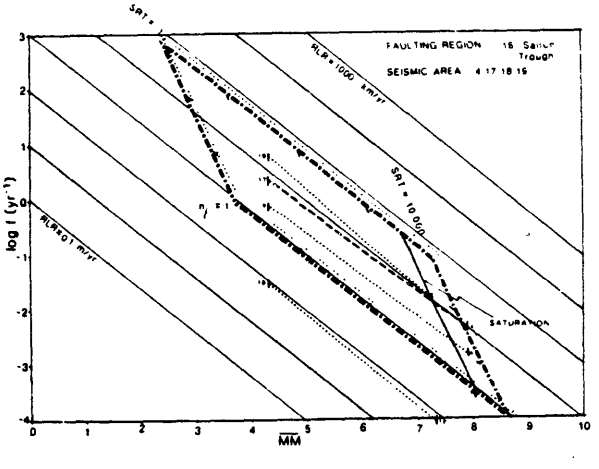
FAULTING REGION 18 Salton Trough
SEISMIC AREA 4 17 18 19
RLR = 1000 km/yr
RLR = 0.1 m/yr
SRT = 10,000
SATURATION
log f (yr⁻¹)
MM

Figure 5.1.-1. (C)

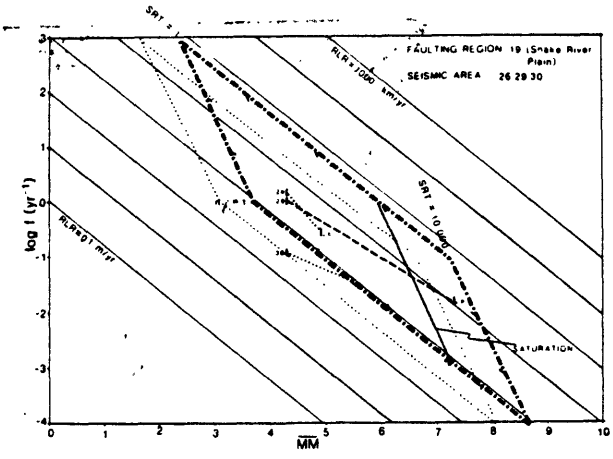
FAULTING REGION 19 (Snake River Plain)
SEISMIC AREA 26 29 30
RLR = 1000 km/yr
RLR = 0.1 m/yr
SRT = 10 000
SATURATION
log f (yr⁻¹)
MM

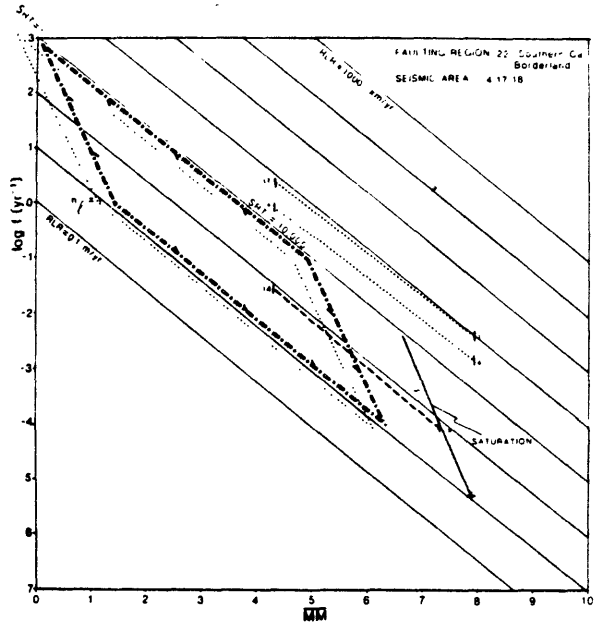
FAULTING REGION 22 Southern Cal Borderland
SEISMIC AREA 4 17 18
RLR = 1000 km/yr
RLR = 0.1 m/yr
SRT = 10 000
SATURATION
log f (yr⁻¹)
MM

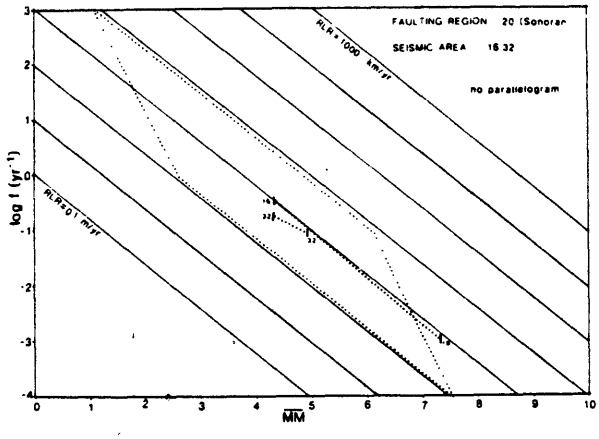
FAULTING REGION 20 (Sonoran
SEISMIC AREA 16 32
no parallelogram
RLR = 1000 km/yr
RLR = 0.1 m/yr
log f (yr⁻¹)
MM

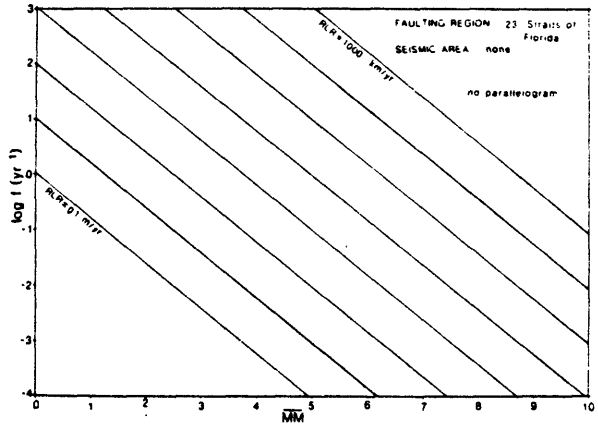
FAULTING REGION 23 Straits of Florida
SEISMIC AREA none
no parallelogram
RLR = 1000 km/yr
RLR = 0.1 m/yr
log f (yr⁻¹)
MM

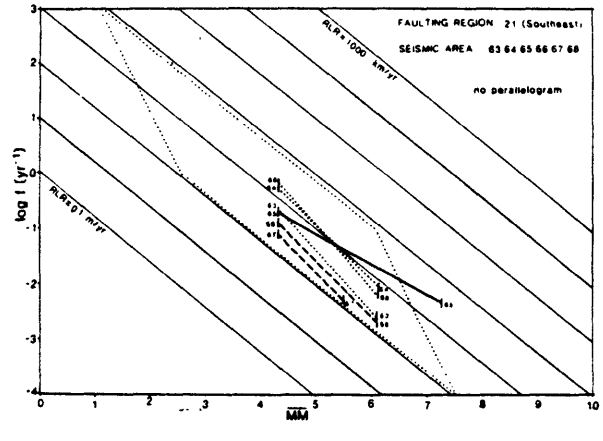
FAULTING REGION 21 (Southeast)
SEISMIC AREA 63 64 65 66 67 68
no parallelogram
RLR = 1000 km/yr
RLR = 0.1 m/yr
log f (yr⁻¹)
MM

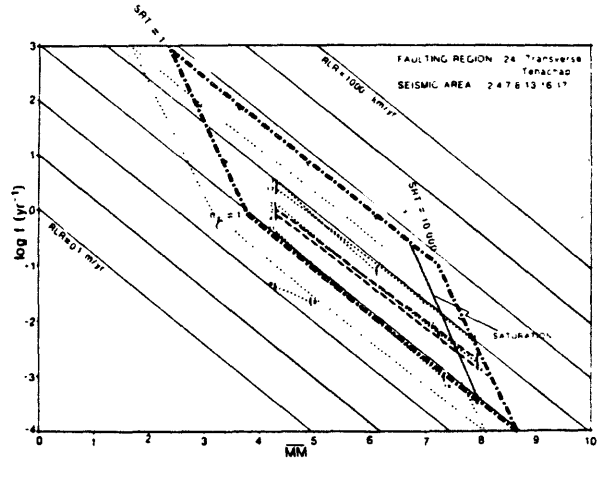
FAULTING REGION 24 Transverse Tenachap
SEISMIC AREA 2 4 7 8 13 16 17
RLR = 1000 km/yr
SRT = 10 000
SATURATION
RLR = 0.1 m/yr
log f (yr⁻¹)
MM

Figure 5.1.-1. (D)

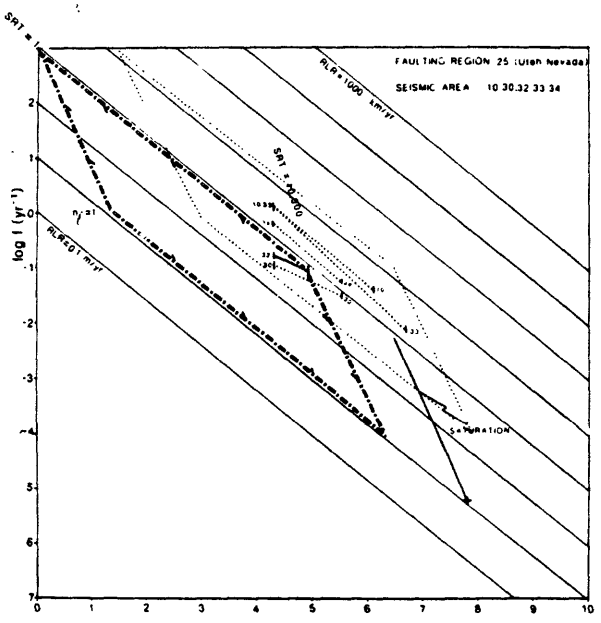
FAULTING REGION 25 (Utah Nevada)
SEISMIC AREA 10 30 32 33 34
RLR = 1000 km/yr
SRT = 10,000
n/s = 1
RLR = 0.1 m/yr
SATURATION
log f (yr⁻¹)

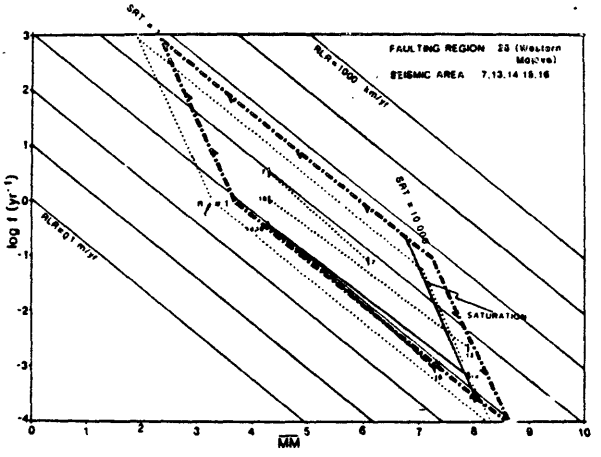
FAULTING REGION 28 (Western Mojave)
SEISMIC AREA 7,13,14,15,16
RLR = 1000 km/yr
SRT = 10,000
n/s = 1
RLR = 0.1 m/yr
SATURATION
log f (yr⁻¹)
MM

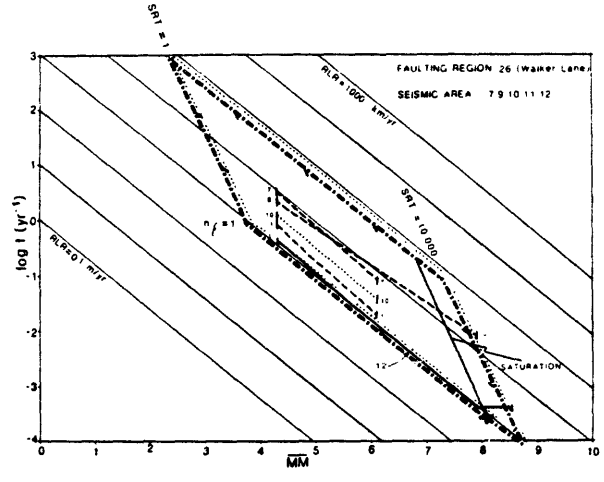
FAULTING REGION 26 (Walker Lane)
SEISMIC AREA 7 9 10 11 12
RLR = 1000 km/yr
SRT = 10,000
n/s = 1
RLR = 0.1 m/yr
SATURATION
log f (yr⁻¹)
MM

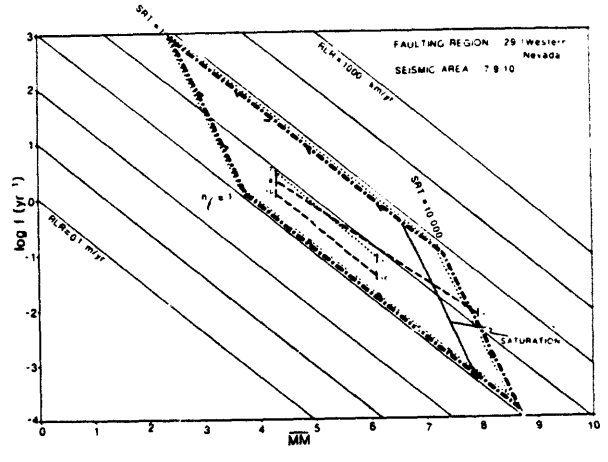
FAULTING REGION 29 (Western Nevada)
SEISMIC AREA 7 9 10
RLR = 1000 km/yr
SRT = 10,000
n/s = 1
RLR = 0.1 m/yr
SATURATION
log f (yr⁻¹)
MM

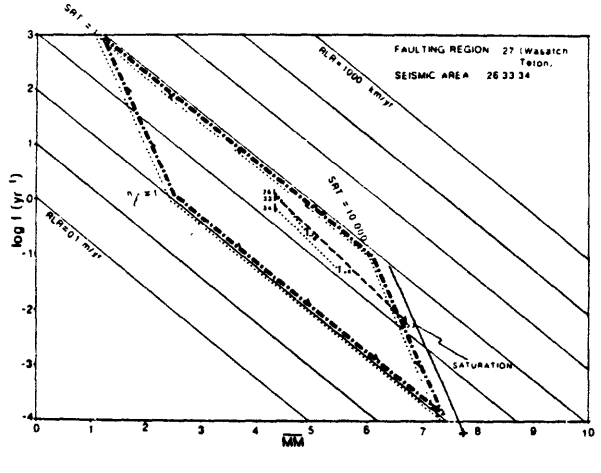
FAULTING REGION 27 (Wasatch Teton)
SEISMIC AREA 26 33 34
RLR = 1000 km/yr
SRT = 10,000
n/s = 1
RLR = 0.1 m/yr
SATURATION
log f (yr⁻¹)
MM

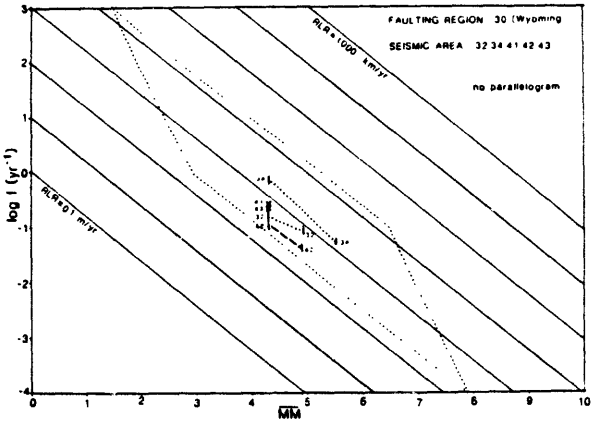
FAULTING REGION 30 (Wyoming)
SEISMIC AREA 32 34 41 42 43
no parallelogram
RLR = 1000 km/yr
RLR = 0.1 m/yr
log f (yr⁻¹)
MM

Figure 5.1.-1(E)

REFERENCES

Algermissen, S. T., 1969, Seismic risk studies in the United States. World Conference on Earthquake Engineering, 4th, Santiago, Chile, January 13-18, 1969, Proceedings, v. 1, p. 14-27.

Algermissen, S. T., and Perkins, D. M., 1976, A probabilistic estimate of maximum acceleration in rock in the contiguous U. S.: U.S. Geological Survey Open-file Report 76-416, 45 p.

Donovan, N. C., Bolt, B. A., and Whitman, R. V., 1978, Development of expectancy maps and risk analysis: Proceedings, American Society Civil Engineers, v. 104, p. 1179-1192.

Hartmann, W. K., 1977, Cratering in the solar system: Scientific American, v. 236, p. 84-99.

Horton, R. E., 1945, Erosional development of streams and their drainage basins; hydrophysical, approach to quantitative morphology: Geological Society of America Bulletin, v. 56, p. 275-370.

Howard, K. A., 1978, Preliminary map of young faults in the United States as a guide to possible fault activity: U.S. Geological Survey Miscellaneous Feild Studies Map MF-916 (Sheet 1 of 2).

Kitagawa, H., and Suzuki, I., 1975, Reliability approaches in fracture mechanics, in A. M. Freudenthal (ed.) Reliability Approaches in Structural Engineering: Tokyo, Maruzen, p. 217-233.

Leopold, L. B., and Langbein, W. B., 1962, The concept of entropy in landscape evolution: U.S. Geological Survey Professional Paper 500-A, 20 p.

Mark, R. K., 1977, Application of linear statistical models of earthquake magnitude versus fault length in estimating maximum expectable earthquakes: Geology, v. 5, p. 464-466.

Mark, R. K., and Bonilla, M. G., 1977, Regression analysis of earthquake magnitude and surface fault length using the 1970 data of Bonilla and Buchanan: U.S. Geological Survey Open-file Report 77-614, 8 p.

Miller, B. R., 1977, Close Packing and Cracking: M.S. thesis, University of Oregon, Eugene, 35 p.

Shreve, R. L., 1966, Statistical law of stream numbers: Journal of Geology, v. 74, p. 17-38.

Stevens, P. S., 1974, Patterns in Nature: Boston, Little Brown, 240 p.

Strahler, A. N., 1952, Hypsometric (area-altitude) analysis of erosional topography: Geological Society of America Bulletin, v. 63, p. 1117-1142.

Strahler, A. N., 1964, Quantitative geomorphology of drainage basins and channel networks, in Ven Te Chow (editor), Handbook of Applied Hydrology: Compendium of Water Resources Technology: New York, McGraw-Hill, p. 39-76.

Thompson, D'Arcy W., 1942, On Growth and Form, 2nd edition: Cambridge, Cambridge University Press.

Vere-Jones, D., 1976, A branching model for crack propagation: Pure and Applied Geophysics, v. 114, p. 711-725.

Woldenberg, M. J., 1966, Horton's laws justified in terms of allometric growth and steady state in open systems: Geological Society of America Bulletin, v. 77, p. 431-434.

Woldenberg, M. J., 1968a, Hierarchical systems: Cities, rivers, alpine glaciers, bovine livers, and trees: Ph.D. Dissertation, Columbia University, New York.

Woldenberg, M. J., 1968b, Energy flow and spatial orders -- mixed hexagonal heirarchies of central places: Geographical Review, v. 58, p. 552-574.

Woldenberg, M. J., 1969, Spatial order in fluvial systems: Horton's laws derived from mixed hexagonal hierarchies of drainage basin areas: Geological Society of America Bulletin, v. 80, p. 97-112.

Woldenberg, M. J., 1971, A structural taxonomy of spatial hierarchies, in M. Chisholm, A. E. Frey, and P. Haggett (eds.) Regional Forecasting: Hamden, Conn., Anchor Books, p. 147-175.

Woldenberg, M. J., and Berry, B. J. L., 1967, Rivers and central places: Analogous systems?: Journal of Regional Science, v. 7, p. 129-139.

Ziony, J. I., Wentworth, C. M., Buchanan-Banks, J. M., and Wagner, H. C., 1974, Preliminary map showing recency of faulting in coastal southern California: U. S. Geological Survey Miscellaneous Field Studies, Map MF-585 (sheets 1 and 2 of 3).